

TOPICS IN CURRENT CHEMISTRY

289

Volume Editor S. Inagaki

Orbitals in Chemistry

 Springer

Topics in Current Chemistry

Editorial Board:

V. Balzani · A. de Meijere · K.N. Houk · H. Kessler

J.-M. Lehn · S. V. Ley · M. Olivucci · S. Schreiber · J. Thiem

B. M. Trost · P. Vogel · F. Vögtle · H. Wong · H. Yamamoto

Topics in Current Chemistry

Recently Published and Forthcoming Volumes

Orbitals in Chemistry

Volume Editor: Satoshi Inagaki
Vol. 289, 2009

Glycoscience and Microbial Adhesion

Volume Editors: Thisbe K. Lindhorst,
Stefan Oscarson
Vol. 288, 2009

Templates in Chemistry III

Volume Editors: Broekmann, P., Dötz, K.-H.,
Schalley, C.A.
Vol. 287, 2009

Tubulin-Binding Agents:

Synthetic, Structural and Mechanistic Insights

Volume Editor: Carlomagno, T.
Vol. 286, 2009

STM and AFM Studies on (Bio)molecular Systems: Unravelling the Nanoworld

Volume Editor: Samorì, P.
Vol. 285, 2008

Amplification of Chirality

Volume Editor: Soai, K.
Vol. 284, 2008

Anthracycline Chemistry and Biology II

Mode of Action, Clinical Aspects and New Drugs
Volume Editor: Krohn, K.
Vol. 283, 2008

Anthracycline Chemistry and Biology I

Biological Occurrence and Biosynthesis,
Synthesis and Chemistry
Volume Editor: Krohn, K.
Vol. 282, 2008

Photochemistry and Photophysics of Coordination Compounds II

Volume Editors: Balzani, V., Campagna, S.
Vol. 281, 2007

Photochemistry and Photophysics of Coordination Compounds I

Volume Editors: Balzani, V., Campagna, S.
Vol. 280, 2007

Metal Catalyzed Reductive C–C Bond Formation

A Departure from Preformed Organometallic Reagents
Volume Editor: Krische, M. J.
Vol. 279, 2007

Combinatorial Chemistry on Solid Supports

Volume Editor: Bräse, S.
Vol. 278, 2007

Creative Chemical Sensor Systems

Volume Editor: Schrader, T.
Vol. 277, 2007

In situ NMR Methods in Catalysis

Volume Editors: Bargon, J., Kuhn, L. T.
Vol. 276, 2007

Sulfur-Mediated Rearrangements II

Volume Editor: Schaumann, E.
Vol. 275, 2007

Sulfur-Mediated Rearrangements I

Volume Editor: Schaumann, E.
Vol. 274, 2007

Bioactive Conformation II

Volume Editor: Peters, T.
Vol. 273, 2007

Bioactive Conformation I

Volume Editor: Peters, T.
Vol. 272, 2007

Orbitals in Chemistry

Volume Editor: Satoshi Inagaki

With Contributions by

S. Inagaki · M. Ishida · J. Ma · Y. Naruse · T. Ohwada · Y. Wang

 Springer

Editor
Satoshi Inagaki
Gifu University
Faculty of Engineering
Department of Chemistry
1-1 Yanagido
Gifu
501-1193 Japan
inagaki@gifu-u.ac.jp

ISSN 0340-1022 e-ISSN 1436-5049
ISBN 978-3-642-01750-6 e-ISBN 978-3-642-01751-3
DOI 10.1007/978-3-642-01751-3
Springer Heidelberg Dordrecht London New York

Library of Congress Control Number: 2009938932

© Springer-Verlag Berlin Heidelberg 2009

This work is subject to copyright. All rights are reserved, whether the whole or part of the material is concerned, specifically the rights of translation, reprinting, reuse of illustrations, recitation, roadcasting, reproduction on microfilm or in any other way, and storage in data banks. Duplication of this publication or parts thereof is permitted only under the provisions of the German Copyright Law of September 9, 1965, in its current version, and permission for use must always be obtained from Springer. Violations are liable to prosecution under the German Copyright Law.

The use of general descriptive names, registered names, trademarks, etc. in this publication does not imply, even in the absence of a specific statement, that such names are exempt from the relevant protective laws and regulations and therefore free for general use.

Cover design: WMXDesign GmbH, Heidelberg, Germany

Printed on acid-free paper

Springer is part of Springer Science+Business Media (www.springer.com)

Volume Editor

Satoshi Inagaki

Gifu University
Faculty of Engineering
Department of Chemistry
1-1 Yanagido
Gifu
501-1193 Japan
inagaki@gifu-u.ac.jp

Editorial Board

Prof. Dr. Vincenzo Balzani

Dipartimento di Chimica "G. Ciamician"
University of Bologna
via Selmi 2
40126 Bologna, Italy
vincenzo.balzani@unibo.it

Prof. Dr. Armin de Meijere

Institut für Organische Chemie
der Georg-August-Universität
Tammanstr. 2
37077 Göttingen, Germany
ameijer1@uni-goettingen.de

Prof. Dr. Kendall N. Houk

University of California
Department of Chemistry and Biochemistry
405 Hilgard Avenue
Los Angeles, CA 90024-1589, USA
houk@chem.ucla.edu

Prof. Dr. Horst Kessler

Institut für Organische Chemie
TU München
Lichtenbergstraße 4
86747 Garching, Germany
kessler@ch.tum.de

Prof. Dr. Jean-Marie Lehn

ISIS
8, allée Gaspard Monge
BP 70028
67083 Strasbourg Cedex, France
lehn@isis.u-strasbg.fr

Prof. Dr. Steven V. Ley

University Chemical Laboratory
Lensfield Road
Cambridge CB2 1EW
Great Britain
Svl1000@cus.cam.ac.uk

Prof. Dr. Massimo Olivucci

Università di Siena
Dipartimento di Chimica
Via A De Gasperi 2
53100 Siena, Italy
olivucci@unisi.it

Prof. Dr. Stuart Schreiber

Chemical Laboratories
Harvard University
12 Oxford Street
Cambridge, MA 02138-2902, USA
sls@slsiris.harvard.edu

Prof. Dr. Joachim Thiem

Institut für Organische Chemie
Universität Hamburg
Martin-Luther-King-Platz 6
20146 Hamburg, Germany
thiem@chemie.uni-hamburg.de

Prof. Dr. Barry M. Trost

Department of Chemistry
Stanford University
Stanford, CA 94305-5080, USA
bmtrost@leland.stanford.edu

Prof. Dr. Pierre Vogel

Laboratory of Glycochemistry
and Asymmetric Synthesis
EPFL – Ecole polytechnique fédérale
de Lausanne
EPFL SB ISIC LGSA
BCH 5307 (Bat.BCH)
1015 Lausanne, Switzerland
pierre.vogel@epfl.ch

Prof. Dr. Fritz Vögtle

Kekulé-Institut für Organische Chemie
und Biochemie
der Universität Bonn
Gerhard-Domagk-Str. 1
53121 Bonn, Germany
voegtle@uni-bonn.de

Prof. Dr. Henry Wong

The Chinese University of Hong Kong
University Science Centre
Department of Chemistry
Shatin, New Territories
hncwong@cuhk.edu.hk

Prof. Dr. Hisashi Yamamoto

Arthur Holly Compton Distinguished
Professor
Department of Chemistry
The University of Chicago
5735 South Ellis Avenue
Chicago, IL 60637
773-702-5059
USA
yamamoto@uchicago.edu

Topics in Current Chemistry Also Available Electronically

Topics in Current Chemistry is included in Springer's eBook package *Chemistry and Materials Science*. If a library does not opt for the whole package the book series may be bought on a subscription basis. Also, all back volumes are available electronically.

For all customers who have a standing order to the print version of *Topics in Current Chemistry*, we offer the electronic version via SpringerLink free of charge.

If you do not have access, you can still view the table of contents of each volume and the abstract of each article by going to the SpringerLink homepage, clicking on "Chemistry and Materials Science," under Subject Collection, then "Book Series," under Content Type and finally by selecting *Topics in Current Chemistry*.

You will find information about the

- Editorial Board
- Aims and Scope
- Instructions for Authors
- Sample Contribution

at springer.com using the search function by typing in *Topics in Current Chemistry*.

Color figures are published in full color in the electronic version on SpringerLink.

Aims and Scope

The series *Topics in Current Chemistry* presents critical reviews of the present and future trends in modern chemical research. The scope includes all areas of chemical science, including the interfaces with related disciplines such as biology, medicine, and materials science.

The objective of each thematic volume is to give the non-specialist reader, whether at the university or in industry, a comprehensive overview of an area where new insights of interest to a larger scientific audience are emerging.

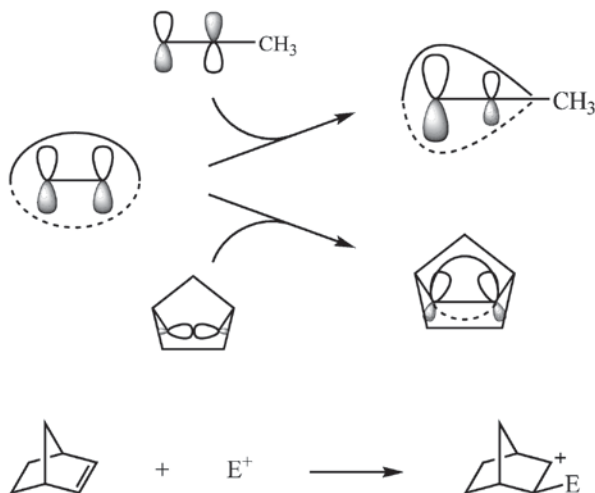
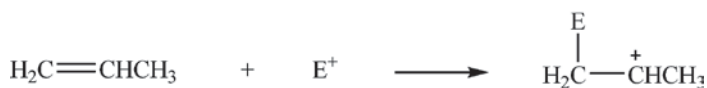
Thus each review within the volume critically surveys one aspect of that topic and places it within the context of the volume as a whole. The most significant developments of the last 5–10 years are presented, using selected examples to illustrate the principles discussed. A description of the laboratory procedures involved is often useful to the reader. The coverage is not exhaustive in data, but rather conceptual, concentrating on the methodological thinking that will allow the non-specialist reader to understand the information presented.

Discussion of possible future research directions in the area is welcome.

Review articles for the individual volumes are invited by the volume editors.

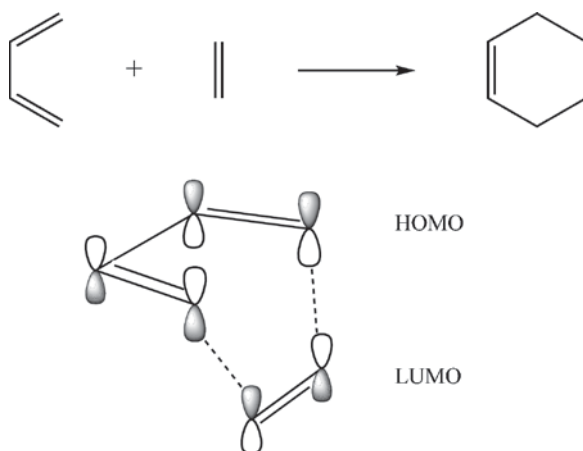
In references *Topics in Current Chemistry* is abbreviated *Top Curr Chem* and is cited as a journal.

Impact Factor 2008: 5.270; Section “Chemistry, Multidisciplinary”: Rank 14 of 125



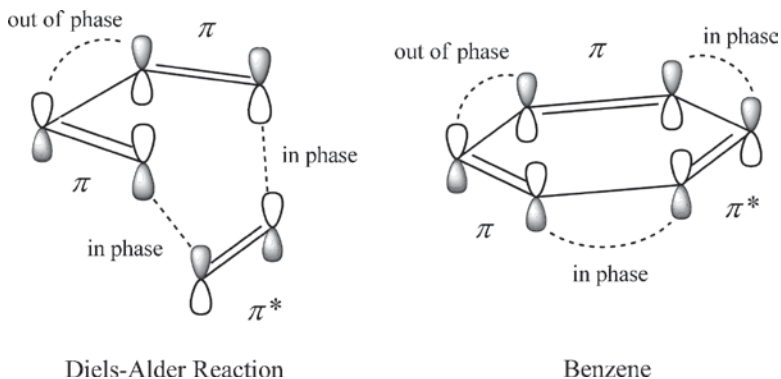
Scheme 2 Orbital mixing changes amplitudes

The history of orbital phase can be traced back to the theory of chemical bond or bonding and antibonding orbitals by Lennard-Jones in 1929. The second milestone was the discovery of the importance of orbital symmetry in chemical reactions, pointed out by Fukui in 1964 (Scheme 3) and established by Woodward and



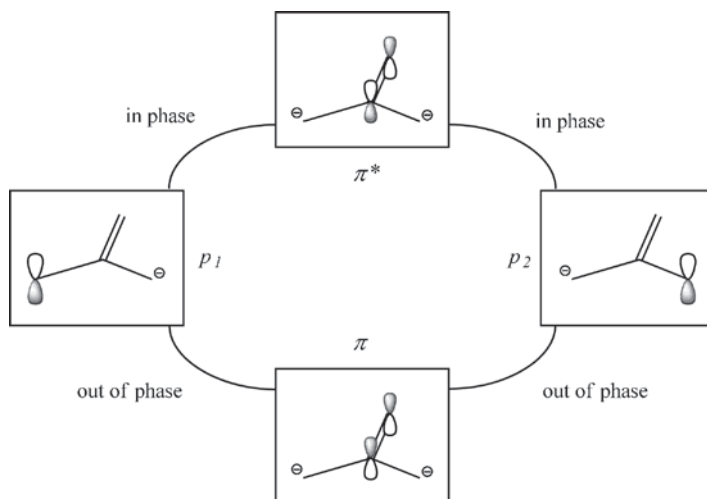
Scheme 3 Orbital symmetry

Hoffmann in 1965. Ten years later, Fukui and Inagaki proposed an orbital phase theory for cyclic molecules and transition states, which includes the Woodward-Hoffmann rule and the Hückel rule for aromaticity (Scheme 4). In 1982 Inagaki



Scheme 4 Orbital phase

and Hirabayashi disclosed cyclic orbital interactions even in noncyclic conjugated systems (Scheme 5). The orbital phase was shown to control noncyclic as well as cyclic systems. The orbital phase theory has since expanded and is still expanding the scope of its applications.



Scheme 5 Cyclic orbital interaction in noncyclic conjugation

One day Fukui sent me an article where Dirac wrote [Dirac PAM (1972) Fields and Quanta, 3:139]:

.... “However, the one fundamental idea which was introduced by Heisenberg and Schroedinger was that one must work with noncommutative algebra.” “The question arises whether the noncommutation is really the main new idea of quantum mechanics. Previously I always thought it was but recently I have begun to doubt it.” “So the real genius of Heisenberg and Schroedinger, you might say, was to discover the existence of probability *amplitudes* containing this *phase* quantity which is very well hidden in nature.” Dirac thought that amplitude and phase are keywords in quantum mechanics. His words encouraged me in the early days, although he was not referring to amplitude and phase of orbitals.

In the first chapter, a theory for the interactions of two orbitals is briefly summarized for students or chemists who are not familiar with orbitals and for readers to understand the theoretical background common to all the other chapters of this volume. In the second chapter, the mechanism of chemical reactions is proposed to form a spectrum composed of a delocalization band – a pseudoexcitation band – a transfer band. In the third chapter, a theory for the interactions of three orbitals is described and applications of orbital mixing rules to stereoselective organic reactions are reviewed. In the fourth chapter, an orbital phase theory for cyclic orbital interactions and its applications are described and reviewed. In the fifth chapter, orbital phase in the environments of reaction centers is shown to control stereoselectivities of organic reactions. In the sixth chapter, π -facial selectivities of Diels-Alder reactions are reviewed. In the seventh chapter, the orbital phase theory is applied to designing persistent singlet localized diradicals. In the eighth chapter, a theory for the relaxation of small ring strains is described and reviewed and in the ninth chapter, the chemical orbital theory is shown to be helpful in thinking about inorganic molecules as well.

The chemical orbital theory has been established almost as described in this volume. The theory is useful and reliable for thinking about molecules and reactions. In the future, applications will shift more and more from understanding to designing molecules and reactions.

I appreciate the help and encouragement offered to me by Prof. Hisashi Yamamoto of the University of Chicago.

Summer 2009

Satoshi Inagaki

Contents

Elements of a Chemical Orbital Theory	1
Satoshi Inagaki	
A Mechanistic Spectrum of Chemical Reactions	23
Satoshi Inagaki	
Orbital Mixing Rules	57
Satoshi Inagaki	
An Orbital Phase Theory	83
Satoshi Inagaki	
Orbital Phase Environments and Stereoselectivities	129
Tomohiko Ohwada	
π-Facial Selectivity of Diels-Alder Reactions	183
Masaru Ishida and Satoshi Inagaki	
Orbital Phase Design of Diradicals	219
Jing Ma, Satoshi Inagaki, and Yong Wang	
Relaxation of Ring Strains	265
Yuji Naruse and Satoshi Inagaki	
Orbitals in Inorganic Chemistry: Metal Rings and Clusters, Hydronitrogens, and Heterocycles	293
Satoshi Inagaki	
Index	317

Elements of a Chemical Orbital Theory

Satoshi Inagaki

Abstract Interaction is important in chemistry. Interactions of atoms form chemical bonds. Bonds interact with each other in molecules to determine the molecular properties. Interactions of molecules give rise to chemical reactions. Electrons control atoms, bonds, and molecules. The behavior of electrons is simply and effectively represented by orbitals, which contain wave properties, i.e., phase and amplitude. In our chemical orbital theory we consider the interactions of the orbitals of atoms, bonds and molecules. The elements of the chemical orbital theory are separated into three groups: (1) interactions of *two* orbitals, (2) interactions of *three* orbitals, and (3) *cyclic* interactions of *more than two* orbitals. Here, general aspects of the interactions of *two* orbitals are summarized to show the background of this volume and assist nonspecialists to read the following chapters. Among the keywords are: phase and amplitude of orbitals, strength of orbital interactions, electron delocalization, electron localization, exchange repulsion, ionization energy, electronic spectrum, frontier orbitals, reactivity, selectivity, orbital symmetry, and so on. The remaining elements of the chemical orbital theory, i.e., orbital mixing rules for the three-orbital interactions and an orbital phase theory for the cyclic interactions, are introduced briefly.

Keywords Chemical orbital theory, Electron delocalization, Frontier orbital, Orbital amplitude, Orbital energy, Orbital interaction, Orbital mixing rule, Orbital phase, Orbital phase continuity, Orbital phase environment, Orbital symmetry, Reactivity, Selectivity

S. Inagaki (✉)
Department of Chemistry, Faculty of Engineering, Gifu University, Yanagido,
Gifu 501-1193, Japan
e-mail: inagaki@gifu-u.ac.jp

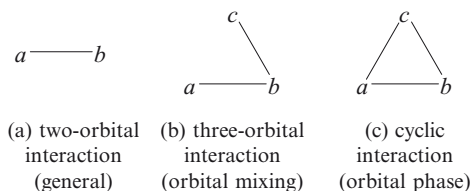
Contents

1	General Rules of Orbital Interactions: Chemical Bonds.....	2
1.1	Phase of Orbitals	3
1.2	Amplitude of Orbitals: Interactions of Different Orbitals	4
1.3	Strength of Orbital Interactions	6
1.4	Electron Delocalization	8
1.5	Exchange Repulsion	9
1.6	Stabilization and Number of Electrons	9
2	Applications to Molecular Properties: Interactions of Bond Orbitals	11
2.1	From Bond Orbitals to Molecular Orbitals	11
2.2	Energy, Phase, and Amplitude of Orbitals	12
2.3	Ionization Energies	13
2.4	Electronic Spectra.....	13
3	Applications to Chemical Reactions: Interactions of Frontier Orbitals.....	13
3.1	Frontier Orbital Theory	14
3.2	From Electron Density to Frontier Orbital Amplitude.....	14
3.3	Reactivity.....	15
3.4	Selectivity	16
3.5	Orbital Symmetry	16
3.6	Orbital Phase Environments	17
3.7	Radical Reactions: Copolymerizations	18
3.8	Photochemical Reactions	19
4	Interactions of More Than Two Orbitals.....	20
4.1	Orbital Mixing Rules.....	21
4.2	An Orbital Phase Theory.....	21
	References.....	21

1 General Rules of Orbital Interactions: Chemical Bonds

The elements of the chemical orbital theory are general rules for interactions of *two* orbitals, orbital mixing rules for interactions of *three* orbitals, and orbital phase rules for *cyclic* interactions of *more than two* orbitals (Scheme 1). Here, we summarize general rules for the two-orbital interactions [1, 2] using an example of atomic orbital interactions to generate bond orbitals.

The bond orbitals contain wave properties, i.e., phase and amplitude. The phase property determines the energy of orbitals. The amplitude determines electron density distributions. Strength of interactions depends on the overlap and the energy gap between the orbitals. The numbers of electrons are crucial to attraction or repulsion. A clear image is given for delocalization of electrons important in chemistry.

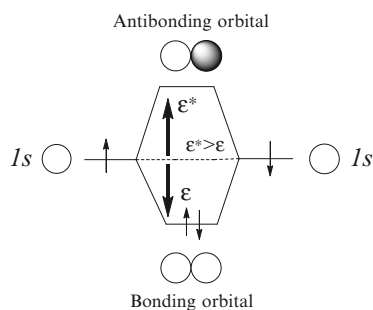


Scheme 1 Interactions of orbitals

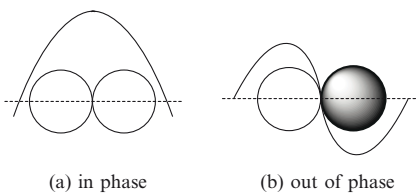
1.1 Phase of Orbitals

The solution of the Schrodinger equation for a hydrogen atom gives atomic orbitals, e.g., *s*-orbitals, *p*-orbitals and so on. There are assumed to be orbitals for the electrons of chemical bonds. The bond orbitals, i.e., the bonding and antibonding orbitals of a hydrogen molecule are illustrated in Scheme 2. The bonding orbital lies lower in energy than the *1s* atomic orbitals, whereas the antibonding orbital lies higher. The *1s* orbitals have the same signs of values in the overlap region or a positive overlap integral in the bonding orbital, and opposite signs or a negative overlap integral in the antibonding orbital. The sign relations suggest a wave property of the electrons in the bond (Scheme 3). The combinations giving the positive (negative) overlaps are referred to as the in-phase (out-of-phase) combination. The phase properties make a difference in the electron distribution as well as the orbital energy. Electron density increases (decreases) in the overlap region of the in-phase (out-of-phase) combined orbitals (Scheme 4). The orbital phase features the bonding and antibonding properties of bond orbitals [3]. A chemical bond forms when both electrons in the atomic orbitals occupy the stabilized or bonding orbital. This is the simplest answer to the question of why neutral hydrogen atoms are bonded to each other. In our chemical orbital theory, a chemical bond is represented by the bonding orbital occupied by a pair of electrons and the vacant antibonding orbital rather than a line between the atoms in the organic electron theory.

More than two electrons cannot occupy the bonding orbital (the Pauli's exclusion principle). Third and fourth electrons occupy the antibonding orbital. The antibonding property overcomes the bonding property ($\epsilon^* > \epsilon$ in Scheme 2) and breaks the bond.



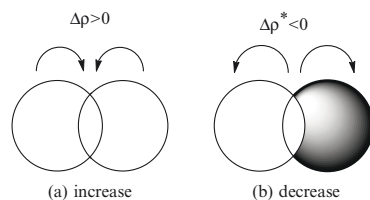
Scheme 2 Bond orbitals of a hydrogen molecule



Scheme 3 Phase of orbitals

(a) in phase

(b) out of phase

Scheme 4 Electron density in the overlap region

This is the case with He_2 , which is known not to exist as a stable molecule. Ethylene $\text{CH}_2=\text{CH}_2$ has a π bond while hydrazine NH_2-NH_2 with two more electrons has no π bond but two lone pairs.

The theory of two-orbital interactions leads to some general rules of orbital interactions:

1. Interactions of two orbitals gives in-phase and out-of-phase combined orbitals
2. The in-phase (out-of-phase) combined orbitals are stabilized (destabilized) and bonding (antibonding)
3. The destabilization (the antibonding property) of the out-of-phase combined orbital overcomes the stabilization (the bonding property) of the in-phase combined orbitals

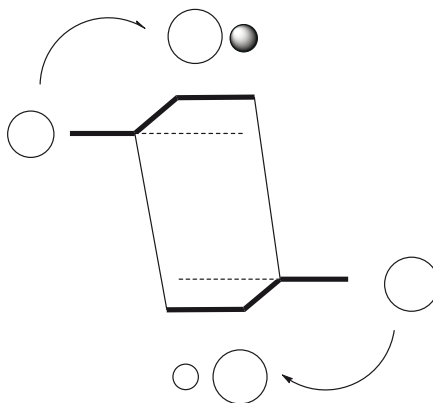
The stabilization of the in-phase combined orbital implies that electrons are more stabilized by the delocalization to the overlap region than by the localization to the interacting orbitals. The relative stability of the out-of-phase combined orbitals has been reported in a few papers [4–6].

1.2 Amplitude of Orbitals: Interactions of Different Orbitals

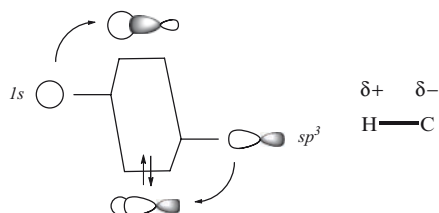
We have learned the interactions of the same orbitals and chemical bonds between the same atoms. The orbital phase plays a crucial role in the energies and the spacial extensions of the bond orbitals. Here we learn interactions of different orbitals and amplitude of orbitals, using an example of polar bonds between different atoms.

The orbital interaction rules described in the Sect. 1.1 are generalized here (Scheme 5):

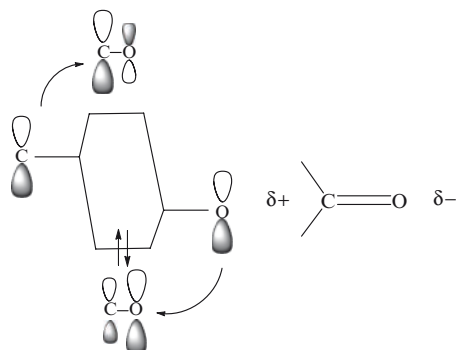
- A low-lying orbital lowers its energy and deforms its spacial extension by mixing a high-lying orbital in phase whereas a high-lying orbital raises its energy and deforms its spacial extension by mixing a low-lying orbital in out of phase. In other words:
 1. The in-phase combined orbital lies lower in energy than the low-lying orbital, whereas the out-of-phase combined orbital lies higher in energy than the high-lying orbital
 2. The in-phase combined orbital has the low-lying orbital as the major component, whereas the out-of-phase combined orbital has the high-lying orbital as the major component

Scheme 5 Interaction between different orbitals

Scheme 6 illustrates the orbitals of the polar σ bond in methane resulting from the interaction between the $1s$ atomic orbitals of a hydrogen atom and a sp^3 hybrid orbital of the carbon atom. The energy (-13.6 eV) of the $1s$ orbital is higher than that (-13.9 eV) of the hybrid orbital. The major component of the bonding orbital is the hybrid orbital on the carbon. This can be compared to the polarized C–H bond with slightly negatively charged carbon atom and positively charged hydrogen atom. The antibonding orbital is polarized in the reverse direction with $1s$ as the major component.

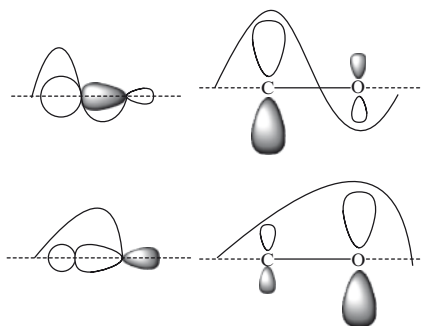
**Scheme 6** Orbitals of a polar σ bond in CH_4

The interaction of the p -orbitals in the carbonyl $\text{C}=\text{O}$ group is illustrated in Scheme 7. The major component of the bonding orbital is the p -orbital of the oxygen atom lower (-17.8 eV) in energy than that (-11.4 eV) of the carbon atom. The carbonyl π bond is polar. The oxygen atom is negatively charged and the carbon atom is positively charged. The antibonding orbital is polarized in the reverse direction. The p -orbital of the carbon atom is the major component. The relative energies of atomic orbitals can be guessed from the electronegativity. The energy decreases with the electronegativity.



Scheme 7 Orbitals of a polar π bond

The bond orbitals of $\sigma_{\text{C-H}}$ and $\pi_{\text{C=O}}$ relate to the other property of waves apart from the phase, that is, the amplitude. The bonding orbitals have large amplitudes on the low-lying atomic orbitals, i.e., on C of $\sigma_{\text{C-H}}$ and on O of $\pi_{\text{C=O}}$ (Scheme 8). The antibonding orbitals have large amplitudes on the high-lying atomic orbitals.

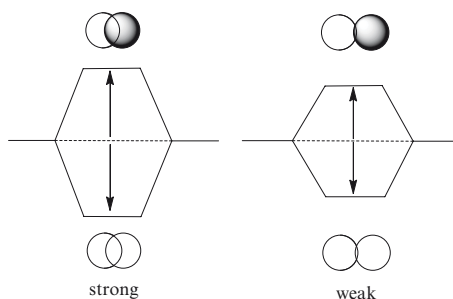


Scheme 8 Amplitudes of orbitals

1.3 Strength of Orbital Interactions

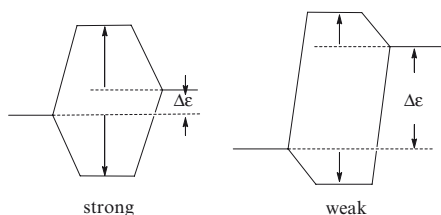
The orbital interactions are controlled by the overlap integrals (Scheme 9) and the energy gap between the orbitals (Scheme 10):

1. The orbital overlap strengthens the interaction
2. The energy gap weakens the interaction



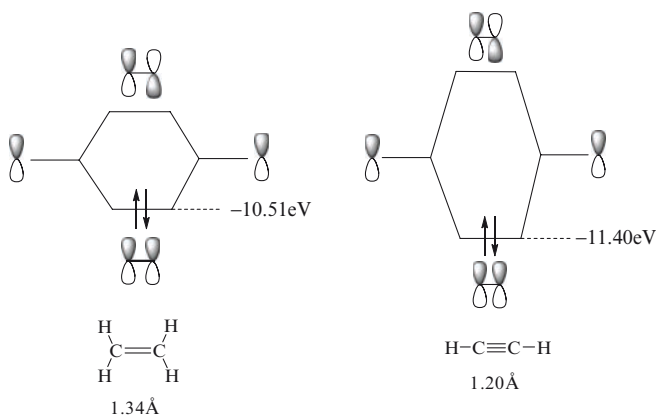
Scheme 9 Overlap strengthens the interaction

Scheme 10 Orbital energy gap $\Delta\epsilon$ weakens the interaction



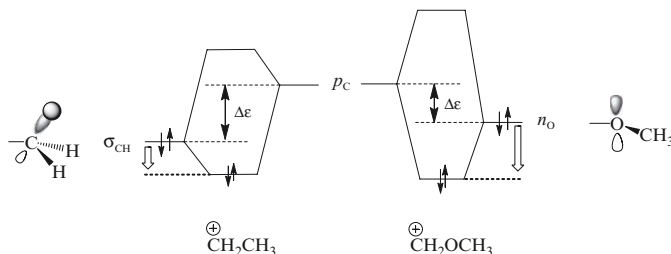
As the interaction is strong, the in-phase combined orbital is stabilized and the out-of-phase combined orbital is destabilized. The energy splitting increases between the in-phase and out-of-phase combined orbitals.

The ionization energies of ethylene and acetylene (Scheme 11) give experimental evidence of the effects of the orbital overlap on the interaction (Scheme 9). The π bonding orbitals result from the interaction of the carbon p orbitals. There is no difference in the energy gap. The strength of the interaction is determined by the overlap. The atomic distance is shorter in acetylene. The p orbitals have greater overlap with each other. The interaction is stronger. It follows that the bonding orbital lies lower in energy and that the ionization energy is higher. This is in agreement with the observed high ionization energy of 11.40 eV for acetylene relative to 10.51 eV for ethylene.



Scheme 11 Experimental evidence of the relation between the overlap and the interaction: the ionization energies of ethylene and acetylene

Substituent effects on the rate constants of S_N1 reactions give experimental evidence of the relation between the energy gap and the interaction. Alkyl substitutions on the carbon atoms bonded to the leaving group X accelerate the reaction. Alkoxy substitutions accelerate it further. The transition state is late. The geometry is close to that of the reaction intermediate carbocation. The rate is qualitatively estimated by the stability of the carbocation. The carbocations are generally planar. There is a vacant p orbital on the carbon atom. The σ_{CH} bonds interact with the ionic center. According to the rule for the interaction of different orbitals, the bonding orbitals of the σ_{CH} bonds interact and mix with vacant p orbital in phase to be lowered in energy (Scheme 12). The σ_{CH} bonds and therefore the carbocation are stabilized. This is the stabilization by the hyperconjugation. In the RO-substituted

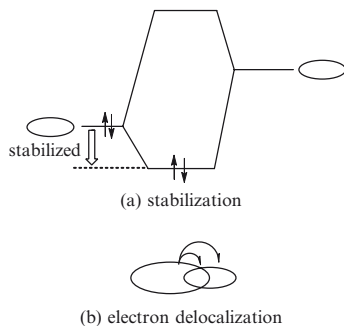


Scheme 12 Experimental evidence of the relation between the energy gap ($\Delta\epsilon$) and the interaction: the substituent effects on the stabilities of the carbocations

carbocations, a lone pair interacts with the cation center. The lone pair orbitals lie higher in energy than σ_{CH} . The ionization energies of the oxygen lone pairs (10.94, 10.64, 10.04, 9.61 eV for CH_3OH , $\text{C}_2\text{H}_5\text{OH}$, $(\text{CH}_3)_2\text{O}$, and $(\text{C}_2\text{H}_5)_2\text{O}$, respectively) are lower than those of the alkanes (13.6, 11.99, 11.51 eV for CH_4 , C_2H_6 , and C_3H_8 , respectively). The oxygen lone pairs are closer in energy to the vacant p -orbital. The narrow energy gap leads to stronger interaction and more stabilization of the in-phase combined orbital as stated above as a rule of the orbital interaction (Scheme 10). This is the stabilization by the resonance.

1.4 Electron Delocalization

Delocalization of electrons is important in chemistry. Electron delocalization is a major factor of the stabilities and the reactivities of molecules. The delocalization occurs through the interaction of an occupied orbital with a vacant orbital (Scheme 13). The two electrons occupy the stabilized orbital. There are no electrons in the destabilized orbital. The stabilization results from the interactions between the occupied and unoccupied orbitals.



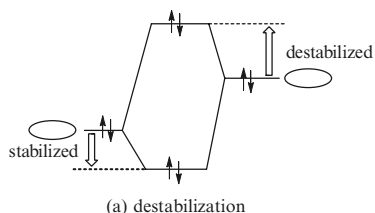
Scheme 13 Electron delocalization and stabilization by the interaction between the occupied and unoccupied orbitals

The electrons occupy the in-phase combined orbital after the interaction. They are distributed not only in the orbital occupied prior to the interaction, but also in the overlap region and the orbital vacant prior to the interaction. The electrons localized in the occupied orbital before the interaction delocalize to the overlap region and the vacant orbital after the interaction (Scheme 13).

Electron delocalization occurs through the interaction between the occupied and unoccupied orbitals and leads to the stabilization.

1.5 Exchange Repulsion

The interaction between the occupied orbitals leads to the destabilization (Scheme 14). The two electrons in the stabilized orbital lead to stabilization, but there are two more electrons, which occupy the destabilized orbitals. The destabilization overcomes the stabilization, and net destabilization results.



Scheme 14 Exchange repulsion and destabilization by the interaction between the occupied orbitals



Two electrons occupy the in-phase combined orbital. The probability density increases in the overlap region. Two more electrons occupy the out-of-phase combined orbital and reduce the density there. The decrease is greater than the increase. The electrons are expelled from the overlap region.

The destabilization is caused by the exchange of electrons between the occupied orbitals through the orbital overlap. The force is then termed exchange repulsion or overlap repulsion. The exchange repulsion is a major cause of the *steric repulsion*. There are many occupied orbitals in the sterically crowded space.

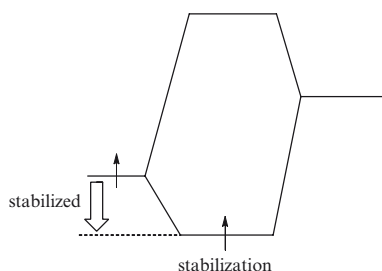
1.6 Stabilization and Number of Electrons

In the interaction of a pair of atomic orbitals, two electrons form a bond and four electrons form no bond (Sect. 1.1). The substituted carbocations are stabilized by the electron delocalization (hyperconjugation and resonance) through the interaction of the doubly occupied orbitals on the substituents with the vacant *p*-orbital on the cation center. The exchange repulsion (Sect. 1.5) is caused by four electrons. Now

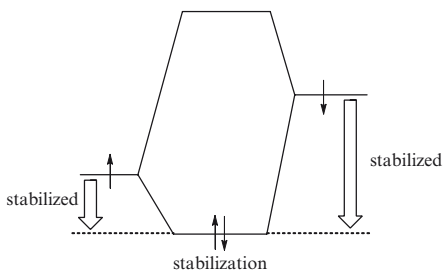
we see that two-electron interaction leads to the stabilization and four-electron interaction leads to the destabilization. The stabilization/destabilization by the orbital interaction is determined by the number of electrons.

Radicals and excited states have an orbital occupied by one electron. The interaction of the singly occupied orbital with a vacant orbital (Scheme 15) and with a singly occupied orbital (Scheme 16) leads to the stabilization. The stabilized orbitals occupy one and two electrons, respectively. There are no electrons in the destabilized orbital. For the interaction with a doubly occupied orbital there are two electrons in the stabilized orbital and one electron in the destabilized orbital (Scheme 17). Although the destabilization of the out-of-phase combined orbital is greater than the stabilization of the in-phase combination, there is one more electron in the stabilized orbital. Net stabilization is then expected.

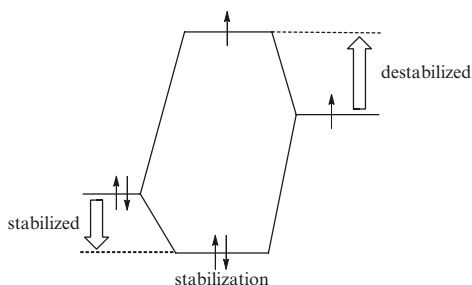
The participation of one through three electrons in the orbital interaction gives rise to stabilization. The destabilization occurs when four electrons participate.



Scheme 15 The stabilization by the interaction between a singly occupied orbital and a vacant orbital



Scheme 16 The stabilization by the interaction between singly occupied orbitals



Scheme 17 The stabilization by the interaction between singly and doubly occupied orbitals

2 Applications to Molecular Properties: Interactions of Bond Orbitals

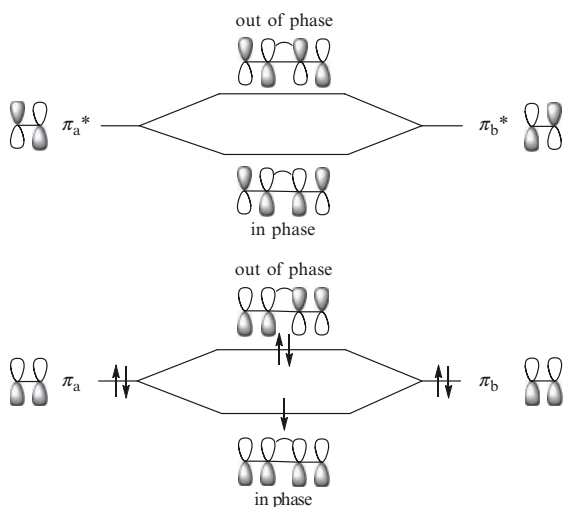
Chemists have developed, established, and advanced an idea of chemical bonds which localize between a pair of atoms. The idea is useful for understanding and designing molecules and chemical reactions. Chemists will never give up the idea of chemical bonds.

We have learned about bond orbitals which represent chemical bonds. In this section, we learn how interactions of bonds determine molecular properties. Interactions of bond orbitals give molecular orbitals, which show behaviors of the electrons in molecules.

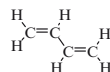
2.1 From Bond Orbitals to Molecular Orbitals

Butadiene has two π bonds. The interaction between the two π bonds is one of the simplest models to derive molecular orbitals from bond orbitals. A π bond in butadiene is similar to that in ethylene. The π bond is represented by the bonding and antibonding orbitals. The interactions occur between the π bonds in butadiene. The bond interactions are represented by the bond orbital interactions.

The bonding orbitals π_a and π_b of ethylenes are combined in phase to be the lowest π molecular orbitals (π_1) of butadiene (Scheme 18). The out-of-phase combined orbital (π_2) is the highest occupied molecular orbital (HOMO). The in-phase combination of



Scheme 18 The π molecular orbitals of butadiene from the bond orbitals

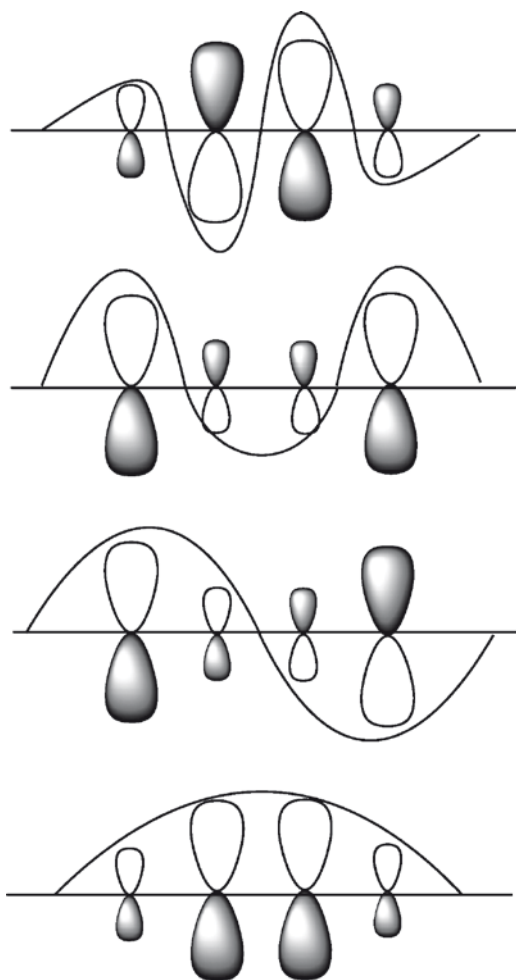


the antibonding orbitals (π_3) gives the lowest unoccupied molecular orbital (LUMO) of butadiene. The out-of-phase combination gives the highest molecular orbital (π_4).

There is energy gaps between the bonding and the antibonding orbitals (between π_a and π_b^* , between π_a^* and π_b), but no gaps between the bonding orbitals π_a and π_b , and between the antibonding orbitals (π_a^* and π_b^*). The $\pi_a-\pi_b^*$ and $\pi_a^*-\pi_b$ interactions are weak relative to the $\pi_a-\pi_b$ and $\pi_a^*-\pi_b^*$ interactions (Sect. 1.3), and can thus be neglected here.

2.2 Energy, Phase, and Amplitude of Orbitals

The energies, the phases and the amplitudes of the π molecular orbitals of butadiene are shown in Scheme 19. The π_1 , π_2 , π_3 , and π_4 orbitals corresponds to half, one,



Scheme 19 The energies, the phases and the amplitudes of the π molecular orbitals of butadiene

one and a half, and two waves, respectively. The energies of the p orbitals increase with the number of waves or with the number of out-of-phase combined neighboring pairs of the atomic orbitals. The amplitudes at the inner and terminal p -orbitals in Scheme 18 are identical to each other because the bond orbitals of ethylene are combined. The actual π molecular orbitals have larger amplitudes at the inner p -orbitals in p_2 and p_3 , and at the terminal p -orbitals in π_1 and π_4 . The difference in the amplitudes cannot be reproduced until the interactions between π and π^* of ethylene are taken into consideration (Chapter “Orbital Mixing Rules”).

The energy, the phase, and the amplitude characterize salient features of orbitals. This can be seen in atomic orbitals and bond orbitals (Sect. 1).

2.3 Ionization Energies

The energy splitting by the orbital interaction is confirmed by the ionization energies of ethylene and butadiene. The ionization energy of ethylene is 10.51 eV. The first and second ionizations are observed at 9.09 and 11.55 eV for butadiene. One is lower than that of ethylene, the other being higher. This is in agreement with the orbital energy ordering: the π_1 and π_2 orbitals of butadiene lie lower and higher than π of ethylenes, respectively. The difference 1.42 eV of π_2 from π is greater than that (1.04 eV) of π_1 from π . This is in agreement with the rule that the out-of-phase orbital (π_2) is destabilized more than the in-phase combined orbital (π_1) is stabilized.

2.4 Electronic Spectra

The π orbitals of butadiene (Scheme 18) qualitatively obtained from the orbitals of ethylenes are also supported by the electronic spectra of polyenes. The HOMO of butadiene is higher than the HOMO of ethylene since the former is the out-of-phase combination of the latter. The LUMO of butadiene is the in-phase combination of the LUMOs of ethylene and lies lower than the LUMO of ethylene. The energy gap between the HOMO and the LUMO is smaller in butadiene. In fact, the wavelength (λ_{\max}) is longer for butadiene (217 nm) than for ethylene (165 nm). The wavelength increases with the chain length of the polyenes.

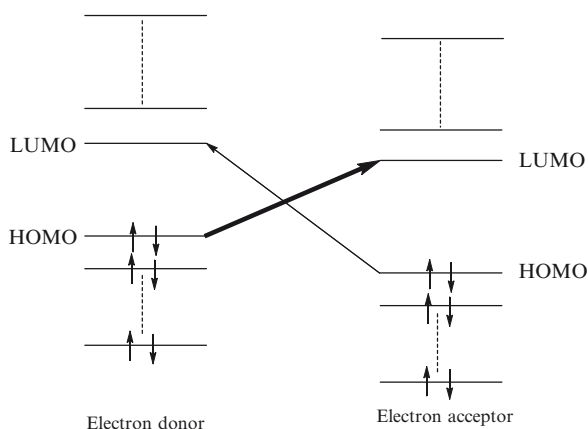
3 Applications to Chemical Reactions: Interactions of Frontier Orbitals

Atomic orbitals interact with each other to give bond orbitals (Sect. 1), which mutually interact to give molecular orbitals (Sect. 2). Here we will examine interactions of molecular orbitals, especially those of frontier orbitals important for chemical reactions.

3.1 Frontier Orbital Theory

There are many occupied and unoccupied molecular orbitals in molecules. Interactions occur between any pair of the molecular orbitals. The strengths of the interactions and the effects on the energies of interacting molecules are different from each other. Some lead to significant stabilization or destabilization, others to only slight stabilization or destabilization.

The frontier orbital theory [7–9] assumes that the stabilization by the electron delocalization could control chemical reactions. The stabilization comes from the interactions between the occupied molecular orbitals of one molecule and the unoccupied molecular orbitals of another (Sect. 1.4). The strong interaction occurs when the energy gap is small (Sect. 1.3). The HOMO and the LUMO are the closest in energy to each other. *The HOMO–LUMO interaction, especially the interaction between the HOMO of electron donors and the LUMO of electron acceptors, controls the chemical reactions* (Scheme 20). The HOMO and the LUMO are termed the “frontier orbitals.”

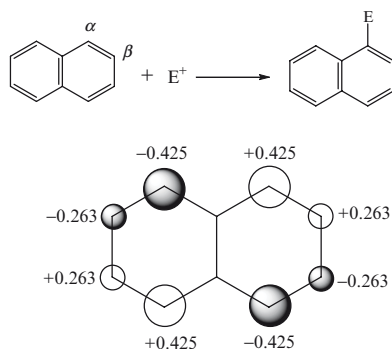


Scheme 20 Frontier orbital interactions

3.2 From Electron Density to Frontier Orbital Amplitude

Naphthalene undergoes electrophilic substitutions at the α rather than β position. The Hückel molecular orbital calculations show that all the carbons have the same π electron density 1.0. This is not in agreement with the theory of organic reactions based on the Coulombic interaction that electrophilic attack occurs on the most negatively charged atom. Fukui [7] proposed the frontier orbital theory for the discrepancy between the theory and the experimental observation. The importance of

Scheme 21 Electrophilic aromatic substitution and the HOMO amplitude of naphthalene

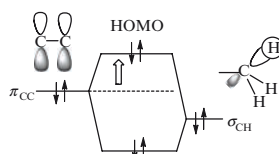


electron density implies that the electrons in each orbital contribute to the same degree. The frontier orbital theory emphasizes the exclusive importance of the electrons in HOMO. The HOMO amplitude (the coefficients of the p orbitals in the HOMO) are larger at the α rather than β position of naphthalene (Scheme 21).

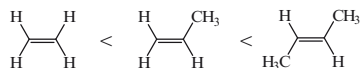
3.3 Reactivity

The energy of the frontier orbitals determines the reactivity. The small energy gap between the HOMO of electron donors and the LUMO of electron acceptors promotes the interaction and stabilizes the transition states. *Electron donors react fast as the HOMO energy is high. Electron acceptors react fast as the LUMO energy is low.*

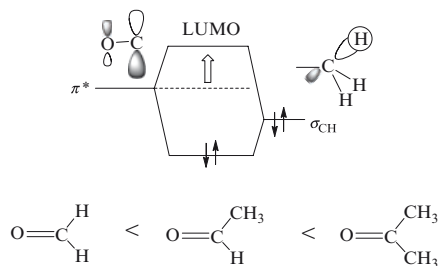
Alkyl substituents accelerate electrophilic addition reactions of alkenes and retard nucleophilic additions to carbonyl compounds. The bonding orbital σ_{CH} of the alkyl groups interacts with the π bonding orbital, i.e., the HOMO of alkenes and raises the energy (Scheme 22). The reactivity increases toward electron acceptors. The σ_{CH} orbital interacts with π^* (LUMO) of carbonyl compounds and raises the energy (Scheme 23). The reactivity decreases toward electron donors.



Scheme 22 The HOMO energy of alkenes raised by alkyl substituents



Scheme 23 The LUMO of carbonyl compounds raised in energy by alkyl substituents

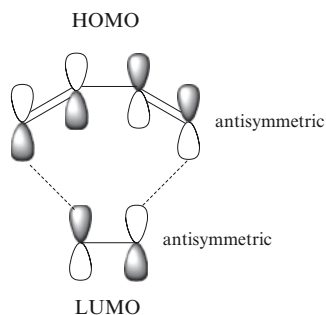


3.4 Selectivity

The amplitude of the frontier orbitals determines the selectivity. The most reactive atom in a molecule has the largest amplitude of the frontier orbitals. The frontier orbitals overlap each other to the greatest extent at the sites with the largest amplitudes. Reactions occur on the atoms in the electron donors and acceptors, where the HOMO and LUMO amplitudes are largest, respectively. Electrophiles prefer the α position of naphthalene, an electron donor, with the larger HOMO amplitude (Scheme 21). Nucleophiles attack the carbons of the carbonyl groups, an electron acceptor, with the larger LUMO amplitude (Scheme 7).

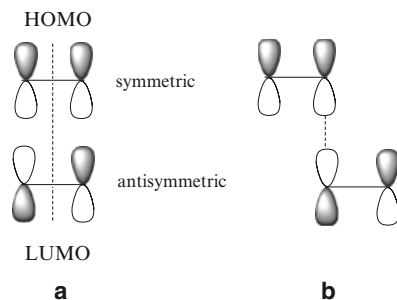
3.5 Orbital Symmetry

The chemical reactions through cyclic transition states are controlled by the symmetry of the frontier orbitals [11]. At the symmetrical (C_s) six-membered ring transition state of Diels–Alder reaction between butadiene and ethylene, the HOMO of butadiene and the LUMO of ethylene (Scheme 18) are antisymmetric with respect to the reflection in the mirror plane (Scheme 24). The symmetry allows the frontier orbitals to have the same signs of the overlap integrals between the p -orbital components at both reaction sites. The simultaneous interactions at the both sites promotes the frontier orbital interaction more than the interaction at one site of an acyclic transition state. This is also the case with interaction between the HOMO of ethylene and the LUMO of butadiene. The Diels–Alder reactions occur through the cyclic transition states in a concerted and stereospecific manner with retention of configuration of the reactants.



Scheme 24 The symmetry-allowed frontier orbital interaction for the Diels–Alder reactions

Scheme 25a,b The symmetry-forbidden (a) and -free (b) frontier orbital interactions for the dimerization of ethylenes



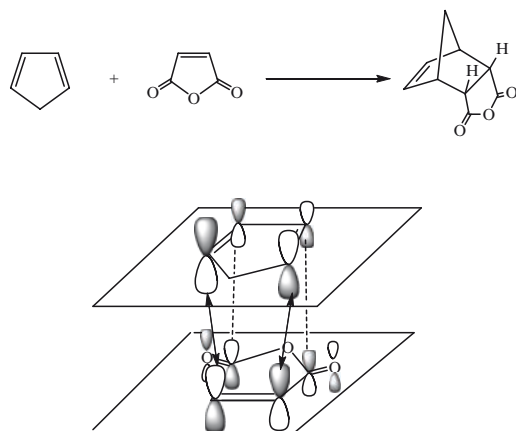
The frontier orbital interaction is forbidden by the symmetry for the dimerization of ethylenes through the rectangular transition state. The HOMO is symmetric and the LUMO is antisymmetric (Scheme 25a). The overlap integrals have the opposite signs at the reaction sites. The overlap between the frontier orbitals is zero even if each overlap between the atomic p -orbitals increases. It follows that the dimerization cannot occur through the four-membered ring transition states in a concerted and stereospecific manner.

The frontier orbital interaction can be free from the symmetry restriction. A pair of the reaction sites is close to each other while the other pair of the sites is far from each other (Scheme 25b). This is the geometry of the transition state leading to diradical intermediates.

Woodward and Hoffmann presented an orbital symmetry rule for pericyclic reactions [12, 13].

3.6 Orbital Phase Environments

The frontier orbital interactions at other than reaction sites can determine the selectivity [14]. The interaction between the HOMO of cyclopentadiene and the LUMO of maleic anhydride is illustrated in Scheme 26. The HOMO of cyclopentadiene has the same phase property as butadiene (Scheme 18). The LUMO of maleic anhydride is an in-phase combined orbital of $\pi^*_{\text{C=C}}$ and $\pi^*_{\text{C=O}}$. At the transition state for the *endo* addition, the phase relation between the p -orbitals on the inner unsaturated carbons of the diene and on the carbonyl carbons of maleic anhydride is the same (in phase) as that between the carbons to be bonded. The interaction between the atoms not to be bonded, that is, the secondary interaction, stabilizes the *endo* transition state. Whether the secondary interaction is attractive or repulsive depends on the orbital phase properties in the environments around the reaction sites. Stereoselectivity can be determined by the orbital phase environments. This topic is reviewed by Ohwada in Chapter "Orbital Phase Environments and Selectivities".

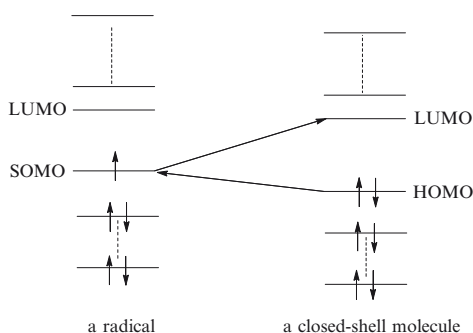


Scheme 26 Endo-selectivity of the Diels–Alder reactions and orbital phase environments

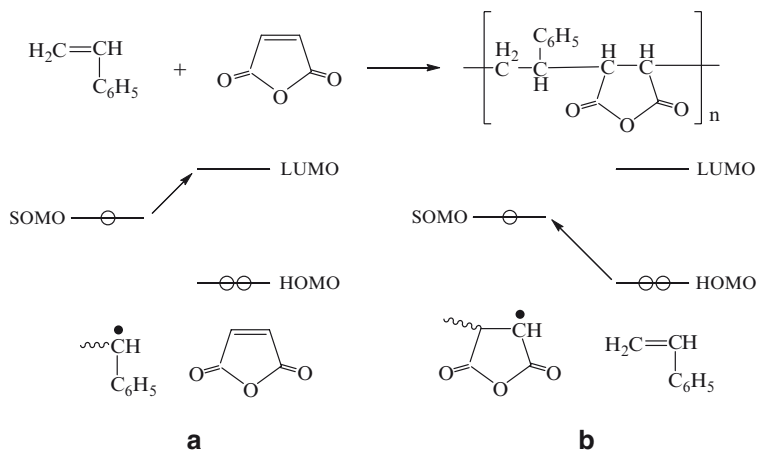
3.7 Radical Reactions: Copolymerizations

A radical has a singly occupied molecular orbital (SOMO). This is the frontier orbital. The SOMO interacts with HOMO and the LUMO of closed-shell molecules to stabilize the transition state (Scheme 27). The radical can be a donor toward a monomer with low LUMO or an acceptor toward one with high HOMO.

The free radical copolymerization of styrene and maleic anhydride results in a nearly perfect alternation of monomer units (Scheme 28) [15]. The end of the growing polymer chain has a radical center. The SOMO is the frontier orbital. The orbital energy is raised by the interaction with the high-lying occupied orbital of the electron donating substituent, i.e., with the HOMO of the phenyl group. The radical is nucleophilic and prefers an acceptor, i.e., maleic anhydride, which has an electron accepting CO group (Scheme 28a). The resulting radical center has the accepting substituent and a low SOMO energy. The radical is electrophilic and reacts with the



Scheme 27 Frontier orbital interaction in the radical reactions



Scheme 28a,b Nucleophilic (a) and electrophilic (b) radical additions in copolymerization

donating monomer, styrene (Scheme 28b). This is the mechanism of the alternation of the monomer units in the polymer chain.

Random copolymerization occurs between butadiene and styrene [15]. There are no appreciable differences in the nucleophilic and electrophilic abilities between the radical centers with the vinyl and phenyl groups at the end of the growing polymer chain or in the donor/acceptor properties between the monomers.

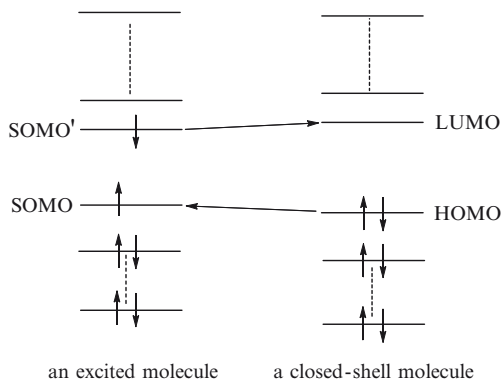
3.8 Photochemical Reactions

There are two SOMOs in the excited states of closed-shell molecules. The SOMOs are the frontier orbitals in the photochemical reactions (Scheme 29). The SOMO interacts with the orbitals, whether occupied or unoccupied, of closed-shell molecules to stabilize the transition states of photochemical reactions. The low-lying SOMO (usually the original HOMO) is close in energy to the HOMO of closed-shell reaction partners in the ground states. The high-lying SOMO' (the original LUMO) is close in energy to the LUMO of the partners. The SOMO–HOMO and SOMO'–LUMO interactions are important in the excited states.

Photochemical reactions of carbonyl compounds with alkenes give the oxetanes (Scheme 30). The stereochemical course depends on the substituents of the alkenes [16]. The reactions proceed with the retention of the configuration of the alkenes for the electron accepting substituent, e.g., CN. The stereochemical integrity is lost for the donating group, e.g., OCH₃.

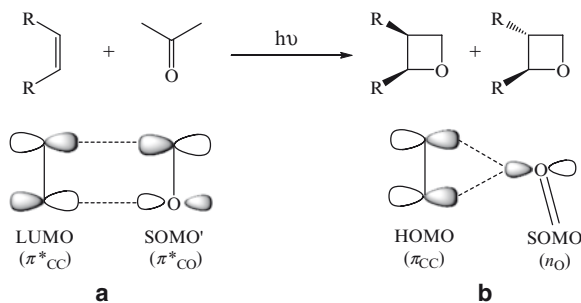
The excited state of the carbonyl compound is the (n, π^*) state where one electron is excited from the HOMO to the LUMO. The SOMO is the n -orbital on the carbonyl oxygen atom. The SOMO' is the antibonding π^* -orbital.

Scheme 29 Frontier orbital interactions in photochemical reactions



The alkene substituted with the electron accepting group has the LUMO (π^*) lowered by the interaction with the vacant orbital of the substituent. The high-lying SOMO' interacts with the LUMO of the alkene more effectively than with the HOMO. The interaction is the symmetry-allowed $\pi^*-\pi^*$ interaction (Scheme 30a). The configuration of the alkene is retained.

The alkene with the electron donating group has the HOMO (π) raised by the interaction with the occupied orbital of the substituent. The low-lying SOMO (n_o) interacts with the HOMO of the alkene more effectively. The frontier orbital interaction is the $n-\pi_{C=C}$ interaction (Scheme 30b), which is impossible at the four-membered ring transition states. This is not good for the retention of the configuration.



Scheme 30a,b [2 + 2] Cycloaddition reactions of excited carbonyl compounds with the alkenes substituted by electron-accepting (a) and -donating (b) groups

4 Interactions of More Than Two Orbitals

The theory of two-orbital interactions has been described in the preceding sections. The elements of the chemical orbital theory also include the theories of *three-orbital interactions* and *cyclic interactions of more than two orbitals* (Scheme 1).

4.1 *Orbital Mixing Rules*

A theory of three-orbital interactions [17–20] is helpful to understand and design molecules and reactions. The orthogonal atomic, bond, or molecular orbitals ϕ_h and ϕ_l are both assumed to interact with a perturbing orbital ϕ_p . The orbitals ϕ_h and ϕ_l cannot interact directly but do so indirectly or mix with each other through ϕ_p . Orbital mixing rules are drawn to predict the phase relations in ϕ_h – ϕ_p – ϕ_l . The orbitals ϕ_h and ϕ_l deform according to the orbital phase relation between ϕ_h and ϕ_l . The deformation determines the direction of favorable interactions.

The orbital mixing rules are described in detail and shown to be powerful for understanding and designing selective reactions in Chapter “Orbital Mixing Rules” and applied in chapter “ π -Facial Selectivities of Diels–Alder reactions”.

4.2 *An Orbital Phase Theory*

Another theory as an important element of the chemical orbital theory is an orbital phase theory for cyclic interactions of more than two orbitals. The cyclic orbital interactions are controlled by the continuity–discontinuity of orbital phase [21–23].

The orbital phase theory includes the importance of orbital symmetry in chemical reactions pointed out by Fukui [11] in 1964 and established by Woodward and Hoffmann [12, 13] in 1965 as the stereoselection rule of the pericyclic reactions via cyclic transition states, and the $4n + 2\pi$ electron rule for the aromaticity by Hueckel. The pericyclic reactions and the cyclic conjugated molecules have a common feature or cyclic geometries at the transition states and at the equilibrium structures, respectively.

In 1982 the present author discovered *cyclic orbital interactions in acyclic conjugation*, and showed that the *orbital phase continuity* controls acyclic systems as well as the cyclic systems [23]. The orbital phase theory has thus far expanded and is still expanding the scope of its applications. Among some typical examples are included relative stabilities of cross vs linear polyenes and conjugated diradicals in the singlet and triplet states, spin preference of diradicals, regioselectivities, conformational stabilities, acute coordination angle in metal complexes, and so on.

The orbital phase theory and its applications are reviewed in Chapter “An Orbital Phase Theory”.

Acknowledgments The author thanks Prof. Hisashi Yamamoto of the University of Chicago for his reading of the manuscript and his encouraging comments, Messrs. Hiroki Murai and Hiroki Shimakawa for their assistance in preparing the manuscript, and Ms. Jane Clarkin for her English suggestions.

References

1. Salem L (1982) *Electrons in chemical reactions*. Wiley, New York
2. Albright TA, Burdett JK, Whangbo M-H (1985) *Orbital interactions in chemistry*. Wiley, New York

3. Lennard-Jones JE (1929) *Trans Faraday Soc* 25:668
4. Whangbo M-H, Hoffmann R (1978) *J Chem Phys* 68:5498
5. Inagaki S, Goto N, Yoshikawa K (1991) *J Am Chem Soc* 113:7144
6. Inagaki S, Takeuchi T (2005) *Chem Lett* 34:750
7. Fukui K, Yonezawa T, Shingu H (1952) *J Chem Phys* 22:722
8. Fukui K (1971) *Acc Chem Res* 4:57
9. Fukui K (1975) *Theory of orientation and stereoselection*, Springer, Berlin Heidelberg New York
10. Fleming I (1976) *Frontier orbitals and organic chemical reactions*. Wiley, London
11. Fukui K (1964) In: Loewdin P-O, Pullman B (eds) *Molecular orbitals in chemistry, physics, and biology*. Academic Press, London, p 513
12. Woodward RB, Hoffmann R (1969) *Angew Chem Int Ed Engl* 8:781
13. Hoffmann R, Woodward RB (1970) *The conservation of orbital symmetry*, Verlag Chemie/Academic, New York
14. Hoffmann R, Woodward RB (1965) *J Am Chem Soc* 87:4388
15. Pine SH (1987) *Organic chemistry* 5th edn. McGraw-Hill, New York, p 956
16. Herndon WC (1974) *Top Curr Chem* 46:141
17. Inagaki S, Fukui K (1974) *Chem Lett* 3:509
18. Inagaki S, Fujimoto H, Fukui K (1976) *J Am Chem Soc* 98:4054
19. Libit L, Hoffmann R (1974) *J Am Chem Soc* 96:1370
20. Imamura A, Hirano T (1975) *J Am Chem Soc* 97:4192
21. Fukui K, Inagaki S (1975) *J Am Chem Soc* 97:4445
22. Inagaki S, Fujimoto H, Fukui K (1976) *J Am Chem Soc* 98:4693
23. Inagaki S, Kawata H, Hirabayashi Y (1982) *Bull Chem Soc Jpn* 55:3724

A Mechanistic Spectrum of Chemical Reactions

Satoshi Inagaki

Abstract The mechanism of chemical reactions between electron donors and acceptors continuously changes with the power of the donors and the acceptors. The interaction between the HOMO (d) of the donors and the LUMO (a^*) of the acceptors or *delocalization* of electrons is important for the reactions. The electron d -to- a^* transferred configuration mixes to a significant extent. As the donors and/or the acceptors are strong, their excited configurations appreciably mixes together with the transferred configuration. The d - a and d^* - a^* orbital interactions are important in addition to the d - a^* interaction. Reactions have features characteristic of the excited-state reactions although the donor–acceptor system is not really excited, but in the ground state. This process is termed *pseudoexcitation*. The a - d - a^* - d^* interaction is important. For much stronger donors and acceptors, the electron transferred configuration is stable and predominant. Covalent bonds do not form but instead ionic pairs, and *electron transfer* results. A mechanistic spectrum of chemical reactions is composed of the delocalization, pseudoexcitation, and electron transfer bands.

Keywords Cycloadditions, Chemical orbital theory, Donor–acceptor interaction, Electron delocalization band, Electron transfer band, Frontier orbital, Mechanistic spectrum, NAD(P)H reactions, Orbital amplitude, Orbital interaction, Orbital phase, Pseudoexcitation band, Quasi-intermediate, Reactivity, Selectivity, Singlet oxygen, Surface reactions

Contents

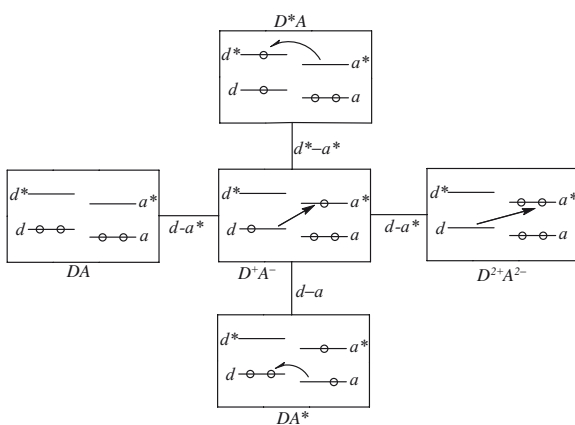
1	Mechanisms of Chemical Reactions Between Electron Donors and Acceptors.....	24
1.1	[2+2] Cycloadditions Between Alkenes	26
1.2	[2+2] Cycloadditions of Carbonyl Compounds	29
1.3	[4+2] Cycloadditions	30
1.4	Cycloisomerization of Conjugate Polyenes	32

S. Inagaki
Department of Chemistry, Faculty of Engineering, Gifu University, Yanagido,
Gifu 501-1193, Japan
e-mail: inagaki@gifu-u.ac.jp

1.5	Electrophilic Aromatic Substitutions.....	33
1.6	Reactions of Indoles with Unsaturated Acceptors.....	34
2	Delocalization Band.....	34
2.1	[4+2] Cycloadditions of a Ketene.....	35
2.2	Exo-addition in Diels–Alder Reactions.....	35
2.3	[4+2] Cycloadditions on Surface.....	36
3	Pseudoexcitation Band.....	36
3.1	Reactions of Singlet Molecular Oxygen O ₂ (¹ Δ _g).....	36
3.2	[2+2] Cycloadditions of Bent Unsaturated Bonds.....	43
3.3	[2+2] Cycloadditions of Ketenes.....	44
3.4	[2+2] Cycloadditions with Surface.....	47
3.5	[2+2] Cycloadditions of Unsaturated Bonds Between Heavy Atoms.....	48
4	Transfer Band.....	49
4.1	NAD(P)H Reactions.....	49
4.2	Reactions of Methyl Benzenes with TCNQ.....	52
4.3	Hydride Equivalent Transfers.....	52
	References.....	53

1 Mechanisms of Chemical Reactions Between Electron Donors and Acceptors

Molecules have some occupied and some unoccupied orbitals. There occur diverse interactions (Scheme 1) when molecules undergo reactions. According to the frontier orbital theory (Sect 3 in Chapter “Elements of a Chemical Orbital Theory” by Inagaki in this volume), the HOMO (d) of an electron donor (D) and the LUMO (a^*) of an electron acceptor (A) play a predominant role in the chemical reactions (delocalization band in Scheme 2). The electron configuration D^+A^- where one electron transfers from d to a^* significantly mixes into the ground configuration DA where



Scheme 1 Electron configurations important for the reactions between electron-donors and -acceptors

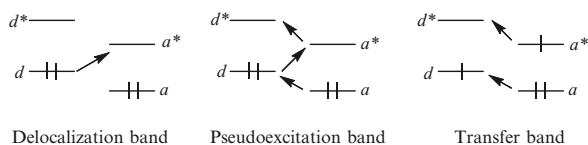
the occupancy of each orbital remains unchanged from those of the reactants. The $d-a^*$ interaction is accompanied by *delocalization* of electrons from d to a^* . Electron delocalization between the reactants is important for the reactions.

Ground-state reactions between strong donors and acceptors have features characteristic to the excited-state reactions [1]. Strong donors have high HOMO and strong acceptors have low LUMO. In chemical reactions between the strong donors and acceptor, the delocalization is greatly promoted from d to a^* . The weight of the electron-transferred configuration, D^+A^- , increases. Electronic rearrangements from D^+A^- are expected to be important and substantial. The electron in a^* of D^+A^- transfers to d^* , giving the locally-excited configuration, D^*A which contains the excited configuration of D . The $D^+A^-D^*A$ configuration interaction is approximated by the d^*-a^* orbital interaction. To the resulting electron hole in d of D^+A^- an electron transfers from a of D^+A^- , giving the locally-excited configuration, DA^* which has the excited configuration of A . The $D^+A^-DA^*$ configuration interaction is approximated by the $d-a$ orbital interaction. In this band of the mechanistic spectrum, the mixing-in of the locally-excited configurations or the HOMO–HOMO and LUMO–LUMO interactions are important even if the reactions take place in the ground states. This band is termed *pseudoexcitation* [1]. The importance of the HOMO–HOMO and LUMO–LUMO interaction has been discussed elsewhere [2–4].

The pseudoexcitation in donors occurs through the $d-a^*-d^*$ interaction. The $a-d-a^*$ orbital interaction causes the pseudoexcitation in the acceptors. The simultaneous pseudoexcitations in the donors and acceptors are caused by the $a-d-a^*-d^*$ interaction (Scheme 2).

Polar reactions, e.g., electrophilic addition reactions, are proposed here to be reactions in the pseudoexcitation band, where the $a-d-a^*-d^*$ orbital interaction is important. Mixing of locally-excited configurations, e.g., D^*A , DA^* , expresses polarizations of reactants, and in polar reactions reactants are highly polarized. Significant mixing of locally-excited configurations is necessary to express the interactions in polar reactions; this is why polar reactions are proposed to be reactions in the pseudoexcitation band. Sordo et al. analyzed the electronic structure of the transition states of the addition of HF and HCl to ethylene [5] to show the importance of the pseudoexcitation of ethylene as well as the delocalization from ethylene to the electrophiles. Interestingly, a second molecule of hydrogen halide is suggested to promote the pseudoexcitation rather than the delocalization as a catalyst.

Much stronger donor–acceptor interactions stabilize D^+A^- too much to give rise to the pseudoexcitation. The electron transferred configuration is stable and predominant. Electrons transfer to generate ion radical pairs or salts. Covalent bonds do not form and *electron transfer* results.



Scheme 2 Change of the frontier orbital interactions with the power of donors and acceptors

With the power of the donors and acceptors, changes occur in the important frontier orbital interactions (Scheme 2) and in the mechanism of chemical reactions. The continuous change forms a mechanistic spectrum composed of the delocalization band to pseudoexcitation band to the electron transfer band.

1.1 [2+2] Cycloadditions Between Alkenes

[2+2] Cycloaddition reactions are forbidden by orbital symmetry in the delocalization band and occur with retention of configurations in the pseudoexcitation band. Ion pair complexes form between alkenes in the transfer band.

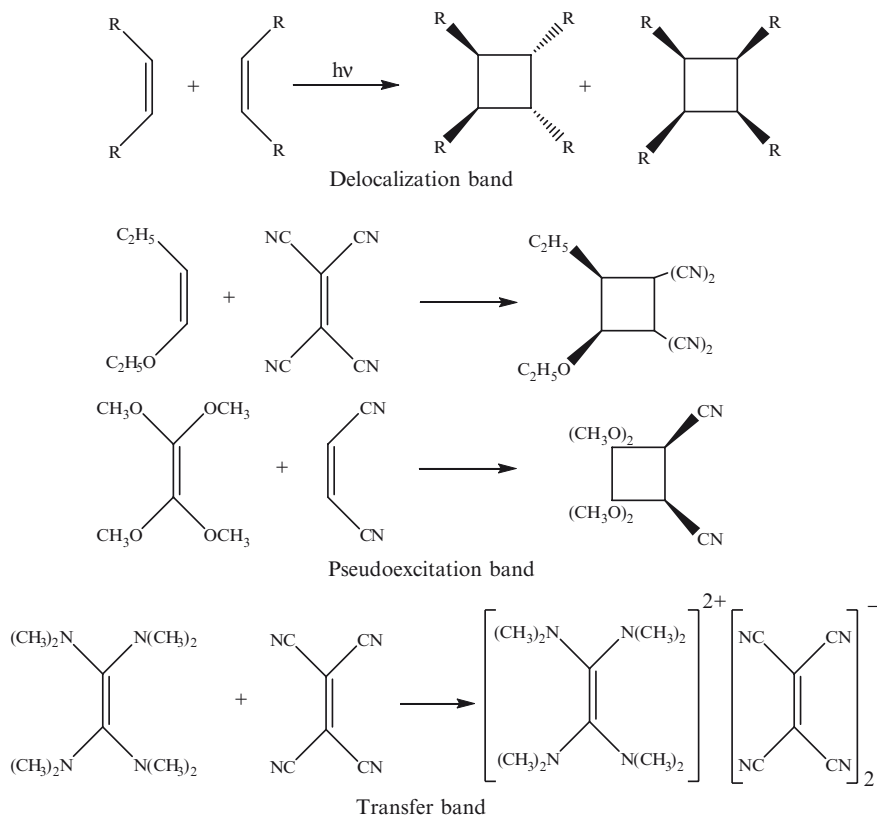
1.1.1 Delocalization Band

Photochemical [2+2] cycloadditions of olefins occur with retention of configuration according to the Woodward–Hoffmann rule [6, 7]. These are excited-state reactions in the *delocalization band of the mechanistic spectrum*. A striking example of the symmetry-allowed reaction was observed when the neat *cis*- and *trans*-butenes were irradiated (delocalization band in Scheme 3) [8].

Thermal dimerization of ethylene to cyclobutane is forbidden by orbital symmetry (Sect 3.5 in Chapter “Elements of a Chemical Orbital Theory” by Inagaki in this volume). The activation barrier is high ($E_{\text{A}}=44$ kcal mol⁻¹) [9]. Cyclobutane cannot be prepared on a preparative scale by the dimerization of ethylenes despite a favorable reaction enthalpy ($\Delta H = -19$ kcal mol⁻¹). Thermal reactions between alkenes usually proceed via diradical intermediates [10–12]. The process of the diradical formation is the most favored by the HOMO–LUMO interaction (Scheme 25b in chapter “Elements of a Chemical Orbital Theory”). The intervention of the diradical intermediates implies loss of stereochemical integrity. This is a characteristic feature of the thermal reactions between alkenes in the delocalization band of the mechanistic spectrum.

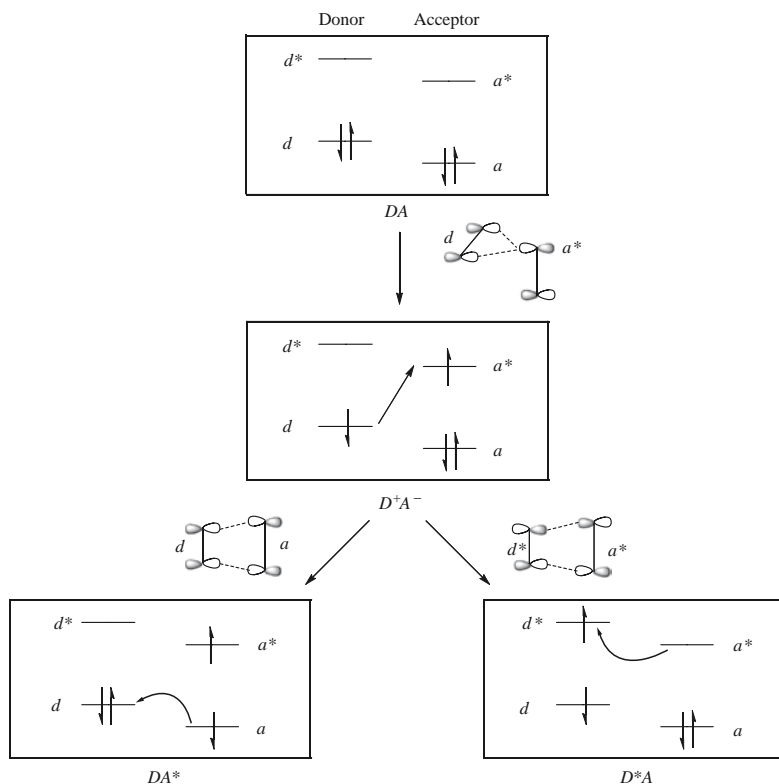
1.1.2 Pseudoexcitation Band

Thermal [2+2]cycloadditions between electron-donating and accepting olefins are stereoselective reactions in the pseudoexcitation band. The mixing-in of the locally-excited configurations or the HOMO–HOMO and LUMO–LUMO interactions are important in addition to the mixing-in of the electron-transferred configuration or the HOMO–LUMO interaction, even if the reactions take place in the ground states. The HOMO or the in-phase combined *p*-orbitals of electron donating unsaturated bond interacts with the LUMO or the out-of-phase combined *p*-orbitals of electron accepting unsaturated bond the most effectively in the geometry (Scheme 4) where a three-centered interaction occurs among the two *p*-orbitals in the HOMO and one *p*-orbital in the LUMO [13]. The transient three-membered ring retains the configuration



Scheme 3 Mechanistic spectrum of [2+2] cycloaddition reactions between alkenes

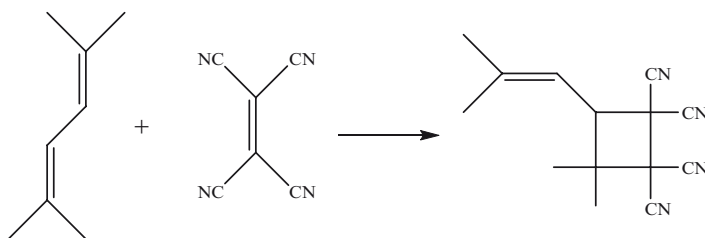
of the donor. In this geometry, the HOMO–HOMO interaction is allowed by symmetry. The pseudoexcitation occurs in the acceptor. The HOMO–HOMO interaction retains the configurations of the acceptor. The LUMO–LUMO interaction or the pseudoexcitation of the donor is not allowed in the symmetrical three-membered ring, but during the deformation to the four-membered ring product with retention of the configurations. Thermal [2+2]cycloaddition reactions between electron-donating and accepting olefins tend to retain the configurations. The stereoselectivities have been well documented. The reaction of ethyl *cis*-butenyl ether with TCNE produced the *cis*-cyclobutane derivative as a predominant (98%) product with retention of the configurations of the donor (pseudoexcitation band in Scheme 3) [14]. High retention of the donor configuration was observed for the reaction in the pseudoexcitation band [15]. Fumaro- and maleonitrile react with tetramethoxyethylene in a stereospecific manner with retention of the configurations of the acceptor (pseudoexcitation band in Scheme 3) [16]. From the geometry for the three-centered interaction, the stereochemical integrity is more likely to be lost on the acceptors. In fact, this stereochemical tendency was observed in the reactions of *cis*- and *trans*-isomers between propyl propenyl ether and 1,2-dicyano-1,2-bis(trifluoromethyl)ethylene [17].



Scheme 4 Thermal [2+2] cycloaddition reactions in the pseudoexcitation band

Unsymmetrical substitution with strong electron donating groups highly polarizes the HOMO. The incipient three-ring collapses earlier to strengthen the HOMO–LUMO interaction between the reaction centers with larger orbital amplitudes. The HOMO–HOMO–LUMO–LUMO interaction occurs more effectively, leading to the formation of zwitterions. Polar additions are reactions in the pseudoexcitation band. Treatment of enamines, $\text{RCH}=\text{CXNR}^1\text{R}^2$, with methylenemalononitriles, $\text{R}^3\text{R}^4\text{C}=\text{C}(\text{CN})_2$, gives stable 1,4-dipolar compounds [18]. Some enamines react with TCNE to generate stable 1,4-dipoles at -40°C which lose HCN at 20°C , giving tricyanobutadiene [19].

A strong acceptor TCNE undergoes [2+2] rather than [4+2] cycloaddition reactions even with dienes. 1,1-Diphenylbutadiene [20] and 2,5-dimethyl-2,4-hexadiene (Scheme 5) [21] afford mainly and exclusively vinyl cyclobutane derivatives, respectively. In the reactions of 2,5-dimethyl-2,4-hexadiene: (1) the observed rate constant, k_{obs} , is greater for chloroform solvent than for a more polar solvent, acetonitrile; (2) the trapping of a zwitterion intermediate by either methanol or *p*-toluenethiol was unsuccessful; (3) radical initiators such as benzyl peroxide, or radical inhibitors like hydroquinone, have no effect on the rate; (4) the entropies of activation are of



Scheme 5 Preference of [2+2] over [4+2] cycloaddition reactions in the pseudoexcitation band

large negative value. These observations are in agreement with the characteristic features expected for the reactions in the pseudoexcitation band.

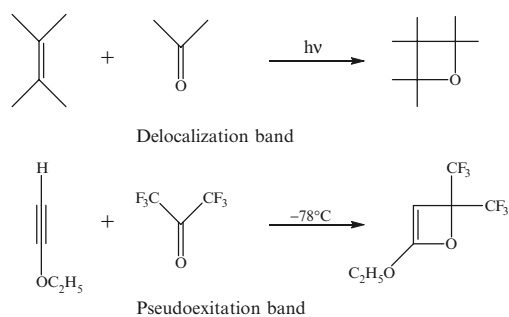
One recent example of preferential [2+2] cycloaddition of dienes is the reaction of 2-siloxybutadienes with allenecarboxylates to afford cyclobutanes used for the preparation of very hindered cyclohexene systems [22].

1.1.3 Transfer Band

Reactions between much stronger donors and acceptors belong to the *electron transfer band*. Such olefins do not form cyclobutanes but ion radical pairs or salts of olefins. *Tetrakis(dimethylamino)ethylene* has an ionization potential as low as Na. The olefin with extraordinary strong electron-donating power is known not to undergo [2+2]cycloaddition reaction, but to give 1:2 complex with TCNE (transfer band in Scheme 3) [23].

1.2 [2+2] Cycloadditions of Carbonyl Compounds

A part of the mechanistic spectrum is supported by the [2+2] cycloaddition reactions between the unsaturated carbon bonds and carbonyl compounds [24].



Scheme 6 Mechanistic spectrum of [2+2] cycloaddition of carbonyl compounds with alkenes and alkynes

1.2.1 Delocalization Band

Four-membered ring formation between unsaturated carbon bonds and carbonyl compounds is a photochemical reaction [25]. This is an excited-state reaction in the delocalization band (Scheme 6).

1.2.2 Pseudoexcitation Band

The [2+2] cycloaddition could occur thermally in the pseudoexcitation band. In fact, an alkyne with electron-donating group, ethoxyacetylene, and electron accepting carbonyl compound, perfluoroacetone, form the oxetene at low temperature (-78°C) without light irradiation (pseudoexcitation band in Scheme 6) [26, 27].

Thermal [2+2] cycloaddition reactions of carbonyl compounds were catalyzed by a Lewis acid. The catalyst forms complexes with the carbonyl compounds and enhances the electron-accepting power. The reaction shifts from the delocalization band to the pseudoexcitation band. Catalyzed [2+2] cycloaddition reactions were observed with acetylenic compounds [28] and ketenes [29–31].

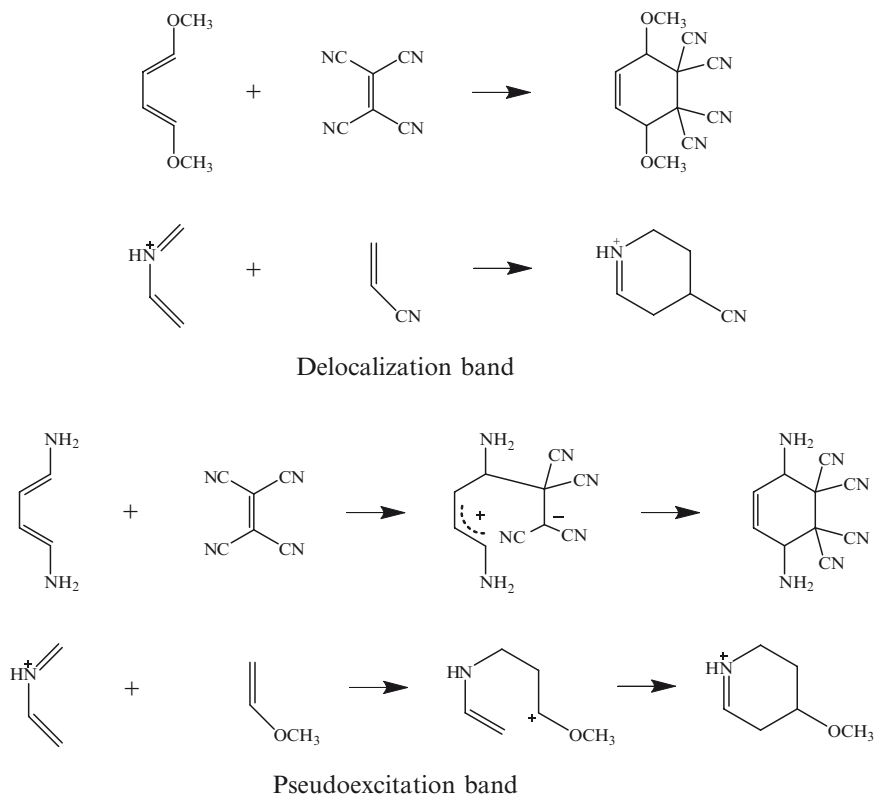
Olefins (enamines) unsymmetrically substituted with strong electron-donating (amino) group and CS_2 generate zwitterions (1,4-dipoles) [32, 33]. Polar additions are proposed here to be reactions in the pseudoexcitation band.

1.3 [4+2] Cycloadditions

The mechanistic spectrum suggests that [4+2] cycloadditions should shift from concerted reactions in the delocalization band to stepwise reactions through intermediates in the pseudoexcitation band. The HOMO–LUMO interactions, important in the delocalization band, are allowed by the orbital symmetry (Sect 3.5 in Chapter “Elements of a Chemical Orbital Theory” by Inagaki in this volume). The reactions occur in a concerted manner. In the pseudoexcitation band the HOMO–HOMO–LUMO–LUMO interaction is important. The HOMO–HOMO and LUMO–LUMO interactions are, however, forbidden by the orbital symmetry at the six-membered ring transition states for the Diels–Alder reactions. The pseudoexcitation band does not prefer concerted [4+2] cycloaddition reactions. The HOMO–HOMO and LUMO–LUMO interactions can be free from the symmetry restriction, when one pair of the reaction sites is closer to each other than another pair of sites (Scheme 7). This geometry leads to a zwitterion intermediate. Even the symmetry-allowed [4+2] cycloaddition reactions can be changed to such polar addition reactions as electrophilic additions when the donors and acceptors are strong. This suggests that polar additions could be reactions in the pseudoexcitation band.

1.3.1 Delocalization Band

An electron donating butadiene with the methoxy substituents at the 1 and 4 positions was calculated to undergo a concerted [4+2] cycloaddition reaction with TCNE as



Scheme 7 Mechanistic spectrum of [4+2] cycloaddition reactions

usual (delocalization band in Scheme 7) [34]. Some calculations [35] showed the [4+2] cycloaddition reaction of the *N*-protonated 2-aza-1,3-butadiene cation with acrylonitrile takes place in a concerted manner (delocalization band in Scheme 7).

1.3.2 Pseudoexcitation Band

A stronger donor, the butadiene with the amino groups in place of the methoxy group in the 1,4-positions, was calculated to react with TCNE via a zwitterion (pseudoexcitation band in Scheme 7) [34]. The loss of the stereochemical integrity was observed in the [4+2] cycloaddition reactions between some strong donors, 1,4-bis(dimethylamino) butadienes, and acceptors, fumaric and maleic dinitriles [36].

In hetero [4+2] cycloaddition (delocalization band in Scheme 7) the cationic diene is a strong acceptor and the dienophile is substituted by an electron accepting group. Replacement with a strong donating substituent in the dienophile shifts the reaction from the delocalization band to the pseudoexcitation band. The methoxy-substituted dienophile gives a zwitterionic intermediate (pseudoexcitation band in Scheme 7) [35]. This is a polar reaction in the pseudoexcitation band.

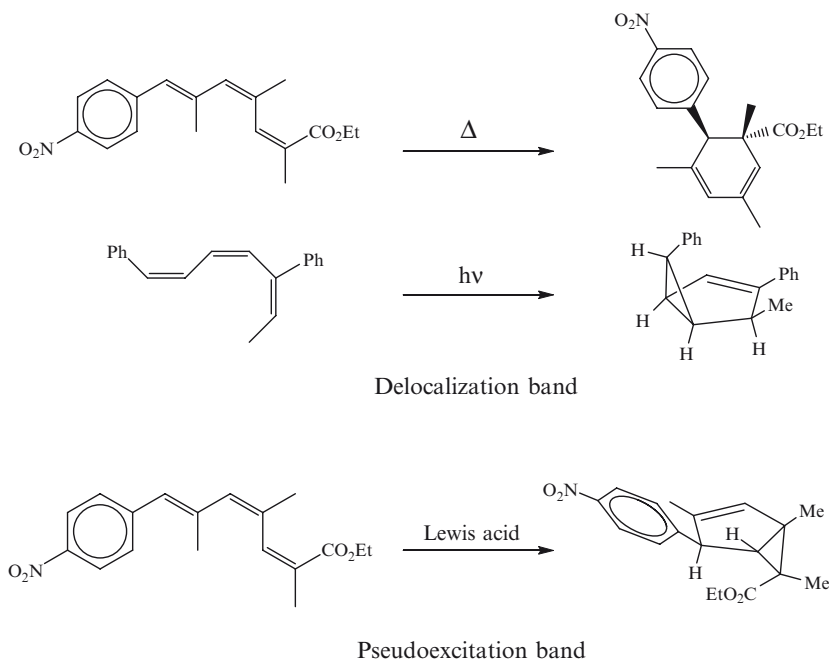
According to the calculations at high levels of theory, the [4+2] cycloaddition reactions of dienes with the singlet ($^1\Delta_g$) oxygen follow stepwise pathways [37, 38]. These results, which were unexpected from the Woodward–Hoffmann rule and the frontier orbital theory, suggest that the [4+2] cycloadditions of the singlet ($^1\Delta_g$) oxygen could be the reactions in the pseudoexcitation band.

1.4 Cycloisomerization of Conjugate Polyenes

According to the Woodward–Hoffmann rule [6, 7], conjugate polyenes with $4n$ and $4n+2$ π electrons undergo cyclizations in conrotatory and disrotatory fashions under the thermal conditions, respectively. Recently, novel cycloisomerizations were found to be catalyzed by Lewis acid and to afford bicyclic products [39] as photochemical reactions do [40]. The new finding supports the mechanistic spectrum of chemical reactions.

1.4.1 Delocalization Band

Hexatrienes undergo disrotatory ring closure by thermal activation to afford cyclohexadienes in agreement with the Woodward–Hoffmann rule (delocalization band in Scheme 8) [41–43]. Photo-irradiation of hexatrienes is known to give bicyclic products in a stereospecific $[4\pi_a+2\pi_a]$ manner (delocalization band in Scheme 8) [40] in contrast to this rule.



Scheme 8 Mechanistic spectrum of cycloisomerizations of hexatrienes

1.4.2 Pseudoexcitation Band

Trauner and colleagues [39] recently found a striking contrast in the thermal and catalyzed reactions of a triene. Thermal reaction of a trienolate readily underwent disrotatory electrocyclozation to afford cyclohexadiene (delocalization band in Scheme 8) in accordance with the Woodward–Hoffmann rule. Surprisingly, treatment of the trienolate with Lewis acid did not result in the formation of the cyclohexadiene but rather gave bicyclo[3.1.0]hexene in a $[4\pi_a+2\pi_a]$ manner (pseudoexcitation band in Scheme 8). The catalyzed reaction is similar to the photochemical reaction in the delocalization band.

The hexatriene is polarized by unsymmetrical substitution with the C=O group, and further activated by coordination with Lewis acid. The catalyzed reaction is polar. The similarity between the catalyzed and the photochemical reactions can be understood if polar reactions belong to the pseudoexcitation band as has been proposed in Sect 1.

1.5 Electrophilic Aromatic Substitutions

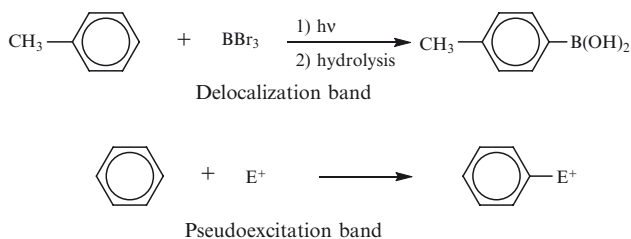
The mechanistic spectrum shed new light on a familiar textbook example of organic reactions, i.e., electrophilic aromatic substitution (Scheme 9).

1.5.1 Delocalization Band

No electrophilic aromatic substitution reactions of toluene, ethylbenzene, and cumene occur with BBr_3 in the dark: the electrophile is too weak for these reactions. The photochemical reactions followed by hydrolysis give the *p*-isomers of the corresponding boronic acids as the major products (delocalization band in Scheme 9) [44].

1.5.2 Pseudoexcitation Band

Electrophilic aromatic substitution reactions take place between aromatic compounds and strong acceptors (pseudoexcitation band in Scheme 9). The substitutions are



Scheme 9 Mechanistic spectrum of electrophilic aromatic substitutions

regarded as reactions in the pseudoexcitation band. Addition of AlCl_3 causes the haloboration with BBr_3 [45]. Complex formation of BBr_3 with AlCl_3 generates a more electrophilic species $[\text{BBr}_2]^+[\text{AlCl}_3\text{Br}]^-$ and shifts the reaction from the delocalization band to the pseudoexcitation band.

1.6 Reactions of Indoles with Unsaturated Acceptors

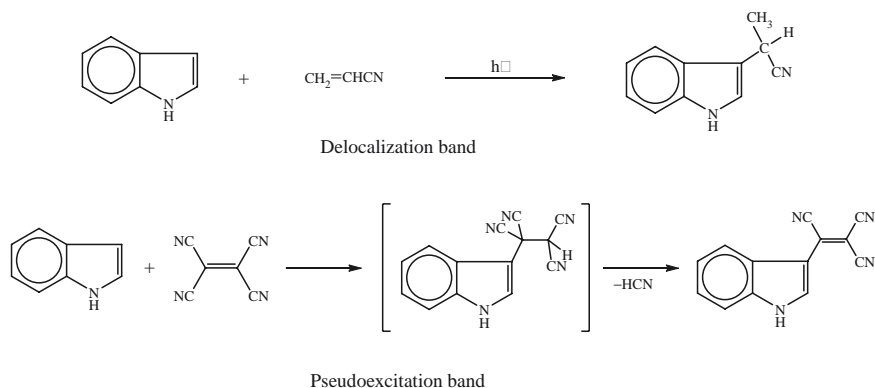
The theory of the mechanistic spectrum generally suggests that photochemical reactions between donors and acceptors in the delocalization band could be similar to thermal reactions between strong donors and acceptors in the pseudoexcitation band. This is further supported by the reactions of indoles with electron-accepting alkenes.

A photochemical reaction of indole with acrylonitrile gave an α -cyanoethylated indole (delocalization band in Scheme 10) [46]. This is a photochemical reaction in the delocalization band.

A stronger acceptor, TCNE, undergoes a similar reaction without irradiation to give tricyanovinylindole after the elimination of HCN by pyridine (pseudoexcitation band in Scheme 10) [47].

2 Delocalization Band

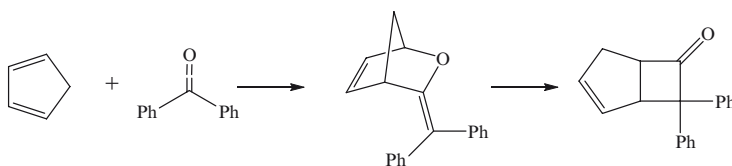
The reactions in this band are controlled by the frontier orbital interactions (Sect 3 in chapter “Elements of a Chemical Orbital Theory”), which were described in detail earlier [48–51]. A few recent interesting advances are reviewed in this section.



Scheme 10 Mechanistic spectrum of the reactions of indoles with unsaturated acceptors

2.1 [4+2] Cycloadditions of a Ketene

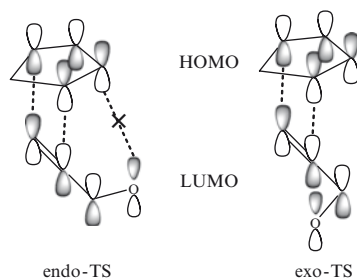
Staudinger observed that the cycloaddition of ketenes with 1,3-dienes afforded cyclobutanones from a formal [2+2] cycloaddition [52] prior to the discovery of the Diels–Alder reaction. The 2+2 cycloadditions were classified into the symmetry-allowed $\pi 2_s + \pi 2_a$ cycloaddition reactions [6, 7]. It was quite momentous when Machiguchi and Yamabe reported that [4+2] cycloadducts are initial products in the reactions of diphenylketene with cyclic dienes such as cyclopentadiene (Scheme 11) [53, 54]. The cyclobutanones arise by a [3, 3]-sigmatropic (Claisen) rearrangement of the initial products.



Scheme 11 [4+2] Cycloaddition reaction of diphenylketene

2.2 Exo-addition in Diels–Alder Reactions

Endo-selectivity of the Diels–Alder reactions of olefinic dienophiles are well understood in terms of the secondary frontier orbital interaction [55]. However, *exo*–*endo* selectivity of the reactions of acetylenic dienophiles was difficult to investigate, since *exo* and *endo* transition states produce diastereomerically identical adducts. Ishihara and Yamamoto [56, 57] reported the first example of an enantioselective Diels–Alder reaction of acetylenic dienophiles with dienes, which have prochiral reactive centers, in the presence of chiral boron Cu(II) catalysts. The secondary orbital interaction is antibonding between the lobes on the 2-position of the dienes and carbonyl oxygen of the dienophiles (Scheme 12). The Diels–Alder reactions of acetylenic aldehydes is resistant to the *endo*-transition structure, in contrast to that of olefinic aldehydes. The predominance of the *exo*-transition structure, confirmed by ab initio calculations, is in agreement with the observed enantioselectivity.



Scheme 12 Orbital phase environment in the Diels–Alder reactions of acetylenic aldehydes: *exo*-selectivity

Similar enantioselective Diels–Alder reactions between cyclopentadiene and α,β -acetylenic aldehydes catalyzed by a chiral super Lewis acid were reported by Corey and Lee [58].

2.3 [4+2] Cycloadditions on Surface

Reactions on the surface are interesting. The adsorptions of unsaturated organic molecules on the surface provide a means for fabricating well-ordered monolayer films. Thin film organic layers can be used for diverse applications such as chemical and biological sensors, computer displays, and molecular electronics.

Diels–Alder reactions are allowed by orbital symmetry in the delocalization band and so expected to occur on the surface. In fact, [4+2] cycloaddition reaction occurs on the clean diamond (100)- 2×1 surface, where the surface dimer acts as a dienophile. The surface product was found to be stable up to approximately 1,000 K [59, 60]. 1,3-Butadiene attains high coverage as well as forms a thermally stable adlayer on reconstructed diamond (100)- 2×1 surface due to its ability to undergo [4+2] cycloaddition [61].

Diels–Alder reactions also take place on the Si(100)- 2×1 [62] and Ge(100)- 2×1 [63, 64] surface. The experiments by Hammers and his colleagues [65] indicate that the [4+2] cycloaddition reactions of 1,3-cyclohexadiene and 1,3-dimethylbutadiene on the Si(001) surface compete with the [2+2] cycloaddition reactions.

3 Pseudoexcitation Band

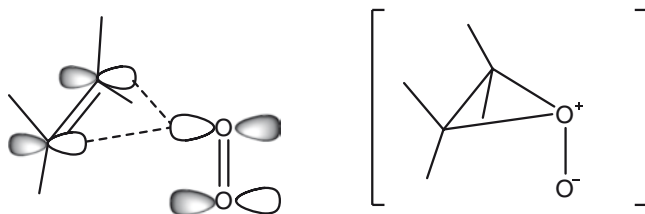
Some typical reactions in the pseudoexcitation band are reviewed in this section. The importance of pseudoexcitation [1] in chemical reactions was supported by the detailed numerical analysis of the electronic structures of the transition states [66]. The concept of pseudoexcitation appeared in physics [67–69].

3.1 Reactions of Singlet Molecular Oxygen $O_2 (^1\Delta_g)$

Singlet molecular oxygen $O_2 (^1\Delta_g)$ is an electron acceptor powerful enough to react with olefins in the pseudoexcitation band. The [2+2] cycloaddition and ene reactions and the stereoselectivities are reviewed in this subsection.

3.1.1 Quasi-Intermediate, Perepoxide

The interaction between the HOMO of alkenes and the LUMO of singlet oxygen 1O_2 (Scheme 4) is the most favored in the perepoxide structure (Scheme 13). This suggests



Scheme 13 Perepoxide quasi-intermediate

a path via the perepoxide intermediate or a perepoxide-like transition state [13]. We earlier predicted the following property and role of perepoxide from the calculated potential surface [70]. If an energy minimum exists (for perepoxide), it is very shallow – we may say, perepoxide itself cannot be isolated; in such a sense, perepoxide cannot be a genuine intermediate. However, if the flat region on the surface (for a perepoxide-like structure) is high, some kinetic and dynamic effects could possibly be observed as if the perepoxide intermediate actually intervened. This property is an attribute of the true intermediate. Such partial but not complete fulfillment of the conditions for reaction intermediate deserves the designation, *quasi-intermediate*.

After 28 years the perepoxide quasi-intermediate was supported by a two-step no intermediate mechanism [71, 72]. The minimum energy path on the potential energy surface of the reaction between singlet molecular oxygen O_2 ($^1\Delta_g$) and d_6 -teramethylethylene reaches a valley-ridge inflection point and then bifurcates leading to the two final products [73].

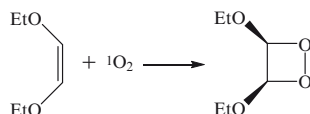
Katsumura, Kitaura and their coworkers [74] found and discussed the high reactivity of vinylic vs allylic hydrogen in the photosensitized reactions of twisted 1,3-dienes in terms of the interaction in the perepoxide structure. Yoshioka and coworkers [75] investigated the effects of solvent polarity on the product distribution in the reaction of singlet oxygen with enolic tautomers of 1,3-diketones and discussed the role of the perepoxide intermediate or the perepoxide-like transition state to explain their results. A recent review of the ene reactions of 1O_2 was based on the significant intervention of the perepoxide structure [76], which can be taken as a quasi-intermediate.

A perepoxide intermediate [77] or a peroxy diradical intermediate [78–81] have been proposed.

3.1.2 [2+2] Cycloaddition Reactions

[2+2] Cycloaddition reactions can occur with retention of configuration in the pseudoexcitation band (Sect 1.1) whereas $[2\pi_s+2\pi_s]$ reactions are symmetry-forbidden in the delocalization band. Experimental evidence is available for the stereospecific [2+2] cycloaddition reactions between $^1\Delta_g O_2$ and olefins with retention of configuration (Scheme 14) [82]. A perepoxide intermediate was reported to be trapped in the epoxide form [83] in the reaction of adamantylideneadamantane with singlet oxygen affording dioxetane derivatives [84].

Scheme 14 Stereospecific [2+2] cycloaddition reactions of $O_2 (^1\Delta_g)$



3.1.3 Concerted/Stepwise Boundary

The concept, quasi-intermediate [70], was introduced in 1975 to symbolize a boundary between concerted and stepwise mechanisms. Recent advances in computer chemistry are allowing us to investigate subtle problems more clearly in the years since 2000. Concerted/stepwise boundary mechanisms were proposed for other diverse reactions than those of singlet molecular oxygen $O_2 (^1\Delta_g)$.

Reactions that would be concerted based on the potential energy surface can nonetheless end up as a stepwise process [85]. The potential energy surface for the rearrangement of $(CH_3)_3C-CHCH_3-OH_2^+$ indicates loss of the water leaving group and migration of the methyl group take place in a concerted manner. However, most trajectories involve a stepwise route. The carbocation prior to the methyl migration can be termed a quasi-intermediate.

A mechanism at the S_N2Ar/S_N1 boundary was proposed for the nucleophilic substitution reaction of aryldiazonium ions in water [86].

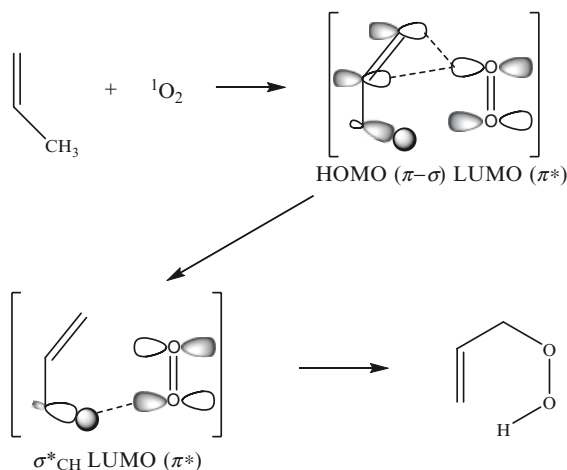
A single transition structure was located on the potential energy surface of the intramolecular bicyclization of protonated and Lewis acid activated (2*E*,4*Z*)-hepta-2,4,6-trienal and the corresponding methyl ester to provide the bicyclo[3.1.0]hexene derivatives [87]. These are models for the reactions in the pseudoexcitation band (Scheme 8). The five-membered ring is formed through the transition structure. The subsequent formation of the three-membered ring is barrierless. The reaction cannot be considered a stepwise process because no intermediate is found along the reaction path. It is not a concerted mechanism because of the timing of the bond-formation process. The five-membered ring structure can be termed a quasi-intermediate.

It is noteworthy that these are the reactions in the pseudoexcitation band if the polar reactions are taken as proposed in Sect 1.

3.1.4 Ene Reactions

Following the discovery of the ene reaction of singlet molecular oxygen $O_2 (^1\Delta_g)$ (Scheme 15) in 1953 by Schenck [88], this fascinating reaction continues to receive considerable mechanistic attention today. The importance of a path via the perepoxide intermediate or a perepoxide-like transition state [13] or the perepoxide quasi-intermediate [70] was proposed for the ene reactions of singlet oxygen 1O_2 with alkenes affording allylic hydroperoxides.

The HOMO of alkenes is an out-of-phase combination of the π and σ_{CH} orbitals. The amplitude is larger on π . The LUMO of singlet oxygen is π^* . The frontier orbital interaction occurs most effectively when the alkenes and the singlet oxygen



Scheme 15 An ene reaction of O_2 ($^1\Delta_g$)

assume a three-membered ring geometry (Schemes 15 and 4). This is a structure of the perepoxide quasi-intermediate. The interaction reduces the σ_{CH} bonding electron density and elongates the σ_{CH} bond. The positively charged and weakened σ_{CH} bond can readily accept electron density from π^* of the oxygen having accepted partial electron density from π . The σ_{CH}^* orbital is lowered enough to interact with π^* . As a result, the partial electron density is promoted (pseudoexcited) from the HOMO (π) to an unoccupied orbital (σ_{CH}^*) of alkenes. The ene reaction is a reaction in the pseudoexcitation band.

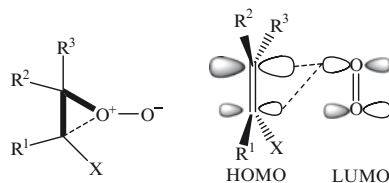
The significant role of the quasi-intermediates is in agreement with the small deuterium isotope effects in the ene reactions ($k_{\text{H}}/k_{\text{D}} = 1.1\text{--}2.4$ for 1-methylcyclohexene relative to the value 12.2 for 1,5-hydrogen shift of *cis*-1,3-pentadiene) [89]. Orfanopoulos and Stephenson [90] interpreted the results of their extensive investigation of the reaction of singlet oxygen with isotopically-labelled 2,3-dimethyl-2-butene to support a reactive intermediate with “structural requirements not dissimilar to those of the perepoxide”. Shuster and coworkers [91] proposed reversible formation of an explex or encounter complex in the first identifiable step, followed by irreversible conversion to a perepoxide in the rate-determining step of the ene reaction.

3.1.5 HOMO Amplitudes, Quasi-Intermediate Structures, and Mode Selectivities

The geometrical structure of the perepoxide quasi-intermediate was suggested to play critical roles in determining diverse selectivities of the reactions of $^1\text{O}_2$ with substituted olefins [92].

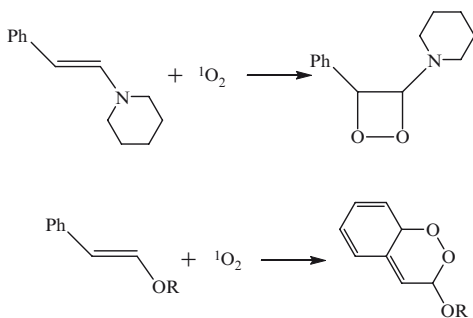
The HOMO amplitude of olefins determines (Sect 3.4 in Chapter “Elements of a Chemical Orbital Theory” by Inagaki in this volume) which carbon atom attracts

the incoming oxygen more strongly. For example, an electron donating substituent X enlarges the HOMO amplitude on the β carbon. This implies unsymmetrical structure of the quasi-intermediate (Scheme 16). The β -attack is preferable. In this case, the exocyclic tailing oxygen in the three-membered ring quasi-intermediate cannot react with the substituents (R^2 , R^3) on the β carbon but with R^1 and/or X . Otherwise, a [2+2] cycloaddition reaction occurs to form a dioxetane.



Scheme 16 HOMO polarized by X deforms peroxide quasi-intermediates

The lone pairs on the nitrogen and oxygen atoms make a significant difference in the chemical reactions (Scheme 17). β -Arylenamines undergo [2+2] cycloaddition reactions [93] whereas β -arylenol ethers undergo [2+2+2] cycloaddition reactions [94]. The mode selectivity was attributed [95] to the HOMO amplitude or the π bond polarity.



Scheme 17 HOMO amplitude controls the selectivities of reaction modes

The nitrogen lone pair enlarges the HOMO amplitude on the β carbon more than the oxygen lone pairs or the aromatic rings since the lone pair orbital of the nitrogen lies higher in energy. In the case of the amino substituent, the transient three-membered ring of the peroxide quasi-intermediate may collapse at an early stage and the incoming oxygen attacks the β carbon of the enamines. The [2+2] cycloaddition reaction results.

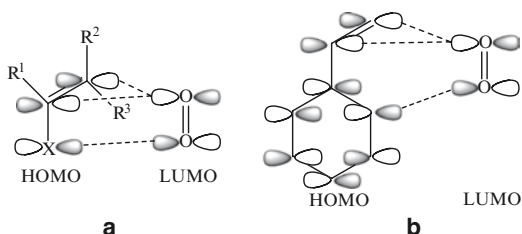
The alkoxy oxygen lone pairs and the phenyl group polarize the HOMO to a similar extent in opposite directions. The HOMO polarization is not significant. The symmetrical peroxide structure cannot collapse at an early stage. The tailing oxygen atom can attack the phenyl ring on the α carbon to undergo the [2+2+2] cycloaddition reactions.

In the photooxygenation of electron-rich olefins with allylic hydrogen atoms, ene reactivity usually dominates [96]. Nevertheless, other reactions become the preferred reaction mode. Inagaki et al. [92] attributed the exclusive [2+2] cycloaddition

reaction of indene [96], the [2+2+2] cycloaddition reaction of diphenylmethylenecyclobutane (no ene reactions) [97], to the HOMO amplitude or to the polarized π bond.

3.1.6 Attraction by Substituents and Selectivities

Attraction of the exocyclic tailing oxygen atom with X steers the oxygen atom to the same side of the double bond [92]. Lone pairs (Scheme 18a) on X and aromatic rings (Scheme 18b) can attract the tailing oxygen. The reactions can take place with X or the substituent R³ on the same side of the double bond rather than with those (R¹, R²) on the opposite side.



Scheme 18 a,b Attraction between $^1\text{O}_2$ and the substituents of alkenes: **a** a lone pair and **b** a phenyl π bond

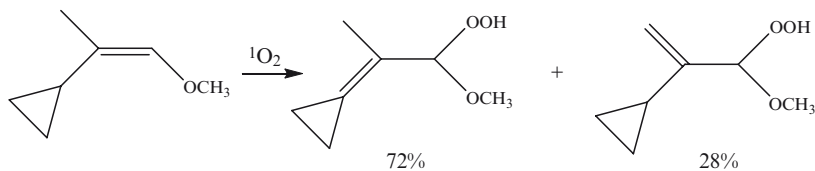
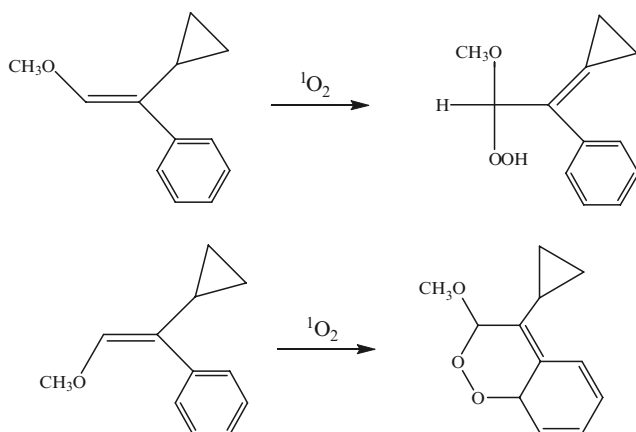
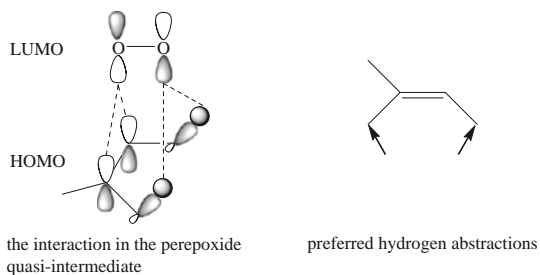
In fact, the hydrogen abstraction in the ene reactions was experimentally substantiated to occur from the group on the same side of the methoxy group (Scheme 19a) [98]. The *E*-isomer of enol ether yielded the hydroperoxide by a process which involves a cyclopropyl H-abstraction, whereas the *Z*-isomer led, via a [2+2+2] cycloadduct, to the epoxide (Scheme 19b) in agreement with the findings by Foote [99] cited in [92]. Recently, a similar effect of an alkenyl nitrogen functionality on the mode selectivity (and the diastereoselectivity) was found for the reactions of singlet oxygen with enecarbamates [100], but in that case the competition occurred between the ene reaction and [2+2] cycloaddition. Such a steering effect is exercised by allylic nitrogen [101] or oxygen [102].

3.1.7 Cis-Effect

The argument of the directing effect of lone pairs on the substituent [92] easily extends to the alkyl cases. The orbital interaction (Scheme 20) [103] in the peroxide quasi-intermediate suggests the stabilization occurs by the simultaneous interaction of $^1\text{O}_2$ with two allylic hydrogens on the same side of the alkene. Photooxygenation of trisubstituted olefins revealed a strong preference for H-abstraction from disubstituted side of the double bond [104, 105].

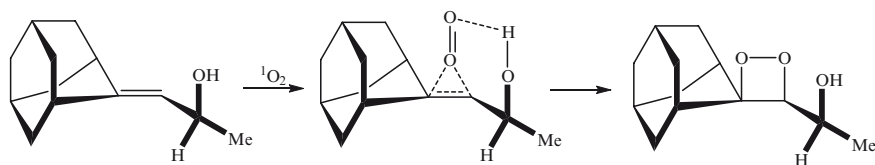
3.1.8 Hydrogen Bonding Effects

Hydrogen bonding to the pendant (tailing) oxygen (Scheme 21) in the peroxide quasi-intermediates controls the facial/diastereoselectivity of the ene reactions of

**a** the regioselectivity**b** the mode selectivity**Scheme 19a,b** Nonbonded attraction controls the regioselectivity (**a**) and the mode selectivity (**b**)**Scheme 20** HOMO–LUMO interaction in the peroxide quasi-intermediate for the cis-effect and the regioselectivity (percent) of the hydrogen abstractions

singlet oxygen with allylic alcohols [106, 107] and amines [108, 109]. The allylic alcohol exhibits a striking diastereoselectivity for the three (S^*S^*) β -hydroxy allylic hydroperoxide while its acylated derivative exhibits a modest erythro (S^*R^*) diastereoselectivity.

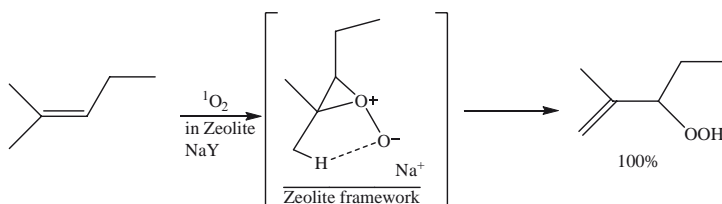
The steering effect of the hydrogen bonding was applied to a highly diastereoselective dioxetane formation from a chiral allylic alcohol (Scheme 21) [110].



Scheme 21 Hydrogen bonding effects

3.1.9 Photooxygenation in Zeolites

In 1996, Ramamurthy reported that photooxygenation of 2-methyl-2-pentene was regioselective and afforded a single allylic hydroperoxide product (Scheme 22) [111]. The result can be explained in terms of the complexation of the cation in the zeolite with the tailing oxygen in the peroxide quasi-intermediate (Scheme 22) [112–114]. The steric interaction keeps the large substituent (ethyl group) away from the zeolite framework. Hydrogen abstraction occurs on the side of the double bond opposite to the large substituent or from the methyl group, favoring formation of the less hindered hydroperoxide. There is no substituent geminal to the ethyl group. Peroxide quasi-intermediate plays an important role in the photooxygenation in zeolites.



Scheme 22 Regioselectivity in zeolites

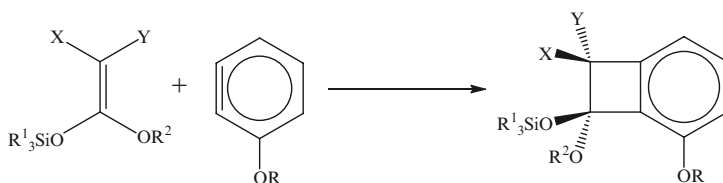
3.2 [2+2] Cycloadditions of Bent Unsaturated Bonds

Bending of unsaturated bonds reduces the overlap between the p -orbitals and weakens the interaction. The π orbital lies high in energy and the π^* orbital lies low. Bent unsaturated bonds are electron acceptors as well as donors. The energy gap between π and π^* is small. Bent unsaturated bonds are readily pseudoexcited to undergo [2+2] cycloaddition reactions.

3.2.1 Reactions of Benzynes

Benzynes share a feature with $^1\Delta_g \text{O}_2$ in the [2+2] cycloaddition reactions. The HOMO–LUMO interaction prefers the three-centered interaction (Scheme 4) [115]. This is in agreement with the calculated reaction path [116].

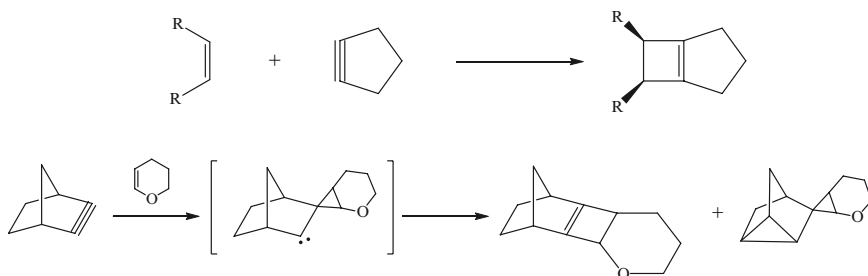
The 2+2 cycloadditions of benzyne to *cis*- and *trans*-propenyl ether gave *cis*- and *trans*-benzocyclobutanes as the main products, respectively [117, 118]. Stereospecific [2+2] cycloaddition reactions were observed between the benzyne species generated by the halogen–lithium exchange reaction of *ortho*-haloaryl triflates and the ketene silyl acetals (Scheme 23) [119].



Scheme 23 Stereospecific [2+2] cycloaddition reaction of a benzyne

3.2.2 Reactions of Cycloalkynes

Reactions of cyclopentyne with alkenes gives [2+2] cycloadduct with complete retention of stereochemistry (Scheme 24) [120]. Laird and Gilbert observed the expected [2+2] cycloadduct along with the polycyclic adduct in the reaction of norbornyne with 2,3-dihydropyran (Scheme 24) [121], and located a cyclopropylcarbene intermediate [122].



Scheme 24 [2+2]Cycloaddition reactions of cycloalkynes

3.3 [2+2] Cycloadditions of Ketenes

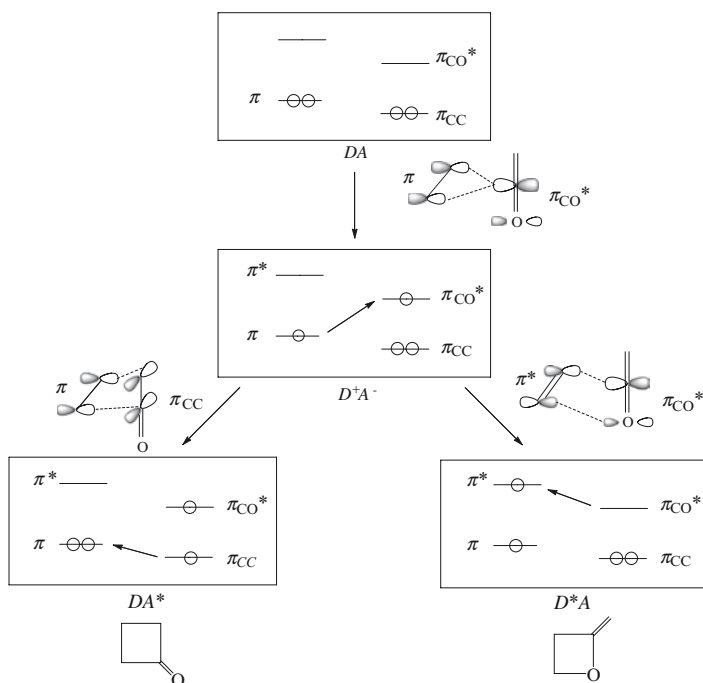
Ketenes have cumulative bonds and can undergo [2+2] cycloaddition reactions across C=C and C=O bonds. Interestingly, most of the products obtained are cyclobutanones rather than oxetanes. Thermal [2+2] cycloaddition reactions in the pseudoexcitation band occur between electron donors and acceptors. Alkenes are donors while ketenes are acceptors. In contrast to the experimental observations,

the reactions are expected to react across the C=O bond. Here, we review [2+2] cycloaddition reactions of ketenes and to present a mechanism of pseudoexcitation unique to ketene reactions to understand their interesting regioselectivity.

3.3.1 Reactions with Alkenes across the C=C Bonds

Cycloaddition reactions of ketenes with alkenes have long been known to give cyclobutanones [123] and to proceed with retention of the configurations [124]. The reactions were classified into the symmetry-allowed $\pi_2 + \pi_2$ cycloaddition reactions together with the 2+2 cycloaddition of vinyl cations [6,7]. However, the 2+2 cycloadditions of ketenes [125] and vinyl cations [126] were proposed to take place via the transient three-membered ring geometry stabilized by the HOMO–LUMO interaction as those of singlet oxygen (Scheme 4). This suggests that the 2+2 cycloadditions of ketenes are reactions in the pseudoexcitation band. The pseudoexcitation can explain a longstanding puzzle of the [2+2] cycloaddition reactions of ketenes with alkenes.

The HOMO and the LUMO of the donors are the π and π^* orbitals of alkenes, respectively. The LUMO of the acceptors is the π_{CO}^* orbital of ketenes. The HOMO of the acceptors is the π_{CC} orbital of ketenes. The localization of the HOMO and LUMO of ketenes on different bonds leads to unique regioselectivity of the [2+2] cycloaddition reactions.



Scheme 25 Pseudoexcitation in the [2+2] cycloaddition reactions of ketenes with alkenes

The primary delocalization occurs from π of alkenes to π_{CO}^* of ketenes (Scheme 25). The pseudoexcitations occur through the HOMO–HOMO and LUMO–LUMO interactions (Scheme 4). The HOMO of the donors is π as usual, whereas the HOMO of the acceptors is not π_{CO} but π_{CC} . The HOMO–HOMO interaction occurs between the C=C bonds of alkenes and ketenes and promotes the reaction across the C=C bond of ketenes. The important DA^* configuration is the intramolecular electron-transferred $\pi_{\text{CC}}\pi_{\text{CO}}^*$ (not $\pi_{\text{CO}}\pi_{\text{CO}}^*$) configuration of the ketene.

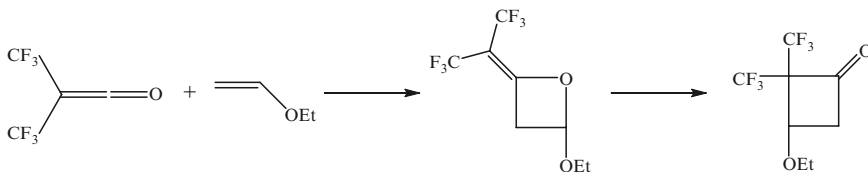
The LUMOs are π^* of alkenes and π_{CO}^* of ketenes. The LUMO–LUMO interaction occurs between the C=C bond of alkenes and the C=O bond of ketenes, promoting the reaction across the C=O bond of ketenes. The important pseudoexcited configuration D^*A is the locally-excited $\pi\pi^*$ configuration of alkenes.

The pseudoexcitation preferentially occurs in ketenes. The energy gap is smaller between π_{CC} and π_{CO}^* of ketenes than between π and π^* of alkenes. The π_{CC} orbital of ketene is raised in energy by the interaction with the n orbital on the carbonyl oxygen above π of alkenes. The π_{CO}^* orbital of ketenes is lower in energy than π^* of alkenes. The pseudoexcitation is preferred in ketenes and occurs through the π – π_{CC} interaction. The [2+2] cycloaddition reactions take place across the C=C bond of ketenes rather than C=O bond.

3.3.2 Reactions with Alkenes across the C=O Bonds

Ketenes can undergo [2+2] cycloaddition reactions across the C=O bonds when substituents lower the π_{CC} energy. The lowering of π_{CC} raises the DA^* ($\pi_{\text{CC}}\pi_{\text{CO}}^*$) energy and suppresses the pseudoexcitation for the reaction across the C=C bonds. Accordingly, such ketenes can react across the C=O bonds as electron accepting unsaturated bonds react in the pseudoexcitation band only if the electron donating partners are sufficiently activated.

Bis(trifluoromethyl)ketene reacts with ethyl vinyl ether across the C=O bond to afford the α -methyleneoxetane, which isomerizes into the oxetanone (Scheme 26) [127]. The transition structure was not located by calculations for the reaction across the C=C bond but for the reaction across the C=O bond. The electron-withdrawing groups on ketenes lower the π_{CC} energy and weaken the promotion from C=C to C=O. The electron donating ethoxy group on the alkene strengthens the HOMO–LUMO interaction enough to pseudoexcite the CO bond.



Scheme 26 [2+2] Cycloaddition reaction of a ketene across the C=O bond

3.3.3 Dimerizations

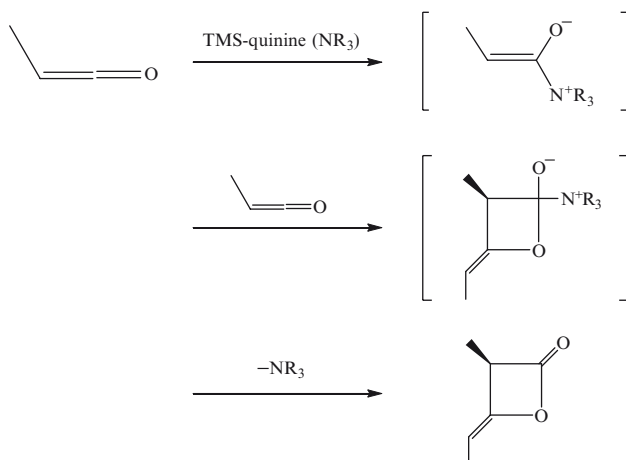
The dimerization of the parent ketene gives the β -lactone. One molecule of ketene reacts across the C=C bond as a donor and the other molecule reacts across the C=O bond as an acceptor. This is similar to the concerted [2+2] cycloaddition reaction between bis(trifluoromethyl)ketene and ethyl vinyl ether to afford the oxetane (Scheme 26) [127]. A lone pair on the carbonyl oxygen in the ketene molecule as a donor activates the C=C bond as the alkoxy group in vinyl ether.

The importance of pseudoexcitation in the dimerization was confirmed by detailed numerical analysis [128].

3.3.4 Catalyzed Dimerizations

Monosubstituted ketenes dimerize into 1,3-cyclobutandiones. The regioselectivity is believed to be determined by the steric repulsions of the substituents. Catalysts change the regioselectivity.

Dimerization of methylketene is catalyzed by an amine, trimethylsilylquinine, to give the β -lactone enantioselectively (Scheme 27) [129]. The catalyst amine attacks the ketene to form an ammonium enolate, an electron donating alkene. The donor is strong enough to react with a ketene across the C=O bond. That is why the β -lactone is obtained instead of the 1,3-cyclobutandione, the uncatalyzed dimerization product of the monosubstituted ketene.



Scheme 27 Amine-catalyzed dimerization of a ketene

3.4 [2+2] Cycloadditions with Surface

Interest in integrating semiconductor technology with organic and biological materials has fueled great interest in understanding how organic molecules react with the

surfaces of diamond, silicon, and germanium. In general, the group IV (001) surface is composed of pairs of atoms, referred to as surface dimers. The dimer atoms are doubly bonded to each other. Analogies can be made between the group IV surface (001) dimers and molecular double bonds, though the surface dimers are strongly bent by virtue of being bonded to the underlying substrate atoms.

Alkenes undergo [2+2] cycloadditions on C(001) [130], Si(001) [131], and Ge(001) [132] surfaces. [2+2] Cycloadditions on the surfaces are taken as reactions in the pseudoexcitation band. In fact, the cycloadditions of alkenes (ethylene, propylene, vinyl chloride, styrene) with a truncated cluster model Si(100)-2 × 1 surface were shown by some calculations to have characteristic features of [2+2] cycloaddition reactions in the pseudoexcitation band [133]. The relative reaction rates (C << Ge < Si) correlate (negatively) with the ordering of the surface-state band gaps (C >> Ge > Si) [130]. The correlation supports that the [2+2] cycloadditions on the C, Si, Ge surfaces are reactions in the pseudoexcitation band since the pseudoexcitation is promoted by the small π - π * splitting of reactants.

Cycloaddition reactions with the Si(100) surface have been investigated for the purpose of designing microelectronics, nonlinear optical materials, sensors, and biologically active surfaces. The features of the [2+2] cycloadditions characteristic of the reactions in the pseudoexcitation band [133] predicts that [2+2] cycloadditions of electron-donating alkenes with Si(100)-2 × 1 surface could proceed with retention of configurations, in agreement with the observation [134]. Such stereospecific functionalizations of surfaces are of potential use for specific applications.

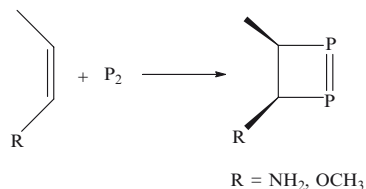
The pseudoexcitation is induced by the delocalization from alkenes to the Si(100)-2 × 1 surface [133]. Electron-accepting alkenes undergo different reactions. For acrylonitrile, a [4+2] cycloaddition reaction was found to be kinetically most favorable [135].

Khanna et al. [136] proposed a mechanism of the reactions of aluminum based clusters with O₂, which lends a physical interpretation as to why the HOMO-LUMO gap of the clusters successfully predicts the oxygen etching behaviors. The importance of the HOMO-LUMO gap strongly suggests that the reactions of the metal clusters belong to the pseudoexcitation band.

Metal surfaces and clusters are readily pseudoexcited. The band gaps of the surface states and the HOMO-LUMO gaps of metal clusters will be found to be important for more and more reactions in future.

3.5 [2+2] Cycloadditions of Unsaturated Bonds Between Heavy Atoms

[2+2] Cycloadditions with the Si(100) surface were theoretically [133] concluded to be reactions in the pseudoexcitation band. The conclusion is applicable to thermal [2+2] cycloaddition reactions of unsaturated bonds between heavy atoms. In fact, Sekiguchi, Nagase et al. confirmed that a Si triple bond underwent the stereospecific reactions with alkenes [137] along the path typical of [2+2] cycloaddition in the pseudoexcitation band. The stereospecific [2+2] cycloadditions of P₂ were designed by Inagaki et al. (Scheme 28) [138].

Scheme 28 [2+2] Cycloadditions of unsaturated heavy-atom bonds

4 Transfer Band

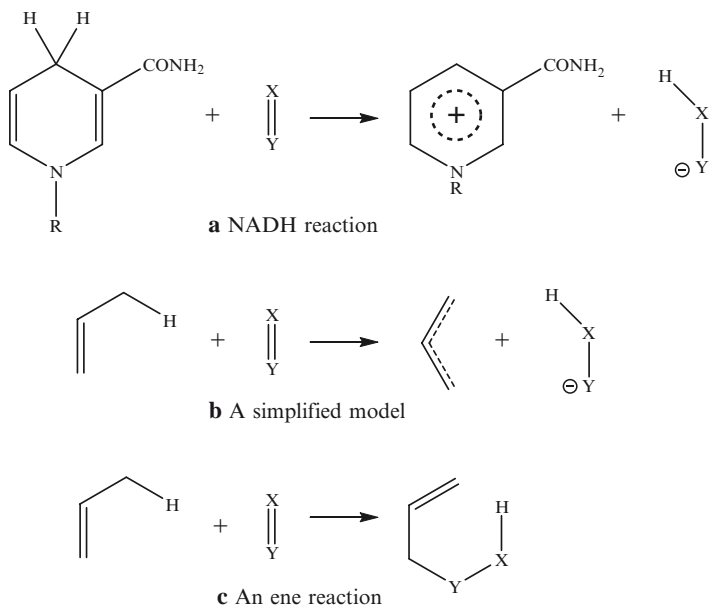
For some pairs of strong donors and acceptors, D^+A^- is too stabilized for the delocalization and for the pseudoexcitation. One electron transfers from the donors to the acceptors instead. No bonds but ion radical pairs or salts form between the donors and acceptors. However, the electron transfers can be followed by reactions. This mechanistic band is here termed simply, “transfer band”.

4.1 NAD(P)H Reactions

Reduced nicotinamide–adenine dinucleotide (NADH) plays a vital role in the reduction of oxygen in the respiratory chain [139]. The biological activity of NADH and oxidized nicotinamideadenine dinucleotide (NAD⁺) is based on the ability of the nicotinamide group to undergo reversible oxidation–reduction reactions, where a hydride equivalent transfers between a pyridine nucleus in the coenzymes and a substrate (Scheme 29a). The prototype of the reaction is formulated by a simple process where a hydride equivalent transfers from an allylic position to an unsaturated bond (Scheme 29b). No bonds form between the π bonds where electrons delocalize or where the frontier orbitals localize. The simplified formula can be compared with the ene reaction of propene (Scheme 29c), where a bond forms between the π bonds.

As is outlined for ene reactions of singlet oxygen in Scheme 15, the prototypical ene reaction starts with the electron delocalization from the HOMO of propene to the LUMO of $X=Y$. The delocalization from the HOMO, a combined π and σ_{CH} orbital with larger amplitude on π , leads to a bond formation between the $C=C$ and $X=Y$ bonds. Concurrent elongation of the σ_{CH} bond enables a six-membered ring transition structure, where partial electron density is back-donated from the LUMO of $X=Y$ having accepted the density, to an unoccupied orbital of propene localized on the σ_{CH} bond. As a result, the partial electron density is promoted (pseudoexcited) from the HOMO (π) to an unoccupied orbital (σ_{CH}^*) of alkenes. This is a reaction in the pseudoexcitation band.

Strong donor–acceptor interaction shifts the reaction from the pseudoexcitation band to the transfer band. Electrons delocalize from the HOMO of propene to the LUMO of $X=Y$ too much to form a bond between the double bonds. One electron transfers and a radical ion pair forms. The negatively charged $X=Y$

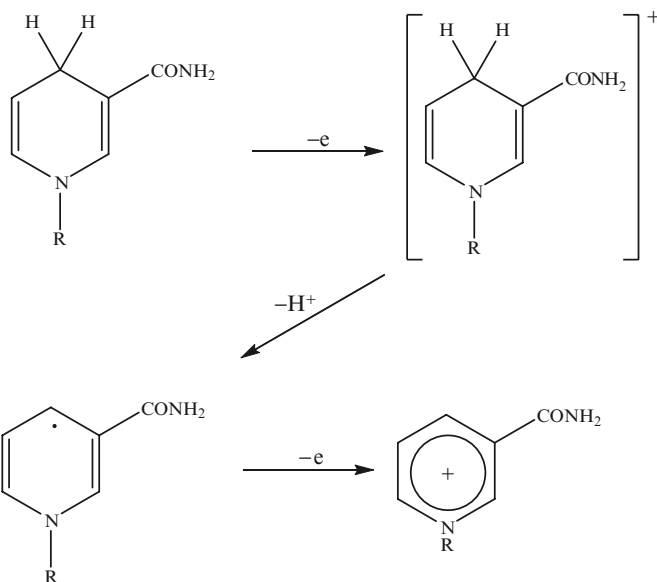


Scheme 29 a,b,c Reaction of NADH (a), a simplified model (b) and its related (ene) reactions (c)

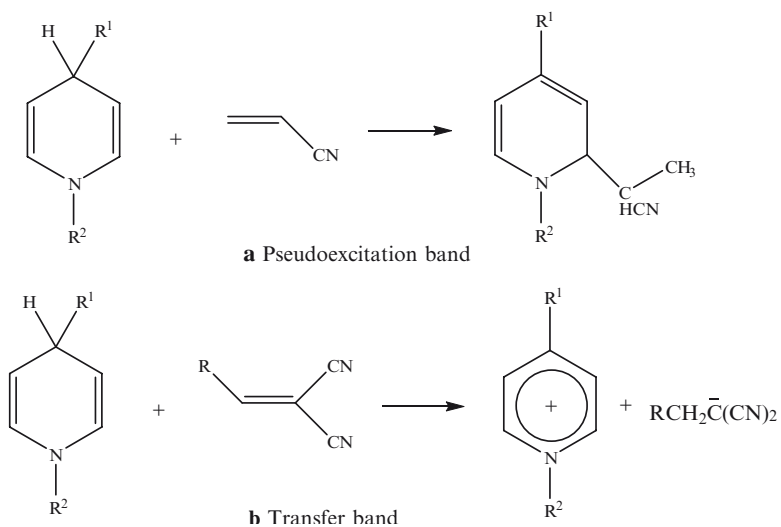
abstracts a proton (protonic entity) from the positively charged propene. Reduction of unsaturated bonds by NADH was theoretically concluded to occur with the nature of a sequential electron–proton–electron shift (Scheme 30) [140]. Electron-donating ability of NADH enhanced by the lone pair on the nitrogen atom of the pyridine ring and high electron acceptability of substrates are key factors of the oxidation of NADH. This is a reaction in the transfer band.

The sequential electron–proton–electron transfer mechanism is in agreement with the experimental observation by Ohno et al. [141]. The mechanism was confirmed by Selvaraju and Ramamurthy [142] from photophysical and photochemical study of a NADH model compound, 1,8-acridinedione dyes in micelles.

A pair of reactions of 1,4-dihydropyridines with electron-accepting alkenes (Scheme 31) shows experimental evidence for the mechanistic spectrum between the pseudoexcitation and transfer bands. Acrylonitrile undergoes an ene reaction [143] (Scheme 31a). This is a reaction in the pseudoexcitation band. A stronger acceptor, alkylidene- and arylmethylidenemalonitriles are reduced [144] (Scheme 31b). This is a reaction in the transfer band, where a hydride equivalent shifts without bond formation between the π bonds of the donors and acceptors.



Scheme 30 Sequential electron-proton-electron transfer

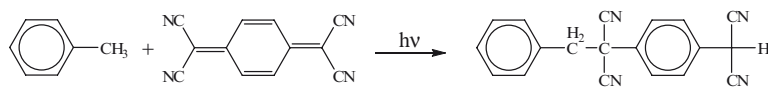


Scheme 31 a,b A mechanistic spectrum of NADH reactions: (a) pseudoexcitation band; (b) transfer band

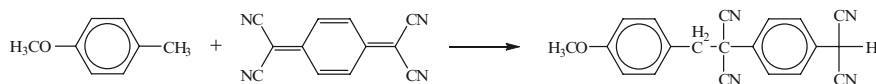
4.2 Reactions of Methyl Benzenes with TCNQ

There are other reactions apart from NADH reduction (Sect 4.1) where the hydride equivalent shifts between electron donors and acceptors without bond formation between the π bonds. The hydride equivalent transfer must be reactions in the transfer band. In fact, a photochemical reaction between donors and acceptors is similar to thermal reactions between strong donors and acceptors. This further supports the mechanistic spectrum (Scheme 32).

Photoirradiation of 7,7,8,8-tetracyanoquinodimethane (TCNQ) in toluene afforded 1,6-addition product (pseudoexcitation band in Scheme 32) [145]. The 1,6-addition thermally occurs with a stronger donor, *p*-methoxytoluene (transfer band in Scheme 32) [146].



a Pseudoexcitation band



b Transfer band

Scheme 32 Mechanistic spectrum of the reactions of methylbenzenes with unsaturated acceptors

4.3 Hydride Equivalent Transfers

Hydrogen is the least electronegative atom except for metal atoms. It is unlikely that the hydrogen atom not bonded to a metal atom is negatively charged. However, there are diverse reactions where a hydride equivalent transfers. Among them are Cannizzaro reactions, Meerwein–Ponndorf–Verley reduction, and so on. It is also unlikely that a hydride directly transfers at the transition states. These hydride equivalent shifts are taken as reactions in the electron transfer band as are those in the preceding sections. In fact, one electron transfer was observed by ESR measurements for Cannizzaro reactions [147], Meerwein–Ponndorf–Verley reduction [148], and the hydride equivalent transfers from Grignard reagents [149] and alkoxides [148].

Acknowledgments The author thanks Prof. Hisashi Yamamoto of the University of Chicago for his reading of the manuscript and his encouraging comments, Messrs. Hiroki Shimakawa and Hiroki Murai for their assistance in preparing the manuscript, and Ms. Jane Clarkin for her English suggestions.

References

1. Inagaki S, Fujimoto H, Fukui K (1975) *J Am Chem Soc* 97:6108
2. Fukui K (1966) *Bull Chem Soc Jpn* 39:498
3. Epiotis ND (1972) *J Am Chem Soc* 94:1924
4. Yamaguchi K, Fueno T, Fukutome H (1973) *Chem Phys Lett* 22:461
5. Mene'ndez MI, Sua'rez D, Sordo JA, Sordo TL (1995) *J Comput Chem* 6:659
6. Woodward RB, Hoffmann R (1969) *Angew Chem Int Ed Engl* 8:781
7. Hoffmann R, Woodward RB (1970) *The conservation of orbital symmetry*. Verlag Chemie/Academic, New York
8. Yamazaki H, Cvetanovic' RJ (1969) *J Am Chem Soc* 91:520
9. Benson SW (1986) *Thermodynamical kinetics*. Wiley, New York, Table A11
10. Bartlett PD, Montgomery LK, Seidel B (1964) *J Am Chem Soc* 86:616
11. Montgomery LK, Schueller K, Bartlett PD (1964) *J Am Chem Soc* 86:622
12. Bartlett PD, Montgomery LK (1964) *J Am Chem Soc* 86:628
13. Inagaki S, Yamabe S, Fujimoto H, Fukui K (1972) *Bull Chem Soc Jpn* 45:3510
14. Huisgen R, Steiner G (1973) *J Am Chem Soc* 95:5054
15. Nishida S, Moritani I, Teraji T (1973) *J Org Chem* 38:1878
16. Hoffmann RW, Bressel U, Gehlhaus J, Hauser H (1971) *Chem Ber* 104:873
17. Proskow S, Simmons HE, Cairns TL (1966) *J Am Chem Soc* 88:5254
18. Gompper R, Elser W, Mueller H-J (1967) *Angew Chem Int Ed Engl* 6:453
19. Gompper R (1969) *Angew Chem Int Ed Engl* 8:312
20. Eisch JJ, Husk GR (1966) *J Org Chem* 31:589
21. Asaad AN, Aksnes G (1988) *Z Naturforsch* 43a:435
22. Jung ME, Nishimura N, Novack AR (2005) *J Am Chem Soc* 127:11206
23. Nelson PL, Ostrem D, Lassila JD, Chapman OL (1969) *J Org Chem* 34:811
24. Inagaki S, Minato T, Yamabe S, Fujimoto H, Fukui K (1974) *Tetrahedron* 30:2165
25. Calvert JG, Pitts JN Jr (1966) *Photochemistry*. Wiley, New York
26. England DC (1961) *J Am Chem Soc* 83:2205
27. Middleton WJ (1965) *J Org Chem* 30:1307
28. Vieregge H, Bos HJT, Arens JF (1959) *Rec Trav Chim Pays-Bas* 78:664
29. Yang HW, Romo D (1999) *Tetrahedron* 55:6403
30. Evans DA, Janey JM (2001) *Org Lett* 3:215
31. Calter MA, Tretyak OA, Flaschenriem C (2005) *Org Lett* 7:1809
32. Gompper R, Wetzel B, Elser W (1968) *Tetrahedron Lett* 5519
33. Gompper R, Elser W (1967) *Angew Chem Int Ed* 6:366
34. Yamabe S, Nishihara Y, Minato T (2002) *J Phys Chem A* 106:4980
35. Ding YQ, Fang DC (2003) *J Org Chem* 68:4382
36. Sustmann R, Luecking K, Kopp G, Rese M (1989) *Angew Chem Int Ed Engl* 28:1713
37. Bobrowski M, Liwo A, Oldziej S, Jeziorek D, Ossowski T (2000) *J Am Chem Soc* 122:8112
38. Sevin F, McKee ML (2001) *J Am Chem Soc* 123:4591
39. Miller AK, Banghart MR, Beaudry CM, Suh JM, Trauner D (2003) *Tetrahedron* 59:8919
40. Courtot P, Salaun JY, Rumin R (1976) *Tetrahedron Lett* 2061
41. Vogel E, Grimme W, Dinne E (1965) *Tetrahedron Lett* 391
42. Marvell EN, Caple G, Schatz B (1965) *Tetrahedron Lett* 385
43. Glass DS, Watthey JWH, Winstein S (1965) *Tetrahedron Lett* 377
44. Ogata Y, Izawa Y, Tomioka H, Ukigai T (1969) *Tetrahedron* 25:1817
45. Olah GA (1973) *Friedel-Crafts chemistry*. Wiley, New York, p 73
46. Yamasaki K, Matsuura T, Saito I (1974) *J Chem Soc Chem Commun* 944
47. Noland WE, Kuryla WC, Lange RF (1959) *J Am Chem Soc* 81:6010
48. Fukui K, Yonezawa T, Shingu H (1952) *J Chem Phys* 22:722
49. Fukui K (1971) *Acc Chem Res* 4:57
50. Fukui K (1975) *Theory of orientation and stereoselection*. Springer, Berlin Heidelberg New York

51. Fleming I (1976) *Frontier orbitals and organic chemical reactions*. Wiley, London
52. Staudinger H (1907) *Liebigs Ann Chem* 40:51
53. Yamabe S, Dai T, Minato T, Machiguchi T, Hasegawa T (1996) *J Am Chem Soc* 118:6518
54. Machiguchi T, Hasegawa T, Ishikawa A, Terashima S, Yamabe S, Dai T, Minato T (1999) *J Am Chem Soc* 121:4771
55. Hoffmann R, Woodward RB (1965) *J Am Chem Soc* 87:4388
56. Ishihara K, Kondo S, Kurihara H, Yamamoto H, Ohashi S, Inagaki S (1997) *J Org Chem* 62:3026
57. Ishihara K, Fushimi M (2008) *J Am Chem Soc* 130:7532
58. Corey EJ, Lee TW (1997) *Tetrahedron Lett* 38:5755
59. Hossain MZ, Aruga T, Takagi N, Tsuno T, Fujimori N, Ando T, Nishijima M (1999) *Jpn J Appl Phys Part 2: Lett* 38:L1496
60. Wang GW, Bent SF, Russell JN Jr, Butler JE, D'Evelyn MP (2000) *J Am Chem Soc* 122:744
61. Ouyang T, Gao X, Qi D, Wee ATS, Loh KP (2006) *J Phys Chem B* 110:5611
62. Teplyakov AV, Kong MJ, Bent SF (1997) *J Am Chem Soc* 119:11100
63. Teplyakov AV, Lal P, Noah YA, Bent SF (1998) *J Am Chem Soc* 120:7377
64. Lee SW, Nelen LN, Ihm H, Scoggins T, Greenlief CM (1998) *Surf Sci* 410:L773
65. Hovis JS, Liu H, Hammers RJ (1998) *J Phys Chem B* 102:6873
66. Mene'ndez MI, Sordo JA, Sordo TL (1992) *J Phys Chem* 96:1185
67. Pathak RK (1985) *Phys Rev A* 31:2806
68. Liu SH (1989) *Phys Rev B* 39:1403
69. Kanada H, Kaneko T, Tang YC (1991) *Phys Rev C* 43:371
70. Inagaki S, Fukui K (1975) *J Am Chem Soc* 97:7480
71. Singleton DA, Hang C, Szymanski MJ, Meyer MP, Leach AG, Kuwata KT, Chen JS, Greer A, Foote CS, Houk KN (2003) *J Am Chem Soc* 125:1319
72. Singleton DA, Hang C, Szymanski MJ, Greenwald EE (2003) *J Am Chem Soc* 125:1319
73. Gonzalez-Lafont A, Moreno M, Lluch JM (2004) *J Am Chem Soc* 126:13089
74. Mori H, Ikoma K, Isoe S, Kitaura K, Katunuma S (1998) *J Org Chem* 63:8704
75. Yoshioka M, Sakuma Y, Saito Y (1999) *J Org Chem* 64:9247
76. Alberti MN, Orfanopoulos M (2006) *Tetrahedron* 62:10660
77. Hotokka M, Roos B, Siegbahn P (1983) *J Am Chem Soc* 105:5263
78. Harding LB, Goddard WA III (1977) *J Am Chem Soc* 99:4520
79. Harding LB, Goddard WA III (1980) *J Am Chem Soc* 102:439
80. Maranzana A, Ghigo G, Tonachini G (2000) *J Am Chem Soc* 122:414
81. Maranzana A, Ghigo G, Tonachini G (2003) *Chem Eur J* 9:2616
82. Bartlett PD, Schaap AP (1970) *J Am Chem Soc* 92:3223
83. Schaap AP, Faler G (1973) *J Am Chem Soc* 95:3381
84. Wieringa JH, Strating J, Wynberg H (1972) *Tetrahedron Lett* 169
85. Ammal SC, Yamataka H, Aida M, Dupuis M (2003) *Science* 299:1555
86. Ussing BR, Singleton DA (2005) *JACS* 127:2888–2899
87. López CS, Faza ON, Alvarez R, de Lera AR (2006) *J Org Chem* 71:4497
88. Schenck GO, Eggert H, Denk W (1953) *Liebigs Ann Chem* 584:177
89. Hoffmann HMR (1969) *Angew Chem* 81:597
90. Grdina B, Orfanopoulos M, Stephenson LM (1979) *J Am Chem Soc* 101:3111
91. Hurst JR, Wilson SL, Schuster GB (1985) *Tetrahedron* 41:2191
92. Inagaki S, Fujimoto H, Fukui K (1976) *Chem Lett* 5:749
93. Foote CS, Lin JWP (1968) *Tetrahedron Lett* 3267
94. Foote CS, Mazur S, Burns PA, Lerdal P (1973) *J Am Chem Soc* 95:586
95. Inagaki S, Fujimoto H, Fukui K, (1976) *J Am Chem Soc* 98:4054
96. Denny RW, Nickon A (1973) In: Dauben WG (ed) *Organic reactions*, vol 20. Wiley, New York, p 133
97. Rio G, Bricout D, Lacombe ML (1973) *Tetrahedron* 29:3553
98. Rousseau G, Le Perchec G, Conia JM (1977) *Tetrahedron Lett* 2517
99. Lerdal D, Foote CS (1978) *Tetrahedron Lett* 3227
100. Adam W, Bosio SG, Turro NJ, Wolff BT (2004) *J Org Chem* 69:1704

101. Matsumoto M, Kitano Y, Kabayashi H, Ikawa H (1996) *Tetrahedron Lett* 45:6191
102. Matsumoto M, Kabayashi H, Matsubara J, Watanabe N, Yamashita S, Oguma D, Kitano Y, Ikawa H (1996) *Tetrahedron Lett* 37397
103. Stephenson LM (1980) *Tetrahedron Lett* 21:1005
104. Shulte-Elte KH, Muller BL, Rautenstrauch V (1978) *Helv Chim Acta* 61:2777
105. Orfanopoulos M, Grdina MB, Stephenson LM (1979) *J Am Chem Soc* 101:275
106. Adam W, Nestler B (1992) *J Am Chem Soc* 114:6549
107. Adam W, Nestler B (1993) *J Am Chem Soc* 115:5041
108. Adam W, Bruenker HG (1993) *J Am Chem Soc* 115:3008
109. Bruenker HG, Adam W (1995) *J Am Chem Soc* 117:3976
110. Adam W, Saha-Moeller CR, Schambony SB (1999) *J Am Chem Soc* 121:1834
111. Li X, Ramamurthy V (1996) *J Am Chem Soc* 118:10666
112. Clennan EL, Sram JP (1999) *Tetrahedron Lett* 40:5275
113. Clennan EL, Sram JP (2000) *Tetrahedron* 56:6945
114. Stratakis M, Froudakis G (2000) *Org Lett* 21369
115. Inagaki S, Fukui K (1973) *Bull Chem Soc Jpn* 46:2240
116. Hayes DM, Hoffmann R (1972) *J Phys Chem* 76:656
117. Tabushi I, Oda R, Okazaki K (1968) *Tetrahedron Lett* 3743
118. Wasserman HH, Solodar AJ, Keller LS (1968) *Tetrahedron Lett* 5597
119. Hosoya T, Hasegawa T, Kuriyama Y, Suzuki K (1995) *Tetrahedron Lett* 36:3377
120. Gilbert JC, Baze ME (1984) *J Am Chem Soc* 106:1885
121. Laird DW, Gilbert JC (2001) *J Am Chem Soc* 123:6704
122. Bachrach SM, Gilbert JC, Laird DW (2001) *J Am Chem Soc* 123:6706
123. Staudinger H (1912) *Die Ketene*. Enke, Stuttgart
124. Huisgen R, Feiler L, Binsch L (1964) *Angew Chem Int Ed Engl* 3753
125. Sustmann R, Ansmann A, Vahrenholt F (1972) *J Am Chem Soc* 94:8099
126. Wagner HU, Gommer R (1971) *Tetrahedron Lett* 4061, 4065
127. Machiguchi T, Okamoto J, Takachi J, Hasegawa T, Yamabe S, Minato T (2003) *J Am Chem Soc* 125:14446
128. Yamabe S, Minato T (1993) *Bull Chem Soc Jpn* 66:3283
129. Calter MA, Orr RK, Song W (2003) *Org Lett* 5:4745
130. Hovis JS, Coulter SK, Hamers RJ, D'Evelyn MP, Russell JN Jr, Butler JE (2000) *J Am Chem Soc* 122:732
131. Bozack MJ, Taylor PA, Choyke WJ, Yates JT Jr (1986) *Surf Sci* 177:L933
132. Hamers RJ, Hovis JS, Greenlief CM, Padowitz DF (1999) *Jpn J Appl Phys* 38:3879
133. Wang Y, Ma J, Inagaki S, Pei Y (2005) *J Phys Chem B* 109:5199
134. Liu H, Hamers RJ (1997) *J Am Chem Soc* 119:7593
135. Wang Y, Ma J (2006) *J Phys Chem B* 110:5542
136. Reber AC, Khanna SN, Roach PJ, Woodward WH, Castleman AW Jr (2007) *J Am Chem Soc* 129:16098
137. Kinjo R, Ichinohe M, Sekiguchi A, Takagi N, Sumimoto M, Nagase S (2007) *J Am Chem Soc* 129:7766
138. Nagasaki S, Inagaki S (2008) *Tetrahedron Lett* 49:3578
139. Bohinski RC (1997) *Modern concepts in biochemistry*, 3rd edn. Allyn & Bacon, Boston
140. Inagaki S, Hirabayashi Y (1977) *Bull Chem Soc Jpn* 50:3360
141. Ohno A, Kito N (1972) *Chem Lett* 1:369
142. Selvaraju C, Ramamurthy P (2004) *Chem Eur J* 102253
143. Sulzbach RA, Iqbal AFM (1971) *Angew Chem* 83:758
144. Wallensfels K, Ertel W, Friedrich K (1973) *Justus Liebig Ann Chem* 1663
145. Yamasaki K, Yonezawa T, Ohashi M (1975) *J Chem Soc Perkin Trans* 1:93
146. Ohashi M, Nakayama N, Yamasaki K (1976) *Chem Lett* 5:1131
147. Ashby EC, Coleman DT III, Gamasa MP (1983) *Tetrahedron Lett* 24:851
148. Ashby EC, Goel AB, Argyropoulos JN (1982) *Tetrahedron Lett* 23:2273
149. Maruyama K (1964) *Bull Chem Soc Jpn* 37:897

Orbital Mixing Rules

Satoshi Inagaki

Abstract A theory of the interaction of *three* orbitals, i.e., the $\phi_h-\phi_p-\phi_l$ interaction, and its chemical applications are reviewed. General rules are drawn to predict the orbital phase relations between ϕ_h and ϕ_l , which do not directly interact with each other but indirectly through a perturbing orbital ϕ_p . When ϕ_h and ϕ_l are orbitals on the same atoms, bonds, or molecules and ϕ_p is a perturbing orbital, ϕ_h deforms by mixing-in of ϕ_l and vice versa. The direction of the orbital deformation is determined by the orbital phase relation between ϕ_h and ϕ_l . The orbital mixing rules are applied to the deformation of the orbitals. The deformation determines favorable interactions with other orbitals. The orbital mixing rule is powerful for understanding and designing selective reactions. The electrostatic orbital mixing by positive and negative electric charges and its chemical consequences are reviewed as well.

Keywords Orbital mixing, Orbital amplitude, Orbital phase, Orbital polarization, Orbital deformation, Regioselectivity, Stereoselectivity, π Facial selectivity

Contents

1	Orbital Mixing Rules	58
1.1	Overlap Mixing	59
1.2	Electrostatic Mixing	62
2	Applications to Regioselectivities.....	64
2.1	Electrophilic Additions.....	64
2.2	Diels–Alder Reactions.....	65
2.3	Electrophilic Aromatic Substitutions	72
3	Applications to π Facial Selectivities.....	76
3.1	Norbornenes	76

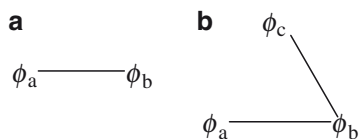
S. Inagaki
Department of Chemistry, Faculty of Engineering, Gifu University,
Yanagido, Gifu 501–1193, Japan
e-mail: inagaki@gifu-u.ac.jp

3.2	7-Alkylidenenorbornenes	77
3.3	Benzobicyclo[2.2.2]octadienes	79
3.4	Cyclohexanones.....	79
4	Recent Related Topics.....	80
	References.....	80

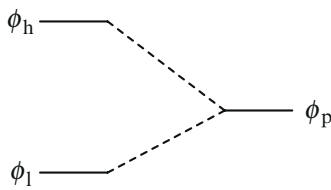
1 Orbital Mixing Rules

The theory of interaction between a pair of orbitals, ϕ_a and ϕ_b (Scheme 1a) is well established (Chapter “Elements of a Chemical Orbital Theory” by Inagaki in this volume) and successfully applied to understanding and designing molecules and reactions (Chapter “A Mechanistic Spectrum of Chemical Reactions” by Inagaki in this volume). Here, we describe a theory of the interaction of *three* orbitals, ϕ_a , ϕ_b , and ϕ_c , (Scheme 1b). The ϕ_a – ϕ_b – ϕ_c interactions include indirect interactions of mutually orthogonal orbitals, ϕ_h and ϕ_l of an atom, a bond, or a molecule at *higher* and *lower* energy levels, respectively, through a perturbing orbital of an external entity (Scheme 2).

The indirect interactions between ϕ_h and ϕ_l via ϕ_p were independently investigated by three groups at almost the same time (1974–1976). Inagaki and Fukui developed orbital mixing rules to understand diverse selectivities of organic reactions, especially π facial selectivities [1, 2]. Imamura and Hirano [3] derived rules of orbital mixing by electric charges as well as through the orbital overlapping to investigate catalytic activity. Libit and Hoffmann [4] disclosed the mechanism of the polarization of the π bond of propene. The orbital mixing rules will be described separately in Sect. 1.1 (through orbital overlapping) and in Sect. 1.2 (by electric charges).



Scheme 1a,b Interactions of two (a) and three (b) orbitals



Scheme 2 Indirect interactions between orthogonal orbitals, ϕ_h and ϕ_l , through a perturbing orbital ϕ_p

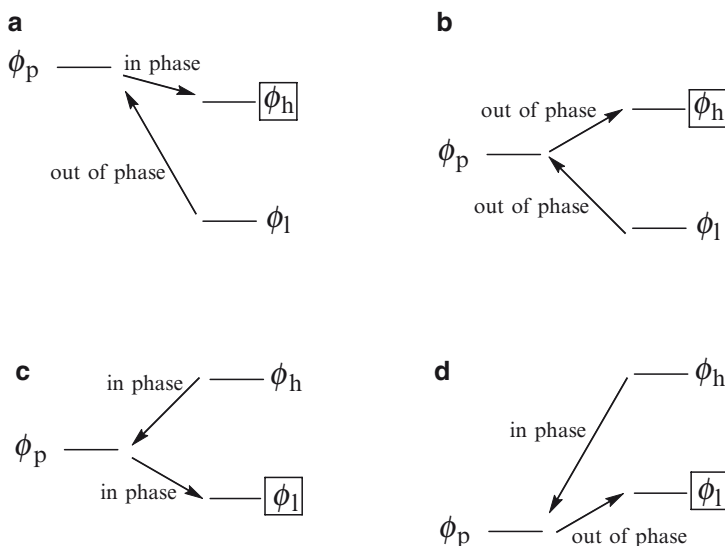
1.1 Overlap Mixing

1.1.1 Rules of Orbital Phase Relations

According to the theory of two-orbital interaction (Sect. 1.2 in the Chapter “Elements of a Chemical Orbital Theory” by Inagaki in this volume), an orbital has higher-lying orbitals mix in phase and lower-lying orbitals mix out of phase. An orbital ϕ_h has ϕ_p mix in phase when ϕ_p lies in energy above ϕ_h (Scheme 3a). It is important in the orbital mixing rules to determine the phase relation between ϕ_h and ϕ_l , which cannot interact directly with each other. A high-lying orbital ϕ_h has a low-lying orbital ϕ_l mix out of phase. The phase relation cannot be taken between ϕ_h and ϕ_l since they do not interact with each other, but between ϕ_l and ϕ_p (Scheme 3a). As a result, the phase relation between ϕ_h and ϕ_l is determined indirectly.

When ϕ_p lies below ϕ_h (Scheme 3b), the high-lying orbital ϕ_h has ϕ_p mix out of phase and a low-lying orbital ϕ_l mix out of phase with ϕ_p (Scheme 3b).

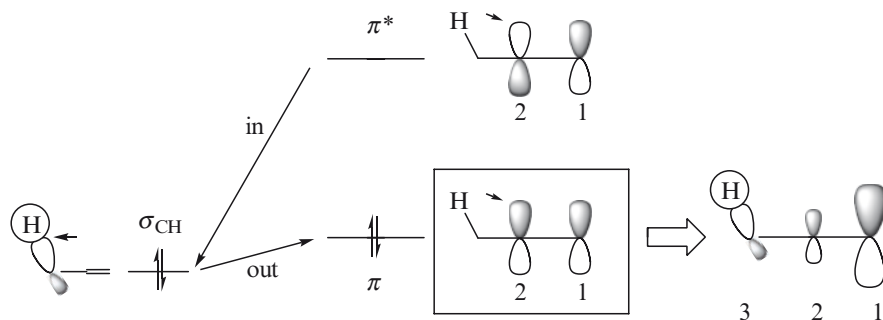
Scheme 3c, d illustrates the orbital phase relation when ϕ_l has ϕ_h mix. An orbital ϕ_l is in phase (out of phase) with ϕ_p at a higher (lower) energy level according to the theory of two-orbital interaction. The orbital ϕ_l has ϕ_h mix in phase with ϕ_p (Schemes 3c,d) because ϕ_l lies below ϕ_h .



Scheme 3 Orbital mixing rules

1.1.2 Orbital Polarization and Regioselectivities

Amplitudes of frontier orbitals are important for regioselectivities of organic reactions (Sect. 3.4 in the Chapter “Elements of a Chemical Orbital Theory” by Inagaki in this volume). Stabilization by the frontier orbital interaction is greatest when it occurs

Scheme 4 The Markovnikov rule**Scheme 5** Orbital polarization

between atoms with the largest amplitudes. Here, a simple application of the orbital mixing rule to regioselectivity is described by using a textbook example of reactions, electrophilic addition of HCl to propene (Scheme 4).

The π orbital amplitudes of ethene are identical on both carbons. Unsymmetrical substitutions polarize the π orbital. Electron acceptors or electrophiles attack the carbon with the larger π amplitude. The polarization of frontier orbitals is important for regioselectivities of reactions. Here, mechanism of the π orbital polarization of ethene by methyl substitution [4] is described (Scheme 5).

The π orbital of ethene mixes a σ_{CH} bonding orbital lying below out of phase, and the high-lying π^* orbital in phase with σ_{CH} (Scheme 5, cf. Scheme 3d). The in-phase and out-of-phase relations are placed where the strongest interactions occur, or between σ_{CH} and the p orbital on the closer carbon (C₂) in π and π^* . The phase relation between π and π^* is uniquely determined. The signs of p orbitals in π and π^* are the same on C₁ and opposite on C₂. The π amplitude increases on C₁ and decreases on C₂. It follows that the HOMO of propene has large amplitude on C₁.

The frontier orbital of an electrophilic reagent, HCl, is the LUMO or the antibonding orbital of the σ bond. The $1s$ orbital energy (-13.6 eV) of hydrogen atom is higher than the $3p$ orbital energy (-15.1 eV) of chlorine atom [5]. The main component of σ_{HCl}^* is $1s$ which mixes $3p_{\text{Cl}}$ out of phase.

The reaction first occurs between C₁ and H with the largest amplitudes of the frontier orbitals, in agreement with the Markovnikov rule.

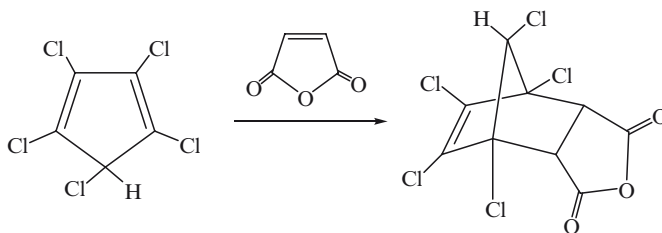
1.1.3 Orbital Deformation and π Facial Selectivities

The π conjugate molecules usually have planar geometries and no difference between the two faces above and below the molecular plane. When substitutions break the symmetry with respect to the plane, π orbitals mix σ orbitals orthogonal prior to the substitution. Rehybridization occurs and the unsaturated bonds have

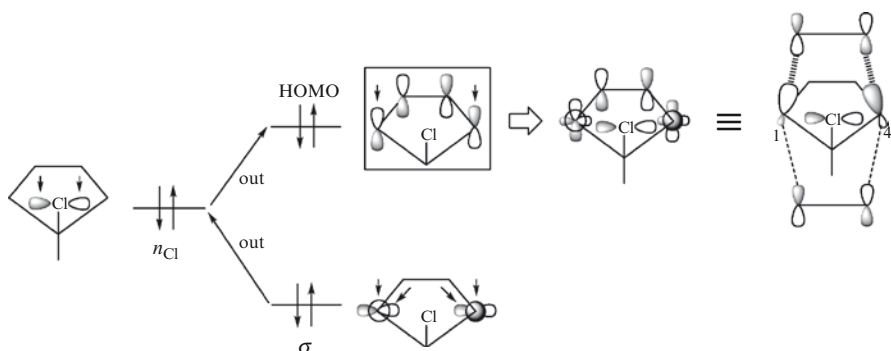
nonequivalent π orbital extensions on the two faces. There arises a question. Which face is more reactive? This is π facial selectivity. The selectivity can be controlled by the direction of the nonequivalent orbital extension [1, 2] determined by the σ - π orbital mixing through the interaction with the substituents. A simple example is shown below.

Williamson and his co-workers [6] demonstrated that Diels–Alder reactions occur preferentially on the sterically hindered face or *syn* to the 5-chlorine atom of 1,2,3,4,5-pentachlorocyclopentadiene to give the *anti*-cycloadduct (Scheme 6).

The HOMO of the diene is antisymmetric with respect to reflection in the plane containing the C_5 -Cl bond. Only a nonbonding orbital on Cl is allowed by symmetry to interact with HOMO. The HOMO mixes the low-lying nonbonding orbital n_{Cl} out of phase, and the low-lying σ orbital for the C–C bonds out of phase with n_{Cl} (Scheme 7, cf. Scheme 3b). The out-of-phase relations are placed between n_{Cl} and the *syn* lobes of p orbitals on C_1 and C_4 in π HOMO, and between n_{Cl} and the σ orbitals represented by the s and p orbital components. As a result, the phase relation between π HOMO and σ is uniquely determined. The signs of the p_π orbital lobes *syn* to Cl are the same as those of the p_σ orbital lobes inside the ring. The *syn* lobes rotate inward the ring. The *anti* lobes rotate outwards. The signs of the s orbitals



Scheme 6 π Facial selectivity



Scheme 7 Orbital deformation

are the same as those of the *syn* lobes. The mixing of the *s* orbitals extends the π HOMO on the *syn* side and contracts this orbital on the *anti* lobes. The inward rotations of the *p* orbitals on the *syn* face and the *syn* HOMO extensions both facilitate the overlapping with the LUMO of dienophiles on the *syn* face. The deformation of the HOMO of the 5-chlorocyclopentadiene favors the attack on the *syn* face by dienophiles.

1.2 Electrostatic Mixing

1.2.1 Rules of Orbital Phase Relations

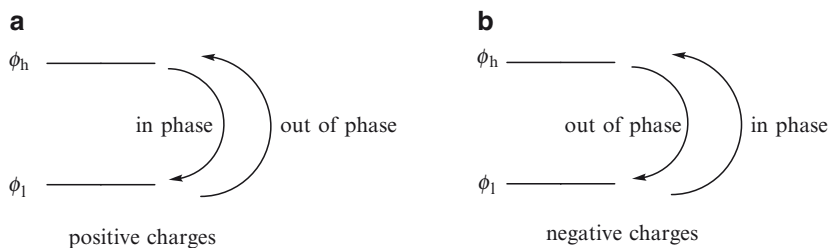
Orthogonal orbitals ϕ_h and ϕ_l are mixed with each other by nearby electric charges [3]. Electrostatic orbital mixing rules state:

1. Near a positive electric charge, a low-lying orbital ϕ_l has a high-lying orbital ϕ_h mix in phase; ϕ_h has ϕ_l mix out of phase (Scheme 8a)
2. Near a negative electric charge, ϕ_l has ϕ_h mix out of phase; ϕ_h has ϕ_l mix in phase (Scheme 8b)

The in-phase and out-of-phase relations mean the same and opposite signs of the atomic orbitals in ϕ_l and ϕ_h nearest to the charge.

Electric charges have another important effect on orbitals. Charges in the vicinity of molecules change the orbital energies:

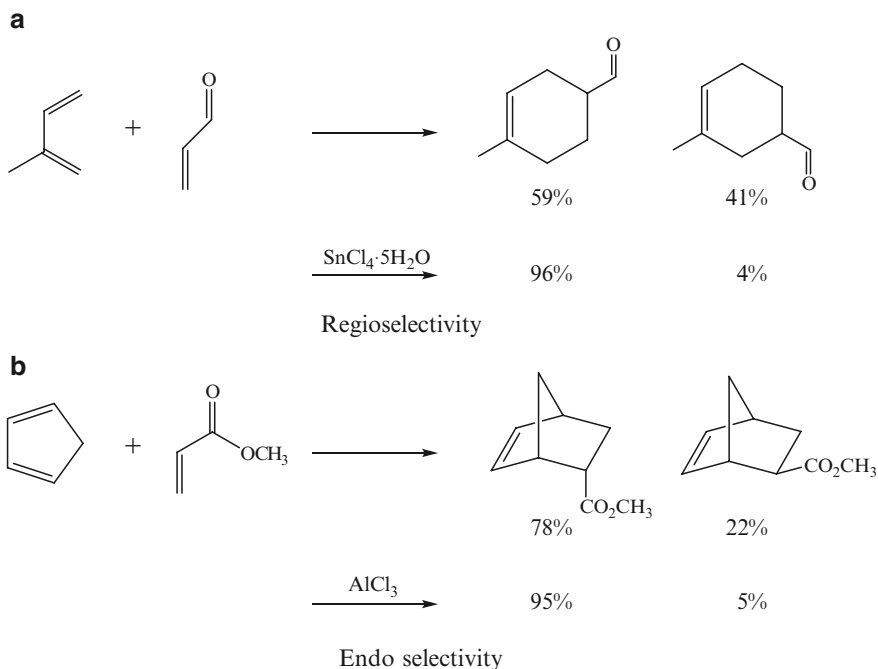
- *Orbital energies are lowered by positive charges and raised by negative charges*



Scheme 8 Orbital mixing by electric charges

1.2.2 Orbital Polarization and Selectivities

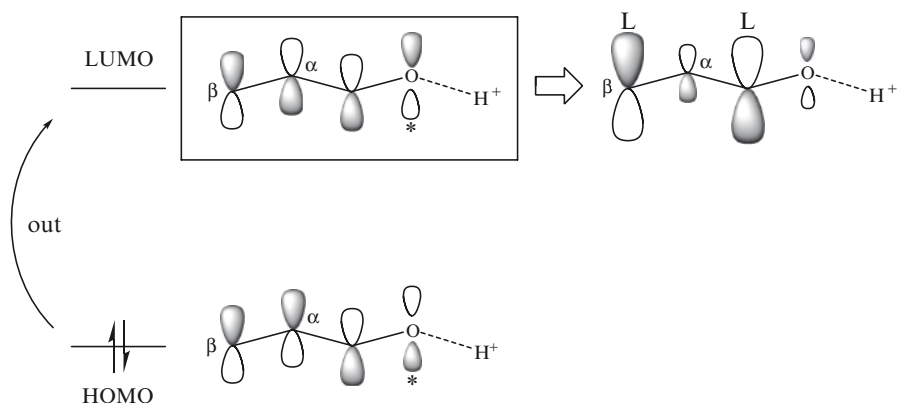
Regioselectivities [7] and *endo* selectivity [8, 9] increase upon Lewis acid catalysis of Diels–Alder reactions (Scheme 9). Houk and Strozier [10] found that protonation on the carbonyl oxygen of acrolein amplifies the LUMO at the terminal and



Scheme 9 Selectivities enhanced by Lewis acid catalysts

carbonyl carbons, in agreement with the enhanced regioselectivity and endo selectivity, respectively.

Imamura and Hirano [3] and Fujimoto and Hoffmann [11] explained the origin of the LUMO polarization in terms of orbital mixing by a positive charge (Scheme 10, cf. Scheme 8a). The LUMO has the HOMO mix by the positive charge of the proton on the carbonyl oxygen. According to the electrostatic orbital mixing rules, a high-lying orbital ϕ_n has a low-lying orbital ϕ_1 mix out of phase at the orbital on the atom nearest to the charge (Scheme 8a). The LUMO has the HOMO mix out of phase at the orbital (indicated by * in Scheme 10) on the carbonyl oxygen. The signs of the atomic orbital components in the LUMO and the HOMO are the same on the terminal β carbon and opposite on the α carbon. The LUMO is amplified on the β carbon. The amplitude relative to that on the α carbon is much larger on protonation. This can account for the regioselectivity enhanced by Lewis acid catalysts. The signs are also the same on the carbonyl carbon. The amplified LUMO on the carbonyl carbon promotes the secondary frontier orbital interaction (Sect. 3.6 in the Chapter “Elements of a Chemical Orbital Theory” by Inagaki in this volume) assisted by the orbital phase environments. This can account for the endo selectivity enhanced by Lewis acid catalysts.



Scheme 10 The LUMO polarization of acrolein on the protonation

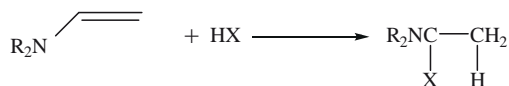
2 Applications to Regioselectivities

The amplitudes of frontier orbitals control regioselectivities of chemical reactions (Sect. 3.4 in the Chapter “Elements of a Chemical Orbital Theory” by Inagaki in this volume). π Orbitals are polarized by substituents. The orbital mixing rules can be applied not only to understanding why the regioselectivities change on the substitutions, but also to designing regioselective reactions as well as enhancing the regioselectivities.

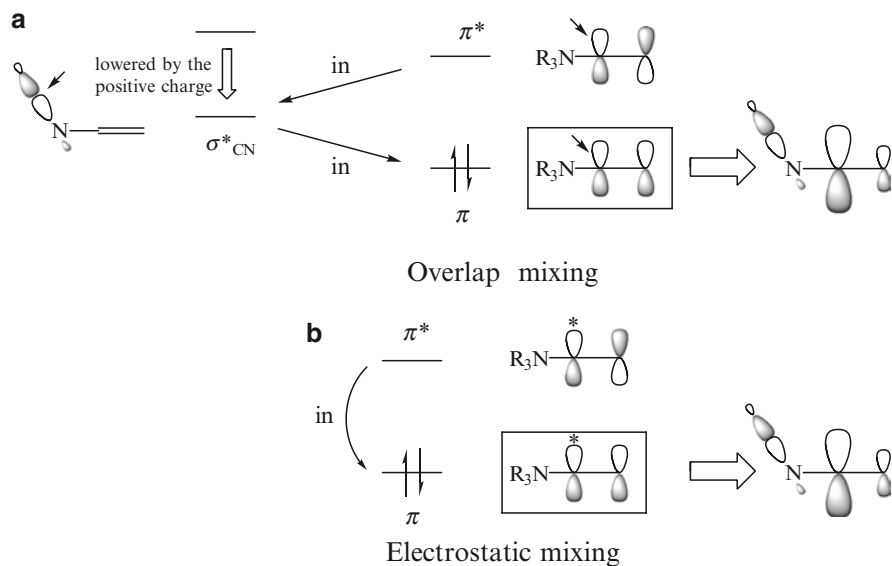
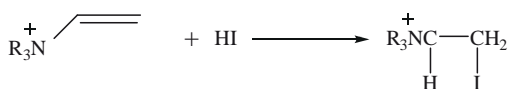
2.1 Electrophilic Additions

The π orbital polarization of ethene on the substitution with an electron donating (methyl) group has been described in Sect. 1.1.2 to show how to apply the orbital mixing rule to understanding the regioselectivity of electrophilic addition reactions of propene. A lone pair on a heteroatom plays the same role as a C–H bond in the methyl group in the π orbital polarization. Enamines have larger HOMO amplitude on the β carbon as propene and undergo electrophilic attacks on this carbon (Scheme 11). Replacement of the amino group by an ammonium group reverses the regioselectivity [12]. A proton attacks the α carbon closer to the positively charged ammonium group. Here, the orbital mixing rules are applied to understanding the reversed regioselectivity.

A positive charge lowers the energies of the bond orbitals in the ammonium group. The σ_{CN}^* orbital is low enough to perturb the π orbital. The π orbital has the high-lying σ_{CN}^* mix in phase, and the high-lying π^* orbital mix in phase with σ_{CN}^* (Scheme 12a, Scheme 3c). The in-phase relations are placed between σ_{CN}^* and the p orbital on the substituted carbon (C_α) in π and π^* indicated by the arrows. The



Scheme 11 Opposite regioselectivities of the electrophilic additions to enamines and their onium ions



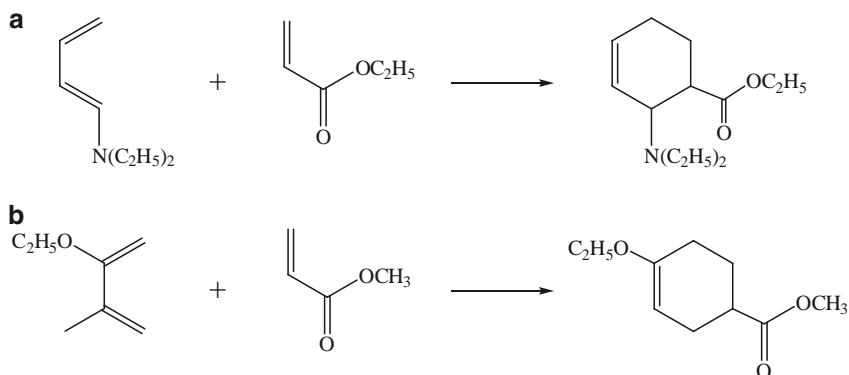
Scheme 12 The π polarization by the orbital mixing

phase relation between π and π^* uniquely determined shows that the signs of p orbitals in π and π^* are the same on C_α and opposite on C_β . The π amplitude increases on C_α and decreases on C_β . It follows that π has larger amplitude on C_α .

The electrostatic mixing by the positive charge polarizes π in the same direction (Scheme 12b, cf. Scheme 8a), possibly more significantly than the overlap mixing. The π orbital is the frontier orbital. The proton attacks on C_α . The regioselectivity is reversed.

2.2 Diels–Alder Reactions

1-Diethylaminobutadiene reacts with ethyl acrylate and exclusively gives 3,4-disubstituted cyclohexene product (Scheme 13a) [13, 14]. The reaction of 2-ethoxybutadiene with methyl acrylate gives exclusively 1,4-disubstituted cyclohexene (Scheme 13b) [13, 14].



Scheme 13 Regioselectivities of the Diels–Alder reactions

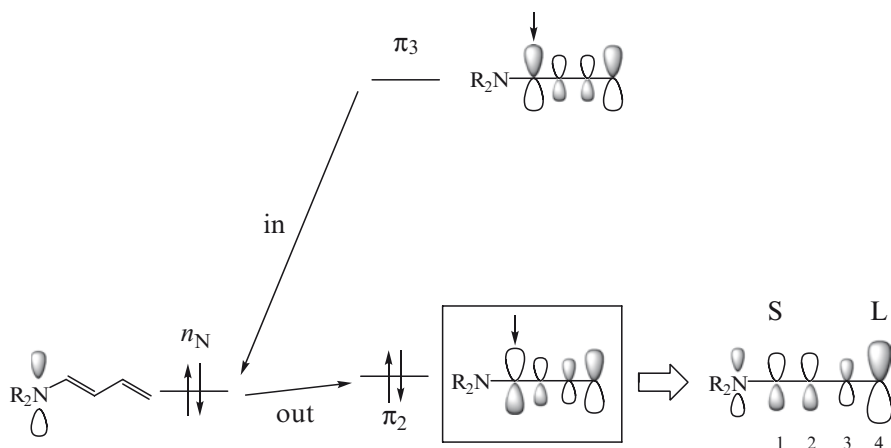
According to the frontier orbital theory, a bond preferentially forms between the atoms with the largest frontier orbital amplitudes (Sect. 3.4 in the Chapter “Elements of a Chemical Orbital Theory” by Inagaki in this volume). This is applicable for the regioselectivities of Diels–Alder reactions [15]. The orbital mixing rules are shown here to be useful to understand and design the regioselectivities.

2.2.1 Polarized HOMO of Substituted Butadienes

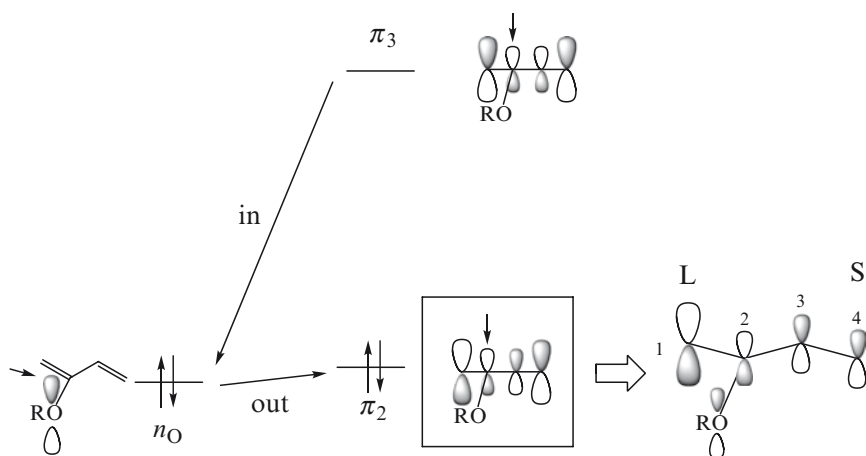
The orbital mixing rule is applied here to the polarization of the HOMO (π_2) of butadiene by the amino substituent on the 1-position (Scheme 14, cf. Scheme 3d). The π_2 orbital has the nonbonding orbital n_N mix out of phase and the high-lying LUMO (π_3) in phase with n_N . The phase relation between π_2 and π_3 shows that the π_2 amplitudes increase on C_4 and decrease on C_1 on the substitution with any electron donating groups at the 1-position. The π_2 orbital is polarized in the opposite direction by any electron donating groups at the 2-position (Scheme 15, cf. Scheme 3d). The amplitudes increase on C_1 and decrease on C_4 .

2.2.2 Polarized LUMO of Ethenes Substituted with a Conjugate Acceptor

The LUMO of alkenes with an electron accepting conjugate group, e.g., a C=O group, is an in-phase combination of π^* and π_{CO}^* according to the theory of two-orbital interaction (Sect. 1.2 in the Chapter “Elements of a Chemical Orbital Theory” by Inagaki in this volume). The π_{CO}^* orbital lies lower in energy than π^* . The main component of LUMO should be π_{CO}^* . This is in agreement neither with the regioselectivity of the Diels–Alder reactions across the C=C bonds nor with the calculated LUMO amplitude (1.2.2). An assumption to solve the problem is a reversal of π^* and π_{CO}^* energy levels in the conjugate system, which could be



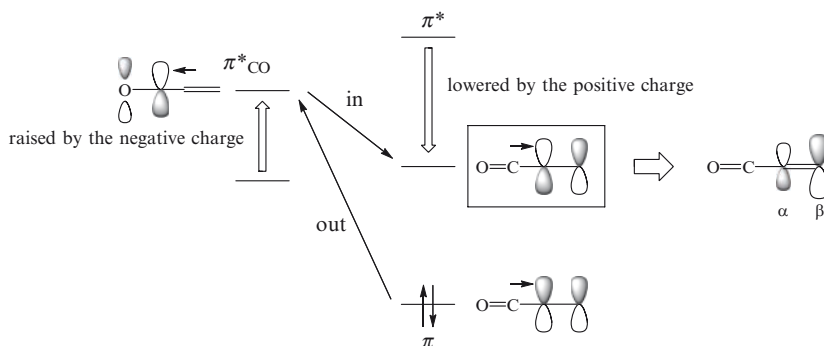
Scheme 14 The HOMO polarization of butadiene by the 1-amino group



Scheme 15 The HOMO polarization of butadiene by the 2-alkoxy group

caused by the electron delocalization from C=C to C=O. The resulting positive charge in the C=C moiety lowers the π^* energy and the negative charge in the C=O group raises the π^*_{CO} energy.

The orbital mixing rules are applied to the polarization of π^* of ethene by a C=O group on the assumption that π^* is lowered below π^*_{CO} . The π^* orbital has π^*_{CO} mix in phase and the low lying π orbital mix out of phase with π^*_{CO} (Scheme 16). As a result, the phase relation between π^* and π is fixed. The amplitude is larger on C $_{\beta}$ than on C $_{\alpha}$ and the carbonyl carbon.

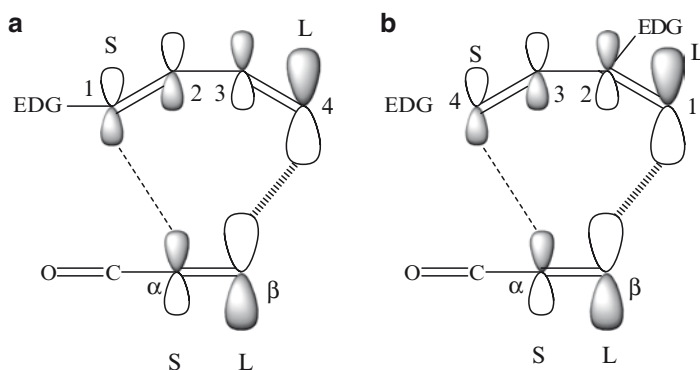


Scheme 16 The LUMO polarization of ethene by an electron accepting conjugate substituent

In fact, the bond model analysis [16–18] at the HF/6–31G* level shows that the π^* coefficient (0.64) is larger than the π^*_{CO} one (0.53) in the LUMO of acrolein. These results support the assumption of π^* being below π^*_{CO} in the conjugate systems.

2.2.3 Frontier Orbital Interactions Directing the Regioselectivities

Butadiene with electron donating group at the 1-position has the largest HOMO amplitude on C_4 (Scheme 14). Dienophiles with electron accepting conjugate groups have the largest LUMO amplitude on C_β (Scheme 16, cf. Scheme 3a). According to the frontier orbital theory, a bond preferentially forms between the atoms with the largest frontier orbital amplitudes (Sect. 3.4 in the Chapter “Elements of Chemical Orbital Theory” by Inagaki in this volume). A bond exclusively forms between C_4 of the dienes and C_β of the dienophiles (Scheme 17a). This is in agreement with the observation that a sole product of the reaction of 1-diethylaminobutadiene with ethyl acrylate is the 3,4-disubstituted cyclohexene (Scheme 13a) [13, 14].



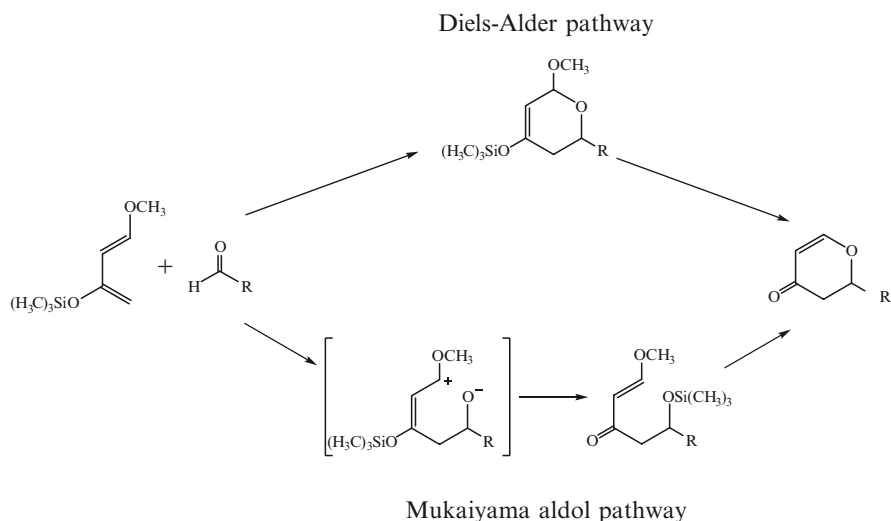
Scheme 17 The polarized frontier orbitals determine the regioselectivity

Butadiene with an electron donating group at the 2-position has the largest HOMO amplitude on C_1 (Scheme 15). A bond forms between C_1 of the dienes and C_β of the dienophiles (Scheme 17b). This is in agreement with the exclusive formation of 1,4-disubstituted cyclohexene in the reaction of 2-ethoxybutadiene with methyl acrylate (Scheme 13b) [13, 14].

2.2.4 Danishefsky's Dienes

Electron donating groups at the 1- and 2-positions of butadiene amplify the HOMO at the 4- and 1-positions, respectively, and direct the regioselectivities of Diels–Alder reactions as has been described above. Two or three electron donating groups at the 1- and 3-positions of butadiene cooperate to polarize the HOMO in the same direction. The HOMO polarization is greater. The HOMO energy is higher. Such 1,3-di(tri) substituted dienes are expected to react more regioselectively with higher reactivity.

Danishefsky's diene [19] is the 1,3-butadiene with a methoxy group at the 1-position and a trimethylsiloxy group at the 3-position (Scheme 18). This diene and Lewis acids extended the scope of hetero-Diels–Alder reactions with aldehydes [20]. This diene reacts with virtually any aldehyde in the presence of Lewis acids whereas dienes usually react with only selected aldehydes bearing strongly electron accepting α -substituents. There are two (Diels–Alder and Mukaiyama aldol) reaction pathways (Scheme 18) identified for the Lewis acids catalyzed reactions of Danishefsky diene with aldehydes [21, 22]. The two pathways suggest that these reactions occur on the boundary between the delocalization band (the pericyclic



Scheme 18 Two pathways of the reactions of Danishefsky's diene with aldehydes

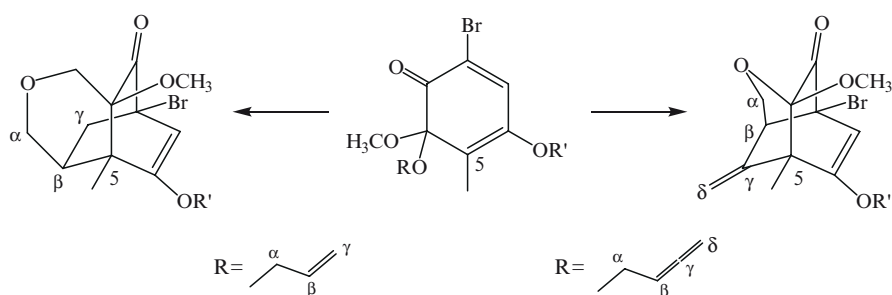
reaction) and the pseudoexcitation band (the aldol reaction). This can be understood in terms of the shift from the delocalization band to the pseudoexcitation band in the mechanistic spectrum of chemical reactions (Chapter “A Mechanistic Spectrum of Chemical Reactions” by Inagaki in this volume) by the enhancement of electron donating power of the diene by the two substituents and that of electron accepting power of the aldehydes by Lewis acid catalysts.

The chemistry of the hetero-Diels–Alder reactions is advancing as one of the most important chiral C–C bond-forming reactions [23].

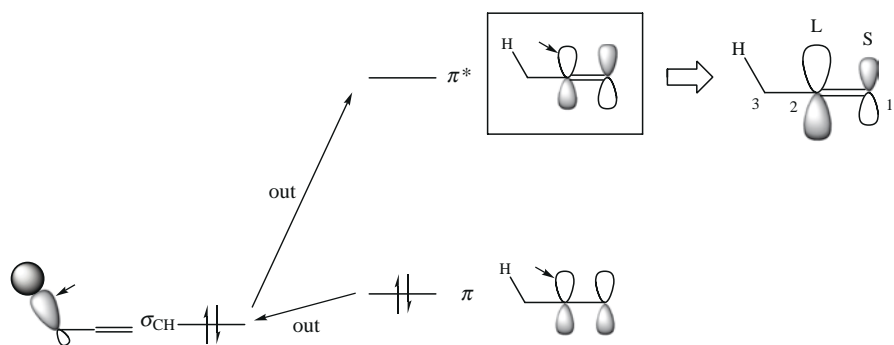
2.2.5 Regioselectivity Reversed by an Allenyl Group

Very recently, Cook and Danishefsky [24] reported an interesting regioselectivity of intramolecular Diels–Alder reactions reversed by the change in the dienophilic moieties from vinyl to allenyl group (Scheme 19). For R = 2-propenyl group, C_β is bonded to the methyl substituted carbon C₅ of the cyclohexadienone ring. For R = 2,3-butadienyl, C_γ is bonded to C₅.

This is understood in terms of the LUMO amplitudes of the dienophilic moieties. A model molecule is propene. The LUMO amplitude is larger on C₂ (Scheme 20, cf.



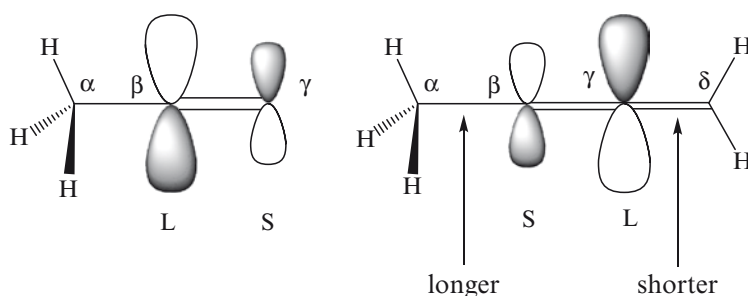
Scheme 19 Regioselectivity reversed by an Allenyl Group



Scheme 20 π* Orbital polarization of propene

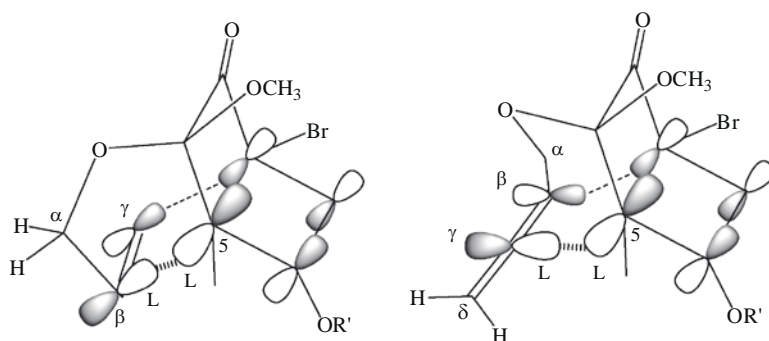
Scheme 3b). The π^* orbital of ethene has a low-lying σ_{CH} bonding orbital mix out of phase, and the low-lying π orbital mix out of phase with σ_{CH} . The relations are placed where the strongest interactions occur, or between σ_{CH} and the p orbital on the closer carbon (C_2) in π and π^* . The phase relation of π^* with π is uniquely determined. The signs of p orbitals in π and π^* are the same on C_2 and opposite on C_1 . The p^* amplitude increases on C_2 and decreases on C_1 . It follows that the LUMO of propene has large amplitude on C_2 .

The allyl ether has larger amplitude at C_β than C_γ (Scheme 21) as propene does at C_2 (Scheme 20). In the 2,3-butadienyl ether the $\text{C}_\beta = \text{C}_\gamma$ π bond is perturbed by the methylene $\text{C}_\delta\text{-H}$ bonds more strongly than by the $\text{C}_\alpha\text{-H}$ bonds because of the shorter distance and the coplanar π^* and σ of $\text{C}_\delta\text{-H}$. The 2,3-butadienyl ether has larger LUMO amplitude C_γ . As a result, the reactive sites are C_β in the allyl group and C_γ in the buta-2,3-dienyl group.



Scheme 21 The LUMO amplitudes of propene and 2,3-butadiene

The most reactive site of the diene part is C_5 of the cyclohexadienone ring with the alkoxy group. This corresponds to C_1 of 2-alkoxybutadiene (Scheme 15), which has the largest HOMO amplitude. The preferable frontier orbital interactions (Scheme 22) are in agreement with the reversed regioselectivities.

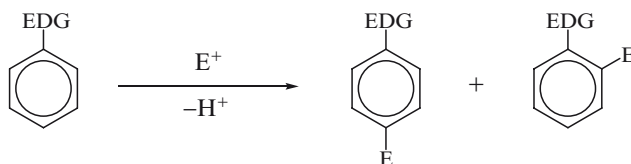


Scheme 22 Preferable frontier orbital interactions reversing the regioselectivities

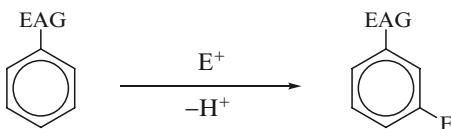
2.3 Electrophilic Aromatic Substitutions

The frontier orbital theory was developed for electrophilic aromatic substitution (Chapter “Elements of a Chemical Orbital Theory” by Inagaki in this volume). Application is successful to the ortho-para orientation (Scheme 23a) for the benzenes substituted with electron donating groups. The ortho and para positions have larger HOMO amplitudes. The meta orientation (Scheme 23b) for the electron accepting groups is under control of both HOMO and the next HOMO [25].

a ortho - para



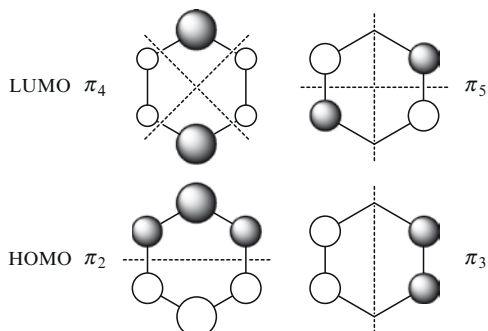
b meta



Scheme 23 Orientation of electrophilic aromatic substitutions

2.3.1 Frontier Orbitals of Benzene

The lowest π_1 orbital of benzene has no nodal plane except for the molecular plane. The HOMOs are degenerate (π_2 and π_3 in Scheme 24). Each has a nodal plane. The LUMOs are also degenerate with two nodal planes (π_4 and π_5). The highest π_6 orbital of benzene has three nodal planes.

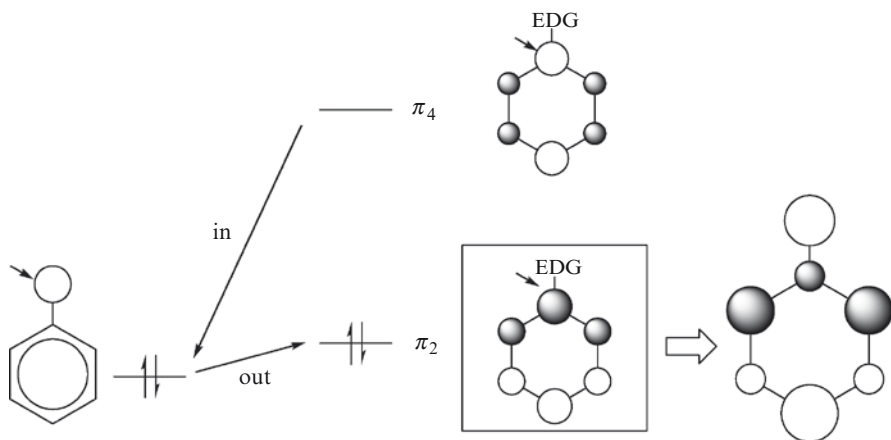


Scheme 24 Degenerate HOMOs and LUMOs of benzene

2.3.2 Orbital Mixing in Benzenes Substituted with an Electron Donating Group

In monosubstituted benzenes there are conventionally supposed to be the substituent on the carbon with the largest amplitude of π_2 and π_4 and with the node of π_3 and π_5 , in order to simplify the following arguments. The substitution does not perturb π_3 and π_5 but does perturb π_2 and π_4 .

When the substituent is an electron donating group, the π_2 energy is raised by the interaction with the substituent orbitals whereas the π_3 energy does not change much. The polarization of π_2 is interesting here for the orientation of electrophilic aromatic substitution. The π_2 orbital has the substituent orbital mix out of phase (Scheme 25) and is destabilized. This is the HOMO to the first approximation. At this stage of the orbital mixing we see the preference for the para selectivity. The meta and ortho positions are not distinguished from each other because π_2 has the same amplitudes at these positions. A difference is made by mixing-in of π_4 . According to the mixing rules (Sect. 1.1.1), π_2 has the high-lying π_4 orbital mix in phase between the p orbital on the ipso position of π_4 and the substituent orbital (Scheme 25, cf. Scheme 3d). The phase relation between π_2 and π_4 is uniquely determined. The signs of the p orbitals on the ortho positions in π_2 is the same as those in π_4 . The HOMO of the benzenes substituted with an electron donating group is amplified at the ortho positions. The HOMO extension is greater than that at the meta positions.



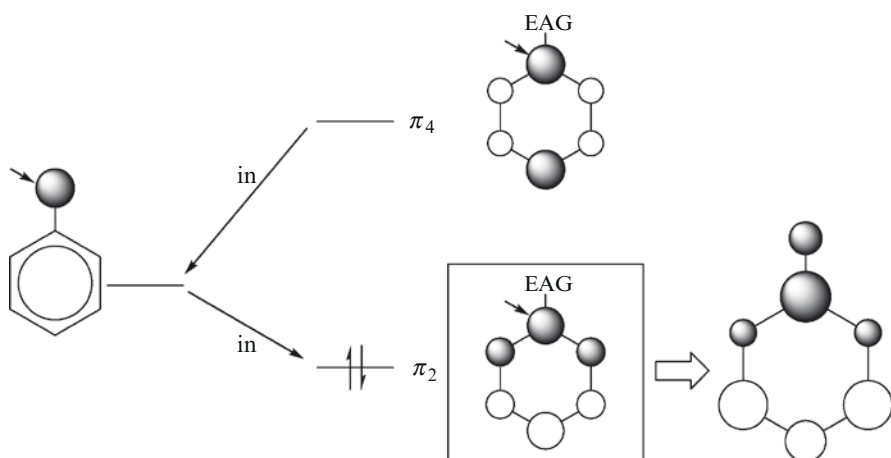
Scheme 25 The polarized HOMO of benzenes with an electron donating substituent

2.3.3 Orbital Mixing in Benzenes Substituted with an Electron Accepting Group

When the substituent is an electron-accepting group, the substituent LUMO is important. The π_2 orbital has the substituent orbital mix in phase and is stabilized. The π_3 energy remains unchanged with the substitution. The HOMO is π_3 , which has the

same amplitudes at the ortho and meta positions. At this stage of the orbital mixing we see no preference for the meta orientation but do for the ortho, meta orientation.

A difference between the meta and para positions is made in the next HOMO or NHOMO by the mixing of π_4 into π_2 . According to the mixing rules, the high-lying π_4 orbital mixes into π_2 in phase with the substituent orbital (Scheme 26, cf. Scheme 3c). The phase relation between π_2 and π_4 is uniquely determined. The signs of the p orbitals on the meta position in π_2 are the same as those in π_4 , whereas those on the ortho positions are opposite to each other. The π_2 orbital of the benzenes substituted with electron-accepting group is amplified at the meta positions. The amplitudes are reduced at the ortho positions. The meta selectivity of electrophilic aromatic substitution is controlled not only by the HOMO but also by the next HOMO [25].



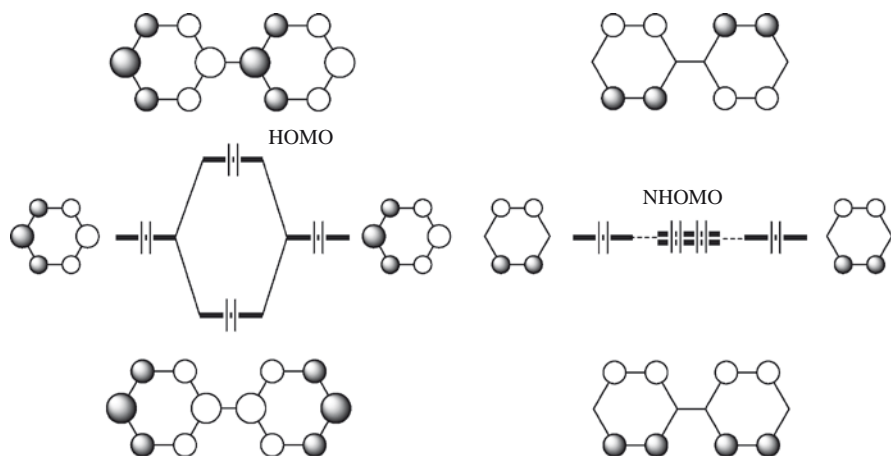
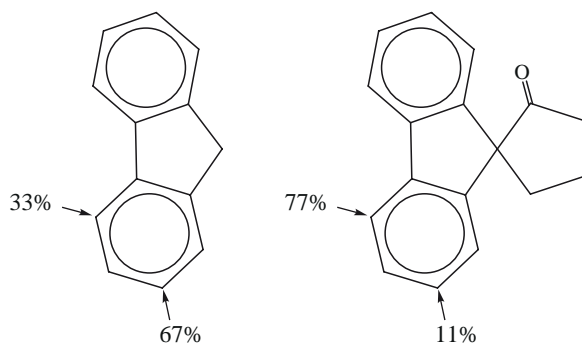
Scheme 26 Next HOMO (NHOMO) polarization of benzenes with an electron accepting group

2.3.4 Regioselectivity of Nitration of Fluorene and Its Reversal by a Spiro Conjugation

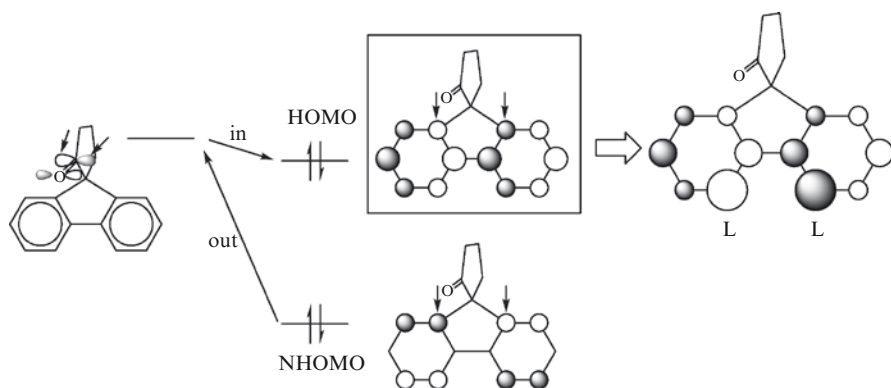
Fluorene undergoes nitrations at the 2-position (67%) and at the 4-position (33%) [26] (Scheme 27). The HOMO of fluorene (Scheme 28) is an out-of-phase combination of the HOMOs (π_2) of benzene (Scheme 24) and lies higher in energy than π_2 . The π_3 orbital of benzene has no amplitude on the carbon bonded to the other phenyl group. The π_3 - π_3 interaction does not occur (Scheme 28). The orbital energy remains unchanged. Neither of the combinations of π_3 can be the HOMO of fluorene. As a result, fluorene has the largest HOMO amplitude at the 2-position in agreement with the regioselectivity [27].

Ohwada and Shudo [26] showed that the regioselectivity of the nitrations was reversed by a remote carbonyl group (Scheme 27). The 4-position is more reactive than the 2-position. The reversed selectivity is explained by the orbital mixing rules. The orbitals closest in energy to the HOMO are the next HOMO (NHOMO), i.e.,

Scheme 27 Reversal of the regioselectivity of nitration by a spiro carbonyl group



Scheme 28 The HOMO and the next HOMO (NHOMO) of fluorene



Scheme 29 The polarized HOMO of fluorene with a spiro carbonyl group

the combined π_3 orbitals. The HOMO has the high-lying π_{CO}^* orbital mix in phase and the NHOMO mix out of phase with π_{CO}^* (Scheme 29, cf. Scheme 3a) [26]. The mixing of NHOMO into HOMO amplifies the HOMO at the 4-position.

3 Applications to π Facial Selectivities

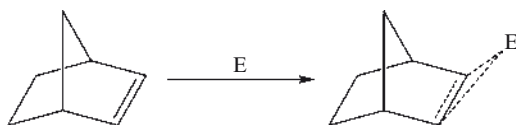
The orbital mixing theory was developed by Inagaki and Fukui [1] to predict the direction of nonequivalent orbital extension of plane-asymmetric olefins and to understand the π facial selectivity. The orbital mixing rules were successfully applied to understand diverse chemical phenomena [2] and to design π facial selective Diels–Alder reactions [28–34]. The applications to the π facial selectivities of Diels–Alder reactions are reviewed by Ishida and Inagaki elsewhere in this volume. Ohwada [26, 27, 35, 36] proposed that the orbital phase relation between the reaction sites and the groups in their environment could control the π facial selectivities and review the orbital phase environments and the selectivities elsewhere in this volume. Here, we review applications of the orbital mixing rules to the π facial selectivities of reactions other than the Diels–Alder reactions.

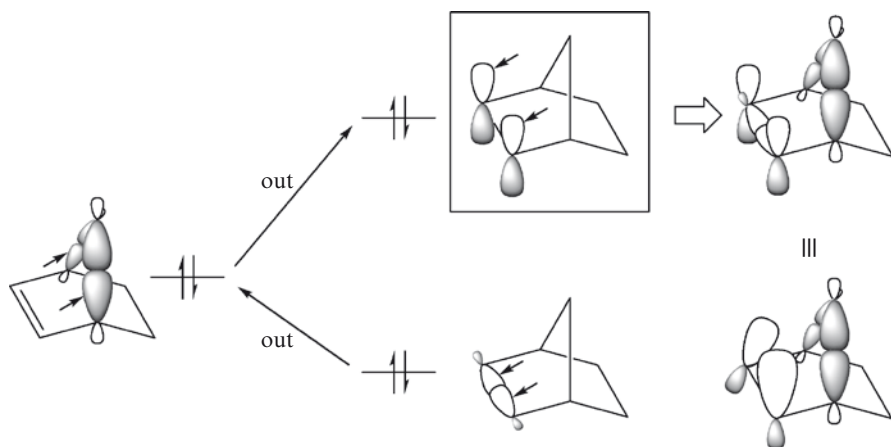
3.1 Norbornenes

Electrophiles are well known to attack the *exo* face of norbornenes (Scheme 30). The π orbital of norbornene extends more in the *exo* direction [1]. According to the orbital mixing rules, the π orbital has the low-lying σ orbital of the methano-bridge mix out of phase and the low-lying σ orbital between the doubly bonded carbons mix out of phase with the methano-bridge orbital (Scheme 31, cf. Scheme 3b). The rehybridization occurs on the unsaturated carbons. The phase relation shows how the π orbital deforms. The mixing of the *s* orbital components extends the *exo* lobes of the p_π orbitals. The p_σ mixing disrotates the p_π axes to make greater overlapping between the p_π orbitals in the *exo* face.

The nonequivalent π orbital extension or the higher electron density in the *exo* face pyramidizes the unsaturated carbons $C_{2(3)}$. The $C_{2(3)}$ –H bonds are bent in the *endo* face. The *endo* pyramidization results in the high *exo* reactivity and, in fact, this pyramidization was confirmed by Wipff and Morokuma [37]. The orbital distortion also implies large negative electrostatic potential in the *exo* face. Very recently, Abbasoglu and Yilmaz [38] calculated a derivative of norbornene, i.e., *endo* tricyclo[3.2.1.0^{2,4}] oct-6-ene and confirmed the *exo* extension of the HOMO accompanied by the *endo* pyramidization, the large negative electrostatic potential on the *exo* face, and the preferential *exo* addition of Br_2 .

Scheme 30 Electrophilic *exo* addition to norbornene





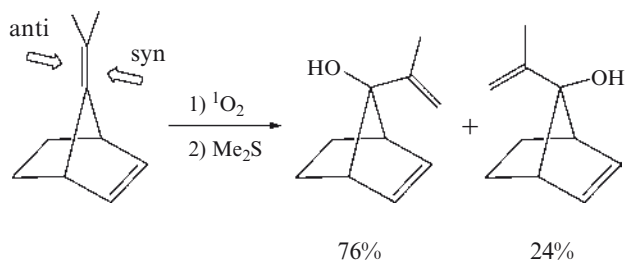
Scheme 31 Nonequivalent *exo* extension of π orbital of norbornene

The *exo* face selectivities are still recent topics of electrocyclic reactions [39] and transition metal catalyzed reactions [40–47].

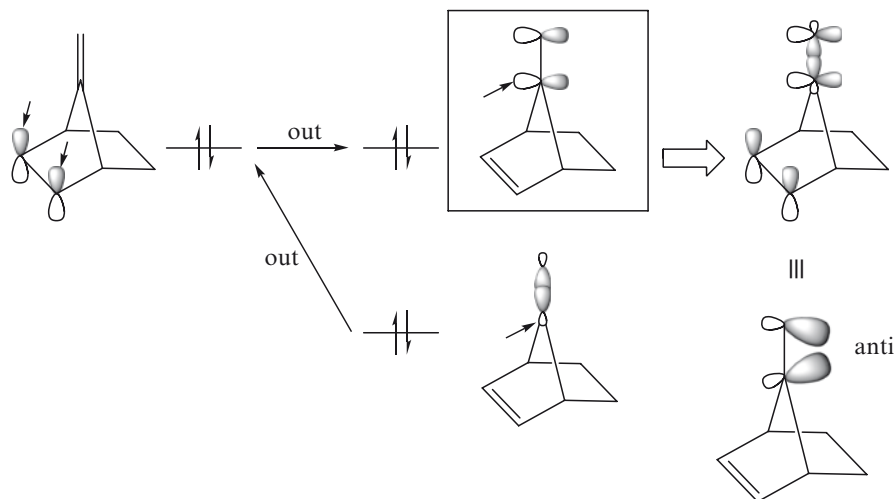
3.2 7-Alkylidenenorbornenes

Okada and Mukai [48] showed a preference for a contrastreric approach of singlet oxygen to *anti* face of 7-isopropylidene double bond in photooxidation of 7-isopropylidenenorbornene followed by reduction with dimethyl sulfide (Scheme 32). They explained the stereoselectivity by applying the orbital mixing rules (Scheme 33). The π orbital of the exocyclic double bond enlarges its extension in the *anti* face.

The HOMO is an out-of-phase combination of the π orbitals of the *exo*- and endocyclic double bonds. According to the orbital mixing rules, the π orbital of the exocyclic double bond has the low-lying exocyclic σ orbital out of phase with the



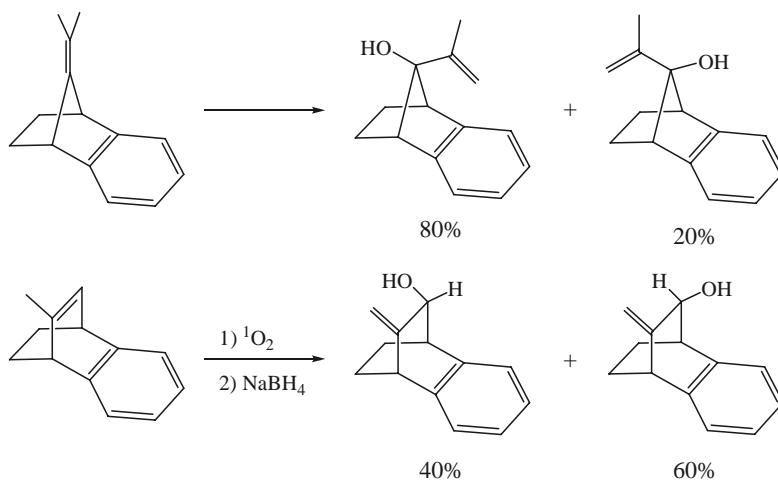
Scheme 32 Contrastreric photooxidations



Scheme 33 Non-equivalent *anti* extension of π orbital of 7-alkyldenenorbornene

endocyclic π orbital. The phase relation is placed between the *exo* lobes of the π orbital and the back lobe of the σ orbital (Scheme 33, cf. Scheme 3b). The rehybridization deforms the π orbital. The mixing of the *s* orbital component extends the *anti* lobes of the p_π orbitals. The p_σ mixing disrotates the p_π axes to make greater overlapping between the p_π orbitals in the *anti* face.

7-Isopropylidenebenzenorbornene is similarly attacked by singlet oxygen predominantly from the *anti* direction (Scheme 34) [49]. This is the case with a substrate



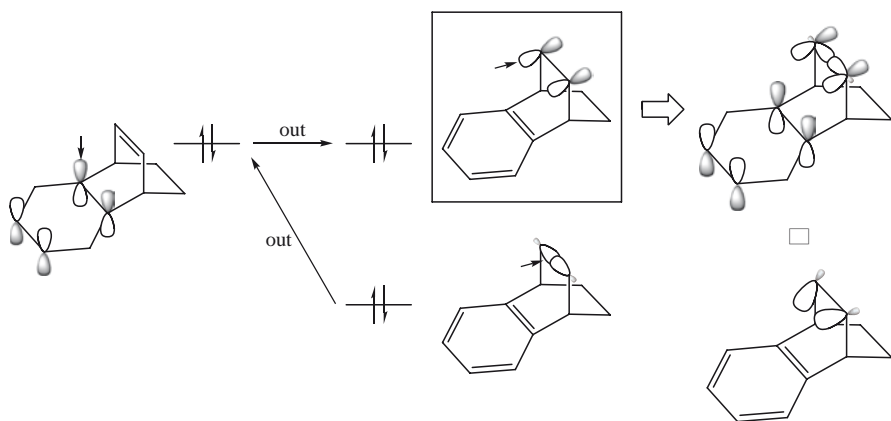
Scheme 34 Opposite π facial selectivities of the photooxidations of the 7-methylenenorbornene and bicyclo[2.2.2]octadiene derivatives

with electron donating methoxy groups on the benzene rings. Perfluorination and perchlorination on the benzene rings reverse the stereoselectivity. This is understood in terms of the π orbital energy of the benzene ring. The perhalogenations lower the π orbital energy too much to perturb and deform the alkylidene π orbital. Singlet oxygens attack the less hindered or *syn* face.

3.3 Benzobicylo[2.2.2]octadienes

2-Methylbenzobicylo[2.2.2]octadiene showed a slight preference for *syn* attack of singlet oxygen [50] in contrast to the *anti* attack on 7-isopropylidenebenzonorbornene (Scheme 34) [49].

According to the orbital mixing rules, the π orbital on the etheno-bridge has the HOMO of the benzene ring mix out of phase and the low-lying σ orbital on the etheno-bridge mix out of phase with the HOMO of the benzene ring. The out-of-phase relation is placed with the front lobe of the σ orbital (Scheme 35, cf. Scheme 3b). The rehybridization deforms the π orbital. The mixing of the *s* orbital components extends the *syn* lobes of the p_π orbitals. The p_σ mixing disrotates the p_π axes to make the overlapping greater between the p_π orbitals in the *syn* face and and to accumulate the electron density in the *syn* face. The orbital mixing increases the reactivity of the *syn* face.



Scheme 35 Nonequivalent *syn* extension of π orbital of benzobicylo[2.2.2]octadiene

3.4 Cyclohexanones

Fukui [51] predicted the deformation of the LUMO of cyclohexanone by the orbital mixing rule [1, 2] and explained the origin of the π facial selectivity of the reduction of cyclohexanone. Tomoda and Senju [52] calculated the LUMO densities on the

axial and equatorial faces outside the repulsive molecular face of cyclohexanones and showed a correlation with the π facial selectivity of hydride reduction. The LUMO distortion was analyzed and explained by the orbital mixing rule.

4 Recent Related Topics

The orbital mixing rules and their chemical consequences have been ongoing for more than 30 years and have provided impact on the studies of molecular properties and chemical reactions [53–56].

Yamabe and Minato [57] applied the orbital mixing rule to explain a stepwise reaction path of acid-catalyzed Diels–Alder reactions between butadiene and acrolein through one C–C bond formation followed by ring closure with a C–O bond formation and subsequent [3,3] sigmatropic rearrangement. They also applied the orbital mixing rules to a diradical process of the reaction of benzyne with trophione [58]. Among recent studies related to the orbital mixing rules include *syn* π face and *endo* selective Diels–Alder reactions of 3,4-di-*tert*-butylthiophene 1-oxide [59] and reversible S₂O-forming retro-Diels–Alder reaction [60] by Nakayama et al., stereoselectivity control by oxaspiro rings during Diels–Alder cycloadditions to cross-conjugated cyclohexadienones by Ohkata et al. [61], mechanism and stereoselectivity of Nazarov reactions of polycyclic dienones by West et al. [62, 63], an adiabatic cycloreversion and a $[2\pi_a + 2\pi_a + 2\sigma_s]$ rearrangement in a triplet state of the biplanophane system, the photoisomer of a 2,11-diaza[3,3](9.10)anthracenoparacyclophane by Kimura et al. [64], the stereochemistry of electrophilic addition reactions, bromination to bisbenzotetracyclo[6.2.2.^{3.6}0^{2.7}]tetradeca-4,9,11,13-tetraene [65], chlorination [66] and bromination [67] to *endo,endo*-tetracyclo[4.2.1.1.^{3.6}0^{2.7}]dodeca-4,9-diene, and bromination to tetracyclo[5.3.0.0.^{2.6}0^{3.10}]deca-4,8-tetraene [68] by Abbasoglu and coworkers, phosphine-Pd interaction and trans influence in the transition metal complexes by Yamanaka et al. [69, 70], Ru- and Rh-catalyzed C–C bond cleavage of cyclobutenones and reconstructive and selective synthesis of 2-pyranones, cyclopentenes, and cyclohexenones by Kondo and Mistudo [71].

Acknowledgements The author thanks Prof. Hisashi Yamamoto of the University of Chicago for his reading of the manuscript and his encouragements, Messrs. Hiroki Murai and Hiroki Shimakawa for their assistance in preparing the manuscript, and Ms. Jane Clarkin for the English suggestions.

References

1. Inagaki S, Fukui K (1974) *Chem Lett* 3:509
2. Inagaki S, Fujimoto H, Fukui K (1976) *J Am Chem Soc* 98:4054
3. Imamura A, Hirano T (1975) *J Am Chem Soc* 97:4192

4. Libit L, Hoffmann R (1974) *J Am Chem Soc* 96:1370
5. Pritchard HO, Skinner HA (1955) *Chem Rev* 55:745
6. Williamson KL, Li Hsu Y-F (1970) *J Am Chem Soc* 92:7385
7. Lutz EF, Bailey GM (1964) *J Am Chem Soc* 86:3899
8. Inukai T, Kojima T (1966) *J Org Chem* 31:2032
9. Sauer J, Kredel J (1966) *Tetrahedron Lett* 731
10. Houk KN, Strozier RW (1973) *J Am Chem Soc* 95:4094
11. Fujimoto H, Hoffmann R (1974) *J Phys Chem* 78:1874
12. Pine SH (1987) *Organic chemistry*, 5th edn. McGraw-Hill, New York, p 522
13. Titov JA (1962) *Russ Chem Rev* 31:267
14. Sauer J (1967) *Angew Chem Int Ed Engl* 6:16
15. Epiotis ND (1973) *J Am Chem Soc* 95:5624
16. Inagaki S, Goto N, Yoshikawa K (1991) *J Am Chem Soc* 113:7144
17. Iwase K, Inagaki S (1996) *Bull Chem Soc Jpn* 69:2681
18. Ikeda H, Inagaki S (2001) *J Phys Chem A* 105:10711
19. Danishefsky S, Kitahara T (1974) *J Am Chem Soc* 96:7807
20. Danishefsky S, Kerwin JF Jr, Kobayashi S (1982) *J Am Chem Soc* 104:358
21. Larson ER, Danishefsky S (1982) *J Am Chem Soc* 104:6458
22. Danishefsky S, Larson ER, Askin D, Kato N (1982) *J Am Chem Soc* 107:1246
23. Lin L, Liu X, Feng X (2007) *Synlett* 2147
24. Cook SP, Danishefsky SJ (2006) *Org Lett* 8:5693
25. Hirao H, Ohwada T (2003) *J Phys Chem A* 107:2875
26. Ohwada T, Shudo K (1991) *Chem Pharm Bull* 39:2176
27. Ohwada T (1992) *J Am Chem Soc* 114:8818
28. Ishida M, Beniya Y, Inagaki S, Kato S (1990) *J Am Chem Soc* 112:8980
29. Ishida M, Aoyama T, Beniya Y, Yamabe S, Kato S, Inagaki S (1993) *Bull Chem Soc Jpn* 66:3493
30. Ishida M, Kobayashi H, Tomohiro S, Wasada H, Inagaki S (1998) *Chem Lett* 27:41
31. Ishida M, Kobayashi H, Tomohiro S, Inagaki S (2000) *J Chem Soc Perkin Trans* 2:1625
32. Ishida M, Sakamoto M, Hattori H, Shimizu M, Inagaki S (2001) *Tetrahedron Lett* 42:3471
33. Ishida M, Hirasawa S, Inagaki S (2003) *Tetrahedron Lett* 44:2178
34. Ishida M, Itakura M, Tashiro H (2008) *Tetrahedron Lett* 49:1804
35. Ohwada T, Okamoto I, Haga N, Shudo K (1994) *J Org Chem* 59:3975
36. Ohwada T, Uchiyama M, Tsuji M, Okamoto I, Shudo K (1996) *Chem Pharm Bull* 44:296
37. Wipff G, Morokuma K (1980) *Tetrahedron Lett* 21:4445
38. Abbasoglu R, Yilmaz SS (2006) *J Mol Model* 12:290
39. Benson CL, West FG (2007) *Org Lett* 9:2545
40. Mitsudo T, Naruse H, Kondo T, Ozaki Y, Watanabe Y (1994) *Angew Chem Int Ed Engl* 33:580
41. Kondo T, Uenoyama S, Fujita K, Mitsudo T (1999) *J Am Chem Soc* 121:482
42. Kondo T, Mitsudo T (2005) *Chem Lett* 34:1462
43. Matsushima Y, Kikuchi H, Uno M, Takahashi S (1999) *Bull Chem Soc Jpn* 72:2475
44. Nakao Y, Yada A, Satoh J, Ebata S, Oda S, Hiyama T (2006) *Chem. Lett* 35:790
45. Nishihara Y, Inoue Y, Nakayama Y, Shiono T, Takagi K (2006) *Macromolecules* 39:9872
46. Nishihara Y, Inoue Y, Izawa S, Miyasaka M, Tanemura K, Nakajima K, Takagi K (2006) *Tetrahedron* 62:9872
47. Cossu S, Peluso P, Alberico E, Marchetti M (2006) *Tetrahedron Lett* 47:2569
48. Okada K, Mukai T (1978) *J Am Chem Soc* 100:6509
49. Paquette L, Hertel LW, Gleiter R, Boehm M (1978) *J Am Chem Soc* 100:6510
50. Paquette L, Bellamy F, Wells GJ, Boehm MC, Gleiter R (1981) *J Am Chem Soc* 103:7122
51. Fukui K (1975) *Theory of orientation and stereoselection*. Springer, Berlin Heidelberg New York
52. Tomoda S, Senju T (1997) *Tetrahedron* 53:9057
53. Dannenberg JJ (1999) *Chem Rev* 99:1225
54. Ohwada (1999) *Chem Rev* 99:1337

55. Mehta G, Chandrasekhar J (1999) *Chem Rev* 99:1437
56. Mehta G, Uma R (2000) *Acc Chem Res* 33:278
57. Yamabe S, Minato T (2000) *J Org Chem* 65:1830
58. Yamabe S, Minato T, Ishikawa A, Irinamihara O, Machiguchi (2007) *J Org Chem* 72:2832
59. Takayama J, Sugihara J, Takayanagi T, Nakayama J (2005) *Tetrahedron Lett* 46:4165
60. Nakayama J, Aoki S, Takayama J, Sakamoto A, Sugihara Y, Ishii A (2004) *J Am Chem Soc* 126:9085
61. Ohkata K, Tamura Y, Shetuni BB, Takagi R, Miyanaga W, Kojima S, Paquette LA (2004) *J Am Chem Soc* 126:16783
62. White TD, West FG (2005) *Tetrahedron Lett* 46:5629
63. Mazzola RD, White TD, Vollmer-Snarr HR, West FG (2005) *Org Lett* 7:2799
64. Okamoto H, Yamaji M, Satake K, Tobita S, Kimura M (2004) *J Org Chem* 69:7860
65. Abbasoglu R (2007) *J. Mol Model* 13:1215
66. Abbasoglu R, Uygur Y (2007) *Ind J Chem A* 46:396
67. Abbasoglu R (2007) *J Mol Model* 13:425
68. Abbasoglu R (2006) *J. Mol Model* 12:991
69. Yamanaka M, Shiga A (2005) *J Theor Comp Chem* 4:345
70. Yamanaka M, Mikami K (2005) *Organometallics* 24:4579
71. Kondo T, Taguchi Y, Kaneko Y, Niimi M, Mitsudo TA (2004) *Angew Chem Int Ed* 43:5369

An Orbital Phase Theory

Satoshi Inagaki

Abstract Cyclic orbital interactions are contained in non-cyclic conjugation as well as cyclic conjugation. For effective interactions, the orbitals are required to meet simultaneously the phase continuity conditions: (1) out of phase relation between electron-donating orbitals; (2) in phase relation between electron-accepting orbitals and between electron-donating and -accepting orbitals. The orbital phase theory is applicable to diverse chemical phenomena of non-cyclic conjugate systems, e.g., relative stabilities of non-cyclic isomers, and selectivities of the reactions through non-cyclic transition structures. The orbital phase theory also includes the rules for cyclic systems, i.e., the Woodward–Hoffmann rule for stereoselection of organic reactions and the Hückel $4n + 2\pi$ electron rule for aromatic molecules. Derivation and applications of the orbital phase theory are reviewed.

Keywords Chemical orbital theory, *Cis*-stability, Cyclic conjugation, Disposition isomers, Diradicals, Donor-acceptor, Electron delocalization, Geminal bond participation, Inorganic heterocycles, Ring strain, Orbital phase, Orbital phase continuity, Polarization, Preferential branching, Reactivity, Selectivity, Stability, Tautomerism, *Z*-selectivity

Contents

1	Introduction.....	84
2	A Theory	85
2.1	Non-Cyclic Conjugation.....	85
2.2	Cyclic Conjugation	94
3	Applications to Non-Cyclic Conjugation.....	98
3.1	Stability and Number of Electrons.....	99
3.2	Regioselectivities of Electrophilic Additions	99
3.3	Electrophilic Aromatic Substitutions.....	100

S. Inagaki
Department of Chemistry, Faculty of Engineering, Gifu University, Yanagido,
Gifu, 501-1193, Japan
e-mail: inagaki@gifu-u.ac.jp

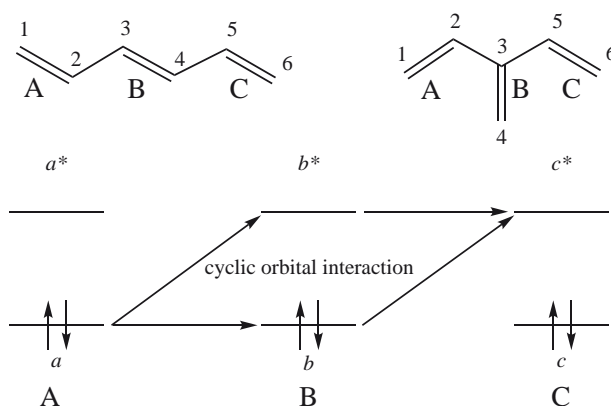
orbital interactions are controlled by orbital phase properties. The phase is required for effective interactions to be continuous. The continuity-discontinuity of the orbital phase has been shown to control a wide variety of molecular structures and reactions. The orbital phase theory has expanded and is still expanding the scope of its applications beyond the cyclic systems. We also describe applications of the orbital phase theory to cyclic systems, which cannot be made by the Woodward–Hoffmann rule or the Hückel rule.

2 A Theory

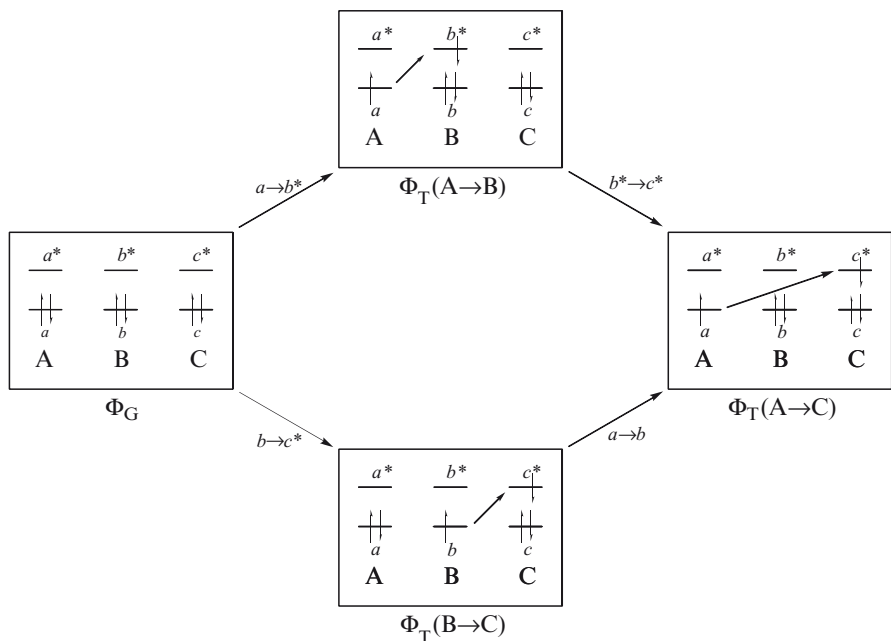
Bonds interact with one another in molecules. The bond interactions are accompanied by the delocalization of electrons from bond to bond and the polarization of bonds. In this section, bond orbitals (bonding and antibonding orbitals of bonds) including non-bonding orbitals for lone pairs are shown to interact in a cyclic manner even in non-cyclic conjugation. Conditions are derived for effective cyclic orbital interactions or for a continuous orbital phase.

2.1 Non-Cyclic Conjugation

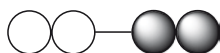
The electron delocalizations in the linear and cross-conjugated hexatrienes serve as good models to show cyclic orbital interaction in non-cyclic conjugation (Schemes 2 and 3), to derive the orbital phase continuity conditions (Scheme 4), and to understand the relative stabilities (Scheme 5) [15].



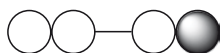
Scheme 2 Cyclic orbital interaction for the electron delocalization between the terminal π bonds in the non-cyclic trienes



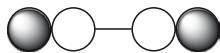
Scheme 3 Electron delocalization and the cyclic interaction of the electron configurations



(i) The electron donating orbitals are out of phase.

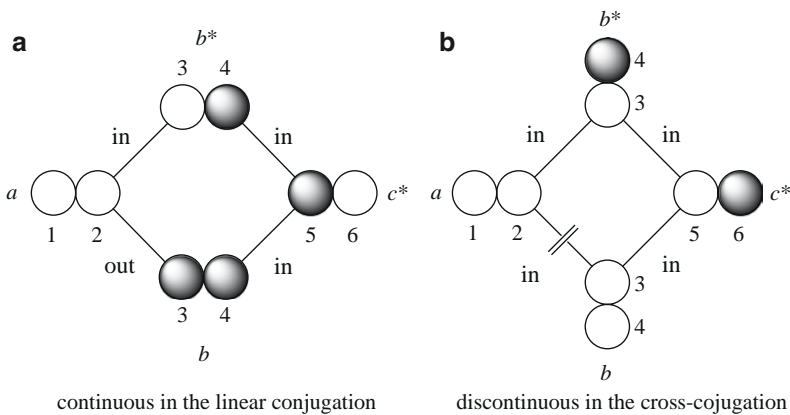


(ii) The electron donating and accepting orbitals are in phase.



(i) The electron accepting orbitals are in phase.

Scheme 4 Conditions for the continuity of orbital phase



Scheme 5 Orbital phase properties of the hexatrienes

2.1.1 Cyclic Orbital Interactions in Non-Cyclic Conjugation

A pair of electrons is assumed to occupy each bonding orbital of the three π bonds in the hexatrienes prior to the bond interactions. Scheme 3 illustrates the mechanism of the delocalization of π electrons from the terminal bond A to the other bond C through the middle bond B. There are paths via the bonding (b) and antibonding (b^*) orbitals of B. Along the b path, an electron shifts from b to c^* through the $b-c^*$ interaction, and the resulting electron hole in b is supplied with an electron by a through the $a-b$ interaction. The $a-b-c^*$ interaction occurs in the b path. Along the b^* path, an electron shifts from a to b^* through the $a-b^*$ interaction and then to c^* through the b^*-c^* interaction: the $a-b^*-c^*$ interaction occurs. As a result, the cyclic $-a-b-c^*-b^*-$ interaction (Scheme 2) surprisingly occurs in the non-cyclic conjugate trienes.

The electron delocalization from A to C can be compared to the two waves starting at the point a , running along different b and b^* paths, and reaching the same point c^* to interfere with each other. The waves in phase strengthen each other and those out of phase weaken each other.

2.1.2 Conditions for Continuous Orbital Phase

Here we derive the conditions of orbital phase for the cyclic orbital interactions. The $A \rightarrow B$ delocalization is expressed by the interaction between the ground configuration Φ_G and the electron-transferred configuration $\Phi_{T(A \rightarrow B)}$ (Scheme 3). A pair of electrons occupies each bonding orbital in Φ_G , which is expressed by a single Slater determinant Φ_G :

$$\Phi_G = | a(1)\alpha(1)a(2)\beta(2)b(3)\alpha(3)b(4)\beta(4)c(5)\alpha(5)c(6)\beta(6) |, \quad (1)$$

where the normalization factor is omitted. In $\Phi_{T(A \rightarrow B)}$, the bonding orbital a in Φ_G is replaced by an antibonding orbital b^* :

$$\begin{aligned} \Phi_{T(A \rightarrow B)} = & | a(1)\alpha(1)b^*(2)\beta(2)b(3)\alpha(3)b(4)\beta(4)c(5)\alpha(5)c(6)\beta(6) | \\ & + | b^*(1)\alpha(1)a(2)\beta(2)b(3)\alpha(3)b(4)\beta(4)c(5)\alpha(5)c(6)\beta(6) |. \end{aligned} \quad (2)$$

The subsequent shift from b^* to c^* is expressed by the $\Phi_{T(A \rightarrow B)} - \Phi_{T(A \rightarrow C)}$ interaction, where

$$\begin{aligned} \Phi_{T(A \rightarrow C)} = & | a(1)\alpha(1)c^*(2)\beta(2)b(3)\alpha(3)b(4)\beta(4)c(5)\alpha(5)c(6)\beta(6) | \\ & + | c^*(1)\alpha(1)a(2)\beta(2)b(3)\alpha(3)b(4)\beta(4)c(5)\alpha(5)c(6)\beta(6) |. \end{aligned} \quad (3)$$

The $\Phi_G - \Phi_{T(A \rightarrow B)} - \Phi_{T(A \rightarrow C)}$ interaction occurs in the b^* path. Similarly, the $\Phi_G - \Phi_{T(B \rightarrow C)} - \Phi_{T(A \rightarrow C)}$ interaction occurs in the b path. The $\Phi_{T(B \rightarrow C)}$ configuration is expressed as

$$\Phi_{T(B\rightarrow C)} = | a(1)\alpha(1)a(2)\beta(2)b(3)\alpha(3)c^*(4)\beta(4)c(5)\alpha(5)c(6)\beta(6) | \quad (4)$$

$$+ | a(1)\alpha(1)a(2)\beta(2)c^*(3)\alpha(3)b(4)\beta(4)c(5)\alpha(5)c(6)\beta(6) |.$$

It follows that the cyclic $-\Phi_G - \Phi_{T(A\rightarrow B)} - \Phi_{T(A\rightarrow C)} - \Phi_{T(B\rightarrow C)}$ configuration interaction occurs in the A \rightarrow C delocalization (Scheme 3).

The overlap integrals between the configurations are approximated to those between the orbitals:

$$S(G, A\rightarrow B) = +s(a, b^*),$$

$$S(A\rightarrow B, A\rightarrow C) = +s(b^*, c^*),$$

$$S(A\rightarrow C, B\rightarrow C) = -s(a, b),$$

$$S(B\rightarrow C, G) = +s(b, c^*).$$

The plus and minus signs imply that electrons accumulate in the overlap region when the orbitals are combined in phase and out of phase, respectively. The cyclic orbital interaction gives rise to stabilization when the orbitals between a and b^* , between b^* and c^* , and between b and c^* are combined in phase and when a and b are combined out of phase. These are the orbital phase conditions for the A \rightarrow C delocalization in the trienes. When all the phase conditions are simultaneously satisfied, the orbital phase is continuous.

In principle, the orbital phase continuity conditions do not necessarily require a definite phase relation between a given pair of orbitals (e.g., in phase relation between a and b^*). The configuration overlap integral $S(G, A\rightarrow B)$ happens to have a plus sign such as $+s(a, b^*)$ since the ground and transferred configurations are expressed as given above. From the property of determinant, overlap integrals of the configurations change signs by an odd number of permutations. The sign of each overlap is arbitrary. However, the sign of the product of all the overlap integrals related to the cyclic interaction is uniquely determined for a given set of configuration functions. The sign of the product is minus in the present case. This requires an odd number of out of phase relations for the electron accumulation between all pairs of the relevant orbitals. The present case meets the requirements if the electron-donating orbitals a and b are combined out of phase while the pairs of the donating and accepting orbitals and those of the accepting orbitals are combined in phase.

The orbital phase continuity conditions are summarized in Scheme 4. Cyclic orbital interactions give rise to stabilization when the orbitals simultaneously satisfy the following conditions:

1. Electron-donating orbitals are combined out of phase
2. Electron-accepting orbitals are combined in phase
3. Electron-donating and -accepting orbitals are combined in phase

Or simply, in other words:

Only neighboring electron-donating orbitals are combined out of phase while any other neighboring orbital pairs are combined in phase.

The conditions are also equivalent to:

An even (odd) number of neighboring donating orbital pairs requires an even (odd) number of out of phase relations.

Electron-donating orbitals are those occupied by electrons, i.e., bonding orbitals of bonds, non-bonding orbitals of lone pairs, HOMOs of molecules, groups and others. Electron-accepting orbitals are vacant orbitals, i.e., antibonding orbitals of bonds, vacant atomic orbitals on cationic centers, LUMOs of molecules, groups, etc.

The orbital phase continuity conditions stem from the intrinsic property of electrons. Electrons are fermions, and are described by wavefunctions antisymmetric (change plus and minus signs) with respect to an interchange of the coordinates of an pair of particles. The antisymmetry principle is a more fundamental principle than Pauli's exclusion principle. Slater determinants are antisymmetric, which is why the overlap integral between $\Phi_{T(A\rightarrow B)}$ and $\Phi_{T(A\rightarrow C)}$ given above has a negative sign. The signs of the overlap integrals are important as described above to derive the conditions for the continuity of orbital phase.

2.1.3 Continuous and Discontinuous Orbital Phases

The orbital phase conditions are applied to the cyclic $-a-b-c^*-b^*-$ interaction (Scheme 2). The linear conjugate triene was found to satisfy the required orbital phase relations (Scheme 5): (1) the donating orbitals a and b are combined out of phase; (2) the accepting orbitals a^* and b^* are combined in phase; (3) the donating orbital a and the accepting orbital b^* are combined in phase; (4) the donating orbital b and the accepting orbital c^* are combined in phase. On the other hand, the cross conjugate triene does not simultaneously satisfy the conditions. In Scheme 5, the in phase relation between the donating orbitals a and b does not meet the requirements while any other pair of orbitals satisfies the conditions. The orbital phase is discontinuous. If the a and b orbitals are combined out of phase as the conditions require, another pair of orbitals cannot satisfy the conditions. The phase remains discontinuous. The continuity-discontinuity property of the orbital phase is uniquely determined for a given cyclic orbital interaction.

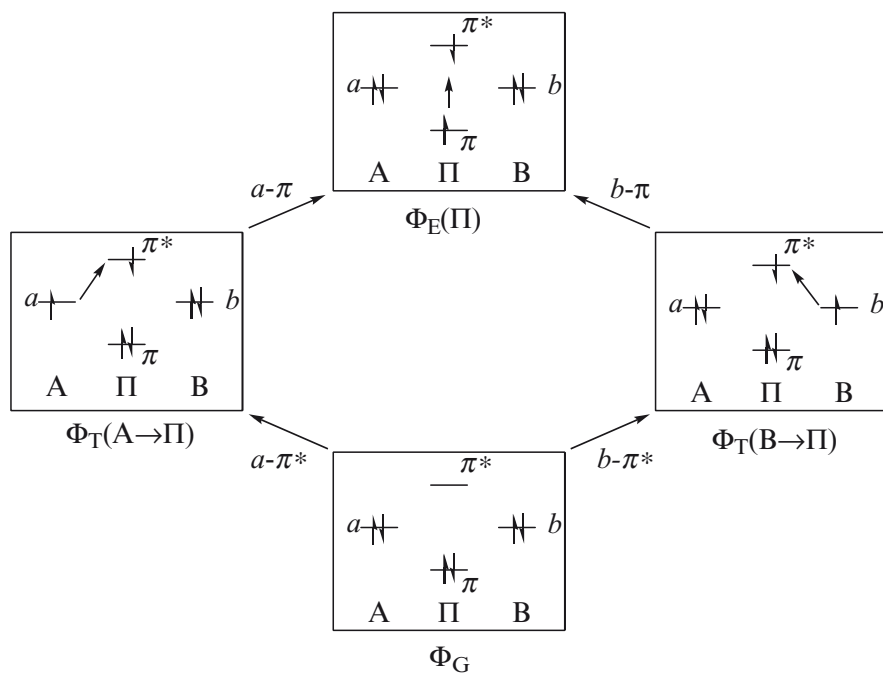
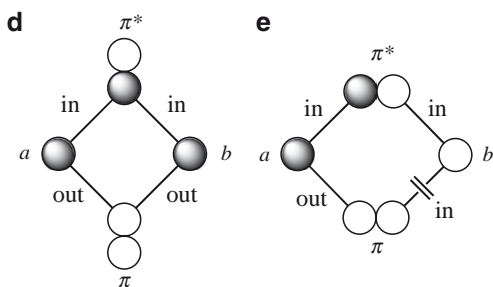
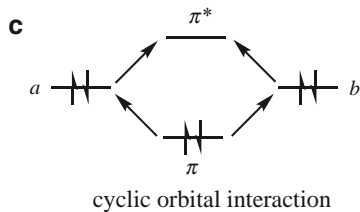
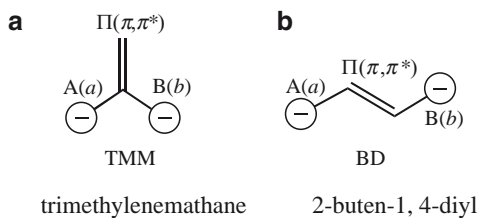
The orbital phase is continuous in the linear conjugate triene and discontinuous in the cross-conjugate triene. The electron delocalization between the terminal bonds is favored in the linear triene and disfavored in the cross-conjugate triene. The linear triene is more stable. The continuity-discontinuity of orbital phase underlies the thermodynamic stabilities of non-cyclic conjugated molecules.

2.1.4 Polarization of Bonds

Interactions polarize bonds. Trimethylenemethane (TMM) and 2-buten-1,4-diyl (BD) dianions (Scheme 6a, b) are chosen as models for linear and cross-conjugated dianions. The bond polarization (Scheme 7) is shown to contain cyclic orbital interaction (Scheme 6c) even in non-cyclic conjugation [15]. The orbital phase continuity-discontinuity properties (Scheme 6d, e) control the relative thermodynamic stabilities.

Scheme 7 illustrates the mechanism of the polarization of the π bond. In one path, an electron in the non-bonding orbital a of the anionic center A is transferred to the antibonding orbital π^* of the double bond Π . The $A\rightarrow\Pi$ delocalization is

Scheme 6 Cross- and linear conjugate dianions



Scheme 7 Polarization of the cross- (TMM) and linear (BD) conjugate dianions

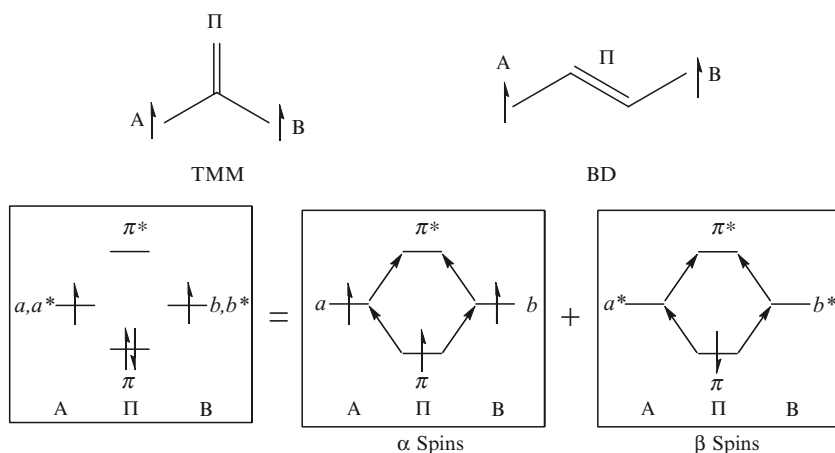
expressed by the $\Phi_G - \Phi_{T(A \rightarrow \Pi)}$ configuration interaction or by the $a - \pi^*$ orbital interaction. The resulting electron hole in a is supplied with an electron by the bonding orbital π . This is expressed by the interaction of $\Phi_{T(A \rightarrow \Pi)}$ with the locally excited configuration $\Phi_{E(\Pi)}$ or by the $a - \pi$ interaction. As a result, the polarization contains the $\Phi_G - \Phi_{T(A \rightarrow \Pi)} - \Phi_{E(\Pi)}$ interaction or the $\pi - a - \pi^*$ interaction. Along the other path, the polarization contains the $\Phi_G - \Phi_{T(B \rightarrow \Pi)} - \Phi_{E(\Pi)}$ interaction or the $\pi - b - \pi^*$ interaction. It follows that the cyclic $-\Phi_G - \Phi_{T(A \rightarrow \Pi)} - \Phi_{E(\Pi)} - \Phi_{T(B \rightarrow \Pi)}$ (Scheme 7) or the $\pi - a - \pi^* - b -$ interaction occurs (Scheme 6c).

The orbital phase continuity conditions (Scheme 4) are applied to the cyclic orbital interactions (Scheme 6d, e). The π and non-bonding orbitals (a and b) are electron-donating orbitals, and π^* is an electron-accepting orbital. The in phase relation is required for the $a - \pi^*$ and $b - \pi^*$ pairs, and the out of phase relation is required for the $a - \pi$ and $b - \pi$ pairs. The cross conjugate dianion satisfies the conditions while the linear conjugate dianion does not. The cross conjugated dianion is more stable than the linear one, in a striking contrast to the trienes. The relative stability is in agreement with the experimental observation [16, 17]. The special stability of the cross conjugate systems has been noted as the Y-delocalization [18].

Similar arguments lead to the prediction that the cross conjugate TMM dication should be more stable than the linear conjugate BD dication. The cyclic orbital interaction is favored by the continuity of orbital phase in the TMM dication, but the orbital phase is discontinuous in the BD dication.

2.1.5 Triplet States

The orbital phase theory has been developed for the triplet states [19]. The orbital phase continuity conditions (Scheme 4) were shown to be applicable. We describe here, for example, the triplet states of the TMM and BD diradicals, with three α spin electrons and one β spin electron. The α and β spins are considered separately (Scheme 8).

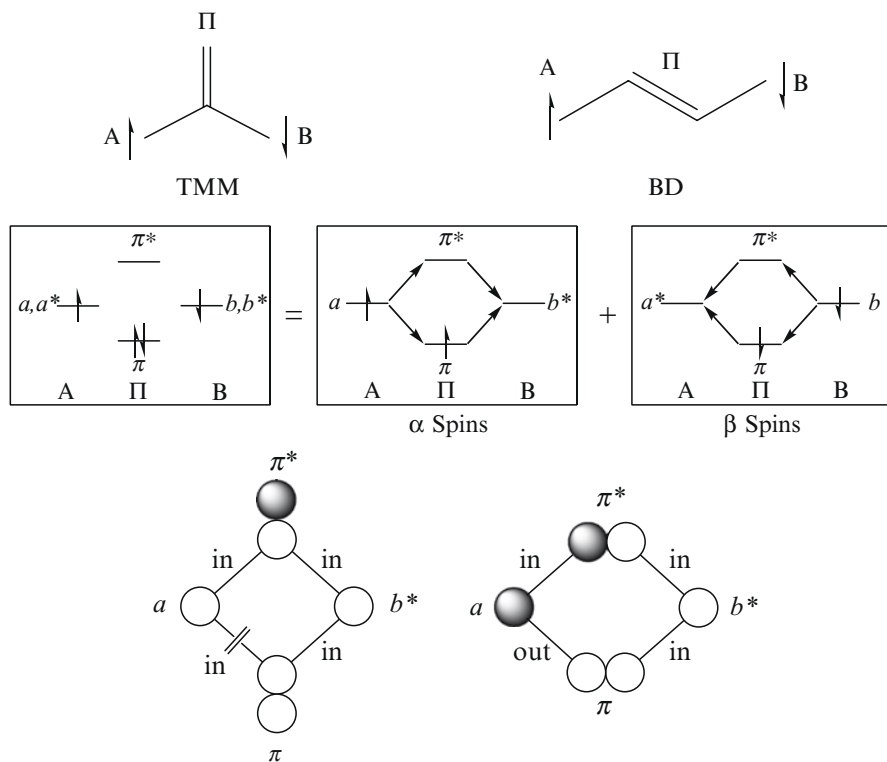


Scheme 8 Electron configuration and polarization in the triplet diradicals

α Spins occupy the π bonding orbital of the double bond and the p orbitals in the radical centers. This is the same as the α spin electron configuration of the dianion. β Spins occupy only π . The p orbitals in the radical centers are not occupied by β spins. This is the same as the β spin electron configuration of the dication. The orbital phase has been shown to be continuous in the cross conjugated dianion and dication. It follows that the cross conjugate diradical is more stable than the linear one in the triplet states.

2.1.6 Singlet Diradicals

The orbital phase theory is applicable to the singlet diradicals [20]. The electron configuration of the singlet states of the cross- (TMM) and linear (BD) conjugate diradicals is shown in Scheme 9, where the mechanism of the delocalization of α and β spins between the radical centers through the double bond are separately illustrated by the arrows. The cyclic $[-a-\pi-b-\pi^*-]$ interaction is readily seen to occur for the spin delocalizations. The p orbital (a) in one radical center and the π orbital are occupied by α spins, and therefore, electron-donating orbitals. The p orbital (b) in the other radical center and the π^* orbital are not occupied by α spins,



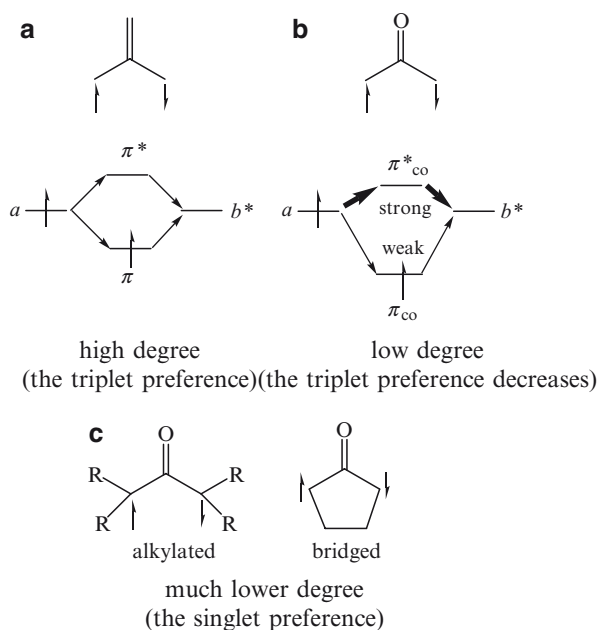
Scheme 9 Electron configuration and delocalization, cyclic orbital interaction, and orbital phase properties in the singlet diradicals

and therefore are electron-accepting orbitals. The orbital phase is discontinuous for the TMM diradical and continuous for the BD diradical in the singlet states (Scheme 9, cf. Scheme 4). The phase properties of the triplet and singlet states of a given diradical are opposite to each other.

The interactions stabilize the ground states and destabilize the corresponding excited states. The phase continuity stabilizes the ground states and destabilizes the excited states. The phase discontinuity does not significantly split the energy levels between the ground and excited states. The energy increases in the order: ground states with the continuous phase < ground or excited states with the discontinuous phase < excited states with the continuous phase. It should be noted that the singlet diradicals of the Kekule molecules (e.g., BD) are the excited states. The ground states correspond to closed-shell molecules (e.g., butadiene). The cross-conjugate (TMM) singlet diradical of the discontinuous phase is more stable than the linear conjugate (BD) diradical destabilized by the phase continuity.

2.1.7 Degree of the Orbital Phase Discontinuity

There is a degree in the continuity and discontinuity of the orbital phase [20]. 2-Oxopropane-1,3-diyl (Scheme 10) is a hetero analog of trimethylenemethane (TMM) where the orbital phase is continuous in the triplet diradical (Sect. 2.1.5) and discontinuous in the singlet diradical (Sect. 2.1.6). The π and π^* orbitals of carbonyl bonds are lower in energy than those of C=C bonds. The lowering strengthens the interaction of the radical orbitals (a , b) with $\pi^*_{C=O}$ and weakens that



Scheme 10 Spin preference and degree of the discontinuity of orbital phase

with $\pi_{\text{C=O}}$. The same is expected from the π bond polarity. The $\pi_{\text{C=O}}$ and $\pi_{\text{C=O}}^*$ orbitals extend less and more on the carbonyl carbon, respectively. The $a-\pi^*-b$ interaction is stronger than the $a-\pi-b$ interaction. The spin delocalization between the radical centers survives the phase discontinuity since the delocalization along the π^* path is greater in magnitude than that along the π path. Consequently, the degree of phase discontinuity in the singlet state is lowered in the 2-oxopropane-1,3-diyl diradical. The weakened $a-\pi$ interaction reduces the effect of the cyclic orbital interaction and therefore the effect of the phase continuity in the triplet state or the triplet preference. This is in agreement with the results of the MCSCF calculations [21]. Alkyl groups on the carbon radical centers and alkanone bridges between the radical centers raise the radical p orbital energy, and also lower the degree of the phase discontinuity in the singlet states. In fact, the ground states of the substituted [22] and bridged [23, 24] derivatives (Scheme 10) are singlets.

2.2 Cyclic Conjugation

Orbitals have been shown in the preceding section to interact in a cyclic manner even in non-cyclic geometry. Cyclic conjugation contains the cyclic orbital interactions because of the cyclic geometry, in addition to those of the non-cyclic subsystems.

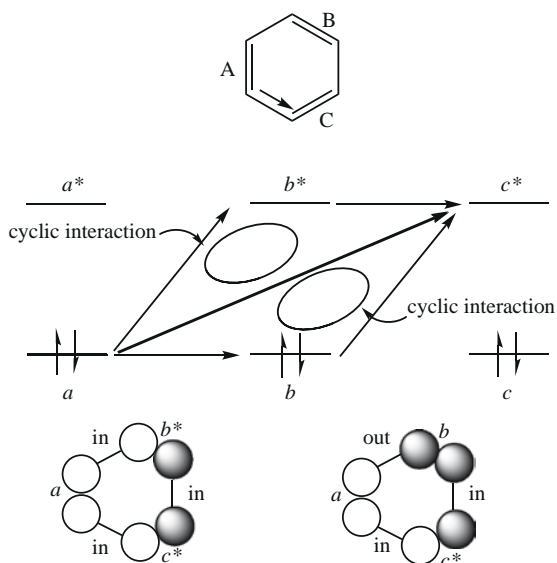
A part of the chemical consequences of the cyclic orbital interactions in the cyclic conjugation is well known as the Hückel rule for aromaticity and the Woodward–Hoffmann rule for the stereoselection of organic reactions [14]. In this section, we describe the basis for the rules very briefly and other rules derived from or related to the orbital phase theory. The rules include *kinetic* stability (electron-donating and accepting abilities) of cyclic conjugate molecules (Sect. 2.2.2) and discontinuity of cyclic conjugation or inapplicability of the Hückel rule to a certain class of conjugate molecules (Sect. 2.2.3). Further applications are described in Sect. 4.

2.2.1 Cyclic Delocalization of Electrons

Benzene (Scheme 11) serves as a simple model to illustrate the cyclic orbital interaction in the cyclic systems.

There are assumed to be three π bonds, A, B, and C, in benzene. Here we consider the electron delocalization from A to C. The electron delocalization via B is the same as that in the linear conjugate hexatriene (Schemes 2 and 3) used as a model of non-cyclic conjugate systems. The cyclic orbital interaction has been shown to be favored by the phase continuity (Scheme 5a). There is an additional path for the delocalization in cyclic geometry, which is the direct path from A to C or from a to c^* . The path gives rise to the cyclic $a-b-c^*$ and $a-b^*-c^*$ interactions. The cyclic orbital interactions satisfy the orbital phase continuity conditions

Scheme 11 Cyclic orbital interactions and the orbital phase continuity



(Scheme 4): (1) out of phase between a and b ; (2) in phase between a^* and b^* , between a and b^* , and between b and c^* . The phase continuity stabilizes benzene.

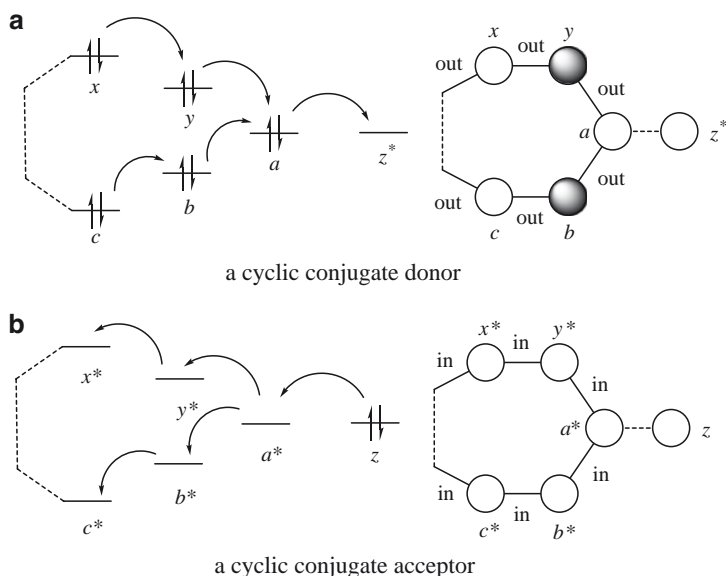
The orbital phase theory can be applied to cyclically interacting systems which may be molecules at the equilibrium geometries or transition structures of reactions. The orbital phase continuity underlies the Hückel rule for the aromaticity and the Woodward–Hoffmann rule for the stereoselection of organic reactions.

2.2.2 Kinetic Instability (Powers as Donors and Acceptors) of Cyclic Conjugate Molecules

The orbital phase continuity underlies the aromaticity or the thermodynamic stability of cyclic conjugated molecules. Kinetic stability of cyclic conjugate molecules is shown here to be also under the control of the orbital phase property. The continuity conditions can be applied to the design of powerful electron donors and acceptors.

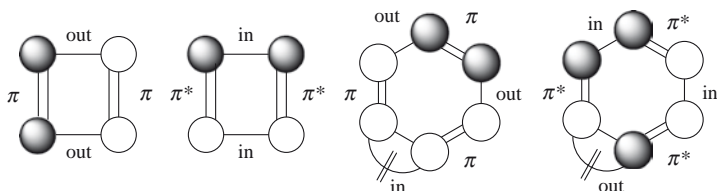
A cyclic conjugate molecule composed of π bonds, A, B, ..., X, and Y interacts at A with a reactant Z (Scheme 12). When the molecule is an electron donor (Scheme 12a), electrons delocalize from a to z^* . The resulting electron hole in a is supplied with an electron by the neighboring b . Similar delocalization sequentially follows from c to b , from d to c and so on. This is also the case with the opposite side Y, X, It follows that the cyclic orbital interaction of $a, b, \dots, x,$ and y is important in the conjugated molecule. The orbitals are all electron-donating orbitals. When each neighboring pair of orbitals is combined out of phase, the interaction of the cyclic

molecules with the acceptor is promoted. The molecules are strong electron donors or kinetically unstable toward electron acceptors. The cyclic conjugated molecules with all pairs of the neighboring electron-accepting orbitals in phase (Scheme 12b) are strong electron acceptors or kinetically unstable toward donors.



Scheme 12 The orbital phase conditions for kinetic instability

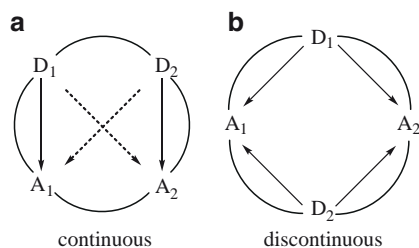
Antiaromatic molecules are kinetically unstable, and aromatic molecules are kinetically stable (Scheme 13). In cyclobutadiene, the π orbitals can be combined out of phase and the π^* orbitals can be combined in phase. Cyclobutadiene is kinetically unstable toward electron donors and acceptors. In benzene, all neighboring pairs of π orbitals cannot be combined out of phase, and all neighboring pairs of π^* orbitals cannot be combined in phase. Benzene is kinetically stable toward donors and acceptors.



Scheme 13 Kinetic instability of antiaromatic molecules and kinetic stability of aromatic molecules

2.2.3 Continuity and Discontinuity of Cyclic Conjugation

The orbital phase continuity conditions or the Hückel $4n + 2 \pi$ electron rule cannot be applied to predicting the thermodynamic stabilities of cyclic ‘conjugate’ molecules where donors and acceptors are alternately disposed along the cyclic chain (Scheme 14b) [25]. The cyclic delocalization of π electrons is disfavored by the donor–acceptor disposition. Electrons delocalize from a donor D_1 to an adjacent acceptor A_1 . The electron accepted by A_1 cannot readily delocalize to the neighbor on the other side because it is not an acceptor but a donor (D_2). On the other hand, the electron hole in D_1 resulting from the electron donation to A_1 cannot be readily supplied by an electron by the neighbor on the other side because it is an acceptor (A_2). Delocalization occurs only between adjacent pairs of donors and acceptors. Electrons cannot delocalize in a cyclic manner. In this sense, cyclic conjugation is discontinuous when donors and acceptors are alternately disposed along the conjugate chain. Thermodynamic stability of discontinuously conjugated molecules is determined neither by orbital phase property nor by number of π electrons, but by the number of the adjacent donor–acceptor pairs.

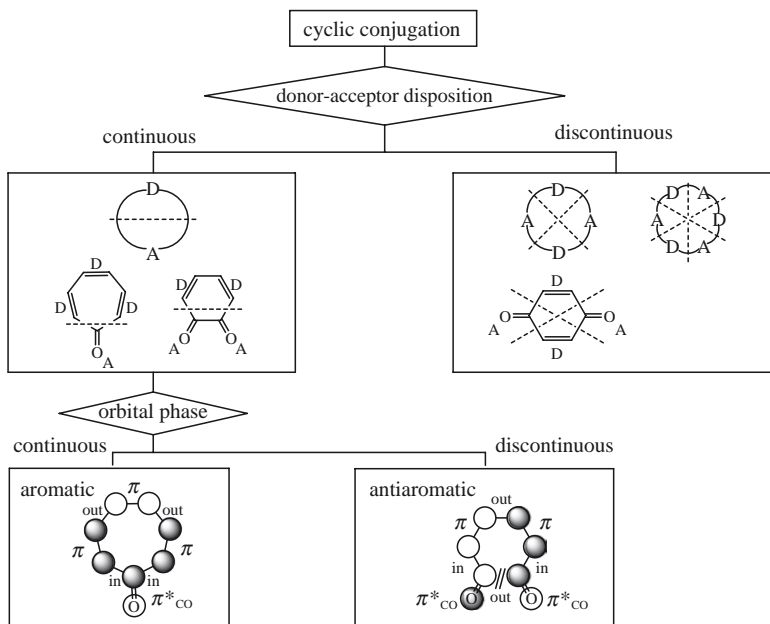


Scheme 14 Cyclic conjugations

The cyclic conjugation is continuous if the donors are on one side of the cyclic chain and the acceptors are on the other side (Scheme 14a). Electrons delocalize from a donor D_1 to A_1 . The electron accepted by A_1 can readily delocalize to the neighbor on the other side because it is an acceptor (A_2). An electron can delocalize from D_1 to A_2 . The delocalization can take place along the other path. D_2 donates an electron to A_2 . The resulting electron hole in D_2 can be supplied with an electron by the neighbor D_1 . This is equivalent to the delocalization from D_1 to A_2 . Electrons can delocalize in a cyclic manner. Thermodynamic stability of continuously conjugated molecules is under control of the orbital phase property or determined by the number of π electrons.

2.2.4 Classification of Cyclic Conjugation

The preceding theory of cyclic conjugation has led to such classification as is summarized in Scheme 15 [25]. Cyclic conjugation is first divided into the continuous and discontinuous conjugations by the donor–acceptor disposition. The stability of



Scheme 15 A classification of cyclic conjugated molecules

continuously conjugated molecules is determined by orbital phase properties. The Hückel $4n + 2\pi$ electron rule can be applied. The continuous conjugate molecules are further divided into aromatic and antiaromatic molecules.

Cyclic conjugation is continuous in *o*-benzoquinone and discontinuous in *p*-benzoquinone (Scheme 15, cf. Scheme 4). The donors (the C=C bonds) are on one side of the cyclic chain and the acceptors (the C=O bonds) are on the other side in *o*-benzoquinone. In *p*-benzoquinone the donors and the acceptors are alternatively disposed along the chain. The thermodynamic stability of *o*-benzoquinone is under control of the orbital phase property. The continuity conditions are not satisfied. *o*-Benzoquinone is antiaromatic. The thermodynamic stability of *p*-benzoquinone is free of the orbital phase (neither aromatic nor antiaromatic) and comes from the delocalization between the four pairs of the neighboring donors and acceptors. In fact, *p*-benzoquinone, which melts at 116 °C, is more stable than *o*-benzoquinone, which decomposes at 60–70 °C.

3 Applications to Non-Cyclic Conjugation

The finding of the cyclic orbital interactions in non-cyclic conjugation opens a way to systematic understanding and designing of molecules and reactions in a unified manner. Here, we apply the orbital phase theory to non-cyclic interactions of bonds, groups, molecules, cationic, anionic, and radical centers, lone pairs, etc.

3.1 Stability and Number of Electrons

The orbital phase theory leads to an analogy with the Hückel rule for cyclic conjugated molecules. Relative stability of the cross- and linear conjugated species with four p orbitals is determined by the number of π electrons, as described in the theoretical sections (Sects. 2.1.4, 2.1.6). For 2π and 6π electrons, the cross-conjugated molecules (e.g., trimethylenemethane TMM dication and dianion) are more stable than linear conjugated molecules (e.g., but-2-ene-1,4-diyl BD dication and dianion). For 4π electrons, linear conjugated molecules (e.g., butadiene) are more stable than cross-conjugated molecules (e.g., the singlet TMM diradical). The cross conjugation prefers $4n + 2$ ($n = 0, 1$) π electrons, while the linear conjugation prefers $4n$ π electrons (Table 1). The cross- and linear conjugations are comparable to the Hückel and Möbius conjugations of the cyclic molecules, respectively [26].

Table 1 Relative stabilities of cross- vs linear conjugated species and number of π electrons

Number of electrons	Conjugation	
	Cross (TMM)	Linear (BD)
2	Stable	Unstable
4	Unstable	Stable
6	Stable	Unstable

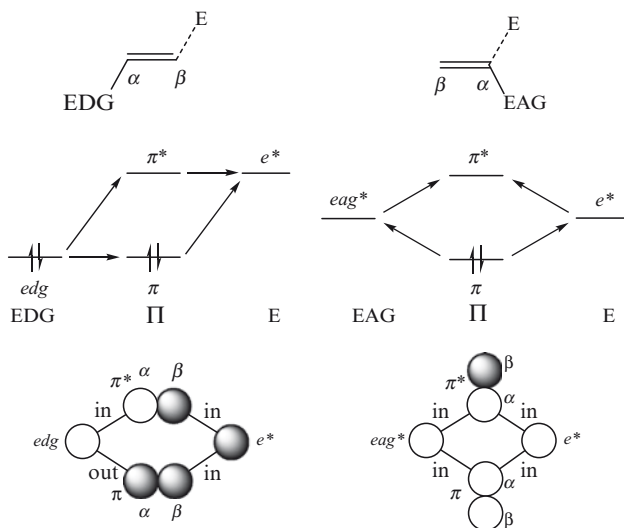
Experimental evidence for the six electron systems has been described in Sect. 2.1.4. Skancke reproduced the relative stability of the cross conjugated systems relative to the linear isomers by calculating the trimethylenemethane and buta-1,4-diyl dianions [27] and their dilithio salts [28]. For the four electron systems butadiene is more stable than trimethylenemethane. Experimental examination of the relative stabilities of two electron systems using the trimethylenemethane and buta-1,4-diyl dications needs to overcome the intrinsic instabilities of dications dissatisfying the octet rule.

3.2 Regioselectivities of Electrophilic Additions

Here, the orbital phase theory sheds new light on the regioselectivities of reactions [29]. This suggests how widely or deeply important the role of the wave property of electrons in molecules is in chemistry.

Additions of an electrophile (E) to the π bond (Π) substituted by an electron-donating group (EDG) and an electron-accepting group (EAG) occur at the β and α positions, respectively. Transition states are considered as non-cyclic E- Π -EDG(EAG) systems (Scheme 16).

The regioselectivities of the reactions of EDG-substituted alkenes are determined by delocalization from R to E via Π . The delocalization contains the cyclic interactions of orbitals, i.e., the electron-donating orbital (edg) of EDG, electron-accepting orbital (e^*) of the electrophile, and the bonding π orbital and the antibonding π^* orbital. For



Scheme 16 The orbital phase continuity controls the regioselectivity

the β additions, the delocalization is favored by the orbital phase continuity whereas the phase is discontinuous for the α additions (Scheme 16, cf. Scheme 4).

For the EAG-substituted alkenes, the transition states are non-cyclic E- Π -EAG systems. Polarization of Π , induced by the delocalization from Π to EAG and E, determines the regioselectivities. The polarization is analogous to that in the TMM dication (Sect. 2.1.4). The cyclic interaction occurs among the electron-accepting orbital (eag^*) of the substituent, e^* , π , and π^* . The α addition is favored by the orbital phase continuity while the β addition is disfavored by the phase discontinuity (Scheme 16).

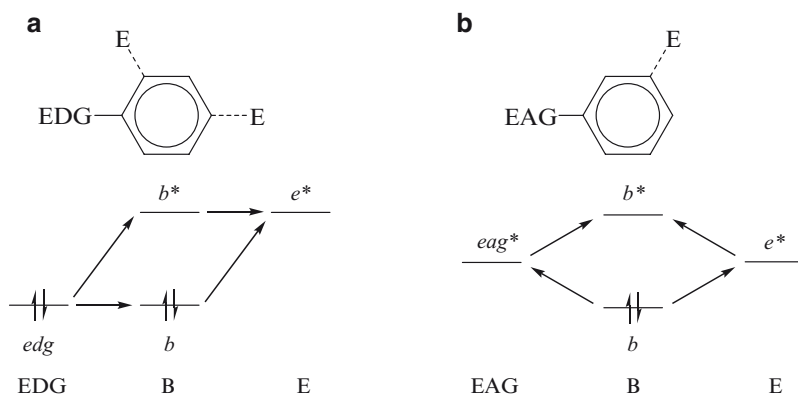
The regioselectivities of Diels–Alder reactions are also understood in terms of the orbital phase continuity [29]. The selectivity is also explained by the frontier orbital amplitude [30].

3.3 Electrophilic Aromatic Substitutions

3.3.1 Kinetic Control

Substitution reactions on a benzene ring (B) with an electron-donating group (EDG) and an electron-accepting group (EAG) by an electrophile (E) occur at the *o*- and *p*-positions and at the *m*-positions, respectively. Transition states are considered as non-cyclic E–B–EDG (EAG) systems (Scheme 17).

The orientation of the reactions of EDG-substituted benzenes is determined by delocalization from EDG to E via B. The delocalization contains the cyclic interactions of the electron-donating orbital (edg) of EDG, electron-accepting orbital (e^*) of the electrophile, and the HOMO (b) and the LUMO (b^*) of the benzene ring (Scheme 17). For the *ortho* and *para* orientations, the delocalization is favored by the orbital phase

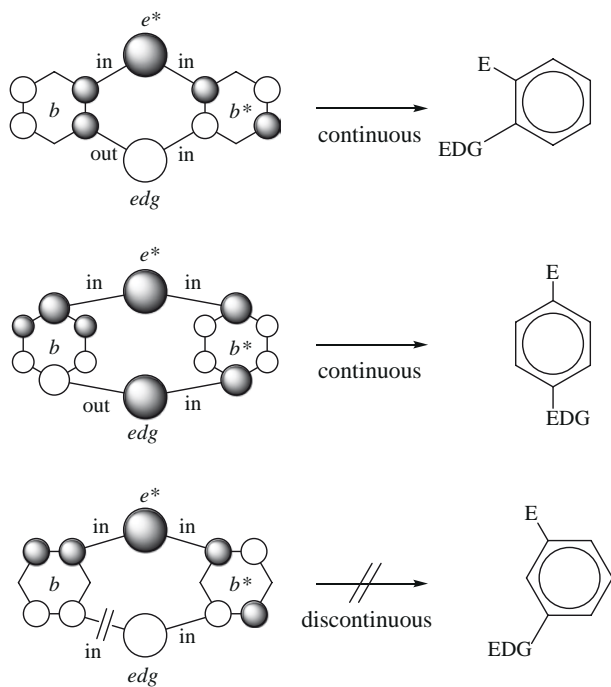


benzenes with an electron donating group benzenes with an electron accepting group

Scheme 17 Cyclic orbital interactions at the transition structures of electrophilic aromatic substitutions

continuity whereas the phase is discontinuous for the *meta*orientation (Scheme 18, cf. Scheme 4).

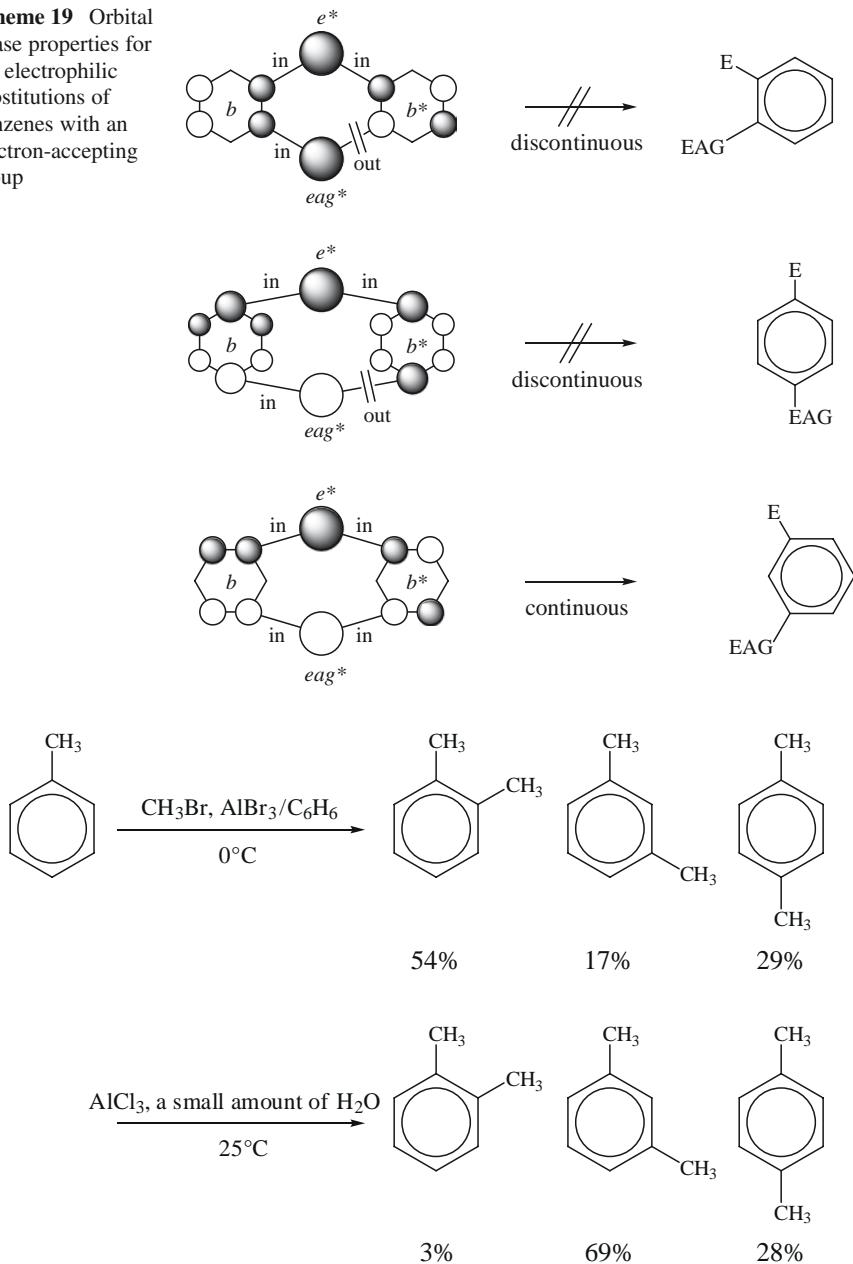
For the EAG-substituted benzenes, the transition states are non-cyclic E-B-EAG systems. Polarization of B, induced by the delocalizations from B to EAG and E



Scheme 18 Orbital phase properties for the electrophilic substitutions of benzenes with an electron-donating group

(Scheme 17), determines the orientations. The cyclic interaction occurs among the electron-accepting orbital (eag^*) of the substituent, e^* , b , and b^* . The *meta*-orientation is favored by the orbital phase continuity while the *ortho* and *para* orientations are disfavored by the phase discontinuity (Scheme 19, cf. Scheme 4).

Scheme 19 Orbital phase properties for the electrophilic substitutions of benzenes with an electron-accepting group

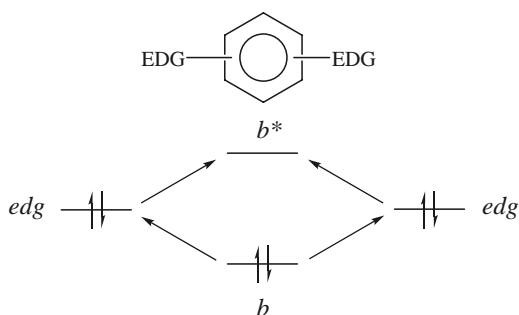


Scheme 20 Kinetic and thermodynamic distributions of the product isomers in the Friedel–Crafts methylations

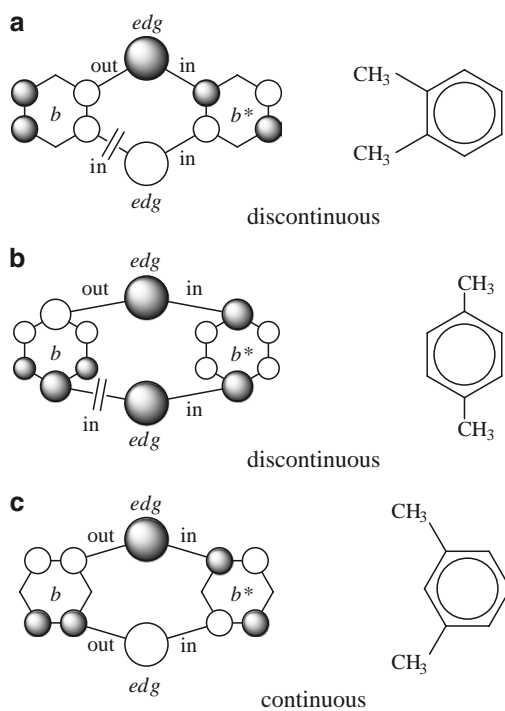
3.3.2 Thermodynamic Control

The thermodynamic product distribution in the Friedel–Crafts methylation (Scheme 20) is in contrast to the kinetic distribution. The reaction kinetically shows the *ortho* and *para* orientations. Thermodynamic stabilities of the products prefer the *meta* isomer as a major product.

The orbital phase theory can be applied to the thermodynamic stability of the disubstituted benzene isomers. The cyclic orbital interaction in the benzene substituted with two EDGs is shown in Scheme 21. The orbital phase is continuous in the *meta* isomer and discontinuous in the *ortho* and *para* isomers (Scheme 22, cf. Scheme 4).



Scheme 21 Cyclic orbital interaction in benzenes with two electron-donating groups



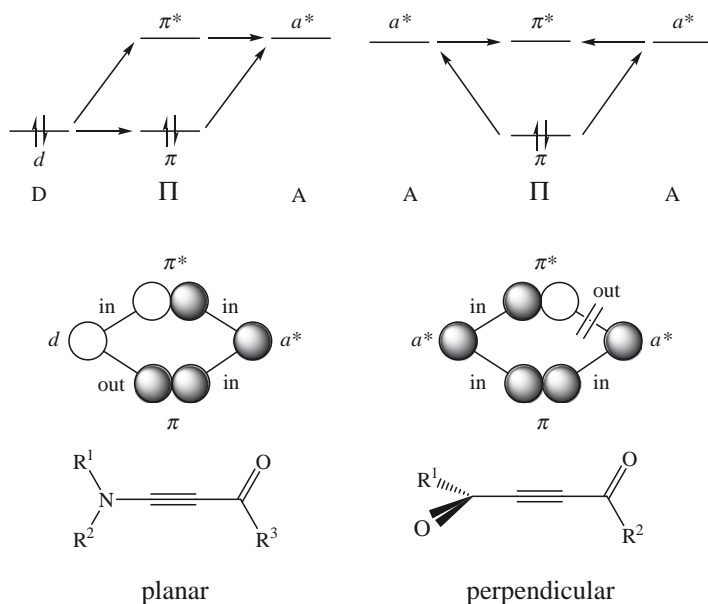
Scheme 22 Orbital phase properties of xylylenes

3.4 Conformational Stability

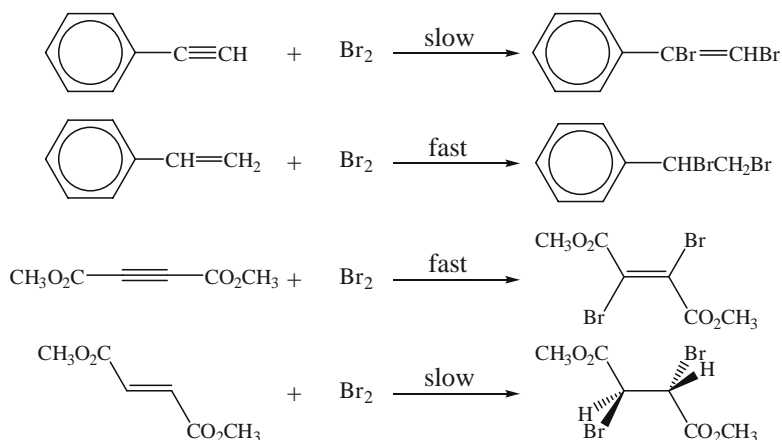
The orbital phase theory was applied to the conformations of alkenes (α - and β -substituted enamines and vinyl ethers) [31] and alkynes [32]. The conformational stabilities of acetylenic molecules are described here.

Acetylenes $XCCY$ with π conjugated substituents, X and Y, on both carbon atoms have planar or perpendicular conformations. The substituents can be electron-donating or -accepting. The planar conformers are linear conjugate D- Π -D, D- Π -A, or A- Π -A systems whereas the perpendicular conformers are composed of Π -D and Π -A not in conjugation with each other. The orbital phase is continuous only in the planar conformations of D- Π -A (Scheme 23, cf. Scheme 4). The acetylenes with X=D (OR, NR₂) and Y=A (RCO, ROCO) prefer planar conformations. When both substituents are electron-donating or accepting, the phase is discontinuous. The acetylenes then prefer perpendicular conformations. The predicted conformational preference was confirmed by ab initio molecular orbital calculations [32]. Diacetylenic molecules show similar conformational preference, which is, however, reduced as expected [32].

Reactivity of electrophilic addition (bromination) of MeO₂CCCCO₂Me [33] suggests the predominance of the perpendicular conformation. Triple bonds are usually less reactive toward electrophiles than double bonds. PhCCH is brominated 3,000 times more slowly than PhCH=CH₂. However, MeO₂CCCCO₂Me is brominated



Scheme 23 Planar and perpendicular conformers of acetylenes



Scheme 24 Unusually high reactivity of the triple bond of acetylene dicarboxylate in the bromination

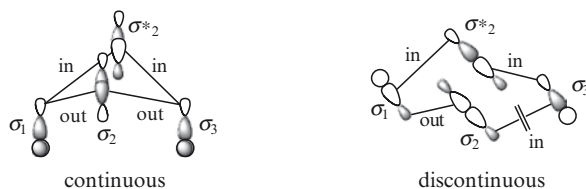
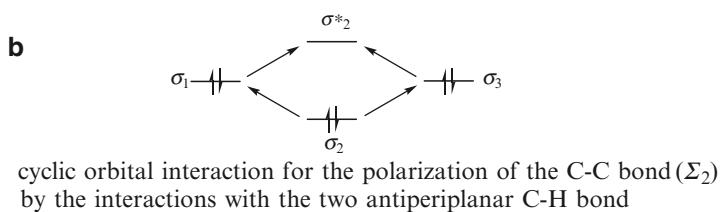
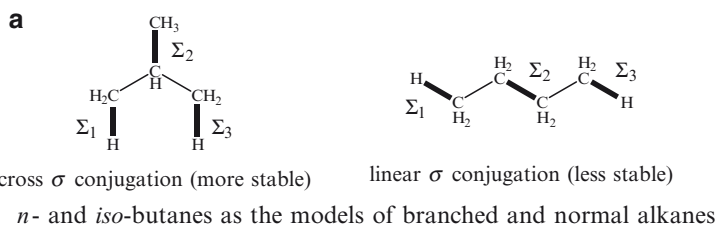
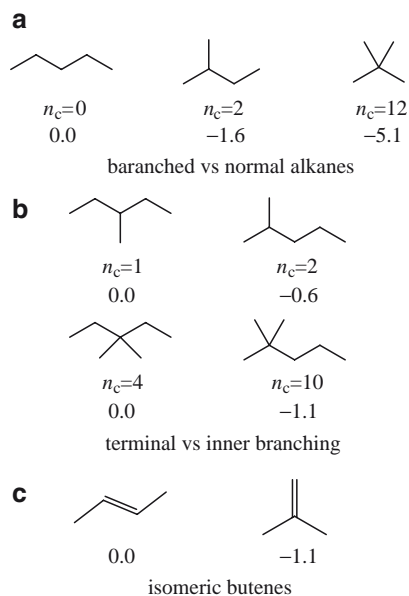
faster than *trans*- $\text{MeO}_2\text{CH}=\text{CHCO}_2\text{Me}$ (Scheme 24). We can easily understand the anomaly when we take the perpendicular conformation of $\text{MeO}_2\text{CCCCO}_2\text{Me}$. A π bond of the acetylene is deactivated by a single CO_2Me group in the perpendicular conformation, while the π bond of $\text{MeO}_2\text{CH}=\text{CHCO}_2\text{Me}$ is deactivated by both CO_2Me groups.

3.5 Preferential Branching of Alkanes

Branching has long been known from the thermochemical data [34, 35] to stabilize alkanes (Scheme 25). The preferential branching seems in disagreement with a familiar rule that steric congestion gives rise to destabilization. The effect of branching on the stability of alkanes has lacked a compelling explanation in the past, though many attempts [36–40] were made. Here, the orbital phase theory is applied to branching effects on the relative stabilities of isomeric alkanes [41].

3.5.1 Origin of Preferential Branching

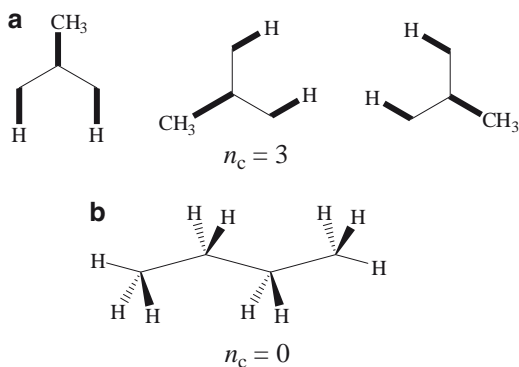
Butanes are chosen as the simplest models for the normal and branched isomers. Both branched and normal isomers contain a C–C bond (Σ_2) interacting with the terminal C–H bonds (Σ_1 and Σ_3) (Scheme 26a). The cyclic $-\sigma_1-\sigma_2^*-\sigma_3-\sigma_2-$ interaction (Scheme 26b) occurs in the polarization of the middle C–C σ -bond by the interactions with the antiperiplanar C–H σ -bonds. The orbital phase is continuous in the branched isomer and discontinuous in the normal isomer (cf. Scheme 4). The branched isomer is more stable. The basic rule of the branching effects on the stability of alkanes is:

Scheme 25 Relative stabilities of branched alkanes (kcal mol⁻¹)**Scheme 26** Orbital phase control over the branching of alkanes

The cross σ conjugation of a C–C bond with two antiperiplanar C–H bonds is more stable than the linear conjugation (Scheme 26).

The number (n_c) of the cross σ conjugations of the trios of a C–C bond and two antiperiplanar C–H bonds is important for the stabilities of alkanes. The cross conjugation number (n_c) of an alkane is defined as that of the conformer where the longest C–C chain has trans a zigzag structure. For example, there are three cross conjugations ($n_c = 3$) in isobutene and none in *n*-butane ($n_c = 0$) (Scheme 27). Isobutane is more stable than *n*-butane [34, 35].

Scheme 27 Numbers (n_c) of the cross σ conjugation trios of a C–C bond and two antiperiplanar C–H bonds in butanes



3.5.2 Rules of Branching

We derived some rules of the branching effects on the stabilities. We used the cross conjugation numbers (n_c).

Rule 1. *Branching stabilizes alkanes: neopentane-type branching stabilizes alkanes more than isobutane-type branching; normal isomers are the least stable.*

There is no cross σ conjugation in normal isomers ($n_c = 0$), while any branching gives rise to at least one cross conjugation ($n_c \neq 0$). For example, the cross conjugation number n_c is 0 for *n*-pentane, 2 for 2-methylbutane, and 12 for neopentane. The stability increases with n_c (Scheme 25).

Rule 2. *Terminal branching stabilizes alkanes more than inner branching.*

Terminal branching gives one more cross conjugation number (n_c) than inner branching (Scheme 25b). For example, the number is 2 for 2-methylpentane and 1 for 3-methylpentane, in agreement with the relative stability. Inner branched isomers have almost the same heat of formation. For example, the difference is very small (0.12 kcal mol⁻¹) between 3- and 4-methylheptanes ($n_c = 1$).

The stability of 2-methylpropene relative to *trans*-2-butene (Scheme 25c) can be understood by the analogy of the cross and linear σ conjugation model. The central

C–C σ bond is replaced by a C=C π bond. The relative stability can also be understood by the analogy of the cross and linear π conjugation in the TMM and BD dianions (Schemes 6 and 7). Lone pair orbitals for the anion centers correspond to the σ_{CH} bonds. The branched butene is more stable than the linear isomer.

The preferential branching in the heavier congeners (E=Si, Ge, and Sn) was confirmed by the ab initio MO and DFT calculations [41].

Five years after our theory of the branching [41], Gronert [42] fit the experimental atomization energies of numerous alkanes within five parameters involving the C–H and C–C bond energies as well as the repulsive geminal bond (C–C–C, C–C–H, H–C–H) interaction energies, and reproduced the effect of branching on the stability of alkanes. Wodrich and Schleyer [43] put forward alternative fits with different parameters including geminal attraction terms. The net attractive character of the most basic 1,3-alkyl-alkyl interaction was evaluated by the bond separation energy procedure to be 2.8 kcal mol⁻¹ stabilization of propane vs methane and ethane. However, the parameter fitting cannot explain why the 1,3-alkyl-alkyl interactions are attractive. The quantities and even the signs associated with the geminal bond interaction energies varied widely and are still disputed. The parameters obtained from the fitting of the experimental data cannot make sense for understanding of nature until the physical base is understood well.

Gronert [42] and Schleyer [43] are not aware of our theory [41]. Branched alkanes are stabilized by the C–C bond polarization by two antiperiplanar C–H bonds. The polarization is favored by the orbital phase continuity. We can predict the relative stabilities of alkanes only by counting the number of the vicinal bond trios. Neither the Gronert nor the Schleyer model contains any vicinal interactions.

Very recently, Zavitsas [44] expressed standard enthalpies of formation of alkanes as a simple sum in which each term consists of the number of hydrogen atoms of different types multiplied by an associated coefficient derived from the known enthalpy of formation of typical molecules.

3.6 *Relative Stabilities of Isomeric Alkyl Species*

It is fairly well known that electronegative groups bind preferentially to tertiary and secondary alkyl groups, whereas electropositive groups prefer primary alkyl groups as was first pointed out for the propyl systems with electronegative groups [45]. The relative stability of carbocations increases in the order: primary < secondary < tertiary species. This is a special example for electronegative groups since the vacant p orbitals on the carbocations are one of the most electron-accepting. The best characterized organometallic systems are the alkyllithium compounds, where, for example, *n*-butyllithium is ca. 2.5 kcal mol⁻¹ more stable than its secondary isomer [46]. Primary alkyl transition metal complexes are usually more stable than secondary and tertiary ones due to the partial carbanionic character of the alkyl group [47].

From the orbital phase theory an outstanding electron-donating (accepting) bond toward both the C–H and C–C bonds is predicted to prefer as long sequential conjugation of mutually antiperiplanar bonds as possible. The electron delocalization

is favored by the orbital phase continuity. This is why electropositive groups prefer primary alkyl groups. The lone pair on the carbanionic center can delocalize through the electron-accepting C–C bonds. Another geminal alkyl chain can similarly promote the electron delocalization. However, the steric congestion between the geminal alkyl chains may destabilize the secondary and tertiary isomers.

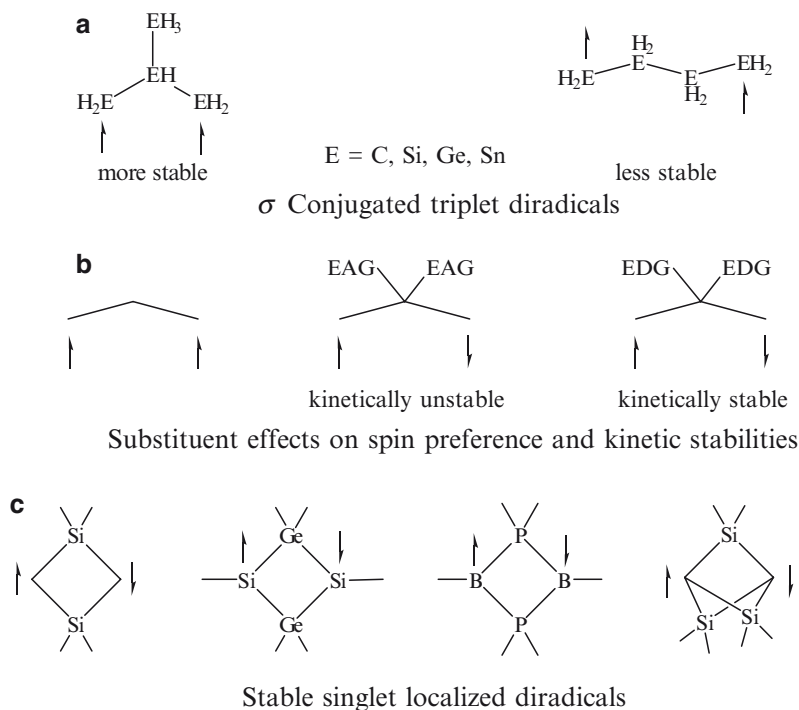
An electron-accepting bond demands donating bonds at the antiperiplanar positions, which are not the C–C bonds but the C–H bonds in the alkyl group. The sequential conjugation is impossible because the hydrogen atom of the C–H bond cannot form any more bonds. The electron-accepting bond then tends to have as many C–H bonds in the antiperiplanar positions as possible. The relative stability increases in the order: primary < secondary < tertiary alkyl compounds. The steric factor is not serious. The conformation with C–H bonds in the antiperiplanar with the electron-accepting bonds does not significantly suffer from steric crowding, as contrasted with the conformation demanded to assume the alkyl chains antiperiplanar with the electron-donating bond.

3.7 Diradicals

Stability of diradicals is important for photochemical reactions. Spin multiplicity of the ground states is critical for the molecular magnetic materials. The relative stability of singlet (triplet) isomers and the spin multiplicity of the ground states (spin preference) [48] has been described to introduce the orbital phase theory in Sects. 2.1.5 and 2.1.6. Applications for the design of diradicals are reviewed by Ma and Inagaki elsewhere in this volume. Here, we briefly summarize the applications.

1. The cross σ conjugated isomers of diradicals E_4H_8 were predicted to be more stable than the linear isomers in the triplet states (Scheme 28a) [49].
2. 2-Substituents of trimethylene diradical change the spin multiplicity of the ground states from the triplet preference of the parent diradical to the singlet preference (Scheme 28b) by lowering the degree (Sect. 2.1.7) of phase discontinuity in the singlet diradical. Electron-accepting groups (e.g., F) at C_2 kinetically destabilize the singlet toward the intramolecular ring closure. The ground states were calculated [50] to be triplet in the parent species and singlet in the disilyl diradical. For the difluoro diradical, the singlet is lower than the triplet in energy, but is a transition state. Recently, C- [51] and Si-centered [52] diradicals (Scheme 28c) were designed and shown to have singlet ground states and to be more stable than the σ bonded bicyclic isomers. Singlet localized B-centered diradicals (Scheme 28c) are known to be indefinitely stable at room temperature both in solution and in the solid state [53]. This unusual stability may be attributed to high electron-donating power of B radicals which lower the degree of the phase discontinuity in the singlet state.
3. Bicyclic localized singlet 1,3- σ -diradicals were theoretically designed by the orbital phase theory (Scheme 28c) [54].

Extensive experimental studies of localized singlet diradicals have been made by Abe and co-workers [55–60]



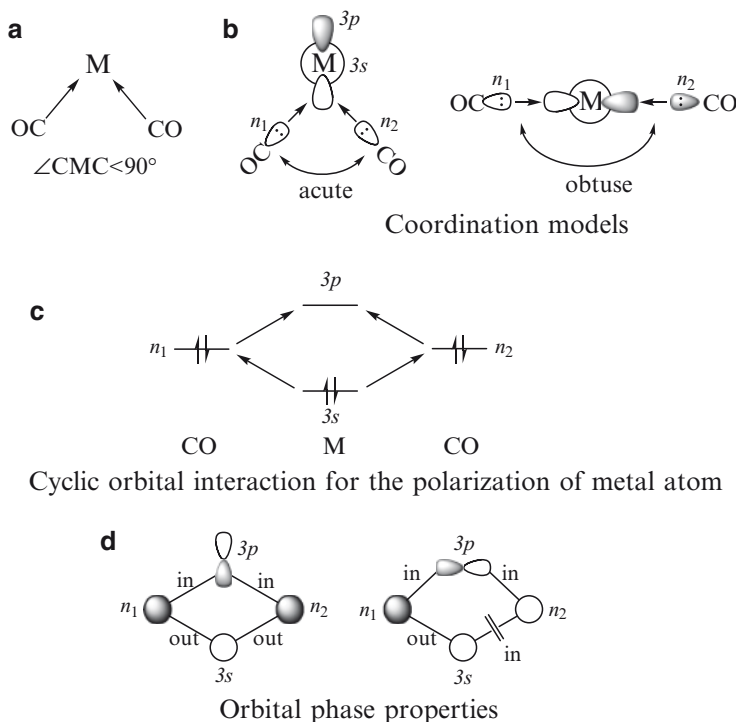
Scheme 28 Spin preference of designed or observed diradicals

3.8 Atomic Polarization for Acute Coordination Angle in Metal Complexes

Matrix isolation spectroscopy showed that the major product of the condensation of Al and CO was not AlCO but Al(CO)₂ [61, 62]. Theoretical studies suggested that the C–Al–C angle in Al(CO)₂ [63] and the C–Si–C angle in Si(CO)₂ [64] should be unusually acute (Scheme 29a). The orbital phase theory accounts for the acute coordination angles and the stability of Al(CO)₂ relative to AlCO [65].

The *n* orbitals on the two CO molecules interact with the same lobe of a vacant 3*p* orbital on a metal atom in the model for the acute angle coordination, and with different lobes for the obtuse angle coordination (Scheme 29b). Cyclic orbital interaction occurs between the occupied 3*s* orbital and the vacant 3*p* orbitals on M and the *n* orbitals, *n*₁ and *n*₂, of the CO molecules (Scheme 29c). The phase is continuous for the same lobe interaction and discontinuous for the different lobe interaction (Scheme 29d, cf. Scheme 4). The acute-angle coordination is favored.

The acute-angle coordinations were similarly predicted for tricoordinated metal complexes [66]. The acute O–Al–O angles of trihydrated aluminum clusters were reported [67].



Scheme 29 Acute coordination angles and atomic polarization in metal complexes $[M(CO)_2]$

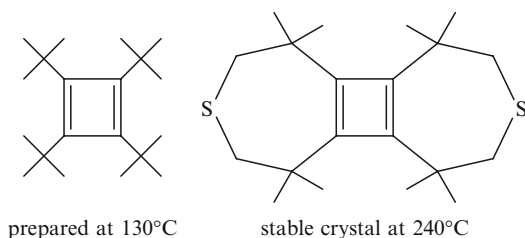
4 Applications to Cyclic Conjugation

Orbitals interact in cyclic manners in cyclic molecules and at cyclic transition structures of chemical reactions. The orbital phase theory is readily seen to contain the Hückel $4n + 2 \pi$ electron rule for aromaticity and the Woodward–Hoffmann rule for the pericyclic reactions. Both rules have been well documented. Here we review the advances in the cyclic conjugation, which cannot be made either by the Hückel rule or by the Woodward–Hoffmann rule but only by the orbital phase theory.

4.1 Kinetic Stability

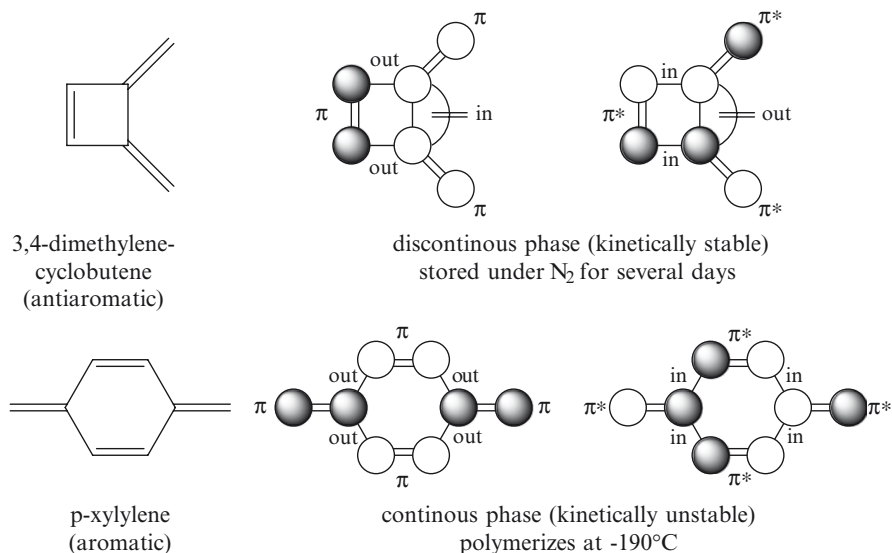
The kinetic stabilities and the donor–acceptor properties of cyclic conjugated molecules [68] have been described (Scheme 12) in the theoretical subsection (Sect. 2.2.2) to be controlled by the phase property. There is a parallelism between the thermodynamic and kinetic stabilities. An aromatic molecule, benzene, is kinetically stable, and an antiaromatic molecule, cyclobutadiene, is kinetically unstable (Scheme 13).

Scheme 30 Kinetically stabilized antiaromatic cyclobutadienes



Cyclobutadiene owes its observed instability much to the kinetic property. Cyclobutadiene dimerizes in the argon matrix above 35 K [69] and only exists for 2–10 ms under low pressure [70, 71]. However, cyclobutadiene is stabilized by bulky substituents (Scheme 30). The *tert*-butyl derivative was quantitatively prepared even at a high temperature (130 °C) [72]. Yellow crystals of the cyclobutadiene fused by two seven-membered rings did not decompose below 240 °C [73].

The parallelism between the thermodynamic and kinetic stabilities is not necessarily found in the cyclic conjugated molecules bearing exocyclic bonds. The calculated resonance energies [74] suggested that 3,4-dimethylenecyclobutene is antiaromatic whereas *o*- and *p*-xylylenes are aromatic. The suggested thermodynamic stability and instability are not in agreement with experimental observations. The cyclobutene derivative can be stored under nitrogen in a refrigerator for several days [75]. *o*-Xylylene photochemically synthesized in rigid glass (−196 °C) dimerizes on melting the glassy solution (ca. −150 °C) [76–79]. *p*-Isomer polymerizes at the moment of condensation at −190 °C [80]. The observed stability/instability can be understood in terms of the kinetic property (Scheme 31, cf. Scheme 4). The phase



Scheme 31 Contrasting thermodynamic and kinetic stabilities

is discontinuous for both bonding and antibonding orbitals in the dimethylenecyclobutene and continuous in the xylylenes. The phase properties show the kinetic stability of dimethylenecyclobutene and the kinetic instability of xylylenes.

Stabilities of cyclic conjugated molecules encountered in the laboratory seem to owe much to kinetic rather than thermodynamic properties. Many unstable conjugated molecules including anti-aromatic molecules are now known to be isolated as stable ones when they are protected by bulky substituents from intermolecular reactions.

4.2 Donor–Acceptor Disposition Isomers

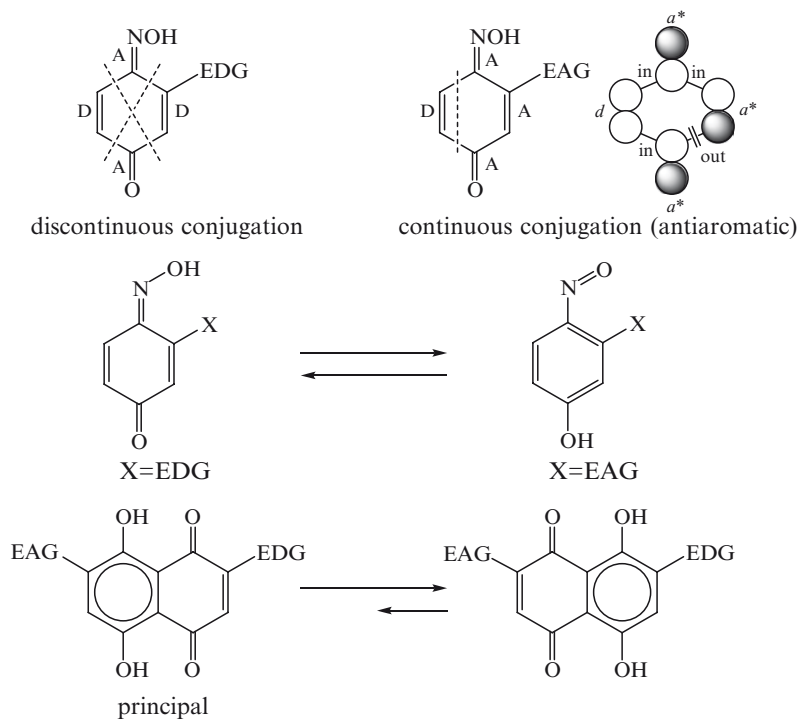
According to the theory of cyclic conjugation, the Hückel rule is applicable only to a continuous cyclic conjugation, but not to a discontinuous one (Schemes 14 and 15). In the discontinuously conjugated molecules, electron donors and acceptors are alternately disposed along the cyclic chain [25]. The thermodynamic stability depends neither on the number of π electrons nor the orbital phase properties, but on the number of neighboring donor–acceptor pairs. Chemical consequences of the continuity-discontinuity of cyclic conjugation are reviewed briefly here.

4.2.1 Tautomerism

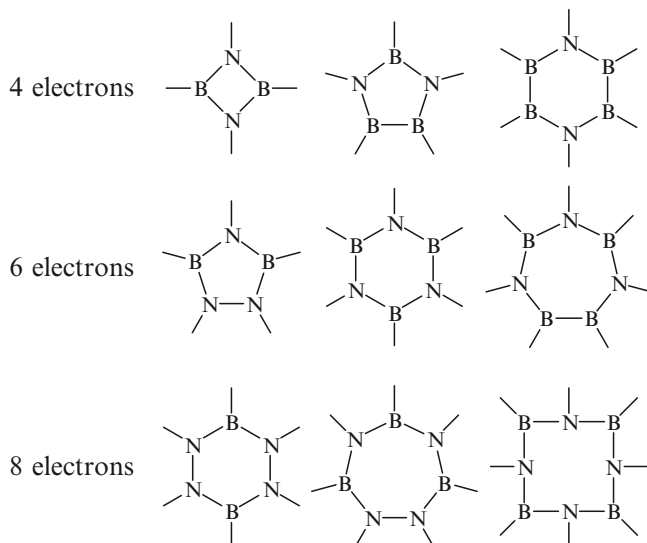
The theory of cyclic conjugation can be applied to the tautomerism (Scheme 32). In 3-substituted 1,4-benzoquinone 4-oximes, the C=C bonds are donors and the C=O and C=N bonds are acceptors. The cyclic conjugation is discontinuous. The orbital phase property is not significant. When an electron-accepting group is introduced on a C=C bond, the C=C bond turns into an acceptor. The cyclic conjugation is continuous and the stability is controlled by the phase property. The phase is discontinuous (cf. Scheme 4). Some destabilization occurs. The nitroso form increases [81]. A similar substituent effect was observed in the naphthazarins [82]. The principal tautomer assumes the quinoid form on the nucleus with an electron-donating group and the benzenoid form on the nucleus with an electron-accepting group.

4.2.2 Inorganic Heterocycles

Almost all known inorganic heterocyclic molecules, where N, O and S atoms with lone pair orbitals are donors while B atoms with vacant p orbitals are acceptors, are classified into discontinuous conjugation. The donors and the acceptors are alternately disposed along the cyclic chain. The thermodynamic stabilities are controlled by the non-cyclic electron delocalization or by the number of neighboring donor–acceptor pairs, but not by the number of π electrons [83]. In fact, both $4n\pi$ and $4n + 2\pi$ electron heterocycles are similarly known [84, 85] (Scheme 33), contradicting the Hückel rule.



Scheme 32 The continuity/discontinuity of cyclic conjugation and the orbital phase determining the equilibrium

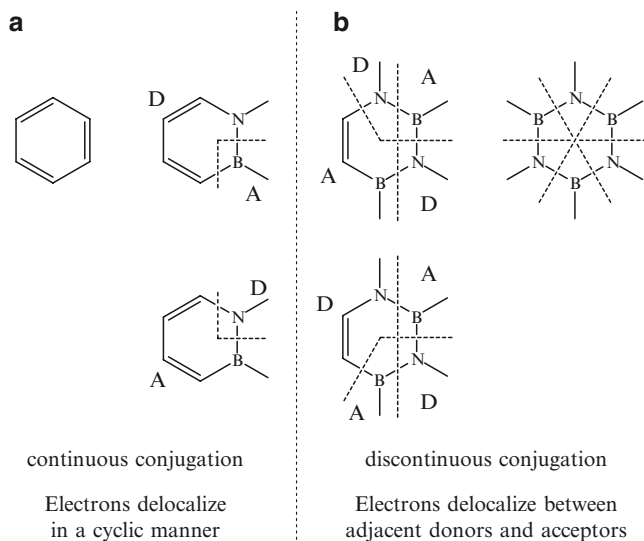


Scheme 33 Known inorganic heterocycles containing N and B atoms

4.2.3 From Aromatic Benzene to Non-Aromatic Borazine

The cyclic conjugation and orbital phase are both continuous in benzene. Electrons delocalize in a cyclic manner. The cyclic conjugation is discontinuous in borazine ($N_3B_3H_6$ in Scheme 33). Electrons cannot delocalize in a cyclic manner, but only between the neighboring pairs of donors and acceptors. There arises a fundamental question how electrons delocalize in the isoelectronic molecules where C=C bonds are replaced with N–B bonds.

Cyclic conjugation is continuous in 1,2-dihydro-1,2-azaborine with one N–B bond (Scheme 34). The nitrogen atom with a lone pair is donor. The B atom with a vacant p orbital is acceptor. Whether the remaining C=C bonds are donors or acceptors, the donors are disposed on one side of the cyclic chain while the acceptors are on the other side. The orbital phase property or the number of electrons is important. The phase continuity or the six π electrons predicts that 1,2-dihydro-1,2-azaborine could be aromatic.



Scheme 34 Cyclic conjugations in benzene and its isoelectronic molecules containing B–N bonds

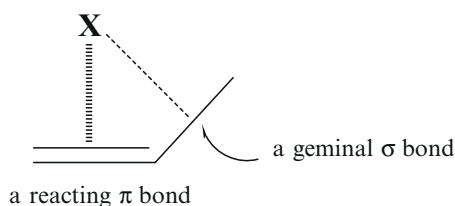
With one more N–B bond, the cyclic conjugation is discontinuous in 1,3,2,4-diazadiborane. The donors and acceptors are alternately disposed along the cyclic chain. Electrons cannot effectively delocalize in a cyclic manner, but between the adjacent donor–acceptor pairs in a non-cyclic manner. The diazadiborane is not predicted to be aromatic.

Ashe has demonstrated that 1,2-azaborines can undergo electrophilic aromatic substitutions [86]. The 1H NMR chemical shifts of 1,2-azaborines are consistent

with the presence of aromatic ring current effects [87]. Liu and co-workers [88] found clear signs of the electron delocalization in the X-ray crystal structures of a derivative of 1,2-hydro-1,2-azaborine, such as a more planar six-membered ring with more homogeneous bond lengths, compared to the partially and fully saturated reference heterocycles.

4.3 Geminal Bond Participation

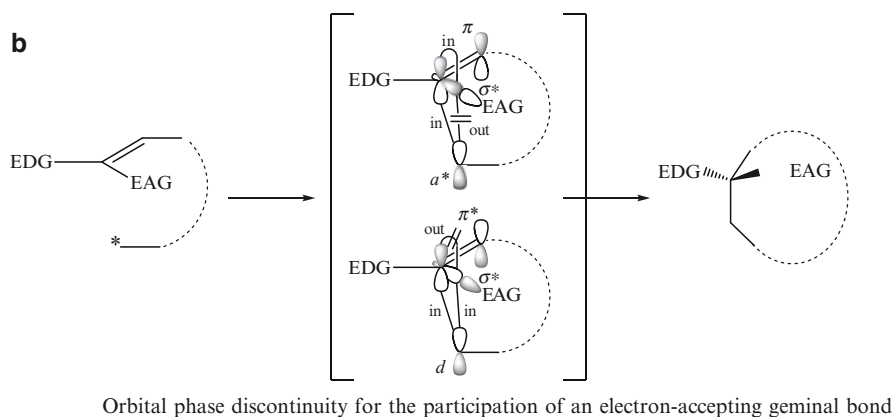
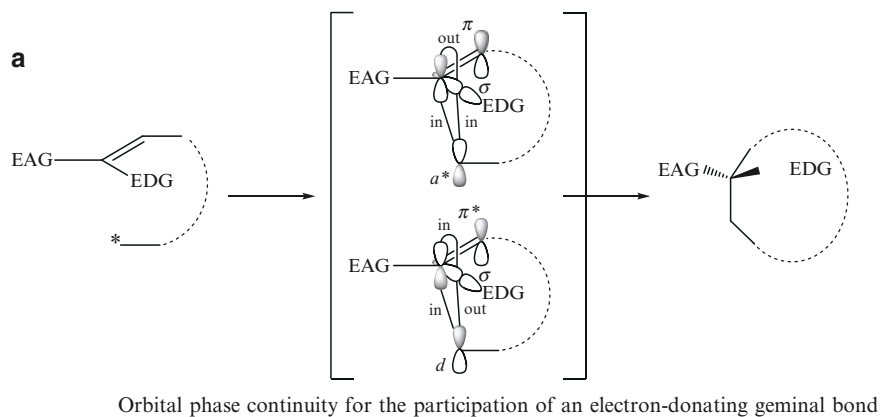
Interactions of vicinal bonds have been extensively studied and are well known as hyperconjugation, resonance, and others [89–91]. The σ bonds *vicinal* to a reacting π bond have been proposed to participate in organic reactions and to control the selectivity [92, 93]. Recently, we noticed the importance of the participation of the σ bonds geminal to a reacting π bond (Scheme 35) [94] and have made extensive applications [95–102]. Here, we present an orbital phase theory for the geminal bond participation and make a brief review.



Scheme 35 Participation of geminal σ bonds

4.3.1 Theory

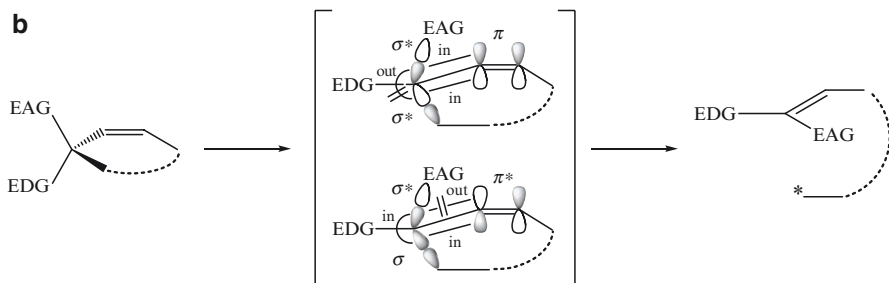
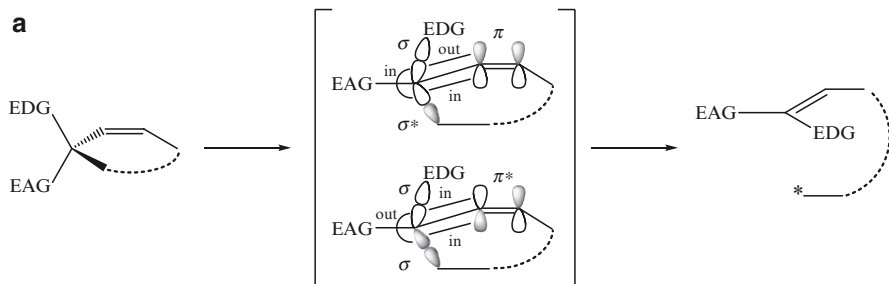
When a π bond reacts, the geminal σ bonds interact not only with a reaction partner but also with the π bond as the reaction center is pyramidized. The cyclic interaction occurs among the π bond, the partner, and the geminal σ bonds. At the cyclic transition states of smaller than a seven-membered ring structure, the geminal σ bond at the *Z*-position preferentially participates due to the geometrical constraint. Delocalization occurs from π to an electron-accepting orbital (a^*) of the partner and from a donating orbital (d) of the partner to π^* . When the geminal σ bond participates as a donor, the orbital phase is continuous (Scheme 36a, cf. Scheme 4). The electron-donating π and σ orbitals combined in phase with a^* are out of phase with each other. The electron-donating d and σ orbitals combined in phase with π^* are also out of phase with each other. The phase relations satisfy the continuity



Scheme 36 Cyclic transition states prefer electron-donating geminal σ bonds at the Z-position in the reactants

conditions. The participation of the electron-donating geminal σ bond is favored by the phase continuity. For the electron-accepting geminal bond, the phase is discontinuous (Scheme 36b) and the participation is disfavored by the phase discontinuity. An electron-donating geminal σ bond at the Z-position of the alkenes accelerates the reaction via a cyclic transition state.

When a π bond forms (Scheme 37), the geminal σ bonds interact with the breaking σ bond and with the π bond next to the reaction center. The cyclic interaction occurs among the breaking σ bond, the geminal σ bonds and the π bond. Main orbital interactions occur between π (π^*) and σ^* (σ) of the breaking bond. The orbital phase is continuous for an electron-donating geminal σ bond (Scheme 37a, cf. Scheme 4) and discontinuous for an electron-accepting geminal bond (Scheme 37b). An electron-donating σ bond prefers the Z-position of the π bond to be formed via cyclic transition states.

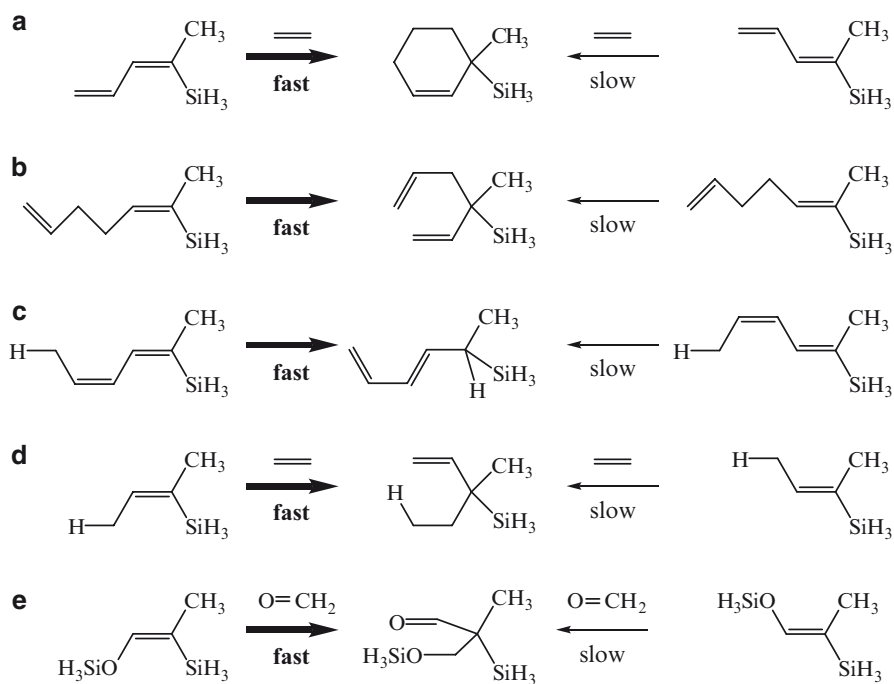


Scheme 37 Electron-donating geminal σ bonds prefer the *Z*-position in products via cyclic transition states

4.3.2 Applications

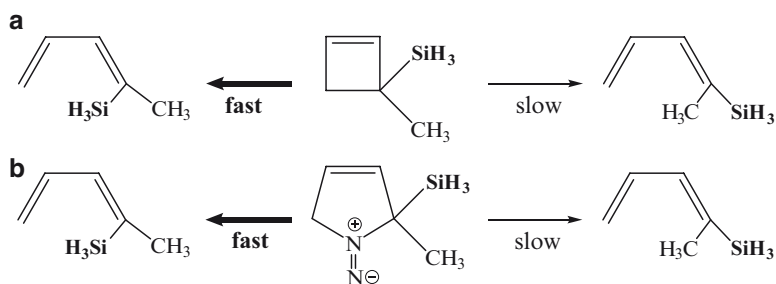
The predictions of the reactivities by the geminal bond participation have been confirmed by the bond model analysis [103–105] of the transition states and the calculations of the enthalpies of activation ΔH^\ddagger of the Diels–Alder reaction [94], the Cope rearrangement [95], the sigmatropic rearrangement [96], the Alder ene reaction [100], and the aldol reaction [101] as are illustrated by the reactions of the methyl silyl derivatives in Scheme 38 [102]. The $\sigma_{\text{C-Si}}$ bond is more electron donating than the $\sigma_{\text{C-C}}$ bond. A silyl group at the *Z*-position enhances the reactivity.

The orbital phase theory for the geminal bond participation is applied to predicting the selectivities. In 2001, the electron-donating geminal σ bonds at the 3-position of cyclobutenes were predicted to rotate inwardly in the ring opening and to occupy the *Z*-position in the products [97]. The cheletropic reactions [100] were also predicted to undergo the inward rotation of the electron-donating geminal σ bonds, affording the *Z*-isomers. The geminal bond participation was supported by the correlation of calculated torquoselectivity ($\Delta\Delta H^\ddagger = \Delta H^\ddagger_{\text{inward}} - \Delta H^\ddagger_{\text{outward}}$) with the σ_{CR} orbital energy of the geminal bonds [99]. The inward rotation is promoted by the electron-donating capability of the σ_{CR} bonds. The torquoselectivity does not



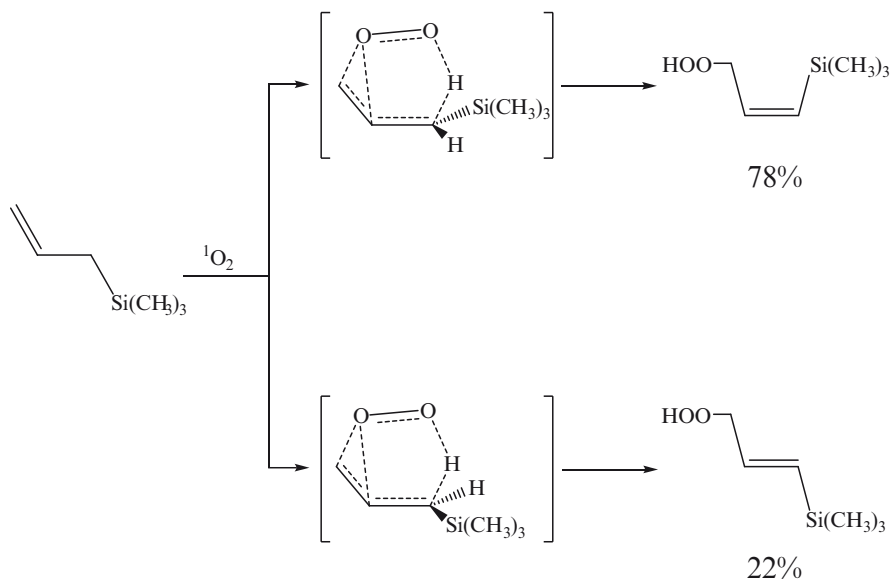
Scheme 38 Geminal bond participation and reactivity

change appreciably for the electronegative substituents, in agreement with the prediction from the geminal bond participation. The σ_{CH} or σ_{CC} bond in the reference substituents is more electron-donating than σ_{CR} and determines the selectivity instead of σ_{CR} . The selectivities of the reactions of the methyl silyl derivatives are illustrated in Scheme 39.



Scheme 39 Geminal bond participation and selectivity

In 1987, more than a decade before our proposal of the geminal bond participation [94], ene reactions of allylsilanes with singlet oxygen was reported to afford the *Z*-isomers more than the *E*-isomers of allylic hydroperoxides (Scheme 40) [106].



Scheme 40 *Z*-Selectivity of ene reactions of allylsilanes with singlet oxygen

The *Z*-selectivity is understood in terms of the geminal bond participation. The C–Si bond, which is more electron-donating than the C–H bond, occupies the *Z*-position.

In 2001, Murakami et al. [107–110] independently reported experimental observation of the inward rotation of the silyl group of the ring opening of cyclobutenes. Shindo and co-workers also observed the preferential inward rotation of the silyl group in the opening of the 3-oxacyclobutene ring [111, 112]. Both groups proposed that the torquoselectivities could be controlled by the vicinal bond participation or the interaction of σ of the breaking σ bond with σ^* of the Si–CH₃ bond in the substituent, according to the Houk hypothesis of the vicinal π bond (lone pair) participation [113–119]: electron-accepting unsaturated groups inwardly rotate due to the attraction with the breaking σ bond whereas the substituents with the lone pair(s) prefer the outward rotation due to the repulsion with the breaking σ bond. Houk and co-workers [119] argued for the vicinal bond participation by Murakami and Shindo. Shindo et al. [120] later emphasized the interaction of the lone pair(s) on the oxygen in the 3-oxacyclobutene ring in place of the breaking σ bond.

The unsaturated substituents with low-lying vacant orbitals were found [99] to favor the inward rotation more than expected from the geminal bond participation.

The additional preference of the inward rotations is expected from vicinal bond participation or Rondan–Houk hypothesis.

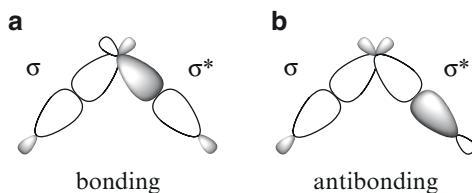
The geminal bond participation [94–102] is expected to advance organic chemistry, but still remains unexplored, especially by experiments.

4.4 Relaxation of Strain of Small Ring Molecules

Strain of small ring molecules cannot be fully understood in terms of the deviation of the bond angles from the ideal ones of the hybrid orbitals. The mechanism of the relaxation of the strain has been proposed. Here, we briefly review σ relaxation by the $\sigma \rightarrow \sigma^*$ interactions between the geminal σ bonds in the rings and π relaxation by the $\pi \rightarrow \sigma^*$ interaction between the endocyclic π bond with the vicinal σ bonds on the ring atoms. A more detailed review is made by Naruse and Inagaki elsewhere in this volume.

4.4.1 σ Relaxation

Interactions of the chemical bonds at the geminal positions are expected to be important although not a great deal of attention has been given to them so far, compared with those at the vicinal positions. Surprisingly, the interaction of the bonding orbital of a σ bond with σ^* of a geminal bond can be antibonding as well as bonding (Scheme 41) [121], depending on the orbital phase relation between σ and σ^* . The bonding and anti-bonding properties of the geminal σ – σ^* interactions lead to a mechanism of σ relaxation of small ring strains [121–127]. The antibonding property decreases with the acuteness of the bond angle. The geminal σ – σ^* interaction has been applied [121] to almost the same strain energies of cyclopropane (27.5 kcal mol⁻¹) and cyclobutane (26.5 kcal) in spite of 2.5 times greater deviation of the bond angle of cyclopropane from the sp³ valence angle. The antibonding property of the geminal σ – σ^* interaction increases in silanes and decreases in phosphanes in agreement with the high strain of cyclosilane and low strain of cyclophosphanes [122]. For the nitrogen ring molecules N_nH_n, the antibonding property of the geminal σ – σ^* interaction is reduced in the three-membered ring and enhanced in the four-membered ring, compared to that in open chain molecules. The three-membered ring is surprisingly less strained than the four-membered ring [123]. Furthermore, the geminal σ – σ^* interaction gives insight into the origins of *inverted tetrahedral configurations* of the bridgehead carbons in the bicyclo[1.1.0]butane frameworks [124], and into the effects of the *inverted bond* on the strains of the [1.1.1]propellane frameworks [125]. Recently, tricyclo[2.1.0.0^{1,3}]pentasilane has been designed and predicted to undergo a novel degenerate rearrangement of distorted three-membered rings [126]. A derivative has been synthesized independently [128]. Introduction of phosphorus atoms into the tricyclo[2.1.0.0^{1,3}]pentane structure has been found to relax the ring strain due to the lone pair effect on the geminal σ – σ^* interaction [127].



Scheme 41 Geminal $\sigma \rightarrow \sigma^*$ interactions

The antibonding properties of the geminal $\sigma\text{--}\sigma^*$ interactions has recently led to a theory of electron *localization* and its successful application to blue-shifting hydrogen bonds [129].

4.4.2 π Relaxation

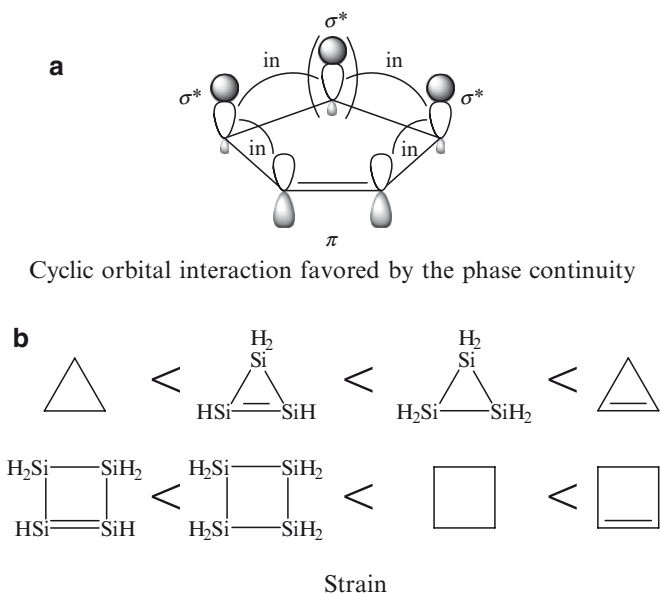
π Relaxation mechanism was also proposed [130–133]. The π relaxation originates from cyclic delocalization of π electrons in the double bond through the hyperconjugation with σ bonds on the saturated ring atoms under control of the orbital phase property [134, 135].

The cyclic (π , σ^* , ... σ^*) interaction is favored by the phase continuity (Scheme 42a, cf. Scheme 4). The cyclic delocalization of π electrons significantly occurs in the molecules with π and σ^* high and low in energy, respectively. The π relaxation is expected to be remarkable in the unsaturated silicon congeners. The electron-donating π orbital of a Si=Si bond is higher in energy than that of a C=C bond, while an electron-accepting σ^*_{SiH} orbital is lower than that of a σ^*_{CH} orbital. In fact, the calculated strain energies showed appreciable π relaxation of the ring strains of the unsaturated silicon congeners (Scheme 42b). Introduction of a double bond into cyclosilanes reduces the ring strain, causing a contrast with cycloalkanes. For example, cyclopropene is more strained than cyclopropane [136]. The relative orders of the ring strain for the monocyclic molecules are applicable to the polycyclic small ring molecules [135]. Some polycyclic silicon molecules have been designed and shown to be thermodynamically stable enough, especially for the unsaturated ones to be synthetic targets. A derivative of spiro[2.2]pentasiladiene has been prepared [132].

Observed geometrical features or stabilities of small ring molecules containing an endocyclic double bond have been explained in terms of the $\pi\text{--}\sigma^*$ interactions [137, 138]. The π relaxation is predicted to stabilize such small ring unsaturated molecules of heavy atoms recently prepared [139–142].

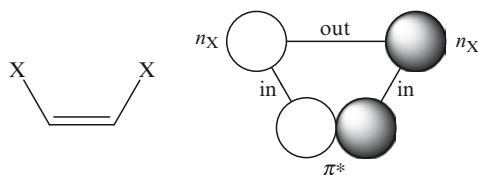
4.5 Relative Stabilities of *cis*-Isomers

Some *cis*-isomers are more stable than the *trans*-isomers. Yamamoto and Tomoda [143] estimated the energies of bond interactions in 1,2-haloethenes and proposed



Scheme 42 π Relaxation of ring strain

that the cyclic delocalization of lone pairs through the $\pi_{C=C}$ bond favored by the orbital phase continuity (Scheme 43) could be the dominant factor in stabilizing the *cis*-isomers. The cyclic delocalization of lone pairs also contributes to the *cis* preference of 1,2-halodiazenes [144].

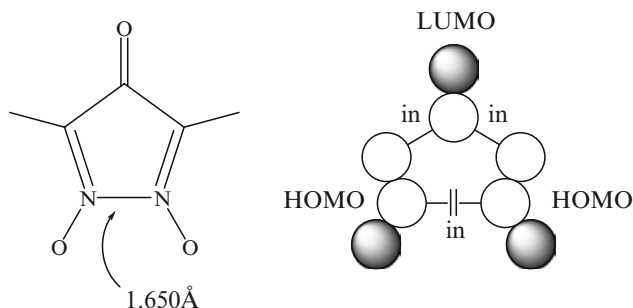


Scheme 43 Orbital phase continuity stabilizes the *cis*-isomers

4.6 Long N–N Bonds in Cyclic Conjugated Molecules

Harano and co-workers [145] showed an unusually long N–N bond (1.65 Å) in 2,5-dimethylpyrazolone-*N,N*-dioxide by X-ray analysis. The pyrazolone *N,N*-dioxide ring was taken as a continuously conjugate system composed of two electron-donating nitrono moieties and an electron-accepting carbonyl group. The orbital phase plays a crucial role in the property of the cyclic conjugate molecule. The phase is discontinuous (Scheme 44, cf. Scheme 4). The long N–N bond was suggested to

stem from the antiaromatic character. Harano et al. [146] also discussed the long N–N bond in the six-membered ring of furazano[3,4-*d*]pyridazine 5,6-dioxide in a similar manner.



Scheme 44 Long N–N bonds and orbital phase discontinuity in pyrazolone *N,N*-dioxides

Note added in proof

A review article on the topics related to the geminal bond partition (Sect. 4.3) has appeared very recently [Shindo M, Mori S (2008) *Synlett* 2231].

Acknowledgements The author thanks Prof. Hisashi Yamamoto of the University of Chicago for his reading of the manuscript and his encouragement, Messrs. Hiroki Murai and Hiroki Shimakawa for their assistance in preparing the manuscript, and Ms. Jane Clarkin for the English suggestions.

References

1. Robinson R (1932) Outline of an electrochemical (electronic) theory of the course of organic reactions. The Institute of Chemistry of Great Britain and Ireland, London
2. Ingold CK (1934) *Chem Rev* 15:225
3. Lennard-Jones JE (1929) *Trans Faraday Soc* 25:668
4. Fukui K (1964) In: Loewdin P-O, Pullman B (eds) *Molecular orbitals in chemistry, physics, and biology*. Academic Press, London, p 513
5. Fukui K (1971) *Acc Chem Res* 4:57
6. Fukui K (1975) *Theory of orientation and stereoselection*. Springer, Berlin Heidelberg New York
7. Woodward RB, Hoffmann R (1969) *Angew Chem Int Ed Engl* 8:781
8. Hoffmann R, Woodward RB (1970) *The conservation of orbital symmetry*. Academic, New York
9. Hoffmann R, Woodward RB (1965) *J Am Chem Soc* 87:4388
10. Hueckel E (1931) *Z Phys* 70:204

11. Zimmerman HE (1971) *Acc Chem Res* 4:272
12. van der Hart WJ, Mulder JJC, Oosteroff LJ (1972) *J Am Chem Soc* 94:5724
13. Fukui K, Inagaki S (1975) *J Am Chem Soc* 97:4445
14. Inagaki S, Fujimoto H, Fukui K (1976) *J Am Chem Soc* 98:4693
15. Inagaki S, Kawata H, Hirabayashi Y (1982) *Bull Chem Soc Jpn* 55:3724
16. Klein J, Medlik A (1973) *J Chem Soc Chem Comm* 275
17. Mills NS, Shapiro J, Hollingworth M (1981) 103:1263
18. Gund P (1972) *J Chem Educ* 49:100
19. Iwase K, Inagaki S (1993) *Chem Lett* 22:1619
20. Iwase K, Inagaki S (1996) *Bull Chem Soc Jpn* 69:2781
21. Osamura Y, Borden WT, Morokuma K (1984) *J Am Chem Soc* 106:5112
22. Coolidge MB, Yamashita K, Morokuma K, Borden WT (1990) *J Am Chem Soc* 112:1751
23. Ichimura AS, Lahti PM, Matlin AR (1990) *J Am Chem Soc* 112:2868
24. Hirano T, Kumagai T, Miyashi T, Akiyama K, Ikegami Y (1991) *J Org Chem* 56:1907
25. Inagaki S, Hirabayashi Y (1977) *J Am Chem Soc* 99:7418
26. Inagaki S, Iwase K, Goto N (1986) *J Org Chem* 51:362
27. Agranat I, Skancke A (1985) *J Am Chem Soc* 107:867
28. Skancke A (1994) *J Phys Chem* 98:5234
29. Inagaki S (1984) *Bull Chem Soc Jpn* 57:3599
30. Epiotis ND (1973) *J Am Chem Soc* 95:5624
31. Inagaki S, Ohashi S (1999) *Theor Chem Acc* 102:65
32. Ohashi S, Inagaki S (2001) *Tetrahedron* 57:5361
33. March J (1992) *Advanced organic chemistry*. Wiley, New York
34. Pedley JB, Naylor BD, Kirby SD (1986) *Thermochemical data of organic compounds*, 2nd edn. Chapman & Hill, London
35. Lide DR, Kehiaian HV (1994) *Handbook of thermophysical and thermochemical data*. CRC Press, Boca Raton
36. Ito K (1953) *J Am Chem Soc* 75:2430
37. Pitzer PS, Catalano E (1956) *J Am Chem Soc* 78:4844
38. Bartell LS (1962) *Tetrahedron* 17:177
39. Wiberg KB, Bader RFW, Lau CDH (1987) *J Am Chem Soc* 109:1001
40. Laidig KE (1991) *J Phys Chem* 95:7709
41. Ma J, Inagaki S (2001) *J Am Chem Soc* 123:1193
42. Gronert S (2006) *J Org Chem* 71:1209
43. Wodrich MD, Schleyer PvR (2006) *Org Lett* 8:2135
44. Zavitsas AA, Matsunaga N, Rogers DW (2008) *J Phys Chem A* 112:5734
45. Robinson GC (1967) *J Org Chem* 32:1963
46. Arnett EM, Moe KD (1991) *J Am Chem Soc* 113:7068
47. Harvey JN (2001) *Organometallics* 20:4887
48. Iwase K, Inagaki S (1996) *Bull Chem Soc Jpn* 69:2781
49. Ma J, Ikeda H, Inagaki S (2001) *Bull Chem Soc Jpn* 74:273
50. Skancke A, Hrovat DA, Borden WT (1998) *J Am Chem Soc* 120:7079
51. Ma J, Ding Y-H, Hattori K, Inagaki S (2004) *J Org Chem* 69:4245
52. Wang Y, Ma J, Inagaki S (2004) *J Phys Org Chem* 20:649
53. Scheschkewitz D, Amii H, Gornitzka H, Schoeller WW, Bourissou D, Bertrand G (2002) *Science* 295:1880
54. Wang Y, Ma J, Inagaki S (2005) *Tetrahedron Lett* 46:5567
55. Abe M, Kawanami S, Ishihara C, Tategami A (2004) *J Org Chem* 69:7250
56. Abe M, Adam W, Borden WT, Hattori M, Hrovat A, Nojima M, Nozaki K, Wirz J (2004) *J Am Chem Soc* 126:574
57. Abe M, Kawanami S, Ishihara C, Nojima M (2004) *J Org Chem* 69:5622
58. Abe M, Kawanami S, Masuyama A, Hayashi T (2006) *J Org Chem* 71:6607
59. Abe M, Hattori M, Takegami A, Masuyama A, Hayashi T, Seki S, Tagawa S (2006) *J Am Chem Soc* 128:8008

60. Abe M, Kube E, Nozaki K, Matsuo T, Hayashi T (2006) *Angew Chem Int E* 45:7828
61. Kasai PH, Jones PM (1984) *J Am Chem Soc* 106:8018
62. Chenier JHB, Hampson CA, Howard JA, Mile B, Sutcliffe R (1986) *J Phys Chem* 90:1524
63. Balaji V, Sunil KK, Jordan KD (1987) *Chem Phys Lett* 136:309
64. Grev RS, Schaefer HF III (1989) *J Am Chem Soc* 111:5687
65. Sakai S, Inagaki S (1990) *J Am Chem Soc* 112:7961
66. Iwase K, Sakai S, Inagaki S (1994) *Chem Lett* 23:1601
67. Watanabe H, Aoki M, Iwata S (1993) *Bull Chem Soc Jpn* 66:3245
68. Inagaki S, Iwase K (1984) *Nouv J Chim* 8:73
69. Chapman OL, McIntosh CL, Pacansky J (1973) *J Am Chem Soc* 95:614
70. Tyerman WJR, Kato M, Kebarle P, Masamune S, Strausz OP, Gunning HE (1967) *Chem Commun* 497
71. Hedaya E, Miller RD, McNeil DW, D'Angelo PF, Schissel P (1969) *J Am Chem Soc* 91:1875
72. Maier G, Pfriem S, Schaefer U, Matusch R (1978) *Angew Chem* 90:552
73. Kimling H, Krebs A (1972) *Angew Chem* 84:952
74. Hess BA, Schaad LJ (1971) *J Am Chem Soc* 93:305
75. Huntsman WD, Wristers HJ (1963) *J Am Chem Soc* 85:3308
76. Migirdicyan E (1968) *C R Acad Sci Ser C* 266:756
77. Flynn CR, Michl J (1973) *J Am Chem Soc* 95:5802
78. Flynn CR, Michl J (1974) *J Am Chem Soc* 96:3280
79. Migirdicyan E, Baudet J (1975) *J Am Chem Soc* 97:7400
80. Auspos LA, Hall LAR, Hubbard JK, Kirk W Jr, Schaeffgen JR, Speck SB (1955) *J Polymer Sci* 15:9
81. Norris RK, Sternhell S (1972) *Aust J Chem* 25:2621
82. Moore RE, Scheuer PJ (1966) *J Org Chem* 31:3272
83. Inagaki S, Hirabayashi Y (1982) *Inorg Chem* 21:1798
84. Finch A, Leach JB, Morris JH (1969) *Organomet Chem Rev A* 4:1
85. Haiduc I (1970) *The chemistry of inorganic ring systems*. Wiley, New York, Part 1
86. Pan J, Kampf JW, Ashe AJ III (2007) *Org Lett* 9:679
87. Ashe AJ III, Fang X, Fang X, Kampf JW (2001) *Organometallics* 20:5413
88. Abbey ER, Zakharov LV, Liu S-Y (2008) *J Am Chem Soc* 130:7250
89. Pine SH (1987) *Organic chemistry*, 5th edn. McGraw-Hill, New York, Chap 7
90. Morrison RT, Boyd RN (1992) *Organic chemistry*, 6th edn. Prentice Hall International, London, Chap 11
91. Kirby AJ (1996) *Stereoelectronic effect*. Oxford University Press, Oxford, Chap 6
92. Cherest M, Felkin H, Prudent N (1968) *Tetrahedron Lett* 2199
93. Anh TD, Eisenstein O (1977) *Nouv J Chim* 1:61
94. Inagaki S, Ikeda H (1999) *J Org Chem* 63:7820
95. Ikeda H, Naruse Y, Inagaki S (1999) *Chem Lett* 28:363
96. Ikeda H, Ushioda N, Inagaki S (2001) *Chem Lett* 30:166
97. Ikeda H, Kato T, Inagaki S (2001) *Chem Lett* 30:270
98. Naruse Y, Hayashi Y, Inagaki S (2003) *Tetrahedron Lett* 44:8509
99. Yasui M, Naruse Y, Inagaki S (2004) *J Org Chem* 69:7246
100. Naruse Y, Suzuki T, Inagaki S (2005) *Tetrahedron Lett* 46:6937
101. Naruse Y, Fukasawa S, Ota S, Deki A, Inagaki S (2007) *Tetrahedron Lett* 48:817
102. Naruse Y, Inagaki S (2007) *Chem Lett* 36:820
103. Iwase K, Inagaki S (1996) *Bull Chem Soc Jpn* 69:2781
104. Inagaki S, Yamamoto T, Ohashi S (1997) *Chem Lett* 26:977
105. Ikeda H, Inagaki S (2001) *J Phys Chem A* 4710:71
106. Shimizu N, Shibata F, Imazu S, Tsuno Y (1987) *Chem Lett* 16:1071
107. Murakami M, Miyamoto Y, Ito Y (2001) *Angew Chem Int Ed* 40:189
108. Murakami M, Miyamoto Y, Ito Y (2001) *J Am Chem Soc* 123:6441
109. Murakami M, Hasegawa M, Igawa H (2004) *J Org Chem* 69:587

110. Murakami M, Usui I, Hasegawa M, Matsuda T (2005) *J Am Chem Soc* 127:1366
111. Shindo M, Matsumoto K, Mori S, Shishido K (2002) *J Am Chem Soc* 124:6840
112. Mori S, Shindo M (2004) *Org Lett* 6:3945
113. Kirmse W, Rondan NG, Houk KN (1984) *J Am Chem Soc* 106:7989
114. Rondan NG, Houk KN (1985) *J Am Chem Soc* 107:2099
115. Rudolf K, Spellmeyer DC, Houk KN (1987) *J Org Chem* 52:3708
116. Buda AB, Wang Y, Houk KN (1989) *J Org Chem* 54:2264
117. Jefford CW, Bernardinelli G, Wang Y, Spellmeyer DC, Buda A, Houk KN (1992) *J Am Chem Soc* 114:1157
118. Nakamura K, Houk KN (1995) *J Org Chem* 60:686
119. Lee PS, Zhang X, Houk KN (2003) *J Am Chem Soc* 125:5072
120. Mori S, Shindo M (2004) *Org Lett* 6:3945
121. Inagaki S, Goto N, Yoshikawa K (1991) *J Am Chem Soc* 113:7144
122. Inagaki S, Yoshikawa K, Hayano Y (1993) *J Am Chem Soc* 115:3706
123. Inagaki S, Ishitani Y, Kakefu T (1994) *J Am Chem Soc* 116:5954
124. Inagaki S, Kakefu T, Yamamoto T, Wasada H (1996) *J Phys Chem* 100:9615
125. Inagaki S, Yamamoto T, Ohashi S (1997) *Chem Lett* 26:977
126. Takeuchi K, Uemura D, Inagaki S (2005) *J Phys Chem A* 109:8632
127. Takeuchi K, Horiguchi A, Inagaki S (2005) *Tetrahedron* 61:2601
128. Scheshcekewitz D (2005) *Angew Chem Int Ed* 44:2954
129. Inagaki S, Takeuchi T (2005) *Chem Lett* 34:750
130. Goller A, Heydt H, Clark T (1996) *J Org Chem* 61:5840
131. Tsutsui S, Sakamoto K, Kabuto C, Kira M (1998) *Organometallics* 17:3819
132. Iwamoto T, Tamura M, Kabuto C, Kira M (2000) *Science* 290:504
133. Göller A, Clark T (2000) *J Mol Model* 6:133
134. Naruse Y, Ma J, Inagaki S (2001) *Tetrahedron Lett* 42:6553
135. Naruse Y, Ma J, Takeuchi K, Nohara T, Inagaki S (2006) *Tetrahedron* 62:4491
136. Cox JD, Plicher G (1970) *Thermochemistry of organic and organometallic compounds*. Academic Press, London
137. Lee VY, Takanashi K, Nakamoto M, Sekiguchi A (2004) *Russ Chem Bull* 53:1102
138. Sase S, Kano N, Kawashima T (2006) *J Org Chem* 71:5448
139. Kira M, Iwamoto T, Kabuto C (1996) *J Am Chem Soc* 118:10303
140. Wiberg N, Auer H, Noth H, Knizek J, Polborn K (1998) *Angew Chem Int Ed* 37:2869
141. Ichinohe M, Matsuno T, Sekiguchi A (1999) *Angew Chem Int Ed* 38:2194
142. Fukawa T, Lee VY, Nakamoto M, Sekiguchi A (2004) *J Am Chem Soc* 126:11758
143. Yamamoto T, Kaneno D, Tomoda S (2008) *Bull Chem Soc Jpn* 81:1415
144. Yamamoto T, Kaneno D, Tomoda S (2008) *J Org Chem* 73:5429
145. Yoshitake Y, Eto M, Harano K (1998) *Tetrahedron Lett* 39:2761
146. Yoshitake Y, Eto M, Harano K (1999) *Chem Pharm Bull* 47:601

Orbital Phase Environments and Stereoselectivities

Tomohiko Ohwada

Abstract Facial selections are reviewed to propose a new theory, *orbital phase environment*, for stereoselectivities of organic reactions. The orbital phase environment is a generalized idea of the secondary orbital interaction between the non-reacting centers and the unsymmetrization of the orbitals at the reacting centers arising from in-phase and out-of-phase overlapping with those at the neighboring non-reacting sites. In this context, the nucleophilic addition preferentially occurs on the face of the carbonyl functionality opposite to the better electron-donating orbital at the β position. In a similar manner to the carbonyl cases, the preferred reaction faces of olefins in electrophilic addition reactions are opposite to the better electron-donating orbitals at the β positions. The orbital phase environments in Diels-Alder reactions are also reviewed.

Keywords Facial selection, Orbital phase, Secondary orbital interaction, Orbital unsymmetrization, Ketones, Olefins, Diels-Alder dienophiles, Diels-Alder dienes, Michael acceptor, Amine nitrogen atom

Contents

1	Orbital Phase Environments.....	130
1.1	Orbital Unsymmetrization by Overlapping	130
1.2	Secondary Orbital Interactions	131
1.3	Orbital Phase Environments	131
2	Stereoselection of Ketones.....	132
2.1	Cycloalkane System: Cyclohexanone Case.....	132
2.2	Orbital Phase Environment Unsymmetrization of Carbonyl π^* Orbitals by Interaction with β - σ Orbitals	133
2.3	π - π Interaction System.....	142
3	Stereoselection of Olefins	145
3.1	Methylenecyclohexane Case.....	145

T. Ohwada

Graduate School of Pharmaceutical Sciences, The University of Tokyo, 7-3-1 Hongo,
Bunkyo-ku, Tokyo, 113, Japan
e-mail: ohwada@mol.f.u-tokyo.ac.jp

3.2	Interaction of σ Orbitals at the β -Position with the Olefin π Orbitals.....	147
3.3	Effects of Different Arrangements of Composite Molecules	153
3.4	Overlapping of Olefin π Orbital with π Orbitals at the β Positions.....	157
3.5	Two π Component System. Validation of Orbital Size Effect on the Magnitude of Facial Selectivity	159
4	Stereoselection of Diels–Alder Reactions: Dienophiles.....	161
4.1	Dienophiles Based on Norbornane Structure.....	162
4.2	Dienophiles Based on Dibenzobicyclo[2.2.2]octatriene Structure.....	164
5	Stereoselection of Diels–Alder Dienes	166
5.1	Cyclopentane Case.....	166
5.2	Cyclohexadiene Case.....	169
6	Stereoselection of Nucleophilic Conjugate Addition	171
6.1	Bicyclic Systems.....	171
7	Detection of Orbital Interactions in Alternative Component.....	172
7.1	Nitration of Fluorene Derivatives	172
8	Orbital Interaction Affects Bond Strength of <i>N</i> -Nitroso Bond.....	174
8.1	Facial Selectivity of Amine Non-Bonding Orbital	174
8.2	N–NO Bond Cleavage of <i>N</i> -Nitrosamines.....	175
9	Conclusion	177
	References.....	177

1 Orbital Phase Environments

sp^2 and sp -carbon atoms such as a carbonyl group and an alkene are reactive centers in many kinds of reactions. The π orbitals of a simple molecule such as ethylene or formaldehyde are symmetric in magnitude and antisymmetric in sign with respect to reflection in the molecular plane. Various attempts have been made to rationalize stereoselectivities, and several general ideas have emerged, including a steric basis and an orbital basis.

Steric repulsions come from two orbital–four electron interactions between two occupied orbitals. Facially selective reactions do occur in sterically unbiased systems, and these facial selectivities can be interpreted in terms of unsymmetrical π faces. Particular emphasis has been placed on the dissymmetrization of the orbital extension, i.e., *orbital distortions* [1, 2]. The orbital distortions are described in (Chapter “Orbital Mixing Rules” by Inagaki in this volume). Here, we review the effects of *unsymmetrization of the orbitals due to phase environment in the vicinity of the reaction centers* [3].

1.1 Orbital Unsymmetrization by Overlapping

Deformation of symmetrical orbital extension of carbonyl or olefin compounds was proposed to be the origin of the facial selectivities. We illustrate the unsymmetrical orbital phase environment of π orbitals of carbonyl and olefin groups and facial selectivities in Fig. 1 [3, 4]. There are in-phase and out-of-phase combinations of

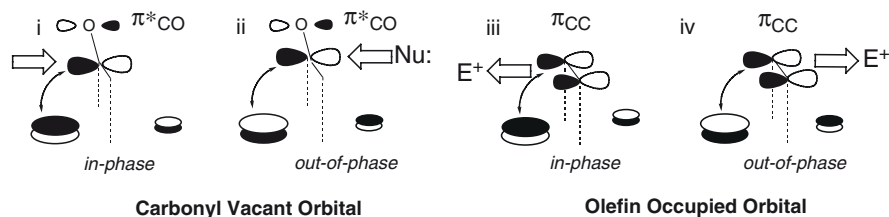


Fig. 1 Unsymmetrical orbital phase environment and preferential attack of reagents

π orbitals at the reaction centers and orbitals of the substituents in the vicinity. Electron “density” in the in-phase combined orbitals increases in the overlap region (i and iii in Fig. 1). The out-of-phase mixing of orbitals (ii and iv in Fig. 1) depletes electron density from the overlap region.

1.2 Secondary Orbital Interactions

Secondary orbital interactions (SOI) (Fig. 2) [5] between the non-reacting centers have been proposed to determine selectivities. For example, cyclopentadiene undergoes a cycloaddition reaction with acrolein **1** at 25 °C to give a norbornene derivative (Fig. 2a) [6]. The *endo* adduct (74.4%) was preferred over the *exo* adduct (25.6%). This *endo* selectivity has been interpreted in terms of the in-phase relation between the HOMO of the diene at the 2-position and the LUMO at the carbonyl carbon in the case of the *endo* approach (Fig. 2c). An unfavorable SOI (Fig. 2d) has also been reported for the cycloaddition of cyclopentadiene and acetylenic aldehyde **2** and its derivatives (Fig. 2b) [7–9]. The *exo*-TS has been proposed to be favored over the *endo*-TS.

1.3 Orbital Phase Environments

The SOI concept is akin to the unsymmetrization of orbitals. The only difference is in the sites of the subsidiary interactions, which occur between the non-reacting centers (positions 3 and 4 in Fig. 3a) in SOI and between the reacting and non-reacting centers (sites 2 and 3 in Fig. 3b) for the unsymmetrization of orbitals (Fig. 1). The *orbital phase environment* around the reaction centers is a general idea.

In this review we will focus on the *unsymmetrization of the orbital phase environment in the vicinity of reacting π systems*, and its effect on *facial selectivities*. This idea can be applied to many kinds of recently observed facial selectivities, such as those involving ketones [10–21], olefins [22–31], dienes [32–46] and others [47–49].

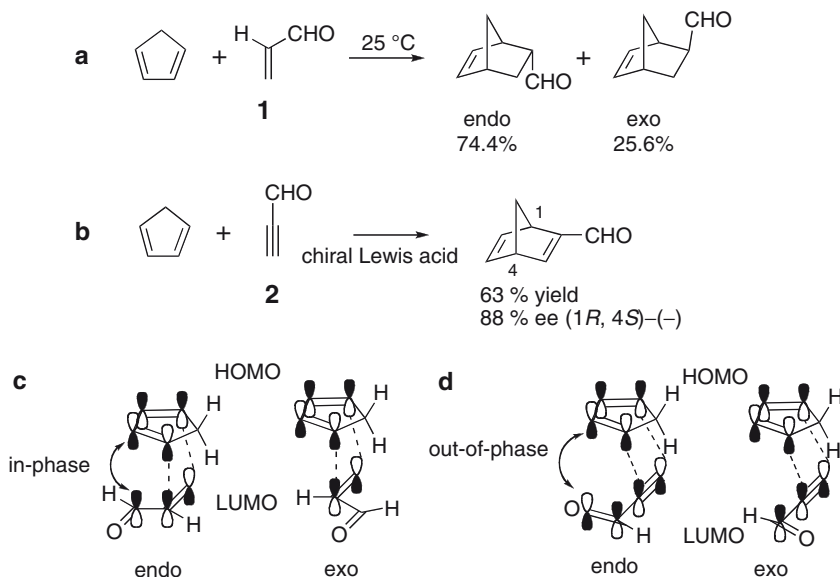


Fig. 2 Secondary orbital interaction (SOI) in Diels–Alder reactions

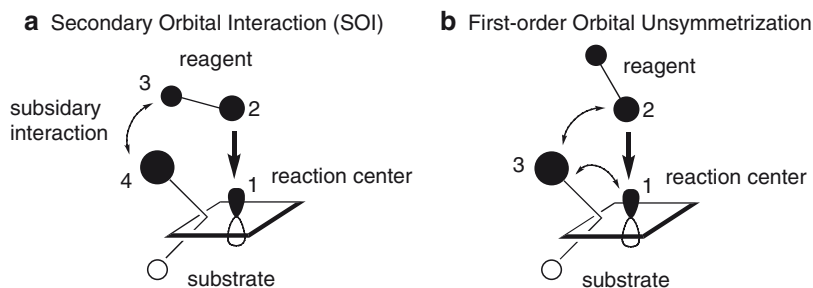


Fig. 3 Orbital interactions of interest in secondary orbital interaction and the unsymmetrization of orbitals

2 Stereoselection of Ketones

2.1 Cycloalkane System: Cyclohexanone Case

Hydride reduction of 4-*tert*-butylcyclohexanone **3** shows a preference for axial addition [axial addition:equatorial addition = 91–88.5:9–11.5 (LiAlH₄) [16, 17, 50, 51] or 87–86:13–14 (NaBH₄) [50, 52]. Addition of acetylide anion, Na(Li or K) C≡CH, also showed a similar axial preference [14, 15, 53].

The LUMO of cyclohexanone **3** is an out-of-phase combination of the carbonyl π* orbital with the σ_{CH} orbital (**5** in Fig. 4). The out-of-phase environment disfavors attack from the face of the σ_{CH} bonds (motif ii in Fig. 1). This leads to the axial attack of nucleophiles. The observed selectivities are in agreement with the orbital

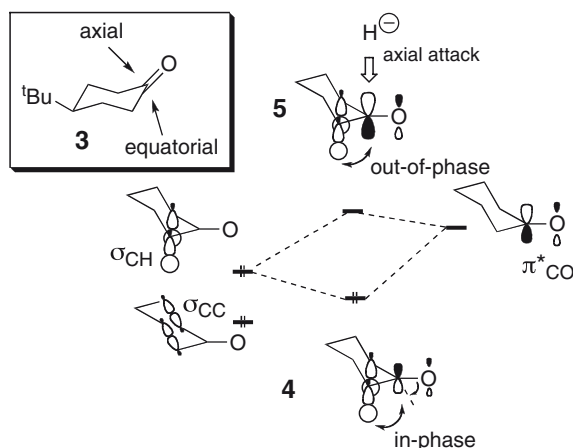


Fig. 4 Orbital unsymmetrization of cyclohexanone

unsymmetrization of the LUMO of the relevant ketone. Frenking et al. [54] supported the predominant mixing of the β - σ_{CH} orbital over that of the β - σ_{CC} orbital in the LUMO of cyclohexanone. *In this context, the nucleophilic addition of the carbonyl functionality as opposed to the better electron-donating (σ) orbital at the β position is favored.* Frenking et al. also demonstrated orbital rehybridization of the carbonyl π^* orbital of cyclohexanone (**3**), resulting in a more diffused orbital amplitude (due to second-order mixing) in an axial direction [54]. This orbital distortion was also discussed in a quantitative manner by Tomoda et al. [10, 55–57]. This is superficially consistent with Klein's model [58].

Fukui applied the orbital mixing rule [1, 2, 59] to the orbital hybridization or the deformation of the LUMO of cyclohexanone to explain the origin of the π -facial selectivity in the reduction of cyclohexanone. Cieplak [60] proposed that electron delocalization occurs from the σ_{CH} bonds into the σ^* orbital of the incipient σ_{CC} bonds at the transition state.

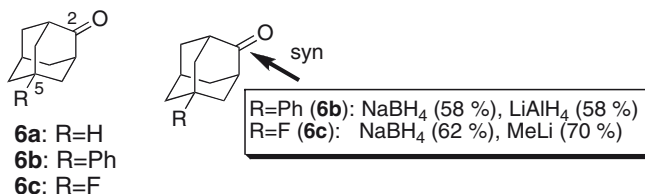
Laube and Hollenstein [21, 61] studied the single crystal structures of cyclohexanone derivatives complexed with a Lewis acid and found pyramidalization of the carbonyl carbon (**4**, Fig. 4), in agreement with the observed selectivity [61].

2.2 Orbital Phase Environment Unsymmetrization of Carbonyl π^* Orbitals by Interaction with β - σ Orbitals

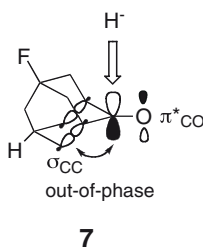
2.2.1 Adamantanone Case

Facial selectivity of 5-substituted adamantan-2-ones (**6**) was initially studied by Giddings and Hudec [62], followed by intensive studies by le Noble's group [63–66]. Electron-withdrawing substituents such as phenyl (**6b**), fluoro (**6c**), hydroxyl and trifluoromethyl groups at the 5 position favored the *syn* addition

of the reducing agent (NaBH_4) (with respect to the substituent at the 5 position) [62, 63]. For example, in the hydride reduction with NaBH_4 of 5-phenyladamantan-2-one **6b**, *syn* addition was favored over *anti* addition (*syn*: *anti* = 58:42).



The carbonyl π face of the adamantan-2-one with an electron-withdrawing group at the 5-position is unsymmetrized by interaction of the β - σ bonds antiperiplanar to the C-H bonds and to the C-R bond. The orbital phase environment of the carbonyl π^* orbital (**7**) is unsymmetrized by the more electron-donating σ_{CC} orbitals at the β -position, which is consistent with the observed *syn* preference.



2.2.2 Cyclopentanone Case

Halterman and McEvoy studied hydride reduction of a functionalized 2,2-diarylcyclopentanone **8** (Fig. 5) containing an unsubstituted phenyl group and a *para*-substituted phenyl group, both geminal substituents being assumed to be sterically equivalent [67]. The stereoselective reduction with sodium borohydride of a

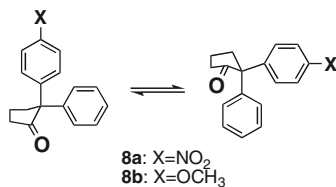
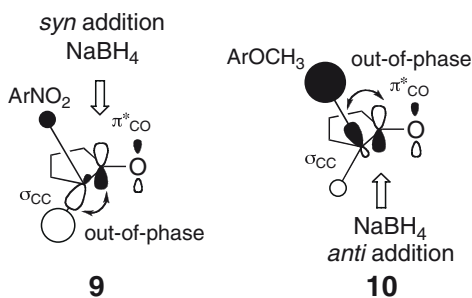


Fig. 5 Puckering of the cyclopentane ring



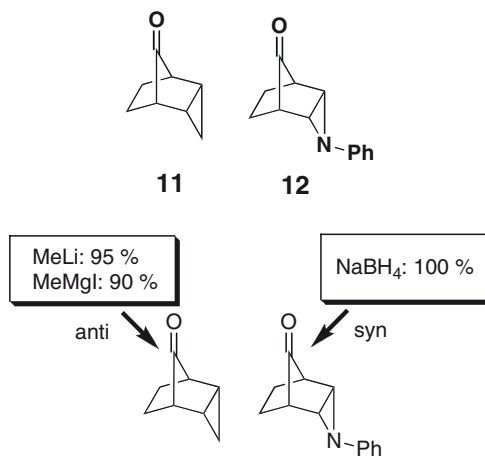
functionalized 2,2-diarylcyclopentane was observed, the preferred direction being dependent on the aromatic substituent. In the case of the electron-withdrawing nitro group (**8a**), *syn* addition of the hydride ion was favored (*syn:anti* = 79:21), whereas the electron-donating methoxy group (**8b**, X=OCH₃) favored *anti*-addition (*syn:anti* = 43:57).



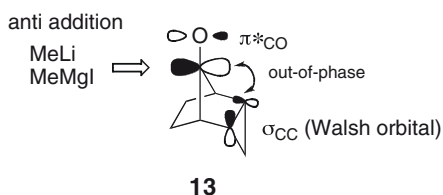
The carbonyl π^* orbital is also assumed to be unsymmetrized arising from the out-of-phase interaction of the σ_{CC} orbital attached to the more electron-donating aryl group (**9** and **10**). These unsymmetrizations of the carbonyl π^* orbital correspond well to *syn* addition (**9**) and *anti* addition (**10**), respectively. Thus, the electron-donation of the β - σ orbitals controls the facial selectivities. The cyclopentane system was more sensitive to stereoelectronic effects, showing larger induced biases, than the adamantanone system [63].

2.2.3 Bicyclic System Case: Small-Ring-Annulated Bicyclo[2.2.1]heptanones

Gassman et al. studied the facial selectivity of 7-norbornanone **11** annulated with an *exo*-cyclopropyl group, i.e., tricyclo[3.2.1.0^{2,4}]octan-8-one [68, 69]. Addition of methyl lithium to **11** gave predominantly the *anti* addition product with respect to the fused cyclopropane ring (*syn* addition:*anti* addition = 5:95). Similarly, addition of methylmagnesium iodide gave a 9:1 mixture of *anti*- and *syn*- adducts (*syn* addition:*anti* addition = 10:90). The carbonyl π^* orbital is subject to out-of-phase coupling with the bonding Walsh orbital at the β -position (**13**).



In the present case, the Walsh orbital will overlap with the π^* orbital of the carbonyl group more efficiently than the β - σ orbitals because of agreement of orbital symmetry and the efficient overlapping. This out-of-phase motif (**13**) is consistent with retardation of *syn* addition with respect to the cyclopropyl group, that is, *anti* preference.

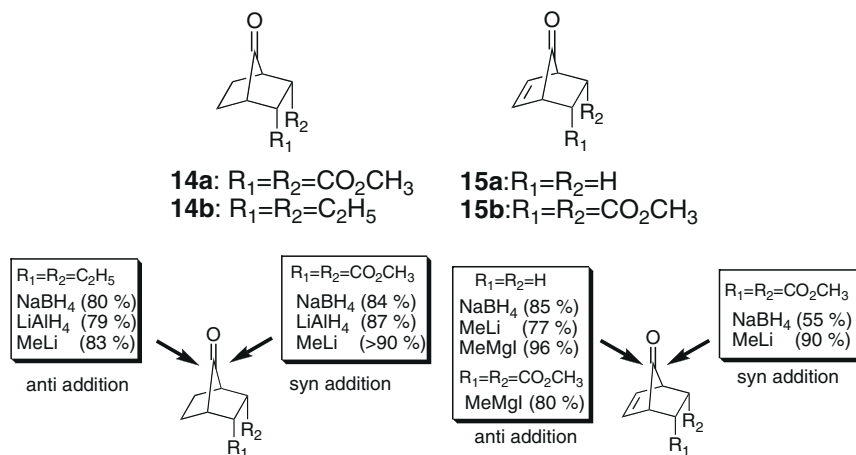


Sodium borohydride reduction of the 7-norbornanone **12**, annulated with an *N*-phenyl aziridine ring, 3-phenyl-3-aza-*endo*-tricyclo[3.2.1.0^{2,4}]octan-8-one, was also studied by Gassman et al. [69], who found a strong *syn* preference with respect to the aziridine group (*syn* addition:*anti*-addition = 100:0). Replacement of the cyclopropyl ring with an aziridine ring diminished the contribution of the Walsh-type orbital to the LUMO of the molecule. Houk et al. rationalized the *anti* preference of a reducing reagent toward **11** in terms of electrostatic repulsion due to the electron-donating cyclopropyl group [70]. Also, the reverse *syn* addition of **12** was rationalized in terms of geometrical distortion of the ethano bridges arising from ring strain due to the aziridine ring, rather than electrostatic interaction [70].

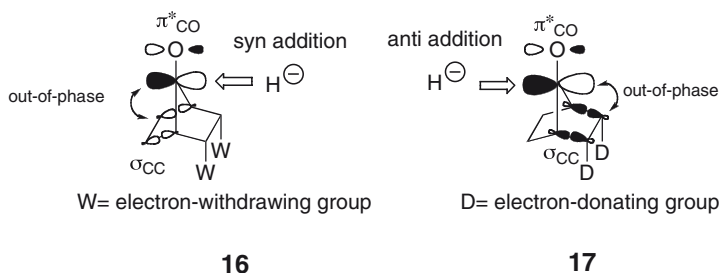
2.2.4 2,3-*exo,exo*-Disubstituted 7-Norbornanones

Facial selectivities in the nucleophilic addition of bicyclic ketones have recently been examined comprehensively [71, 72]. Mehta and his colleagues studied the facial selectivities of 2,3-*exo,exo*-disubstituted 7-norbornanones **14a** and **14b** [73–75]. In the reduction of **14a** and **14b** with sodium borohydride, lithium aluminum hydride,

and the bulky lithium tri-*tert*-butoxyaluminum hydride, a very significant variation in face selectivity as a



function of 2,3-*exo,exo* substitution was found, the most dramatic being the reversal in *syn:anti* ratio (with respect to the substituent) in going from **14a** (bismethoxycarbonyl, 84:16) to **14b** (bisethyl, 20:80). The asymmetry of the π face of the 2,3-disubstituted 7-norbornanones **14a** and **14b** arises from the first-order orbital unsymmetrization of the carbonyl π^* orbital (**16** in **14a** and **17** in **14b**).

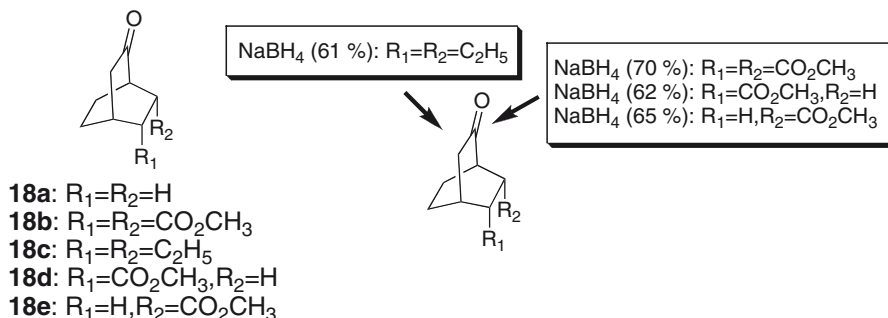


Mehta et al. also studied the facial selectivities of *exo*-substituted 7-norbornenones **15a** and **15b**, which exhibit steric bias with respect to the *anti* side of the π face (with respect to the *exo* substituent) [76, 77]. In the reduction with sodium borohydride, high *anti* preference (more than 85%) was observed in the parent derivative **15a**. Weak electron-withdrawing substituents (CH_2OCH_3 , CH_2OAc , COONa) also showed *anti* preference, the magnitude being comparable to that in the case of the parent compound (**15a**); this is indicative of the steric bias of **15a**. In the case of a strong electron-withdrawing substituent (di- or mono- CO_2CH_3 , CN), the *syn* preference of addition was increased, becoming predominant in some cases (di- CO_2CH_3 (**15b**) *syn:anti* = 55:45; mono- CO_2CH_3 *syn:anti* = 32:68; mono- CN *syn:anti* =

56:44). This is consistent with the intrinsic *syn* preference of 7-norbornanones **14a** substituted with potent electron-withdrawing groups. The *syn* preference of strong electron-withdrawing groups is even greater in the addition of methyl lithium: the diester derivative **15b** exhibited a high *syn* preference (*syn:anti* = 90:10), while *anti* preference was found in the parent (**15a**) and diether derivative (CH₂OCH₃) (*syn:anti* = 26:74). On the other hand, electrostatic attraction was proposed as a rationale for the observed facial preferences of **14a** and **14b** by Houk et al. [70] and Mehta et al. [75].

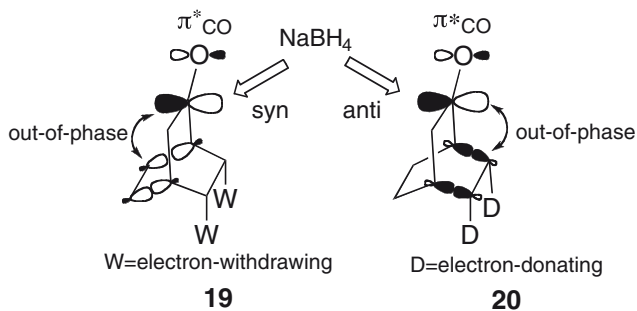
2.2.5 5,6-*exo,exo*-Disubstituted Bicyclo[2.2.2]octan-2-ones

Mehta et al. also studied the facial selectivities of 5,6-*exo,exo*-disubstituted bicyclo[2.2.2]octan-2-ones **18** [75, 78]. These systems are related to the 2,3-*exo,exo*-disubstituted 7-norbornanones **14**, but differ in the direction of the carbonyl π face. Hydride reduction of 5,6-*exo,exo*-disubstituted bicyclo[2.2.2]octan-2-ones (**18**) with NaBH₄ and DIBAL-H and methylation with MeLi were studied [75, 78].



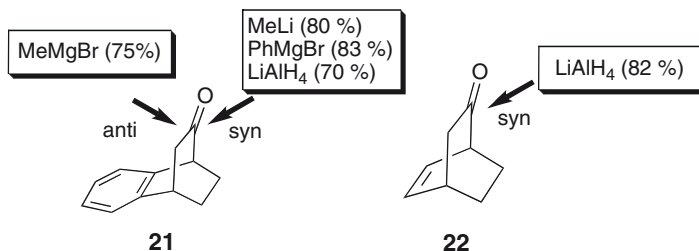
The remote *exo*-substituents have a profound bearing on the face-selectivity in nucleophilic additions to these ketones. The *syn* preference (with respect to the *exo* substituent) of the bismethoxycarbonyl substituents (**18b**) is completely reversed in favor of *anti* face addition in the bisethyl substrate **18c**. On the other hand, relatively modestly inductive *exo*-substituents (R₁ and/or R₂ in **18**), such as methoxymethyl and vinyl groups, exhibit no facial bias. These results are generally consistent with those obtained for the 2,3-*exo,exo*-disubstituted 7-norbornanone derivatives **14a** and **14b** [73, 74], and therefore there seems to be no significant effect of bicyclic systems on the facial selectivities. The facial selectivities observed in both bicyclic systems (**14a** and **14b** and **18b** and **18c**) are compatible with the Cieplak model. These preferences can also be rationalized in terms of orbital unsymmetrization of the carbonyl π^* orbital arising from out-of-phase mixing of the vicinal σ_{CC} orbital of the bicyclo[2.2.2]octene systems **18** (**19** (for **18b**) and **20** (for **18c**)). The latter proposal is compatible with the observation that both **18d** (R₁=CO₂CH₃, R₂=H) and **18e** (R₁=H,

$R_2=CO_2CH_3$) exhibit little difference in face selectivity, i.e., *syn* selectivity when subjected to $NaBH_4$ (*syn:anti* = 65:35 in **18d**; 62:38 in **18e**) and DIBAL-H (*syn:anti* = 66:34 in **18d**; 61:39 in **18e**) reduction. The behavior of **18d** and **18e** is also consistent with orbital unsymmetrization, as in **19**. On the other hand, Mehta et al. suggested the presence of significant electrostatic contributions from *exo*-electron-withdrawing groups, rationalizing the *syn* face selectivity in **18b** [75].

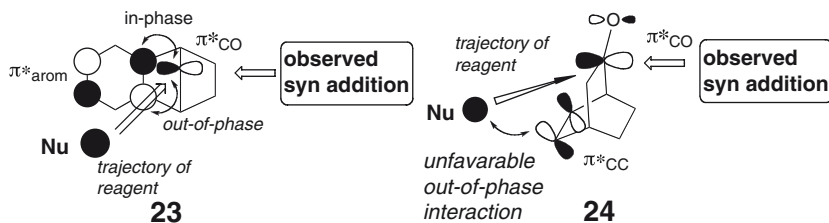


2.2.6 Benzobicyclo[2.2.2]octan-2-ones

The facial selectivity of the parent benzobicyclo[2.2.2]octan-2-one **21**, studied by Pudzianowski et al. [79], is rather unexpected. Addition of organometallic reagents such as methyl lithium and Grignard reagents exhibited *syn* preference (with respect to the ethano bridge), which is the more sterically hindered side. In the reduction of bicyclo[2.2.2]octenone **22** with $LiAlH_4$, *syn* addition is also favored (82:18 (*syn:anti*, with respect to the ethano bridge)), the rate of *syn* attack being enhanced (in a ratio of 2.6) over that observed in the saturated derivative, bicyclo[2.2.2]octanone **18a** [80]. This is in sharp contrast to the *anti* preference (with respect to the ethano bridge) of bicyclo[2.2.1]hepten-7-one **15a** [73] and 7-benzonorbornanone [81, 82]. Therefore, the facial selectivities depend on the bicyclic systems. In the parent benzobicyclo[2.2.2]octan-2-one **21** and bicyclo[2.2.2]octenone **22** the carbonyl π^*_{CO} orbitals interact with the aromatic π^* orbital (**23**) or the olefin π^* orbital (**24**) in the in-phase manner, implying *anti* preferences in both systems.

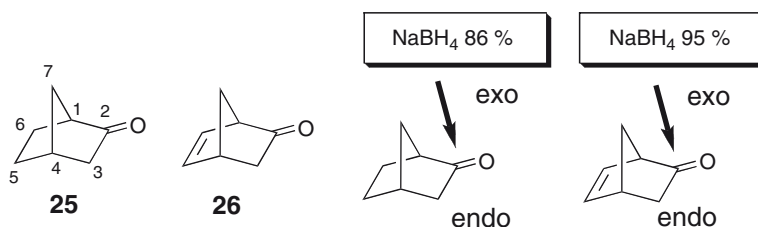


Thus, the predictions seem to be in conflict with the observed *syn* biases. However, along the trajectory of attack of the nucleophile to the carbonyl group of the bicyclo[2.2.2]octane structures (indicated in **23** and **24**), out-of-phase interactions between the reagent and the substrate are involved, and this is different from the situation in the bicyclo[2.2.1]heptane structures (**15a**) [83–87]. Thus, attack on the side opposite to the unsaturated moiety will be favored. This is a kind of SOI (Fig. 3a) which unsymmetrizes the π face.

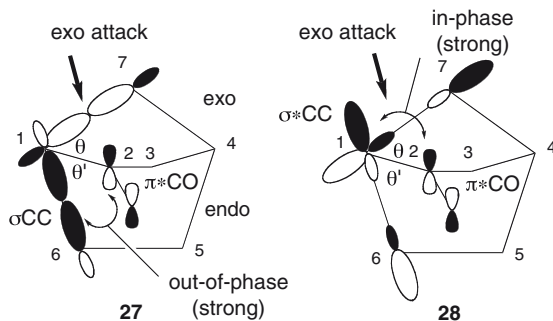


2.2.7 Classical Case: 2-Norbornanone

The *exo* reactivity of 2-norbornanone **25** in nucleophilic addition (such as reduction with hydride) is a classical example of the facial selectivity of carbonyl groups in bicyclic systems [80].



In a similar manner to orbital unsymmetrization of the relevant bicyclic ketones (for example **14** and **18**), the π^*_{CO} of the carbonyl moiety of norbornanone **25** can interact with CC framework orbitals of the methano and ethano bridges, i.e., σ_{CC} orbitals of the vicinal CC bonds, judging from the small energy difference (see **27**). Owing to the higher energy level, the π^*_{CO} orbital mixes out-of-phase with the occupied σ_{CC} orbitals of the vicinal C–C bonds ($\text{C}_1\text{--C}_6$ and $\text{C}_4\text{--C}_3$ in the ethano bridge; $\text{C}_1\text{--C}_7$ and $\text{C}_4\text{--C}_7$ in the methano bridge) to give an energetically deactivated LUMO (**27**). This mixing involves a π type overlap of these orbitals whose magnitude exhibits dihedral angle-dependence.



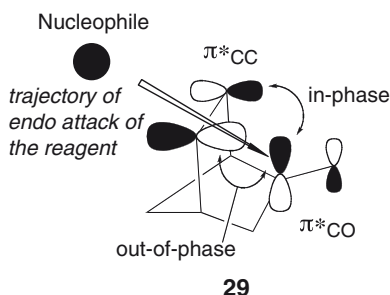
Because of the better π -type overlapping of the carbonyl π^* orbital with the σ bonds of the ethano bridge as compared with that of the methano bridge in **27** (i.e., θ (dihedral angle, $\angle C_7C_1C_2C_3$ or $\angle C_7C_4C_3C_2$) $<$ θ' (dihedral angle $\angle C_6C_1C_2C_3$ or $\angle C_5C_4C_3C_2$)), out-of-phase mixing of the σ_{CC} orbital of the ethano bridge is more predominant for the π^*_{CO} orbital of the carbonyl group, i.e., on the *endo* face, leading to *exo* addition of nucleophiles. This reflects the difference between the orbital interaction of the carbonyl π^* orbital with the methano bridge and that with the ethano bridge [88]. Significant intervention of the σ_{CC} orbital of the methano bridge was also discussed in connection with orbital distortion [1].

While the present interaction involves occupied σ orbitals, we can also consider the intervention of vacant σ^* orbitals. In this context, another mechanism of unsymmetrization of the carbonyl π^* orbital has been proposed, arising from the in-phase combination of the vacant σ^*_{CC} orbitals [88]. Because of the small difference in energy, the π^* orbital can interact with the vacant C–C σ^* orbitals (i.e., σ^*_{C-C} bond orbitals) of the methano and ethano bridges (see **28**). The π^*_{CO} orbital can interact with the back-side lobes of the σ^*_{C-C} orbitals centered on the bridgehead carbon atom (C_1) in an in-phase manner. The magnitude of the interaction is also dihedral angle-dependent: the greater the angle (θ), the greater the overlap of the orbitals. Thus, the in-phase mixing with less acute orbitals (θ') of the ethano bridge to the carbonyl π^*_{CO} orbital resulted in a larger build-up of the virtual internuclear bonding region on the *exo* face which is to be attacked by electrons of an occupied orbital of a nucleophilic reagent. This orbital unsymmetrization is also consistent with the experimental *exo* reactivity of norbornanone **25**. This interaction motif bears a close resemblance to orbital interactions in the transition state associated with back-side nucleophilic attack (S_N2) on a tetrahedral carbon center of α -haloketones [89, 90].

Various theoretical interpretations of the bias of norbornanone **25** have been proposed. Two basic explanations have been suggested, i.e., torsion-based arguments [91] and stereoelectronic arguments [1, 92–95].

2-Norbornenone **26** undergoes reduction by sodium borohydride under kinetic conditions to produce 5% *exo*- (i.e., *endo* attack) and 95% *endo*- (i.e., *exo* attack) 2-norborneol. This leads to the partial rate constants of 11.4 for *exo* and 0.6 for *endo* attack (relative rate with respect to the rate of $LiAlH_4$ reduction of cyclopentanone (1.00)) [80]. In the saturated 2-norbornanone **25**, the values are 4.55 for *exo* and 0.74 for *endo* attack. Thus, the introduction of the double bond enhances the

exo attack, while the *endo* attack is rather unaffected. The carbonyl π^* orbital is subject to in-phase combination with the vacant olefinic π^* orbital (**29**), and the orbital level is lowered, which is consistent with the acceleration of

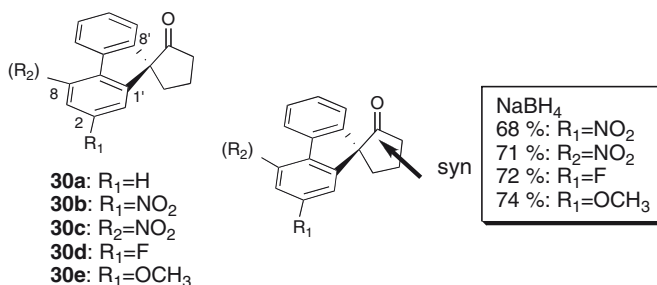


the reduction. However, the trajectory of the addition again involves unfavorable out-of-phase orbital interaction (SOI, **29**), in a similar manner to **23** and **24**, and thus the *endo* addition is not favored.

2.3 π - π Interaction System

2.3.1 Spirocyclopentanone Case

The unsymmetric π face of carbonyl groups is postulated to be attributable to orbital interactions between a σ -fragment and a π -fragment. Interactions between two π fragments in a carbonyl molecule can also lead to an unsymmetrical orbital phase environment [3].



Facial selectivities of spiro[cyclopentane-1,9'-fluorene]-2-ones **30a–30e** were studied by Ohwada [96, 97]. The carbonyl π orbital can interact with the aromatic π orbital of the fluorene in a similar manner to spiro conjugation [98–102]. The ketones **30** were reduced to alcohols by the action of sodium borohydride in methanol at -43 °C. The *anti*-alcohol, i.e., the *syn* addition product of the reducing reagent with respect to the substituent, is favored in all cases, irrespective of the substituent at C-2 or C-4 of the fluorene ring (2-nitro **30b** (*syn:anti* = 68:32), 4-nitro

30c (*syn:anti* = 71:29), 2-fluoro **30d** (*syn:anti* = 72:28) and 2-methoxyl **30e** (*syn:anti* = 74:26) groups). This lack of substituent effects is in sharp contrast to the situation in the 2,2-diarylcyclopentanones **8** [67].

In fluorenes bearing a spiro carbonyl group, π orbitals of fluorenes (**32**) and those of the carbonyl group (**31**) can interact predominantly through the *ipso* (C-1' and C-8') positions of the fluorene ring (**30**), i.e., the π orbitals at the β position of the carbonyl group (see Fig. 6). This type of interaction involves σ -type overlaps of the π orbitals in spiro geometry, in a similar manner to spiro conjugation [98, 99]. The π^*_{CO} orbital (**31**) interacts preferentially with the next-LUMO (NLUMO) (**32**) of the fluorene derivative, rather than the LUMO: the LUMOs bear the orbitals at the *ipso* (C-1' and C-8') positions, symmetric in sign with respect to the plane passing through C-9 and the carbonyl group (i.e., non-interaction because of orbital phase symmetry); the NLUMOs and π^*_{CO} are antisymmetric in sign (Fig. 6). The NLUMOs have coefficients largely localized on one of the benzene rings, the one bearing the nitro, fluoro, or even methoxyl substituent (for example, at C-1' rather than at C-8'). At the points of interaction (at C-1' and C-8'), different amplitudes of the wave functions of the NLUMO of the fluorene result in different build-up of the virtual bonding region between nuclei (**33**) [93]. A larger vacant bonding region captures the incoming electrons of a nucleophile more efficiently. Therefore, the π^*_{CO} fragment favors the interaction with the HOMO of the hydride ion on the side of the substituent, resulting in a biased reduction product (see Fig. 1, motif i). Furthermore, in-phase combination of the NLUMO of the fluorene (for example, 2-nitrofluorene) and π^*_{CO} orbital (**32**, Fig. 6) lowered the energy of the π^*_{CO} fragment, so activating it for attack of a nucleophile. Unexpectedly a similar orbital distribution was found in the case of the NLUMO of 2-methoxyfluorene, which will lead to a similar orbital unsymmetrization of the ketone of **30e**. In the present example, the π orbitals at the β position of the carbonyl functionality also affected the facial selectivity. This is a similar interaction to that found in the cases of β - σ orbitals.

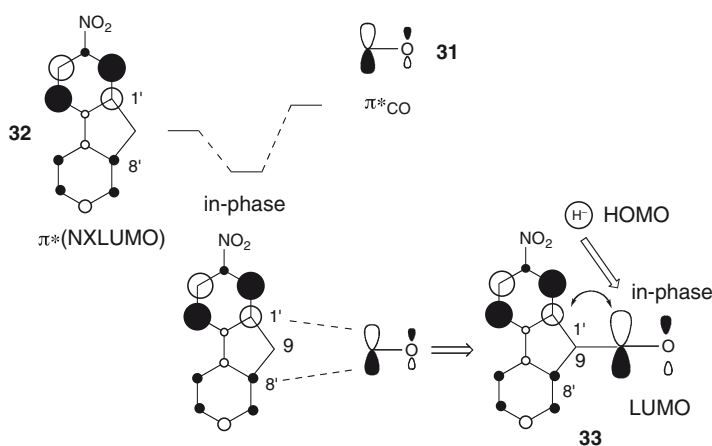
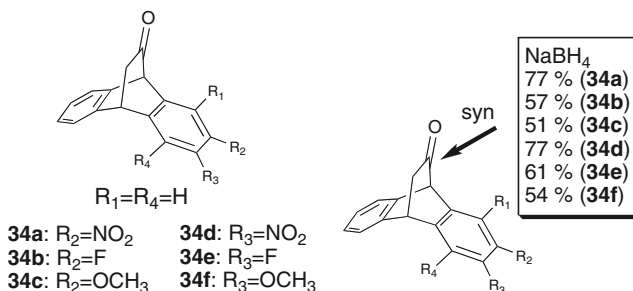


Fig. 6 Orbital unsymmetrization of the carbonyl π^* orbital

2.3.2 Dibenzobicyclo[2.2.2]octadienone Case

Dibenzobicyclo[2.2.2]octadienones (**34**) bearing an aromatic substituent were designed to probe the unsymmetrization of the carbonyl π^* orbital arising from the aromatic π orbitals [103, 104]. Reduction of the carbonyl moiety of 2- ($R_2 \neq H$) and 3-substituted ($R_3 \neq H$) dibenzobicyclo[2.2.2]octadienones (**34**) was studied by using sodium borohydride in methanol at -43°C . The 2- (**34a**) and 3-nitrodibenzobicyclo[2.2.2]octadienones (**34d**)



preferentially gave *anti*-alcohols (with respect to the nitrobenzene moiety) on reduction with hydride ion, i.e., *syn*-attack with respect to the nitrobenzene moiety (*syn:anti* = 77:23), with values of diastereomeric excess of 54% (**34a**) and 54% (**34d**). A fluoro substituent (in **34b** and **34e**) also favors *syn* addition to give an *anti*-alcohol (for **34b**:*syn:anti* = 57:43; for **34e**:*syn:anti* = 61:39). Substituent effects were found to be similar in both 2- and 3-substituted ketones, although the substituent is remote from the reaction center and is different in direction. On the other hand, a methoxy group (in **34c** and **34f**) showed only a negligible preference in the reduction reaction, giving a slight excess of the *anti*-products.

The low-lying vacant orbitals of the dihydroanthracene fragment bearing components at the *ipso* (C-1', C-4', C-5' and C-8') positions can participate in mixing with the π^*_{CO} orbital. An electron-withdrawing substituent such as a nitro or a fluoro group perturbs the π face of the carbonyl group. The lower-lying vacant aromatic π^* orbital of dihydroanthracenes substituted with an electron-withdrawing nitro group (for example, **35**) has coefficients largely localized on the benzene ring bearing the nitro group, because the relevant vacant aromatic π^* orbital (**35**) is predominantly derived from the LUMO of nitrobenzene. The resultant in-phase mixing lowers the energy of the π^*_{CO} fragment, activating it for attack of a nucleophile. Simultaneously, the in-phase overlap results in build-up of a virtual bonding region between nuclei (**35**). Therefore, the π^*_{CO} fragment favors the interaction with the HOMO of the hydride ion on the side of the substituent (motif i in Fig. 1), resulting in the biased reduction product (*syn* alcohol) observed for the 2- and 3-nitro derivatives (**34a** and **34d**). On the other hand, the lowest-lying vacant aromatic π^* orbital (LUMO) of the dihydroanthracene substituted with an electron-donating hydroxyl group (**36**, OH instead of OCH_3) has orbital amplitudes at the *ipso* (C-1' and C-4'; C-5' and C-8') positions that are approximately symmetric in sign and in magnitude with respect to the plane passing through C-9 and C-10 (Fig. 7). The

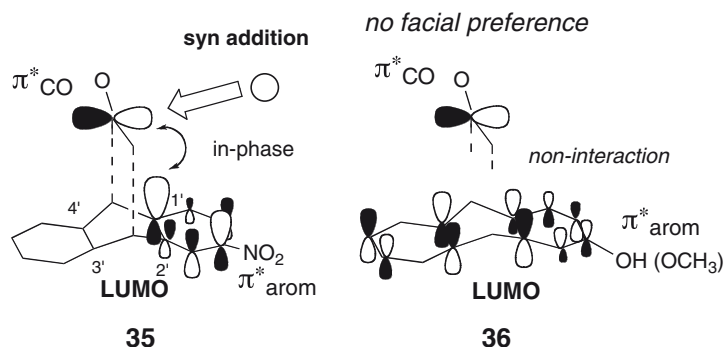


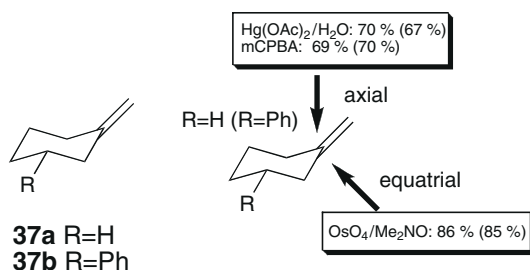
Fig. 7 Orbital unsymmetrization of the carbonyl π^* orbital

NXHOMO of the hydroxy-substituted dihydroanthracene is also symmetric in sign. Therefore, the antisymmetric π^*_{CO} orbital does not interact significantly with these vacant π orbitals of **36**, resulting in an unperturbed π face of the carbonyl π^* orbital. This motif is regarded as an example of orbital *non-interaction* [105]. Thus, the reduction of 2-methoxy and 3-methoxydibenzobicyclo[2.2.2]octadienones (**34c** and **34f**) should intrinsically show little or no bias.

3 Stereoselection of Olefins

3.1 Methylenecyclohexane Case

Klein showed that axial reaction of the parent methylenecyclohexane **37** is preferred in hydroboration [106]. The experimental data on the parent methylenecyclohexanone **37a** accumulated by Senda et al. [107] and the more recent systematic studies by Cieplak et al. [108, 109] on π -facial selectivities of 3-substituted methylenecyclohexanes **37** have characterized the intrinsic features of the facial selection of methylenecyclohexanes. That is, axial preference of unsubstituted and 3-substituted methylenecyclohexanes was observed in oxymercuration [107] and epoxidation reactions [110]. There is also an increase in the proportion of axial attack with increase in the electronegativity of the remote 3-equatorial



substituent (R) [108, 109]. On the other hand, in the dihydroxylation with osmium tetroxide [111], equatorial preference was observed in the parent and 3-aryl-substituted methylenecyclohexanes in a similar manner to that in the hydroboration.

The inherent axial preference can be rationalized in terms of orbital unsymmetrization arising from first-order mixing (Fig. 8). Because of more efficient overlap, the olefin π orbital interacts with the σ_{CH} orbitals to a greater extent than with the σ_{CC} orbitals. The HOMO of methylenecyclohexanone is, thus, generated by out-of-phase combination of the olefin π orbital and the σ_{CH} orbitals (**39**), the composition being similar to that of cyclohexanone (see **5**), but the occupation by electrons being different [112]. This asymmetry of the olefin π orbital is consistent with the axial preference of methylenecyclohexane **37a** (motif iii in Fig. 1). The HOMO of methylenecyclohexane **37a** in fact involves out-of-phase combinations of the olefin π orbital with the σ_{CH} orbitals and the σ_{CC} orbitals (**40**), the former component being larger.

In this context, *the preferred reaction faces are opposite to the better-electron-donating σ orbitals at the β positions, in a similar manner to the carbonyl cases.* Electron-withdrawing substitution at C-(3), which attenuates the contribution of the σ_{CC} orbitals in **40**, thereby increases the percentage of the axial approach.

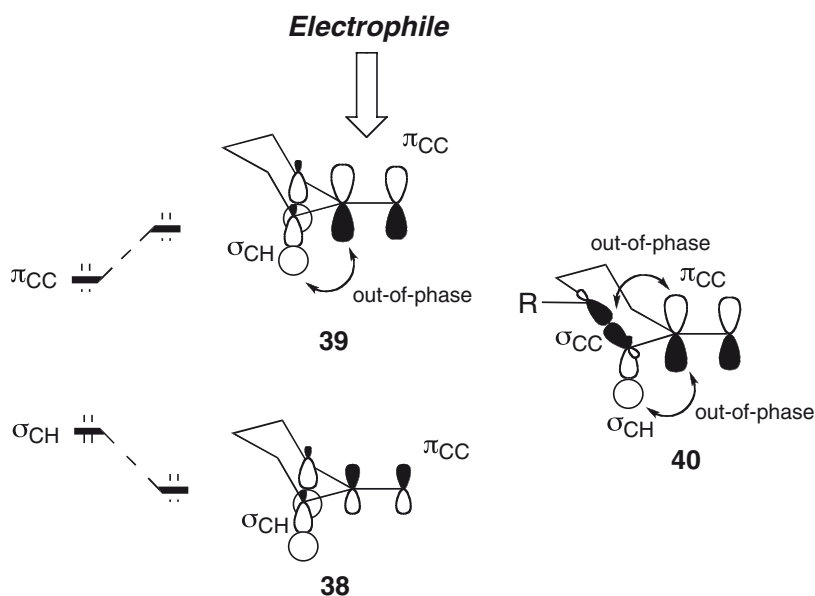
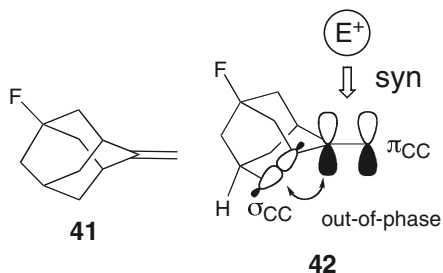


Fig. 8 Orbital unsymmetrization in methylenecyclohexane

3.2 Interaction of σ Orbitals at the β -Position with the Olefin π Orbitals

3.2.1 2-Vinylideneadamantanes Case

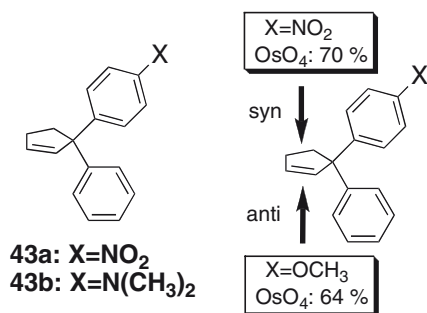
le Noble et al. and others have reported facial selectivities arising from remote substituents in the case of the 2-vinylideneadamantane derivative **41** [23, 113]. Epoxidation of 5-fluoro-2-methyleneadamantane **41** with mCPBA gave a



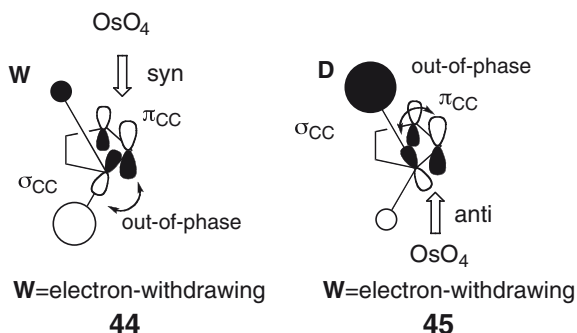
mixture of epoxy products (*syn:anti* (with respect to the fluoro group) 66:34). A 60:40 ratio was obtained in the addition of dichlorocarbene. Similar *syn* preference was obtained in the addition of dibromocarbene and in hydroboration. Oxymercuration of **41** with mercuric acetate favored *syn* addition (>95% *syn* alcohol), while addition of trifluoroacetic acid furnished >99% *syn* ester, and HCl gas gave >>99% *syn* dihalide. The olefin π orbital of 5-fluoro-2-methyleneadamantane **41** is also subject to unsymmetrization arising from out-of-phase combination of the relevant σ_{CC} orbitals (**42**), the addition on the side of the fluorine being favored.

3.2.2 Cyclopentene Case

The stereoselective osmium-catalyzed dihydroxylation of a functionalized 2,2-diarylcyclopentene **43** containing an unsubstituted phenyl group and a *para*-substituted phenyl group were also examined by Halterman and McEvoy [114]. The electron-withdrawing nitro substituent (**43a**, X=NO₂) favored *syn* addition with respect to the substituted benzene ring (*syn:anti* = 70:30), whereas the electron-donating *N,N*-dimethylamino group (**43b**, X=N(CH₃)₂) favored *anti*-addition with respect to the substituted benzene ring (*syn:anti* = 36:64). The present facial selectivity obtained in the reaction of the corresponding olefin **43** is similar to that in the reduction of the relevant cyclopentanone derivatives **8** [67]. Addition opposite the more electron-rich aromatic ring was favored, which appears to be in agreement with the Cieplak hypothesis. Essentially, the olefin π orbital is



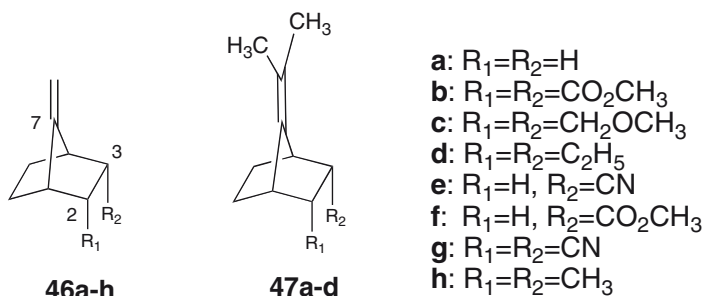
unsymmetrized due to the unequal contributions of the relevant σ_{CC} orbitals in an out-of-phase manner (**44** and **45**). This out-of-phase motif with respect to the olefin π orbital is in agreement with the observed facial selectivities: *syn* with respect to the electron-withdrawing group (**44** in **43a**) and *anti* with respect to the electron-donating substituent (**45** in **43b**).

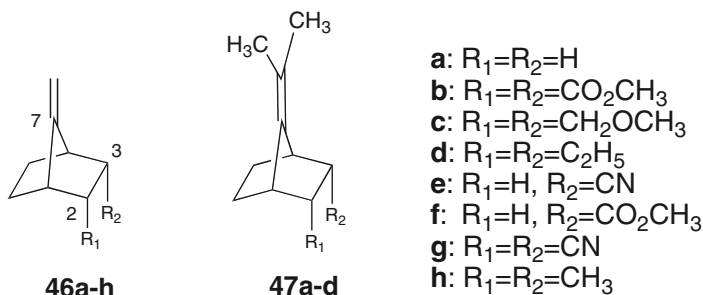


3.2.3 Unsaturated Bicyclo[2.2.1]heptane Case

1. 2,3-*exo,exo*-Disubstituted Bicyclo[2.2.1]heptane Derivatives

Mehta et al. studied 2,3-*exo,exo*-disubstituted 7-methylenenorbornanes **46** [115] and 2-*exo*-monosubstituted 7-isopropylidenenorbornanes **47** [29, 77, 116]. The 7-

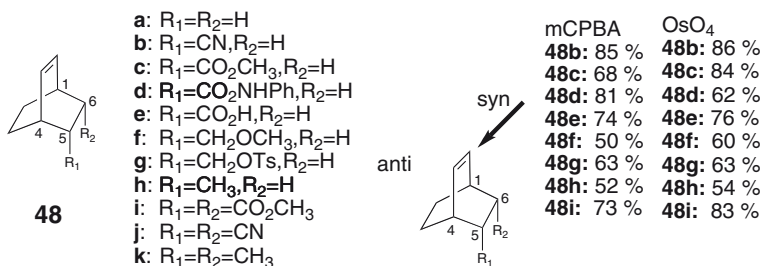




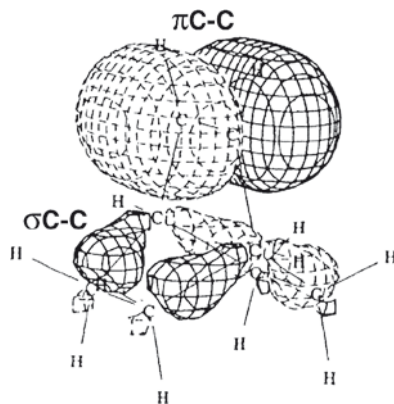
methylene-norbornanes **46** bearing *exo*-electron-withdrawing substituents were subject to epoxidation, hydroboration and oxymercuration reactions, which showed consistent *syn* facial selectivities (with respect to the *exo* substituent). In the case of disubstitution of methoxycarbonyl groups (**46b**), *syn* addition of the reagent is favored in epoxidation, with *syn:anti* addition = 74:26. The dimethoxymethyl compound **46c** showed rather *anti* preference, and the diethyl substrate **46d** showed a greater *anti* preference in epoxidation, with *syn:anti* addition = 30:70. Owing to the electron-donating methyl groups on the olefin, the isopropylidene derivatives **47** undergo the addition of dichlorocarbene, as well as singlet oxygen addition, epoxidation and reaction with the bromine (I) cation. A single *endo* electron-withdrawing substituent, as in **47e** ($R=CN$) and **47f** ($R=CO_2CH_3$), also favored *syn* addition (with respect to the *exo* substituent). Orbital unsymmetrization of the olefin π orbital of 7-methylenenorbornane **46** and 7-isopropylidenenorbornane **47** is involved, as in the case of bicyclo[2.2.2]octenes (**48**). These are discussed together in the following section.

2. Bicyclo[2.2.2]octene Case

Jones and Vogel investigated the substituent effect of a 5,6-bis(methoxycarbonyl) group in bicyclo[2.2.2]octene (**48i**) [117]. The substituent effect of a single 5-*exo* substituent on the facial selectivities of bicyclo[2.2.2]octenes **48b–48h** was also characterized by our group [118]. Epoxidation and dihydroxylation of the olefin moiety of 5-*exo*-substituted



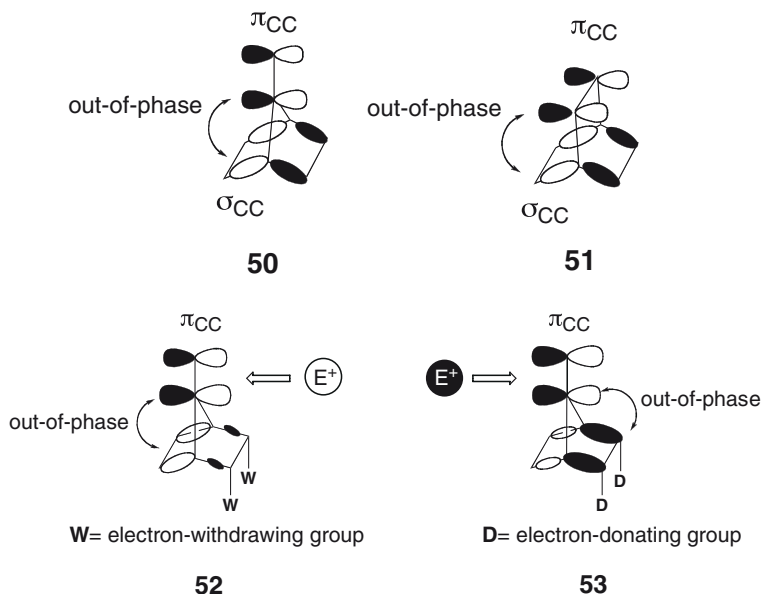
bicyclo[2.2.2]octenes (**48b–48h**) were investigated. 5-*exo*-Cyanobicyclo[2.2.2]octene **48b** underwent preferential *syn*-addition (with respect to the face of the cyano group) of peroxidic reagents, i.e., *m*-chloroperbenzoic



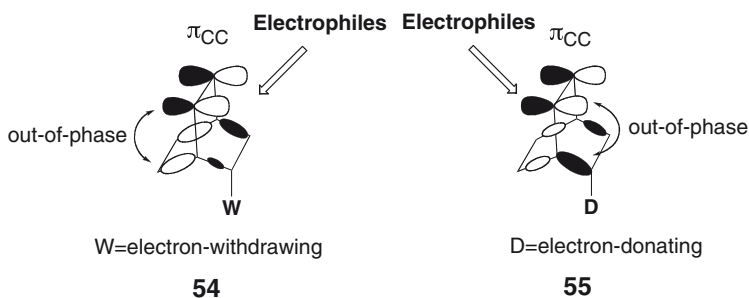
acid (mCPBA) and osmium tetroxide. In the epoxidation of **48b** with mCPBA, the *syn* epoxide is favored over the *anti* epoxide. In the dihydroxylation with osmium tetroxide, the *syn* diol is also favored over the *anti* diol. Values of diastereomeric excess observed in these reactions ranged from 70% (*syn:anti* = 85:15) to 72% (*syn:anti* = 86:14). 5-*exo*-Methoxycarbonyl-bicyclo[2.2.2]octene **48c** also preferentially gave the *syn*-epoxide (d.e. 36%) (*syn:anti* = 68:32) and the *syn*-diol (d.e. 68%) (*syn:anti* = 84:16). Electron-withdrawing nature of the substituent is important for *syn*-preference, as judged from the findings that benzanilide (**48d**) and carboxylic acid (**48e**) substituents distorted the olefinic π face similarly to the methoxycarbonyl group, whereas the methoxymethyl group (**48f**) imparted weaker (in the case of dihydroxylation, d.e. 20%) or absent (in the case of epoxidation) selectivity. Tosylation of the methyl alcohol functionality (**48g**) restored the *syn*-selectivity to some extent in hydroxylation and particularly in the epoxidation. On the other hand, the 5-methyl derivative **48h** showed a negligible preference in both reactions.

The *syn* preference arising from electron-withdrawing groups is consistent with the preference observed in the case of the bis(methoxycarbonyl) group (**48i**) (*syn:anti* = 73:27 in the epoxidation; *syn:anti* = 83:17 in the dihydroxylation). A single substituent is sufficient to perturb the π face in the bicyclo[2.2.2]octene system **48**. Furthermore, the bicyclo[2.2.2]octane system **48** exhibited the same preference as those found in 7-methylidene- (**46**) and 7-isopropylidenenorbornanes (**47**), except for the effect of electron-donating alkyl groups: in 7-vinylidenenorbornane (**47d**) the ethyl substituent favored *anti*-addition in the epoxidation with mCPBA.

The HOMOs of unsubstituted vinylidenenorbornane **47a** and unsubstituted bicyclo[2.2.2]octene **48a** are intrinsically comprised of similar components, i.e., the π orbital of the ethylene and the σ -orbitals of the ethano bridges, the coupling being in an out-of-phase fashion (**50** and **51**), though the arrangement of the components is different. The contour plot (**49**) of the HOMO of **48a** is consistent with these orbital interactions (**50**).

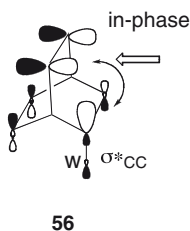


An electron-withdrawing group significantly lowers the energy of the σ orbital and an electron-donating group raises the energy of the σ orbital. Thus, substitution of an electron-withdrawing group decreases the contribution of the vicinal σ_{C-C} orbital (C–C–W bond) to the HOMO of the whole 7-vinylidenenorbornane (**52**) or bicyclo[2.2.2]octene molecule (**54**). Therefore, the antibonding phase environment is diminished on the side of the substituent, and so *syn* addition is favored. A similar orbital interaction diagram applies in the case of the substitution of an electron-donating group in 5-substituted 7-methylidenenorbornane **46** and bicyclo[2.2.2]octane **48**: an electron-donating group enhances the contribution of the electron-rich σ bond (C–C–D bond) to the HOMOs of the olefin molecules (**53** and **55**), and thus *anti* preference will be observed.



Additional $\sigma^*-\pi$ coupling (see **56**) can also participate in the facial selectivities [118]. That is, substitution of an electron-withdrawing group (W) makes the rele-

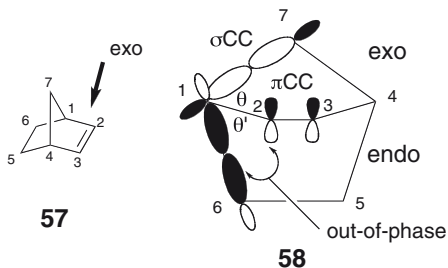
vant carbon atom (C–W) more electronegative, which leads to a situation where the σ bonding orbitals are weighted more heavily on the atom W and the σ antibonding orbitals are weighted more heavily on the relevant carbon atoms (**56**) [119]. The π orbital of the olefin in **48b–48e** can interact efficiently with the $exo\text{-}\sigma_{CW}^*$ orbital in an in-phase manner, which provides a more extended



bonding region on the side of the substituent (**56**) in the cases of electron-withdrawing substituents. This reinforces the *syn*-preference [120].

3.2.4 Classical Case of 2-Norbornene

The *exo* reactivity of norbornene **57** [25–28, 30] has been rationalized in terms of the torsional strain [91, 121] and orbital distortion of the olefin π orbital [1, 2, 93–95, 122].



In norbornene **57** the π_{CC} of the olefin moiety can interact with CC framework orbitals of the methano and ethano bridges (**58**), i.e., σ_{CC} orbitals of the vicinal CC bonds. The π_{CC} orbital is mixed out-of-phase with the occupied σ_{CC} orbitals of the vicinal C–C bonds (C1–C6 and C4–C5 in the ethano bridge; C1–C7 and C4–C7 in the methano bridge) to give an energetically raised HOMO (**58**), whose magnitude of interaction exhibits dihedral angle-dependence [88]. In out-of-phase mixing, the greater the angle, the stronger the interaction: the less acute angle of the σ bonds of the ethano bridge (θ (dihedral angle, $\angle C_7C_1C_2C_3$ or $\angle C_7C_4C_3C_2$) $<$ θ' (dihedral angle $\angle C_6C_1C_2C_3$ or $\angle C_5C_4C_3C_2$)) in **57** leads to out-

of-phase mixing of the π_{CC} orbital with the σ_{CC} orbital of the *ethano bridge* predominantly over that of the *methano bridge*, resulting in favoring *exo* addition of electrophiles.

3.3 Effects of Different Arrangements of Composite Molecules

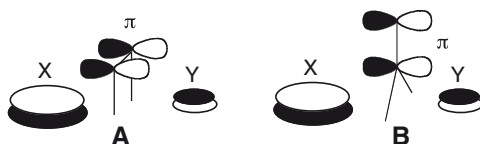
As discussed in connection with the facial selectivities of 7-methylenenorbornane **46** and bicyclo[2.2.2]octene **48**, the components of the molecules, i.e., π functionality and two interacting σ orbitals at the two β positions, are the same, but the connectivity of these fragments, i.e., the topology of the π systems, is different (**A** and **B**, Fig. 9). A similar situation was found in the case of spiro[cyclopentane-1,9'-fluorene] **68** [96, 97] and 11-isopropylidenedibenzonorbornadienes **71** (see 3.4.1 and 3.4.2) [123]. In these systems, the π faces of the olefins are subject to unsymmetrization due to the difference of the interacting orbitals at the β positions. In principle, consistent facial selectivities were observed in these systems.

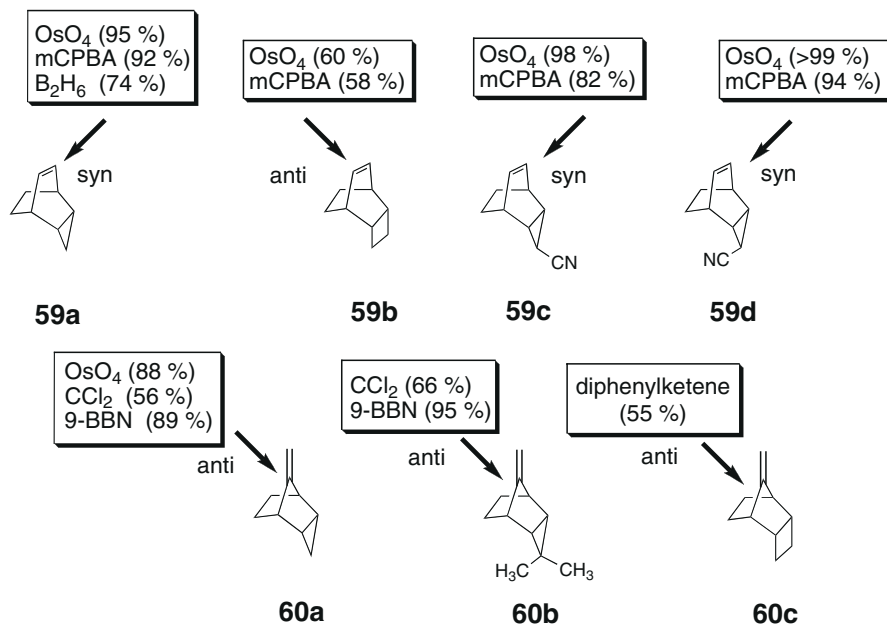
Recently a reverse perturbation effect of a cyclopropyl group on facial selectivities was described in two bicyclic systems, bicyclo[2.2.2]octane **59** and norbornane (bicyclo[2.2.1]heptane) **60** [124]. Bicyclo[2.2.2]octane **59a**, annulated with an *exo*-cyclopropyl group, i.e., *exo*-tricyclo[3.2.2.0^{2,4}]non-6-ene, and 7-methylenenorbornane **60a**, annulated with an *exo*-cyclopropyl group, i.e., 8-



methylene-*exo*-tricyclo[3.2.1.0^{2,4}]octane, are isomers wherein the olefin group is faced with the same structural units, while the orientations of the olefin are different (**59** as in **A**, and **60** as in **B**, Fig. 9).

Fig. 9 Different arrangements of (**A** and **B**) composite molecules (x, y and π)





Dihydroxylation of **59a** with osmium tetroxide in pyridine and epoxidation of **59a** with *m*-chloroperbenzoic acid (mCPBA) both showed high *syn* preference of the addition (OsO₄ *syn:anti* = 95:5; mCPBA *syn:anti* = 92:8). This preference is in sharp contrast to the *anti* preference of **60a** (*syn:anti* = 12:88), observed under similar dihydroxylation conditions with osmium tetroxide in pyridine.

The *anti* facial preference of the norbornane **60a** was previously found in the additions of dichlorocarbene (*syn:anti* = 44:56) [125, 126] and of 9-BBN (*syn:anti* = 11:89) [125, 126]. The *anti*-preference was also observed in the reactions of methylenebicyclo[2.2.1]heptane (**60b**) bearing an *endo*-dimethylcyclopropyl group (R₁, R₂ = C(CH₃)₂) [125, 126] with dichlorocarbene (*syn:anti* = 34:66) and 9-BBN (*syn:anti* = 5:95). Therefore, we can conclude that the *anti*-preference, induced by a cyclopropyl group, is intrinsic to 7-methylenenorbornane **60a**. The *anti* preference was also observed in alkyl-substituted **46d** (R₁ = R₂ = Et), supporting the idea that a cyclopropyl group behaves as an electron-donating substituent [78].

On the other hand, the observed *syn* preference of **59a** is consistent with a study of hydroboration of **59a** with diborane by Schueler and Rhodes [127], who obtained a mixture of the monoalcohols (*syn:anti* = 74:26) upon oxidative work-up. A similar magnitude of *syn*-preference was found (*syn:anti* = 73:27) in the hydroboration with a bulkier borane, 2,3-dimethyl-2-butylborane (thexyl borane) [127]. This lack of effect of the bulk of the reagent in the hydroboration of **59a** is consistent with the idea that the π face of **59a** is free from steric bias [127], and that the *syn* preference of **59a** found in dihydroxylation and epoxidation is non-sterically determined [128].

The *syn*-preference of **59a** is concluded to be attributable to the fused cyclopropyl ring, based on the observation that the bicyclo[2.2.2]octene (**59b**) fused with a

cyclobutane ring ($R_1, R_2 = (\text{CH}_2)_2$) changes the preference to the *anti* direction, in both dihydroxylation (*syn:anti* = 40:60) and epoxidation (*syn:anti* = 42:58). The *anti*-preference of the 7-methylenenorbornane **60a** is also diminished when the cyclopropyl ring is replaced with a cyclobutane ring (**60c**); in the attack of diphenylketene, the *syn:anti* ratio is 45:55 [120, 129].

A cyclopropyl group is known to act as a strong π donor due to a high-lying occupied Walsh orbital [130], which is frequently regarded as an equivalent of a double bond (i.e., **67**, Fig. 11) [131–139]. The previous account of the observed *anti* facial preference of **60a** was based on this interaction, in particular, out-of-phase interaction of the relevant orbitals (**63** in Fig. 11) [125–129, 131]. However, the corresponding out-of-phase interaction of the olefinic π orbital with the Walsh orbital of the cyclopropyl group (**65** in Fig. 11) seems not to be relevant to **59a**, because the 2p–2p σ orbital (**66**), the major component of the Walsh orbital, overlaps with the olefinic π orbital at the nodal positions. As shown in the contour plots (Fig. 10), the β – σ orbitals of the cyclopropyl group made a smaller contribution than other β – σ orbitals to the HOMO (**61**), i.e., there is a marked out-of-phase interaction with the olefin π_{CC} orbital (**64**) (Fig. 11). Thus, the effect of the cyclopropyl

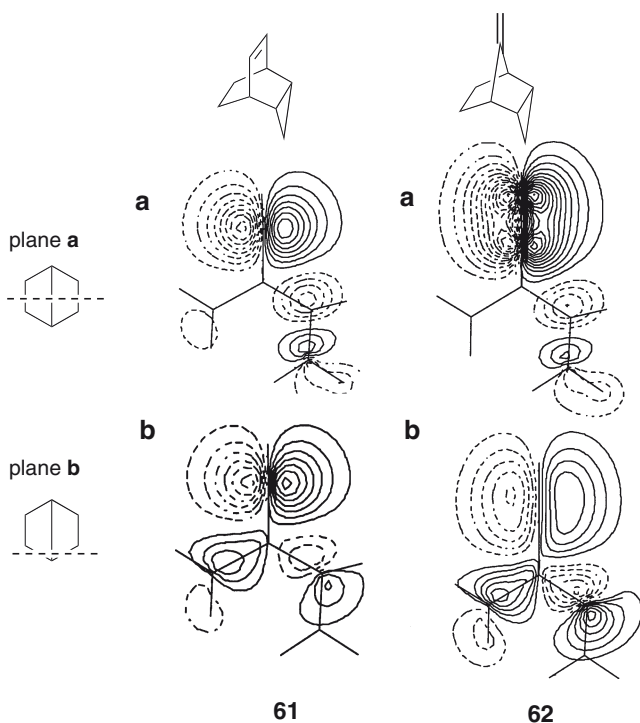


Fig. 10 Contour plots of π orbitals of olefins in unsymmetrical phase environments

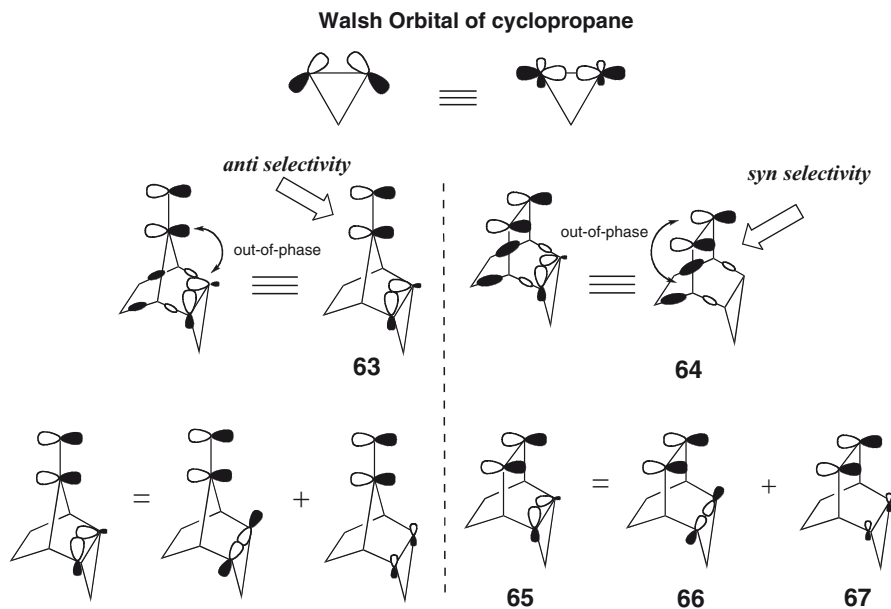


Fig. 11 Different orbital interactions in the different arrangements

group observed in the bicyclo[2.2.2]octene (**59a**) is equivalent to that of an electron-withdrawing substituent, such as a cyano (**48b**) or a methoxycarbonyl (**48c**) group, which is consistent with *syn* preference in dihydroxylation and epoxidation [118]. This notion is in sharp contrast to the conventional understanding of this group as strongly electron-donating [70, 140, 141]. Wiberg and Bader proposed that on the basis of “atoms in molecule” theory, hydrogen is more electronegative than carbon in hydrocarbons with no geometrical strain, and the order of the relative electron-withdrawing abilities of the groups is $H > CH_3 > CH_2 > CH > C$ [142]. The electronegativity of a carbon increases with an increase in geometrical strain as measured by the decrease in its bond path angles from the normal values. This view at least partially explains why the strained cyclopropyl structure of **59a** behaves like an electron-withdrawing group.

This notion is also supported by the following experimental observations. Because substitution of a cyano group on the cyclopropane ring lowers the energy of the Walsh orbital of the cyclopropyl group, the resultant attenuation of the interaction of the olefin orbital with the Walsh orbital, if this interaction is indispensable, would reduce the facial selectivity. However, substitution of a cyano group on the cyclopropyl group, as in *exo*-cyano **59c** and *endo*-cyano **59d**, essentially does *not* modify the *syn*-preference in dihydroxylation and epoxidation, but even increases the *syn* preference (**59c** (98:2) and **59d** (>99:<1)) in the case of dihydroxylation.

3.4 Overlapping of Olefin π Orbital with π Orbitals at the β Positions

3.4.1 Spiro[cyclopentane-1,9'-fluorene]-2-enes

Epoxidation of substituted spiro[cyclopentane-1,9'-fluorene]-2-enes **68** with a peroxidic reagent was studied [98]. The spiro olefins react with *m*-chloroperbenzoic acid (mCPBA) in chloroform at 3 °C to give a mixture of the epoxides. In all cases (2-nitro (**68b**), 4-nitro (**68c**), 2-fluoro (**68d**) and 2-methoxyl (**68e**) groups), the *syn*-epoxides, i.e., the *syn* addition of the peroxidic reagent with respect to the substituent, is favored. For example, for **68b**:*syn:anti* = 63:37; for **68c**:*syn:anti* = 65:35. Thus, a similar bias is observed in both the reduction of the carbonyl derivatives of **30** and the epoxidation of the derivatives of **68**.

In the epoxidation of an olefin with a peracid, the occupied π orbital of the olefin group (π_{CC} , HOMO) interacts with the vacant orbital (LUMO) of the peracid [143, 144]. The higher-lying aromatic π orbital of the substituted fluorenes (**69**) can interact with the π_{CC} orbital in a similar manner to spiro conjugation (Fig. 12).

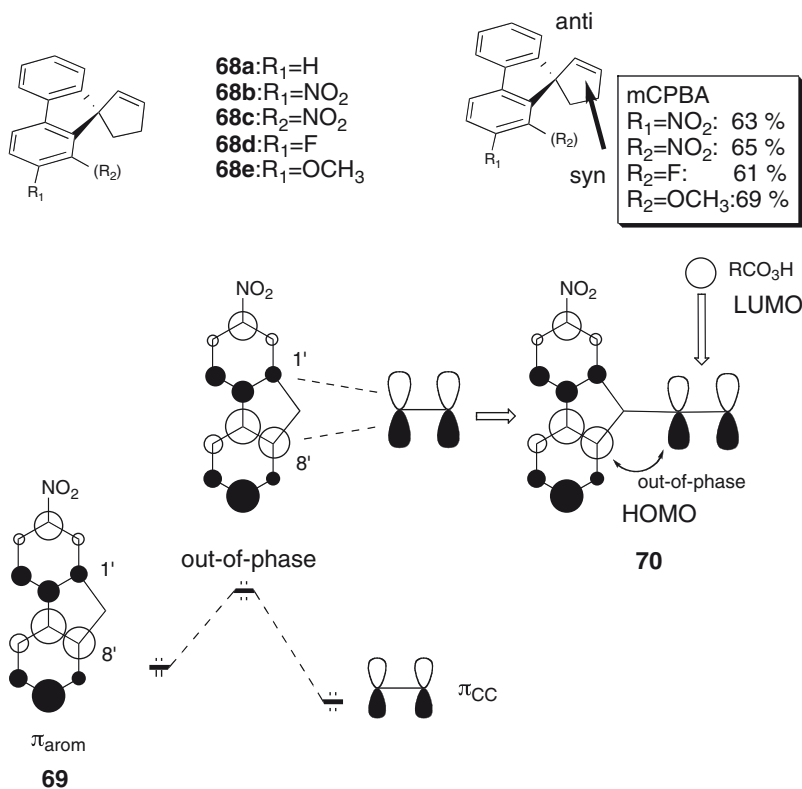
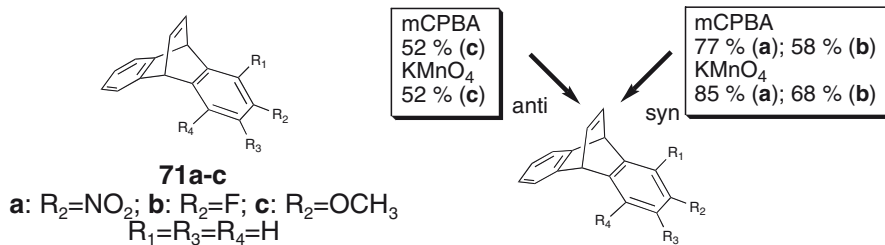


Fig. 12 Orbital unsymmetrization of the olefin π orbital

Out-of-phase combination of π_{CC} with the aromatic π orbital (**69**) of the substituted fluorene raises the energy so as to activate the π_{CC} fragment of the olefin to the attack of an electrophile. The relevant aromatic π orbital of substituted fluorenes, for all substituents studied, has biased orbital coefficients at the points of interaction: the coefficient of C-8' is larger than that of C-1' (see **69**). These different overlaps result in divergent amplitudes of the antibonding region between nuclei (**70**). The antibonding unsymmetrization, arising from the orbital bearing a larger coefficient, greatly reduces the electron-donating ability toward the attack of the electron-deficient orbital of an electrophile (motif iii in Fig. 1). Unexpectedly, a similar orbital distribution was found in the case of 2-methoxyfluorene. Thus, the π_{CC} fragment favors the attack of an electrophile on the side of the substituent, providing a reasonable interpretation of the observed biased epoxidation of the olefin in the cases of both a nitro and a methoxy substituent. In the present π - π interaction system, the electron-donating ability of the orbitals at the β position with respect to the olefin group will determine the facial selectivity of the olefin, i.e., the opposite side to the better-electron-donating π orbital is favored.

3.4.2 Dibenzobicyclo[2.2.2]octatrienes

Epoxidation and dihydroxylation of the olefin moiety of 2-substituted dibenzobicyclo[2.2.2]octatrienes (**71**) were studied [103, 104].



2-Nitrodibenzobicyclo[2.2.2]octatriene **71a** undergoes preferential *syn*-addition (with respect to the nitro group) of peroxidic reagents, i.e., *m*-chloroperbenzoic acid, osmium tetroxide and potassium permanganate. In the epoxidation of **71a** with mCPBA, the *syn*-epoxide is favored over the *anti*-epoxide. In the dihydroxylation with osmium tetroxide or potassium permanganate, the *syn*-diol is also favored over the *anti*-diol. 2-Fluorodibenzobicyclo[2.2.2]octatriene **71b** also preferentially gave the *syn*-epoxide and the *syn*-diol. On the other hand, the 2-methoxy substrate **71c** showed only a small preference in the reactions, giving a slight excess of the *anti*-products. The olefin π orbital interacts with the aromatic π orbital of the dihydroanthracene in convex geometry (like **72**). The combination is in an out-of-phase fashion. The HOMO (**72**) of 2-nitrodihydroanthracene is essentially localized on the unsubstituted benzene moiety, stemming predominantly from the HOMO of the benzene, which is higher in energy than the HOMO of the nitrobenzene (Fig. 13). Therefore,

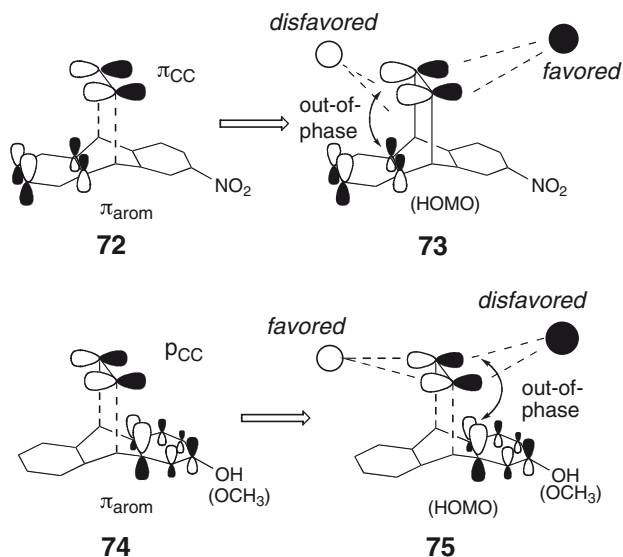


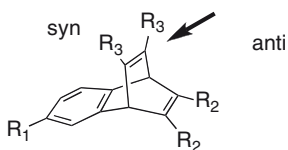
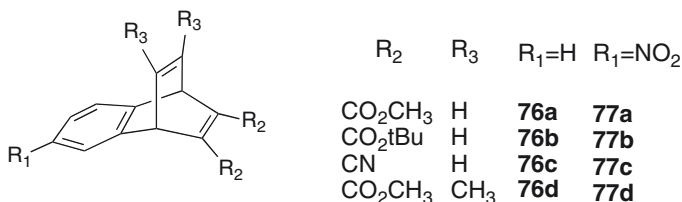
Fig. 13 Unsymmetrization of the olefinic π orbital

electrophilic oxidative reagents attack the olefinic π lobe opposite the out-of-phase environment, that is, from the same side (syn) as the substituent (motif iii in Fig. 1). In the case of an electron-donating hydroxyl group, an out-of-phase combination of π_{CC} of the olefin with the HOMO of hydroxydihydroanthracene (instead of OCH_3 , **74**) raises the energy so as to activate the π_{CC} fragment to the attack of an electrophile. The HOMO of 2-hydroxydihydroanthracene (**74**) also has biased orbital amplitudes localizing on the phenol moiety, not on the benzene moiety. Therefore, the attack of an electrophile on the side opposite the hydroxyl group is favored. However, the HOMO of hydroxydihydroanthracene (**74**) increases the energy separation from the HOMO of ethylene by 13.63 kcal mol⁻¹ (PM3) as compared with the case of the nitro substituent (**72**). The large energy gap of these interactive fragments would decrease the effect of asymmetrization in **75**. This is consistent with the small, but consistent preference for *anti*-attack of the reagents in 2-methoxy-dibenzobicyclo[2.2.2]octatriene **71c**.

3.5 Two π Component System. Validation of Orbital Size Effect on the Magnitude of Facial Selectivity

The dibenzobicyclo[2.2.2]octatriene system (**71**) essentially involves interaction of three composite π orbitals, i.e., the olefinic π orbital as the reaction center, and two aromatic π orbitals. A simplified interaction network, i.e., *two π component systems free from steric bias*, is intriguing. In this context the facial selectivities of

benzobicyclo[2.2.2]octatrienes (**76** and **77**) bearing two electron-withdrawing groups at one of the olefin groups were studied [145]. Remote substituents do not change facial preference, but do change the magnitude of the selectivity.



R ₂	R ₃	Reagent	R ₁ = H		R ₁ = NO ₂			
			Ratio(<i>anti</i> : <i>syn</i>)	d.e.	Ratio(<i>anti</i> : <i>syn</i>)	d.e.		
CO ₂ CH ₃	H	mCPBA	76a	86:14	72	77a	60:40	20
CO ₂ <i>t</i> Bu	H	mCPBA	76b	63:37	26	77b	54:46	8
CN	H	mCPBA	76c	94:6	88	77c	79:21	58
CO ₂ CH ₃	CH ₃	mCPBA	76d	79:21	58	77d	61:39	22
CO ₂ CH ₃	H	OsO ₄	76a	99<:1>	98<	77a	84:16	68
CO ₂ <i>t</i> Bu	H	OsO ₄	76b	95:5	90	77b	73:27	46

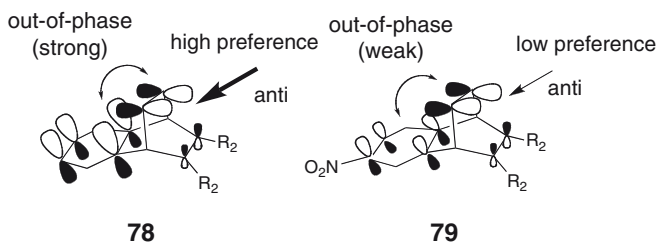
Unsubstituted benzobicyclo[2.2.2]octatriene **76a** bearing two methoxycarbonyl groups at the C₂ and C₃ positions exhibited strong *anti* preference (with respect to the benzene moiety) with two oxidative electrophilic reagents, *m*-chloroperbenzoic acid (mCPBA) and osmium tetroxide.

The diastereomeric excess (d.e.) of **76a** reached 72% (epoxidation) and 98% (dihydroxylation). Nitro substitution on the aromatic ring (as in **77a**) significantly reduced the selectivity (increased the *syn* proportion), although *anti* preference was still retained in epoxidation (20% d.e.) and in dihydroxylation (68% d.e.).

The *anti* face, i.e., the *syn* side with respect to the diester groups, seems to suffer from steric congestion owing to the out-of-plane conformations of the proximate diester functional groups. This is supported by the results with the bis(*tert*-butoxycarbonyl) compound **76b**: the sterically demanding *tert*-butyl groups did reduce the selectivity in both epoxidation (26% d.e.) and dihydroxylation (90% d.e.). However, *anti* preference survived, indicating that the intrinsic nature of the benzobicyclo[2.2.2]octatriene motif is as proposed. An aromatic nitro group (**77b**) also reduced (46% d.e. in dihydroxylation) or almost abrogated

(8% d.e. in epoxidation) the selectivity. Therefore, the selectivity is determined by non-sterical bias.

The HOMO of benzotrienes **76** and **77** can be represented as a combination of the three π orbitals, i.e., $\Psi_{\text{HOMO}} = a\pi_{\text{olefin}} + b\pi_{\text{aromatic}} + c\pi_{\text{olefin(R}_2)}$. However, owing to the low energy of the π orbital (π_{R_2}) of the ethylene substituted with electron-withdrawing groups, the HOMO of **76** and **77** can be approximated as a two π interacting system (i.e., the first two terms, see



78 and **79**): the orbital components are assumed to involve the π orbital (π_{olefin}) of the ethylene (as the reaction center) and that (π_{arom}) of the aromatic ring. In this system, the remote nitro substituent significantly weakened the out-of-phase interaction of the aromatic π orbital with the olefin π orbital (**79**). Thus, the amplitude of the out-of-phase region exposed to the π reaction center can determine the magnitude of facial selectivity. This experiment provided support for the notion that the magnitude of facial selectivities depends on the magnitude of overlap of the interacting orbitals.

4 Stereoselection of Diels–Alder Reactions: Dienophiles

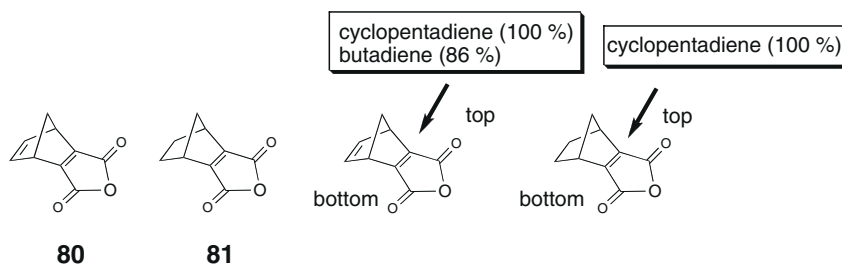
Although there have been many experimental and theoretical studies on the behavior of facially perturbed dienes (see below), only a few systematic experiments have been carried out to characterize facially perturbed dienophiles. Dienophiles embedded in the norbornane or norbornene motif have been rather intensively studied [146–150]. In most cases, steric effect controls selectivity, but in some cases the reactions are considered to be free from steric bias, and the selectivity has been explained in terms of other factors, such as orbital effects [151, 152].

During the past decade, many papers have dealt with the facial selectivities of Diels–Alder reactions, particularly in relation to dienes [153–159], and various attempts have been made to rationalize the origins of the selectivities [160]. The facial selectivities of Diels–Alder reactions are discussed in detail in Chapter “ π -Facial Selectivity of Diels–Alder Reactions” by Ishida and Inagaki in this volume. In this and the following section, we will consider the facial selectivities of Diels–Alder reactions in terms of orbital phase environment.

4.1 Dienophiles Based on Norbornane Structure

4.1.1 Maleic Anhydride Embedded in Norbornadiene Derivative

Edman and Simmons [146] synthesized bicyclo[2.2.1]hepta-2,5-diene-2,3-dicarboxylic anhydride **80** as a facially perturbed dienophile on the basis of the norbornadiene motif, and its top selectivity in Diels–Alder reactions with cyclopentadiene (top-*exo*:top-*endo* = 60~70:1) was observed by Bartlett (Fig. 14) [147]. The most preferred addition was top-*exo* addition, along with the minor addition modes, top-*endo* >> bottom-*endo* addition (Fig. 14). The addition of butadiene to this anhydride preferentially afforded the top-adduct (top:bottom = 6:1). In the addition of anthracene, a top-adduct was formed exclusively.



Cycloaddition of bicyclo[2.2.1]hept-2-ene-2,3-dicarboxylic anhydride **81** with cyclopentadiene was also studied by Bartlett et al., who found exclusive top addition, the top-*endo*/top-*exo* ratio being 3:2 [147]. The *endo*/*exo* ratio is significantly different from that of **80** (60–70:1). The observed top selectivity in norbornadiene (**80**) and norbornene (**81**) derivatives is consistent with the inherent top reactivity of norbornanone **25** and norbornene **57**. Orbital unsymmetrization of the dienophile

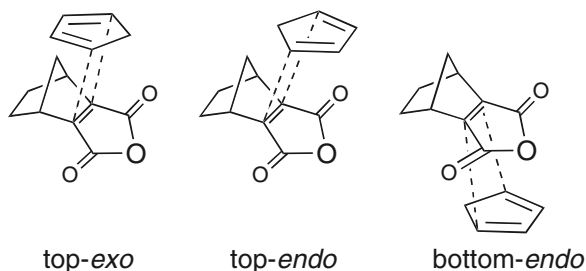
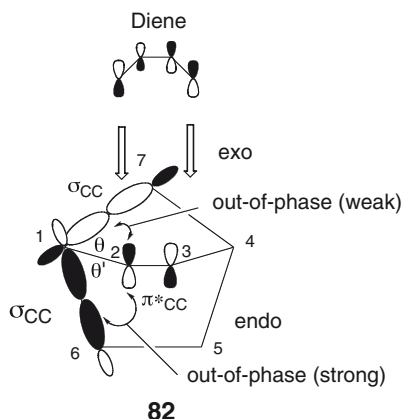


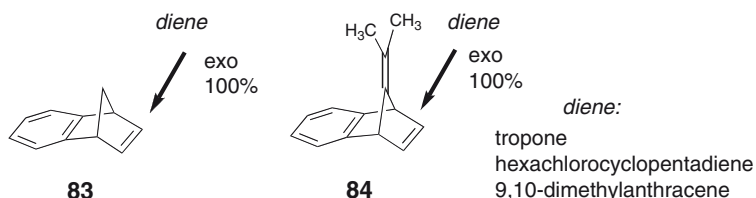
Fig. 14 Addition modes of cyclopentadiene

vacant π orbital arising from out-of-phase σ - π^* coupling (**82**) is proposed to participate in the top (*exo*) preference.

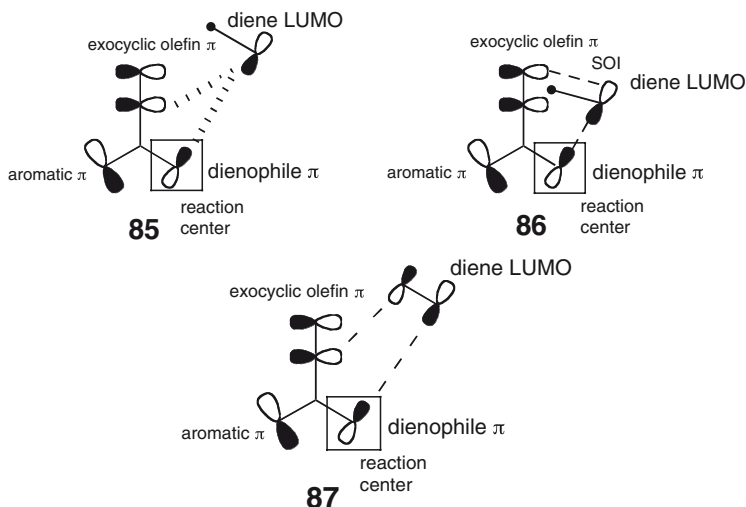


4.1.2 Benzonorbornadienes

Diels–Alder cycloadditions involving norbornene **57** [34], benzonorbornene (**83**), 7-isopropylidenenorbornadiene and 7-isopropylidenebenzonorbornadiene (**84**) as dienophiles are characterized as inverse-electron-demand Diels–Alder reactions [161, 162]. These compounds react with electron-deficient dienes, such as tropone. In the inverse-electron-demand Diels–Alder reaction, orbital interaction between the HOMO of the dienophile and the LUMO of the diene is important. Thus, orbital unsymmetrization of the olefin π orbital of norbornene (**57**) is assumed to be involved in these top selectivities in the Diels–Alder cycloaddition.



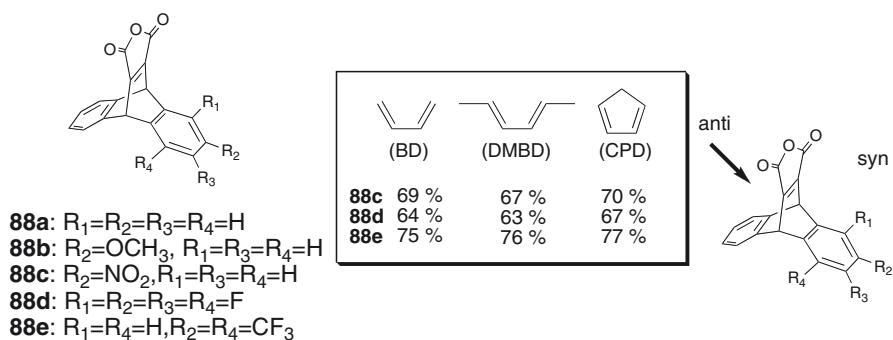
Furthermore, large rate acceleration was encountered in these Diels–Alder cycloadditions of 7-isopropylidenebenzo-norbornadiene (**84**) as compared with benzonorbornadiene (**83**) in the reaction of tropone [161]. As pointed out by Haselbach and Rossi [162], the initial orbital interaction of the HOMO of **84** and the LUMO of the diene is a non-interacting one (**85**) because of the orbital symmetry disagreement, leading to decreased reactivity of **84**. Thus, the observed large acceleration and high *exo*-selectivity of **84** can be rationalized in terms of



favorable π^* back-lobe interaction of the diene (the LUMO) with the π orbital of the terminal carbon atom of the exocyclic olefin (SOI) of **84** (**86**). The secondary orbital interactions (**87**) [161], though sterically congested, may attenuate the initial unfavorable orbital interaction at the reaction centers.

4.2 Dienophiles Based on Dibenzobicyclo [2.2.2]octatriene Structure

The Diels–Alder reactions of anhydrides based on a dibenzobicyclo[2.2.2]octatriene motif **88a–88e**, as non-sterically biased dienophiles, were studied [151].



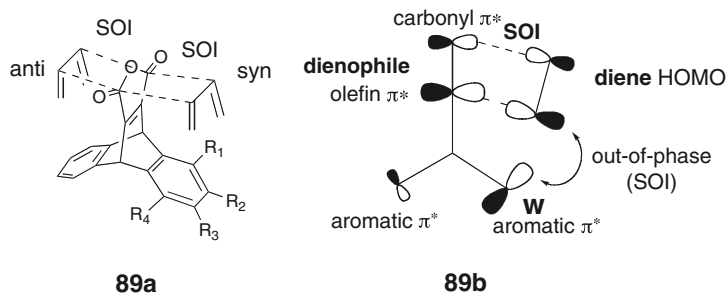
The cycloaddition reactions of the anhydrides (**88a–88e**) with acyclic dienes (butadiene and 1,4-dimethylbuta-1,3-diene) were conducted at 23 °C in dichlo-

romethane as a co-solvent. While the electron-donating methoxy-substituted dienophile **88b** showed no facial selectivity in the cycloaddition, the nitro-substituted **88c** did exhibit facial selectivity, i.e., *anti*-addition (with respect to the substituted benzene ring) is favored over *syn*-addition. The perturbing effect of an electron-withdrawing substituent is larger in 1,2,3,4-tetrafluoro- (**88d**) and 2,3-bis(trifluoromethyl)-substituted anhydrides (**88e**). Both substrates (**88d** and **88e**) also favored *anti*-addition over *syn*-addition: the tetrafluoro compound (**88d**) exhibited a similar bias (*syn:anti* = 36:64) to the nitro compound, and the bis(trifluoromethyl) compound (**88e**) exhibited a bias as large as 25:75 (*syn:anti*).

The relative rates of cycloaddition of **88b–88e** were measured in comparison with that of the parent **88a** as a reference. The methoxy substituent has practically no effect on the reaction rate. However, it is apparent that electron-withdrawing substituents (**88b**, **88c** and **88e**) significantly accelerate the *anti*-addition, whereas in *syn*-addition the acceleration is not as large; the rate is comparable to that of the reference compound (**88a**). In the reactions of the tetrafluoro-substituted dienophile **88d**, we found significant rate acceleration on both sides, though *anti*-side addition was still substantially favored.

Therefore, the preference of the cycloadditions is opposite in direction to the biases observed in nucleophilic additions of 2-substituted 9,10-dihydro-9,10-ethanoanthracen-11-ones (**34**) (dibenzobicyclo[2.2.2]octadienones) and in electrophilic additions of 2-substituted 9,10-dihydro-9,10-ethenoanthracenes (dibenzobicyclo[2.2.2]octatrienes) **71** [103].

We postulate that the attack on both sides is accelerated by positive SOI (**89a**), but an unfavorable orbital interaction along the *syn* attack trajectory (**89b**) cancels the acceleration at the *syn* face [151]: as the diene approaches the anhydride moiety (preferentially in *endo* fashion), unfavorable out-of-phase interaction (SOI) of the π lobes at C₁ and C₄ of the diene with the π^* lobes of the aromatic moiety of the dienophile occurs (**89**). The unexpected *anti*-selectivity stems from unfavorable SOI on the *syn* side.

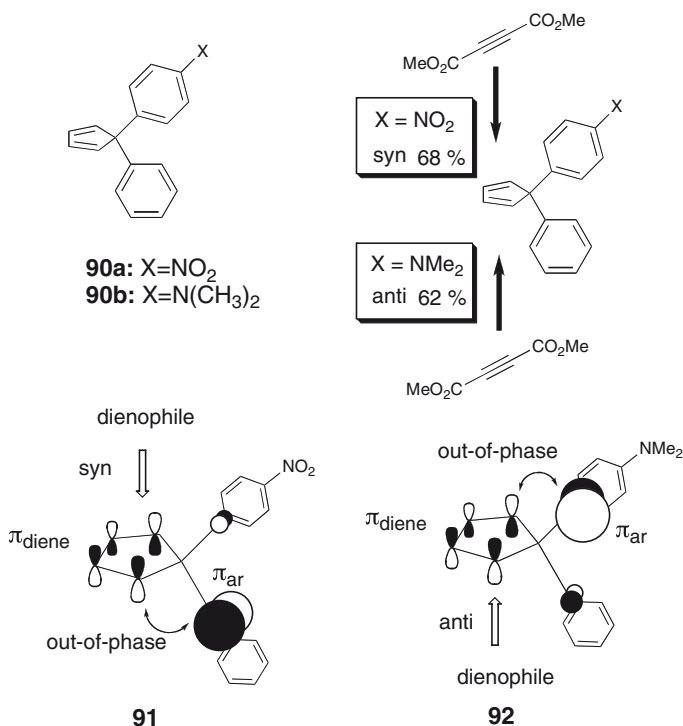


5 Stereoselection of Diels–Alder Dienes

5.1 Cyclopentane Case

5.1.1 5,5-Diaryl-1,3-Cyclopentadienes

The sterically unbiased dienes, 5,5-diarylcyclopentadienes **90**, wherein one of the aryl groups is substituted with NO_2 , Cl and $\text{N}(\text{CH}_3)_2$, were designed and synthesized by Halterman et al. [163] Diels–Alder cycloaddition with dimethyl acetylenedicarboxylate at reflux (81°C) was studied: *syn* addition (with respect to the substituted benzene) was favored in the case of the nitro group (**90a**, $\text{X} = \text{NO}_2$) (*syn:anti* = 68:32), whereas anti addition (with respect to the substituted benzene) is favored in the case of dimethylamino group (**90b**, $\text{X} = \text{N}(\text{CH}_3)_2$) (*syn:anti* = 38:62). The facial preference is consistent with those observed in the hydride reduction of the relevant 2,2-diaryl-cyclopentanones **8** with sodium borohydride, and in dihydroxylation of 3,3-diarylcyclopentenes **43** with osmium trioxide. In the present system, the interaction of the diene π orbital with the σ bonds at the β positions (at the 5 position) is symmetry-forbidden. Thus, the major product results from approach of the dienophile from the face opposite the better π electron donor at the β positions, in a similar manner to spiro conjugation. Unsymmetrization of the diene π orbitals is inherent in **90**, and this is consistent with the observed facial selectivities (**91** for **90a**; **92** for **90b**).



Facial selectivities of cycloaddition reactions of 5,5-disubstituted cyclopentadienes have been studied by Inagaki and Ishida [32, 44, 45] and other groups [40].

5.1.2 Spiro-1,3-Cyclopentadienes

Benzo[*a*]- (a), benzo[*b*]- (b) and benzo[*c*]fluorenes (c) bearing a diene group (**93**) in spiro geometry are three possible combinatorial isomers wherein the direction of fusion of the naphthalene is different (Fig. 15). The π reaction centers of the diene groups are subject to spiro-conjugation [98, 99, 102] with the planar aromatic π system. The effect of perturbation arising from spiro-conjugation on

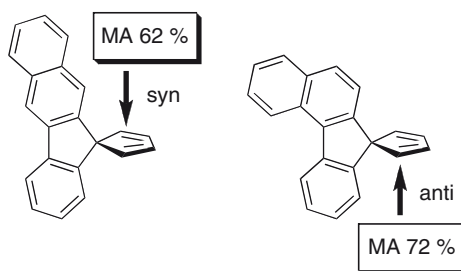
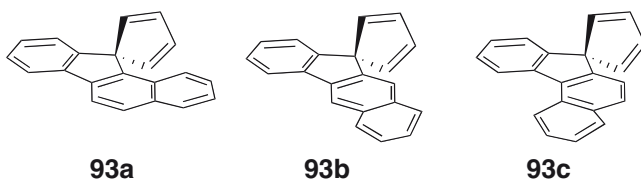
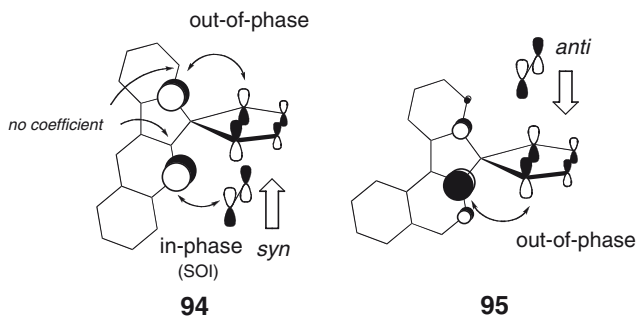


Fig. 15 Possible combinatorial isomers

the chemical reactivities, in particular the facial selectivities, were investigated [164]. With respect to the π faces of the relevant reaction centers, the first aromatic system is sterically biased (i.e., sterically unsymmetrical), while the latter two systems are assumed to be free from steric bias. These dienes react as Diels–Alder dienes with several dienophiles (maleic anhydride, *N*-phenylmaleimide and *N*-phenyl-1,3,5-triazoline-2,4-dione). The *endo* isomers of the adducts were predominantly formed. The direction of fusion of the aromatic ring changes the facial preference. The diene (**93b**) bearing benzo[*b*]fluorene favored *syn* addition of the dienophiles (*syn:anti* = 62:38 (for maleic anhydride)) with respect to the naphthalene ring, whereas the diene **93c** (benzo[*c*]fluorene) showed a reverse *anti* preference for the additions (*syn:anti* = 28:72 (for maleic anhydride)). The diene systems involve complete spiro-conjugation, leading to an effective overlap of the diene π orbital and the aromatic π orbital. The observed preferences of the diene (*syn* (**94**) and *anti* (**95**)) seem to be consistent with this idea.

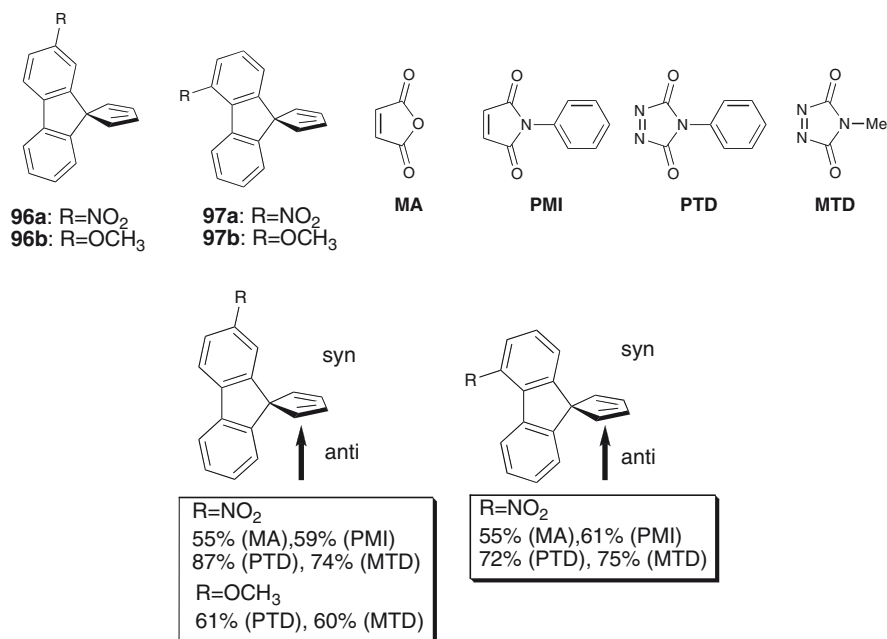




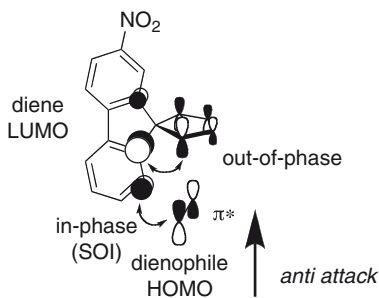
In the presence of out-of-phase spiro interaction of the dienes, there was also a large subsidiary in-phase orbital interaction on the naphthalene moiety of **93a** (**94**). The syn addition observed in the case of **93a** can be accounted for in terms of the additional intervention of this SOI.

5.1.3 Spirofluorene-Diene System

In order to study the effect of perturbation arising from spiro-conjugation on the chemical reactivities, in particular the facial selectivities, sterically unbiased dienes (**96** and **97**) based on fluorenes in spiro geometry have been synthesized [165]. These dienes react as Diels–Alder dienes with several dienophiles (maleic anhydride (MA), *N*-phenylmaleimide (PMI), *N*-phenyl-1,3,5-triazoline-2,4-dione (PTD) and *N*-methyl-1,3,5-triazoline-2,4-dione (MTD)).



In the cases of the 2-nitro-substituted (**96a**) and 4-nitro-substituted dienes (**97a**), *anti* addition of the dienophiles with respect to the nitro substituent was favored. The reactions of **96a** and **97a** with PTD and MTD proceed readily even at low temperature (below $-43\text{ }^{\circ}\text{C}$), and the facial selectivity (*anti:syn*) is as large as 87:13 (**96a** in the case of PTD) or 75:25 (**97a** in the case of MTD). When the reaction of **96a** with PTD was carried out at a higher temperature ($0\text{ }^{\circ}\text{C}$), the facial selectivity was reduced (*anti:syn* = 76:24), though *anti* preference was retained. In the reactions of **96a** with less reactive dienophiles (MA and PMI), which required high reaction temperature and long reaction time, *anti* preference of the addition of PMI was observed, although the magnitude of the facial selectivity decreased, i.e., *anti:syn* = 59:41, and in the case of MA the selectivity almost disappeared. In the case of the 2-methoxy-substituted diene **96b**, *anti* preference of the addition was observed, but the magnitude of the facial selectivity was reduced (*anti:syn* = 60:40), even in the reactions of the reactive dienophiles (PTD and MTD). On the other hand, the 4-methoxy-substituted diene **97b** showed no significant facial selectivity in the reactions of the dienophiles, PTD and MTD. This divergent behavior of **96b** and **97b** is in contrast to the similar behaviors of the 2- (**96a**) and 4-nitro-substituted dienes (**97a**) in terms of *syn* facial preference. The present *syn* selectivity is probably due to the in-phase interaction of the approaching diene with the peripheral orbital of the unsubstituted benzene moiety, that is, a kind of SOI (**98**), in a similar manner to the benzofluorene case (**89** and **94**).



5.2 Cyclohexadiene Case

5.2.1 Heterocyclic Propellanes

The cycloaddition reaction of heterocyclic propellanes **99** ($X = \text{O}$ and S) with *N*-phenyltriazolinedione (NN) (Fig. 16) affords the *anti* adduct with respect to the bridge [166–168]. Replacement of the $\alpha\text{-CH}_2$ groups by carbonyls (that is **100**),

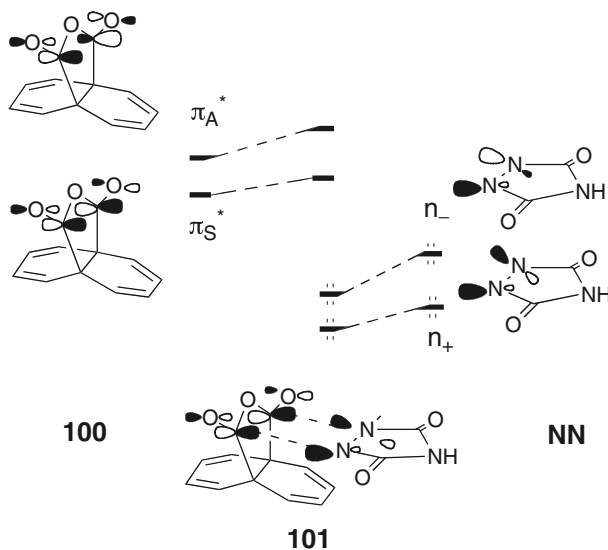
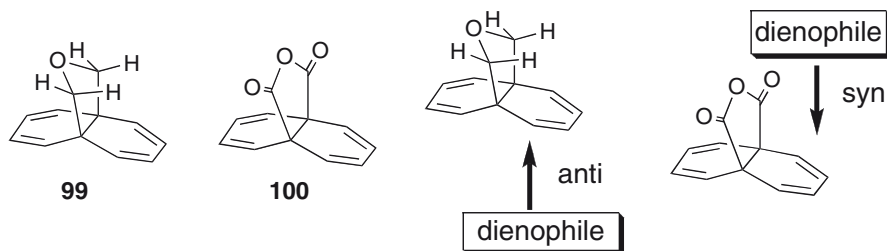


Fig. 16 Secondary orbital interaction (SOI)

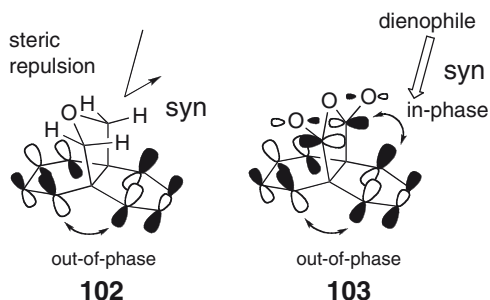


instead, resulted in the formation of only *syn* products. Secondary orbital interactions (SOI) were considered to be responsible for the reverse *syn* addition of triazolinediones to anhydride **100** (Fig. 16) [168].

When the carbonyl groups are present, the transition state for *syn* attack is stabilized by interactions between the in-phase combination of the NN lone pairs and the antisymmetric π^* orbital of the CO-X-CO bridge (**100**). Although the secondary effect (SOI) operates only during *syn* approach and contributes added stabilization to this transition state, the primary orbital interaction (see **103**) between the HOMO of the cyclohexadiene moiety of **100** and the π^* orbital of the dienophile (NN, Fig. 16) is differentiated with respect to the direction of attack, i.e., *syn* or *anti*, of triazolinedione (NN, Fig. 16).

The stereochemical course of the first reaction of **99** can be rationalized in terms of the relative steric contributions of the flanking bridge, in particular of methylene

protons and the puckering oxygen atom (**102**). In terms of orbital interactions, both systems, **99** and **100**, involve the essential out-of-phase orbital interaction motif between two π components of the two butadiene units (**102** and **103**), and therefore, the *anti* addition is intrinsically unfavorable in these systems. Replacement of the flanking methylenes with the trigonal planar carbon atoms as

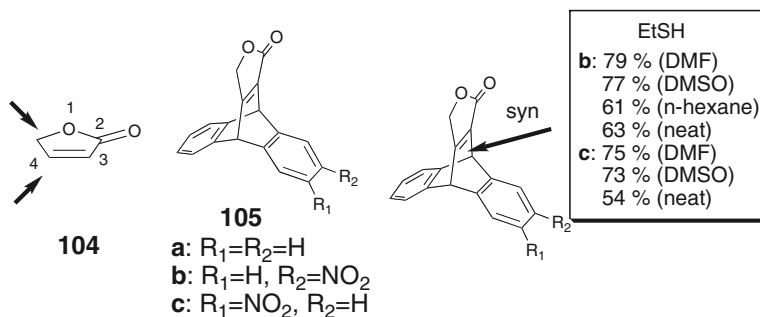


in **100** retrieves the genuine steric unbiased, exhibiting the inherent *syn* addition arising from the orbital unsymmetrization (**103**). The contribution of the in-phase motif of the vacant carbonyl π^* orbital of the anhydride moiety (**103**) to the HOMO of the molecule **100** also encourages *syn* addition.

6 Stereoselection of Nucleophilic Conjugate Addition

6.1 Bicyclic Systems

In 1,4-conjugate additions toward cyclic unsaturated lactones, facial selectivity

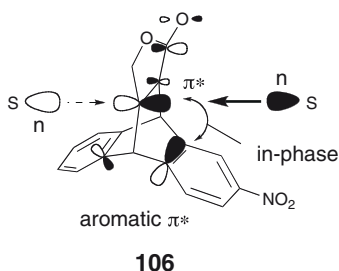


of the 2(*5H*)-furanone (**104**) embedded in a dibenzobicyclo[2.2.2]octatriene frame (**105a–105c**) was studied [169]. The base-catalyzed 1,4-addition of ethanethiol to **105a–105c** in a variety of aprotic solvents at 23 °C for 75 h was studied.

The 3-nitro lactone (**105b**) favors *syn*-addition rather than *anti*-addition in all cases (with respect to the nitro group). The 2-nitro lactone (**105c**) also favors *syn*-addition, though the ratio obtained in neat reaction is smaller than that of **105b**. In both cases (**105b** and **105c**), it was found that the magnitude of the *syn*-preference increased with increasing solvent polarity: the *syn/anti* ratio of **105b** and that of **105c** reached 79:21 and 75:25, respectively, in DMF. On the other hand, the reaction in a non-polar solvent, such as *n*-hexane, showed a smaller selectivity than that in polar solvents, though *syn*-preference was still observed. These results indicate intrinsic *syn*-preference of attack of the nucleophilic reagent on **105b** and **105c**.

The *syn*-preference of **105b** and **105c** is similar to those observed in the reduction of the related ketones, **34** and in the epoxidation and dihydroxylation of the related olefins **71** [104]. Although the trajectories of the attacking reagents are considered to be different in these reactions [83–87, 170, 171], all three types of reactions favor *syn*-addition, which excludes a predominant role of divergent trajectories in these dibenzobicyclic systems.

The substituent effect of the aromatic nitro group can be accounted for in terms of π orbital unsymmetrization. The LUMO of the dibenzobicyclic lactone (**106**) can be analyzed as an in-phase combination of three vacant π^* orbitals, i.e., those of benzene, nitrobenzene and the 2(5*H*)-furanone moiety. The energetically



lower-lying π^* orbital of the nitrobenzene fragment contributes significantly to the LUMO of the whole molecule, rather than the π^* orbital of the non-substituted benzene. Thus, the LUMO of the 2(5*H*)-furanone is unsymmetrized (**106**). Therefore the *syn*-attack of the nucleophilic reagent is favored because of the additional *in-phase* interaction of the π^* lobe of the nitrobenzene motif.

7 Detection of Orbital Interactions in Alternative Component

7.1 Nitration of Fluorene Derivatives

Interactions between two fragments (i.e., two functional groups) in a molecule would be subject to efficient reciprocal perturbations, reminiscent of “action and reaction” in dynamics. Few studies have paid attention to such reciprocal interactions,

which can modify the reactivities inherent to the respective functional groups. The following example serves highlight the significance of reciprocal interactions in the nitration of the fluorene ring of spiro ketones **30**.

In the spiro systems **30**, the aromatic orbitals unsymmetrize the carbonyl orbital. Simultaneously, the carbonyl group can perturb the orthogonal aromatic ring. Nitration of the fluorene derivatives (**30**) bearing a spiro substituent was studied (Fig. 17) [96, 97].

The reactivities of **30** can be interpreted in terms of the reciprocal perturbation of the aromatic ring arising from the bisected carbonyl group. Fluorene **107** exhibits greater nucleophilicity at C-2 than at C-4, due to increased conjugation of the aromatic rings and steric congestion at C-4. In the nitration of the parent fluorene **107** at $-43\text{ }^{\circ}\text{C}$ with acetyl nitrate, the isomer distribution was observed to be 67% at C-2 and 33% at C-4. Figure 17 also shows the 4-/2-nitration ratios. A spiro-substitution, on the other hand, was found to have a large effect on the nitration, resulting in a great change in the distribution of products: instead of the 2-nitro derivative (11%), spiro[cyclopentane-1,9'-fluorene]-2-one **30** predominantly gave the 4-nitro derivative (77% yield) with the nitrating reagent at $-75\text{ }^{\circ}\text{C}$. A similar divergence in the distributions of nitrated compounds was also observed in the case of the reactions of the spiro fluorene bearing a six-membered ring, spiro[cyclohexane-1,9'-fluorene]-2-one **108**. The bisected carbonyl group of **30** and **108** plays a significant role in these divergent nitrations: the nitration of spiro[cyclopentane-1,9'-fluorene] **109** and spiro[cyclohexane-1,9'-fluorene] **110**, the decarbonylated compounds, resulted in the commonly expected distributions of nitrated fluorenes. Judging from the ratios of 4-/2-nitration, a less flexible conformation, i.e., a more rigid planarity of the five-membered ring of **30** and **109**, strongly perturbed the nitration. Neither the cyclohexane ring nor the cyclopentane ring, in the spiro-geometry, encouraged the nitration at C-4, or rather both enhanced the reactivities at the C-2 position of the fluorene ring. These results also exclude possible steric congestion around the C-2 position owing to the spiro-substitution of the C-9 position. Moreover, the nitration of

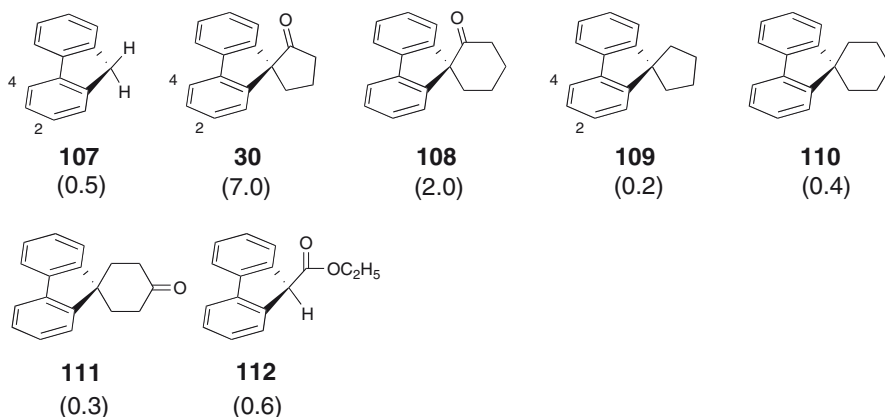


Fig. 17 Reciprocal perturbations in nitrations ratios of 4-/2-nitration are shown in parentheses

spiro[cyclohexane-1,9'-fluorene]-4-one **111** also favored the 2-nitro derivative (65%) rather than the 4-nitro derivative (17%), suggesting that proximity is requisite for interaction between the carbonyl and the aromatic moieties. An indirect effect on the nitration reaction arising from a carbonyl substituent at the C-9 position of the fluorene was indicated by the nitration of 9-ethoxycarbonylfluorene **112**. The 4-/2-ratio (0.6) is very similar to that of fluorene **107** (0.5). All the results, therefore, indicate perturbation of the fluorene ring arising from the bisected carbonyl group of **30**.

8 Orbital Interaction Affects Bond Strength of *N*-Nitroso Bond

8.1 Facial Selectivity of Amine Non-Bonding Orbital

A non-bonding orbital of amines is rapidly inverted at ambient temperature. In this context, the non-bonding orbital constitutes a π face. In the 7-azabicyclo[2.2.1]heptane (**113**) substituted with exo dangling CF_3 groups, the π face of the nitrogen non-bonding orbital is dissymmetrized. We studied the facial selectivity of oxidative electrophilic reaction, i.e., oxidation of the amine **113** with mCPBA, and observed high syn preference of the attack (syn (**114a**):anti (**114b**) = 94:6) (Fig. 18) [171]. Because of the presence of the exo- CF_3 substituents, the amine inversion process can be biased. That is, in CD_2Cl_2 , an equilibrium of the two amine structures (**113a** and **113b**) can be frozen out at -83°C and the ratio of the conformers was 59:41 (conformer assignment was not carried out). Although the amines **113a** and **113b** are present in a slight biased distribution at low temperature, the observed facial selectivity was more overwhelming (Fig. 18). Thus, the dangling CF_3 group

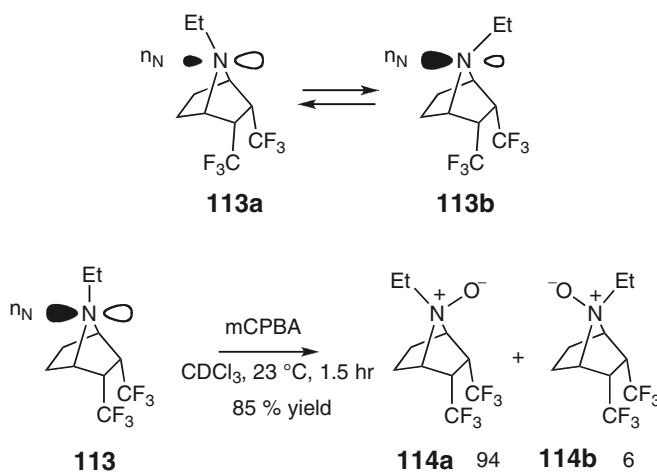
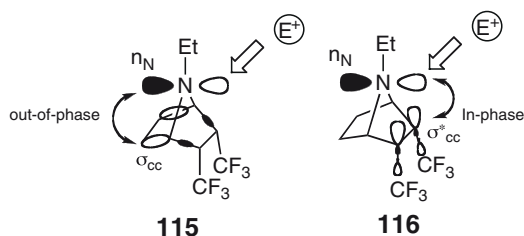


Fig. 18 Oxidative electrophilic reaction of amine

induced facial selectivity in the oxidative electrophilic reaction of the relevant amine nitrogen non-bonding orbital.



The unsymmetrization of the nitrogen non-bonding orbital (n_N) was due to out-of-phase interaction of the electron-rich σ orbital at the β positions (**115**), which leads to *syn* addition. Furthermore, in-phase interaction of the nitrogen non-bonding orbital (n_N) with the low-lying vacant σ^* orbitals (**116**, due to the electron-withdrawing CF_3 groups) can contribute to the *syn* preference.

8.2 N–NO Bond Cleavage of N-Nitrosamines

Orbital interaction described in Sect. 8.1 can also be detected experimentally in terms of the bond strength. The N–NO bond cleavage of *N*-nitrosamines can be controlled by a remote substituent. Two possible modes of cleavage of the N–NO bond of *N*-nitrosamines, i.e., homolytic and heterolytic cleavages, are well recognized (Fig. 19). Aromatic *N*-nitrosamines and aromatic *N*-nitrosoureas were demonstrated to undergo homolytic cleavage of the N–NO bond to give NO (nitric oxide). Aromatic *N*-nitrosoureas and *N*-nitrososulfonamides were also shown to be heterolytically cleaved to give NO^+ (nitrosonium ion) in solution. Thus, some aromatic *N*-nitroso compounds can act as donors of NO or NO^+ . On the other hand, aliphatic *N*-nitrosoureas do not release NO, and there has been no report of aliphatic *N*-nitrosamines that readily undergo N–NO bond cleavage. Although N–NO bond cleavage was not detected in the case of the monocyclic aliphatic *N*-nitrosamine (**121**) with five-membered rings under acidic conditions (under Griess assay conditions), the N–NO bond of the *N*-nitroso derivatives of the 7-azabicyclo[2.2.1]heptane motif (**117–119**) was shown to be cleaved under similar conditions

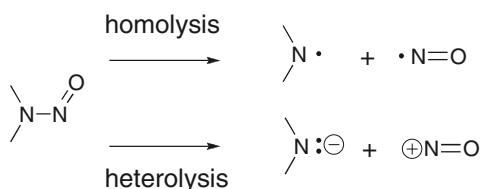


Fig. 19 Two possible modes of N–NO bond cleavage of *N*-nitrosamines

(Fig. 20) [172, 173]. Enhanced N–NO bond cleavage of the *N*-nitroso derivatives of the 7-azabicyclo[2.2.1]heptanes as compared with the unsubstituted derivatives (**120**) was found in the cases of substitution of electron-withdrawing groups, such as an aromatic nitro group (**117**), ester groups (**118**) and the *N*-phenylimido group (**119**). Reduction of resonance in the N–NO group (Fig. 21) of the bicyclic derivatives (**117–120**) is important for promoting N–NO bond cleavage. Electron delocalization arising from the interaction of the nitrogen nonbonding orbital with the vacant aromatic π^* orbital (**122**, Fig. 22a), or from the interaction of the aromatic π orbital with the vacant antibonding $\sigma^*_{\text{N-N}}$ orbital (**123**, Fig. 22b) can weaken the N–NO bond (Fig. 21). Such interactions would account for the facile bond cleavage of **117–119**, which bear a benzo group or electron-withdrawing substituents. This delocalization was facilitated by the *N*-pyramidalization of the relevant bicyclic *N*-nitrosamines. The interaction **122** is exactly similar to **116**.

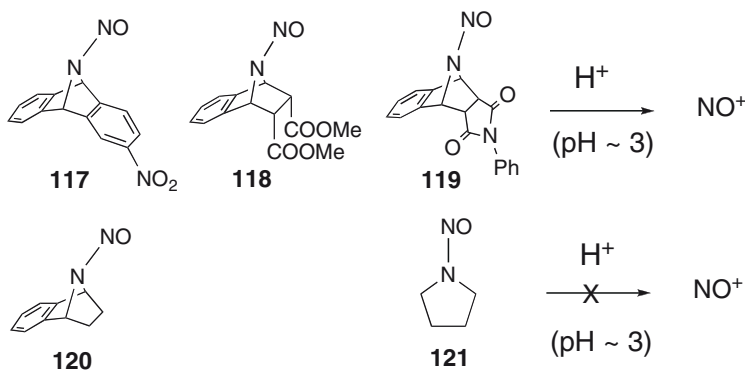


Fig. 20 Weak N–NO bond of bicyclic *N*-nitrosamines

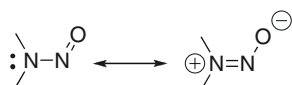


Fig. 21 *N*-Nitrosamine resonance

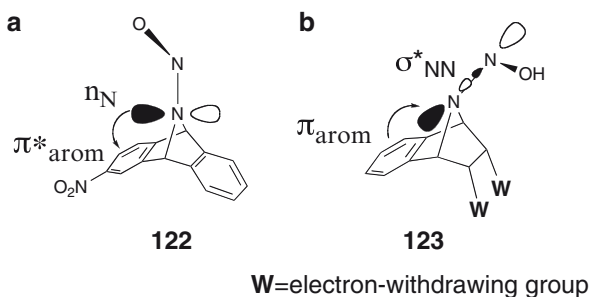


Fig. 22 Orbital interactions which weaken the N–NO bond

9 Conclusion

This reviews contends that, throughout the known examples of facial selections, from classical to recently discovered ones, a key role is played by the unsymmetrization of the orbital phase environments of π reaction centers arising from first-order perturbation, that is, the unsymmetrization of the orbital phase environment of the relevant π orbitals. This asymmetry of the π orbitals, if it occurs along the trajectory of addition, is proposed to be generally involved in facial selection in sterically unbiased systems. Experimentally, carbonyl and related olefin compounds, which bear a similar structural motif, exhibit the same facial preference in most cases, particularly in the cases of adamantanes. This feature seems to be compatible with the Cieplak model. However, this is not always the case for other types of molecules, or in reactions such as Diels–Alder cycloaddition. In contrast, unsymmetrization of orbital phase environment, including SOI in Diels–Alder reactions, is a general concept as a contributor to facial selectivity. Other interpretations of facial selectivities have also been reviewed [174–180].

References

1. Inagaki S, Fukui K (1974) *Tetrahedron Lett* 15:509–514
2. Inagaki S, Fujimoto H, Fukui K (1976) *J Am Chem Soc* 98:4054–4061
3. Ohwada T (1999) *Chem Rev* 99:1337–1376
4. Ohwada T, Shudo K (1994) *Yuki Gosei Kagaku Kyokaiishi* 52:596–607
5. García J, Mayorai JA, Salvatella L (2000) *Acc Chem Soc* 33:658–664
6. Kobuke Y, Fueno T, Durukawa (1970) *J Am Chem Soc* 92:6548–6553
7. Ishihara K, Kondo S, Kurihara H, Yamamoto H, Ohashi S, Inagaki S (1997) *J Org Chem* 62:3026–3027
8. Corey EJ, Lee TW (1997) *Tetrahedron Lett* 38:5755–5758
9. Ishihara K, Fushimi M (2008) *J Am Chem Soc* 130:7532–7533
10. Suzuki Y, Kaneno D, Miura M, Tomoda S (2008) *Tetrahedron Lett* 49:4223–4226
11. Carr JA, Snowden TS (2008) *Tetrahedron* 64:2897–2905
12. Moraleda D, Ollivier C, Santelli M (2006) *Tetrahedron Lett* 47:5471–5474
13. Kreiselmeyer G, Frey W, Fohlisch B (2006) *Tetrahedron* 62:6029–6035
14. Kobler C, Bohrer A, Effenberger F (2004) *Tetrahedron* 60:10397–10410
15. Lindsay HA, Salisbury CL, Cordes W, McIntosh MC (2001) *Organic Lett* 3:4007–4010
16. Luibrand RT, Taigounov IR, Taigounov AA (2001) *J Org Chem* 66:7254–7262
17. Rosenberg RE, Abel RL, Drake MD, Fox DJ, Ignatz AK, Kwiat DM, Schaal KM, Virkler PR (2001) *J Org Chem* 66:1694–1700
18. Chao I, Shih JH, Wu HJ (2000) *J Org Chem* 65:7523–7533
19. Frackenhohl J, Hoffmann HMR (2000) *J Org Chem* 65:3982–3996
20. Salvatella L, Ruiz-Lopez MF (1999) *J Org Chem* 121:10772–10780
21. Laube T (1999) *J Org Chem* 64:8177–8182
22. Tanaka K, Tanaka M, Suemune H (2005) *Tetrahedron Lett* 46:6053–6056
23. Chu JH, Li WS, Chao I, Chung WS (2004) *Tetrahedron* 60:9493–9501
24. Lu CD, Chen ZY, Liu H, Hu WH, Mi AQ, Doyle MP (2004) *J Org Chem* 69:4856–4859
25. Mayo P, Tam W (2002) *Tetrahedron* 58:9513–9525
26. Mayo P, Tam W (2002) *Tetrahedron* 58:9527–9540

27. Mayo P, Orlova G, Goddard JD, Tam W (2001) *J Org Chem* 66:5182–5191
28. Mayo P, Tam W (2001) *Tetrahedron* 57:5943–5952
29. Kobayashi T, Miki K, Nikaen B, Ohta A (2001) *J Chem Soc Perkin Trans 1*:1372–1385
30. Jordan RW, Tam W (2000) *Organic Lett* 2:3031–3034
31. Mayo P, Poirier M, Rainey J, Tam W (1999) *Tetrahedron Lett* 40:7727–7730
32. Ishida M, Itakura M, Tashiro H (2008) *Tetrahedron Lett* 49:1804–1807
33. Lahiri S, Yadav S, Banerjee S, Patil MP, Sunoj RB (2008) *J Org Chem* 73:435–444
34. Liu P, Jordan RW, Kibbee SP, Goddard JD, Tam W (2006) *J Org Chem* 71:3793–3803
35. Lahiri S, Yadav S, Chanda M, Chakraborty I, Chowdhury K, Mukherjee M, Choudhury AR, Row TNG (2005) *Tetrahedron Lett* 46:8133–8136
36. Ohkata K, Tamura Y, Shetuni BB, Takagi R, Miyanaga W, Kojima S, Paquette LA (2004) *J Am Chem Soc* 126:16783–16792
37. Paquette LA, Shetuni BB, Gallucci JC (2003) *Org Lett* 5:2639–2642
38. Mehta G, Le Droumaguet C, Islam K, Anoop A, Jemmis ED (2003) *Tetrahedron Lett* 44:3109–3113
39. Ishida M, Hirasawa S, Inagaki S (2003) *Tetrahedron Lett* 44:2187–2190
40. Pye CC, Xidos JD, Burnell DJ, Poirier RA (2003) *Can J Chem* 81:14–30
41. Martinez R, Jimenez-Vazquez HA, Delgado F, Tamariz (2003) *J Tetrahedron* 59:481–492
42. Ujaque G, Lee PS, Houk KN, Hentemann MF, Danishefsky S (2002) *J Chem Eur J* 8:3423–3430
43. Hou HF, Peddinti RK, Liao CC (2002) *Organic Lett* 4:2477–2480
44. Ishida M, Sakamoto M, Hattori H, Shimizu M, Inagaki S (2001) *Tetrahedron Lett* 42:3471–3474
45. Ishida M, Kobayashi H, Tomohiro S, Inagaki S (2000) *J Chem Soc Perkin Trans 2* 1625–1630
46. Carreno MC, Garcia-Cerrada S, Urbano A, Di Vitta C (2000) *J Org Chem* 65:4355–4363
47. Tanimoto H, Saito R, Chida N (2008) *Tetrahedron Lett* 49:358–362
48. Kulkarni SS, Liu YH, Hung SC (2005) *J Org Chem* 70:2808–2811
49. Alabugin IV, Manoharan M (2004) *J Org Chem* 69:9011–9024
50. Eliel EL, Senda Y (1970) *Tetrahedron* 26:2411
51. Rei M-H (1979) *J Org Chem* 44:2760
52. Wigfield DC, Phelps DJ (1976) *J Org Chem* 41:2396
53. Hennion GF, O'Shea FX (1958) *J Am Chem Soc* 80:614
54. Frenking G, Köhler KF, Reetz MT (1991) *Angew Chem Int Ed* 30:1146–1149
55. Senju T, Tomoda S (1997) *Chem Lett* 26:431–432
56. Tomoda S, Senju T (1997) *Tetrahedron* 53:9057–9066
57. Tomoda S (1999) *Chem Rev* 99:1243–1264
58. Klein J (1973) *Tetrahedron Lett* 44:4307–4310
59. Fukui K (1975) *Theory of orientation and stereoselection*. Springer, Berlin Heidelberg New York
60. Cieplak AS (1981) *J Am Chem Soc* 103:4540–4552
61. Laube T, Hollenstein S (1992) *J Am Chem Soc* 114:8812–8817
62. Giddings MR, Hudec J (1981) *Can J Chem* 59:459–467
63. Cheung CK, Tseng LT, Lin M-H, Srivastava S, le Noble WJ (1986) *J Am Chem Soc* 108:1598–1605
64. Lin M-H, Boyd MK, le Noble WJ (1989) *J Am Chem Soc* 111:8746–8748
65. Lau J, Gonikberg EM, Hung J-T, le Noble WJ (1995) *J Am Chem Soc* 117:11421–11425
66. Kaselj M, le Noble W (1996) *J Org Chem* 61:4157–4160
67. Halterman RL, McEvoy MA (1990) *J Am Chem Soc* 112:6690–6695
68. Gassman PG, Schaffhausen JG, Raynolds PW (1982) *J Am Chem Soc* 104:6408–6411
69. Gassman PG, Schaffhausen JG, Starkey FD, Raynolds PW (1982) *J Am Chem Soc* 104:6411–6414
70. Paddon-Row MN, Wu Y-D, Houk KN (1992) *J Am Chem Soc* 114:10638–10639
71. Priyakumar UD, Sastry GN, Mehta GN (2004) *Tetrahedron* 60:3465–3472

72. Ganguly B, Chandrasekhar J, Khan JFA, Mehta G (1993) *J Org Chem* 58:1734–1739
73. Mehta G, Khan FA (1990) *J Am Chem Soc* 112:6140–6142
74. Mehta G, Praveen M (1992) *Tetrahedron Lett* 33:1759–1762
75. Ganguly B, Chandrasekhar J, Khan FA, Mehta G (1993) *J Org Chem* 58:1734–1739
76. Mehta G, Khan FA (1992) *Tetrahedron Lett* 33:3065–3068
77. Mehta G, Khan FA, Gadre SR, Shirsat RN, Ganguly B, Chandrasekhar J (1994) *Angew Chem Int Ed* 33:1390–1392
78. Mehta G, Khan FA, Ganguly B, Chandrasekhar J (1992) *J Chem Soc Chem Commun* 1711–1712
79. Pudzianowski AT, Barrish JC, Spergel SH (1992) *Tetrahedron Lett* 33:293–296
80. Brown HC, Muzzio J (1966) *J Am Chem Soc* 88:2811–2822
81. Okada K, Tomita S, Oda M (1986) *Tetrahedron Lett* 27:2645–2648
82. Okada K, Tomita S, Oda M (1989) *Bull Chem Soc Jpn* 62:459–468
83. Bürgi HB, Dunitz JD, Shefter E (1973) *J Am Chem Soc* 95:5065–5067
84. Bürgi HB, Dunitz JD, Lehn JM, Wipff G (1974) *Tetrahedron* 30:1563–1572
85. Bürgi HB, Lehn JM, Wipff G (1974) *J Am Chem Soc* 96:1956–1957
86. Bürgi H-B (1975) *Angew Chem Int Ed* 14:460–473
87. Cieplak AS (1999) *Chem Rev* 99:1265–1336
88. Ohwada T (1993) *Tetrahedron* 49:7649–7656
89. Dedieu A, Veillard A (1972) *J Am Chem Soc* 94:6730
90. Anh NT, Minot C (1980) *J Am Chem Soc* 102:103
91. Schleyer PVR (1967) *J Am Chem Soc* 89:701
92. Spanget-Larsen J, Gleiter R (1982) *Tetrahedron Lett* 23:2435–2438
93. Spanget-Larsen J, Gleiter R (1983) *Tetrahedron* 39:3345–3350
94. Ito S, Kakehi A (1982) *Bull Chem Soc Jpn* 55:1869–1873
95. Mazzocchi PH, Stahly B, Dodd J, Rondan NG, Domelsmith LN, Roseboom MD, Caramella P, Houk KN (1980) *J Am Chem Soc* 102:6482–6490
96. Ohwada T, Shudo K (1991) *Chem Pharm Bull* 39:2176–2178
97. Ohwada T (1992) *J Am Chem Soc* 114:8818–8827
98. Simmons HE, Fukunaga T (1967) *J Am Chem Soc* 89:5208–5215
99. Semmelhack MF, Foos JS, Katz S (1973) *J Am Chem Soc* 95:7325–7336
100. Tajiri A, Nakajima T (1971) *Tetrahedron* 27:6089–6099
101. Bischof P, Gleiter R, Haider R (1978) *J Am Chem Soc* 100:1036–1042
102. Gordon MD, Fukunaga T, Simmons HE (1976) *J Am Chem Soc* 98:8401–8407
103. Ohwada T, Okamoto I, Haga N, Shudo K (1994) *J Org Chem* 59:3975–3984
104. Haga N, Ohwada T, Okamoto I, Shudo K (1992) *Chem Pharm Bull* 40:3349–3351
105. Hoffmann R, Mollère PD, Heilbronner E (1973) *J Am Chem Soc* 95:4860–4862
106. Klein J (1974) *Tetrahedron* 30:3349–3353
107. Senda Y, Kamiyama S, Imaizumi S (1978) *J Chem Soc Perkin Trans 1* 530
108. Johnson CR, Tait BD, Cieplak AS (1987) *J Am Chem Soc* 109:5875–5876
109. Cieplak AS, Tait BD, Johnson CR (1989) *J Am Chem Soc* 111:8447–8462
110. Carlson RG, Behn NS (1987) *J Org Chem* 52:1363
111. Patrick DW, Truesdale LK, Biller SA, Sharpless KB (1978) *J Org Chem* 43:2628
112. Lessard J, Saunders JK, Viet MTP (1982) *Tetrahedron Lett* 23:2059–2062
113. Srivastava S, le Noble WJ (1987) *J Am Chem Soc* 109:5874–5875
114. Halterman R, McEvoy MA (1992) *J Am Chem Soc* 114:980–985
115. Mehta G, Khan FA (1991) *J Chem Soc Chem Commun* 18–19
116. Mehta G, Gunasekaran G, Gadre SR, Shirsat RN, Ganguly B, Chandrasekhar J (1994) *J Org Chem* 59:1953–1955
117. Jones G, Vogel P (1993) *J Chem Soc Chem Commun* 769–771
118. Ohwada T, Uchiyama M, Tsuji M, Okamoto I, Shudo K (1996) *Chem Pharm Bull* 44:296–306
119. Imamura A (1968) *Mol Phys* 15:225–238
120. Imamura A, Hirano T (1975) *J Am Chem Soc* 97:4192–4198

121. Hoffmann R (1971) *Acc Chem Res* 4:1–9
122. Houk KN, Rondan NG, Brown FK, Jorgensen WL, Madura JD, Spellmeyer DC (1983) *J Am Chem Soc* 105:5980–5988
123. Paquette LA, Klinger F, Hertel LW (1981) *J Org Chem* 46:4403–4413
124. Tsuji M, Ohwada T, Shudo K (1997) *Tetrahedron Lett* 38:6693–6696
125. Hoffmann RW, Haul N, Landmann B (1983) *Chem Ber* 116:389–403
126. Hoffmann RW, Haul N (1979) *Tetrahedron Lett* 20:4959–4962
127. Schueler PE, Rhodes YE (1974) *J Org Chem* 39:2063–2069
128. Maasa W, Birkhahn M, Landmann B, Hoffmann RW (1983) *Chem Ber* 116:404–408
129. Becherer J, Hoffmann RW (1978) *Tetrahedron* 34:1193–1197
130. Hoffmann R, Davidson RB (1971) *J Am Chem Soc* 93:5699–5705
131. Hoffmann RW, Kurz HR, Becherer J, Reetz MT (1978) *Chem Ber* 111:1264–1274
132. Srinivasan R, Ors JA, Brown KH, White LS, Rossi AR (1980) *J Am Chem Soc* 102:5297–5302
133. Rhodes YE, Scheler PE, DiFate VG (1970) *Tetrahedron Lett* 11:2073–2076
134. Günther H, Herrig W, Seel H, Tobias S (1980) *J Org Chem* 45:4329–4333
135. Haywood-Farmer JS, Pincock RE (1969) *J Am Chem Soc* 91:3020–3028
136. Martin HD, Heller C, Haider R, Hoffmann RW, Becherer J, Kurz HR (1977) *Chem Ber* 110:3010
137. Bischof P, Heilbronner E, Prinzbach H, Martin HD (1971) *Helv Chim Acta* 54:1072–1080
138. Bruckmann P, Klessinger M (1972) *Angew Chem Int Ed* 11:524–525
139. Hoffmann RW, Schüttler R, Schäfer W, Schweig A (1972) *Angew Chem Int Ed* 11:512–513
140. Christl M (1975) *Chem Ber* 108:2781–2791
141. Christl M, Herbert R (1979) *Chem Ber* 112:2022–2027
142. Wiberg KW, Bader RFW, Lau CHH (1987) *J Am Chem Soc* 109:1001–1012
143. Singleton DA, Merrigan SR, Liu J, Houk KN (1997) *J Am Chem Soc* 119:3385–3386
144. Houk KN, Liu J, DeMello NC, Condroski KR (1997) *J Am Chem Soc* 119:10147–10152
145. Ohwada T, Tsuji M, Okamoto I, Shudo K (1996) *Tetrahedron Lett* 37:2609–2612
146. Edman JR, Simmons HE (1968) *J Org Chem* 33:3808–3816
147. Bartlett PD, Blakeney AJ, Kimura M, Waatson WH (1980) *J Am Chem Soc* 102:1383–1390
148. Mehta G, Padma S, Pattabhi V, Pramanik A, Chandrasekhar J (1990) *J Am Chem Soc* 112:2942–2949
149. Mehta G, Padma S, Karra SR (1989) *J Org Chem* 54:1342–1346
150. Carreño MC (1995) *Chem Rev* 95:1717–1760
151. Okamoto I, Ohwada T, Shudo K (1996) *J Org Chem* 61:3155–3166
152. Paddon-Row MN, Patney HK, Warrener RN (1979) *J Org Chem* 44:3908–3917
153. Hoffmann R, Woodward RB (1965) *J Am Chem Soc* 87:4388–4389
154. Ishida M, Kobayashi H, Tomohiro S, Wasada H, Inagaki S (1998) *Chem Lett* 27:41–42
155. Xidos JD, Poirier RA, Pye CC, Burnell DJ (1998) *J Org Chem* 63:105–112
156. Xidos JD, Poirier RA, Burnell DJ (2000) *Tetrahedron Lett* 41:995–998
157. Yadav V, Senthil G, Babu KG, Parvez M, Reid JL (2002) *J Org Chem* 67:1109–1117
158. Morrison CF, Vaters JP, Miller DO, Burnell DJ (2006) *Org Biomol Chem* 4:1160–1165
159. Ogbomo S, Burnell DJ (2006) *Org Biomol Chem* 4:3838–3848
160. Mehta G, Uma R (2000) *Acc Chem Res* 33:278–286
161. Pfändler HRHT, Haselbach E (1974) *Helv Chim Acta* 57:383–394
162. Haselbach E, Rossi M (1976) *Helv Chim Acta* 59:278–290
163. Halterman R, McCarthy BA, McEvoy MA (1992) *J Org Chem* 57:5585–5589
164. Tsuji M, Ohwada T, Shudo K (1998) *Tetrahedron Lett* 39:403–406
165. Igarashi H, Sakamoto S, Yamaguchi K, Ohwada T (2001) *Tetrahedron Lett* 42:5257–5260
166. Gleiter R, Paquette LA (1983) *Acc Chem Res* 16:328–334
167. Böhm MC, Eiter RG (1980) *Tetrahedron* 36:3209–3217
168. Gleiter R, Ginsburg D (1979) *Pure Appl Chem* 51:1301–1315

169. Okamoto I, Ohwada T, Shudo K (1997) *Tetrahedron Lett* 38:425–428
170. Baldwin JE (1976) *J Chem Soc Chem Commun* 738–741
171. Okamoto I, Ohwada T, unpublished result
172. Ohwada T, Miura M, Tanaka H, Sakamoto S, Yamaguchi K, Ikeda H, Inagaki S (2001) *J Am Chem Soc* 123:10164–10172
173. Yanagimoto T, Toyoda T, Matsuki N, Makino Y, Uchiyama S, Ohwada T (2007) *J Am Chem Soc* 129:736–737
174. Mengel A, Reiser O (1999) *Chem Rev* 99:1191–1224
175. Dannenberg J (1999) *J Chem Rev* 99:1225–1242
176. Gung BW (1999) *Chem Rev* 99:1377–1386
177. Kaselj M, Chung W-S, le Noble WJ (1999) *Chem Rev* 99:1387–1414
178. Adcock W, Trout NA (1999) *Chem Rev* 99:1415–1436
179. Mehta G, Chandrasekhar (1999) *J Chem Rev* 99:1437–1468
180. Wipf P, Jung J-K (1999) *Chem Rev* 99:1469–1480

π -Facial Selectivity of Diels-Alder Reactions

Masaru Ishida and Satoshi Inagaki

Abstract Diels-Alder reaction is one of the most fundamental and important reactions for organic synthesis. In this chapter we review the studies of the π -facial selectivity in the Diels-Alder reactions of the dienes having unsymmetrical π -plane. The theories proposed as the origin of the selectivity are discussed.

Keywords π -Facial selectivity, σ/π Interaction, CH/ π Interaction, Ciplak effect, Diels-Alder reaction, Electrostatic interaction, Orbital mixing rule, Orbital phase environment, Secondary orbital interaction, Steric repulsion, Torsional control

Contents

1	Introduction.....	183
2	Origin of π -Facial Selectivity.....	185
2.1	Orbital Interaction.....	185
2.2	Steric Repulsion.....	205
2.3	Torsional Control.....	207
2.4	Electrostatic Interaction.....	207
2.5	CH/ π or π/π Interaction.....	211
3	Diels-Alder Reaction of Thiophene 1-Oxides.....	213
4	Conclusion.....	217
	References.....	217

1 Introduction

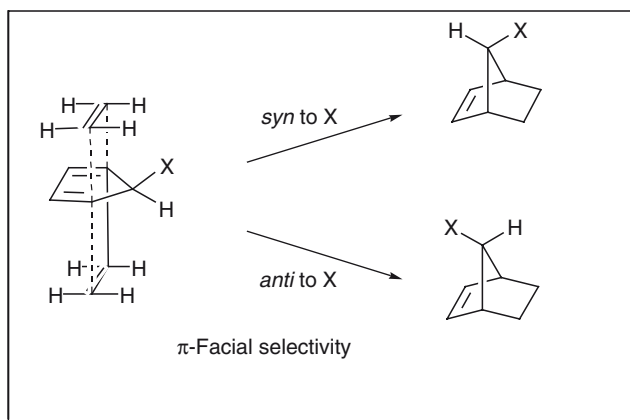
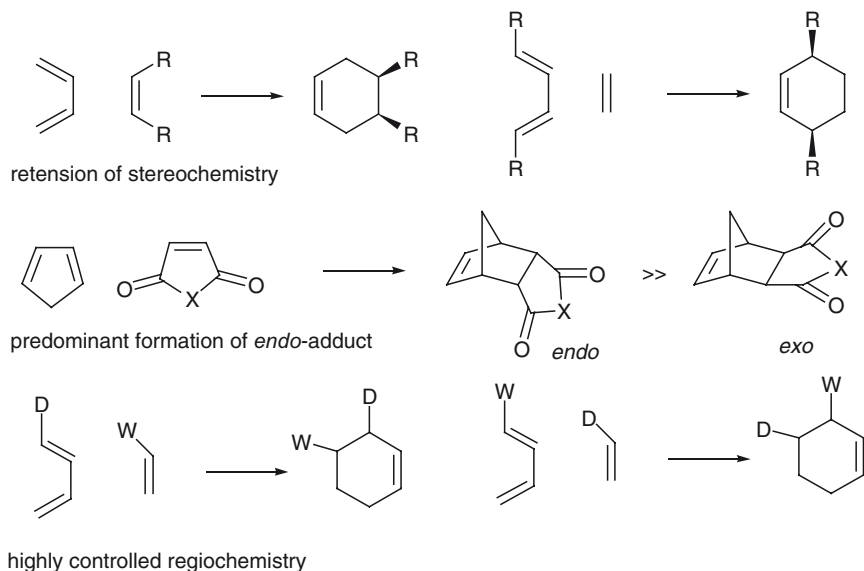
Diels-Alder reaction is one of the most fundamental reactions for organic synthesis. Its synthetic utility is unquestioned. The stereochemistry of the reactions has attracted much attention. The retention of stereochemistry in the diene and the dienophile, the predominant formation of *endo*-attack products in the reactions of cyclic dienes, and highly controlled regioselectivity in the reactions of substituted dienes and

M. Ishida (✉) and S. Inagaki (✉)

Department of Chemistry, Faculty of Engineering, Gifu University, Yanagido,
Gifu, 501-1193, Japan

e-mails: m_ishida@gifu-u.ac.jp; inagaki@gifu-u.ac.jp

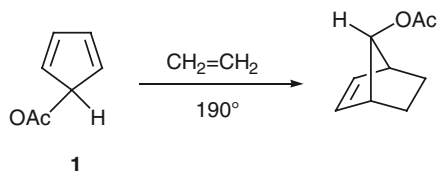
dienophiles have been well established textbook issues, where frontier orbital interaction plays a main role. Incorporation of π -facially unsymmetrical factor to the diene or dienophile opened a new frontier of stereochemistry. 5-Substituted cyclopentadiene Cp-X is the simplest diene having an unsymmetrical π -plane (Scheme 1).



Scheme 1 Stereochemistry in Diels-Alder reactions

In principle, the diene can react with dienophiles at either of its faces. *Anti* π -facial selectivity with respect to the substituent at 5-positions was straightforwardly predicted on the basis of the repulsive interaction between the substituent and a dienophile, however, there were some counter examples. The first of them is the *syn* π -facial selectivity observed in the reaction between 5-acetoxy-1,3-cyclopentadiene **1** and ethylene reported by Woodward and coworkers in 1955

(Scheme 2) [1]. Since acetoxy moiety is much larger than hydrogen, the steric factor due to the substituent was obviously overwhelmed by other factors.



Scheme 2 Diels-Alder reaction between 5-acetoxy-1,3-cyclopentadiene and ethylene

It becomes intriguing to inquire what leads to the observed contrasteric reactivity. Intensive studies to disclose the origin of π -facial selectivity examined various dienes having unsymmetrical π -plane, since their reactions potentially generate five or more consecutive stereocenters with one operation. In this chapter, we review the theories to disclose the origin of π -facial selectivity in Diels-Alder reactions of the substrates having unsymmetrical π -planes. Recent works are discussed.

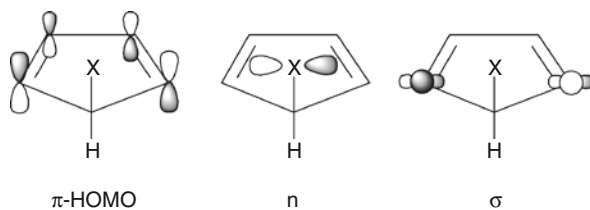
2 Origin of π -Facial Selectivity

2.1 Orbital Interaction

2.1.1 Deformation of Frontier Molecular Orbital (Orbital Mixing Rule)

Inagaki, Fujimoto and Fukui demonstrated that π -facial selectivity in the Diels-Alder reaction of 5-acetoxy- and 5-chloro-1,3-cyclopentadienes, **1** and **2**, can be explained in terms of deformation of a frontier molecular orbital FMO [2]. The orbital mixing rule was proposed to predict the nonequivalent orbital deformation due to asymmetric perturbation of the substituent orbital (Chapter “Orbital Mixing Rules” by Inagaki in this volume).

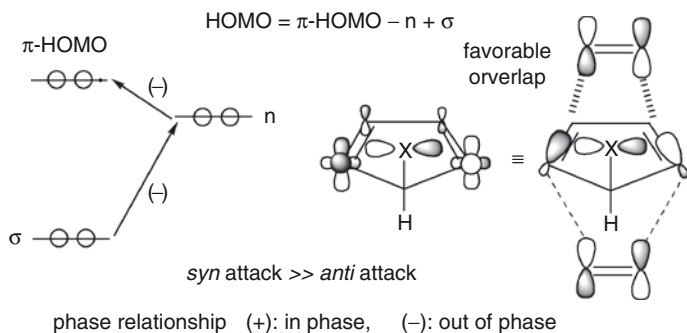
The FMO of the diene having substituent X at the 5-positions is comprised of three molecular orbitals, namely, π -HOMO of the diene part, σ -orbital of carbon framework, and the nonbonding (n) orbital of X (Scheme 3). The FMO of the diene for Diels-Alder reactions should mainly consist of π -HOMO. The π -HOMO is antisymmetric with respect to reflection in the plane containing C5 carbon and its substitu-



Scheme 3 Components of FMO

ent X and H. The same symmetry is required for the σ orbital and the perturbing orbital n on X.

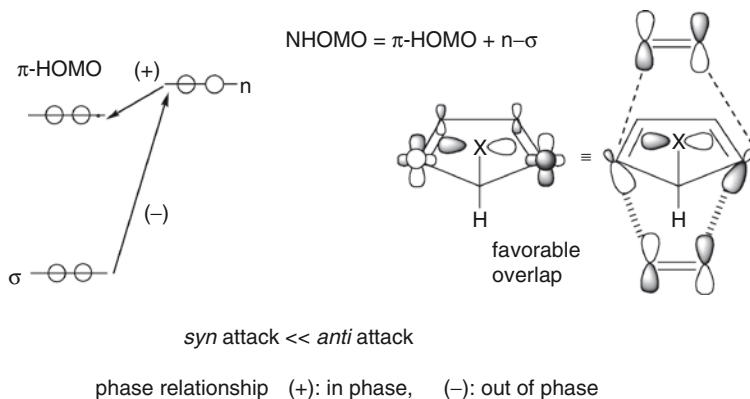
The orbital mixing rule demonstrates that the direction of the FMO extension is controlled by the relative energies of the π -HOMO (ϵ_π) and the n-orbital of X (ϵ_n). In the case of 5-acetoxy- and 5-chloro-1,3-cyclopentadienes, the π -HOMO lies higher than n ($\epsilon_\pi > \epsilon_n$). In this case, the π -HOMO mainly contributes to the HOMO of the whole molecule by an out-of-phase combination with the low-lying n. The mixing of σ -orbital takes place so as to be out-of-phase with the mediated orbital n. The HOMO at C1 and C4 extends more and rotates inwardly at the *syn* face with



Scheme 4 Direction of nonequivalent extension of the HOMO of Cp-X where $\epsilon_\pi > \epsilon_n$

respect to the substituent. The HOMO is suitable for the reactions on the *syn* face of the diene with respect to the substituent (Scheme 4).

The rule was then applied for the cyclopentadienes having substituent X of high-lying n-orbitals ($\epsilon_\pi < \epsilon_n$) [3, 4]. In this case the HOMO is not the FMO for Diels-Alder reactions since the n-orbital predominantly contributes to the HOMO of the whole molecule. The NHOMO should be the FMO. The NHOMO consists mainly of π -HOMO with the combination with high-lying n in in-phase relationship. Mixing of σ orbital takes place by out-of-phase relationship with respect to n. The NHOMO



Scheme 5 Direction of nonequivalent extension of the NHOMO of Cp-X where $\epsilon_n > \epsilon_\pi$

deforms in a way opposite to the HOMO and is suitable for the reactions on the *anti* face of the diene with respect to the substituent (Scheme 5).

These predictions were well consistent with the selectivity in the reactions of series of cyclopentadiene having substituents of group 16 elements (O, S, Se). There were reported several examples of the reactions of the cyclopentadienes having oxygen substituents such as hydroxy or acetoxy moiety, where $\epsilon_\pi > \epsilon_n$, to react with dienophiles with highly *syn* π -facial selectivity [1, 5]. 5-Phenylselenocyclopentadiene **3**, which was categorized to the latter case ($\epsilon_\pi < \epsilon_n$), was found to react exclusively with *anti* π -facial selectivity. 5-Phenylthiocyclopentadiene **4**, which can be classified as the middle case ($\epsilon_\pi \approx \epsilon_n$), was found to react with dienophiles with the ratio of *syn/anti*= 40:60 (Table 1) [3, 4, 6].

Fallis and coworkers studied π -facial selectivity in the reactions of series of 5-substituted 1,2,3,4,5-pentamethylcyclopentadienes Cp*-X. They reported that the diene **5** (Cp*-X: X = SCH₃) with maleic anhydride proceeded more slowly than that of the 5-oxygen substituted cyclopentadienes **6** and **7** (Cp*-X: X = OH, OCH₃), where the HOMO of the diene **5** lies higher than those of **6** and **7** [7, 8] (Table 2). These results seemed to suggest that in the case of the reaction of **5** the NHOMO considerably contributed to the reactions.

In the case of cyclopentadienes having halogen substituents at 5-positions, *syn* π -facial selectivity is expected since the dienes are classified into the case of

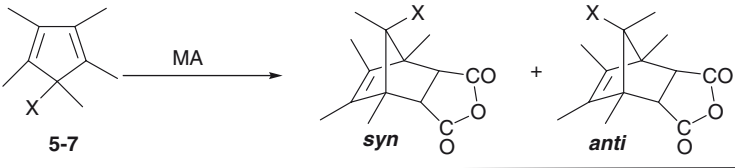
Table 1 π -Facial selectivity in the reactions of cyclopentadienes having the substituents of group 16 elements at 5-positions

The reaction scheme shows a 5-substituted cyclopentadiene (with substituent X and H at the 5-position) reacting with dienophiles to produce two bicyclic products: a *syn* product (with H and X on the same side) and an *anti* product (with H and X on opposite sides).

3: X=PhSe
4: X=PhS

X	n-Orbital level[eV] ^a	M.O. Calculation coefficients ^b	$C_{p\pi}$	C_n	Selectivity mixing rule	observed
OAc	10.04 ($\epsilon_\pi > \epsilon_n$)	HOMO NHOMO	0.523 0.081	0.137 0.829	<i>syn</i>	<i>syn</i>
SPh	8.71 ($\epsilon_\pi \approx \epsilon_n$)	HOMO NHOMO	0.368 0.384	0.730 0.693	<i>syn/anti</i>	<i>syn/anti</i>
SePh	8.40 ($\epsilon_\pi < \epsilon_n$)	HOMO NHOMO	0.319 0.426	0.804 0.605	<i>anti</i>	<i>anti</i>
H	8.57	(HOMO Level of cyclopentadiene)				

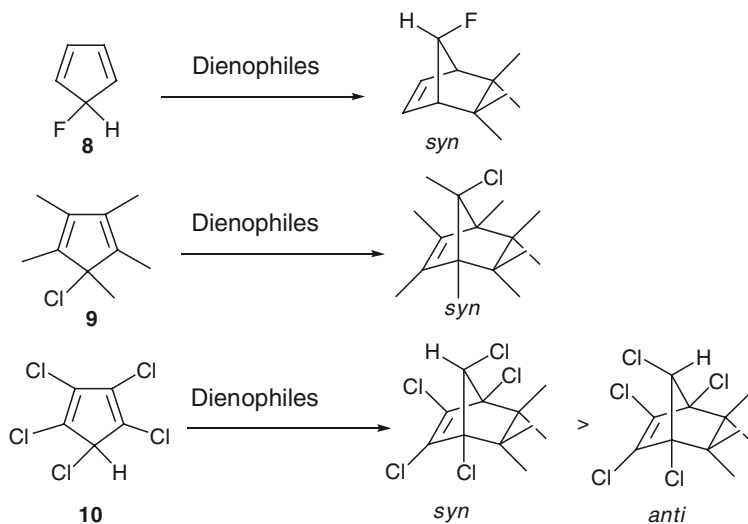
^aEvaluated from ionization potentials of dimethyl derivatives. ^bSTO-3G. ^c $C_{p\pi}$ is the component of p-atomic orbital at the reaction center.

Table 2 Reactions of Cp*-X with maleic anhydride (MA)


Diene	X	Reaction time	HOMO [eV] ^a	Selectivity (<i>syn/anti</i>)
5	SCH ₃	27.5 h	7.26	10 : 90
6	OH	< 10 min	7.52	100 : 0
7	OCH ₃	< 3.5 h	7.42	100 : 0 ^b

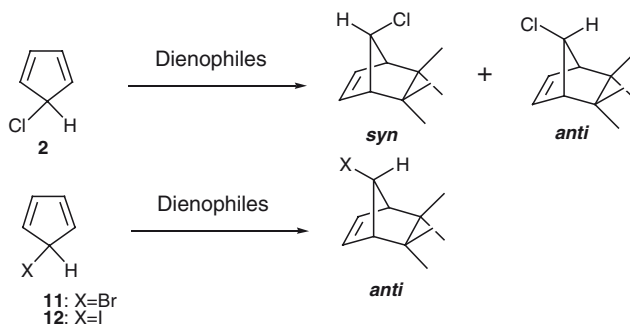
^aPhotoelectron spectra.^bDienophile: N-Phenylmaleimide

$\epsilon_{\pi} > \epsilon_n$. However the selectivities observed were dependent on the substituents. 5-Fluorocyclopentadiene and 5-chloropentamethylcyclopentadiene, **8** and **9**, reacted with *syn* π -facial selectivity [9, 7]. 1,2,3,4,5-Pentachlorocyclopentadiene **10** reacted with *syn* π -facial preference (Scheme 6) [10].

**Scheme 6** π -Facial selectivity in the reactions of the cyclopentadienes **8–10**

In contrast, 5-chlorocyclopentadiene **2** gave *syn/anti* mixture and 5-bromo- and 5-iodocyclopentadienes **11** and **12** reacted with *anti* π -facial selectivity [11, 12]. In these cases, repulsive interaction between the substituents and dienophiles cannot be excluded (Scheme 7).

The orbital mixing rule was recently applied to the prediction and design of cyclopentadienes having substituents of π -system at 5-positions (Scheme 8) [13, 14].



Scheme 7 π -Facial selectivity in the reactions of the cyclopentadienes **2** and **11–12**

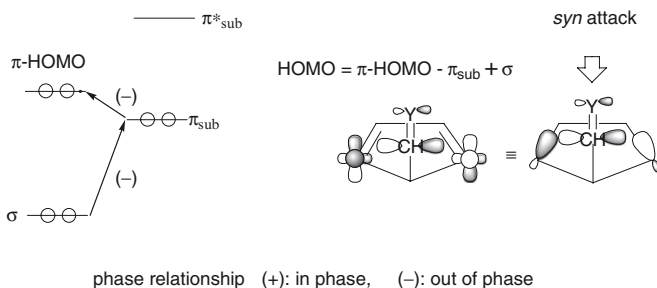


13: X = C \equiv CH **14:** X = C \equiv N **15:** X = CH=CH₂ **16:** X = CH=NOH **17:** X = CH=O

Scheme 8 Cyclopentadienes having substituents of π -system at 5-positions

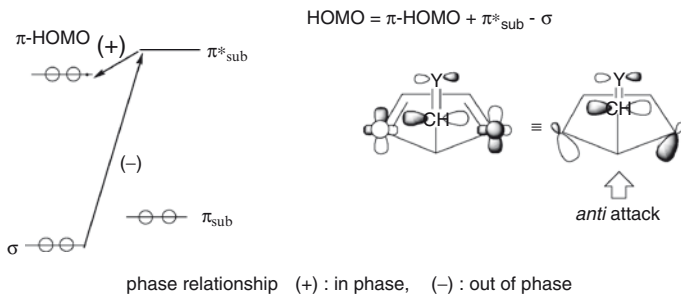
Application of the orbital mixing rule to such a system was classified into two categories, again depending on the relative orbital energies of π -HOMO and substituents orbitals π_{sub} and π_{sub}^* . When the π_{sub}^* orbital lies much higher than the π -HOMO, the participation of the π_{sub}^* orbital in the orbital mixing is negligible. The π -HOMO of the diene combines with the low-lying π_{sub} orbital out-of-phase and mixes the σ orbital of carbon framework out-of-phase with respect to the π_{sub} orbital. The resulting FMO distorts to favor the reaction at *syn* side of the substituent (HOMO = π -HOMO - π_{sub} + σ) (Scheme 9).

On the other hand, when the π_{sub}^* orbital lies low enough to interact with the π -HOMO, the participation of the π_{sub}^* orbital needs to be taken into account.



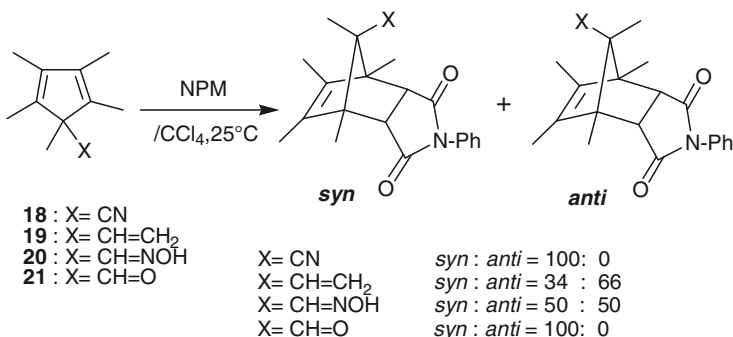
Scheme 9 Direction of nonequivalent extension of the HOMO of Cp-CH=Y where $\epsilon_{\pi_{\text{sub}}} \gg \epsilon_{\pi\text{-HOMO}}$

Combination of the π -HOMO with the high-lying π^*_{sub} orbital in phase, followed by mixing of the σ orbital out-of-phase with the π^* orbital gives the FMO, which distorts to favor the reaction at *anti* side of the substituent (HOMO = π -HOMO + $\pi^*_{\text{sub}} - \sigma$) (Scheme 10).



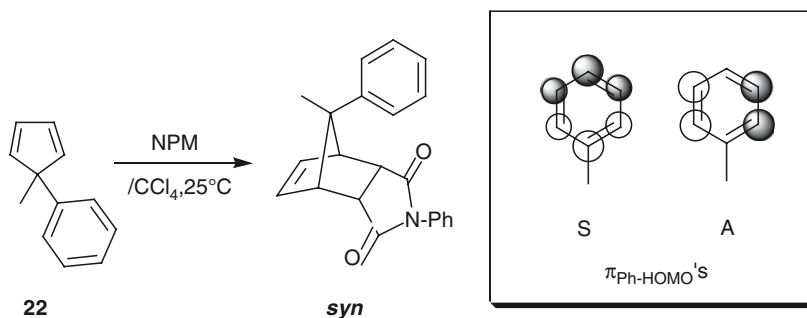
Scheme 10 Direction of nonequivalent extension of the HOMO of Cp-CH=Y where $\epsilon_{\pi^*_{\text{sub}}}$ lies low

The cyclopentadiene having substituents of C \equiv CR and C \equiv N are typical examples of the former case ($\epsilon_{\pi^*_{\text{sub}}} \gg \epsilon_{\pi\text{-HOMO}}$). Theoretical calculation showed that the diene **13** is expected to react with highly *syn* π -facial selectivity [15]. Experimental study of the selectivity in the reactions of the pentamethylcyclopentadiene derivatives **18–21** is particularly of interest (Scheme 11). Exclusive formation of *syn* attack product in the reaction of the diene **18** is well consistent with the prediction [16]. In the case of the dienes **19–21**, the efficiency of the orbital mixing mediated by π_{sub} or π^*_{sub} orbital was dependent on the conformation of the substituents. However, the selectivity observed was well consistent with the theory. In the reactions of the dienes **19** and **20** where $\epsilon_{\pi^*_{\text{sub}}} \gg \epsilon_{\pi\text{-HOMO}}$, considerable formation of *syn* attack products was observed. In the reactions of the diene **21** where $\epsilon_{\pi^*_{\text{sub}}}$ is low, exclusive formation of *anti* attack products was observed [14, 16, 17].



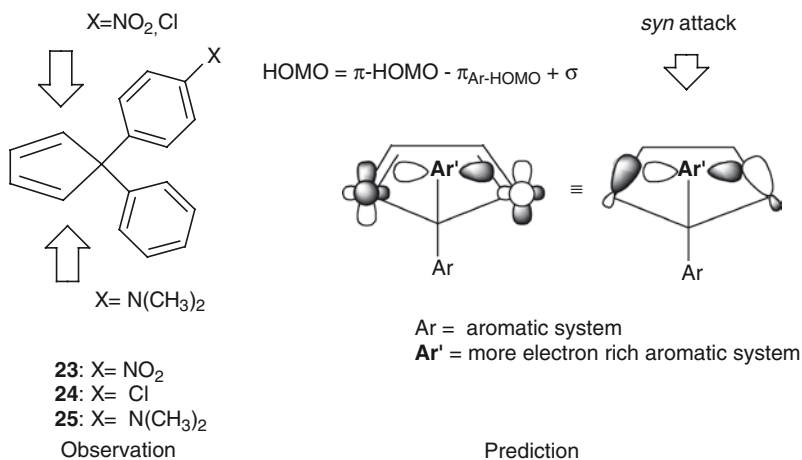
Scheme 11 π -Facial selectivity in the reactions of the cyclopentadienes **18–21**

Recently we pointed out that the cyclopentadiene having phenyl moiety at the 5-position is the diene of $\epsilon_{\pi^*_{\text{sub}}} \gg \epsilon_{\pi\text{-HOMO}}$. The phenyl moiety can mediate orbital mixing through its degenerated $\pi_{\text{Ph-HOMO}}$'s almost independently on the conformation around the phenyl moiety. The reactions between 5-methyl-5-phenylcyclopentadiene **22** and *N*-phenylmaleimide were observed to proceed exclusively with *syn* π -facial selectivity [18] (Scheme 12).



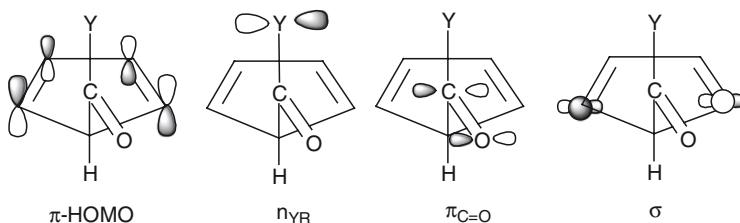
Scheme 12 π -Facial selectivity in the reaction of the cyclopentadiene **22**

Halterman et al. reported that 5-aryl-5-phenylcyclopentadienes **23–25** reacted with dienophiles to favor the reactions on the *anti* side of the more electron rich aromatic system [19]. The orbital mixing rule failed to predict this selectivity, since orbital mixing is expected to take place mainly by mediation of the $\pi_{\text{Ar-HOMO}}$'s of more electron rich aromatic system (Scheme 13). Destabilization due to the orbital phase environment or stabilization due to Cieplak effects can be responsible for the selectivity (See Sects. 2.1.2 and 2.1.3).



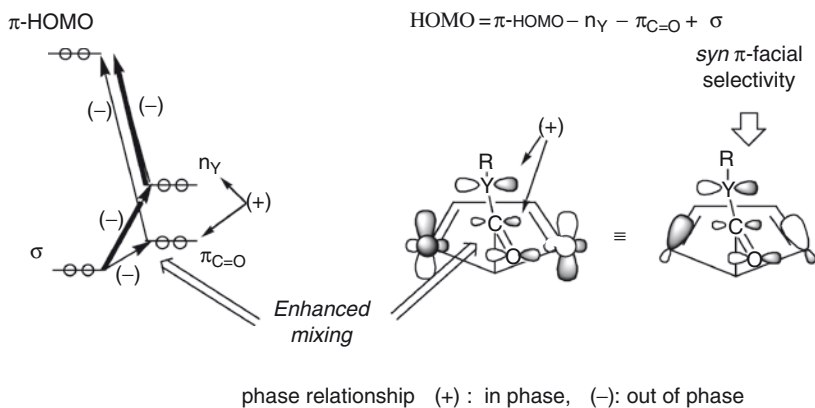
Scheme 13 Prediction and observation of π -facial selectivity in the reactions of 5-aryl-5-phenylcyclopentadienes **23–25**

In the prediction of the FMO of the cyclopentadienes having C(=O)YR substituent at 5 positions, the interactions between the four molecular orbitals, π -HOMO, σ , n_{YR} , and $\pi_{C=O}$ should be taken into account (Scheme 14) [20]. The deformation of FMO takes place by the mixing of π -HOMO and σ mediated by the substituent orbital n_{YR} . Participation of the second substituent orbital $\pi_{C=O}$ perturbs this mixing with dependence on the relative orbital energy between π -HOMO and n_{YR} .



Scheme 14 Component orbitals of the FMO

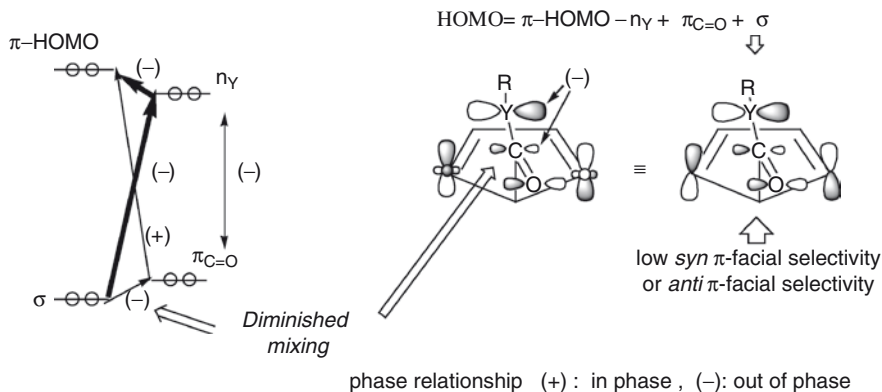
When π -HOMO is high, π -HOMO combines both of the low-lying substituent orbitals, n_{YR} and $\pi_{C=O}$, out-of-phase. The mixing of σ to π -HOMO takes place in an out-of-phase manner with n_{YR} and $\pi_{C=O}$. Since $\pi_{C=O}$ has the same phase as n_{YR} , the mixing of σ is enhanced to give the FMO, which favors the reaction at the *syn* side of the substituents (in the case where $\epsilon_{\pi\text{-HOMO}} \gg \epsilon_{nY} > \epsilon_{\pi\text{C=O}}$: $\text{HOMO} = \pi\text{-HOMO} - n_Y - \pi_{\text{C=O}} + \sigma$) (Scheme 15).



Scheme 15 Direction of nonequivalent extension of the FMO of the cyclopentadiene having C(=O)YR substituent where $\epsilon_{\pi\text{-HOMO}} \gg \epsilon_{nY} > \epsilon_{\pi\text{C=O}}$

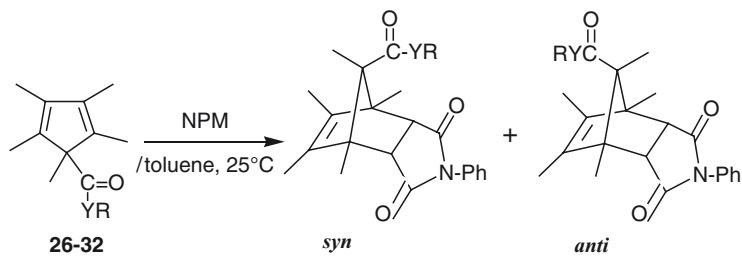
On the other hand, when n_Y lies close to π -HOMO, the interaction between π -HOMO and n_Y is strong. Both orbitals contribute considerably to FMO. The combined orbital, π -HOMO - n_Y is a component of FMO. The $\pi_{C=O}$ orbital interacts with the n_Y more strongly than with the π -HOMO due to the spatial proximity. The phase of $\pi_{C=O}$ is determined by the relation with n_Y rather than π -HOMO so as to be out-of-phase with n_Y (viz. in phase with π -HOMO). As a result, $\pi_{C=O}$ is the opposite

phase with n_Y , while the orbitals are in phase with each other in the former case where $\epsilon_{\pi\text{-HOMO}} \gg \epsilon_{n_Y} > \epsilon_{\pi\text{C=O}}$. The mixings of σ , caused by the interaction with $\pi_{\text{C=O}}$ and n_Y , are diminished by each other. The deformation of FMO is predicted to be reduced (in the case where $\epsilon_{\pi\text{-HOMO}} \approx \epsilon_{n_Y} > \epsilon_{\pi\text{C=O}}$: HOMO = $\pi\text{-HOMO} - n_Y + \pi_{\text{C=O}} + \sigma$) (Scheme 16).



Scheme 16 Direction of nonequivalent extension of the FMO of the cyclopentadiene having C(=O)YR substituent where $\epsilon_{\pi\text{-HOMO}} \approx \epsilon_{n_Y} > \epsilon_{\pi\text{C=O}}$

The prediction was substantiated experimentally by the reactions of pentamethylcyclopentadienes **26–32**. The dienes **26–29** of the former case reacted with highly *syn* π facial preference, while the dienes **30–32** of the latter case reacted with low-*syn* or *anti* π -facile selectivity (Scheme 17).



C(=O)YR where $\epsilon_{\pi\text{-HOMO}} \gg \epsilon_{n_Y} > \epsilon_{\pi\text{C=O}}$

- 26:** YR= OH *syn* : *anti* = 78 : 22
27: YR= OCH₃ *syn* : *anti* = 84 : 16
28: YR= OPh *syn* : *anti* = 83 : 17
29: YR=O(4-CH₃O-Ph) *syn* : *anti* = 84 : 16(in CCl₄)

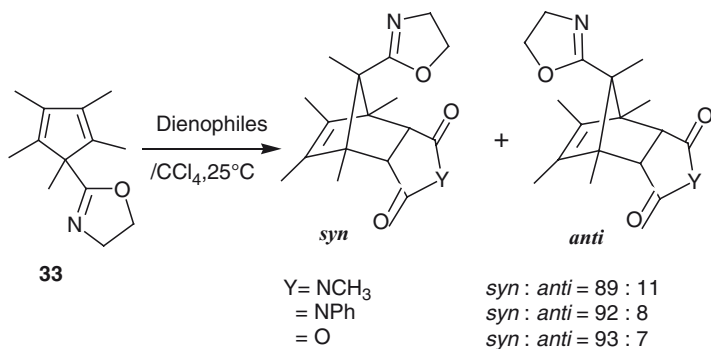
C(=O)YR where $\epsilon_{\pi\text{-HOMO}} \approx \epsilon_{n_Y} > \epsilon_{\pi\text{C=O}}$

- 30:** YR= NH₂ *syn* : *anti* = 27 : 73
31: YR= SCH₃ *syn* : *anti* = 1 : 99
32: COYR= CS₂CH₃ *syn* : *anti* = 0 : 100

Scheme 17 π -Facial selectivity in the reactions of the cyclopentadienes **26–29**

Simple modification of the substituent changes the selectivity due to the orbital energy relationship. The diene **30** where $\epsilon_{\pi\text{-HOMO}} \approx \epsilon_{n_Y} > \epsilon_{\pi\text{C=O}}$ reacted with *anti* π -facial preference as already stated, while the reactions of the diene **33** where

$\epsilon_{\pi\text{-HOMO}} \gg \epsilon_{nY} > \epsilon_{pC=N}$ showed considerable enhancement of *syn* π -facial selectivity in agreement with the prediction. This success showed an example of an application of the theory for the design of the reaction of contrasteric fashion overwhelming the steric hindrance due to the substituent [21] (Scheme 18).



Scheme 18 π -Facial selectivity in the reactions of the cyclopentadiene **33**

Although there are a few exceptions, the prediction on the basis of the orbital mixing rule was not only well consistent with the observed selectivities but also can give a direction for designing and controlling π -facial selectivity overwhelming steric hindrance.

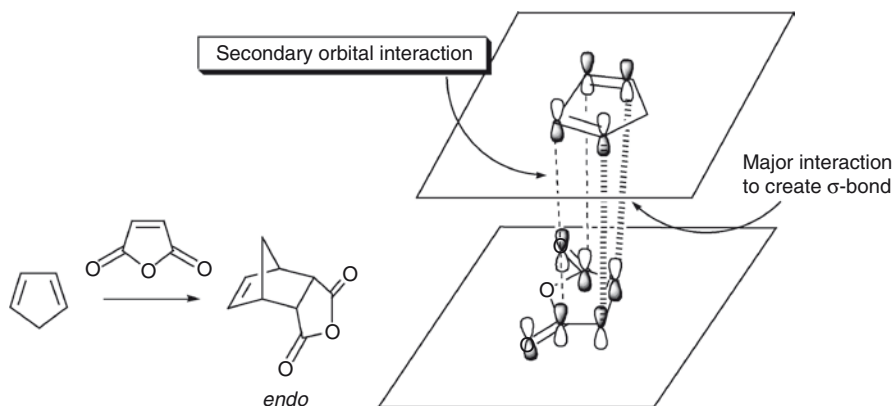
2.1.2 Orbital Phase Environment

Secondary orbital interaction had been proposed to explain predominant formation of *endo* attack products in Diels Alder reaction of cyclopentadiene and dienophiles by Hoffmann and Woodward [22]. According to this rule, the major stereoisomer in Diels-Alder reactions is that it is formed through a maximum accumulation of double bonds. In the Diels-Alder reactions, secondary orbital interaction consists of a stabilizing two-electron interaction between the atoms not involved in the formation or cleavage of σ bonds (Scheme 19).

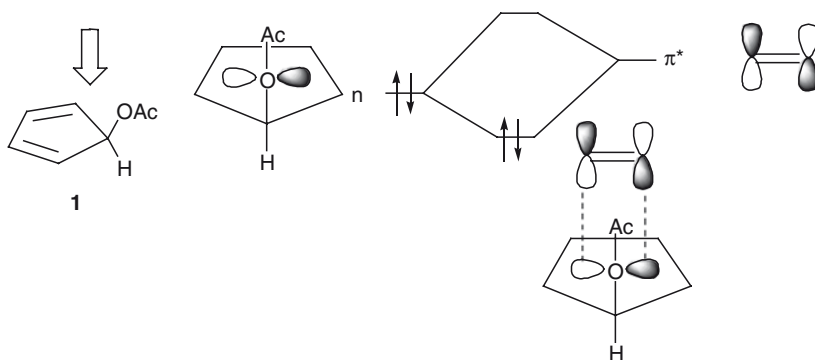
The secondary orbital interaction has been applied to explain enantioselective catalytic Diels-Alder reactions of cyclic dienes and acetylenic dienophiles [23, 24].

There were proposed some applications of secondary orbital interaction to explain the π -facial selectivity. Anh proposed that the selectivity in the reactions of 5-acetoxycyclopentadiene **1** was ascribed to the stabilization by the interaction between the LUMO of a dienophile and n-orbital of the alkoxy oxygen of the acetoxy moiety [25] (Scheme 20).

According to Anh's theory, the cyclopentadienes having substituents of second and third row elements such as SR and SeR at the 5-positions are expected to react with *syn* π facial selectivity since the stabilization due to $n\text{-}\pi^*$ interaction in such systems is larger than **1**. The observation contradicted the prediction [3, 4, 7]. We and Ohwada



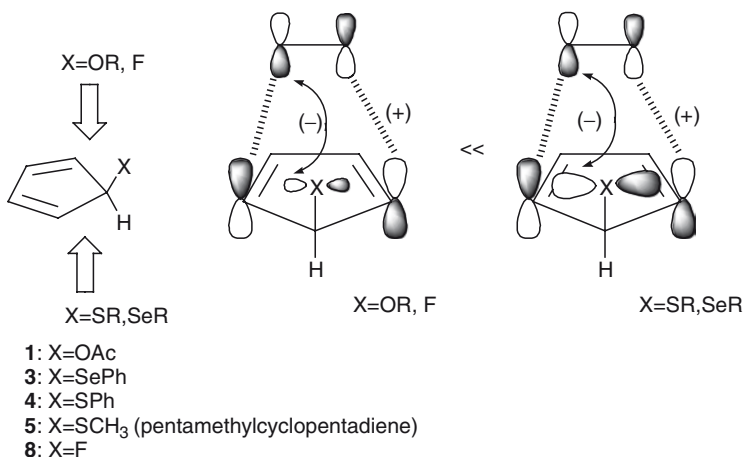
Scheme 19 Secondary orbital interaction in Diels-Alder reaction of cyclopentadiene with maleic anhydride



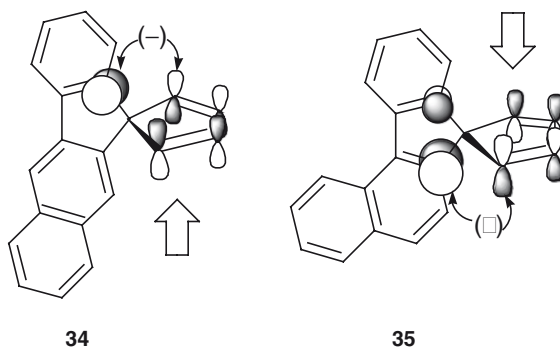
Scheme 20 Anh's model stabilization due to n - π^* orbital interaction

pointed out that the theory is mistaken [26, 27]. The LUMO of dienophile and the π -HOMO of the diene are in phase in Diels-Alder reactions. Thus, the LUMO of dienophile and the n -orbital are out-of-phase since the HOMO of the substituted diene is an out-of-phase combination of the π -HOMO and the n -orbital. The out-of-phase relation between the n -orbital and the dienophile LUMO suggests destabilization. The Anh model cannot be the origin of *syn* π -facial selectivity (Scheme 21).

Ohwada extends his theory, unsymmetrization of π orbitals, to "Orbital Phase Environment" including the secondary orbital interaction (Chapter "Orbital Phase Environments and Stereoselectivities" by Ohwada in this volume). The reactions between the cyclopentadienes bearing spiro conjugation with benzofluorene systems with maleic anhydride exemplified the importance of the phase environment. The reactions proceed avoiding the out-of-phase interaction between dienophile LUMO and the HOMO at the aromatic rings. The diene **34** with benzo[b]fluorene favored *syn* addition with respect to the naphthalene ring, whereas the diene **35** with benzo[c]fluorene showed the reverse *anti* preference (Scheme 22) [28].



Scheme 21 Destabilization due to $n-\pi^*$ orbital interaction

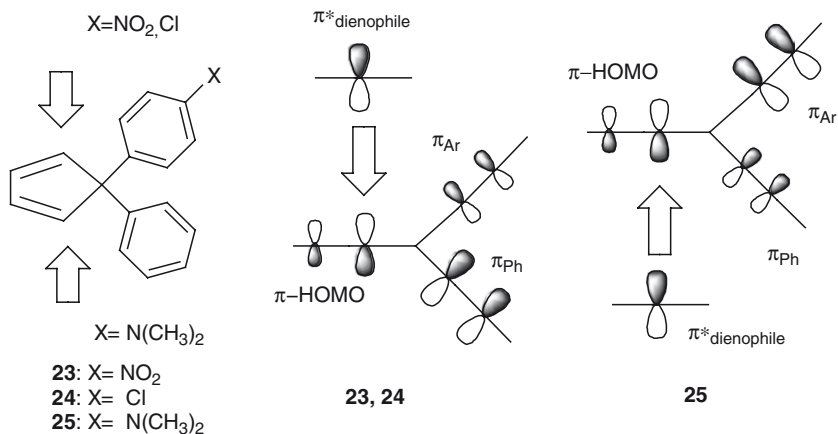


Scheme 22 π -Facial selectivity in the reactions of the dienes **34–35**

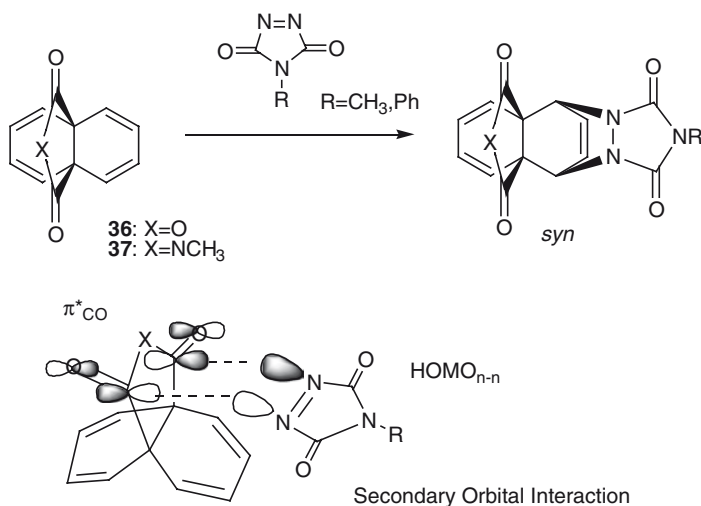
The reactions of 5-aryl-5-phenylcyclopentadiene **23–25** occur on the *anti* side of the more electron rich aromatic system [19]. The selectivity is also consistent with the orbital phase environments. The dienophiles avoid stronger out-of-phase interaction with the aromatic ring with higher HOMO. Halterman and coworkers ascribed the selectivity to the Cieplak effect (Scheme 23).

Gleiter and Ginsburg found that 4-substituted-1,2,4-triazoline-3,5-dione reacted with the propellanes **36** and **37** at the *syn* face of the cyclohexadiene with respect to the hetero-ring. They ascribed the selectivity to the secondary orbital interaction between the π^*_{CO} orbitals (LUMO) of **36** and **37** with antisymmetrical combination of lone pair orbitals ($HOMO_{n-n}$) of the triazolinediones (Scheme 24) [29].

They tested this theory by using dienophiles and substrates where such interaction cannot occur. The dienophiles containing a $C=C$ moiety instead of an $N=N$ moiety such as maleic anhydride and *N*-methylmaleimide exclusively reacted with

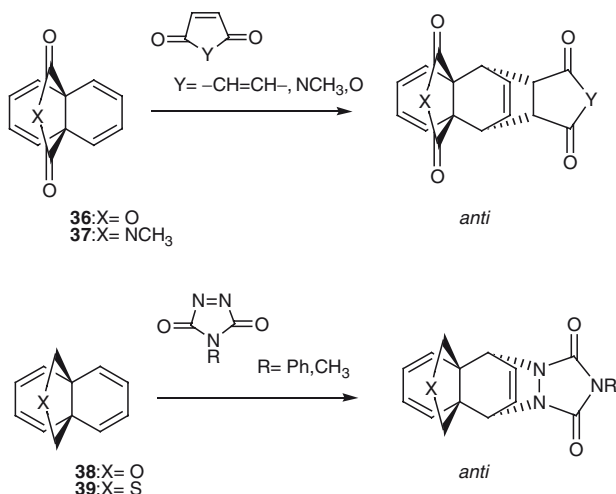


Scheme 23 π -Facial selectivity in the reactions of 5-aryl-5-phenylcyclopentadienes **23–25**



Scheme 24 π -Facial selectivity in the reactions of the propellanes **36–37**

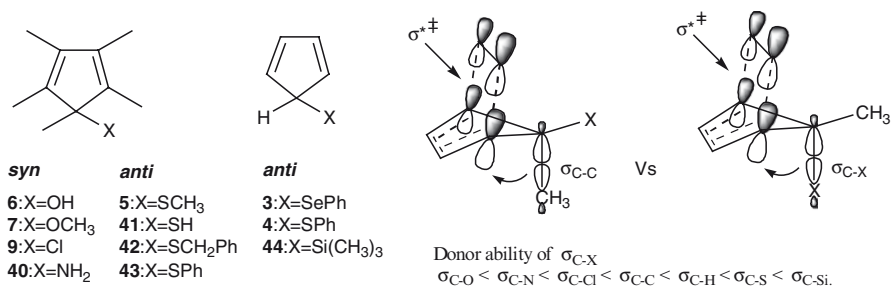
the propellanes **36** and **37** at the *anti* face [30]. The propellanes **38** and **39** containing no $\text{C}=\text{O}$ moieties exclusively reacted with triazolinediones at the *anti* face (Scheme 25). These results supported that the reactions of **36** and **37** with triazolinediones are controlled by the secondary orbital interaction. The origin of the *anti* selectivity observed in the reactions of **36** and **37** with $\text{C}=\text{C}$ dienophiles and of **38** and **39** with triazolinediones is not clear. They ascribed the selectivity to the steric interaction between the hetero-ring and dienophiles [31].



Scheme 25 π -Facial selectivity in the reactions of the propellanes **36–39**

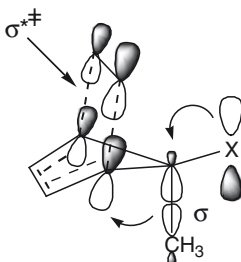
2.1.3 Hyperconjugative Electron Delocalization (Cieplak Effect)

Cieplak proposed that the most important interaction controlling π -face selection overriding steric factors is usually electron delocalization from the σ (hyperconjugation) or π (homoconjugation) orbitals of the stereogenic center into the incipient bond $\sigma^{*\ddagger}$, the low-lying LUMO of transition state [32, 33]. Fallis et al. applied this theory to the interpretation of π -facial selectivity in the Diels-Alder reactions of 5-substituted pentamethylcyclopentadienes [7]. They stated that the cycloaddition of the cyclopentadienes is expected to display a preference for *anti* addition to the antiperiplanar σ bond that is the better donor. *Syn* π facial selectivity observed in the reactions of the pentamethylcyclopentadienes having hydroxy, methoxy, amino, and chloro substituents at 5 positions is well consistent with the theory since addition *anti* to the better σ donor (σ_{C-C}) would be preferable. *Anti* π facial selectivity observed in the reactions of the cyclopentadienes having sulfur, selenium and silicon substituents at the 5 positions is also well consistent with the theory since σ_{C-X} ($X = S, Se, \text{ and } Si$) is a better donor than σ_{C-C} or σ_{C-H} [3, 4, 6, 34] (Scheme 26).



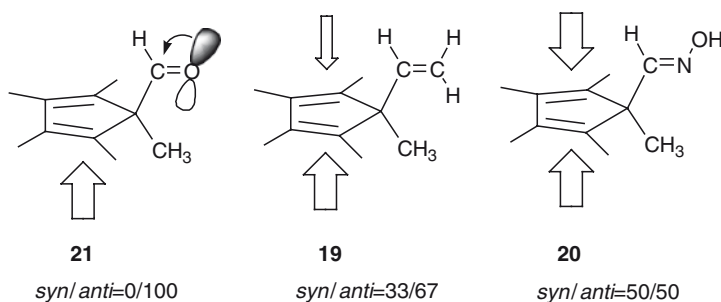
Scheme 26 Hyperconjugative stabilization (Cieplak effect)

Cieplak stated that the lone pair back-donation of C5 substituent also stabilizes the transition state during the *syn* approach since it improves hyperconjugation of the C5–H bond (extended hyperconjugation). He pointed out that for the cyclopentadienes having C5 substituents such as hydroxy, methoxy, amino, and chloro moiety, the hyperconjugative stabilization and the back-donation work in the same direction (Scheme 27).



Scheme 27 Back donation of lone pair of C5 substituent

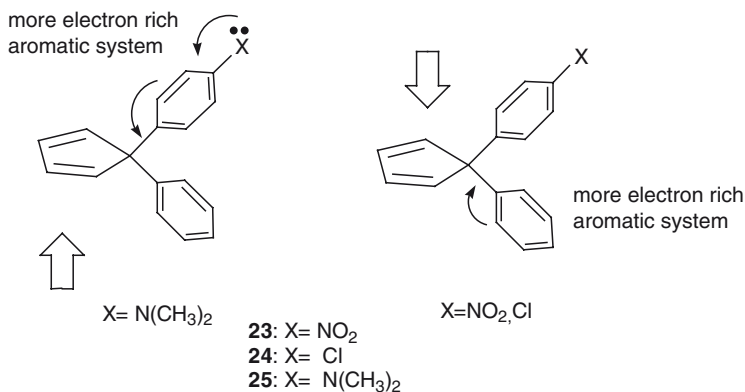
Cieplak applied this effect to the explanation of the shift of selectivity in the reactions of the pentamethylcyclopentadienes **21**, **19**, and **20** having substituents of formyl, vinyl, and (hydroxyimino)methyl moiety at the 5-positions [14]. He pointed out that the observed result is consistent with the notion that in the case of formyl moiety the hyperconjugative effect is enhanced by lone pair back-donation due to the formyl moiety, while we predicted the shift by the orbital mixing rule (Scheme 28).



Scheme 28 Back-donation of lone pair of the formyl moiety

Halterman et al. agreed with this proposal to show the selectivity of 5-aryl-5-phenylcyclopentadiene favoring the reactions on the *anti* side of a more electron rich aromatic system with significant correlation between the Hammett constants for the aromatic substituents and the facial selectivity [19] (Scheme 29).

Coxon et al. also reported that AM1 calculation of the transition states for the reactions between ethylene and 5-methylcyclopentadienes **45–49** bearing the



Scheme 29 Cieplak effect in the reactions of the cyclopentadienes **23–25**

substituents of methyl, chloro, hydroxy, methoxy, and methylthio moiety at the 5-positions was consistent with the Cieplak effect [35]. The bond distance between C5 and substituent X for the *anti* attack is longer than that for the *syn* attack (Table 3). For example, when the reaction occurs at the *syn* side of the chlorine atom of the diene **46**, the C5–Cl bond length is calculated as 1.764 Å, while for the reaction at the *anti* side the C5–Cl bond lengthens to 1.802 Å. Coxon and coworkers concluded that such a lengthening of the C5–X bond is consistent with σ – σ^* interaction in the Cieplak effect (see Scheme 26).

Table 3 Bond lengths of C5–X and C5–CH₃ at the transition states in Diels–Alder reactions between 5-methyl-5-X-cyclopentadienes and ethylene (AM1)

Diene:X	<i>syn</i> attack		<i>anti</i> attack	
	C5–X(Å)	C5–CH ₃ (Å)	C5–X(Å)	C5–CH ₃ (Å)
45 :CH ₃	1.509	1.531	1.531	1.509
46 :Cl	1.764	1.522	1.802	1.503
47 :OH	1.415	1.524	1.434	1.514
48 :OCH ₃	1.423	1.523	1.443	1.513
49 :SCH ₃	1.782	1.514	1.816	1.499

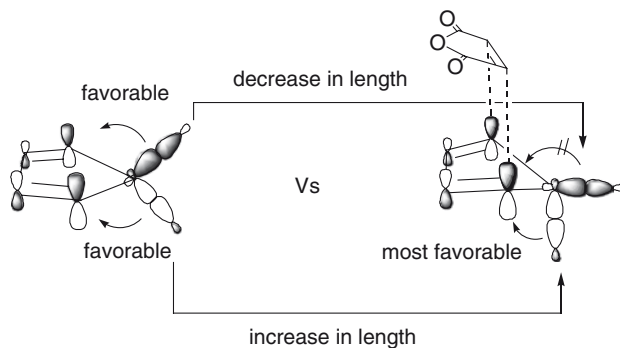
Semi empirical calculations reported by us [4] and by Werstiuk and Ma [36] provided no support for the Cieplak effect. We reported the calculation of the reactions of 5-substituted cyclopentadienes Cp–X (**50**:X = NH₂, **51**:X = PH₂, **52**:X = AsH₂, **53**:X = SbH₂, **54**:X = OH, **55**:X = SH, **56**:X = SeH, **57**:X = TeH, **8**:X = F, **2**:X = Cl, **11**:X = Br, and **12**:X = I) with maleic anhydride at PM3 level of theory. Although lengthening of C5–X and C5–H bonds *anti* to the incipient bonds is in accord with the Cieplak

Table 4 PM3 calculation of 5-X-cyclopentadienes at the transition states of Diels-Alder reactions with maleic anhydride

		Bond length (Å)			
Diene:X	bond	Diene	<i>syn</i> TS(% extrn $\Delta_{TS-Diene}$)		<i>anti</i> TS(% extrn $\Delta_{TS-Diene}$)
50:NH₂	C5-X	1.477	1.470 (-0.47)	<	1.479 (0.13)
	C5-H	1.117	1.121 (0.36)	>	1.114 (-0.27)
54:OH	C5-X	1.400	1.391 (-0.64)	<	1.400 (0.00)
	C5-H	1.112	1.118 (0.54)	>	1.110 (-0.31)
8:F	C5-X	1.360	1.357 (-0.22)	<	1.368 (0.59)
	C5-H	1.112	1.114 (0.54)	>	1.109 (-0.27)
2:Cl	C5-X	1.770	1.756 (-0.79)	<	1.778 (0.45)
	C5-H	1.112	1.117 (0.45)	>	1.110 (-0.18)

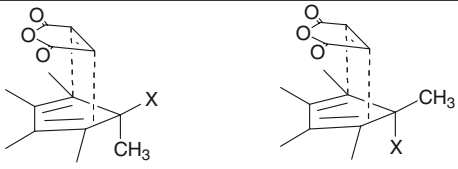
effect, the most noteworthy feature is that the bond length of C5–X and C5–H *syn* to the incipient bonds is short in comparison with those of the starting diene (Table 4).

We pointed out that these results can be attributable to the σ – π^* interaction. At the transition state, the σ orbital at C5 on the *anti* side of the dienophile is parallel with the π^* orbital, the σ bond electrons are able to delocalize much more effectively than that on the *syn* side. Since the electron donating σ bond on the *anti* side stabilizes the transition state, the σ – π^* interaction can contribute to π -facial selectivity. These results suggested that the bond lengthening cannot necessarily be convincing evidence for the Cieplak effect, but can be explained in terms of the σ – π^* interaction without assuming the incipient σ bonds at the transition state (Scheme 30).

**Scheme 30** σ – π^* Interaction at the starting diene and the transition state

Werstiuk and Ma [36] reported that AM1 calculation of the reactions of maleic anhydride and C5-substituted pentamethylcyclopentadienes $\text{Cp}^*\text{-X}$ (**40**:X = NH_2 , **58**:X = NHCOCH_3 , **6**:X = OH, **7**:X = OCH_3 , **5**:X = SCH_3 , **59**:X = H, **60**:X = SiH_3 , **61**:X = CH_3 , **62**:X = $\text{Si}(\text{CH}_3)_3$, **63**:X = CF_3 , **64**:X = NH_3^+). Typical examples are shown in Table 5.

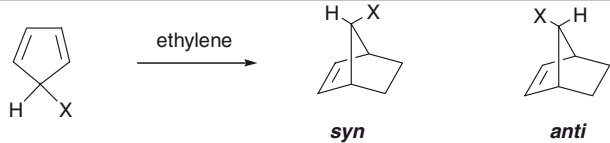
Table 5 AMI Calculation of the transition states in Diels-Alder reactions between 5-X-pentamethylcyclopentadienes and maleic anhydride



Bond length (Å)						
Diene:X	bond	Diene	<i>syn</i> TS		<i>anti</i> TS	difference of length
6 :OH	C5-X	1.420	1.414	<	1.435	0.021
	C5-H	1.521	1.526	>	1.514	0.012
7 :OCH ₃	C5-X	1.427	1.421	<	1.443	0.022
	C5-H	1.518	1.524	>	1.512	0.012

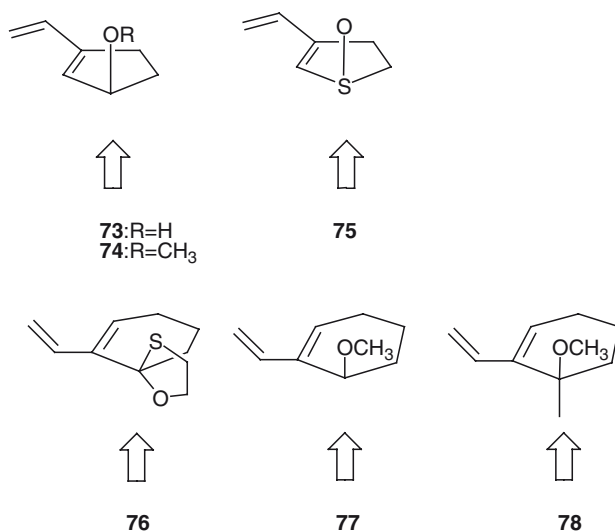
They found marginal lengthening of C5–X and C5–CH₃*anti* to the incipient bonds in accord with the Cieplak effect. The bond lengths of C5–X and C5–CH₃*syn* to the incipient bonds are short in comparison with those of the starting diene, similar to our report. They focused on the difference in the C5–X bond lengths which is larger than the difference computed for C5–CH₃ bonds. For example, the difference in the C5–OH bond lengths is 0.021 Å which is larger than that in C5–CH₃ lengths (0.012 Å). Because of the larger donating ability of $\sigma_{\text{C-C}}$ compared to $\sigma_{\text{C-O}}$, Werstiuk and Ma pointed out that it is unlikely that the difference in the length is related to the major factors responsible for the *syn* π facial selectivity.

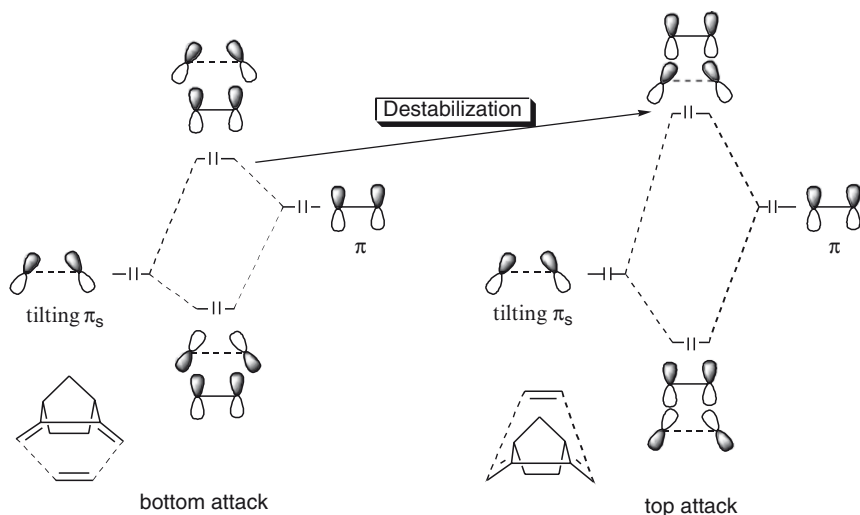
Ab initio calculation of Diels-Alder reactions of a series of 5-heteroatom substituted cyclopentadienes Cp-X (**65**:X = NH^- , **50**:X = NH_2 , **64**:X = NH_3^+ , **67**:X = O^- , **54**:X = OH, **68**:X = OH_2^+ , **69**:X = PH^- , **51**:X = PH_2 , **70**:X = PH_3^+ , **71**:X = S^- , **55**:X = SH, **72**:X = SH_2^+) with ethylene at HF/6-31++G(d)//HF/6-31++G(d) level by Burnell and coworkers [37] provided counterexamples of the Cieplak effect. The calculation showed that ionization of substituents has a profound effect on the π facial selectivity: deprotonation enhances *syn* addition and protonation enhances *anti* addition. The transition states for *syn* addition to the deprotonated dienes are stabilized relative to those of the neutral dienes, while those for *anti* addition are destabilized relative to those of the neutral dienes. On the other hand, activation energies for *syn* addition to the protonated dienes are similar to those of the neutral dienes, but those for *anti* addition are very much lowered relative to neutral dienes (Table 6).

Table 6 Activation energies and π -facial selectivity in the Diels-Alder reactions of 5-X-cyclopentadienes with ethylene


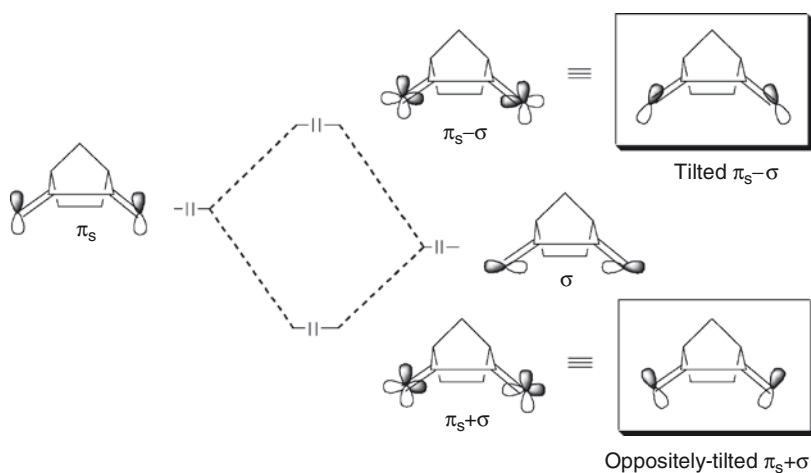
Diene:X	Activation energies (kJ/mol)			Diene:X	Activation energies (kJ/mol)		
	ΔE_{syn}	ΔE_{anti}	<i>syn</i> / <i>anti</i>		ΔE_{syn}	ΔE_{anti}	<i>syn</i> / <i>anti</i>
65 :NH ⁻	161.0	180.6	100 : 0	69 :PH ⁻	192.7	187.7	10 : 90
50 :NH ₂	170.3	178.6	97 : 3	51 :PH ₂	193.8	179.8	0 : 100
64 :NH ₃ ⁺	170.3	153.4	0 : 100	70 :PH ₃ ⁺	193.3	156.8	0 : 100
67 :O ⁻	138.9	182.1	100 : 0	71 :S ⁻	173.6	186.1	100 : 0
54 :OH	162.3	173.7	99 : 1	55 :SH	182.7	179.5	19 : 81
68 :OH ₂ ⁺	162.9	139.3	0 : 100	72 :SH ₂ ⁺	178.7	148.8	0 : 100

Overman, Hehre and coworkers reported *anti* π -facial selectivity in Diels-Alder reactions of vinylcyclopenten **73**, **74** and 4,5-dihydro-3-ethynylthiophen S-oxide **75** [38] (Scheme 31). These results are not in agreement with the Cieplak effect, at least in Diels-Alder reactions of the dienes having unsymmetrical π -plane. Yadav and coworkers reported that the reactions between the vinylcyclohexene **76** and dienophiles favor the reactions *syn* to oxygen, while **77** and **78** favor the reaction *anti* to oxygen substituents [39]. They discuss the Cieplak effect but the reactions are not suitable.

**Scheme 31** π -Facial selectivity in the reactions of the dienes **73–78**



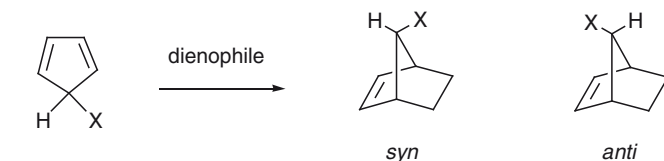
Scheme 34 Diagram of the interaction between the tilting π_s of the model diene with π of dienophile



Scheme 35 Orbital mixing of π_s and σ of the diene unit

2.2 Steric Repulsion

π -Facial selectivities in the Diels-Alder reactions of 5-substituted 1,3-cyclopentadienes Cp-X (**83**:X = H, **84**:X = BH₂, **85**:X = CH₃, **50**:X = NH₂, **54**:X = OH, **8**:X = F, **86**:X = SiH₃, **51**:X = PH₂, **55**:X = SH, **2**:X = Cl, **87**:X = GeH₃, **52**:X = AsH₂, **56**:X = SeH, **11**:X = Br, **88**:X = SnH₃, **53**:X = SbH₂, **57**:X = TeH, **12**:X = I) were calculated at the ab initio HF/6-31G* level by Burnell and coworkers [44] (Scheme 36).



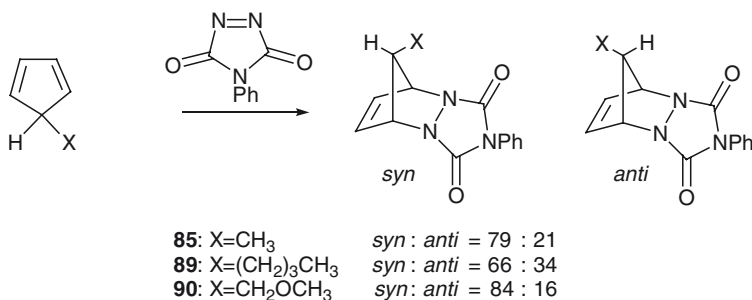
Dienophile = Ethylene

83: X= H	<i>syn</i> : <i>anti</i> = 50 : 50	87: X= GeH ₃	<i>syn</i> : <i>anti</i> = 0 : 100
84: X= BH ₂	<i>syn</i> : <i>anti</i> = 1 : 99	52: X= AsH ₂	<i>syn</i> : <i>anti</i> = 0 : 100
85: X= CH ₃	<i>syn</i> : <i>anti</i> = 20 : 80	56: X= SeH	<i>syn</i> : <i>anti</i> = 2 : 98
50: X= NH ₂	<i>syn</i> : <i>anti</i> = 95 : 5	11: X= Br	<i>syn</i> : <i>anti</i> = 7 : 93
54: X= OH	<i>syn</i> : <i>anti</i> = 99 : 100	88: X= SnH ₃	<i>syn</i> : <i>anti</i> = 0 : 100
8: X= F	<i>syn</i> : <i>anti</i> = 100 : 0	53: X= SbH ₂	<i>syn</i> : <i>anti</i> = 0 : 100
86: X= SiH ₃	<i>syn</i> : <i>anti</i> = 0 : 100	57: X= TeH	<i>syn</i> : <i>anti</i> = 0 : 100
51: X= PH ₂	<i>syn</i> : <i>anti</i> = 0 : 100	12: X= I	<i>syn</i> : <i>anti</i> = 0 : 100
55: X= SH	<i>syn</i> : <i>anti</i> = 11 : 89		
2: X= Cl	<i>syn</i> : <i>anti</i> = 71 : 29		

Scheme 36 π -Facial selectivity in the reactions of 5-substituted cyclopentadienes with ethylene

They estimated the steric factor [45]: X = F (0.478) < OH (0.616) < NH₂ (0.778) < Cl (0.899) < CH₃ (0.996) < H (1.013) < Br (1.0509) < SH (1.075) < SeH (1.223) < PH₂ (1.283) < I (1.304) < BH₂ (1.362) < AsH₂ (1.433) < TeH (1.490) < SiH₃ (1.525) < GeH₃ (1.600) < SbH₂ (1.734) < SnH₃ (1.926).

The values of X = NH₂, OH, F, Cl, and CH₃ are smaller than that of X = H, in accordance with the observed selectivity. Excellent correlation was found for all other cyclopentadienes described above. *Syn* π -facial selectivity in the reactions between 4-phenyl-1,2,4-triazoline-3,5-dione and cyclopentadiene having simple alkyl group at 5 positions are reported by Burnell and coworkers [46] (Scheme 37).



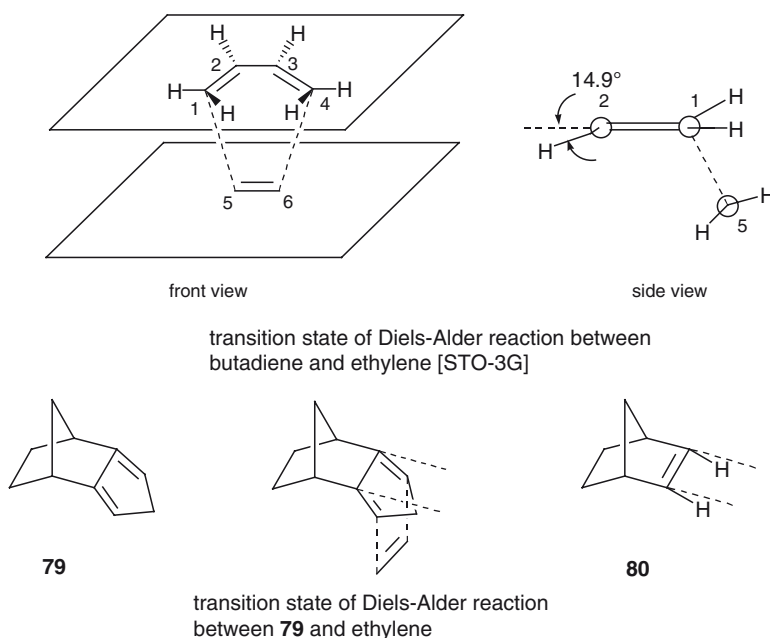
Scheme 37 π -Facial selectivity in the reactions of the cyclopentadienes **85** and **89–90**

They pointed out that the results are consistent with an explanation based on their “steric hindrance,” although the orbital mixing rule already predicted the deformation of the FMO of **85** to favor the reaction at the *syn* side [2].

The steric factor proposed by Burnell and coworkers cannot be applicable for ionic substituents X (see Table 6).

2.3 Torsional Control

In contrast with *exo* (top) facial selectivity in the additions to norbornene **80** [41], Diels-Alder reaction between isodicyclopentadiene **79** takes place from the bottom [40] (see Scheme 32). To solve this problem, Houk and Brown calculated the transition state of the parent Diels-Alder reaction of butadiene with ethylene [47]. They pointed out that of particular note for isodicyclopentadiene selectivity issue is the 14.9° out-of-plane bending of the hydrogens at C2 and C3 of butadiene. The bending is derived from C1 and C4 pyramidalization and rotation inwardly to achieve overlap of p-orbitals on these carbons with the ethylene termini. To keep the π -bonding between C1–C2 and C3–C4, the p-orbitals at C2 and C3 rotate inwardly on the side of the diene nearest to ethylene. This is necessarily accompanied by C2 and C3 hydrogen movement toward the attacking dienophile. They proposed that when norbornene is fused at C2 and C3, the tendency of *endo* bending of the norbornene framework will be manifested in the preference for bottom attack in Diels-Alder reactions (Scheme 38).

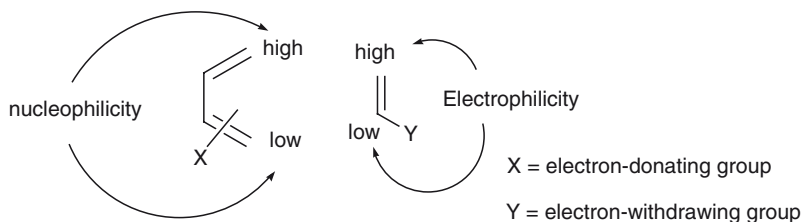


Scheme 38 Torsional control of π -facial selectivity in the reactions of isodicyclopentadiene **79**

2.4 Electrostatic Interaction

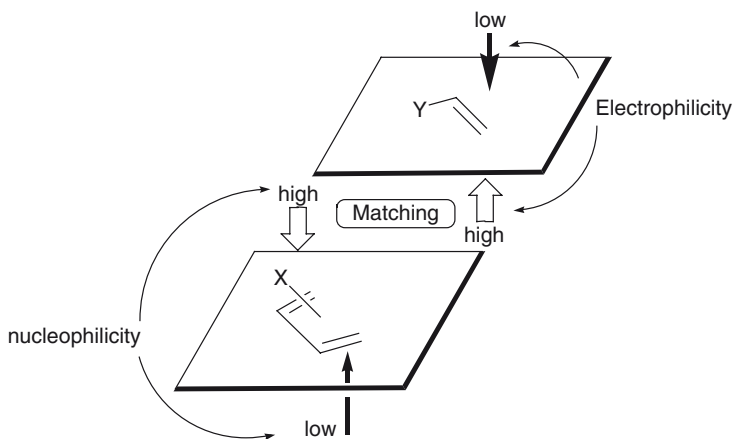
Kahn and Hehre stated that the regiochemistry of Diels-Alder reactions of electron-rich dienes and electron-withdrawing dienophiles follows from matching the nucleophilicity of the dienes and the electrophilicity of the dienophiles, although it has

been accepted that only frontier orbital interactions are important in dictating regiochemistry. They pointed out that this suggests that electrostatic interaction plays a major role (Scheme 39) [48].



Scheme 39 Regioselectivity predicted on the basis of matching of the nucleophilicity of the diene having electron-donating group X and the electrophilicity of the dienophile having electron-withdrawing group Y

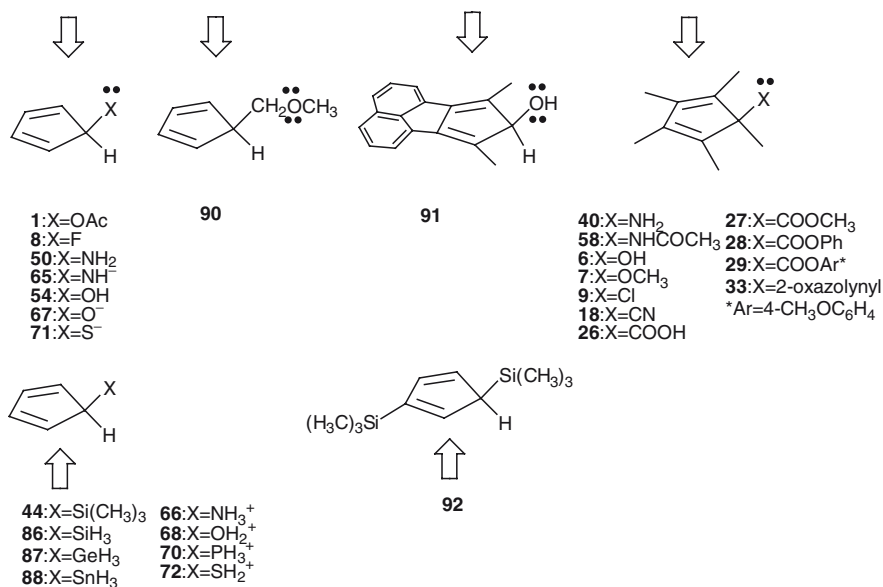
Kahn and Hehre straightforwardly extended this idea to the description of π -facial selectivity in Diels Alder reactions. They simply stated “cycloaddition involving electron-rich dienes and electron-poor dienophiles should occur preferentially onto the diene face which is the more nucleophilic and onto the diene face which exhibits the greater electrophilicity” (Scheme 40) [49].



Scheme 40 Facial selectivity predicted on the basis of matching of the nucleophilicity of the diene having electron-donating group X and the electrophilicity of the dienophile having electron-withdrawing group Y

Here the nucleophilicity of the dienes was evaluated from the electrostatic potential; the energy accounts only for Coulombic interactions, between a “test” electrophile (a proton) and the dienes. The electrophilicity of the dienophiles was evaluated from electrostatic potential between a “test” nucleophile (a hydride) and the dienophiles. They stated that, in the case of the reaction of 5-substituted cyclopentadienes, the approach of dienophile (an electrophile) will occur at the *syn* side of the substituents having lone pairs, and at the *anti* side of electropositive substituents. There are some

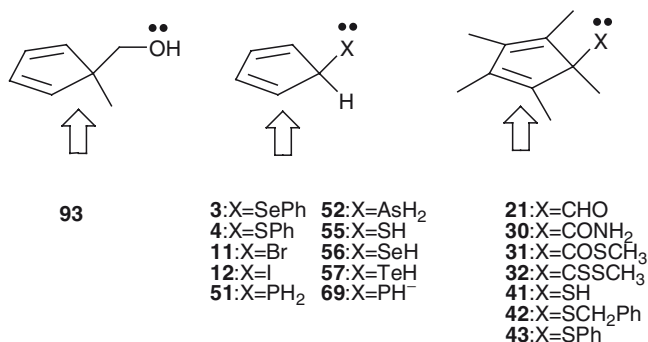
examples of experimental and theoretical support (Scheme 41). For example, *syn* π -facial selectivity observed in the reactions of the cyclopentadienes **1**, **8**, **90**, and **91** and pentamethylcyclopentadienes **6**, **7**, **9**, **18**, **26–29**, **33**, **40**, and **58** and the



Scheme 41 Experimental and theoretical supports for the electrostatic interaction

computational study of the reactions of the dienes **50**, **54**, **65**, **67**, and **71** are consistent with the electrostatic interaction, although the orbital mixing rule gives similar prediction [5, 7–9, 13, 16, 20, 37, 44, 46]. *Anti* π -facial selectivity observed in the reactions of **44** and **92** and computational study for the reactions of **66**, **68**, **70**, **72**, and **86–88** is also consistent with the electrostatic interaction [34, 37, 44, 50].

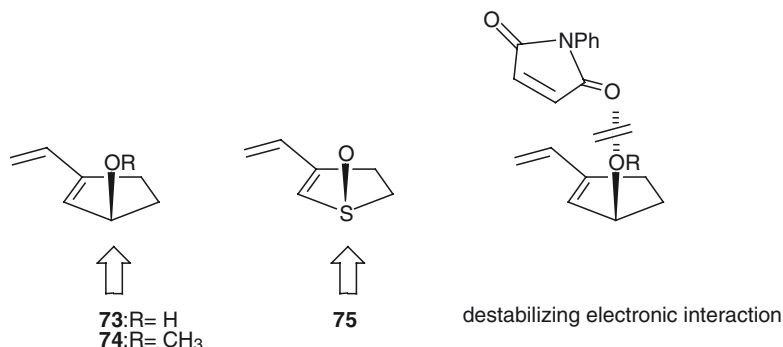
There were reported to be some counterexamples (Scheme 42). 5-(Hydroxymethyl)-5-methylcyclopentadiene **93**, the homologue of 5-hydroxycyclopentadiene **54**, was



Scheme 42 Counter examples of the electrostatic interaction

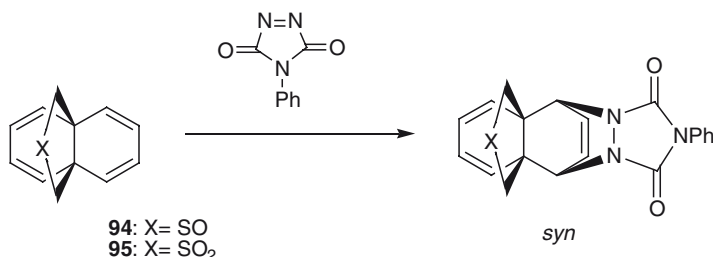
reported by Paquette and coworkers to react with dienophiles at the *anti* side of hydroxymethyl moiety [51]. The cyclopentadienes **3**, **4**, **11**, **12** and the pentamethylcyclopentadienes **21**, **30–32**, **41–43** reacted with *anti* π -facial selectivity [4, 7, 11–14, 20]. The computational study of the reactions of the dienes **51–52**, **55–57**, and **69** also showed *anti* π -facial selectivity [37, 44].

Overman, Hehre and coworkers also reported *anti* π -facial selectivity in Diels-Alder reactions of the vinylcyclopentenes **73**, **74** and 4,5-dihydro-3-ethynylthiophen *S*-oxide **75**. They attributed the selectivity to destabilizing electronic interaction between the allylic heteroatom and dienophile in the *syn* attack transition state (Scheme 43) [38].



Scheme 43 π -Facial selectivity in the reactions of the dienes **73–75**

Ginsburg and coworkers found that the sulfoxide **94** and sulfone **95** reacted with *N*-phenyltriazolinedione at the *syn* side of sulfoxide and sulfone moiety respectively [52] (Scheme 44). These results strongly contradict the *anti* selectivity observed in the reaction of the sulfide **39** (see Scheme 25).

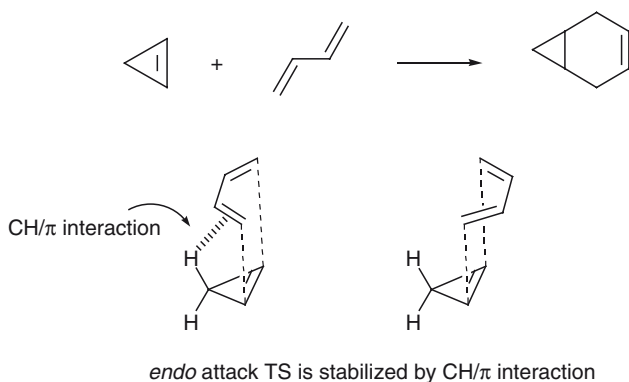


Scheme 44 π -Facial selectivity in the reactions of the propellanes **94–95**

They stated that the observed selectivity may be charge-controlled, since the molecular orbital calculation of the triazorine and the sulfone **95** showed a strongly negative field around the lone pairs of the azo moiety of the triazorine and a strongly positive field around the sulfur of the sulfone group [29].

2.5 CH/ π or π / π Interaction

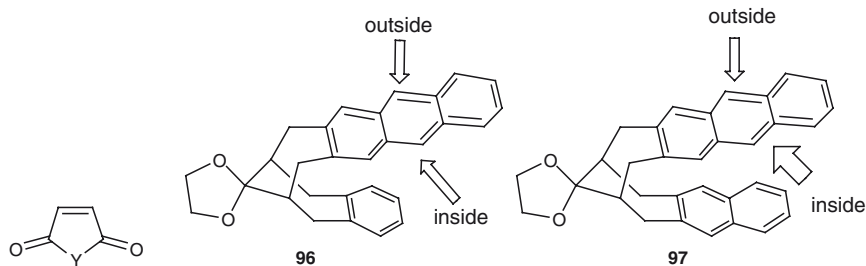
The CH/ π interaction is the weakest extreme of hydrogen bonds which occurs between CH and π -system. The energy of a typical CH/ π hydrogen bond is ca. 0.5–2.5 kcal mol⁻¹. Participation of CH/ π hydrogen bond in the transition states of competing reactions causes the difference in the Gibbs energy and can result in an acceptable selectivity [53]. For example, Dannenberg and coworkers reported the theoretical study of *endo/exo* selectivity of the Diels-Alder reaction between cyclopropene and butadiene using HF, CASSCF, QCISD(T) methods. All calculations showed that the *endo* product of the reaction should be favored. They ascribed the selectivity to a stabilizing CH/ π interaction at the *endo* attack transition state [54] (Scheme 45).



Scheme 45 CH/ π Interaction in the Diels-Alder reaction between cyclopropene and butadiene

Mataka and coworkers reported the studies of the Diels-Alder reactions of [3.3] orthoanthracenophanes **96** and **97**, of which anthraceno unit, the potential diene, has two nonequivalent faces, inside and outside. The reactions of **96** with dienophiles gave the mixtures of inside and outside adducts with the ratios between 1:1 and 1:1.5. However, the ratio changes drastically, in favor of the inside adducts, when **97** reacts with dienophiles such as maleic anhydride, maleimide and naphthoquinone [55] (Scheme 46). Mataka suggested that the π -facial selectivity is controlled by an orbital interaction between the electron-poor dienophiles and the π -orbital of the facing aromatics, which would lead to a stabilization of the transition state, while Nishio suggested that the selectivity is due to the attractive π / π or CH/ π interaction [53].

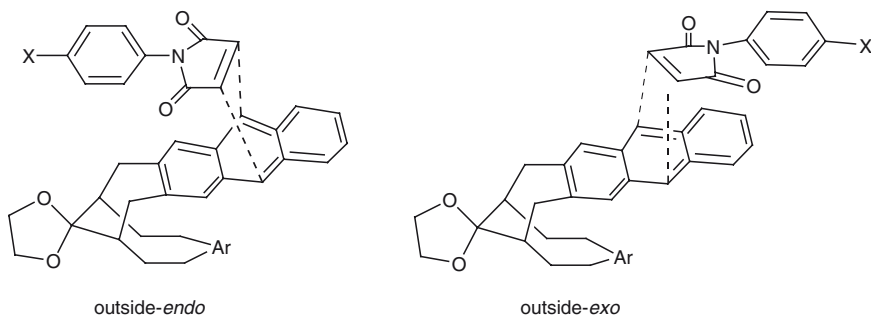
Mataka and coworkers further studied the *exo/endo* selectivity of outside attack products in the reactions of **96** and **97** with *N*-(5-*X*-phenyl)maleimides [56]. They found that the *endo/exo* selectivity is markedly dependent on the electronic nature of the substituent *X* (Scheme 47). The electro-withdrawing substituents such as NO₂ and Cl enhance *endo*-selectivity. The relative order of the *endo*-selectivity is NO₂ > Cl > H > OCH₃.



Dienophile:	Y=	inside/outside*	inside/outside*
N-phenylmaleimide	NPh	52 : 48	50 : 50
maleic anhydride	O	56 : 44	86 : 14
maleimide	NH	60 : 40	88 : 12
naphthoquinone	-C ₆ H ₄ -	—	100 : 0

*outside adducts are *exo/endo* mixtures

Scheme 46 π -Facial selectivity in the reactions of [3.3]orthoanthracenophanes **96–97**



96: Ar=C₆H₄

X=OCH₃ *endo/exo*=60/40

X=H *endo/exo*=60/40

X=Cl *endo/exo*=67/33

X=NO₂ *endo/exo*=67/33

97: Ar=C₁₀H₆

X=OCH₃ *endo/exo* = 83/17

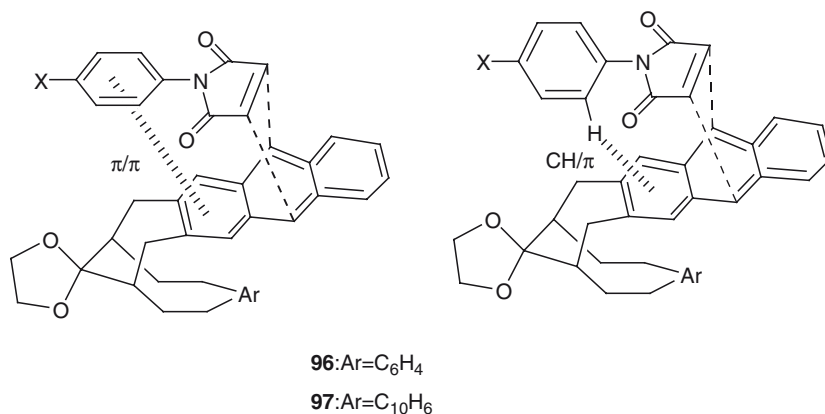
X=H *endo/exo* = 100/0

X=Cl *endo/exo* = 100/0

X=NO₂ *endo/exo* = 100/0

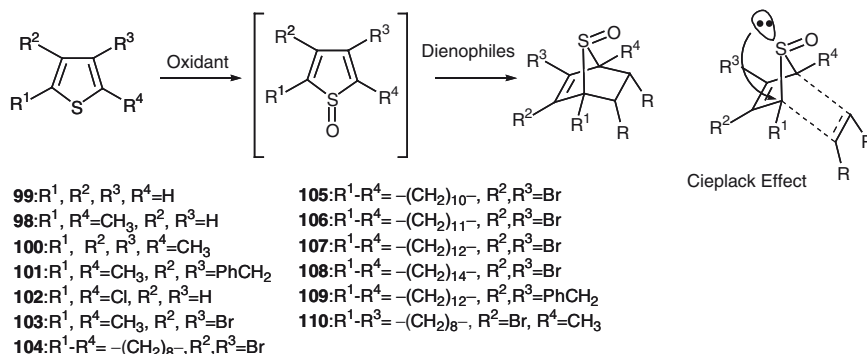
Scheme 47 *Endo/exo* selectivity in the reactions of [3.3]orthoanthracenophanes **96–97**

Mataka ascribed the selectivity to π/π interaction between the phenyl moiety of dienophiles and most closely stacked aromatic part of the anthracenophanes **96** and **97**, while again Nishio stated that the selectivity is due to the attractive CH/ π interaction [53] (Scheme 48).

**Scheme 48** π/π and CH/ π Interactions

3 Diels-Alder Reaction of Thiophene 1-Oxides

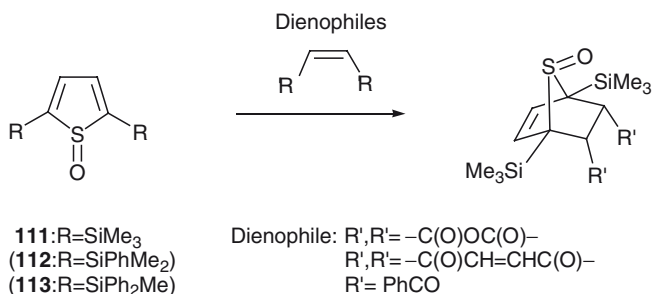
π -Facial selectivity in the Diels-Alder reactions of thiophene 1-oxides has recently attracted keen attention (Scheme 49). Fallis and coworkers reported in situ generated 2,5-dimethylthiophene 1-oxide **98** reacted with various electron-deficient dienophiles exclusively at the *syn* face with respect to sulfoxide oxygen [57].

**Scheme 49** Diels-Alder reactions of in situ generated thiophene 1-oxides with dienophiles

The π -facial selectivity was explained by the “Cieplak Effect” due to back-donation of lone pair electrons on sulfur (Scheme 49). Mansuy and coworkers reported that in situ generated thiophene 1-oxide **99** could be trapped by 1,4-benzoquinone to afford the corresponding *syn* attack product [58]. Tashiro and coworkers also reported that in situ generated thiophene 1-oxide derivatives **98**, **100–103** and

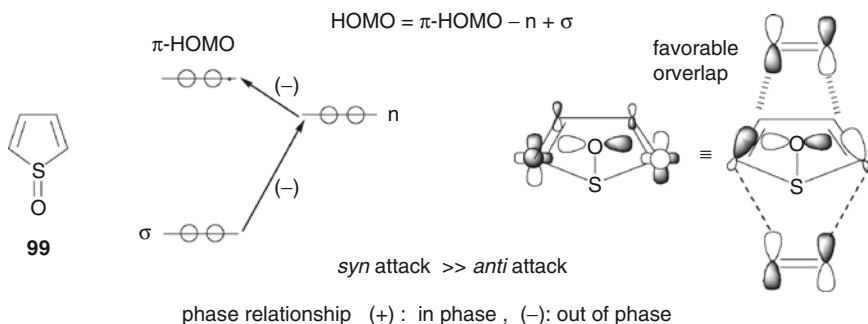
thiophenophane *S*-oxides **104–110** with electron-deficient dienophiles in the presence of $\text{BF}_3 \cdot \text{Et}_2\text{O}$ catalyst gave similar results [59, 60].

Furukawa and coworkers reported preparation and isolation of thiophene 1-oxides **111–113**. Diels-Alder reaction of **111** with maleic anhydride, benzoquinone, and *cis*-1,2-dibenzoyl ethylene gave the corresponding *syn* adducts exclusively [61] (Scheme 50).



Scheme 50 Diels-Alder reactions of thiophen 1-oxide **111** with dienophiles

The *syn* addition mode was also confirmed by ab initio calculation of the reaction between thiophene 1-oxide **99** and ethylene. They stated that the selectivity can be explained by the orbital mixing rule (Scheme 51). The π -HOMO of the diene part of **99** is modified by an out-of-phase combination with the low lying n-orbital of

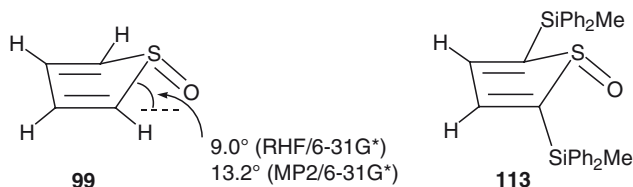


Scheme 51 FMO deformation of thiophen 1-oxide **99**

oxygen to give the HOMO of the whole molecule. σ -Orbitals then mixed in such a way that σ and n are out-of-phase to give the distorted FMO so as to favor *syn* addition. The calculated HOMO of **99** is distorted in this way.

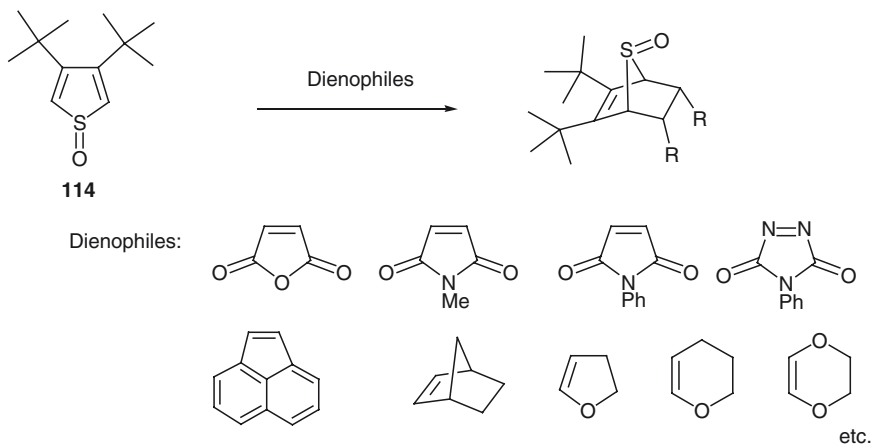
They also pointed out that the carbon atoms C2 and C5 of **99** are already distorted so as to conform to the *syn* addition. The sulfur atom protrudes out of the C2–C3–C4–C5 plane in the opposite direction to the oxygen atom. The C4–C5–C2–S1

dihedral angle is calculated to be 9.0° and 13.2° by the RHF/6-31G* and MP2/6-31G* methods, respectively. X-ray crystallographic analysis of **113** showed that the structure of **113** is a half envelop and the S=O bond is tilted ca. 13.6° out of the C2–C3–C4–C5 plane of thiophene ring (Scheme 52).



Scheme 52 Structures of thiophene 1-oxides **99** and **113**

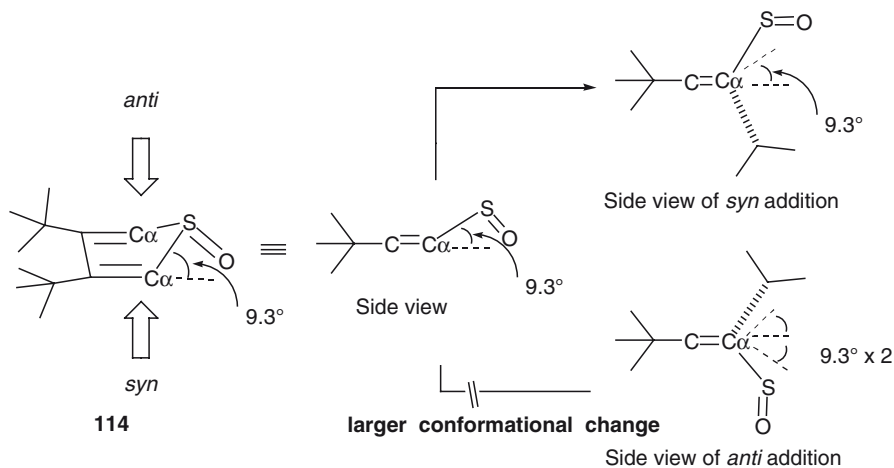
Nakayama and coworkers reported that 3,4-di-*tert*-butylthiophene 1-oxide **114** is thermally stable but still an extremely reactive substrate. They reported that the Diels-Alder reactions of **114** with varieties of electron-deficient and electron-rich dienophiles took place exclusively at the *syn*- π -face of the diene with respect to the S=O bond (Scheme 53) [62, 63].



Scheme 53 Diels-Alder reactions of 3,4-di-*tert*-butylthiophene 1-oxide **114** with varieties of dienophiles

They reported that the DFT calculations of **114** at the B3LYP/6-31G* level showed that the π -HOMO lobes at the α -position are slightly greater for the *syn*- π -face than for the *anti* face. The deformation is well consistent with the prediction by the orbital mixing rule. However, the situation becomes the reverse for the π -LUMO lobes, which are slightly greater at the *anti* than the *syn*- π -face. They concluded that the *syn*- π -facial selectivity of the normal-electron-demand Diels-Alder reactions

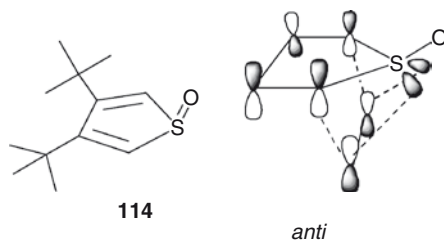
with electron-deficient dienophiles is in harmony with the nonequivalent extension of π -HOMO, whereas the *syn* π -facial selectivity of the reverse-electron-demand Diels-Alder reactions with electron-rich dienophiles cannot be explained in a similar way. Thus, they ascribed the latter case to the energies required for the conformational change of **114**. The *anti* addition transition state will encounter about 18.6° ($9.3^\circ \times 2$) larger change in bond angle around C_α carbons than will the *syn* addition transition state (Scheme 54).



Scheme 54 Difference of conformational change of the thiophene 1-oxide at the *anti* and *syn* addition transition states

In the case of the reverse-electron-demand Diels-Alder reactions, the secondary orbital interaction between the π -HOMO of dienophile and the LUMO of **114** or the effect of the orbital phase environments (Chapter “Orbital Phase Environments and Stereoselectivities” by Ohwada in this volume) cannot be ruled out as the factor controlling the selectivity (Scheme 55).

Hetero Diels-Alder reactions of **114** with thioaldehydes and thioketones were also reported to give the *syn* addition products exclusively [64].



Scheme 55 Destabilization due to n - π orbital interaction

4 Conclusion

Anti π -facial selectivity with respect to the sterically demanded substituent in the Diels-Alder reactions of dienes having unsymmetrical π -plane has been straightforwardly explained and predicted on the basis of the repulsive interaction between the substituent and a dienophile. However, there have been many counter examples, which have prompted many chemists to develop new theories on the origin of π -facial selectivity. We have reviewed some theories in this chapter. Most of them successfully explained the stereochemical feature of particular reactions. We believe that the orbital theory will give us a powerful way of understanding and designing of organic reactions.

Acknowledgement The authors thank Ms. Jane Clarkin for her English suggestions.

References

1. Winstein S, Shatavsky M, Norton C, Woodward RB (1955) *J Am Chem Soc* 77:4183
2. Inagaki S, Fujimoto H, Fukui K (1976) *J Am Chem Soc* 98:4054
3. Ishida M, Beniya Y, Inagaki S, Kato S (1990) *J Am Chem Soc* 112:8980
4. Ishida M, Aoyama T, Beniya Y, Yamabe S, Kato S, Inagaki S (1993) *Bull Chem Soc Jpn* 66:3430
5. Jones DW (1980) *J Chem Soc Chem Commun* 789
6. Ishida M, Aoyama T, Kato S (1989) *Chem Lett* 663
7. Macaulay JB, Fallis AG (1990) *J Am Chem Soc* 112:1136
8. Werstiuk NH, Ma J, Macaulay JB, Falls AG (1992) *Can J Chem* 70:2798
9. McClinton MA, Sik V (1992) *J Chem Soc Perkin Trans* 1:1891
10. Williamson KL, Hsu YFL (1970) *J Am Chem Soc* 92:7385
11. Breslow R, Hoffman JM Jr, Perchonock C (1973) *Tetrahedron Lett* 14:3723
12. Franck-Neumann M, Sedrati M (1983) *Tetrahedron Lett* 24:1391
13. Ishida M, Kobayashi H, Tomohiro S, Wasada H, Inagaki S (1998) *Chem Lett* 41
14. Ishida M, Kobayashi H, Tomohiro S, Inagaki S (2000) *J Chem Soc Perkin Trans* 2:1625
15. Poirier RA, Pye CC, Xidos JD, Burnell DJ (1995) *J Org Chem* 60:2328
16. Ishida M, Tomohiro S, Shimizu M, Inagaki S (1995) *Chem Lett* 739
17. Adam W, Jacob U, Prein MJ (1995) *Chem Soc Chem Commun*:839
18. Ishida M, Itakura M, Tashiro H (2008) *Tetrahedron Lett* 49:1804
19. Halterman RL, McCarthy BA, McEvoy MA (1992) *J Org Chem* 57:5585
20. Ishida M, Sakamoto M, Hattori H, Shimizu M, Inagaki S (2001) *Tetrahedron Lett* 42:3471
21. Ishida M, Hirasawa S, Inagaki S (2003) *Tetrahedron Lett* 44:2187
22. Hoffmann R, Woodward RB (1965) *J Am Chem Soc* 87:4388
23. Ishihara K, Kondo S, Kurihara H, Yamamoto S, Ohashi S, Inagaki S (1997) *J Org Chem* 62:3026
24. Ishihara K, Fushimi M (2008) *J Am Chem Soc* 130:7532
25. Anh NT (1973) *Tetrahedron* 29:3227
26. Ohwada T (1999) *Chem Rev* 99:1337
27. Ishida M, Inagaki S (1994) *Org Synth Chem* 52:649
28. Tsuji M, Ohwada T, Shudo K (1998) *Tetrahedron Lett* 39:403
29. Gleiter R, Ginsburg D (1979) *Pure Appl Chem* 51:1301
30. Kaftory M, Peled M, Ginsburg D (1979) *Helv Chim Acta* 62:1326

31. Ginsburg D (1983) *Tetrahedron* 39:2095
32. Cieplak AS, Tait BD, Johnson CR (1989) *J Am Chem Soc* 111:8447
33. Cieplak AS (1999) *Chem Rev* 99:1265
34. Magnus P, Carins PM, Moursounidis J (1987) *J Am Chem Soc* 109:2469
35. Coxon JM, McDonald DQ (1992) *Tetrahedron Lett* 33:651
36. Werstiuk NH, Ma J (1994) *Can J Chem* 72:2493
37. Xidos JD, Poirier RA, Burnell DJ (2000) *Tetrahedron Lett* 41:995
38. Fisher MJ, Hehre WJ, Kahn SD, Overman LE (1988) *J Am Chem Soc* 110:4625
39. Yadav VK, Senthil G, Babu KG, Parvez M, Reid JL (2002) *J Org Chem* 67:1109
40. Sugimoto TK, Kobuke Y, Furukawa J (1976) *J Org Chem* 41:1457 and references cited in [42] and [49]
41. Freeman F (1975) *Chem Rev* 75:439 and references cited in [2] and [49]
42. Gleiter R, Paquette LA (1983) *Acc Chem Res* 16:328
43. Albright TA, Burdett JK, Whangbo MH (1985) *Orbital interactions in chemistry*. Wiley, New York
44. Xidos JD, Poirier RA, Pye CC, Burnell DJ (1998) *J Org Chem* 63:105
45. Robb MA, Haines WJ, Csizmadia IG (1973) *J Am Chem Soc* 95:42
46. Letourneau JE, Wellman MA, Burnell DJ (1997) *J Org Chem* 62:7272
47. Brown FK, Houk KN (1985) *J Am Chem Soc* 107:1971
48. Kahn SD, Pau CF, Overman LE, Hehre WJ (1986) *J Am Chem Soc* 108:7381
49. Kahn SD, Hehre WJ (1987) *J Am Chem Soc* 109:663
50. Fleming I, Williams RV (1981) *J Chem Soc Perkin Trans 1* 684
51. Paquette LA, Vanucci C, Rogers RD (1989) *J Am Chem Soc* 111:5792
52. Kalo J, Vogel E, Ginsburg D (1977) *Tetrahedron* 33:1183
53. Nishio M (2005) *Tetrahedron* 61:6923
54. Sodupe M, Rios R, Branchadell V, Nicholas T, Oliva A, Dannenberg JJ (1997) *J Am Chem Soc* 119:4232
55. Mataka S, Ma J, Thiemann T, Rudziński JM, Sawada T, Tashiro M (1995) *Tetrahedron Lett* 36:6105
56. Mataka S, Ma J, Thiemann T, Mimura T, Sawada T, Tashiro M (1997) *Tetrahedron* 53:6817
57. Naperstkw AM, Macaulay JB, Newlands MJ, Fallis AG (1989) *Tetrahedron Lett* 30:5077
58. Treiber A, Dansette PM, Amri HE, Girault J-P, Ginderow D, Mornon J-P, Mansuy D (1997) *J Am Chem Soc* 119:1565
59. Li Y, Thiemann T, Sawada T, Mataka S, Tashiro M (1997) *J Org Chem* 62:7926
60. Li Y, Thiemann T, Mimura K, Sawada T, Mataka S, Tashiro M (1998) *Eur J Org Chem* 1841
61. Furukawa N, Zhang S, Horn E, Takahashi O, Saito S (1998) *Heterocycles* 47:793
62. Otani T, Takayama J, Sugihara Y, Ishii A, Nakayama J (2003) *J Am Chem Soc* 125:8255
63. Takayama J, Sugihara Y, Takayanagi T, Nakayama J (2005) *Tetrahedron Lett* 46:4165
64. Takayama J, Fukuda S, Sugihara Y, Ishii A, Nakayama J (2003) *Tetrahedron Lett* 44:5159

Orbital Phase Design of Diradicals

Jing Ma, Satoshi Inagaki, and Yong Wang

Abstract Over the last three decades the rational design of diradicals has been a challenging issue because of their special features and activities in organic reactions and biological processes. The orbital phase theory has been developed for understanding the properties of diradicals and designing new candidates for synthesis. The orbital phase is an important factor in promoting the cyclic orbital interaction. When all of the conditions: (1) the electron-donating orbitals are out of phase; (2) the accepting orbitals are in phase; and (3) the donating and accepting orbitals are in phase, are simultaneously satisfied, the system is stabilized by the effective delocalization and polarization. Otherwise, the system is less stable. According to the orbital phase continuity requirement, we can predict the spin preference of π -conjugated diradicals and relative stabilities of constitutional isomers. Effects of the intramolecular interaction of bonds and unpaired electrons on the spin preference, thermodynamic and kinetic stabilities of the singlet and triplet states of localized 1,3-diradicals were also investigated by orbital phase theory. Taking advantage of the ring strains, several monocyclic and bicyclic systems were designed with appreciable singlet preference and kinetic stabilities. Substitution effects on the ground state spin and relative stabilities of diradicals were rationalized by orbital interactions without loss of generality. Orbital phase predictions were supported by available experimental observations and sophisticated calculation results. In comparison with other topological models, the orbital phase theory

J. Ma and Y. Wang

Institute of Theoretical and Computational Chemistry, Key Laboratory of Mesoscopic Chemistry of MOE, School of Chemistry and Chemical Engineering
Nanjing University, Nanjing 210093, People's Republic of China
e-mail: majing@nju.edu.cn

S. Inagaki

Department of Chemistry, Gifu University, 1-1 Yanagido, Gifu,
501-1193, Japan
e-mail: inagaki@gifu-u.ac.jp

has some advantages. Orbital phase theory can provide a general model for both π -conjugated and localized diradicals. The relative stabilities and spin preference of all kinds of diradicals can be uniformly rationalized by the orbital phase property. The orbital phase theory is applied to the conformations of diradicals and the geometry-dependent behaviors. The insights gained from the orbital phase theory are useful in a rational design of stable 1,3-diradicals.

Keywords Diradical, Kinetic stability, Orbital phase theory, Spin preference

Contents

1	Introduction.....	221
2	Fundamental Concepts of Orbital Phase Theory	222
2.1	Importance of Orbital Phase	222
2.2	Target Questions for Diradicals	223
3	Orbital Phase Design of Diradicals.....	225
3.1	A General Model of Diradicals.....	225
3.2	Cyclic Orbital Interactions in Diradicals	227
3.3	Orbital Phase Continuity Conditions	229
3.4	Orbital Phase Properties of Diradicals.....	233
4	π -Conjugated Diradicals	235
4.1	Kekulé vs Non-Kekulé Diradicals: Typical Examples.....	235
4.2	Extension to Cyclic π -Conjugated Diradicals	238
4.3	Hetero-Atom Effects.....	240
4.4	Comparison with Other Topological Models.....	241
5	Localized Diradicals	243
5.1	Acyclic 1,3-Diradicals: Modulation of S–T Gaps by Substituents.....	244
5.2	Monocyclic 1,3-Diradicals: Taking Advantage of Ring Strain.....	249
5.3	σ -Type Bicyclic Diradicals	252
5.4	Comparison with Experiments.....	256
6	Concluding Remarks.....	258
	References.....	260

Abbreviations

4MR	Four-membered ring
5MR	Five-membered ring
A	Electron-accepting group
D	Electron-donating group
DMCBD	Dimethylenecyclobutadiene
HOMO	Highest occupied molecular orbital
LUMO	Lowest unoccupied molecular orbital
NBMO	Nonbonding molecular orbital
OXA	Oxyallyl
S	Singlet state
SOMO	Singly occupied molecular orbital
S–T gap	Energy gap between the lowest singlet and triplet states

T	Triplet state
TM	Trimethylene
TME	Tetramethylenethane
TMM	Trimethylenemethane

1 Introduction

Theoretical and computational chemistry has grown rapidly and has had significant influence on a wide range of chemistry. The past several decades have witnessed an accelerating pace in the development of quantum chemical methods and computational techniques, the rapid expansion of computational power, and the increasing popularity of user-friendly software packages. Nowadays computational results that surge out of the computer are extensively applied to understand molecular behavior and experimental phenomena. Experimental chemists, coming from almost all sub-fields of chemistry, have also recognized the importance of theoretical predictions on electronic structures of novel species and possible pathways of reactions in their designs of new experiments.

However, there is much to be harvested by seeking the underlying rules governing molecular properties of a similar family and distinguishing those rules from the sophisticated numerical results for individual molecules. For this purpose, qualitative theories are still desirable to provide useful concepts for elucidating intriguing molecular structures and chemical reactions, and more importantly, to predict the observable properties of new molecules before we carry out resource-consuming computations or experiments.

The period 1930–1980s may be the “golden age” for the growth of qualitative theories and conceptual models. As is well known, the frontier molecular orbital theory [1–3], Woodward–Hoffmann rules [4, 5], and the resonance theory [6] have equipped chemists well for rationalizing and predicting pericyclic reaction mechanisms or molecular properties with fundamental concepts such as orbital symmetry and hybridization. Remarkable advances in creative synthesis and fine characterization during recent years appeal for new conceptual models.

Radicals draw intensive attention due to their versatile features and wide occurrence in organic reactions and biological processes [7–14]. They are invoked as not only transient intermediates in many important thermal and photochemical reactions but also the building blocks for organic magnetic materials. However, the fleeting existence of radicals makes them rather difficult to be traced and handled experimentally. The rational design of diradicals is thus a challenging topic. Some simple models are desirable to gain a clear understanding of essential thermodynamic and kinetic features of radicals. Among qualitative theories, orbital phase theory [15–17], which has been developed for the cyclic orbital interactions underlying various chemical phenomena [18–28], was applied to give a general model for diradicals [29–33]. The orbital phase predictions on the properties of various diradicals were confirmed by experiments and calculation results. Several design strategies for stable 1,3-diradicals were suggested.

In this chapter we will review some recent progress in theoretical design of diradicals, with an emphasis on the successful applications of orbital phase theory [Chapter “An Orbital Phase Theory” by Inagaki in this volume]. The important role of orbital Phase in governing spin preference, relative stabilities, and reactivities of a broad branch of diradicals (ranging from π -conjugated to σ -localized systems, with and without heteroatoms or substituents) has been revealed. The rest of this chapter is organized as follows. In Sect. 2 some important concepts of orbital phase theory are briefly introduced. Subsequently, a general model for diradicals is presented in Sect. 3 in the language of the orbital phase theory. The orbital phase properties for the cyclic orbital interactions involved in through-bond and through-space couplings are addressed. The applications of orbital phase theory in π -conjugated and localized diradicals are collected in Sects. 4 and 5, respectively. A comprehensive comparison with theoretical and experimental results is also made in these two sections. Finally, we draw some general rules for designs of diradicals and make an emphasis on the features of the orbital phase theory in Sect. 6.

2 Fundamental Concepts of Orbital Phase Theory

2.1 Importance of Orbital Phase

The wave-particle duality of electrons forms the basis of quantum mechanisms. The information of a particle is hidden in its complicated wave functions. In fact, the phase of an orbital is a consequence of the wave-like behavior of electrons. The orbital phase of an atomic orbital (AO) can be graphically illustrated either by plus/minus signs or by shading/unshading on the lobes. For a molecular system, the wave functions are expressed as a linear combination of atomic orbitals. The sign of the orbital phase itself does not have any physical meaning. Only when atomic orbitals are mixed to form molecular orbitals does the phase become a crucial factor. Take dihydrogen (H_2) as an example. In the minimum basis set, two 1s AOs can overlap in two ways depending on their phase relationship, as shown in Fig. 1. Just like the light waves, atomic orbitals also interact with each other *in phase* or *out of phase*. *In-phase* interaction leads to an increase in the intensity of the negative charge between two nuclei, lowering the potential energy. The resulted molecular orbital in such a way is called bonding orbital. In contrast, *out-of-phase* interaction causes a decrease in the intensity of the negative charge, destabilizing the bond between atoms and consequently being labeled as antibonding orbital.

At the equilibrium inter-atomic distance R , two paired electrons of H_2 occupy the bonding orbital with a closed-shell low-spin singlet ($S = 0$). When the bond length is further increased, the chemical bond becomes weaker. The dissociation limit of H_2 corresponds to a diradical with two unpaired electrons localized at each atom (Fig. 1). In this case, the singlet (**S**: spin-antiparallel) and triplet (**T**: spin-parallel) states are nearly degenerate. Different from such a “pure” diradical with

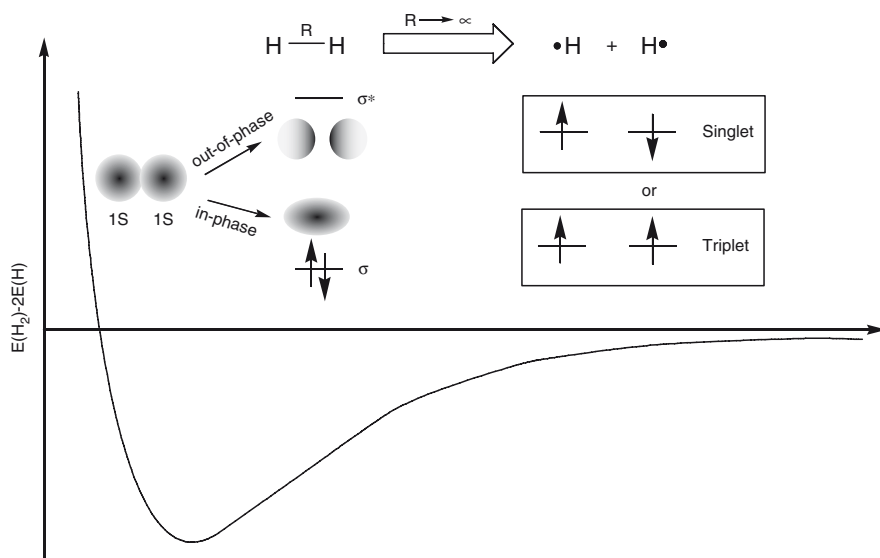
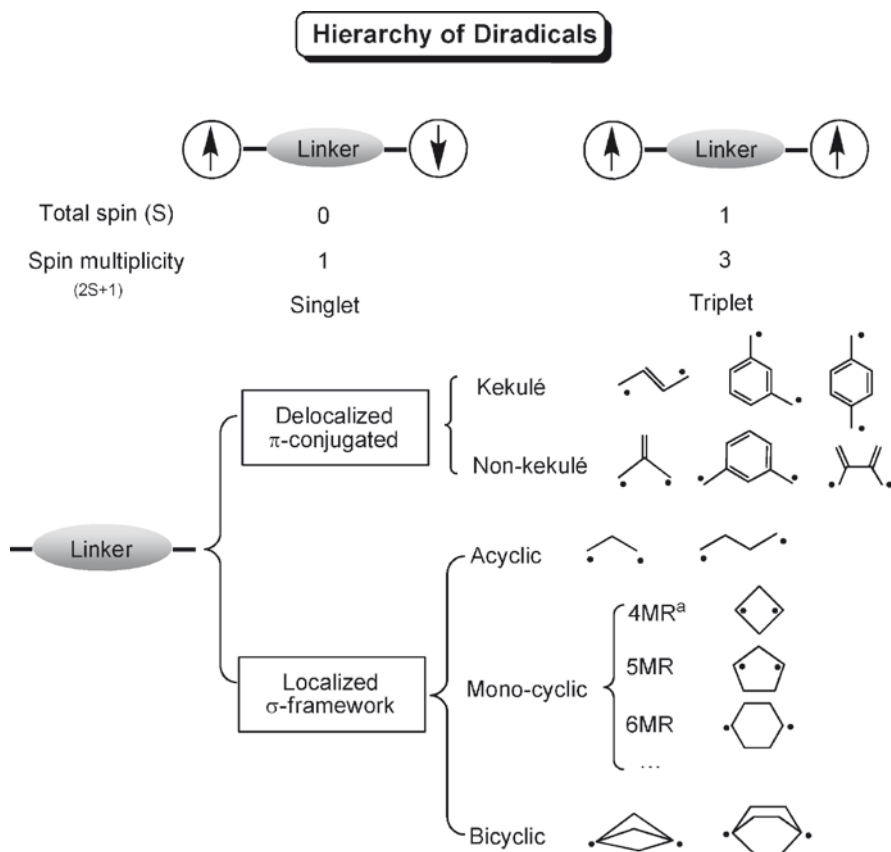


Fig. 1 A schematic illustration of the in-phase and out-of-phase combinations of the atomic orbitals into the bonding and antibonding molecular orbitals, respectively. The dissociation limit of a H₂ molecule corresponds to a “pure” diradical with degenerate singlet and triplet states

100% unpaired spin density confined to each radical site, real diradicals with weak coupling between the radical centers through various types of linkers (as shown in Fig. 2) are named “biradicaloids” [34, 35]. Their ground states can be either singlet (with $S = 0$) or triplet ($S = 1$). The diversity of “spacers” makes the diradical chemistry versatile. Different linkers (π -conjugated vs σ -localized), different topology (acyclic vs cyclic), and various substituents (electron-donating or -withdrawing) of diradicals have been applied to fine tune the spin multiplicity of ground states.

2.2 Target Questions for Diradicals

What are fundamental questions about the interplay between the electronic structures and thermodynamic/kinetic stabilities of diradicals? Borden et al. [36] has already mentioned some. Here, Fig. 3 illustrates two issues of main concern in this review: (1) which is a ground state, singlet or triplet, and (2) whether it is easy or not for a diradical to undergo ring closure. Following our chemical intuitions, we got used to thinking of these two questions from through-bond and through-space interactions, respectively. The competition between the singlet and triplet ground states is dominated by the nature of through-bond interactions, mediated by the π -



^a4MR represents four-membered ring in this review.

Fig. 2 A hierarchy of diradicals

or σ -bridges between two radical centers. Thus, the energy gap between the lowest singlet and triplet states, $\Delta E_{S-T} = E_S - E_T$, is applied to describe the spin preference of ground state. When $\Delta E_{S-T} < 0$, a singlet ground state is favored, and if $\Delta E_{S-T} > 0$, the ground state is predicted to be triplet. The through-space interaction between reactive radical centers leads to facile occurrence of ring-closure reactions, in which the activation energy (E_a) and the energy difference between the diradical and its σ -bonded isomer ($\Delta E_{S-S'} = E_S - E_{S'}$) are key factors for describing the kinetic and thermodynamic stabilities of a diradical, respectively. In the following subsections, we will apply the orbital phase theory to answer the above questions for diradicals of interest.

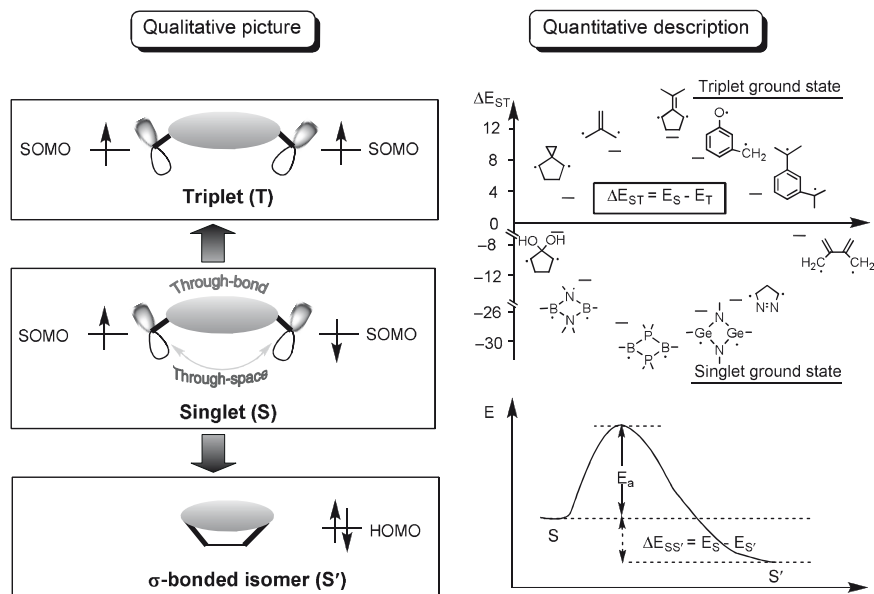


Fig. 3 A schematic illustration of through-bond and through-space interactions between the radical centers. The singlet–triplet energy gap, ΔE_{S-T} , the activation energy (E_a), and the energy difference between the singlet diradical and its σ -bonded isomer, $\Delta E_{S,S'}$ are key parameters for evaluating the spin preference of a diradical, and the kinetic and thermodynamic stabilities against the ring closure in the singlet

3 Orbital Phase Design of Diradicals

3.1 A General Model of Diradicals

The hierarchy of diradicals, as displayed in Fig. 2, shows various types of open-shell systems, for which a systematic classification might be desired. Usually they are classified into two types, delocalized and localized diradicals, depending on the linkage between the radical centers, a π -conjugated unit or σ -framework. Here, according to the dominating mode involved in orbital interactions, we generally divide a variety of diradicals into σ -type and π -type interactions, shown in Fig. 4. It should be mentioned that the assignment of σ -type or π -type diradicals is judged by the type of radical orbitals and hence the nature of orbital interactions between the radical and “linker” orbitals.

The well-established prototypes of 1,3-diradicals, trimethylenemethane (TMM, **1**) and trimethylene (TM, **2**) are selected to illustrate our idea. The diradical is assumed to have two singly occupied orbitals, p and q, of nearly the same energy on two radical centers (P and Q in Fig. 4). As addressed in Sect. 2, it is possible for

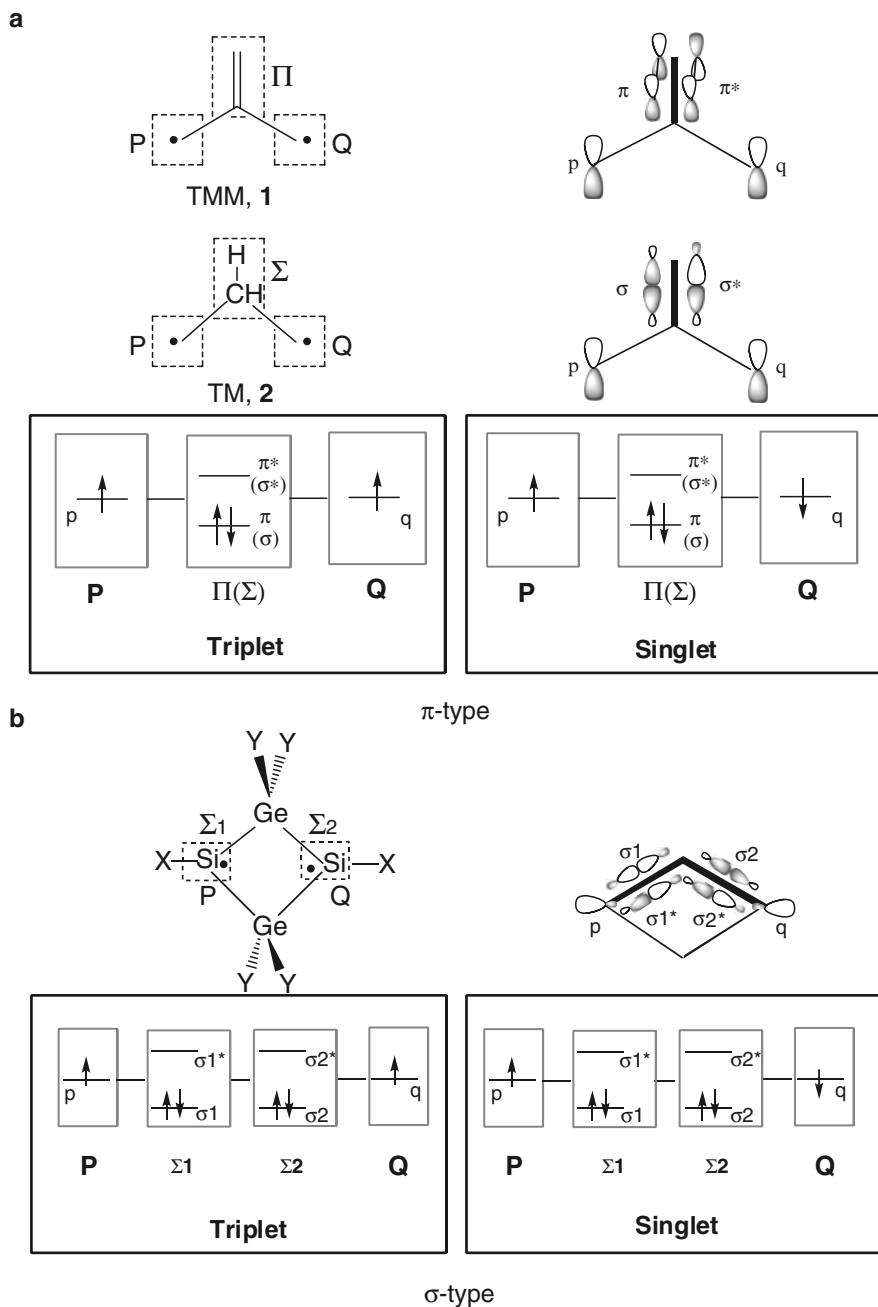


Fig. 4a, b General models for (a) π -type and (b) σ -type diradicals, in which the radical orbitals are mainly of the p-character and sp^n hybrid, respectively

the unpaired electrons of diradicals to interact with each other through the bonds or through space. Let us first consider the through-bond interaction.

If the radical orbitals are mainly of the p -character (e.g., a p -orbital of carbon in TMM), they interact with each other through the π bond, labeled Π (Fig. 4a). This kind of π -conjugated diradicals with p -type radical orbitals is classified as the π -type diradicals. Interestingly, in the language of orbital phase theory, the simplest 1,3-localized diradical, TM (2) also belongs to the π -type family provided its radical orbitals are dominated by the p -character. The only difference between the TMM (Fig. 4a, left) and TM (Fig. 4a, right) lies in the fact that the radical orbitals of TM interact with each other through the σ bond (labeled Σ) instead of the π bond in TMM.

What is the σ -type diradical? Take a cyclic 1,3-diradical, with a four-membered-ring (4MR) structure as an example, the σ -type radical orbitals interact with each other through the intervening chain of the σ bonds, Σ_1 and Σ_2 (Fig. 4b). The cyclic interaction occurs among the radical orbitals, p and q , σ_1 and σ_2 , and σ_1^* and σ_2^* orbitals.

3.2 Cyclic Orbital Interactions in Diradicals

A closer look is then taken at the involved orbitals. Bonding π (or σ) orbitals are doubly occupied, and the antibonding π^* (or σ^*) orbitals are vacant. As is well known, the doubly occupied bonding orbitals can play a role as an electron-donor, and the empty antibonding orbitals are electron-acceptors. In the triplet state, the orbitals, p and q , are singly occupied by α -spin electrons; whereas in the singlet state, an α -spin electron occupies one of p and q , and a β -spin electron occupies the other (Fig. 4a). So, the singly occupied radical orbital has dual roles, donating an electron to the vacant antibonding orbital or accepting one electron from the bonding orbital. Such a situation is called the ground configuration, G, as shown in Fig. 5a.

The delocalization of excessive α - (or β -) spins and the bond polarization can take place among radical orbitals, p and q , and the central π (or σ) and π^* (or σ^*) orbitals, resulting in the electron transferred configurations (T) and locally excited configurations (E), respectively (Fig. 5a). The delocalization-polarization mechanisms are different between singlet and triplet states, as addressed in the following subsections.

3.2.1 Triplet State

When one α -spin electron in p shifts to vacant π^* (or σ^*) through the interaction of the ground configuration 3G with the transferred configuration 3T_1 , the electron delocalization from the radical center to the middle π (or σ) bond takes place by the mixing of the transferred configuration. This configuration interaction is approximated by the p - π^* (p - σ^*) orbital interaction. The resulting hole in the radical orbital p is then supplemented by another α -spin electron from the bonding π (σ) orbital via an interaction between the transferred configuration, 3T_1 , and the locally

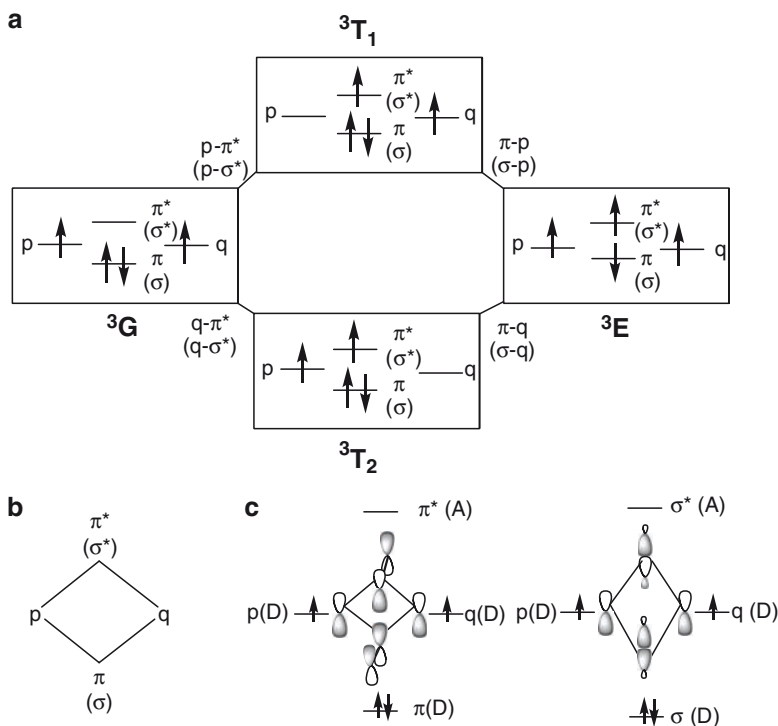


Fig. 5a–c Through-bond interactions in the triplet state of 1,3-diradical. **a** Mechanism of electron delocalization and polarization of α -spin electrons. **b** Cyclic orbital interaction. **c** Orbital phase continuity

excited configuration, 3E , which is approximated by the π - p (σ - p) interaction. The mixing of the excited configuration polarizes the central π (σ) bond. In short, 3G - 3T_1 - 3E or π - p - π^* (σ - p - σ^*) interaction is involved in the electron delocalization-polarization process between radical centers and the π (σ) bond. The similar delocalization-polarization process through another radical orbital q contains the 3G - 3T_2 - 3E or π - q - π^* (σ - q - σ^*) interaction. Consequently, the cyclic 3G - 3T_1 - 3E - 3T_2 - configuration (Fig. 5a) or $-\pi$ - p - π^* - q - ($-\sigma$ - p - σ^* - q -) orbital interaction (Fig. 5b) occurs in the triplet state.

3.2.2 Singlet State

The delocalization-polarization mechanism in the singlet state is more complicated than that in triplet. Similar to the triplet state, there also exists a cyclic 1G - 1T_1 - 1E - 1T_2 - configuration or $-\pi$ - p - π^* - q - ($-\sigma$ - p - σ^* - q -) orbital interaction in the singlet (Fig. 6). In the singlet state, however, the radical orbital q is an electron-accepting orbital (A) for the α -spin electron (rather than the donating orbital in triplet). Thus, there is an additional path of α -spin electron delocalization, 1G - 1T_1 - 1T_3 - 1T_2 - or

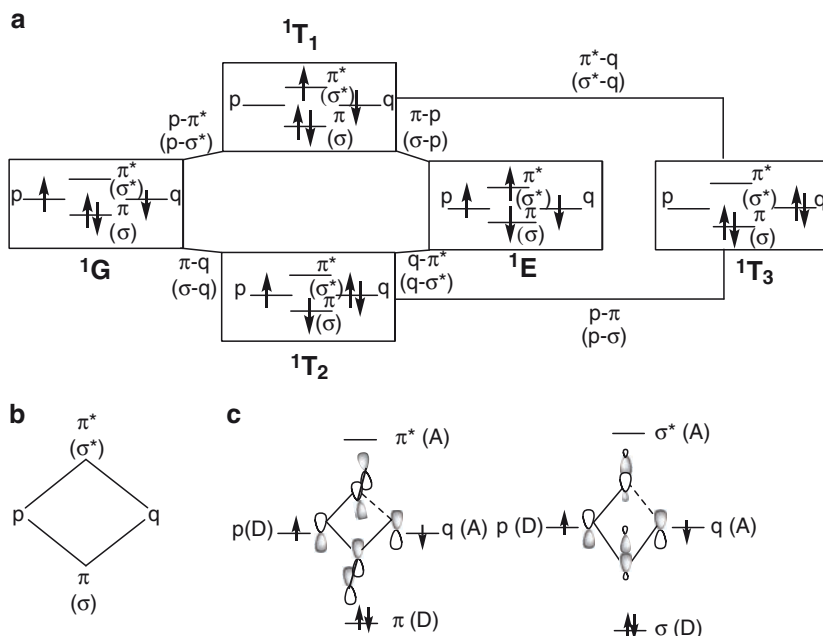


Fig. 6a–c Through-bond interactions in the singlet state of 1,3-diradical. **a** Mechanism of electron delocalization and polarization of α -spin electrons. **b** Cyclic orbital interaction. **c** Orbital phase discontinuity (denoted by the *dotted lines*)

$-p-\pi^*-q-\pi-$ ($-p-\sigma^*-q-\sigma-$) in the singlet state. A similar delocalization-polarization mechanism also exists for the β -spin in the singlet state. Throughout this chapter, we will address only those processes for the α -spins for conciseness.

3.3 Orbital Phase Continuity Conditions

As mentioned above, the cyclic interaction occurs among the radical orbitals, p and q , π (or σ), and π^* (or σ^*) orbitals in both singlet and triplet states. The orbital phase is a crucial factor in promoting the cyclic orbital interaction. Recalling the important role of phase relationship between the atomic orbitals in forming an energetically favorable bonding molecular orbital (Fig. 1), there are also some rules of phase relationship for the favorable orbital interaction in stabilizing the diradical systems. The orbital phase requirements for an effective occurrence of the cyclic configuration interaction have been derived from electron distribution [28, 29] as the sign of the product of the overlap integrals between the configurations involved in the above-mentioned delocalization-polarization processes. This is the same as that obtained from the perturbation energy [15–17]. Here, we briefly describe the derivation of the orbital phase continuity conditions by using an example of four electrons in four orbitals.

Triplet state. The spin eigenfunctions of the triplet state, with M_s (z -component of the total spin) = 1, are written as [29]

$$\begin{aligned} {}^3G &= \frac{1}{\sqrt{4!}} |\pi\bar{\pi}\rho q| \\ {}^3T_1 &= \frac{1}{\sqrt{4!}} |\pi\bar{\pi}\pi * q| \\ {}^3T_2 &= \frac{1}{\sqrt{4!}} |\pi\bar{\pi} p\pi *| \\ {}^3E &= x({}^3E_1) + y({}^3E_2) + z({}^3E_3), \end{aligned} \quad (1)$$

where

$$\begin{aligned} {}^3E_1 &= \frac{1}{2\sqrt{4!}} (|\bar{\pi}\pi * p q| + |\pi\bar{\pi} * p q| - |\pi\pi * \bar{p} q| - |\pi\pi * p\bar{q}|) + \dots \\ {}^3E_2 &= \frac{1}{2\sqrt{4!}} (|\bar{\pi}\pi * p q| - |\pi\bar{\pi} * p q| + |\pi\pi * \bar{p} q| - |\pi\pi * p\bar{q}|) + \dots \\ {}^3E_3 &= \frac{1}{2\sqrt{4!}} (|\bar{\pi}\pi * p q| - |\pi\bar{\pi} * p q| - |\pi\pi * \bar{p} q| + |\pi\pi * p\bar{q}|) + \dots \\ x^2 + y^2 + z^2 &= 1. \end{aligned} \quad (2)$$

The effective cyclic configuration interaction is required for an enhancement of the delocalization-polarization processes via different radical centers. The requirement is satisfied when any pair of the configuration interactions simultaneously contributes to stabilization or to accumulation of electron density in the overlap region. The condition is given by the overlap integrals, S , between the configurations (3G , 3T_1 , 3E_1 , and 3T_2) involved in the proposed delocalization-polarization processes (Fig. 5). Therefore, an effective cyclic configuration interaction needs

$$S({}^3G, {}^3T_1)S({}^3T_1, {}^3E_1)S({}^3E_1, {}^3T_2)S({}^3T_2, {}^3G) > 0 \quad (3)$$

The configuration overlaps, S , are approximately represented by the orbital overlaps, s , if the higher-order terms are neglected [29]:

$$\begin{aligned} S({}^3G, {}^3T_1) &\approx s(p, \pi^*) \\ S({}^3T_1, {}^3E_1) &\approx s(p, \pi) \\ S({}^3T_1, {}^3E_2) &\approx 0 \\ S({}^3T_1, {}^3E_3) &\approx s(p, \pi) \\ S({}^3E_1, {}^3T_2) &\approx s(q, \pi) \\ S({}^3T_2, {}^3T_2) &\approx s(q, \pi) \\ S({}^3E_3, {}^3T_2) &\approx 0 \\ S({}^3T_2, {}^3G) &\approx s(q, \pi^*) \end{aligned} \quad (4)$$

The product of the overlap integrals of the cyclically interacting configurations, 3G , 3T_1 , 3E_1 , and 3T_2 is then approximately expressed as

$$S({}^3G, {}^3T_1)S({}^3T_1, {}^3E_1)S({}^3E_1, {}^3T_2)S({}^3T_2, {}^3G) \approx s(p, \pi^*)s(\pi^*, q)s(q, \pi)s(\pi, p) \quad (5)$$

The configurations 3E_2 and 3E_3 do not participate in any cyclic interactions, since $S({}^3T_1, {}^3E_2) = 0$ and $S({}^3E_3, {}^3T_2) = 0$.

Thus, the requirement in (3) can be rewritten as

$$s(p, \pi^*)s(\pi^*, q)s(q, \pi)s(\pi, p) > 0 \quad (6)$$

The same inequality is derived for the triplet states with $M_S = 0, -1$.

Let us translate the inequality (6) into a more direct way that closely relates to the interacting orbitals. For convenience, the electron-donating orbitals are denoted by D, while the accepting orbitals are denoted by A. The effective occurrence of the cyclic orbital interactions requires the simultaneous satisfaction of the following conditions [15–17]: (1) the electron-donating orbitals (denoted by D–D) are out of phase; (2) the accepting orbitals (denoted by A–A) are in phase; and (3) the donating and accepting orbitals (D–A) are in phase. Figure 7 illustrates all these orbital phase continuity conditions. If the orbital phase relationship of interacting orbitals can meet these requirements simultaneously, the orbital phase is continuous, implying that the delocalization takes place effectively. The system is hence stabilized.

Let us return to the phase relationship of a triplet state. Both of the radical orbitals, p and q , are donating (D) orbitals for α -spin electrons. The bonding π and antibonding π^* orbitals are electron-donating (D) and -accepting (A), respectively. If all the continuity conditions are satisfied in a triplet state, i.e., D–A in phase: $s(p, \pi^*) > 0$

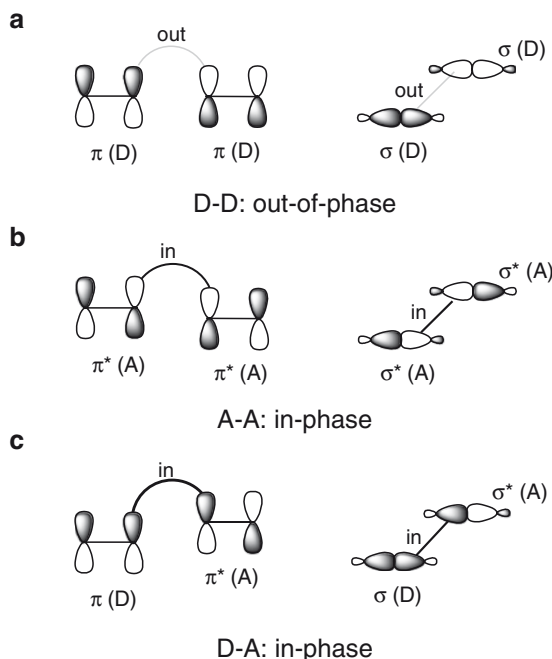


Fig. 7a–c Phase continuity requirements. **a** Electron-donating orbitals (denoted by D–D) are out of phase. **b** Accepting orbitals (denoted by A–A) are in phase. **c** Donating and accepting orbitals (D–A) are in phase

and $s(\pi^*, q) > 0$; D-D out of phase: $s(\pi, p) < 0$ and $s(q, \pi) < 0$, the inequality (6) is also satisfied. In other words, both delocalization and polarization can effectively occur, provided that the conditions are satisfied. Such a case is called the continuous orbital phase. Otherwise, we will say that the orbital phase is discontinuous.

Single state. Similarly, the singlet state can be represented as [29]

$$\begin{aligned} {}^1G &= \frac{1}{\sqrt{2 \cdot 4!}} (|\pi\bar{\pi}p\bar{q}\rangle - |\pi\bar{\pi}\bar{p}q\rangle) \cdots \\ {}^1T_1 &= \frac{1}{\sqrt{2 \cdot 4!}} (|\pi\bar{\pi}\pi^* \bar{q}\rangle - |\pi\bar{\pi}\pi^* q\rangle) \cdots \\ {}^1T_2 &= \frac{1}{\sqrt{2 \cdot 4!}} (|\pi\bar{\pi} p\bar{\pi}^*\rangle - |\pi\bar{\pi} \bar{p}\pi^*\rangle) \cdots \\ {}^1E &= x({}^1E_1) + y({}^1E_2), \end{aligned} \quad (7)$$

where

$$\begin{aligned} {}^1E_1 &= \frac{1}{2\sqrt{4!}} (|\pi\bar{\pi}^* pq\rangle + |\pi\bar{\pi}^* \bar{p}\bar{q}\rangle - |\bar{\pi}\pi^* \bar{p}q\rangle - |\bar{\pi}\pi^* p\bar{q}\rangle) + \cdots \\ {}^1E_2 &= \frac{1}{\sqrt{12 \cdot 4!}} (|\pi\bar{\pi}^* pq\rangle + |\pi\bar{\pi}^* \bar{p}\bar{q}\rangle + |\bar{\pi}\pi^* \bar{p}q\rangle + \\ &|\bar{\pi}\pi^* p\bar{q}\rangle - 2|\bar{\pi}\pi^* \bar{p}\bar{q}\rangle - 2|\pi\bar{\pi}^* \bar{p}q\rangle) + \cdots \\ &x^2 + y^2 = 1. \end{aligned} \quad (8)$$

The overlap integrals of the configurations (S) are approximately related to the orbital overlaps, s , i.e. [29]

$$\begin{aligned} S({}^1G, {}^1T_1) &\approx s(p, \pi^*) \\ S({}^1T_1, {}^1E_1) &\approx -\frac{1}{\sqrt{2}} s(p, \pi) \\ S({}^1T_1, {}^1E_2) &\approx -\sqrt{\frac{3}{2}} s(p, \pi) \\ S({}^1E_1, {}^1T_2) &\approx \sqrt{2} s(q, \pi) \\ S({}^1E_2, {}^1T_2) &\approx 0 \\ S({}^1T_2, {}^1G) &\approx s(q, \pi^*). \end{aligned} \quad (9)$$

We obtain a non-zero product of the cyclically interacting configurations:

$$S({}^1G, {}^1T_1)S({}^1T_1, {}^1E_1)S({}^1E_1, {}^1T_2)S({}^1T_2, {}^1G) \approx (-1)s(p, \pi^*)s(\pi^*, q)s(q, \pi)s(\pi, p). \quad (10)$$

The orbital overlaps involved are the same as those in the equation for the triplet state (5), while the sign is opposite. This gives the following inequality [29]:

$$(-1)s(p, \pi^*)s(\pi^*, q)s(q, \pi)s(\pi, p) > 0 \quad (11)$$

It is interesting that the sign of the left side of inequality (11) is opposite to that of inequality (6) for the triplet state. That means the phase continuity properties of the singlet and triplet states of a given diradical are opposite to each other. It should be

mentioned that, differing from the same role of two radical orbitals as electron-donating in the triplet, one radical orbital (say, p) is an electron-donating orbital and the other (q) is accepting in the singlet state. So, in this case, when all the continuity conditions are satisfied, i.e., D–A in phase: $s(p, \pi^*) > 0$ and $s(q, \pi) > 0$; A–A in phase: $s(\pi^*, q) > 0$; D–D out of phase: $s(\pi, p) < 0$, the inequality (11) is held.

3.4 Orbital Phase Properties of Diradicals

3.4.1 Through-Bond Interaction

As mentioned above, the unpaired electrons of diradicals may interact with each other through bonds. The orbital phase relationships between the involved orbitals control the effectiveness of the cyclic orbital interactions underlying the through-bond coupling.

Orbital phase continuity in triplet state. The orbital phase properties are depicted in Fig. 5c. For the triplet, the radical orbitals, p and q , and bonding π (σ) orbital are donating orbitals (labeled by D in Fig. 5c) for α -spin electrons, while the antibonding π^* (σ^*) orbital (marked by A) is electron-accepting. It can be seen from Fig. 5c that the electron-donating (D) radical orbitals, p and q , can be in phase with the accepting π^* (σ^*) orbital (A), and out of phase with the donating orbital, π/σ (D) at the same time for the triplet state. So the orbital phase is continuous, and the triplet state of 1,3-diradical (e.g., TMM and TM) is stabilized by the effective cyclic orbital interactions [29, 31].

Orbital phase discontinuity in singlet state. In contrast to the triplet state, orbital phase continuity conditions cannot be satisfied simultaneously (denoted by the dashed line in Fig. 6c) in the singlet. Thus, the singlet 1,3-diradical suffers from the orbital phase discontinuity. According to the orbital phase properties, the triplet states of TMM (1) and TM (2) were predicted to be more stable than their singlet states by the orbital phase theory [29, 31].

Singlet σ -type diradical. Figure 8 shows the phase relationship between the electron donating and accepting orbitals in a σ -type diradical (Scheme 4b). It can be seen that the cyclic $-p-\sigma_1^*-\sigma_2^*-q-\sigma_2-\sigma_1-$ orbital interaction satisfies the continuity requirements in the singlet state (Fig. 8): the neighboring orbitals in $p(\text{D})-\sigma_1^*(\text{A})-\sigma_2^*(\text{A})-q(\text{A})-\sigma_2(\text{D})$ are all in phase while those in the sequence $p(\text{D})-\sigma_1(\text{D})-\sigma_2(\text{D})$ are all out of phase. The phase is continuous for the cyclic interaction.

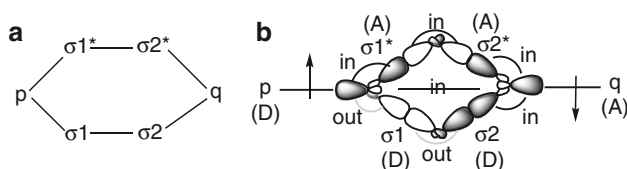


Fig. 8a, b The cyclic orbital interaction (a) and orbital phase continuity (b) in the singlet state of σ -type 1,3-diradical

Moreover, the radical orbitals, $p(D)$ and $q(A)$ are in phase. The direct through-space interaction between the radical centers, i.e., the $p\dots q$ interaction, thermodynamically stabilizes the singlet 1,3-diradicals in addition to the cyclic orbital interactions through the bonds. However, the through-space interaction can also stabilize the transition states of the bond formation between the radical centers and kinetically destabilize the diradicals (which will be discussed in Sect. 3.4.2).

3.4.2 Through-Space Interaction

In the singlet state of π -type 1,3-diradical (e.g., TM, **2**), there may also exist the through-space interaction between radical centers, i.e., $p\dots q$ interaction (Fig. 9), in addition to the previously addressed cyclic $-p-\sigma^*-q-\sigma-$ orbital interactions (Fig. 6). The through-space interaction is indispensable for the bond formation between the radical centers. The corresponding delocalization of the α -spin electron is shown in Fig. 9a. Clearly, the involvement of the through-space $p\dots q$ interaction gives rise to two cyclic orbital interactions, $-p-\sigma^*-q-$ and $-p-\sigma-q-$. From Fig. 9, one can find that the cyclic $-p-\sigma^*-q-$ orbital interaction can satisfy the phase continuity requirements: for the α -spin electron the electron-donating radical orbital, $p(D)$ can

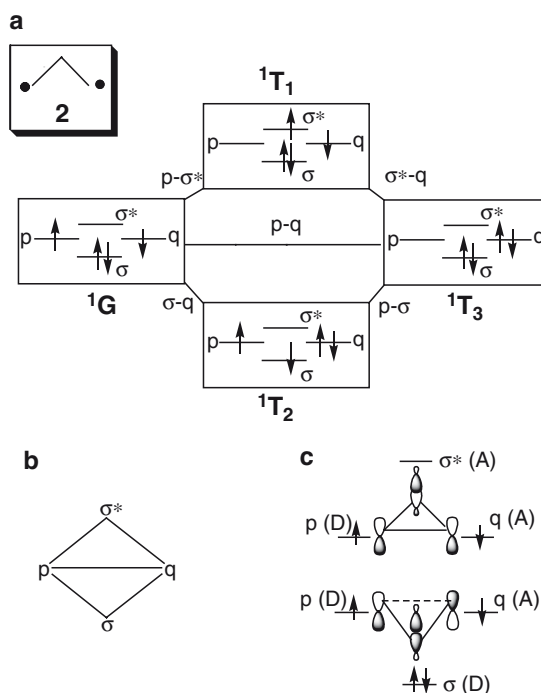


Fig. 9a–c Through-space interactions in the singlet state of π -type 1,3-diradical. **a** Mechanism of electron delocalization of α -spin electrons. **b** Cyclic orbital interactions. **c** Orbital phase properties

simultaneously be in phase with the σ^* antibonding orbital (A) and the other accepting radical orbital, q (A), which are in phase with each other. The tendency of ring closure through the p...q interaction is thus promoted by the effective cyclic $-p-\sigma^*-q-$ orbital interaction. The other cyclic orbital interaction, $-p-\sigma-q-$, does not obey the phase continuity requirements, since the electron-donating radical orbital, p (D) cannot be out of phase with the σ bonding orbital (D) and in phase with the other radical orbital, q (A) at the same time for the α -spin, while σ (D) and q (A) are in phase with each other.

The cyclic orbital interaction of p and q with σ^* or with σ can significantly occur at the transition state of the ring closure of 1,3-diradicals. The continuous orbital phase for the cyclic orbital interaction with σ^* implies effective stabilization of the transition states when the σ bonds are electron acceptors.

To summarize, the properties of triplet and singlet diradicals are closely related to the effectiveness of through-bond and through-space interactions, which are governed by the orbital phase continuity/discontinuity properties. In the next two sections, we will utilize this simple model to predict the spin preference and intramolecular reactivity for a broad range of diradicals.

4 π -Conjugated Diradicals

4.1 *Kekulé vs Non-Kekulé Diradicals: Typical Examples*

The π -conjugated diradicals have been classified into two classes, Kekulé and non-Kekulé diradicals [29]. Among them, 2-methylidenepropane-1,3-diyl (also called TMM, **1**) and 2-butene-1,4-diyl diradical (**3**), are the simplest examples of these two groups, respectively. Although TMM (**1**) is fully conjugated, each of its Kekulé structures has at least two non- π -bonded atoms. Such a kind of diradicals is termed the “non-Kekulé” system. In contrast, we can write out the standard Kekulé structure with the alternating double and single bonds in **3**, so it is called Kekulé diradical. Here, we will show the difference in their orbital phase properties.

As shown in Fig. 10, the triplet state of TMM (**1**) is stabilized by the phase continuity, while its Kekulé-type isomer **3** suffers from the phase discontinuity in the triplet. Consequently, the triplet state of **1** is thermodynamically more stable than **2**. This is in good agreement with the computational results that the total energy of triplet TMM (**1**) is lower than that of its isomer **3** (MCSCF(4,4)/STO-3g: 15.3 kcal mol⁻¹; PPP model: 13.3 kcal mol⁻¹) [29, 37–39]. The phase continuity properties of the singlet and triplet states of a given diradical are opposite each other. So, the singlet TMM is phase discontinuous, but the singlet state of **3** is favored by the phase continuity. The PPP results supported the orbital phase predictions: the singlet state of **3** (the ground state of butadiene) is much lower in energy than that of **1** [29, 38, 39]. The singlet diradical of **1** is an excited state destabilized by the phase continuity [29]. The orbital phase theory is indeed a topological

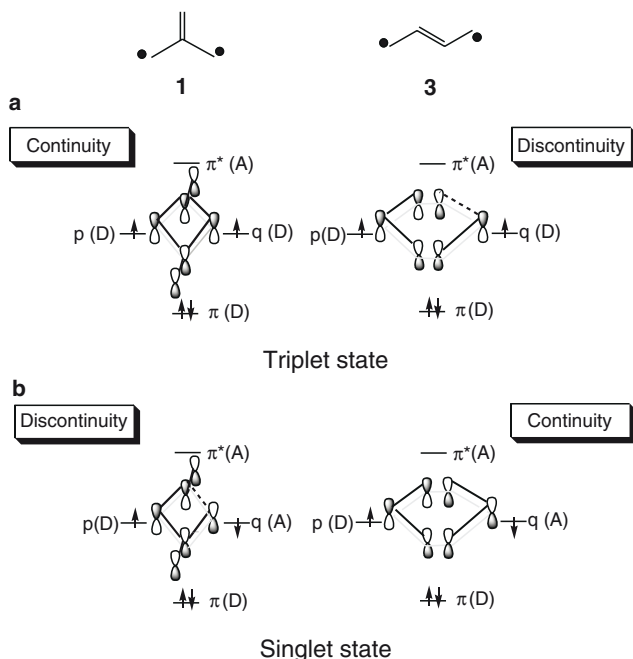


Fig. 10a, b The orbital phase properties of the cross (**1**) and linear (**3**) conjugated 1,3-diradicals for (a) triplet and (b) singlet states

method: the phase properties of diradicals **1** and **3** are essentially the same as those of dianion and dication counterparts of **1** and **3** [40]. The radical cation of TMM displays radical-type reactivity, which distinguishes it from 1,3-butadiene radical cation [41]. This can be explained in terms of the orbital phase discontinuity in TMM radical cation and the continuity in radical cation of **3** for the delocalization between the cation and radical centers.

For higher homologues, four isomeric C_6H_8 diradicals **4–7** with different topological structures were investigated using the orbital phase theory [29]. Figure 11 describes the orbital phase properties of C_6H_8 isomers. Since the phase continuity/discontinuity properties of the singlet states are just the opposite of the triplets, we only depict the orbital phase relationship of the triplet (with α -spins) in the following figures in this section. In comparison with the simplest π -conjugated diradicals **1** and **3**, a little more complicated cyclic six-orbital interaction is involved in **4**, **5**, and **7**. Among these isomers, only the triplet state of isomer **5** is favored by the phase-continuity (Fig. 11). The phase discontinuity makes the triplet straight isomer **4** be less stable than the branched diradical **5**. Interestingly, diradical **6** shares the same substructure and hence the same topology of the four-orbital interaction with diradical **3**, so that the phase of triplet isomer **6** is also discontinuous. These orbital phase predictions are supported by theoretical calculations at various levels, as shown in Table 1 (where a comprehensive comparison with available experiments and other calculations is made for the selected π -conjugated diradicals).

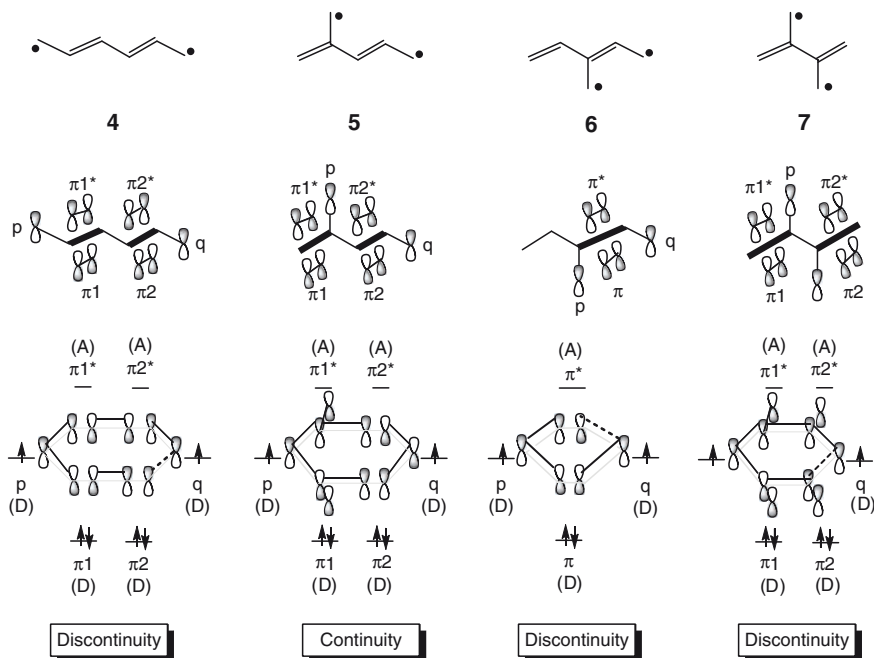


Fig. 11 The phase properties of the triplet states of C_6H_8 isomers

Table 1 Spin preference of ground state and the calculated singlet–triplet energy separation ΔE_{S-T} of some selected π -conjugated diradicals

Species	Spin preference		ΔE_{ST} (kcal mol ⁻¹)		References
	Theory ^a	Exptl.	Calc.		
1	T	T [42–44, 135–139]	16.1 ± 0.1 (exptl. by photoelectron spectra)	[140, 141]	
			16.1 (CASPT2N(10,10)/ccpvtz)	[142]	
			21.1 (MCSCF(4,4)/sto-3g)	[29]	
			9.30 (UCCSD(T)/6-31G)	[48]	
			16.5 (AM1/CI)	[49, 50]	
3	S	–	11.1 (INDO/S-CI)	[51]	
			–73.9 (PPP-CI)	[37]	
4	S	–	–54.5 (UB3LYP/6-31G(d,p))	this work	
			–61.3 (PPP-CI)	[37]	
5	T	–	12.7 (MCSCF(6,6)/STO-3g)	[29]	
			11.5 (PPP-CI)	[37]	
			7.23 (UB3LYP/6-31G(d,p))	this work	
6	S	–	–43.11 (UB3LYP/6-31G(d,p))	this work	
7	S	T, or degenerate S and T, [52–54]	–3.0 ± 0.3 (exptl. by photoelectron spectra)	[55]	
			–1.49 (UCCSD(T)/6-31G)	[48]	
			–0.89 (CAS(6,6)/6-31 + G [*])	[56]	
			0.1 (SD-CI/TZ2P//CAS(6,6)/3-21G)	[57, 58]	
			–3.1 (MCSCF(6,6)/sto-3g)	[29]	

(continued)

Table 1 (continued)

Species	Spin preference		ΔE_{ST} (kcal mol ⁻¹)		References
	Theory ^a	Exptl.	Calc.		
8	T	–	1.6 (B3LYP/6-311G**, non-planar)	[59]	
			–5.3 (AM1/CI)	[49, 50]	
			–0.6 (INDO/S-CI)	[51]	
			8.8 (PPP-CI)	[37]	
9	T	T	1.0 (AM1/CI)	[50]	
			8.9 (AM1/CI)	[118]	
			4.9 (MCSCF(8,8)/6-31G*)	[143]	
			3.4 (AM1/CI)	[118]	
10	T	T [144–148]	5.3 (PPP-CI)	[37]	
			2.5 (VB)	[73, 74, 119]	
			18.2 (MR- σ -S, π -SD CI)	[64]	
			23.6 (ab initio/CI)	[78]	
11	T	T [42–47, 139]	23.2 (AM1/CI)	[50]	
			20.7 (PPP-SCI)	[79]	
12	S	–	10.9 (UCCSD(T)/4-31G)	[48]	
13	T	T [149, 150]	–21.4 (PPP-CI)	[37]	
			–28.3 (UB3LYP/6-31G*)	this work	
14	S	–	9.6 \pm 0.2 (exptl. by photoelectron spectra)	[149]	
			13.8 (EOM-SF-CCSD/6-31G*)	[151]	
			13.4 (UCCSD/6-31G*)	[152]	
			13.2 (UB3LYP/6-31G*)	[152]	
			10.5 (MCSCF(6,6)/sto-3g)	[29]	
15	S	T [62, 63] degenerate S and T [60, 61]	–22.4 (PPP-CI)	[37]	
			–20.1 (UB3LYP/6-31G*)	this work	
16	T	–	–0.84 (UCCSD(T)/4-31G)	[48]	
			5.8 (AM1/CI)	[50]	
17	S	–	3.9 (UB3LYP/6-31G*)	this work	
			–0.7 (AM1/CI)	[49]	
			–2.0 (MCSCF(6,6)/sto-3g)	[29]	
18	T	–	–1.2 (UB3LYP/6-31G*)	this work	
			4.4 (CAS- π MCSCF)	[153]	
			1.6 (MR-SDQ CI)	[153]	
19	T	T [144–148]	5.5 (AM1/CI)	[50]	
			7.7 (MR- σ -S, π -SD CI)	[64]	
20	S	–	–20.7 (MR- σ -S, π -SD CI)	[64]	
			–22.8 (PPP-CI)	[154]	

^aPredicted by orbital phase theory

4.2 Extension to Cyclic π -Conjugated Diradicals

The preceding orbital phase predictions of some topological units (like **1**, **4–6**) can be easily extended to more complex cyclic diradicals [29], as shown in Fig. 12. On the basis of TMM sub-structure (**1**), diradicals **8–11** are predicted to be phase continuous in their triplet states. Such a triplet preference in their ground states is in agreement with calculation results and available experiments, as listed in Table

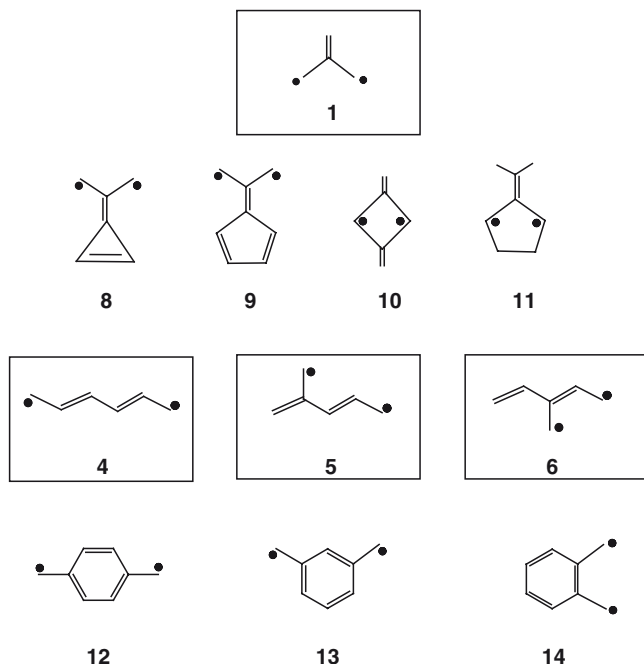


Fig. 12 The extension of some topological units into the more complex cyclic π -conjugated diradicals

1. Among those TMM-based triplet diradicals, the Berson-type TMM (**11**) was found to have longer lifetime than the parent TMM [42–47], probably due to the reluctance in ring-closure within the framework of the five-membered ring (as discussed in Sect. 5.2). Another typical set of π -conjugated diradicals are phenylenebis-methylenes (**12**–**14**). The *p*- (**12**), *m*- (**13**), and *o*- (**14**) isomers contain the acyclic subunits of **4**, **5**, and **6**, respectively. In analogy with the orbital phase properties of **4**–**6**, the triplet state of *m*-isomer **13** stands out from this family with a continuous cyclic six-orbital phase relationship [29]. So the triplet **13** is more stable than the other two isomers, in consistence with the calculation results [37].

Among the non-Kekulé diradicals, tetramethyleneethane (TME, **7**) has evoked lasting attention during the last two decades due to the controversy over its spin preference in the ground state between experiments and theoretical predictions [48–59]. Now TME is known to be a slightly favored singlet diradical with a negligible S–T gap (cf. references collected in Table 1). This correlates well with a disfavored cyclic six-orbital interaction by the phase discontinuity in the triplet state of **7** [29] (shown in Fig. 11). In addition, TME is an important topological unit which appears frequently in many non-Kekulé diradicals (as exemplified by **15**–**17** in Fig. 13).

Like TME, the diradical **15** was shown to have nearly degenerate singlet and triplet states by magnetic susceptibility [60, 61], although the early works by Dowd identified a triplet ground state on the basis of ESR spectrum [62, 63]. The UCCSD(T) calculations predicted a singlet ground state with a small S–T gap of

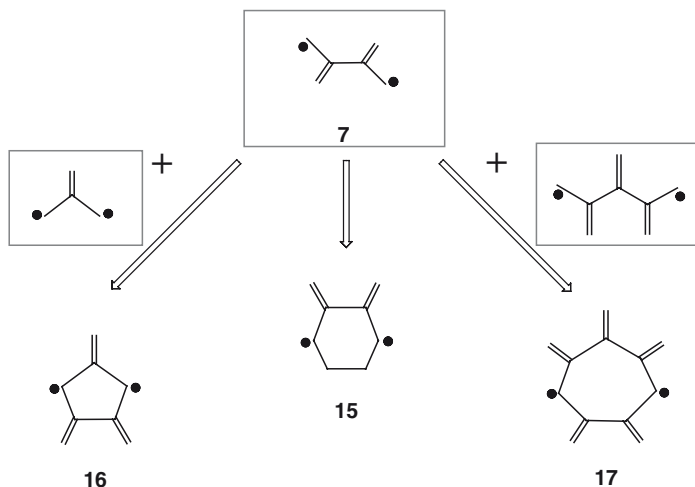


Fig. 13 Selected cyclic π -conjugated diradicals on the basis of tetramethylethane (TME) unit

$-0.85 \text{ kcal mol}^{-1}$ [48], which can also be rationalized by the unfavorable phase properties in the triplet of **15**.

What will happen when the phase-discontinuity triplet TME-substructure is combined with the phase-continuity TMM-unit? The diradical **16** is one of such multi-subunit systems. Which is the dominant substructure, TMM or TME? It was suggested that the four-orbital phase continuity in **1** is more effective than the six-orbital discontinuous one in **7** [29]. Thus, the ground state of **16** is predicted to be triplet, in agreement with calculation results in Table 1. Diradical **17** also consists of two substructures, TME and its longer homologues, in favor of the six-orbital continuous singlet and eight-orbital continuity in triplet, respectively. Since the phase continuity in the singlet TME is more effective than the eight-orbital interaction in the triplet state, the ground state of **17** is predicted to be a singlet. This orbital phase prediction is supported by the calculation results (Table 1).

4.3 Hetero-Atom Effects

The introduction of heteroatoms into the hydrocarbon diradicals is a frequently applied strategy to tune the spin preference and relative stabilities of diradicals. The heteroatoms may change the energies of donor or acceptor orbitals, and consequently affect the donor-acceptor interaction involved in the cyclic orbital interaction. Take 2-oxopropane-1,3-diyl, or so-called oxyallyl (OXA, **18**) as an example [29]. It is a hetero analog of TMM, as shown in Fig. 14. The replacement of CH_2 with oxygen in the central Π unit leads to a decrease in energies of π and π^* orbitals. This may enhance the orbital interaction through one path (denoted by bold lines) and weaken that via the other (denoted by wavy lines) relative to the continuous cyclic orbital interaction in the parent species **1** (Fig. 14). As a result, the $p-\pi^*-q$

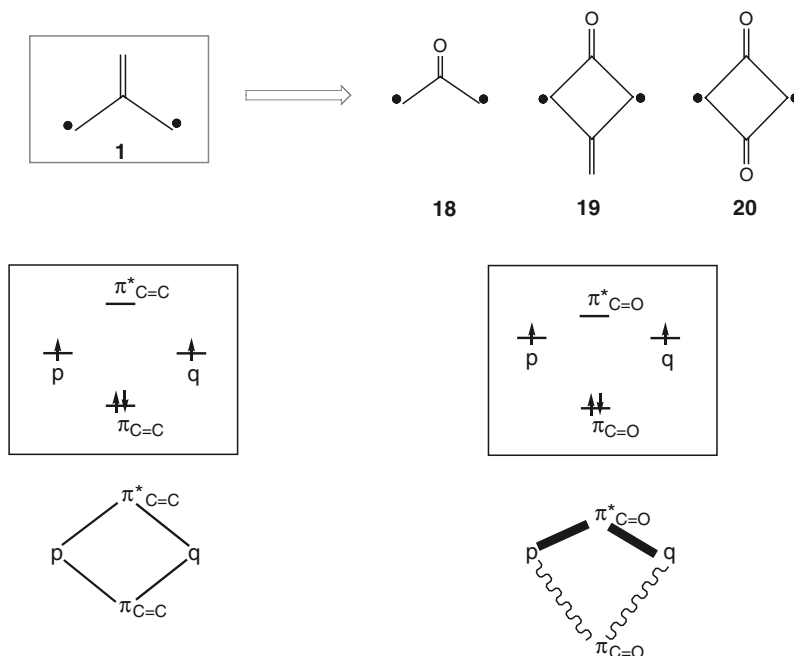


Fig. 14 The heteroatom-containing 1,3-diradicals, where the triplet stabilization is depressed by the strengthening of $p-\pi^*-q$ (denoted by *bold lines*) and weakening of $p-\pi-q$ (wavy lines) interaction path

interaction is more effective than the $p-\pi-q$ one in **18**. The degree of the phase discontinuity in the singlet state and the continuity in the triplet state are lowered [Chapter “An Orbital Phase Theory” in this volume]. The singlet–triplet energy gap of **18** should be smaller than that of **1**. Calculation results (in Table 1) indicate that the S–T gap of TMM (**1**) is nearly four times that of OXA (**18**).

Such an orbital phase picture in Fig. 14 is also applicable to rationalize the relative S–T gaps of hetero diradicals **19** and **20**. In comparison with their parent system, 1,3-dimethylenecyclobutadiene (DMCBD, **10**), the introduction of oxygen atoms does destabilize the triplet state. The calculated energy gap between singlet and triplet states, ΔE_{ST} decreases in the order **10** (18.2 kcal mol⁻¹) > **19** (7.7 kcal mol⁻¹) > **20** (-20.7 kcal mol⁻¹) [64]. These results supported the orbital phase predictions.

4.4 Comparison with Other Topological Models

The classification into Kekulé and non-Kekulé diradicals is mainly based on the difference in their resonance structures. From the proceeding discussions, however, such a classification does not closely relate to the relative stabilities and spin preference of π -conjugated diradicals. For example, some non-Kekulé diradicals, such as **1** and **8**, prefer a triplet ground state, but some others (like **7**) have a singlet ground

state. Some simple rules have been proposed to predict the ground-state spin. Here, we make comparison with some typical models.

It is well known that Hund's rule is applicable to atoms, but hardly so to the exchange coupling between two singly occupied molecular orbitals (SOMOs) of a diradical with small overlap integrals. Several MO-based approaches were then developed. Diradicals were featured by a pair of non-bonding molecular orbitals (NBMOs), which are occupied by two electrons [65–67]. Within the framework of Hückel MO approximation, the relationship between the number of NBMOs, N_{NBMO} , and the number of starred (n) and unstarred (n^*) atoms in the alternate hydrocarbon systems was established as $N_{\text{NBMO}} = n^* - n$. Longuet-Higgins gave a simple way to predict the ground-state spin multiplicity, $2S + 1$, which equals $N_{\text{tot}} - 2T + 1$ (where N_{tot} and T represent the total number of π -sites and the maximum number of double bonds in resonance structures, respectively). As a result, the ground state of a Kekulé diradical is predicted to be a singlet ($S = 0$). For the non-Kekulé or non-alternate diradicals, some modifications have been made [68–70]. In contrast to these models that rely on the counting of N_{NBMO} , Borden and Davidson gave predictions on the basis of the localizability of NBMO [71]. According to whether the Hückel NBMOs can be confined to disjoint sets of atoms, the π -conjugated diradicals were classified into two types. If the NBMOs can span separately on π -sites, the singlet state may be favored over the triplet; if, in contrast, the NBMOs cannot be localized to a disjoint group of atoms, the triplet is predicted to be ground state.

An alternative stream came from the valence bond (VB) theory. Ovchinnikov judged the ground-state spin for the alternant diradicals by half the difference between the number of starred and unstarred π -sites, i.e., $S = (n^* - n)/2$ [72]. It is the simplest way to predict the spin preference of ground states just on the basis of the molecular graph theory, and in many cases its results are parallel to those obtained from the NBMO analysis and from the sophisticated MO or DFT (density functional theory) calculations. However, this simple VB rule cannot be applied to the non-alternate diradicals. The exact solutions of semi-empirical VB, Hubbard, and PPP models shed light on the nature of spin correlation [37, 73–77].

As addressed in many articles, each of those MO- and VB-based models has its own merits and limitations [50, 64, 71, 75–80]. Keeping these in mind and conceiving the importance of the odd-chain unit in ferromagnetic interaction, Radhakrishnan suggested some simple rules according to odd/even in the length of shortest coupling path [49, 50].

Encouragingly, the orbital phase predictions on ground-state spin of the alternant hydrocarbon diradicals, **1**, **5**, **7**, and **13**, are in agreement with those proposed by Borden and Davidson [64, 71, 78–80], by Ovchinnikov [72], and by Radhakrishnan [49, 50]. For the non-alternant systems and hetero-derivatives, **16–20**, the orbital phase theory performs as well as the Radhakrishnan's rule [49, 50].

Despite the success of these simple rules in the π -conjugated diradicals, most of them cannot be directly applied to the localized diradicals within the σ -framework. In Sect. 5, we will demonstrate that the orbital phase theory works effectively for the localized 1,3- and 1,4-diradicals as well.

5 Localized Diradicals

Within the framework of the orbital phase theory, the topology and continuity/discontinuity of orbital phase interactions govern the relative stability and spin preference of a diradical, no matter whether it is a π -conjugated system or a localized diradical. Being stimulated by the successful application of this theory in π -conjugated diradicals, we further explored the role of the orbital phase in understanding the properties (such as spin preference, relative thermodynamic and kinetic stabilities) of localized radicals. As mentioned in Sect. 3.1, some localized diradicals (e.g., **2**) follow the same orbital phase rules as those for their π -conjugated counterparts (like **1**) if the radical orbitals are of p -character (Fig. 4). Another good example is the orbital phase control of relative stability of the crossed (**21**) vs linear (**22**) triplet E_4H_8 ($E = C, Si, Ge, Sn$) diradicals [30], as illustrated in Fig. 15. In comparison with their π -conjugated analogues, **1** and **3** (shown in Fig. 10), the branched and linear E_4H_8 isomers (where the radical centers are connected with saturated E–E bonds) take the same orbital phase properties in triplet states: continuity in the cross-conjugation (**21**) and discontinuity in the linear one (**22**), respectively. Thus, the branched triplet diradicals are predicted to be more stable than the linear isomers. This has been confirmed by MP2 and DFT calculations. Confidence was hence gained to design some novel localized singlet 1,3-diradicals, with acyclic or cyclic geometry.

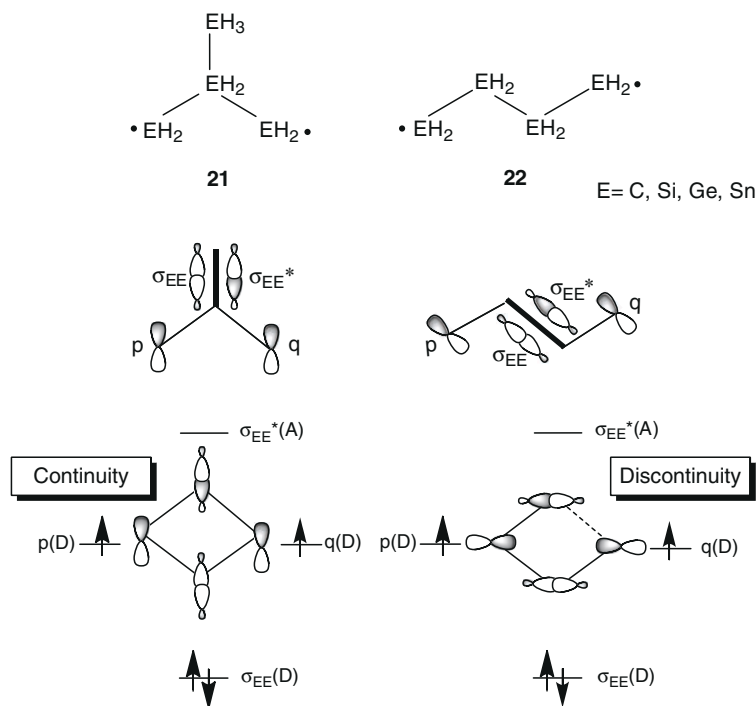


Fig. 15 The orbital phase control of relative stability of triplet E_4H_8 ($E = C, Si, Ge, Sn$) diradicals

5.1 Acyclic 1,3-Diradicals: Modulation of S–T Gaps by Substituents

In recent years, both experimental [7, 8, 81–105] and theoretical [96, 98–117] interests in localized 1,3-diradicals have grown rapidly. Detections of the localized diradicals, especially for the singlet states, are extremely difficult due to their higher reactivities and short lifetimes [81–85]. The orbital phase theory (Figs. 4–6, and 9) as well as several theoretical calculations [106, 107] predicted a triplet ground state for the simplest localized 1,3-diradical, trimethylene (TM, **2**) and indicated little or no barrier to ring closure in the singlet state. The exploration of the persistent, localized singlet 1,3-diradicals is the focus of theoretical and experimental works.

Theoretical designs of stable 1,3-diradical are necessary prior to experiments. In contrast with the foregoing topological rules that have been developed for understanding the ground spin states and stabilities of π -conjugated diradicals [36, 49, 50, 64, 71–74, 78–80, 118, 119], simple theories for the localized diradicals are rare. Here, we employ the orbital phase theory to predict the substitution effects on spin preferences, S–T energy gaps, and kinetic stabilities of the localized 1,3-diradicals. Several factors such as substitution effects and the ring strain drawn from experience and intuition are helpful to guide the future exploration of some new singlet 1,3-diradicals. Substitution influences (both electronic and steric) on the ground-state multiplicity and lifetime of a diradical have evoked intensive works [83, 96, 108–111, 115]. In this subsection, we emphasize the tuning of the S–T gaps by changing substituents on both the geminal (or bridge) position and radical centers (Fig. 16).

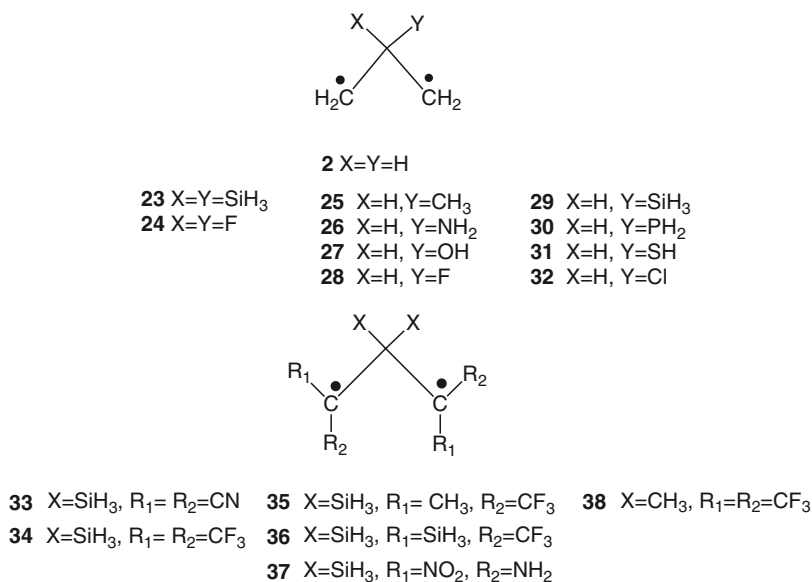


Fig. 16 Acyclic 1,3-diradicals

5.1.1 Substituent Effects on Conformations and S–T Gaps

In addition to the orbital phase, the relative energy between the electron-donating and accepting orbitals is another important factor for the effective cyclic orbital interaction. Energies of σ and σ^* orbitals are changed by substituents (X or Y) at the C_2 . Replacement of C–H bonds by strongly electron-donating groups X raises the energy of σ_{C-X} orbital (Fig. 17a). The increase in the energy of σ_{C-X} strengthens interactions of radical center orbitals, p and q (shown by bold lines in Fig. 17a), rendering more effective $p-\sigma_{C-X}-q$ interaction than the $p-\sigma_{C-X}^*-q$ one. However, the balance between these two through-bond interactions is important for the effective cyclic orbital interaction. Upon substitution with electron-donating groups, the phase discontinuity in the singlet state is mitigated by the more effective $p-\sigma_{C-X}-q$ interaction, so that the singlet diradicals gain some stabilization. This contributes to a decrease in ΔE_{ST} or even to a reversion of the spin preference. Strongly electron-accepting substituents will lower σ_{C-X}^* , leading to the much stronger $p-\sigma_{C-X}^*-q$ interaction than the $p-\sigma_{C-X}-q$ interaction (Fig. 17b). The singlet stabilization also occurs in this case, contributing to a reduction of ΔE_{ST} or even a singlet preference. On the other hand, the triplet stabilization is related to the polarization of the C–X bonds, i.e., the $\sigma_{C-X}-p-\sigma_{C-X}^*$ and $\sigma_{C-X}-q-\sigma_{C-X}^*$ interactions. The energy gap between σ_{C-X} and σ_{C-X}^* is important for evaluating the polarizability of a C–X bond. Thus, the triplet states are stabilized by the bond polarizability or with the decrease in the $\sigma_{C-X}-\sigma_{C-X}^*$ energy gap. To test these orbital phase predictions, TM (**2**) and its geminally disubstituted diradicals with silyl and fluoro groups (**23** and **24**, respectively) and monosubstituted derivatives **25–32** are selected to probe the substitution influence.

Relative to the “rigid” π -conjugated systems, the localized diradicals are complicated by various possible conformations due to low barriers in rotations of σ bonds.

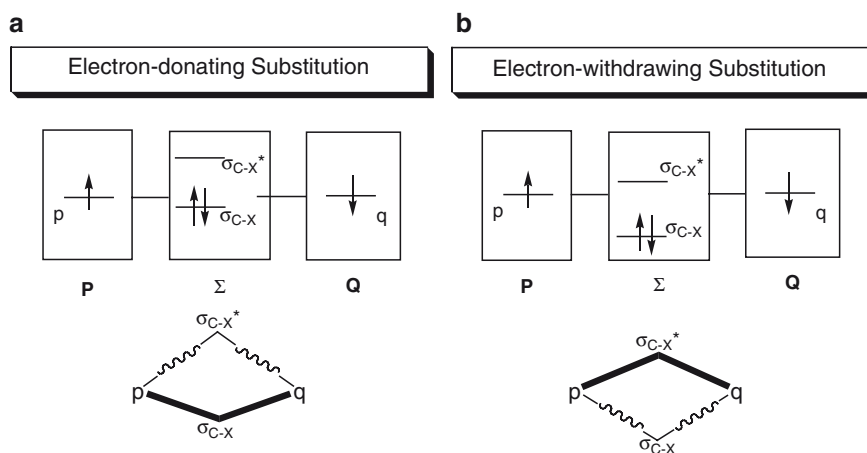


Fig. 17a, b Substituent effects on the cyclic orbital interactions: the (a) $p-\sigma_{C-X}-q$ and (b) $p-\sigma_{C-X}^*-q$ interactions are strengthened (shown by *bold lines*) by the electron-donating and -withdrawing substituents, respectively

The (6,6)CASSCF and (2,2)CASPT2N calculations of TM (**2**) indicated that both the singlet and triplet states prefer conrotatory conformers (**b** in Fig. 18) [31, 110], where the terminal methylene groups are rotated in a conrotatory manner out of the plane defined by the three carbon atoms. Since radical centers interact with different C–H bonds, there is no cyclic orbital interaction. The more favored conrotatory conformation of the singlet state is in agreement with the orbital phase discontinuity for the cyclic orbital interaction in the disrotatory conformers. The similar conformation of the triplet suggests that energies of σ and σ^* of C–H bonds are too low and high, respectively, to polarize the C–H bonds. Primary stabilization in the triplet comes from the interaction between the pair of p (q) and σ^* orbitals; there are thus no effects of cyclic orbital interaction on the preference of the singlet and triplet

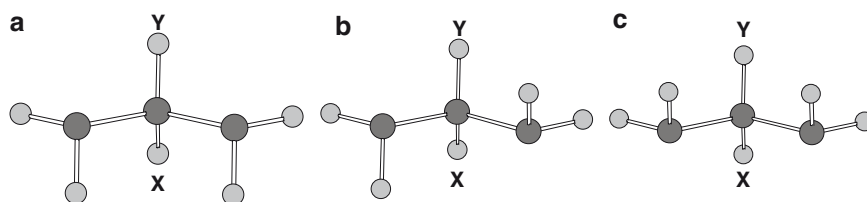


Fig. 18 Typical conformations of acyclic localized 1,3-diradicals, including disrotatory conformers **a** and **c**, and conrotatory conformer **b**

Table 2 Energy differences between the lowest singlet and triplet states (ΔE_{S-T}) of the trimethylene-based 1,3-diradicals calculated by (6,6)CASSCF and (6,6)CAS-MP2 methods with the 6-31G* basis sets

Geminal substitutions	Conformer ^a		ΔE_{S-T} (kcal mol ⁻¹)	
	S	T	CASSCF ^b	CAS-MP2 ^b
X = Y = H (2)	b	b	0.90	1.05, 0.7 ^c
<i>Di-substituted TM</i>				
X = Y = SiH ₃ (23)	a	a	-5.09	-11.2, -11.9 ^e , -11.1 ^d
X = Y = F (24)	NL ^e	b	–	–
<i>Mono-substituted TM</i>				
X = H, Y = CH ₃ (25)	b	a	1.45	1.09
X = H, Y = NH ₂ (26)	b	a	1.54	1.81
X = H, Y = OH (27)	a	b	-0.03	-0.44
X = H, Y = F (28)	NL ^f	a	–	–
X = H, Y = SiH ₃ (29)	c	c	-0.88	-10.5
X = H, Y = PH ₂ (30)	b	c	1.83	1.79
X = H, Y = SH (31)	b	c	0.36	5.86
X = H, Y = Cl (32)	NL ^f	c	–	–

^aThe most stable conformations of singlets (S) and triplets (T) are roughly described by **a**, **b**, and **c** (Fig. 18). The disrotatory conformers, **a** and **c**, are identical to each other for TM (**2**) and its disubstituted derivatives **23** and **24**

^bThe 6-311G** results are given in parentheses

^cThe (2,2)CASPT2N results [110]

^dThe (10,10)CASPT2N result [110]

^eNot located as the local minimum

states in **b** conformation. This is confirmed by a very small gap ($\Delta E_{S-T} = 0.7\text{--}1.05$ kcal mol⁻¹ in Table 2) with the singlet lying slightly above the triplet state.

Slightly different from the parent species, **2**, the singlet and triplet states of the 2,2-disubstituted silyl derivative **23** were found to be favorable in a slightly disrotatory conformation (**a** in Fig. 18), where the radical orbitals interact with the same C–Si bond. Such a conformation provides a chance for the cyclic orbital interaction (as depicted in Fig. 5) to occur in **23**. The conformational change in the triplet states from **b** for **2** to **a** for **23** can be understood in terms of the polarizability of C–X bond, as reflected by the energy gap between σ_{C-X} and σ_{C-X}^* . The energy gap is smaller for C–Si (1.22 a.u.) than for C–H (1.45 a.u.), suggesting the C–Si bond is more polarizable than the C–H bond. The disrotatory conformation allows **23** to gain the stabilization from the phase continuity of the cyclic orbital interaction in the triplet state. On the other hand, the disrotatory conformation **a** of the singlet state may be ascribed to the strong donating capability of silyl groups in **23**. The high σ_{C-Si} energy strengthens the $p\text{--}\sigma_{C-Si}\text{--}q$ interaction relative to the $p\text{--}\sigma_{C-Si}^*\text{--}q$ interaction (c.f. Fig. 17a). The effect of the acyclic $p\text{--}\sigma_{C-Si}\text{--}q$ interaction free from the phase requirements is predominant over that of the unfavorable phase for the cyclic $p\text{--}\sigma_{C-Si}\text{--}q\text{--}\sigma_{C-Si}^*\text{--}$ interaction. Thus the singlet state may be stabilized by the acyclic $p\text{--}\sigma_{C-Si}\text{--}q$ interaction. In fact, the results of calculation of 2,2-disilyl substituted TM, **23** by others and our own show that the singlet ground state is favored (Table 2). In addition, the separation between the terminal carbon atoms (2.570 Å by CASSCF) in the singlet of **23** is longer than that of the parent **2** by 0.052 Å and is about 68% longer than the typical C–C single bond (1.530 Å).

The most stable conformations of the mono-substituted 1,3-diradicals exhibit interesting trends. Most of the singlet conformers of the substituted 1,3-diradicals have conrotatory conformations, **b**, where the cyclic orbital interaction is not effective. In the disrotatory conformers, **a** and **c**, two radical centers are in conjugation with C–X (X = H) and C–Y (Y = CH₃, NH₂, OH, F, SiH₃, PH₂, SH, Cl) bonds, respectively, so that the cyclic orbital interactions in these conformations are disfavored by the orbital phase discontinuity in singlets. An exception is a disrotatory conformation **a** for **27** with an electron-withdrawing substituent, Y = OH. In the conrotatory conformation, at least one of the radical orbitals interacts with a σ_{C-O}^* orbital which is quite low in energy. This may lead finally to the kinetic instability of the conrotatory conformer of **27** (Fig. 9). Otherwise, the σ_{CH}^* energy may be lowered by the inductive effect of the geminal OH group enough to lead to thermodynamic stabilization by the $p\text{--}\sigma_{CH}^*\text{--}q$ interaction (Fig. 17b) but insufficiently for the ring closure. Another exception is a disrotatory conformation **c** for **29** with X = SiH₃. Strong donating group SiH₃ reduces the disadvantage by the phase discontinuity in the disrotatory conformer **c** by enhancing the $p\text{--}\sigma\text{--}q$ path of the cyclic interaction relative to the other part, $p\text{--}\sigma^*\text{--}q$ (cf. Fig. 17a).

Most of the triplet diradicals have disrotatory conformations, in which the cyclic orbital interactions are favored by the phase continuity. 1,3-Diradicals with the second-row substituents, **25–28**, prefer the conformer **a** with the central C–H bond in conjugation (except for the conrotatory conformation **b** in **27**), whereas those substituted by the third-row groups, **29–32** favor the disrotatory conformations **c**

with the C–Y bond in the conjugation. Two radical orbitals prefer to interact with a more polarizable σ bond at C₂ to effectuate the cyclic orbital interaction favored by the phase continuity in the triplet.

The calculated ΔE_{S-T} values (Table 2) consistently show the triplet preference for the mono-substituted TM diradicals though the S–T gap is small and close to that of the parent species **2** (Y = H). However, the ΔE_{S-T} values show slight singlet preference of **27** (Y = OH) and **29** (Y = SiH₃). The singlet states are stabilized by the p– σ_{Csi}^* –q interaction (Fig. 17a) in **29** and probably by the p– σ_{CH}^* –q interaction in **27**, where σ_{CH}^* is lowered in energy by the inductive effect by the geminal OH group (Fig. 17b).

5.1.2 Substituent Effects on Stability

The kinetic stability against the ring closure is also a crucial factor to be considered in the design of persistent localized 1,3-diradicals. As shown in Fig. 9, the transition state for the formation of σ -bonded isomer is stabilized by the continuous orbital phase for the cyclic –p– σ^* –q– orbital interaction. This implies that electron-withdrawing substituents X (e.g., X = F or Cl) at the bridge site kinetically destabilize the singlet 1,3-diradicals and facilitate the ring closure. In fact, all attempts at searching for the singlet 2,2-difluoro-TM (**24**) failed and led to the formation of the σ -bonded isomer, 1,1-difluorocyclopropane. Electron-releasing groups (e.g., X = SiH₃) do not exhibit such kinetic effects due to the discontinuous orbital phase for the cyclic orbital interaction of p and q with σ . These predictions are supported by the sophisticated ab initio calculation results [31, 110].

All the singlet diradicals **23–32** are less stable than their σ -bonded isomers with the corresponding relative energy differences, $\Delta E_{S-S'}$, larger than 40 kcal mol^{–1}. How can we increase the stabilities of singlet diradicals relative to their ring-closure products? To achieve this goal, substituents at the radical centers were employed. Although the singlet preference was not enhanced in comparison with that of 2,2-disilyl-TM (**23**) [31], stabilities of the singlet 1,3-diradicals relative to the cyclopropane isomers were much improved. The 2,2-disilyl-TM (**23**) diradical is 54.0 (51.4) kcal mol^{–1} less stable than 1,1-disilylcyclopropane at the CASSCF(10,10)/6-31G* (CASPT2N(10,10)/6-31G*) level [110]. The instabilities of the singlet diradicals (**33–38**) relative to the cyclopropane isomers are reduced to 14.0, 34.3, 42.4, 37.8, 2.9, and 38.0 kcal mol^{–1}, respectively [31]. In these diradicals, the separations between the unpaired electron centers are enlarged by around 60–69% relative to the corresponding C–C bond lengths in their σ -bonded isomers, indicating diradical characters [120, 121].

All the above-mentioned acyclic 1,3-diradicals are less stable than the σ -bonded isomers. Therefore, in addition to using various substituents, other factors should be further considered in our design of persistent singlet 1,3-diradicals. In Sect. 5.2, ring structure is taken into account. Strain prevents the ring closure in the singlet state. Two linkers between the radical centers multiply the through-bond interactions.

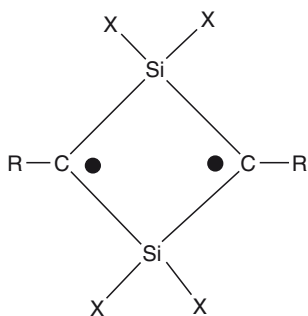
5.2 Monocyclic 1,3-Diradicals: Taking Advantage of Ring Strain

Since the ring strain disfavors the formation of a covalent bond between radical centers, we take the four-membered ring as an alternative motif to design stable localized 1,3-diradicals. The four-membered ring (4MR) not only hinders the formation of the σ -bonded isomer more effectively than larger rings (such as the five- and six-membered rings), but also multiplies the through-bond interactions between the radical centers. It is well recognized that the bonded isomer with bicyclo[1.1.0]butane framework has a higher strain than the three-membered ring. Silicon atoms introduced into the four-membered ring can further enhance the strain effects [122]. So, it is natural to search for the stable singlet diradicals on the basis of 2,4-disilacyclobutane-1,3-diyl (**39**) motif where the saturated carbon atoms are replaced with silicon atoms (Fig. 19).

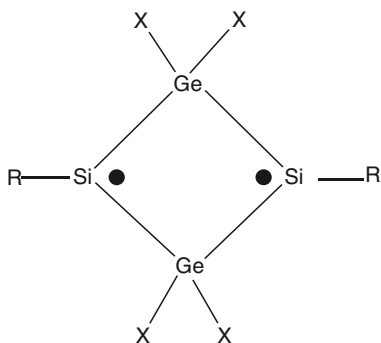
5.2.1 Carbon-Centered Cyclic Diradicals

The lowest singlet of the parent diradical **39** has a long C–C bond (1.664 Å) [31]. We employ the substituents to elongate the C–C bond. Electron-withdrawing groups on the saturated carbon atoms (C₂ and C₄) were previously reported to elongate the C₁–C₃ bond between the bridgeheads in bicyclo[1.1.0]butane [123]. In addition, the electron-withdrawing substituents have been predicted in Sect. 5.1 to stabilize the triplet diradicals to a lesser extent due to the low polarizability of the C–X bonds and the singlet diradicals to a greater extent by the p– σ^* –q interaction (Fig. 17b). Thus, 2,4-disilacyclobutane-1,3-diyls with electron-withdrawing groups on the silicon atoms and electron-donating groups on the radical centers are candidates for stable singlet diradicals. As expected, in the case of CH₃–, NH₂–, OH–, and F–derivatives (**42**–**45**), local energy minima were not located for the σ -bonded isomers but for the singlet diradicals. The four-membered rings are planar for R = NH₂ (**43**), OH (**44**), and F (**45**), and puckered for R = CH₃ (**42**). The non-bonded C...C distance increases in the order of R = CH₃ (2.286 Å) < R = F (2.388 Å) < R = OH (2.448 Å) < R = NH₂ (2.509 Å). The singlet preference increases in the same order, i.e., R = CH₃ ($\Delta E_{s-T} = -14.4$ kcal mol⁻¹) < R = F (-19.1 kcal mol⁻¹) < R = OH (-22.0 kcal mol⁻¹) < R = NH₂ (-24.7 kcal mol⁻¹). These trends are in parallel with the tendency in the π -donating ability of substituents at the radical centers.

It is also interesting to investigate effects of geminal substitutions (X = CH₃, NH₂, OH, and F) on the silicon atoms in 2,4-disilacyclobutane-1,3-diyls with R = F. The non-bonded C...C distances of **45**–**47** increase with the σ -electron withdrawing ability of substituents, which is in agreement with our predictions. The singlet preference is greater for 1,3-diradicals with the stronger withdrawing σ -bonds ($\Delta E_{s-T} = -19.1$ kcal mol⁻¹ for R = F and $\Delta E_{s-T} = -19.6$ kcal mol⁻¹ for R = OH) than that for those with the weaker withdrawing groups ($\Delta E_{s-T} = -16.3$ kcal



- | | |
|-----------------------------------|----------------------------------|
| 39 X=H, R=H | 42 X=F, R=CH ₃ |
| 40 X=H, R=F | 43 X=F, R=NH ₂ |
| 41 X=H, R=SiH ₃ | 44 X=F, R=OH |
| | 45 X=F, R=F |
| 46 X=OH, R=F | |
| 47 X=NH ₂ , R=F | |
| 48 X=CH ₃ , R=F | |



- | | |
|---|------------------------------------|
| 49 X=H, R=H | |
| 50 X=F, R=H | 55 X=CH ₃ , R=H |
| 51 X=F, R=CH ₃ | 56 X=OH, R=H |
| 52 X=F, R=SiH ₃ | 57 X=NH ₂ , R=H |
| 53 X=F, R=C(CH ₃) ₃ | 58 X=SiH ₃ , R=H |
| 54 X=F, R=NH ₂ | |
| 59 X=SiH ₃ , R=CH ₃ | |

Fig. 19 The cyclic 1,3-diradicals

mol⁻¹ for R = CH₃ and $\Delta E_{S-T} = -16.2$ kcal mol⁻¹ for R = NH₂) [31]. This trend supports the predicted substitution effects on S-T gaps.

Stable localized singlet 1,3-diradicals are built on 2,4-disilacyclobutane-1,3-diyls with electron-withdrawing σ -bonds on the silicon atoms and π -electron

donating groups on the carbon atoms (**40**, **42–47**), especially those (**43–46**) of planar geometry. Recently, a five-membered ring version of 2,4-disilacyclobutane-1,3-diyls, 2-metallacyclopentane-1,3-diyls ($M = \text{Si}, \text{Ge}$), were also calculated to have singlet ground states [46].

5.2.2 Silicon-Centered 1,3-Diradicals

Similar to the cyclic carbon-centered 1,3-diradicals (**42–47**), the singlet states of silicon-centered diradicals, $\text{RSi}(\text{GeX}_2)_2\text{SiR}$ ($R = \text{H}, \text{CH}_3, \text{SiH}_3, \text{C}(\text{CH}_3)_3, \text{NH}_2$; $X = \text{H}, \text{CH}_3, \text{OH}, \text{NH}_2, \text{SiH}_3$, **49–59**, shown in Fig. 19b), are predicted to be more stable than the triplet states with appreciable singlet–triplet splittings and the bicyclic σ -bonded isomers, 1,3-disila-2,4-digermabicyclo [1.1.0] butanes. We choose a heavy atom, Ge, to connect the Si radical centers. The Ge atom is larger than the Si atom, keeping the Si radical centers far from each other and reluctant to form a bond. Also, the ring strain of the σ -bonded isomers, the competitors of the singlet diradicals, are increased upon the introduction of Ge atom in the three-membered ring [33].

There exists a difference in the geometries between the carbon- and silicon-centered diradicals. The lowest singlet diradicals **49–59** were found to have *cis*-conformations with the Si–R bonds significantly bent from the four-membered rings (Fig. 20). The radical centers are in conjugation with Si–Ge ring bonds, implying that the singlet states prefer the σ -type diradicals (Fig. 21a) to the π -type diradicals. The lowest triplet states of **50–55**, **58** and **59** have the π -radical centers at both Si atoms, which interact with the Ge–X bonds rather than with the Si–Ge ring bonds. This is in agreement with the orbital phase prediction (Fig. 21b). The exceptions are **56** and **57**, which have the σ -type radical on one Si atom and the π -type radical on the other Si atom. All the lowest triplet states of **49–59** have *trans*-conformations, as expected from the low polarizability of the Ge–X bonds and the partial σ -type diradical character disfavored by the phase discontinuity.

All the designed silicon-centered 1,3-diradicals prefer the four-membered ring structures to the bicyclic σ -bonded isomers, and the singlet states are more stable than the triplet states. The non-bonded distances of **49–59** are considerably longer than the Si–Si bond lengths of known disiliranes (2.27–2.33 Å) [124–127]. The π -electron-donating groups on the silicon radical centers like **54** are candidates for stable singlet diradicals.

To summarize this subsection, the singlet preference is appreciable for 1,3-diradicals containing the four-membered ring. In these monocyclic systems, the four-membered ring functions as an important motif to multiply the through-bond interactions, to destabilize the transition states of the σ -bond formation by the ring strain, and to strain the σ -bonded isomers by the bicyclic geometries. A systematic way is naturally pointing to the bicyclic 1,3-diradicals, which are the topic of the next subsection.

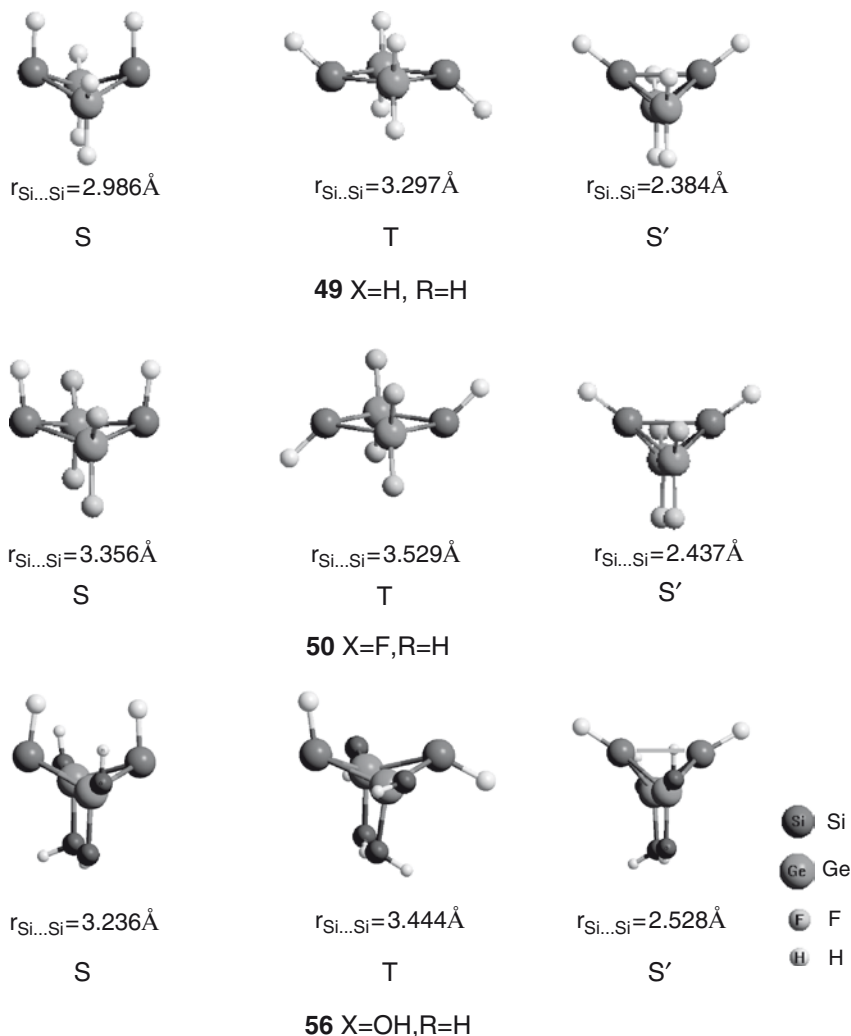


Fig. 20 The optimized geometries of the lowest singlet (S) and triplet (T) states and the σ -bonded isomer (S') for some selected silicon-centered diradicals

5.3 σ -Type Bicyclic Diradicals

As demonstrated above, the most stable singlet silicon-centered monocyclic diradicals are the σ -diradicals where the radicals interact with each other through the Si–Ge bonds, whereas the most stable triplet diradicals are π -diradicals where the radicals interact with each other through the Ge–X bonds. However, for the bicyclic diradicals, **60** and **61**, the conformations are fixed to exclude possibility of π -diradicals (Fig. 22).

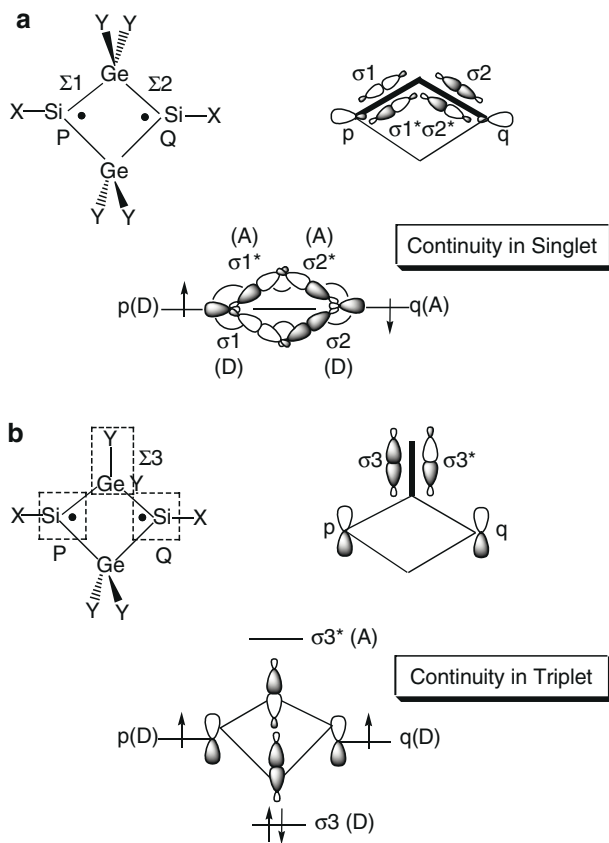


Fig. 21a, b Orbital phase properties on singlet and triplet localized silicon-centered 1,3-diradicals. **a** σ -Type. **b** π -Type

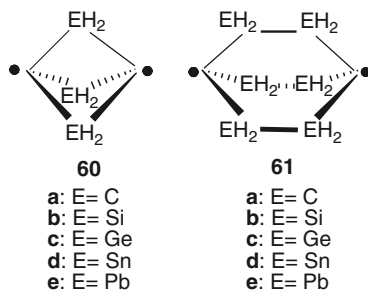


Fig. 22 The bicyclic 1,3- and 1,4-diradicals

As shown in Fig. 23, the radical orbitals interact with each other through σ bond chain, Σ_1 and Σ_2 , in 1,3- σ -diradicals (**60**), while delocalization in 1,4- σ -diradicals (**61**) involves Σ_1 , Σ_2 , and Σ_3 bonds. From the phase properties depicted in Fig. 23,

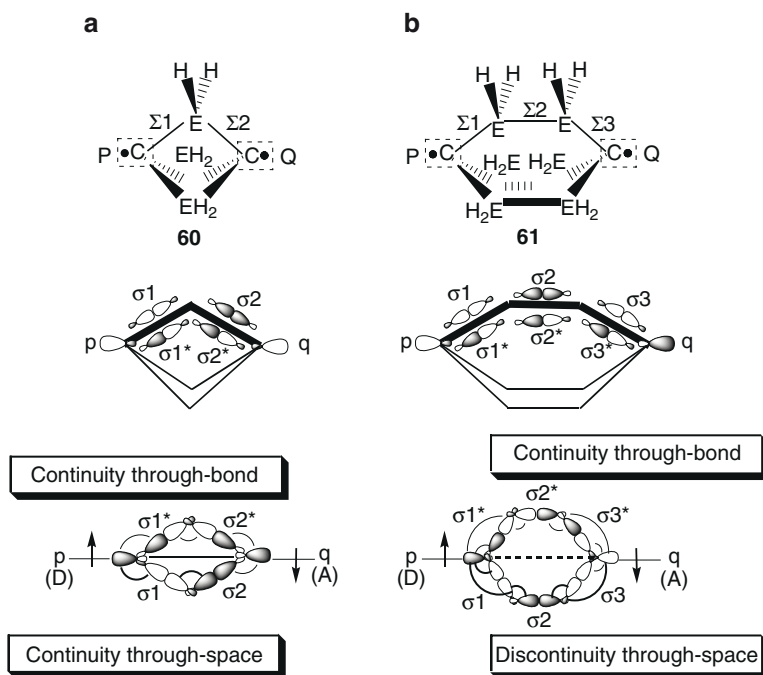


Fig. 23 Orbital phase properties of 1,3- and 1,4-bicyclic singlet diradicals

one can find that cyclic orbital interactions through bonds satisfy the phase continuity requirement in singlet states of **60** and **61** [32]. Thus, 1,3- and 1,4- σ -diradicals were predicted to prefer singlet ground states. However, the through-space interactions between donating p and accepting q orbitals are in-phase (continuity) and out-of-phase (discontinuity) in **60** and **61**, respectively. Thus, the through-space coupling enhances the stability of singlet state of **60** but not that of **61**. Such a difference causes a more outstanding singlet preference in 1,3- σ -diradicals (**60**) than that in 1,4-diradicals (**61**). These predictions were confirmed by our calculations, as addressed below.

5.3.1 1,3- σ -Diradicals

The singlet states of **60** (E = C, Si, Ge, Sn, Pb) have been found to be lower in energy than triplet states [32]. For **60a**, $C(CH_2)_3C$, energy differences of ΔE_{S-T} and $\Delta E_{S-S'}$ are -77.13 and 12.72 kcal mol $^{-1}$, respectively (at the level of UB3LYP/6-31G*). The singlet diradical of **60a** is less stable than its σ -bonded isomer. For other higher congeners **60b–e**, the singlet preference has been revealed by the values of ΔE_{S-T} (**60b**: -55.67 kcal mol $^{-1}$, **60c**: -47.50 kcal mol $^{-1}$, **60d**: -41.78 kcal mol $^{-1}$, **60e**: -40.76 kcal mol $^{-1}$). Most importantly, the σ -bonded isomers were not located for the bicyclic 1,3- σ -diradicals when E = Si, Ge, Sn, or Pb, presumably due to high ring strains in

polycyclic three-membered rings containing heavy group 14 atoms. The bicyclic 1,3- σ -diradicals **60b–e** were promising candidates for singlet diradicals.

5.3.2 1,4- σ -Diradicals

At the level of UB3LYP/6-31G*, we failed to localize the singlet state of $C(C_2H_4)_3C$ (**61a**) except for its σ -bonded isomer. The prediction of less remarkable singlet preference of 1,4- σ -diradicals was confirmed by calculations on **61b–e**. The absolute values of ΔE_{S-T} of 1,4- σ -diradicals were smaller (**61b**: 7.91 kcal mol⁻¹, **61c**: 6.06 kcal mol⁻¹, **61d**: 0.44 kcal mol⁻¹, **61e**: 3.13 kcal mol⁻¹) than those of 1,3- σ -diradicals. Distances between radical centers were elongated by 97.9–164.9% relative to those in the σ -bonded isomers. Different from the 1,3-diradicals, σ -bonded isomers are more stable than singlet 1,4- σ -diradicals by 8.99 kcal mol⁻¹ (**61b**), 14.33 kcal mol⁻¹ (**61c**), 21.49 kcal mol⁻¹ (**61d**), and 31.86 kcal mol⁻¹ (**61e**), respectively. In order to survey kinetic stabilities of singlet diradicals, transition states (TS) in transformations from singlet diradicals to corresponding σ -bonded isomers of **61b–61e** were located at the level of UB3LYP/LANL2DZ, as shown in Fig. 24.

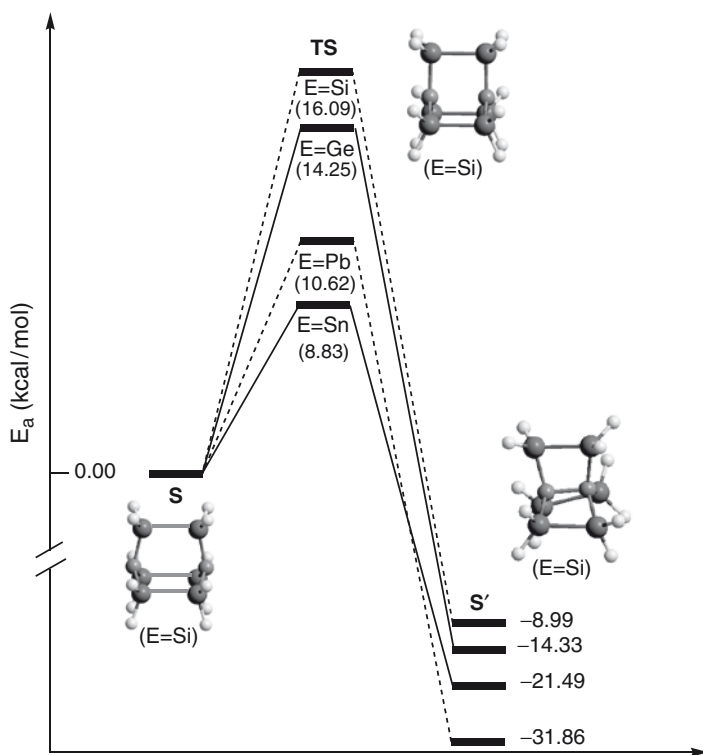


Fig. 24 Reaction barriers for transformations from singlet 1,4-diradicals **61** (E = Si, Ge, Sn, Pb) to their σ -bonded isomers at the level of UB3LYP/LANL2DZ

The activation energies, E_a , were found to be 16.09 (**61b**), 14.25 (**61c**), 8.83 (**61d**), and 10.62 (**61e**) kcal mol⁻¹, respectively. Thus, singlet 1,4-diradicals would be easily transformed to corresponding σ -bonded isomers.

5.4 Comparison with Experiments

Singlet diradicals are usually extremely short-lived intermediates. For example, trimethylene (TM, **2**) was observed to have a fast decay time of 120 fs by femto-second spectroscopy [84, 85]. Since the localized 1,3-cyclopentenediyl diradical (**62**) was characterized by Buchwalter and Closs in 1975 [81, 82], experimental efforts have been made to prepare and characterize the persistent, localized singlet 1,3-diradicals. Some experimental achievements of the localized diradicals are collected in Fig. 25 and Table 3. It should be mentioned that the literature of experimental studies selected here is not exhaustive and more related references can be found in [83–115] and others.

According to the orbital phase theory, the Closs's diradical **62** is predicted to have a triplet ground state due to the same orbital-phase topology as the TM (**2**). In derivatives of **62**, electronic and steric effects of various substituents as well as ring strains in the cyclic diradicals have successfully been applied to modulate the

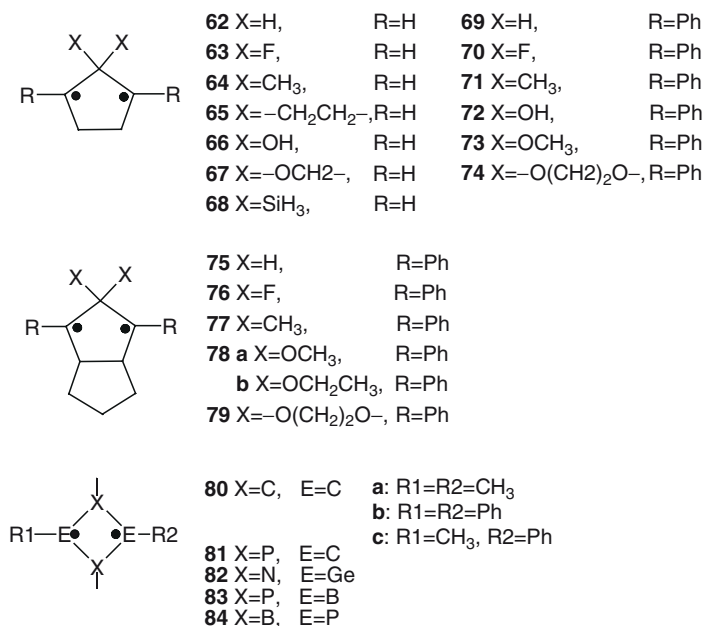


Fig. 25 Some localized 1,3-diradicals observed in experiments

Table 3 A brief collection of some experiments for localized 1,3-diradicals

Species	Experimental observations	References
<i>1,3-Cyclopentadiyl-based diradicals</i>		
62	A triplet ground state was observed by ESR spectrum at 1.3 K, $\tau = 93 \mu\text{s}$ (<i>n</i> -heptane/8 °C)	[14, 81, 82, 87]
63		
64	$\tau < 0.1 \text{ ns}$ (CFCl_3 /-20 °C)	[14, 88]
65	An intermediate in photolysis	[155]
66		
67	An intermediate with a finite lifetime	[91]
68	Generation and reactivity of 2-silylcyclopentane-1,3-diyls were investigated	[128, 129]
69	$\tau = 16 \pm 2 \mu\text{s}$ (20 °C); $\tau = 27 \mu\text{s}$ (acetonitrile/25 °C); $\tau = 30 \mu\text{s}$ (benzene/25 °C)	[14, 87, 130, 156–160]
70	Experimental electronic absorption spectra	[94]
71	$\tau = 1.3 \pm 0.1 \mu\text{s}$ (20 °C);	[87, 156–158]
72		
73	Experimental electronic absorption spectra	[94]
74	Experimental electronic absorption spectra	[94]
75	$\tau = 11.4 \mu\text{s}$ (benzene) 12.0 μs (acetonitrile), with NO_2 -substituted Ph	[89]
76	$\tau = 80 \text{ ns}$ (293 K, in <i>n</i> -pentane), $\lambda = 530 \text{ nm}$	[92, 94]
77	Experimental electronic absorption spectra	[87, 94]
78a	$\tau = 320 \text{ ns}$ (293 K in benzene), up to $\sim 1,050 \text{ ns}$ (dependent on substituents at the para position of phenyl rings)	[93, 96]
78b	$\tau = 880 \text{ ns}$ (293 K in benzene), $\lambda_{\text{max}} = 550 \text{ nm}$	[94, 96]
79	Experimental electronic absorption spectra	[94]
<i>1,3-Cyclobutanediyl-based diradicals</i>		
80a	EPR spectrum triplet ground state observed at very low temperature	[83, 130, 132]
80b	EPR spectrum, electronic absorption spectra	[87, 94]
80c	EPR spectrum, electronic absorption spectra	[87, 94]
81	Singlet diradical was isolated	[99–104, 161]
82	Singlet ground state was characterized by NMR, IR, UV spectroscopy and single-crystal X-ray	[162]
83	Indefinitely stable at room temperature	[98, 133, 163, 164]
84		[134]

spin preference and kinetic stability against the ring closing between the radical centers. The 2,2-difluoro geminal substitution (**63**) and 1,3-diphenyl substituents at radical centers (**69–74**) were frequently utilized in experiments. For example, the transient existence of singlet diradical (**69**: X = H, R = Ph) with a duration of 20 ps was detected, though its ground state prefers a triplet [92]. In addition, generation and reactivity of 2-silylcyclopentane-1,3-diyls (**68**) have been investigated by Abe et al. [128]. These observed fluoro- and silyl-substitution effects on stabilities are in good agreement with the orbital phase predictions (Sects. 5.1 and 5.2).

The 1,3-cyclopentane-diyl (**62**) motif has been further expanded into a bicyclic module containing two fused five-membered rings. The 2,2-disubstituted

1,3-diphenyl-1,3-cyclopentenediyl diradicals (**75–79**, shown in Fig. 25) have longer lifetimes than those 1,3-cyclopentenediyl derivatives. Here, we just mention several examples. The 2,2-difluoro and 2,2-diethoxy derivatives of 1,3-diphenyl-1,3-cyclopentenediyl diradicals have lifetimes of up to microseconds [92–96]. The dimethoxy-substituted diradical prefers a singlet ground state with a 3.73- μ s lifetime in chloroform at room temperature [96]. Recently, regioselective 1,2-migration of **78** was observed by Abe et al., indicating the contribution of hyperconjugation to stabilizing the singlet state [95]. An extremely long-lived singlet 4,4-dimethoxy-3,5-diphenyl-pyrazolidine-3,5-diyl derivative was generated with a lifetime of 9.67 ms at 298 K in toluene [129].

In 1984, Dougherty reported the spectroscopic observation of the triplet 1,3-dimethyl-1,3-cyclobutanediyl (**80a**) for the first time [130]. Soon thereafter, his systematic study on a wealth of substituted 1,3-cyclobutanediyl diradicals indicated that the cyclobutanediyl framework is much more robust for building the localized diradicals than the cyclopentenediyl ones [83]. Within the framework of the four-membered ring, more experimental and theoretical works have shown evidence of long-bond compounds and bond-stretch isomers [99–105, 113–115, 131, 132], which exhibited diradical characters to some extent. Most recently, the biradicaloid form of the 1,2-diphosphinodiboranes (**83**) with a planar PBPB ring structure and sterically demanding substituents has been found to be stable even at room temperature [98]. A variation of the phosphorus and boron substituents was demonstrated to influence the ground-state geometry [133] and S–T gaps [134] of derivatives of **83**.

In reviewing this literature, one can find that the experimental progress of locating novel 1,3-diradicals with desired spin preference and long lifetime cannot be separated from the elegant theoretical works. More encouragingly, all the observed localized 1,3-diradicals with a variety of substituents are in good agreement with our orbital phase predictions, both on spin multiplicity of ground state and kinetic stability relative to ring closure of singlet.

Substantial advances have been made in understanding, preparing, and detecting the carbon-centered delocalized or localized diradicals. But the silicon-centered diradicals are much less explored. Search for other stable localized singlet diradicals remains a goal of experimental and theoretical scientists.

6 Concluding Remarks

In this chapter, the orbital phase theory was applied to develop a theoretical model of diradicals, to predict the substituent effects on the spin preference and S–T gaps, and to design some new 1,3-diradicals.

On the basis of the orbital phase continuity/discontinuity in the involved cyclic orbital interactions, some general rules were drawn for the π -conjugated and localized diradicals:

1. For the π -conjugated systems as well as the π -type diradicals, the triplet branched isomers are more stable than the linear ones (e.g., **1** vs **3**; **5** vs **4**; **21** vs **22**).
2. The singlet Kekulé diradicals, i.e., the excited state of Kekulé molecules, are destabilized by the orbital phase continuity while the triplet Kekulé diradicals and the singlet and triplet non-Kekulé diradicals are stabilized by the orbital phase continuity.
3. The substituents and heteroatoms can be used to tune the spin preference of the acyclic diradicals by changing the energy levels of electron-donating and -accepting orbitals and hence the donor–acceptor interaction.
4. The cyclic 1,3-diradicals containing four-membered ring structures are kinetically more stable than the acyclic species due to the depression of the ring closing to form highly strained bicyclic rings and the multiplication of the through-bond interactions. The cyclic species with various substituents are suggested to be promising targets for future experimental synthesis of persistent localized singlet diradicals.
5. Bicyclic 1,3- σ -diradicals (**60**) prefer singlet ground states with significant S–T gaps. The kinetic stability of such singlet diradicals is also outstanding in all the studied diradicals.

The orbital phase predictions were confirmed by available experiments and calculation results. In comparison with other simple models, the orbital phase theory has advantages in three aspects. (1) It can provide a general model for diradicals no matter whether they are π -conjugated (Kekulé or non-Kekulé; alternate or non-alternate) systems or localized diradicals. The relative stabilities and spin preference of all kinds of diradicals can be uniformly rationalized by the orbital phase property. Some rules concerning the substituent effects can be gained without loss of generality. (2) The orbital phase theory can be easily applied in predicting the spin preference and kinetic stability of the localized 1,3-diradicals, but all the other topological models were only applicable to the π -conjugated systems. (3) The orbital phase theory is directly related to the conformations of diradicals and applicable to understand the conformation-dependent behaviors. This differs from most other topological models, which are mainly based on the connectivity of the molecular graph regardless of the difference in conformations.

In summary, we have theoretically designed some delocalized and localized diradicals. Although the identity of the simple theory is gradually being overwhelmed by the popularity of computational “experiments” using the efficient software packages and powerful computers, especially for the audience of young researchers, we believe that insights for designing stable 1,3-diradicals raised by the orbital phase theory should be of lasting value.

Acknowledgements The authors thank Prof. Hisashi Yamamoto of the University of Chicago for his reading of the manuscript and his encouragements. The authors express their gratitude to Ms. Jane Clarkin for the English revision. J. Ma acknowledges her financial support received from the National Natural Science Foundation of China (Grant No. 20433020 and 20573050), the Ministry of Education (NCET-05-0442), and the Fok Ying Tong Education Foundation (No. 111013).

References

1. Fukui K (1971) *Acc Chem Res* 4:57
2. Fukui K, Fujimoto H (eds) (1997) *Frontier orbitals and reaction paths: Selected papers of Kenichi Fukui*. World Scientific, Singapore
3. Fleming I (1976) *Frontier orbitals and organic chemical reactions*. Wiley, New York
4. Woodward RB, Hoffmann R (1970) *The conservation of orbital symmetry*. Academic Press, London
5. Woodward RB, Hoffmann R (1969) *Angew Chem Int Ed* 8:781
6. Wheland GW (1955) *Resonance in organic chemistry*. Wiley, New York
7. Berson JA (1994) *Science* 266:1338
8. Wentrup C (2002) *Science* 295:1846
9. Rajca A (1994) *Chem Rev* 94:871
10. Rajca A (1993) *Acc Chem Res* 94:871
11. Borden WT (ed) (1982) *Diradicals*. Wiley, New York
12. Dougherty D (1991) *Acc Chem Res* 24:88
13. Little RD (1996) *Chem Rev* 96:93
14. Adam M, Grabowski S, Wilson RM (1990) *Acc Chem Res* 23:165
15. Fukui K, Inagaki S (1975) *J Am Chem Soc* 97:4445
16. Inagaki S, Fujimoto H, Fukui K (1976) *J Am Chem Soc* 98:4693
17. Inagaki S, Kawata H, Hirabayashi Y (1982) *Bull Chem Soc Jpn* 55:3724
18. Inagaki S, Iwase K (1984) *Nouv J Chim* 8:73
19. Ma J, Inagaki S (2000) *J Phys Chem A* 104:8989
20. Naruse Y, Ma J, Inagaki S (2001) *Tetrahedron Lett* 42:6553
21. Ma J, Hozaki A, Inagaki S (2002) *Inorg Chem* 41:1876
22. Ma J, Hozaki A, Inagaki S (2002) *Phosphorus, sulfur and silicon* 177:1705
23. Inagaki S, Iwase K, Kawata H (1984) *Bull Chem Soc Jpn* 57:3599
24. Inagaki S, Iwase K, Kawata H (1985) *Bull Chem Soc Jpn* 58:601
25. Sakai S, Inagaki S (1990) *J Am Chem Soc* 112:7961
26. Iwase K, Sakai S, Inagaki S (1994) *Chem Lett* 23:1601
27. Inagaki S, Ohashi S (1999) *Theor Chem Acc* 102:65
28. Ma J, Inagaki S (2001) *J Am Chem Soc* 123:1193
29. Iwase K, Inagaki S (1996) *Bull Chem Soc Jpn* 69:2781
30. Ma J, Ikeda H, Inagaki S (2001) *Bull Chem Soc Jpn* 74:273
31. Ma J, Ding Y, Hattori K, Inagaki S (2004) *J Org Chem* 69:4245
32. Wang Y, Ma J, Inagaki S (2005) *Tetrahedron Lett* 46:5567
33. Wang Y, Ma J, Inagaki S (2007) *J Phys Org Chem* 20:649
34. Dewar MJS, Healy EF (1987) *Chem Phys Lett* 141:521
35. Grutzmacher H, Breher F (2002) *Angew Chem Int Ed* 41:4006
36. Hrovat DA, Murcko MA, Lahti PM, Borden WT (1998) *J Chem Soc Perkin Trans* 2:1037
37. Döhnert D, Koutecký J (1980) *J Am Chem Soc* 102:1789
38. Dixon DA, Dunning TH Jr, Eades RA, Kleier DA (1981) *J Am Chem Soc* 103:2878
39. Aoyagi M, Osamura Y, Iwata S (1985) *J Chem Phys* 83:1140
40. Inagaki S, Iwase K, Kawata H (1985) *Bull Chem Soc Jpn* 58:601
41. Chou PK, Gao L, Tichy SE, Painter SL, Blackstock SC, Kenttämaa HI (2000) *J Phys Chem A* 104:5530
42. Berson JA, Bushby RJ, McBride JM, Tremelling M (1971) *J Am Chem Soc* 93:1544
43. Berson JA (1978) *Acc Chem Res* 11:446
44. Platz MS, McBride JM, Little RD, Harrison JJ, Shaw A, Potter SE, Berson JA (1976) *J Am Chem Soc* 98:5725
45. Abe M, Kawanami S, Masuyama A, Hayashi T (2006) *J Org Chem* 71:6607
46. Abe M, Kawanami S, Ishihara C, Tãgegami A (2004) *J Org Chem* 69:7250
47. Adam W, Finsel R (1992) *J Am Chem Soc* 114:4563
48. Datta SN, Mukherjee P, Jha PP (2003) *J Phys Chem A* 107:5049

49. Prasad BLV, Radhakrishnan TP (1992) *J Phys Chem* 96:9232
50. Radhakrishnan TP (1991) *Chem Phys Lett* 181:455
51. Lahti PM, Rossi AR, Berson JA (1985) *J Am Soc Chem* 107:2273
52. Dowd P (1970) *J Am Chem Soc* 92:1066
53. Dowd P, Chang W, Paik YH (1986) *J Am Chem Soc* 108:7416
54. Roth WR, Kowalczyk U, Maier G, Reisenauer HP, Sustmann R, Muller W (1987) *Angew Chem Int Ed* 26:1285
55. Clifford EP, Wenthold PG, Lineberger WC, Ellison GB, Wang CX, Grabowski JJ, Vila F, Jordan KD (1998) *J Chem Soc Perkin Trans 2*:1015
56. Rodriguez E, Reguero M, Caballol R (2000) *J Phys Chem A* 104:6253
57. Nachtigall P, Jordan KD (1992) *J Am Chem Soc* 114:4743
58. Nachtigall P, Jordan KD (1993) *J Am Chem Soc* 115:270
59. Filatov M, Shaik S (1999) *J Phys Chem A* 103:8885
60. Matsuda K, Iwamura H (1997) *J Am Chem Soc* 119:7412
61. Matsuda K, Iwamura H (1998) *J Chem Soc Perkin Trans 2*: 1023
62. Dowd P, Chang W, Paik YH (1987) *J Am Chem Soc* 109:5284
63. Roth VWR, Erker G (1973) *Angew Chem* 85:510
64. Du P, Hrovat DA, Borden WT (1989) *J Am Chem Soc* 111:3773
65. Coulson CA, Longuet-Higgins HC (1947) *Proc R Soc A* 191:39
66. Coulson CA, Longuet-Higgins HC (1947) *Proc R Soc A* 192:16
67. Coulson CA, Longuet-Higgins HC (1947) *Proc R Soc A* 193:447
68. Tyutyulkov N, Polansky OE (1987) *Chem Phys Lett* 139:281
69. Karabunarliev S, Tyutyulkov N (1989) *Theor Chim Acta* 76:65
70. Tyutyulkov N, Karabunarliev S, Ivanov C (1989) *Mol Cryst Liquid Cryst* 176:139
71. Davidson ER, Borden WT (1977) *J Am Chem Soc* 99:4587
72. Ovchinnikov A (1978) *Theor Chim Acta* 47:297
73. Li S, Ma J, Jiang Y (1996) *J Phys Chem* 100:4775
74. Li S, Ma J, Jiang Y (1997) *J Phys Chem A* 101:5567
75. Maynau D, Said M, Malrieu JP (1983) *J Am Chem Soc* 105:5244
76. Klein DJ, Nelin CJ, Alexander SA, Masten FA (1982) *J Chem Phys* 77:3101
77. Alexander SA, Klein DJ (1988) *J Am Chem Soc* 110:3401
78. Davidson ER, Borden WT, Smith J (1978) *J Am Chem Soc* 100:3299
79. Pranata J, Dougherty DA (1987) *J Am Chem Soc* 109:1621
80. Zhang DY, Borden WT (2002) *J Org Chem* 67:3989
81. Buchwalter SL, Closs GL (1975) *J Am Chem Soc* 97:3857
82. Buchwalter SL, Closs GL (1979) *J Am Chem Soc* 101:4688
83. Jain R, Sponsler MB, Coms FD, Dougherty DA (1988) *J Am Chem Soc* 110:1356
84. Pedersen S, Herek JL, Zewail AH (1994) *Science* 266:1359
85. Zewail AH (2000) *Angew Chem Int Ed* 39:2586
86. Adam W, Harrer HM, Kita FW, Nau M (1997) *Pure Appl Chem* 69:91
87. Adam W, Harrer HM, Heidenfelder T, Kammel T, Kita F, Nau WM, Sahin C (1996) *J Chem Soc Perkin Trans 2*: 2085
88. Adam W, Günther E, Hössel P, Platsch H, Wilson RM (1987) *Tetrahedron Lett* 28:4407
89. Kita F, Adam W, Jordan P, Nau WM, Sahin C (1999) *J Am Chem Soc* 121:9265
90. Abe M, Adam W (1998) *J Chem Soc Perkin Trans 2*:1063
91. Abe M, Adam W, Nau WM (1998) *J Am Chem Soc* 120:11304
92. Adam W, Borden WT, Burda C, Foster H, Heidenfelder T, Heubes MD, Hrovat A, Kita F, Lewis SB, Scheutzw D, Wirz J (1998) *J Am Chem Soc* 120:593
93. Abe M, Adam W, Borden WT, Hara M, Hattori M, Majima T, Nojima M, Tachibana K, Tojo S (2002) *J Am Chem Soc* 124:6540
94. Abe M, Adam W, Borden WT, Hattori M, Hrovat A, Nojima M, Nozaki K, Wirz J (2004) *J Am Chem Soc* 126:574
95. Abe M, Hattori M, Takegami A, Masuyama A, Hayashi T, Seki S, Tagawa S (2006) *J Am Chem Soc* 128:8008
96. Abe M, Adam W, Heidenfelder TW, Nau M, Zhang X (2000) *J Am Chem Soc* 122:2019

97. Adam W, Baumgarten M, Maas W (2000) *J Am Chem Soc* 122:6735
98. Scheschewitz D, Amii H, Gornitzka H, Schoeller WW, Bourissou D, Bertrand G (2002) *Science* 295:1880
99. Grützmacher H, Breher F (2002) *Angew Chem Int Ed* 41:4006
100. Niecke E, Fuchs A, Nieger M, Schoeller WW (1995) *Angew Chem Int Ed* 34:555
101. Schmidt O, Fuchs A, Gudat D, Nieger M, Hoffbauer W, Niecke E, Schoeller WW (1998) *Angew Chem Int Ed* 37:949
102. Niecke E, Fuchs A, Nieger M (1999) *Angew Chem Int Ed* 38:3028
103. Sebastian M, Nieger M, Szieberth D, Nyulászi L, Niecke E (2004) *Angew Chem Int Ed* 43:637
104. Gandon V, Bourg J-B, Tham FS, Schoeller WW, Bertrand G (2008) *Angew Chem Int Ed* 47:155
105. Iwamoto T, Yin D, Kabuto C, Kira M (2001) *J Am Chem Soc* 123:12730
106. Hoffmann R (1968) *J Am Chem Soc* 90:1475
107. Hoffmann R, Swaminathan S, Odell BG, Gleiter R (1970) *J Am Chem Soc* 92:7091
108. Getty SJ, Davidson ER, Borden WT (1992) *J Am Chem Soc* 114:2085
109. Getty SJ, Hrovat DA, Xu JD, Barker SA, Borden WT (1994) *J Chem Soc Faraday Trans* 90:1689
110. Skancke A, Hrovat DA, Borden WT (1998) *J Am Chem Soc* 120:7079
111. Zhang DY, Hrovat DA, Abe M, Borden WT (2003) *J Am Chem Soc* 125:12823
112. Baldwin JE, Yamaguchi Y, Schaefer HF III (1994) *J Phys Chem* 98:7513
113. Krogh-Jespersen K, Cremer D, Dill JD, Pople JA, Schleyer PVR (1981) 103:2589
114. Budzelaar PHM, Kraka E, Cremer D, Schleyer PVR (1986) *J Am Chem Soc* 108:561
115. Schoeller WW, Begemann C, Niecke E, Gudat D (2001) *J Phys Chem A* 105:10731
116. Jung Y, Head-Gordon M (2003) *J Phys Chem A* 107:7475
117. Jung Y, Head-Gordon M (2003) *Chem Phys Chem* 4:522
118. Radhakrishnan TP (1993) *Chem Phys Lett* 207:15
119. Li S, Ma J, Jiang Y (1997) *J Phys Chem A* 101:5587
120. Clark AE, Davidson ER (2002) *J Phys Chem A* 106:6890
121. Statroverov VN, Davidson ER (2000) *J Am Chem Soc* 122:186
122. Inagaki S, Ishitani Y, Kakefu T (1994) *J Am Chem Soc* 116:5954
123. Inagaki S, Kakefu T, Yamamoto T, Wasada H (1996) *J Phys Chem* 100:9615
124. Ishikawa M, Sugisawa H, Kumada M, Higuchi T, Matsui K, Hirotsu K, Iyoda J (1983) *Organometallics* 2:174
125. Masamune S, Murakami S, Tobita H, Williams DJ (1983) *J Am Chem Soc* 105:7776
126. Yokelson HB, Millevolte AJ, Haller KJ, West R (1987) *J Chem Soc Chem Commun*:1605
127. Tan RP, Gillette GR, Powell DR, West R (1991) *Organometallics* 10:546
128. Abe M, Kawanami S, Ishihara C, Nojima M (2004) *J Org Chem* 69:5622
129. Abe M, Kube E, Nozaki K, Matsuo T, Hayashi T (2006) *Angew Chem Int Ed* 45:7828
130. Jain R, Snyder GJ, Dougherty DA (1984) *J Am Chem Soc* 106:7294
131. Boatz JA, Gordon MS (1989) *J Phys Chem* 93:2888
132. Nguyen KA, Gordon MS, Boatz JA (1994) *J Am Chem Soc* 116:9241
133. Scheschewitz D, Amii H, Gornitzka H, Schoeller WW, Bourissou D, Bertrand G (2004) *Angew Chem Int Ed* 43:585
134. Seierstad M, Kinsinger CR, Cramer CJ (2002) *Angew Chem Int Ed* 41:3894
135. Dowd P (1966) *J Am Chem Soc* 88:2587
136. Dowd P, Gold A, Sachdev K (1966) *J Am Chem Soc* 90:2715
137. Dowd P, Sachdev K (1967) *J Am Chem Soc* 89:715
138. Baseman RJ, Pratt DW, Chow M, Dowd P (1976) *J Am Chem Soc* 98:5726
139. Dowd P (1972) *Acc Chem Res* 5:242
140. Wenthold PG, Hu J, Squires RR, Lineberger WC (1996) *J Am Soc Chem* 118:475
141. Wenthold PG, Hu J, Squires RR, Lineberger WC (1999) *J Am Soc Mass Spectrom* 10:800
142. Cramer CJ, Smith BA (1996) *J Phys Chem* 100:9664
143. Nachtigall P, Dowd P, Jordan KD (1992) *J Am Chem Soc* 114:4747
144. Dowd P, Paik YH (1986) *J Am Chem Soc* 108:2788
145. Snyder GJ, Dougherty DA (1985) *J Am Chem Soc* 107:1774

146. Snyder GJ, Dougherty DA (1986) *J Am Chem Soc* 108:299
147. Snyder GJ, Dougherty DA (1989) *J Am Chem Soc* 111:3927
148. Snyder GJ, Dougherty DA (1989) *J Am Chem Soc* 111:3942
149. Wenthold PG, Kim JB, Lineberger WC (1997) *J Am Chem Soc* 119:1354
150. Neuhaus P, Grote D, Sander W (2008) *J Am Chem Soc* 130:2993
151. Wang T, Krylov AI (2005) *J Chem Phys* 123:104304
152. Zhang G, Li S, Jiang Y (2003) *J Phys Chem A* 107:5573
153. Coolidge MB, Yamashita K, Morokuma K, Borden WT (1990) *J Am Chem Soc* 112:1751
154. Gleiter R, Hoffmann R (1969) *Angew Chem Int Ed* 8:214
155. Rakesh J, Lisa MW, Dennis AD (1988) *J Am Chem Soc* 110:552
156. Adam W, Reinhard G, Platsch H, Wirz J (1990) *J Am Chem Soc* 112:4570
157. Adam W, Grabowski S, Platsch H, Hannemann K, Wirz J, Wilson RM (1989) *J Am Chem Soc* 111:751
158. Adam W, Platsch H, Wirz J (1989) *J Am Chem Soc* 111:6896
159. Coms FD, Dougherty DA (1988) *Tetrahedron Lett* 29:3753
160. Coms FD, Dougherty DA (1989) *J Am Chem Soc* 111:6894
161. Sugiyama H, Ito S, Yoshifuji M (2003) *Angew Chem Int Ed* 42:3802
162. Cui C, Brynda M, Olmstead MM, Power PP (2004) *J Am Chem Soc* 126:6510
163. Amii H, Vranicar L, Gornitzka H, Bourissou D, Bertrand G (2004) *J Am Chem Soc* 126:1344
164. Rodriguez A, Tham FS, Schoeller WW, Bertrand G (2004) *Angew Chem Int Ed* 43:4876

Relaxation of Ring Strains

Yuji Naruse and Satoshi Inagaki

Abstract Relaxation of strain in small ring molecules is reviewed in terms of two mechanisms – σ -relaxation and π -relaxation. The σ -relaxation occurs in in-plane interaction of the ring σ bonds. Previously proposed σ -aromaticity and surface delocalization are briefly discussed. The geminal interaction theory for the σ -relaxation of ring strains is discussed and applied. The geminal interaction is less antibonding or more bonding with decrease in the bond angle, when the hybrid orbital has low s-character for the ring bonds or has an s-rich lone pair (lone pair effect). π -Relaxation of unsaturated ring molecules results from the cyclic delocalization of π electrons through the σ bonds on the saturated ring atoms. The two mechanisms of the σ - and π -relaxation are shown to be necessary for better understanding of ring strains.

Keywords π -Relaxation • σ -Relaxation • Geminal interaction • Inverted bond • Lone pair effect • Orbital phase continuity • Ring strain

Contents

1	Introduction.....	266
2	Theories for the Relaxation of the Ring Strains.....	268
2.1	σ -Relaxation	268
2.2	π -Relaxation.....	271
3	Application of the σ -Relaxation	272
3.1	Homoatomic Ring Molecules	272
3.2	Heteroatomic Ring Molecules	274
3.3	Polycyclic Molecules: Inverted Bonds.....	276
4	Applications of the π -Relaxation	284
4.1	Cycloalkenes and Cyclopolysilenes.....	284
4.2	Cyclic Unsaturated N ₃ H and P ₃ H Molecules	286
4.3	Polycyclic Oligosilenes.....	286
4.4	Related Experimental Observations.....	287
	References.....	290

Y. Naruse and S. Inagaki (✉)

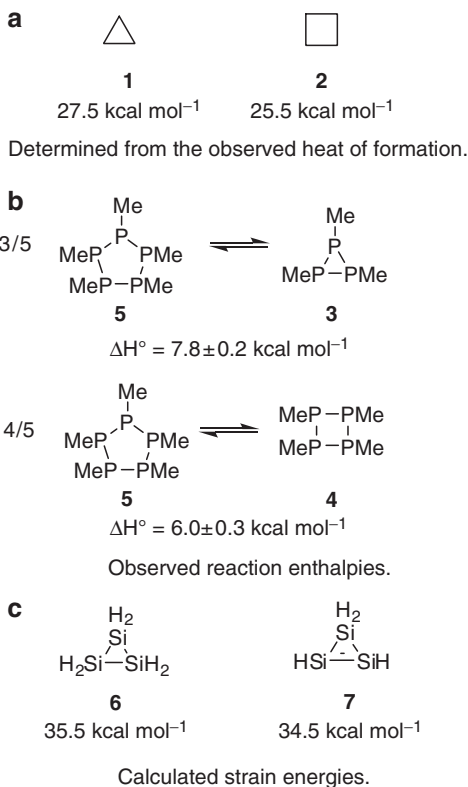
Department of Chemistry, Faculty of Engineering, Yanagido Gifu, 501-1193, Japan
e-mail: inagaki@gifu-u.ac.jp

Abbreviations

IBE	Interbond energy
IBP	Interbond population
NBO	Natural bond orbital
SE	Strain energy

1 Introduction

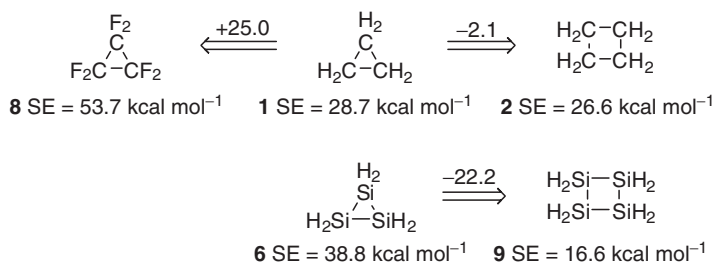
Strain in a molecule is first referred as the deviations of the bond angles from the ideal ones, which is the origin of the strain energy – the excess internal energy from destabilization of the smaller and larger ring molecules which is liberated in combustion [1]. In the small ring systems, more acute bond angles increase the strain with deviation from 109.5° for sp^3 or from 120° for sp^2 hybrid orbital [2]. Baeyer's theory has advanced the chemistry of small-ring molecules. However, there is evidence against the overwhelming predominance of Baeyer's strain. Cyclopropane **1** has the strain energy (SE) of $27.5 \text{ kcal mol}^{-1}$ as determined from the observed heat of formation (Scheme 1a) [3]. Cyclobutane **2** has the SE of $25.5 \text{ kcal mol}^{-1}$,



Scheme 1 Little difference in the ring strain between the three- and four-membered ring molecules

which is only a little ($2.0 \text{ kcal mol}^{-1}$) [3] lower than **1**, while the bond angle decreases by 30° . Baulder obtained the differences in the reaction enthalpies ΔH° of 7.8 and $6.0 \text{ kcal mol}^{-1}$ for $(\text{PCH}_3)_3$ **3** and $(\text{PCH}_3)_4$ **4**, respectively, from the experimental study of the equilibria with $(\text{PCH}_3)_5$ **5** (Scheme 1b) [4]. This suggests little difference in the strain between the three- and four-membered rings of phosphorus compounds. Some unsaturated ring molecules have strain energies similar to the saturated molecules (Scheme 1c)[5]. Something relaxes the Baeyer ring strain.

Furthermore, there are some intriguing trends in the strain (Scheme 2). The calculated SEs are dramatically changed with substitutions. Hexafluorocyclopropane **8** is more strained than **1** by $25.0 \text{ kcal mol}^{-1}$ [6] (Scheme 2). Carbon and



Scheme 2 Calculated strain energies (RHF/6-31G(d))

silicon belong to Group 14, and methane and silane possess the bond angle of 109.5° . However, the SE of cyclotrisilane **6** is $38.8 \text{ kcal mol}^{-1}$, which is higher by $22.2 \text{ kcal mol}^{-1}$ than cyclotetrasilane **9** ($\text{SE} = 16.6 \text{ kcal mol}^{-1}$) (Scheme 2) [7]. Large difference in strain between the three- and four-membered ring makes a sharp contrast to the carbon congeners. There are apparently other important factors of the ring strains than the deviation of the bond angles.

For almost the same strain energies of **1** and **2**, Dewar [8] and Cremer [9] proposed σ -aromaticity of **1** and surface delocalization in **1**, respectively. A geminal interaction theory was developed by us for the ring strain relaxation [10–12]. Interaction between the geminal ring σ -bonds was proposed to relax the ring strain. The geminal interaction theory has been successfully applied to diverse problems with the ring strains [13]. On the other hand, delocalization of π -electrons has been proposed to relax the strains of some unsaturated three-membered ring molecules [14–18]. An orbital phase theory has been applied to the ring strain relaxation of unsaturated molecules including molecules larger than three-membered rings [19, 20]. Here we review the relaxations of the ring strain by σ - and π -electrons (σ -relaxation and π -relaxation, respectively).

2 Theories for the Relaxation of the Ring Strains

2.1 σ -Relaxation

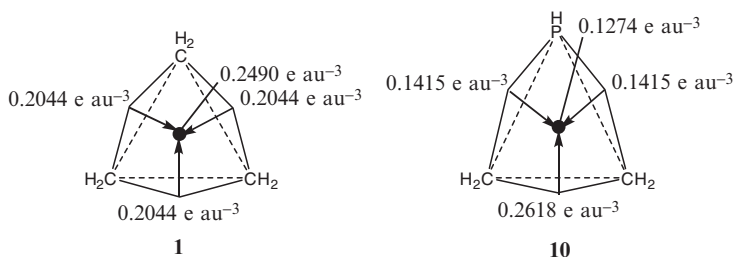
2.1.1 σ -Aromaticity

Dewar proposed that the relatively low ring strain of **1** originates from the delocalization between the three ring bonds [8]. It was called σ -aromaticity. There are six electrons in three σ -bonds of the cyclopropane ring. Delocalization of the six electrons, which is the same electron count as the π -electrons in benzene, might produce significant stabilization. The electron delocalization is accompanied by the loss of electron density from the bonding orbitals and the acceptance of the electron density by the antibonding orbitals. The bonds are elongated by the delocalization. However, the bond lengths of **1** are shorter than the normal C–C bond. As mentioned in the Introduction, high strain energies of cyclotrisilane **6** and hexafluorocyclopropane **8**, which have the same number (six) of σ -electrons as **1**, are not rationalized with σ -aromaticity. Cremer argued against the σ aromaticity [21]. The C–C bonds in cyclobutane **2** are equal, and the same is true for many other cycloalkanes with no bond length alternation. The anisotropy effect of a bent bond, which is caused by the electron flow among the bonds, is not known.

2.1.2 Surface Delocalization

Cremer proposed that the higher electron density inside the ring would relax the strain [9]. The “surface delocalization” stabilizes the lowest orbital of the ring system, which might relax the ring strain.

Bachrach has argued against the surface delocalization by comparing the electron density at the centers of the banana bonds to that of the centers of cyclopropane **1** and phosphirane **10** (Scheme 3) [22]. Density is spread over the ring in **1**, but not



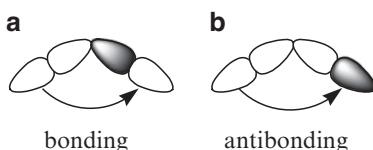
Scheme 3 The electron density at the bond critical points and the center of **1** and **10**

to the extent that it is in **10**. Phosphirane **10** (SE = 20.1 kcal mol⁻¹) is less strained than **1** (SE = 27.8 kcal mol⁻¹). However, phosphirane **10** has a lower electron density

inside the ring than **1**. The surface delocalization theory failed to explain the relative strain energies.

2.1.3 Geminal interaction

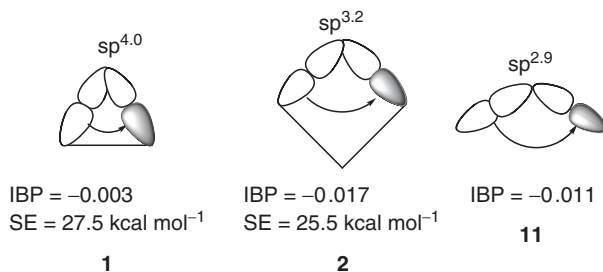
Interaction of the doubly occupied bonding orbital of a σ bond with the vacant antibonding σ^* -orbital of another bond at the geminal position was theoretically shown to be bonding (Scheme 4a) and antibonding (Scheme 4b) when the s-character



Scheme 4 Geminal σ - σ^* interaction

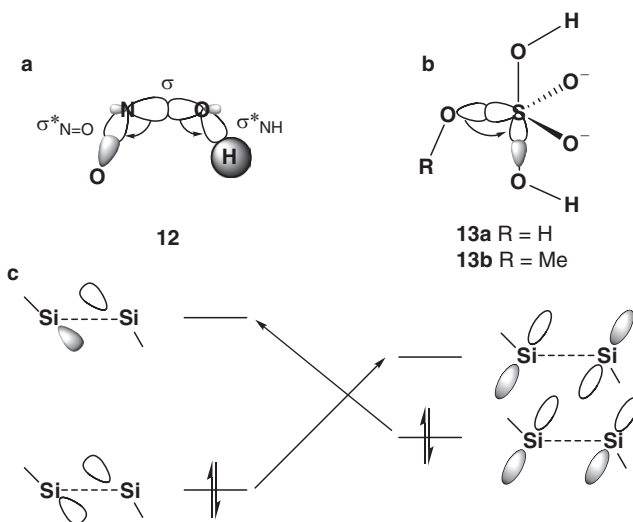
of the hybrid orbitals on the central atom is low and high, respectively [10]. It is surprising that the interaction between the occupied and unoccupied orbitals is antibonding in some cases.

The geminal interaction theory shed new light on the strains of small ring molecules [10]. The hybrids of the ring bonds are $sp^{4.0}$ and $sp^{3.2}$ for **1** and **2**, respectively. The s-characters are appreciably lower in **1** and a little lower in **2** than that of the C-C bond in propane ($sp^{2.9}$). The interbond population (IBP) [10, 11] between the geminal σ and σ^* orbitals shows less antibonding in **1** (-0.003) than propane **11** (IBP = -0.011) (Scheme 5). The antibonding property (IBP = -0.017) of cyclobutane is greater than propane. The low antibonding property of the geminal σ - σ^* delocalization relative to that of propane relaxes the ring strain of **1**.



Scheme 5 The hybrids and interbond population (IBP) between the geminal σ and σ^* orbitals and the SEs

Interactions between the geminal bonds have not yet been extensively studied. Magnasco developed a method with the bond orbital approach in analyzing interactions [23–27] and showed that the geminal delocalizations from $\sigma_{\text{N-O}}$ to $\sigma_{\text{N=O}}^*$ and $\sigma_{\text{O-H}}^*$ (Scheme 6a) significantly depend on the rotation around ON–OH in nitrous acid (HNO_2) **12** [28].



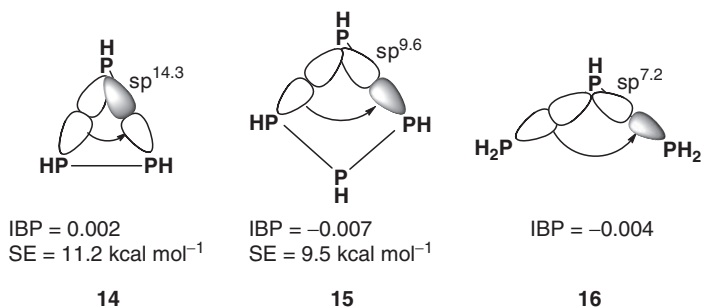
Scheme 6 Other geminal interactions studied

Cameron and Thatcher discussed the geminal delocalization of $\sigma_{\text{SO}} \rightarrow \sigma_{\text{SO}}^*$ in pentaoxasulfurane **13** (Scheme 6b) [29]. Takahashi and Sakamoto noted the importance of unusual delocalization between geminal bonds [30]. The geminal delocalization from one bond to the other between the unsaturated Si atoms was found in the results of the NBO analysis [31] to be essential for the stability of the bent structures (Scheme 6c).

2.1.4 Effects of Lone Pairs

Lone pairs tend to be rich in s-character to lower the energy of the molecules. The σ bonds should have low s-character of the hybrid orbitals on the atom X with the lone pair(s). The geminal σ – σ^* interaction between the ring bonds sharing X is less antibonding or bonding. *Lone pairs on ring atoms reduce strains through the σ -relaxation.*

As mentioned in the Introduction, trimethyltriphosphirane **3** and tetramethyltetraphosphetane **4** have almost the same strain energies. We subjected the parent molecules, triphosphirane **14** and tetraphosphetane **15**, to the bond model analysis



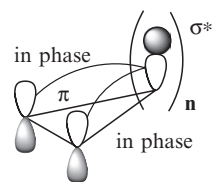
Scheme 7 The hybrids and the interbond population (IBP) between the geminal σ and σ^* orbitals and the SEs

(Scheme 7) [32–36]. The hybrid orbitals for the ring bonds have low s-characters: $sp^{14.3}$ (**14**) and $sp^{9.6}$ (**15**). The IBP value between the geminal σ and σ^* orbitals shows a bonding character in **14** ($\text{IBP}_{\sigma\sigma^*} = 0.002$) and antibonding character ($\text{IBP}_{\sigma\sigma^*} = -0.004$) in **16**. The three-membered ring strain is relaxed. The geminal σ – σ^* interaction is antibonding ($\text{IBP}_{\sigma\sigma^*} = -0.007$) in **15**. No σ -relaxation is expected. As a result, the difference between the three- and four-membered phosphorus ring in the strain is reduced (See Sect. 4.2).

2.2 π -Relaxation

In the ring molecules containing a π bond, delocalization of π electrons occurs through the interaction with σ^* orbitals [19].

Cyclic orbital interaction is needed to meet the orbital phase continuity conditions (Chapter “An Orbital Phase Theory” by Inagaki in this volume) [37, 38]: (1) electron-donating orbitals are out of phase; (2) an electron-donating orbital and an electron-accepting orbital are in phase; (3) electron-accepting orbitals are in phase. In the case of an electron-donating π bond, the phase of π , $\sigma_1^* \cdots \sigma_n^*$ is continuous (Scheme 8). The electron-donating π orbital is combined in phase with electron-accepting σ_1^* and σ_n^* orbitals. The σ_1^* and σ_n^* orbitals are in phase with each other. These relationships meet the orbital phase continuity conditions. The cyclic (π , $\sigma_1^* \cdots \sigma_n^*$) interaction is favored by the phase continuity. Cyclic delocalization of π -electrons stabilizes small ring molecules and relaxes the ring strains [19].



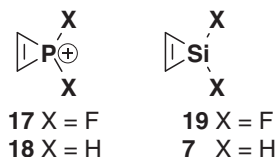
Scheme 8 The orbital phase relationship of the continuity in the (π , $\sigma_1^* \cdots \sigma_n^*$) interaction

Regitz noted the importance of the resonance (Scheme 9) in pentacoordinated phosphirenes for the short C–P bonds and the long C=C bond [39] as compared to the corresponding bonds in 1*H*-phosphirene.

Scheme 9 Resonance structure of penta-coordinated phosphirene



Clark [15] reported relaxation of the strain in the three-membered rings of fluorosubstituted phosphirenium **17** and silirene **19** by the π – σ^* interaction in comparison with the compounds **18** and **7**.

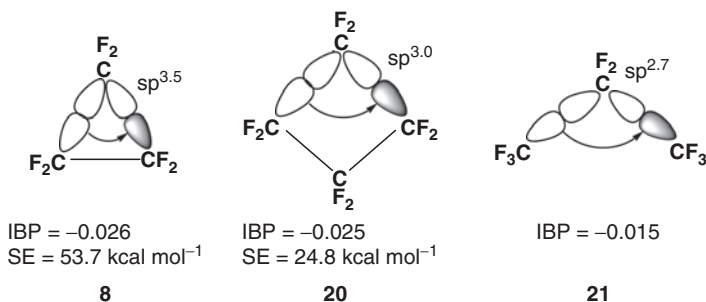


Kira et al. investigated the π → σ^* interaction in silacyclopropene (see Sect. 4.4.1) [5,16].

3 Application of the σ -Relaxation

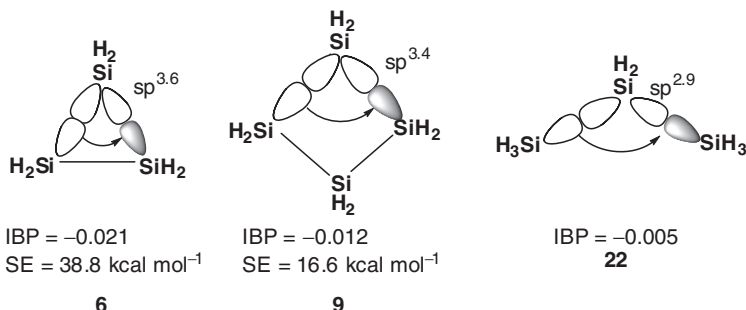
3.1 Homoatomic Ring Molecules

The σ – σ^* interaction of the geminal C–C bonds is antibonding in an open chain molecule, propane **11** (Scheme 5). The antibonding character is lowered for an acute bond angle. The σ -relaxation occurs in cyclopropane **1** to a significant degree. Cyclopropane **1** has almost the same strain energy as cyclobutane **2** [3]. Perfluorination considerably increases the SE of the three-membered ring (53.7 kcal mol⁻¹ [6, 40]) relative to that of the four-membered ring (24.8 kcal mol⁻¹ [6]). Liebman reported that fluorination of cyclopropane resulted in increase of the SE [41]. Fluorine is more electronegative than carbon whereas hydrogen is less electronegative. Thus, a C–F bond is polarized in the opposite direction, and the hybrid on C in the C–F bond is low in s-character. The hybrids of the ring bonds in **8** are then high in s-character, so that the geminal σ – σ^* interaction is more antibonding. In fact, the hybrid orbitals for the ring bonds have high s-characters: sp^{3.5} (**8**) and sp^{3.0} (**20**) (scheme 10) [12], compared with sp^{4.0} in **1** and sp^{3.2} in **2** [10] (Scheme 5). The geminal σ – σ^* interactions between the ring σ -bonds have high antibonding character in **8** (IBP _{$\sigma\sigma^*$} = –0.026) and in **20** (IBP _{$\sigma\sigma^*$} = –0.025), respectively, which are larger than that in perfluoropropane **21**.



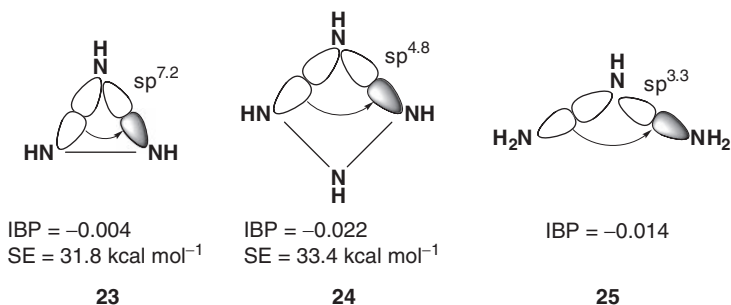
Scheme 10 The hybrids and antibonding character of the geminal $\sigma\text{-}\sigma^*$ interaction and the SEs

In the Si–H bond the Si atom is positively charged and the H atom is negatively charged. The polarization is similar to that in the C–F bond. The three-membered ring molecule, cyclotrisilane **6**, is expected to be more strained than the cyclotetrasilane **9** as is the case with the perfluorinated ring molecules. In fact, the antibonding property increases for Si–Si bonds as the bond angle decreases (Scheme 11) [11]. The hybrid orbitals for the ring bonds have high s-characters: $\text{sp}^{3.6}$ (**6**) and $\text{sp}^{3.4}$ (**9**). The geminal $\sigma\text{-}\sigma^*$ interaction between the ring bonds is highly antibonding in **6** ($\text{IBP}_{\sigma\sigma^*} = -0.021$) and **9** ($\text{IBP}_{\sigma\sigma^*} = -0.012$), which is more antibonding than trisilane **22**. Cyclotrisilane **6** is appreciably more strained than cyclotetrasilane **9** as is expected from the bond angles.



Scheme 11 The hybrids and antibonding character of the geminal $\sigma\text{-}\sigma^*$ interaction and the SEs

In triaziridine **23**, the σ -relaxation is appreciable due to the lone pair effect (Sect. 2.1.4) as is the case with triphosphirane **14** which has almost the same SE as tetraphosphetane **15**. Triaziridine **23** has lower SE ($31.8 \text{ kcal mol}^{-1}$) than tetraazetidene **24** ($\text{SE} = 33.4 \text{ kcal mol}^{-1}$) (Scheme 12) [12]. Lone pairs on nitrogen atoms have high s-character. The hybrid orbitals for the N–N bonds have lower s-character ($\text{sp}^{7.2}$) in **23** than that ($\text{sp}^{3.3}$) in triazane **25** [12]. The geminal $\sigma\text{-}\sigma^*$ interaction is less antibonding in **23** ($\text{IBP}_{\sigma\sigma^*} = -0.004$) than in **25** ($\text{IBP}_{\sigma\sigma^*} = -0.014$). The geminal $\sigma\text{-}\sigma^*$ interaction in **24** ($\text{IBP}_{\sigma\sigma^*} = -0.022$) is more antibonding than in **25**.



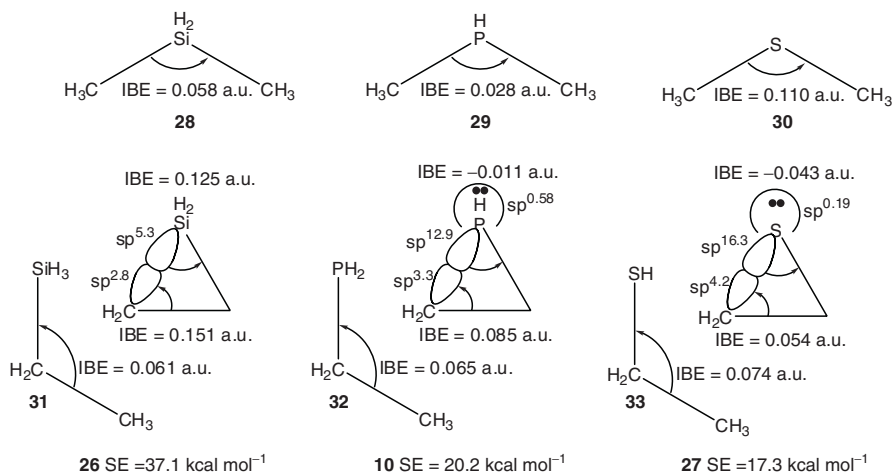
Scheme 12 The hybrids and antibonding character of the geminal σ - σ^* interaction and the SEs

3.2 Heteroatomic Ring Molecules

3.2.1 Three-Membered Ring Molecules

Ring strains decrease in the order of silirane **26** > phosphirane **10** > thiirane **27** (Scheme 13) [13]. Lone pairs tend to increase the s-character for the stabilization. The lone pair effect (Sect. 2.1.4) lowers the s-character of the hybrids of the ring bonds on the heteroatoms X in **10** and **27**. There is no lone pair on Si in **26**. The s-character of the hybrid orbital on X for the C-X bond decreases in the order **26** ($\text{sp}^{5.3}$) > **10** ($\text{sp}^{12.9}$) > **27** ($\text{sp}^{16.3}$). The energy between the geminal σ_{CX} and σ_{XC}^* orbitals termed interbond energy (IBE) [42] is positive (0.125 a.u.) in **26**, leading to destabilization. The positive value of the destabilization is greater than that in dimethylsilane **28** (0.058 a.u.). The σ -relaxation is ineffective. The geminal interaction lowers the energy (-0.011 a.u.) of **10**, but raises the energy of the open chain molecule **29** (0.028 a.u.). In thiirane **27**, the geminal $\sigma_{\text{CX}}-\sigma_{\text{XC}}^*$ interaction more significantly lowers the energy (-0.043 a.u.), but the geminal interaction destabilizes the open chain molecule **30** (0.110 a.u.). The σ -relaxation is effective in **10** and more effective in **27**. The tendency of the σ -relaxation due to the σ - σ^* interaction between the geminal bonds on the heteroatoms is in agreement with that of the ring strain.

The geminal $\sigma_{\text{CC}}-\sigma_{\text{CX}}^*$ interactions support the relative strain energies. The geminal $\sigma_{\text{CC}}-\sigma_{\text{CSiP}}^*$ interaction destabilizes **26** (0.151 a.u.) more than the open chain molecule **31** (0.061 a.u.). The destabilization of **10** (0.085 a.u.) by the geminal interaction is a little greater than that of the open chain molecule **32** (0.065 a.u.). In contrast, the destabilization (0.054 a.u.) of **27** is smaller than that of the open chain molecule **33** (0.074 a.u.). The tendency of the effect of the geminal interactions is in agreement with the order of the s-character of the hybrid orbital on the carbon for the C-X bond ($\text{sp}^{2.8}$ for SiH_2 ; $\text{sp}^{3.3}$ for PH; $\text{sp}^{4.2}$ for S). This order is readily predicted from the electronegativity of X. The σ -relaxation due to the geminal $\sigma_{\text{CC}}-\sigma_{\text{CX}}^*$ interaction increases in the order of **26** < **10** < **27**, with the decrease of the s-character on C for the C-X bond.



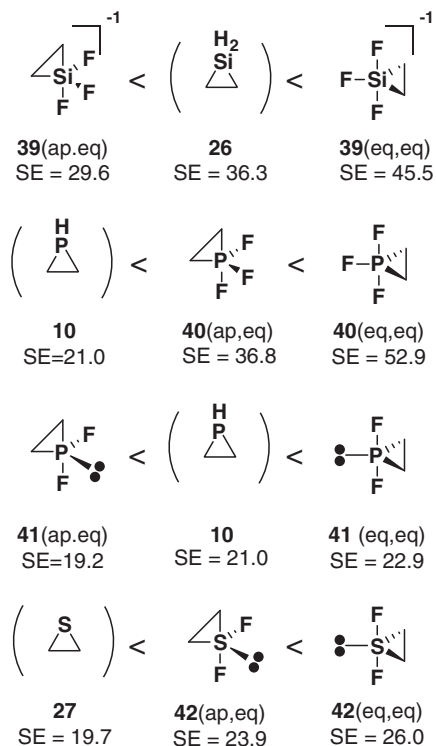
Scheme 13 σ -Relaxation, energies between bond orbitals (Interbond energy: IBE) and hybrids

A similar tendency of the heteroatom (Si, P, S) effects on the ring strains has been obtained [13] for the diaza analogs (NH_2X : **34** ($\text{X} = \text{SiH}_2$: SE = 50.4 kcal mol⁻¹) > **35** ($\text{X} = \text{PH}$: SE = 35.4 kcal mol⁻¹) > **36** ($\text{X} = \text{S}$: 33.1 kcal mol⁻¹) and for the disila analogues (SiH_2X : **6** ($\text{X} = \text{SiH}_2$: SE = 38.9 kcal mol⁻¹) > **37** ($\text{X} = \text{PH}$: SE = 30.7 kcal mol⁻¹) > **38** ($\text{X} = \text{S}$: SE = 28.1 kcal mol⁻¹).

3.2.2 Three-Membered Ring Molecules with a Hypervalent Atom

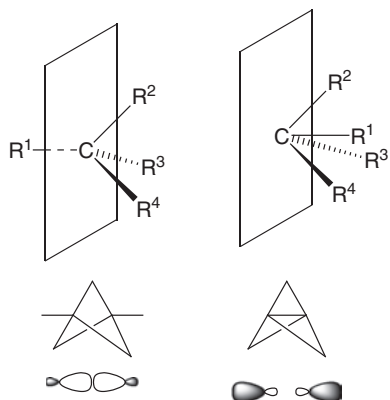
For the three-membered ring molecules (**39–42**) with a hypervalent atom in the ring, the (ap,eq) conformations are less strained than the (eq,eq) conformations (Scheme 14) [36]. The angle is 90° between the apical and equatorial bonds and 120° between the two equatorial bonds in the trigonal bipyramid. The (ap,eq) conformation is more suitable for the bond angles in a small ring. Silirane **26**, phosphirane **10** and thiirane **27** are predicted from the deviation of the ideal bond angles to be more strained than the (ap,eq) isomer. The relative SEs [36] of **26** and **39** and those of **10** and **41** substantiate the prediction. However, **10** is less strained than **40**, and **27** (SE = 19.7 kcal mol⁻¹) has a much smaller SE than the (ap,eq) conformer of **42** [36]. These unexpected relative strains are understood in terms of the lone pair effect (See Sect. 2.1.4). Phosphirane **10** has a lone pair while the pentacoordinated phosphorus has no lone pairs in **40**. Thiirane **27** has two lone pairs while the tetracoordinated sulfur has only one lone pair in **42**. The lone pairs lower the s-character of the ring bonds, weaken the antibonding property of the geminal $\sigma\text{--}\sigma^*$ interaction, and promote the σ -relaxation of the ring strain.

Scheme 14 SEs (in kcal mol⁻¹) of hypervalent three-membered rings (MP2/6-311 + G**) [36]



3.3 Polycyclic Molecules: Inverted Bonds

A saturated carbon atom usually forms at least a bond on one side of the plane with the carbon on it and three bonds on the other side (Scheme 15). However, there are some molecules (e.g., tricyclo[1.1.1.0^{1,3}]pentane), where the carbon atom has an

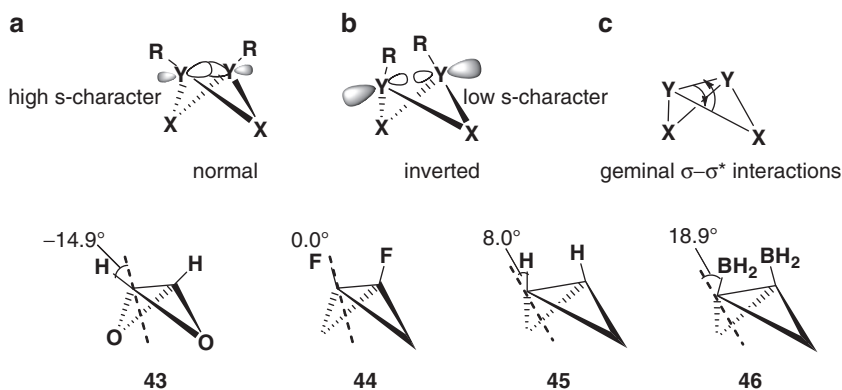


Scheme 15 Normal and inverted bonds

inverted tetrahedral configuration [35, 42]. In the molecules with the inverted configuration, all four bonded atoms or substituents are located on one side of a plane. The hybrid orbital on C for the C–R¹ bond extends in the direction opposite to the bond. Such a bond was tentatively termed an inverted bond [42], e.g., the bond between the bridgehead atoms in tricyclo[1.1.1.0^{1,3}]pentane frameworks.

3.3.1 Bicyclo[1.1.0]butane Derivatives

The bond between the bridgehead carbons of bicyclo[1.1.0]butanes can be either normal or inverted [35]. The normal bond is stabilized by the high s-character (Scheme 16a). In this case, the hybrids on the bridgeheads Y have low s-character for the bridging Y–X bonds. Electronegative atoms X or substituents R at Y stabilize

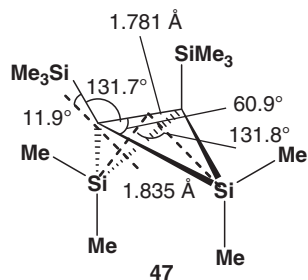


Scheme 16 The normal (a) and inverted (b) bonds between the bridgeheads, important geminal σ – σ^* interactions (c) and inverted angles of some compounds

the normal bond between the bridgeheads. In fact, 2,4-dioxabicyclobutane **43** and 1,3-difluorobicyclobutane **44** have been calculated to have the inversion angle of -14.9° and almost 0° , respectively [35]. Inverted bonds stabilize the bicyclobutane structure by the σ -relaxation due to low s-character of the bridgehead bond. Electropositive bridging atoms X or substituents R at Y invert the bridgehead configurations and increase the bonding property of the geminal σ – σ^* interaction between the central and side bonds (Scheme 16c). In fact, calculated inversion angles increase in the order of **44** < bicyclobutane **45** < 1,3-diborylbicyclobutane **46**. The interaction of the bridgehead bond with the vacant p-orbitals on the boron atom also promotes the inversion.

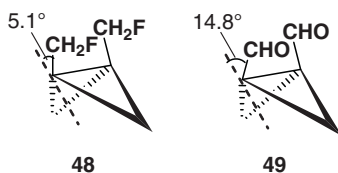
The inversion angle of 2,4-disilabicyclo[1.1.0]butane derivative **47** was calculated from the geometrical parameters by the X-ray analysis [43] to be larger (11.9°) (Scheme 17) than **45**. This supports the prediction of the dependence of the inversion

Scheme 17 The inversion angle and X-ray geometrical parameters used to calculate



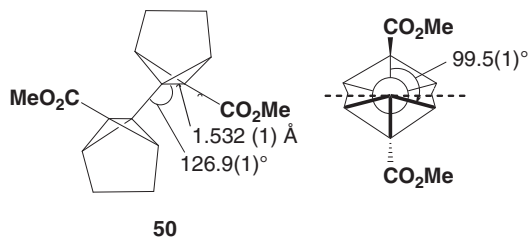
angle on the electronegativity of X and R on Y. Both are electropositive Si atoms, in contrast to **43** and **44**. Theoretical calculations and analysis showed that the diradicaloid picture of the Si...Si would be more appropriate than an existing Si-Si bond [44].

The electron-withdrawing vicinal bonds weaken the central bond and reduce the s-character. The bicyclo[1.1.0]butane frameworks tend to increase the bonding properties of the geminal σ - σ^* interaction between the central and side bonds. Thus, the inverted configuration is preferred. This is the case with the bicyclobutane (**48**) with fluoromethyl groups at the bridgehead (Scheme 18) [42]. The large inversion angle



Scheme 18 Inversion angles of **48** and **49**

of **49** is also due to the interaction of the bridgehead σ bond with $\pi^*_{C=O}$. In fact, the electron-withdrawing CO_2Me group weakens the bridgehead bond, lowers the s-character, and prefers the inverted configuration at the bridgeheads of bis(6-(methoxycarbonyl)tricyclo[2.1.1.0^{5,6}]hex-5-yl) **50** (Scheme 19) [45, 46]. X-ray

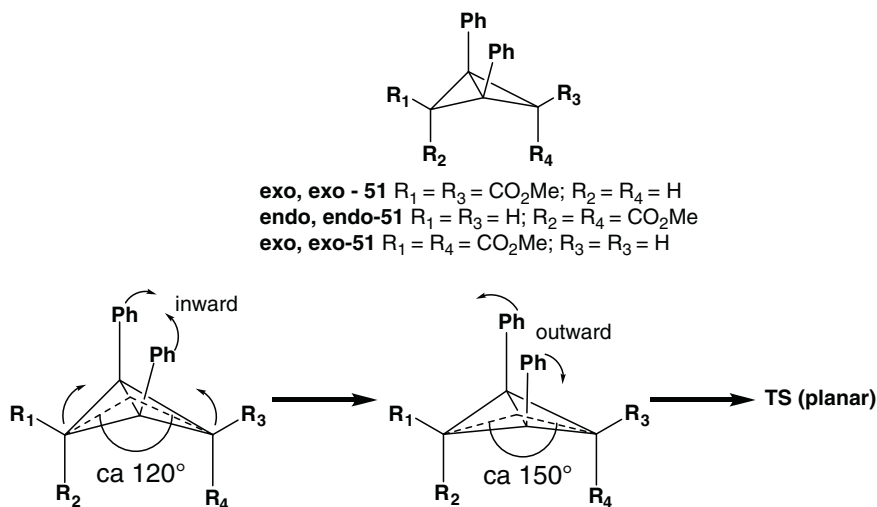


Scheme 19 Inverted configuration indicated by the dihedral angle (99.5°) together with selected bond length and bond angle

analysis showed that C-C bond length between the bridgeheads is long (1.532 \AA) and that the dihedral angle between the bridgehead bond and the side bond of the other bicyclobutane wing is 99.5° . The three bonds (bold in Scheme 19) of the

bicyclobutane ring are located below the plane (the dotted line in Scheme 19) containing the bond between the two tricyclohexane moieties. The tetrahedral configuration of the bridgehead atoms are inverted.

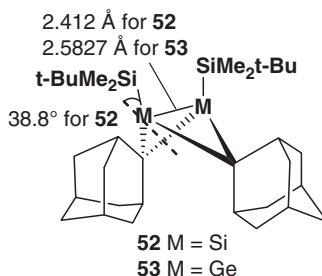
The inversion barrier of 1,3-diphenyl-2,4-bis(methoxycarbonyl)bicyclo[1.1.0]butane **51** has been calculated to be as low as 4 kcal mol⁻¹ [47]. Interestingly, the



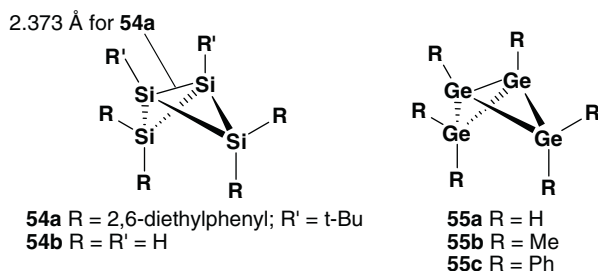
Scheme 20 Motion of phenyl groups of **51** by way of the inversion TS

phenyl groups initially move inward to be close to each other (Scheme 20) and then cease their inward migration at an interflap angle (the angle between the two cyclopropane systems) of ca. 150°, and subsequently move outward. The bridgehead bond should break at the interflap angle of 150°. This observation is in a good accordance with the σ -relaxation by inverting bridgehead bonds of bicyclo[1.1.0]butanes. The inward movement of the phenyl groups assists breaking of the bridgehead bonds by enhancing the σ -relaxation of the ring strain.

The disila- **52** [48, 49] and digermabridged **53** [50] were synthesized and their X-ray analyses were performed. The inversion angle of 38.8° for **52** and extremely long M–M (M=Si, Ge) bond lengths were observed (Scheme 21). The inverted configuration was consistent with both the NMR data and the simulation.



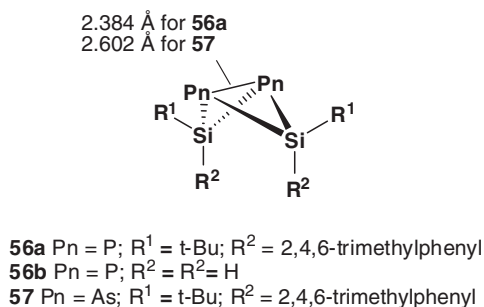
Scheme 21 Inverted angle calculated from the X-ray geometrical parameters and bond lengths of the bridgehead bond



Scheme 22 Tetrasila- and tetragermabicyclo [1.1.0] butanes

A derivative **54a** of the silicon congener Si_4H_6 **54b** was prepared (Scheme 22) [51, 52]. Theoretical calculations by Schleyer [53] showed that **54b** also has two isomers. Hydrido, methyl or phenyl substitution at the 1,3-position prefers the isomer with a long bridgehead bond [54]. The SE of **54b** is less than twice that of cyclotrisilane **6**, and the extremely long bridgehead bond is rich in p-character ($\text{sp}^{64.8}$), while the peripheral bond is rich in s-character at the bridgehead ($\text{sp}^{1.0}$) [55]. These results are in accordance with the inverted configuration. Only the inverted configuration is located for the germanium congener **55** [56].

1,3-Diphospha- and 1,3-diarsena-2,4-disilabicyclo[1.1.0]butanes **56a**, **57** were synthesized and analyzed by X-ray [57–59]. The (exo,exo)-isomers have unusually long P–P or As–As bond lengths and extremely short Si–P and Si–As bond lengths (Scheme 23) [57, 58]. Furthermore, the inversion barrier of **56b** is high (51.0 kcal

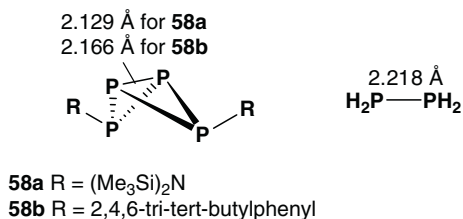


Scheme 23 1,3-diphospha- and diarsena-2,4-disilabicyclo[1.1.0]butanes

mol^{-1}) [58]. The high barrier can be ascribed to the lone pair effect on the σ relaxation of the ring strain (Sect. 2.1.4).

Tetraphosphabicyclo[1.1.0]butane **58** (Scheme 24) has been reported [60, 61]. The SE is much higher than cyclotriphosphane **14** or P_4 (see Sect. 3.3.4), but still lower than bicyclo[1.1.0]butane **45** [62, 63], in agreement with the lone pair effect (see Sect. 2.1.4). Interestingly, the bridgehead bonds have been observed to be shorter than a normal P–P bond (2.218 Å in diphosphine) [64]. The related

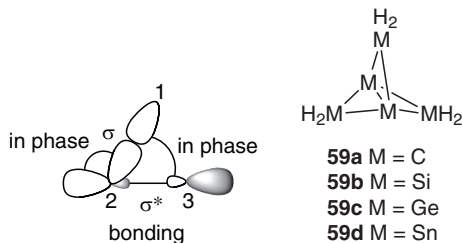
Scheme 24 The short P–P bridgehead bond lengths



1,3-diarsa-2,4-diphospha- and 2,4-diphospha-1,3-distibinobicyclo[1.1.0]butane derivatives also have shorter As–As (2.380 Å) and Sb–Sb (2.723 Å) bond lengths than the normal As–As (2.44 Å) and normal Sb–Sb (2.86 Å) bond lengths [65]. A high π -bond character of the bridgehead bond was proposed to account for these short bond lengths [62]. The reason for the short Pn–Pn (Pn=P, As, Sb) bond lengths is still under discussion.

3.3.2 [1.1.1] Propellane (Tricyclo[1.1.1.0^{1,3}]pentane Framework)

The bond between the bridgehead atoms is inverted in the [1.1.1]propellane system **59**. The hybrid orbitals are directed away from each other. In the geminal σ – σ^* interaction, the greater lobes of the geminal hybrid orbitals at the bridgehead atom can be in phase with each other, while the front lobes of the hybrid orbitals of the normal and inverted bonds at the 1,3-positions are in phase with each other

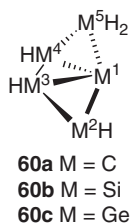


Scheme 25 Bonding geminal σ – σ^* interaction with the inverted bond in the propellane **59**

(Scheme 25) [42]. The geminal delocalization to the inverted bond is bonding. This is in contrast to the geminal σ – σ^* interaction between the normal bonds. The phase relations between the geminal lobes and between the 1,3-lobes are opposite to each other (Scheme 4), indicating the antibonding properties of the geminal σ – σ^* interaction. The bonding character of the geminal delocalization to the inverted bond is enhanced by the s-character of the hybrid orbitals on the bridgehead. The increasing order of s-character is C < Si < Ge < Sn, since the hybridization is difficult for the heavier atoms. In fact, the s-character of the hybrids at the bridgehead atom increases in the order: **59a**: pure p; **59b** –sp^{9.9}; **59c**: –sp^{7.3}; **59d**: –sp^{4.3}; (where the negative sign denotes the inverted bond.) and the SEs (kcal mol^{–1}) are reduced in that order: **59a**: 109.6; **59b**: 64.6; **59c**: 59.5; **59d**: 52.6 [42].

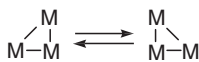
3.3.3 Tricyclo[2.1.0.0^{1,3}]Pentasilane

Tricyclo[2.1.0.0^{1,3}]pentasilane **60b** and -pentagermane **60c** was recently designed (Scheme 26) [66]. Interestingly, the molecule **60b** has the structure of C₁ symmetry instead of C₂-symmetry. The two fusion Si¹–Si³ and Si¹–Si⁴ bonds have different



Scheme 26 Tricyclo [2.1.0.0^{1,3}]pentane and its heavy congeners

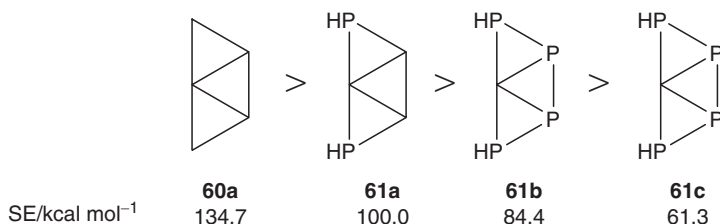
bond lengths, resulting in a new degenerate rearrangement of a distorted three-membered ring (Scheme 27). The enthalpy of the activation is low for **60b** (7.2 kcal mol⁻¹), while it is so high (22.3 kcal mol⁻¹) for **60c** that the reaction can be



Scheme 27 Degenerate rearrangement of the three-membered ring

experimentally observed. The Si¹ atom has an inverted tetrahedral configuration. The geminal σ – σ^* interaction between the fusion bonds is significantly bonding like that in the propellane (Scheme 25). The ring strain is reduced by σ -relaxation. This effect is more remarkable on **60b** than on **60a** as has been discussed in Sect. 3.3.2. The molecule **60b** (the calculated SE: 86.4 kcal mol⁻¹) is less strained than the carbon congener tricyclo[2.1.0.0^{1,3}]pentane **60a** (SE 134.7 kcal mol⁻¹) [66]. Scheshekewitz [67] independently synthesized a derivative of **60b** in 2005 when it was designed [66].

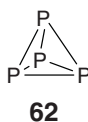
We designed less strained analogs of **61a–c** by applying the lone pair effects (Sect. 2.1.4) [68]. Substitution of carbons with phosphorus atoms relaxes the strain (Scheme 28). Notably, substitution at the 3- and 4-positions in tricyclo[2.1.0.0^{1,3}]pentane resulted in greater relaxation than substitution at the 2- and 5-positions.



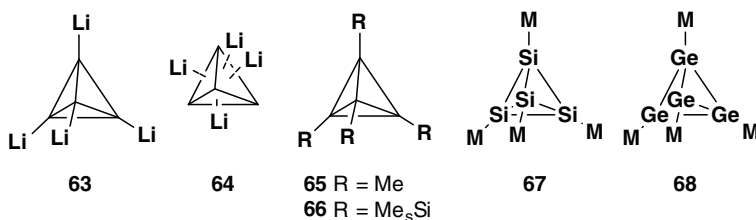
Scheme 28 The lone pair effect for the designing of less strained molecules

3.3.3 P₄ and Other Tetrahedrane Framework

Phosphorus exists as P₄ **62** under ambient conditions and is very stable while the framework is constituted of four triangles. The lone pair on the phosphorus is rich in s-character so that the framework σ -bonds possess low s-character [10]. Considerable σ -relaxation can thus be expected.



Schleyer reported preparation of the tetrahedral C₄Li₄ **63** (Scheme 29) from dithioacetylene by [2 + 2] photoaddition [69]. Interestingly, the structure **64** where lithiums are located above the center of the triangle plane is calculated to be more stable than that where lithiums are located at the vertices of tetrahedron [69]. The lone pair character on C is more suitable for σ -relaxation. Dill proposed that the σ -donating substituents could stabilize small ring compounds because of large stabilization by the bonding of the ring with the substituent in contrast to small stabilization with a σ -withdrawing substituent [70]. Attempt at replacing Li in **63** with a methyl group [69] to prepare **65** (R=Me) [70] failed whereas replacement



Scheme 29 Tetrahedranes **63–66**, M₄Si₄ **67** (M=Na, K, Rb, Cs) and M₄Ge₄ **68**

with the electropositive trimethylsilyl groups was successful [71]. Silicon as well as lithium is more electropositive than carbon atom. The hybrids on C of the C–Si are rich in s-character, so that the tetrahedrane bonds possess a low s-character. Considerable σ -relaxation stabilizes these molecules. This is also the case with M_4Si_4 **67** (M=Na, K, Rb, Cs) and M_4Ge_4 tetrahedra **68**, which were studied with X-ray analysis [72,73], followed by IR [74]. Ba_2Si_4 has also a tetrahedral framework of Si_4 [75].

3.3.5 Cage Compounds

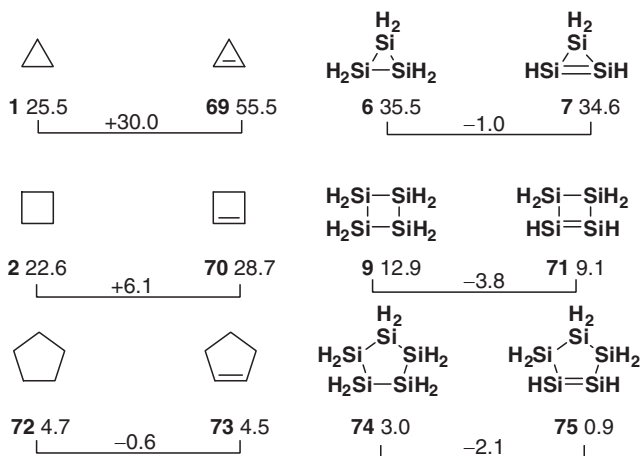
There is an interesting tendency of the ring strains of the large cage molecules. Persiladodecahedrane $Si_{12}H_{12}$ (SE = 32.3 kcal mol⁻¹) is less strained than the carbon congener, dodecahedron $C_{12}H_{12}$ (SE = 43.6 kcal mol⁻¹) [76, 77]. Low strain of silicon congener is more apparent for persilafullerane $Si_{60}H_{60}$ (SE = 114 kcal mol⁻¹) in comparison to fullerane $C_{60}H_{60}$ (SE = 530 kcal mol⁻¹) [78]. Interestingly, $M_{60}H_{60}$ (M=C, Si), where all the hydrogens are located outside of the cage, show the largest SEs per MH unit. Larger perhydrogenated fullerene or persilafullerene show lower energy per MH unit where some hydrogens are located inside of the cage [79].

4 Applications of the π -Relaxation

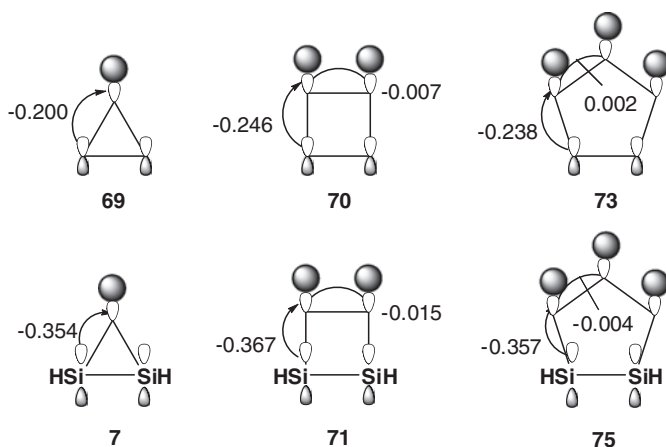
4.1 Cycloalkenes and Cyclopolysilenes

Strains of small ring molecules can be relaxed by the cyclic delocalization of π -electrons through the σ bonds on the saturated atoms in the ring (Scheme 8) [19]. The delocalization significantly occurs in the molecules with π and σ^* high and low in energy, respectively. The π relaxation is expected to be remarkable in cyclooligosilenes (e.g., **7**, **71**, **75**). The electron-donating π orbital of a Si=Si bond is higher in energy than that of a C=C bond, while an electron-accepting σ^*_{SiH} orbital is lower than a σ^*_{CH} orbital. In fact, it was confirmed by calculation at the B3LYP/6-311++G(3df,2p)//B3LYP/6-31G(d) level that cyclooligosilenes **7** [19], **71** and **75** (SE = 34.6, 9.1, and 0.9 kcal mol⁻¹) are less strained than the saturated analogs **6**, **9** and **74** (SE = 35.5, 12.9, and 3.0 kcal mol⁻¹), respectively (Scheme 30). These results show the appreciable relaxation of the strain of the monocyclic oligosilenes.

The π - σ^* interactions are found in Scheme 31 to stabilize **7** ($IBE_{\pi_{SiSi}-\sigma^*_{SiH}} = -0.354$ a.u.) more than **69** (-0.200 a.u.). This results from the high π -orbital energy (-0.278 a.u.) and low σ^* -orbital energy (0.442 a.u.) in **7** relative to the corresponding energies in **69** (-0.371 and 0.767 a.u.). Similar results were obtained for the



Scheme 30 Calculated SEs (in kcal mol⁻¹)



Scheme 31 Interbond energies (IBE/a.u.) in the unsaturated rings

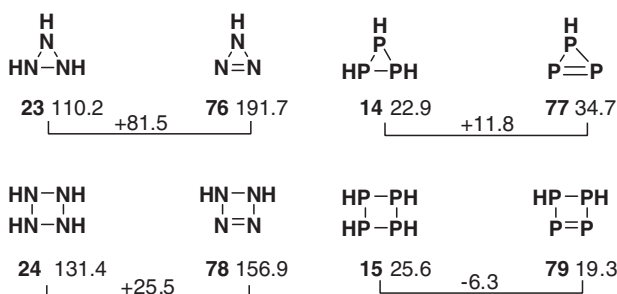
four-membered ring **71**. The delocalization between two σ^*_{SiH} orbitals in **71** is more bonding (IBE $_{\sigma^*_{\text{SiH}}-\sigma^*_{\text{SiH}}} = -0.015$ a.u.) than that between the σ^*_{CH} orbitals in **70** (IBE $_{\sigma^*_{\text{CH}}-\sigma^*_{\text{CH}}} = -0.007$ a.u.). The cyclic orbital interaction occurs more effectively in **71**. The $\pi-\sigma^*$ interaction in **75** is greater (IBE $_{\pi_{\text{CC}}-\sigma^*_{\text{CH}}} = -0.238$ a.u.) than that in **73** (IBE $_{\pi_{\text{CC}}-\sigma^*_{\text{CH}}} = -0.238$ a.u.). The $\sigma^*-\sigma^*$ interactions of the distant $\sigma_{\text{Si-H}}$ bonds are bonding in **75** (IBE $_{\sigma^*_{\text{SiH}}-\sigma^*_{\text{SiH}}} = -0.004$ a.u.), while they are antibonding in **73** (IBE $_{\sigma^*_{\text{CH}}-\sigma^*_{\text{CH}}} = 0.002$ a.u.).

Decrease of the SE in **71** is the largest of the three cyclopolysilenes. The cyclic (σ , σ , π^*) interaction is also favored by the orbital phase continuity [37] and effective

for the ring strain relaxation in addition to the cyclic (π , σ^* , σ^*) interaction in the four-membered ring with a double bond. Both of the mechanisms contribute to the largest relaxation in **71**.

4.2 Cyclic Unsaturated N_3H and P_3H Molecules

Three- and four-membered ring molecules of nitrogen and phosphorus are investigated (Scheme 32) [80]. The unsaturated four-membered ring molecule, tetracyclophosphene **79** is less strained than the saturated molecule, tetracyclophosphane **15**



Scheme 32 Calculated SE (in kJ mol^{-1}) at 0 K

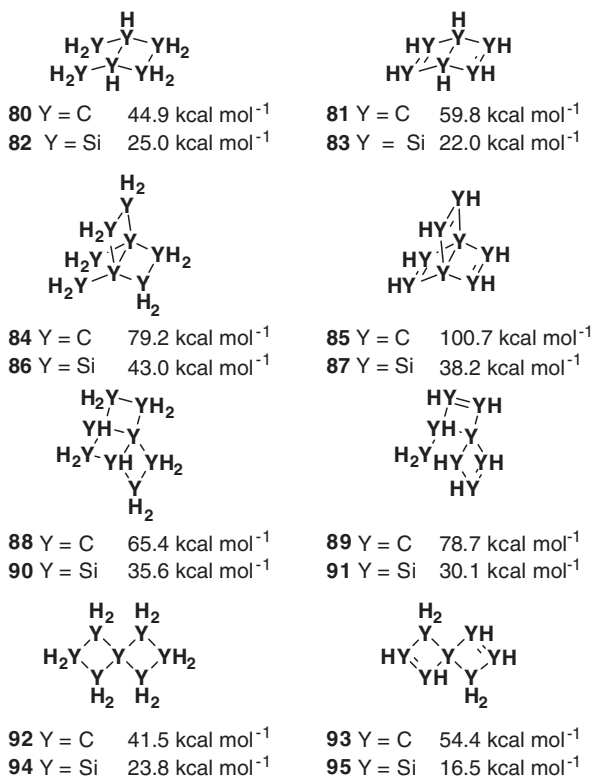
in agreement with the π -relaxation. For the three-membered ring, introduction of double bond increases the strain energies.

P_3H_3 **14** and P_3H **77** molecules are less strained than the nitrogen congeners. As mentioned earlier (Sect. 2.1.4), the lone pair on phosphorus atoms is richer in s-character. The lone pair effect on σ -relaxation is more remarkable.

Interestingly, tetrazetene **78** and tetracyclophosphene **79** are $6e$ π systems, but p-systems, but not planar, and saturated N and P atoms are pyramidalized. The lone pair must be pyramidalized to have high s character for the σ -relaxation.

4.3 Polycyclic Oligosilenes

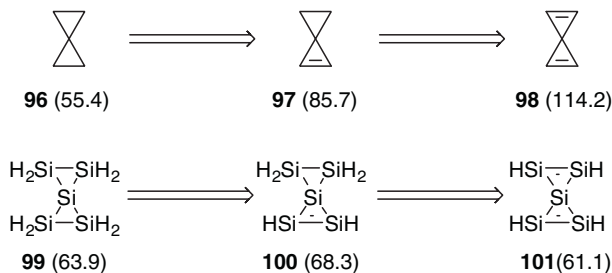
The strain of polycyclic oligosilenes was investigated (Scheme 33) [20]. Highly strained polycyclic molecules are synthetic targets because of unique chemical bonding and function. Some unsaturated silicon congeners have lower strain due to the π relaxation. They can be the next targets for the syntheses. Few experimental reports have appeared for the polycyclic silicon congeners studied here, whereas some carbon congeners have been synthesized.

Scheme 33 SEs of polycyclic molecules

4.4 Related Experimental Observations

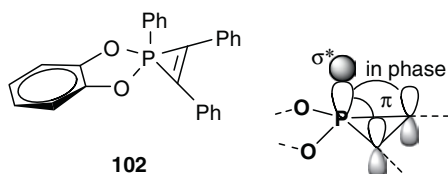
4.4.1 Spiropentasiladiene Derivatives

Kira reported the synthesis of a derivative of spiro[2.2]pentasiladiene **101** [5, 16]. The spiropentasiladiene derivative is stable with a melting point of 216–218 °C, whereas spiropentadiene **98** decomposes even below –100 °C [81]. The carbon congeners are more strained with introduction of the double bond(s), while the silicon derivatives possess almost the same SE (Scheme 34) [5].

**Scheme 34** SE (in parenthesis in kcal mol⁻¹) of spiropentane and spiropentasilane derivatives

4.4.2 Pentacoordinated 1*H*-Phosphirene

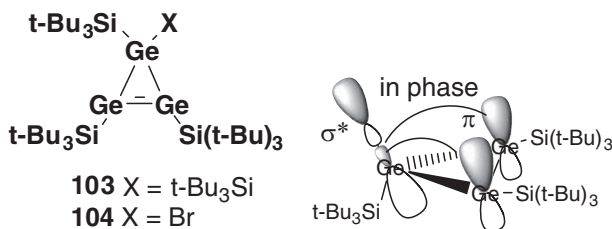
Kawashima reported the structure of 1-phenyl-1*H*-phosphirene **102** which has a distorted square-pyramidal structure (Scheme 35) [82, 83]. The observed elongation of the C=C bond has been interpreted in terms of the π - σ^* interaction in similar ways by Regitz [39] for cyclic phosphirene and by Clark [14] for phosphirenium ions **17**.



Scheme 35 π - σ^* interaction in **102**

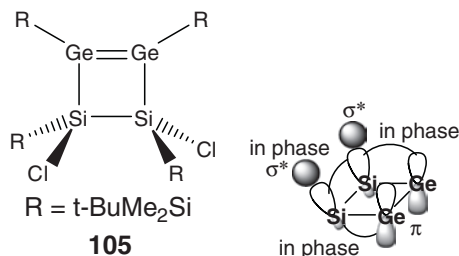
4.4.3 Trigermene and $^3\Delta$ -1,2,3,4-Disiladigermetene

Recently, Sekiguchi reported that substitution of silyl group with bromine resulted in the bond lengthening of the Ge=Ge double bond of the cyclotrigermene [84]. The bond lengths of the Ge=Ge bond in tetrakis(tri-*tert*-butylsilyl)cyclotrigermene **103** and 1-bromo-1,2,3-tris(tri-*tert*-butylsilyl)cyclotrigermene **104** are 2.239(4) Å and 2.2743(8) Å, respectively. The σ^* -orbital of the Ge-Br bond lower in energy than that of the Ge-Si enhances delocalization from π -bond (Scheme 36).



Scheme 36 π - σ^* Interactions more significant in **104** than in **103**

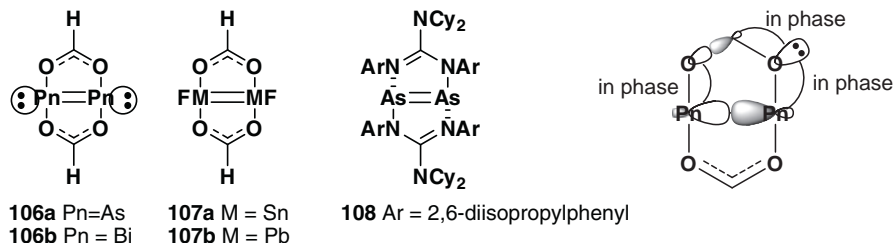
Sekiguchi also reported a synthesis of $^3\Delta$ -1,2,3,4-disiladigermetene **105** from tetra(*tert*-butyldimethylsilyl)disilagermetene [85–87]. The Ge=Ge double bond is the longest (2.2911 Å) among all known cyclic digermanes (2.239–2.274 Å). In contrast, the endocyclic Si-Ge bonds are very short (2.3576 and 2.3589 Å), shorter than the endocyclic Si-Si bond (2.372 Å). The Si-Cl bonds are elongated (2.133 and 2.135 Å), and are considerably longer than a normal Si-Cl bond (2.050 Å). Long Ge=Ge and Si-Cl bond lengths and short Ge-Si bond length resulted from the π -relaxation (Scheme 37).



Scheme 37 Cyclic (π , σ^* , σ^*) interaction in **105**

4.4.4 Design of Doubly Bonded Hypervalent Atoms

We have designed molecules **106** with a double bond between hypervalent atoms [88] by applying the lone pair effect (Sect. 2.1.4), and the pentagon stability [89, 90] (Chapter “Orbitals in Inorganic Chemistry” by Inagaki in this volume), together with the $4n + 2\pi$ electron rule for aromaticity. The pnictogen atoms have lone pairs which relax the strain by nearly 90° angles of O–Pn=Pn. The group 14 element molecules **107** has no lone pairs, and have been calculated to be unstable. The five-membered ring structures are stabilized not only by the pentagon stability (Scheme 38) but also by 6π electrons, i.e., $2e$ from the double bond, $4e$ from two lone pairs on the oxygens, and



Scheme 38 Pentagon stability by cyclic delocalization of a lone pair through vicinal σ bonds favored by the orbital phase continuity

vacant p orbital on C. In the same year, Jones and Stasch reported the synthesis of guanidinato-bridged As=As double bond **108** [91]. The structure, however, is not symmetrical. One N–As bond is covalent, the other is a coordination bond. The As atoms in molecule **108** are not taken as hypervalent atoms.

Acknowledgments The authors thank Ms. Jane Clarkin for her English suggestions.

References

1. von Baeyer A (1885) *Ber Dtsch Chem Ges* 18:2269
2. March J (1992) *Advanced organic chemistry*, 4th edn. Wiley, New York, pp 150–161
3. Cox JD, Plicher G (1970) *Thermochemistry of organic and organometallic compounds*. Academic, London
4. Baulder M, Hahn J, Clef E (1984) *Z Naturforsch* 39b:438
5. Iwamoto T, Tamura M, Kabuto C, Kira M (2000) *Science* 290:504
6. Liebman JF, Dolbier WR Jr, Greenberg A (1986) *J Phys Chem* 90:394
7. Nagase S (1989) *Angew Chem Int Ed Engl* 28:329
8. Dewar MJS (1979) *Bull Soc Chim Belg* 88:967
9. Cremer D, Kraka E (1985) *J Am Chem Soc* 107:3811
10. Inagaki S, Goto N, Yoshikawa K (1991) *J Am Chem Soc* 113:7144
11. Inagaki S, Yoshikawa K, Hayano Y (1993) *J Am Chem Soc* 115:3706
12. Inagaki S, Ishitani Y, Kakefu T (1994) *J Am Chem Soc* 116:5954
13. Naruse Y, Ma J, Inagaki S (2003) *J Phys Chem A* 107:2860
14. Goeller A, Heydt H, Clark T (1996) *J Org Chem* 61:5840
15. Goeller A, Clark T (2000) *J Mol Model* 6:133
16. Tsutsui S, Sakamoto K, Kabuto C, Kira M (1998) *Organometallics* 17:3818
17. Iwamoto T (2005) *Bull Chem Soc Jpn* 78:393
18. Kira M, Iwamoto T (2006) *Adv Organometal Chem* 54:73
19. Naruse Y, Ma J, Inagaki S (2001) *Tetrahedron Lett* 42:6553
20. Naruse Y, Ma J, Takeuchi K, Nohara T, Inagaki S (2006) *Tetrahedron* 62:4491
21. Cremer D (1988) *Tetrahedron* 44:7454
22. Bacharach SM (1989) *J Phys Chem* 91:7780
23. Musso GF, Magnasco V (1982) *J Chem Soc Faraday* 2 78:1609
24. Musso GF, Figari G, Magnasco V (1983) *J Chem Soc Faraday* 2 79:931
25. Musso GF, Figari G, Magnasco V (1983) *J Chem Soc Faraday* 2 79:1283
26. Musso GF, Magnasco V (1984) *Chem Phys Lett* 107:585
27. Musso GF, Magnasco V (1984) *Mol Phys* 53:615
28. Musso GF, Figari G, Magnasco V (1985) *J Chem Soc Faraday* 2 81:1243
29. Cameron DR, Thatcher GRJ (1993) In: Thatcher GRJ (ed) *The anomeric effect*. ACS Symposium 539, American Chemical Society, Washington DC, pp 256–276
30. Takahashi M, Sakamoto K (2004) *J Phys Chem A* 108:5710
31. Glendening ED, Reed AE, Carpenter JE, Weinhold F NBO program. University of Wisconsin (1975–1990)
32. Iwase K, Inagaki S (1996) *Bull Chem Soc Jpn* 69:2781
33. Inagaki S, Ikeda H (1998) *J Org Chem* 63:7820
34. Inagaki S, Goto N (1987) *J Am Chem Soc* 109:3234
35. Inagaki S, Kakefu T, Yamamoto T, Wasada H (1996) *J Phys Chem* 106:9615
36. Ikeda H, Inagaki S (2001) *J Phys Chem A* 47:10711
37. Fukui K, Inagaki S (1975) *J Am Chem Soc* 97:4445
38. Inagaki S, Fujimoto H, Fukui K (1976) *J Am Chem Soc* 98:4693
39. Ehle M, Wagner O, Bergstraesser U, Regitz M (1990) *Tetrahedron Lett* 31:3429
40. Bomse DS, Berman DW, Bauchamp JL (1981) *J Am Chem Soc* 103:3967
41. Zeiger DN, Liebman JF (2000) *J Mol Struct* 556:83
42. Inagaki S, Yamamoto T, Ohashi S (1997) *Chem Lett* 24:977
43. Fritz G, Wartanessian S, Matern E, Hoenle W, von Schering HG (1981) *Z Anorg Allg Chem* 475:87

44. Savin A, Flad H-J, Flad J, Preuss H, von Schering HG (1992) *Angew Chem Int Ed Engl* 31:185
45. Ermer O, Bell P, Scafer J, Szeimies G (1989) *Angew Chem Int Ed Engl* 28:473
46. Galasso V, Carmichael I (2000) *J Phys Chem A* 104:6271
47. Gassman PG, Greenlee ML, Dixon DA, Richsmeiere S, Gougoutas JZ (1983) *J Am Chem Soc* 105:5865
48. Iwamoto T, Yin D, Kabuto C, Kira M (2001) *J Am Chem Soc* 123:12730
49. Kira M (2004) *J Organometal Chem* 689:4475
50. Iwamoto T, Yin D, Boomgaarten S, Kabuto C, Kira M (2008) *Chem Lett* 37:520
51. Masamune S, Kabe Y, Collins S, Williams DJ, Jones R (1985) *J Am Chem Soc* 107:5552
52. Jones R, Williams DJ, Kabe Y, Masamune S (1986) *Angew Chem Int Ed Engl* 25:173
53. Schleyer PvR, Sax AF, Kalcher J, Janoschek R (1987) *Angew Chem Int Ed Engl* 26:364
54. Koch R, Bruhn T, Weidenbruch M (2004) *J Mol Struct (Theochem)* 680:91
55. Dabisch T, Schoeller WW (1986) *J Chem Soc Chem Commun* 896
56. Koch R, Bruhn T, Weidenbruch M (2005) *J Mol Struct (Theochem)* 714:109
57. Driess M, Pritzcow H, Reisgys M (1991) *Chem Ber* 124:1923
58. Driess M, Janoschek R, Pritzcow H (1992) *Angew Chem Int Ed Engl* 31:460
59. Driess M, Pritzcow H, Rell S, Janoschek R (1997) *Inorg Chem* 36:5212
60. Niecke E, Rueger R, Krebs B (1982) *Angew Chem* 94:553
61. Riedel R, Hausen H-J, Fluck E (1985) *Angew Chem Int Ed Engl* 24:1056
62. Schoeller WW, Staemmler V, Rademacher P, Niecke E (1986) *Inorg Chem* 25:4382
63. Schoeller WW, Lerch C (1983) *Inorg Chem* 22:2992
64. Beagley B, Conrad AR, Freeman JM Monogham JJ, Norton BG (1972) *J Mol Struct* 11:371
65. Jutzi P, Meyer U, Opeila S, Olmstead MM, Power PP (1990) *Organometallics* 9:1459
66. Takeuchi K, Uemura D, Inagaki S (2005) *J Phys Chem A* 109:8632
67. Sheshchekewitz D (2005) *Angew Chem Int Ed* 44:2954
68. Takeuchi K, Horiguchi A, Inagaki S (2005) *Tetrahedron* 61:2601
69. Rauscher G, Clark T, Poppinger D, Scheyer PvR (1978) *Angew Chem Int Ed Engl* 17:276
70. Dill JD, Greenberg A, Liebman JF (1979) *J Am Chem Soc* 101:6814
71. Sekiguchi A, Tanaka M (2003) *J Am Chem Soc* 125:12684
72. Busmann E (1961) *Z Anorg Allg Chem* 313:90
73. Witte J, Schnering HG (1964) 327:260
74. Buerger H, Eujen R (1972) *Z Anorg Allg Chem* 394:19
75. Janzon KH, Schaefer H, Weiss A (1970) *Z Anorg Allg Chem* 372:87
76. Nagase S, Kobayashi K, Kudo T (1994) *Main Group Metal Chem* 17:171
77. Nagase S (1995) *Acc Chem Res* 18:469
78. Linnolahti M, Karttunen AJ, Pakkanen TA (2006) *ChemPhysChem* 7:1661
79. Karttunen AJ, Linnolahti M, Pakkanen TA (2007) *J Chem Phys C* 111:2545
80. Glukhovtsev MN, Bach RD, Laiter S (1997) *Int J Quant Chem* 62:373
81. Billups WE, Haley MM (1991) *J Am Chem Soc* 113:5084
82. Sase S, Kano N, Kawashima T (2006) *J Org Chem* 71:5448
83. Kawashima T (2003) *Bull Chem Soc Jpn* 76:471
84. Sekiguchi A, Ishida Y, Fukaya N, Ichinohe M, Takagi N, Nagase S (2002) *J Am Chem Soc* 124:1158
85. Lee VY, Takanashi K, Ichinohe M, Sekiguchi A (2003) *J Am Chem Soc* 125:6012
86. Lee VY, Takahashi K, Nakamoto M, Sekiguchi A (2004) *Russ Chem Bull* 53:1102
87. Sekiguchi A, Lee VY (2003) *Chem Rev* 103:1429
88. Kameyama H, Naruse Y, Inagaki S (2007) *Organometallics* 23:5543
89. Ma J, Hozaki A, Inagaki S (2002) *Inorg Chem* 41:1876
90. Ma J, Hozaki A, Inagaki S (2002) *Phosphorus Sulfur Silicon* 177:1705
91. Green SP, Jones C, Jin G, Stasch A (2007) *Inorg Chem* 46:8

Orbitals in Inorganic Chemistry: Metal Rings and Clusters, Hydronitrogens, and Heterocycles

Satoshi Inagaki

Abstract A chemical orbital theory is useful in inorganic chemistry. Some applications are described for understanding and designing of inorganic molecules. Among the topics included are: (1) valence electron rules to predict stabilities of three- and four-membered ring metals and for those of regular octahedral M_6 metal clusters solely by counting the number of valence electrons; (2) pentagon stability (stability of five- relative to six-membered rings in some classes of molecules), predicted and applied for understanding and designing saturated molecules of group XV elements; (3) properties of unsaturated hydronitrogens N_mH_n in contrast to those of hydrocarbons C_mH_n ; (4) unusually short nonbonded distances between metal atoms in cyclic molecules.

Keywords Valence electron rule, Metal ring, Metal cluster, $4N + 2$ valence electron rule, $8N + 6$ valence electron rule, $6N + 14$ valence electron rule, Pentagon stability, Cyclopentaphosphane, Hydronitrogen, Polynitrogen, Triazene, 2-Tetrazene, Tetrazadiene, Pentazole, Hexazine, Nitrogen Oxide, Disiloxane, Disilaoxirane, 1,3-Cyclodisiloxane, Metallacycle, Inorganic heterocycle

Contents

1	Introduction.....	294
2	Valence Electron Rules.....	294
2.1	Three- and Four-Membered Atomic Rings.....	294
2.2	Alkali and Alkaline Earth Metals: $4N + 2$ Valence Electron Rule.....	299
2.3	Larger Rings: Preference for Small Rings.....	299
2.4	Regular Octahedrons of M_6 Clusters.....	300

S. Inagaki
Department of Chemistry, Faculty of Engineering, Gifu University, Yanagido,
Gifu, 501-1193, Japan
e-mail: inagaki@gifu-u.ac.jp

3	Pentagon Stability	302
3.1	Theory	302
3.2	Applications	303
4	Hydronitrogens and Polynitrogens	304
4.1	Triazene $\text{HN}=\text{NNH}_2$ and 2-Tetrazene $\text{H}_2\text{NN}=\text{NNH}_2$	305
4.2	Tetraazabutadiene (Tetrazadiene) $\text{HN}=\text{NN}=\text{NH}$	306
4.3	Pentazole RN_5 and Hexazine N_6	306
4.4	Nitrogen Oxides	307
5	Short Atomic Distances in Metallacycles	308
5.1	Small Ring Molecules Containing Si–O Bonds	309
5.2	Related Metallacycles	310
6	π -Conjugation in B–N and Related Systems	310
	References	312

1 Introduction

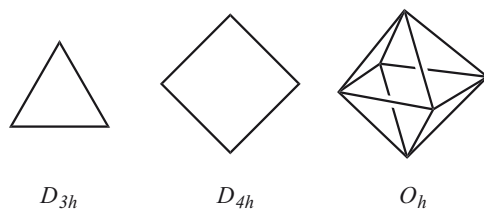
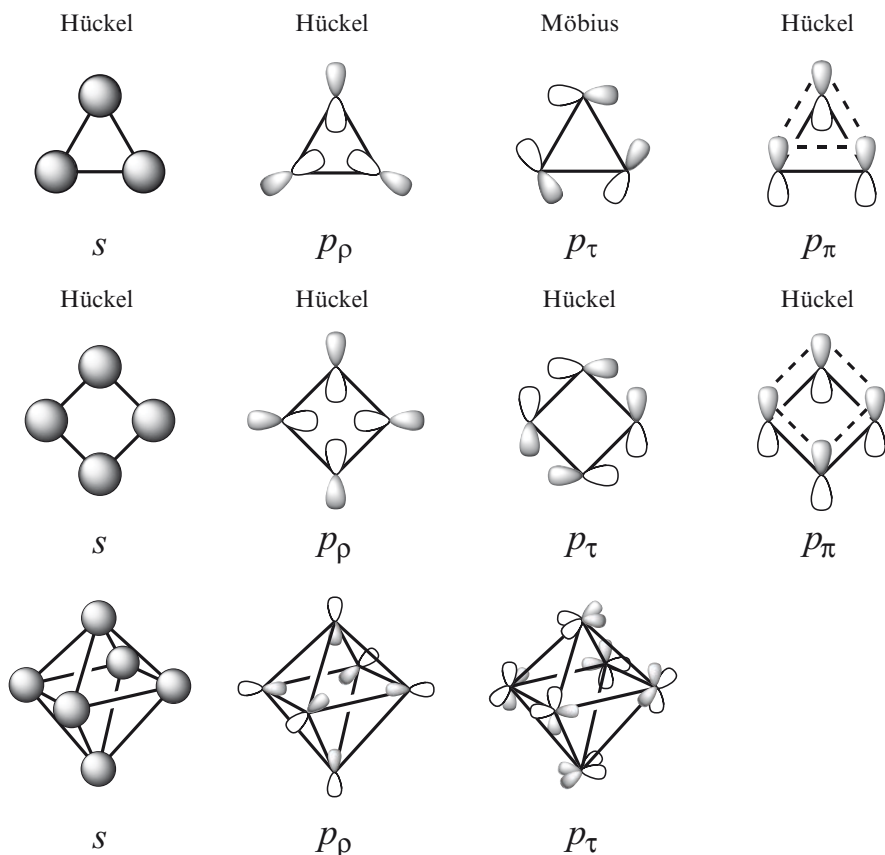
The importance of phase and amplitude of orbitals (wave property of electrons in organic molecules and reactions) has been reviewed in the preceding chapters of this volume. Our orbital theory is as powerful in inorganic chemistry as in organic chemistry for understanding and designing molecules and reactions. This is shown in this chapter by the description of topics on valence electron rules for stabilities of three- and four-membered metal rings and regular octahedral metal clusters, stability of five- relative to six-membered rings, unique molecular properties of unsaturated hydronitrogen and polynitrogens, and unusually short nonbonded distances between metal atoms in cyclic molecules.

2 Valence Electron Rules

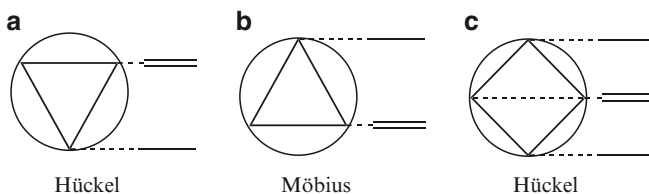
The number of valence electrons is important in chemistry. Useful related rules are the octet rule for first-row atoms in molecules [1], the 18 electron rule for transition-metal complexes [2], the Wade rule for clusters [3, 4], the Hückel rule for aromatic molecules [5], and the Woodward–Hoffman rule for organic reactions [6]. We review here the valence electron rules for three- and four-membered rings [7] and regular octahedrons [8] (Scheme 1) of high-row representative elements in the singlet states. Symmetries (D_{3h} , D_{4h} , and O_h) of these ring and polyhedron structures facilitate derivation of valence electron rules by allowing us to separate the basis set of atomic p -orbitals into radial (p_ρ), tangential (p_τ) and perpendicular (p_π) orbitals (Scheme 2).

2.1 Three- and Four-Membered Atomic Rings

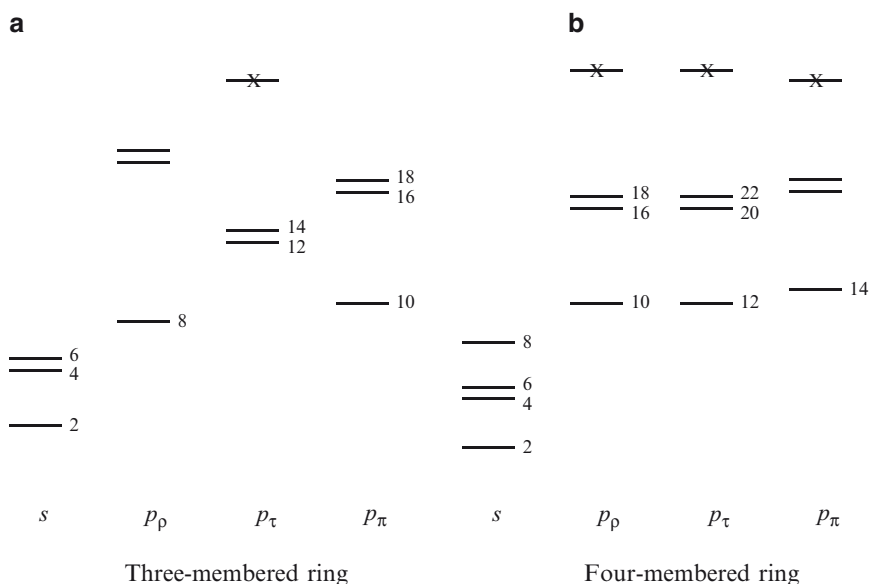
Valence electron rules have been theoretically proposed for three- and four-membered atomic rings [7]. The p_ρ , p_τ and p_π orbital arrays are of the Hückel or Möbius conjugation (Scheme 2) [9, 10]. The splitting patterns of the energy levels are well known

**Scheme 1** Symmetries of metal clusters for (ρ , τ , π) approach**Scheme 2** Hückel or Möbius conjugation of the arrays of s -orbitals and radial (p_ρ), tangential (p_τ), and perpendicular (p_π) p -orbitals

(Scheme 3). The qualitative energy levels (Scheme 4) show the number of valence electrons necessary to obtain closed-shell electronic structures. Each orbital in the s -orbital set is assumed to be occupied by a pair of electrons since the s -orbital energies are low and separate from those of the p -orbital ones, especially for heavy atoms. The total number of valence electrons for the closed-shell structures



Scheme 3 Energy splittings of three- and four-orbital arrays



Scheme 4 Orbital energy levels

is $4N+2$ for the three-membered rings and $8N+6$ for the four-membered rings [7]. The valence electron rules have been supported by ab initio calculations (Tables 1 and 2) [7].

2.1.1 $4N$ Valence Electron rule

$4N$ valence electrons do not allow regular polygons (D_{3h} and D_{4h}) as the ground states of trimers and tetramers [7].

There are no exceptions in Tables 1 and 2 [7]. For $4N$ electron systems, the singlet ground states of trimers and tetramers do not assume three- and four-membered ring structures of D_{3h} and D_{4h} symmetry, respectively.

Table 1 Ground state geometries of trimers^a

Number of valence electrons						
4N+2			4N			
10	14	18	8	12	16	20
Al ₃ ⁻ (<i>D</i> _{3h})	Si ₃ ²⁻ (<i>D</i> _{3h})	S ₃ (<i>C</i> _{2v})	Al ₃ ⁺ (<i>D</i> _{∞h})	Si ₃ (<i>C</i> _{2v})	P ₃ ⁻ (<i>D</i> _{∞h})	S ₃ ²⁻ (<i>C</i> _{2v})
Ga ₃ ⁻ (<i>D</i> _{3h})	Ge ₃ ²⁻ (<i>D</i> _{3h})	Se ₃ (<i>D</i> _{3h})	Ga ₃ ⁺ (<i>D</i> _{∞h})	Ge ₃ (<i>C</i> _{2v})	As ₃ ⁻ (<i>D</i> _{∞h})	Se ₃ ²⁻ (<i>C</i> _{2v})
	P ₃ ⁺ (<i>D</i> _{3h})				S ₃ ²⁺ (<i>C</i> _{2v})	
	As ₃ ⁺ (<i>D</i> _{3h})				Se ₃ ²⁺ (<i>C</i> _{2v})	

^aCalculated at the UB3LYP/6-31 + G(d) level [7]**Table 2** Ground state geometries of tetramers^a

Number of valence electrons								
4N+2					4N			
8N+2			8N+6					
10	18	26	14	22	12	16	20	24
Al ₄ ²⁺ (<i>D</i> _{∞h})	Si ₄ ²⁻ (<i>D</i> _{2d})	S ₄ ²⁻ (<i>C</i> ₂)	Si ₄ ²⁺ (<i>D</i> _{4h})	P ₄ ²⁻ (<i>D</i> _{4h})	Al ₄ (<i>C</i> _{2h})	Si ₄ (<i>D</i> _{2h})	P ₄ (<i>T</i> _d)	S ₄ (<i>D</i> _{2d})
Ga ₄ ²⁺ (<i>D</i> _{∞h})	Ge ₄ ²⁻ (<i>D</i> _{2d})	Se ₄ ²⁻ (<i>C</i> ₂)	Ge ₄ ²⁺ (<i>D</i> _{4h})	As ₄ ²⁻ (<i>D</i> _{4h})	Ga ₄ (<i>C</i> _{2h})	Ge ₄ (<i>D</i> _{2h})	As ₄ (<i>T</i> _d)	Se ₄ (<i>D</i> _{2d})
	P ₄ ²⁺ (<i>D</i> _{2d})		Al ₄ ²⁻ (<i>D</i> _{4h})	S ₄ ²⁺ (<i>D</i> _{4h})				
	As ₄ ²⁺ (<i>D</i> _{2d})		Ga ₄ ²⁻ (<i>D</i> _{4h})	Se ₄ ²⁺ (<i>D</i> _{4h})				

^aCalculated at the UB3LYP/6-31 + G(d) level [7]

Triphosphorus anion P₃⁻ (16e) was calculated to be linear (*D*_{∞h}). [11]. Honea et al. [12] prepared and isolated Si₄ (16e) by low-energy deposition into a solid nitrogen matrix, and carried out a Raman spectra study to show that Si₄ is a planar rhombus (*D*_{2h}). The Al₄⁴⁻ tetraanion (16e) stabilized by the three Li⁺ ions in the most stable structure of Li₃Al₄⁻ is rectangular in a capped octahedral arrangement [13].

2.1.2 4N+2 Valence Electron Rule

Equilateral triangles (D_{3h}) with 4N + 2 valence electrons in the singlet states are the ground states of trimers [7].

The rule is applicable to all but S₃ in Table 1 [7]. The most stable is thiozone (*C*_{2v}), whereas Se₃ has *D*_{3h} symmetry [14]. The lone pair repulsion may destabilize the S₃ ring and is weaker in the Se₃ ring due to the smaller overlap between the nonbonding orbitals.

Kuznetsov and Boldyrev [15] provided theoretical evidence that the B₃⁻, Al₃⁻, and Ga₃⁻ anions (10e) have geometrical (cyclic, planar) and electronic (two delocalized π electrons) properties to be considered as aromatic systems. Positive cations of all group XV trimers (14e), P₃⁺ As₃⁺ Sb₃⁺ and Bi₃⁺, have *D*_{3h} equilateral-triangular ground states [16].

2.1.3 $8N+2$ Valence Electron Rule

$8N+2$ valence electrons do not allow square (D_{4h}) as singlet ground states for tetramers.

The $8N+2$ rule has been completely substantiated by the calculated ground state geometries of tetramers in Table 2 [7]. The Al_4^{2+} cluster (10e) is linear ($D_{\infty h}$) [17]. The Si_4^{2-} cluster (18e) has a butterfly structure (D_{2d}) [18].

2.1.4 $8N+6$ Valence Electron Rule

Square structures with $8N+6$ valence electrons are the ground states of tetramers.

The $8N+6$ valence electron rule has been completely substantiated by the calculated four-membered species in Table 2 [7]. Boldyrev, Wang, and their collaborators presented experimental and theoretical evidence of aromaticity in the Al_4^{2-} [19] Ga_4^{2-} [20], In_4^{2-} [20] and isoelectronic heterosystems, XAl_3 [21]. The Al_4^{2-} unit (14e) was found to be square planar and to possess two π electrons, thus conforming to the $(4n+2)$ π electron counting rule for aromaticity. The π electron counting rule would be more powerful if we could predict the number of π electrons of metal atomic rings in an unequivocal manner. Our $8N+6$ electron rule only requires the number of valence electrons in Al_4^{2-} , which is easy to count.

Sundholm and co-workers [22] showed that (1) the square-shaped Al_4^{2-} ring sustains a very large diatropic ring current in an external magnetic field; (2) the group XIII analogs, B_4^{2-} , Ga_4^{2-} , In_4^{2-} , and Tl_4^{2-} also exist and have D_{4h} symmetry. Fowler and co-workers [23] found that σ electrons rather than π electrons contribute to the delocalized diamagnetic current in Al_4^{2-} induced by a perpendicular magnetic field shielding and concluded that Al_4^{2-} is both σ - and π -aromatic. Zhan et al. [24] theoretically emphasized the importance of the number of σ electrons as well as that of π electrons for unusual stability of Al_3^- and Al_4^{2-} .

The Si_4^{2+} cluster (14e) was shown to be square-planar (D_{4h}) analogous to the Al_4^{2-} cluster [25].

The ground states of P_4^{2-} [26, 27] and As_4^{2-} [28] have D_{4h} structures. Molecular orbital analysis revealed that the square planar P_4^{2-} dianion exhibits the characteristic of π -aromaticity with six π -electrons [29]. The term lone pair aromaticity was proposed for P_4^{2-} [30]. Wang, Boldyrev, and their co-workers [26] presented theoretical and experimental evidence for the square-planar structures of $\text{Na}^+\text{Pn}_4^{2-}$ ($\text{Pn} = \text{P, As, Sb}$). The Sb_4^{2-} [31] and Bi_4^{2-} [32] dianions were prepared and shown to be square-planar (D_{4h}).

The structures of the ground states of the S_4^{2+} [33, 34] and As_4^{2+} [35] dications (22e) have D_{4h} symmetry.

Although initially the aromaticity of Al_4^{2-} was attributed to the two π electrons, [19] it is now recognized that the contribution to aromaticity coming from the four σ electrons is more important than that from the π electrons [36–39].

2.2 Alkali and Alkaline Earth Metals: $4N + 2$ Valence Electron Rule

The s -orbital array of three and four-membered rings is of the Hückel conjugation. (Scheme 2). The splitting patterns of the orbital energy levels (Scheme 3) show that the total number of valence electrons for the closed-shell structures is $4N + 2$ for the three- ($N=0$) and four-membered rings ($N=0, 1$).

2.2.1 Three-Membered Rings

The simplest metal cluster Li_3 with two electrons ($N=0$) is known to have a triangular structure (D_{3h}) as its global minimum, whereas Li_3 of four electrons is linear [40].

The structure of the most stable, singlet states of Be_3 with $4N + 2$ valence electrons ($N=1$) is an equilateral triangle [41]. The Mg_3 [42] clusters (6e) is a van der Waals complex of D_{3h} symmetry. All of the three bonding and antibonding molecular orbitals are occupied by a pair of electrons. No bonding nature can appear between the atoms. The electronic structure is represented by three lone pairs in the s -orbitals. This is the reason the $4N + 2$ valence electron rule is applicable only for $N=0$ in the case of three-membered rings. Mixing-in of p -orbitals significantly contributes to the D_{3h} structures.

2.2.2 Four-Membered Rings

The Li_4^{2+} dication with two electrons ($4N + 2$, $N=0$) adopts a tetrahedral structure [42]. The single molecular orbital composed of four s -orbitals at the lowest energy level in the tetrahedron is lower than that in the square. The number of the in-phase relations between the s -orbitals is greater in the tetrahedron.

The global minimum of a neutral Li_4 molecule with $4N$ valence electrons ($N=1$) does not adopt a square structure (D_{4h}) but a rhombus structure (D_{2h}) [43]. The Raman spectroscopy supported the rhombic structure for the Li_4 [44], Na_4 and K_4 clusters [45, 46].

The Mg_4^{2+} dication [42] with $4N + 2$ ($N=1$) valence electrons has a stable D_{4h} structure in agreement with the rule, but this is a local energy minimum. The linear structure is more stable because it minimizes the Coulomb repulsion. This is in contrast to the tetrahedral structure of the Li_4^{2+} dication with two electrons ($N=0$). The six electron systems cannot form closed-shell structures in the tetrahedron, but the two electron systems can do.

2.3 Larger Rings: Preference for Small Rings

π Bonds between heavy atoms are well known to be unstable relative to σ bonds. *Large monocyclic rings tend to transform into polycyclic structures by forming stable σ bonds between unstable π bonds.*

Density functional calculations showed transitions from planar to nonplanar structures at $n = 5$ with increasing size of Al_n and Ga_n clusters [47]. Both Si and Al tend to build three-dimensional structures rather than two- or one-dimensional structures, except for $n = 3$ or 4 [48].

The planar cyclic P_5^- anion isoelectronic with cyclopentadienyl anion has been prepared in the form of M^+P_5^- salts ($\text{M} = \text{Li}, \text{Na}$) by Baudler et al. [49]. The pentaphosphole anion P_5^- favors planar D_{5h} geometry [50] while the most stable structure of P_5^+ is square-pyramidal [51]. The negatively charged pentamers Sb_5 and Bi_5 are planar rings [52, 53].

2.4 Regular Octahedrons of M_6 Clusters

There are Wade rules for metal clusters, [3, 4] which have been extended by Teo [54, 55], Mingos [56, 57], and Jemmis [58, 59]. These general rules give only a *single* number of electrons for a given polyhedron to be stabilized. The valence electron rules for the three- and four-membered metal rings in the singlet states (Sects. 2.1, 2.2) suggested that there could be more than one number of electrons. A valence electron rule was recently proposed for the regular octahedron of high-row representative elements in the singlet states [8].

Atomic orbitals are separated into the s -orbitals, the radial (ρ), and tangential (τ) p -orbitals (Scheme 2) [7]. The Hückel theory was applied to the s -orbitals, the radial (ρ), and tangential (τ) p -orbitals of the regular octahedron. The qualitative energy levels (Scheme 5) [8] show that the number of valence electrons is $6N + 14$ for the closed-shell structures when all the s -orbitals are occupied by two electrons. The t_{1u} p -orbitals at the nonbonding level are allowed to interact with the bonding p_τ -orbitals of the same symmetry and are raised in energy above the nonbonding level. The upper limit of the number of electrons is 26 ($N = 2$).

The M_6 clusters with $6N + 14$ ($N = 0-2$) valence electrons assume regular octahedrons, whereas those with the other numbers of valence electrons do not.

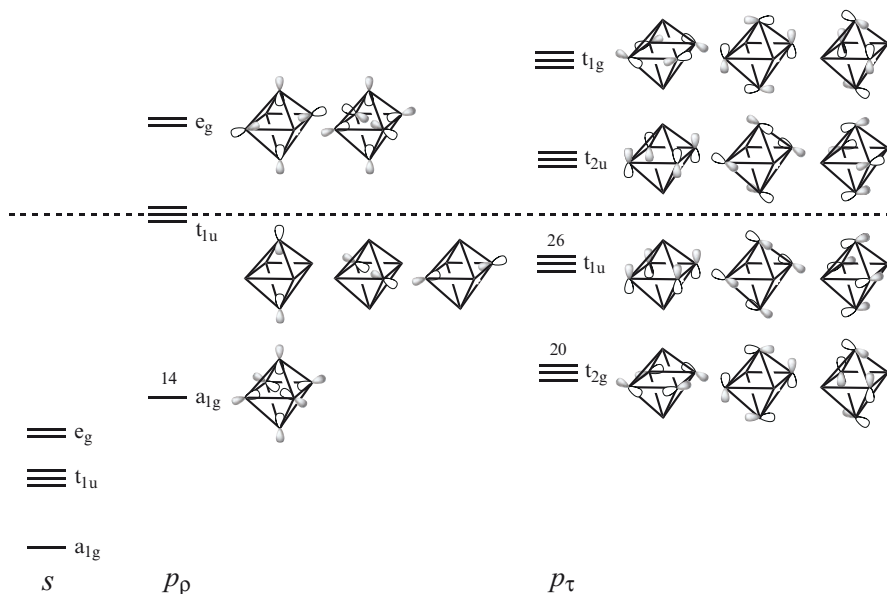
The $6N + 14$ ($N = 0-2$) valence electron rule was supported by the results of the calculations of the M_6 clusters of the third and fourth row elements at the UB3LYP/6-31 + G(d) (Table 3) [8]. The regular octahedrons were located as the energy minima for the 14 ($N = 0$) electron systems, Mg_6^{2-} and Ca_6^{2-} , for the 20 ($N = 1$) electron system, Al_6^{2-} , and for the 26 ($N = 2$) electron systems, Si_6^{2-} and Ge_6^{2-} . No energy minima were located for the regular octahedrons with $6N + 14$ ($N \geq 3$) or the other numbers of valence electrons than $6N + 14$.

The $6N + 14$ valence electron rule is based on the assumption that neighboring p_ρ -orbitals interact with each other more strongly than neighboring p_τ -orbitals, or that the a_{1g} p_ρ -orbital is lower in energy than the t_{2g} p_τ -orbitals (Scheme 5). When the interactions occur to a similar degree, the octahedral geometry of the 20 ($N = 1$) electron systems is unstable. When the interaction between the p_τ -orbitals is stronger, the regular octahedron prefers 18 and 20 ($N = 0, 1$) valence electron systems. The relative magnitudes of the interactions between the p_ρ - and p_τ -orbitals depend on the atoms.

Table 3 Number of valence electrons and regular octahedrons^a

14	16	18	20	22	24	26	28	30	32	34	36	38
Mg ₆ ²⁻	Al ₆ ²⁺	Al ₆	Al ₆ ²⁻	Si ₆ ²⁺	Si ₆	Si ₆ ²⁻	P ₆ ²⁺	P ₆	P ₆ ²⁻	S ₆ ²⁺	S ₆	S ₆ ²⁻
+	-	-	+	-	-	+	-	-	-	-	-	-
Ca ₆ ²⁻	Ga ₆ ²⁺	Ga ₆	Ga ₆ ²⁻	Ge ₆ ²⁺	Ge ₆	Ge ₆ ²⁻	As ₆ ²⁺	As ₆	As ₆ ²⁻	Se ₆ ²⁺	Se ₆	Se ₆ ²⁻
+	-	-	-	-	-	+	-	-	-	-	-	-

^aThe success and the failure in locating the regular octahedral geometries as energy minima at the UB3LYP/6-31 + G(d) levels are denoted by the plus (+) and minus (-) signs, respectively

**Scheme 5** Orbital energy levels of the regular octahedron

The Al₆²⁻ and Ga₆²⁺ dianions have 20 (= 6 × 1 + 14) valence electrons and satisfy the 6*N* + 14 valence electron rule. The Al₆²⁻ dianion possesses an O_h geometry [60]. Wade rules are not applicable to the stable O_h geometry of Al₆²⁻. The instability of the O_h geometry of Ga₆²⁺ in disagreement with the rule can be attributed to similar magnitudes of the interaction between the *p_ρ*-orbitals and that between the *p_τ*-orbitals which gives a very small HOMO-LUMO gap [8].

According to the 6*N* + 14 valence electron rule, the regular octahedron is not stable for 18 (= 4 + 14) electron systems. The most stable forms of Al₆ [47, 48, 61] and Ga₆ [47] were calculated to be distorted octahedrons. However, the result of the calculation by Pettersson et al. [62] showed the regular octahedron as the most stable structure of Al₆, suggesting a reverse ordering of the strength of the neighboring *p_τ*- and *p_ρ*-orbital interactions or the energy levels of the a_{1g} *p_ρ*-orbitals above the t_{2g} *p_τ*-orbitals.

The 24 (10 + 14) electron systems cannot be of O_h geometry. Honea et al. [12] prepared and isolated Si₆ by low-energy deposition into a solid nitrogen matrix, and showed by Raman spectroscopy that the octahedron is distorted, in agreement with

the rule. The tetragonal bipyramid (D_{4h} symmetry) was computed by Zhao and Balasubramanian as the ground states of the Si_6 [63] and Ge_6 clusters [64], in accord with the suggested experimental assignments by Fuke et al. [65, 66].

For 26 ($6 \times 2 + 14$) electron systems, a regular octahedron (O_h) is predicted to be stable. However, the Ge_6^{2-} dianion has been observed to assume a distorted octahedron (D_4) in [$\{(\text{CO})_5\text{Cr}\}_6\text{Ge}_6\{\text{P}(\text{C}_6\text{H}_5)_4\}_2$] [67]. The distortion may be caused by the effects of the ligands and cannot be taken as evidence against the prediction.

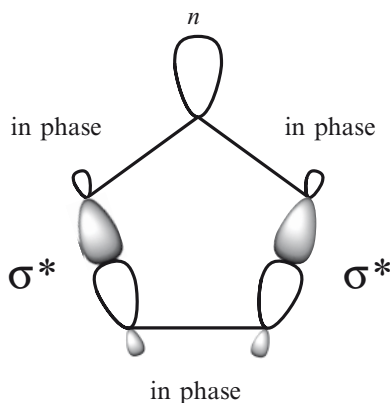
The octahedron is classified into the *closo*-structure by Wade [3,4]. Closo-structures with n skeletal atoms are stable when they have $4n + 2$ valence electrons. Wade's rules predict that the 26 ($= 4 \times 6 + 2$) valence electrons could stabilize the regular octahedrons since n is 6 for the octahedron. This prediction is contained in our $6N + 14$ ($N = 2$) valence electron rule. Our rule also predicts the stability of octahedral metal clusters with the other numbers (14 and 20) of valence electrons.

3 Pentagon Stability

For hydrocarbons, six-membered rings are thermodynamically preferred whether they are saturated or unsaturated. Cyclohexane is free from ring strain. Benzene is stabilized by cyclic delocalization of six π electrons. Here we show that five-membered rings are more stable in a class of molecules. This is termed pentagon stability. We apply the pentagon stability to understanding some interesting chemical phenomena of five-membered ring molecules and to designing some polycyclic molecules stable with little ring strain.

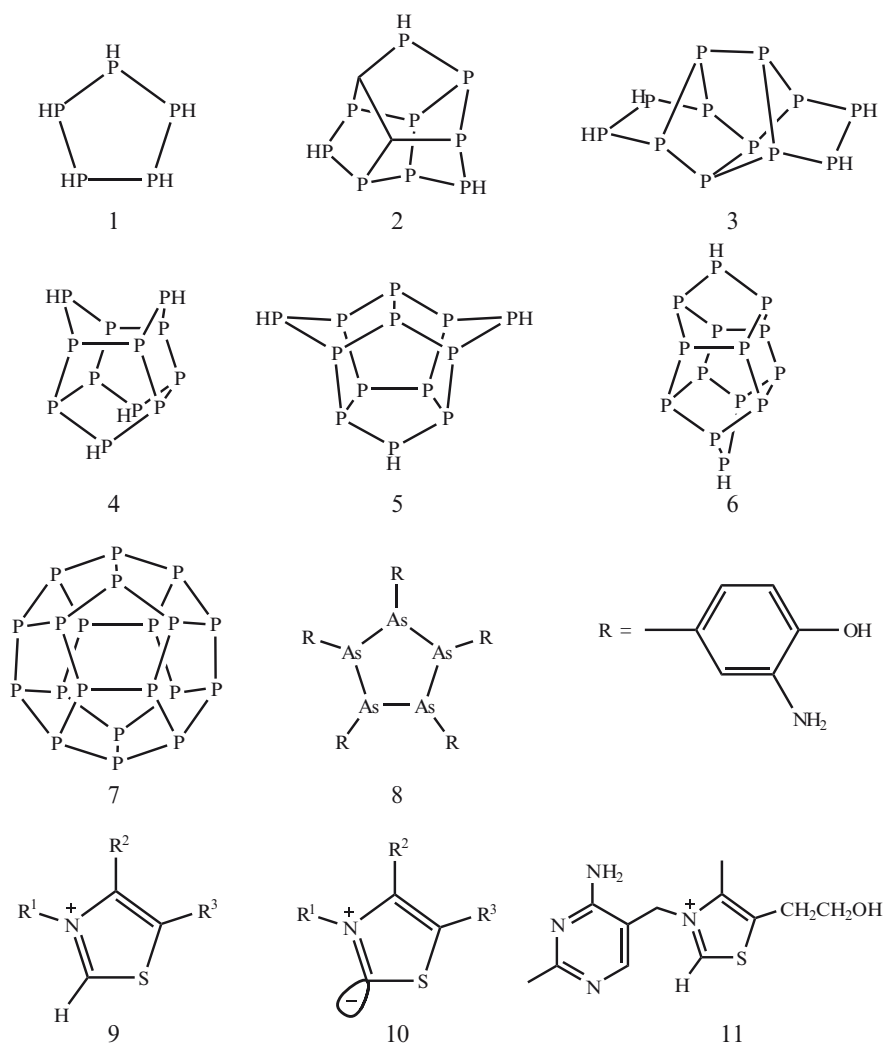
3.1 Theory

The orbital phase theory (Chapter "An Orbital Phase Theory" by Inagaki in this volume) shows that some saturated cyclic molecules with lone pairs on the ring



Scheme 6 Phase continuity of the n , σ , and σ^* orbitals for cyclic delocalization of a lone pair

atoms could prefer the five- to six-membered ring [68]. Cyclic delocalization of the lone pair electrons on the five-membered ring atoms through the vicinal σ bonds is favored by the orbital phase properties (Scheme 6). The resulting stability is outstanding in the saturated phosphorus five-membered rings in the puckered conformation (Scheme 7). The five-membered ring molecule **1** has a *negative* ring strain energy [68–70]. The stability of the five- relative to six-membered phosphorus rings was also noted elsewhere [71].



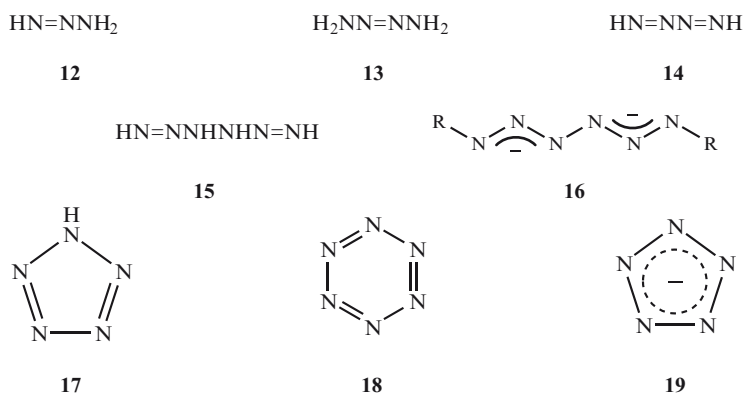
Scheme 7 Cyclopentaphosphane and its related molecules

3.2 Applications

The stability of cyclopentaphosphanes (PR_5) is in agreement with some experimental observations by Baudler [72–74]. The parent compound $(\text{PH})_5\mathbf{1}$ has been isolated and characterized by spectroscopic methods, while the six-membered ring molecule P_6H_6 is still unknown. The pentagon stability is in agreement with the Baudler rule of the maximum number of five-membered ring units [72–74]. The strain energies of **2** and **3** are *negative* [68]. Two stable conformers exist in solution [74]. The derivatives are known. Many polycyclic phosphanes containing the five-membered ring units are derived from the structure rule by Häser [75, 76]. The unknown polycyclic phosphanes **4–6** have low strain energies [68] due to having many puckered pentagon units in them and can be synthetic targets. The low stability of the dodecahedron P_{20} (**7**) was suggested by the high strain energy due to its planar pentagon units [68]. The relative stability of the five-membered rings is significant in the saturated As ring molecules [77] but not in the saturated nitrogen ring molecules [68] due to the greater energy gap between the n and σ^* orbitals.

A textbook error of the structure $\text{RAS} = \text{AsR}$ of salvarsan, asphenamine, Ehrlich 606 [78] has been revised. The main component has a structure of a five-membered As ring (**8**) [79], which is favored by the pentagon stability.

The pentagon stabilization has been found in a biochemical phenomenon [80]. The hydrogen on the thiazolium ring **9** (Scheme 7) is easily ionized to afford the corresponding carbene **10**, a key catalyst in enzymatic reactions for which thiamine (vitamin B-1, **11**) pyrophosphate is the cofactor. The pentagon stability is expected to contribute to this unusual deprotonation. A lone pair generated on the carbon atom in **10** can similarly delocalize through the vicinal C–N and C–S σ bonds in a cyclic manner.



Scheme 8 Hydronitrogens and polynitrogens

4 Hydronitrogens and Polynitrogens

Nitrogen atoms can form molecules isoelectronic to hydrocarbons (Scheme 8). Hydronitrogens N_mH_n are well known to have unique and useful properties. The smallest hydronitrogen is ammonia (NH_3) containing no N–N bond. Hydrazine NH_2NH_2 and diazene $NH=NH$ with one N–N bond (the former a single bond, the latter a double) are widely used to reduce unsaturated functional groups in organic molecules [81]. Hydronitrogens and/or their derivatives with the three nitrogen atoms sequentially bonded (triazane NH_2NHNH_2 , [82] triazene $NH_2NH=NH$ **12** [83] and hydrazoic acid HN_3 [84], are known. For hydronitrogens with four nitrogen atoms sequentially bonded, 2-terazene $NH_2NH=NHNH_2$ **13** [85] has been isolated. Tetrazane $NH_2NH_2NH_2NH_2$ [86] and tetrazadiene $NH=NN=NH$ **14** [87] have been postulated as reaction intermediates. The first pentazole was synthesized as a phenyl derivative of **17** in 1954 [88]. Very recently, unstable HN_5 , the parent pentazolic acid, has been released in solution by the treatment of *N*-(*p*-anisyl)pentazole with cerium(IV) ammonium nitrate [89].

Polynitrogens N_m are recently of great interest as high-energy density materials [90, 91]. The high-energy content arises from an unusual property of nitrogen: its single and double bond energies are considerably less than one-third and two-thirds, respectively, of its triple bond energy. Therefore, the decomposition of polynitrogen species to N_2 is accompanied by a large release of energy. Beyond N_2 , N_3^- , N_3^+ [92], N_4^+ [93], and diazidyl N_6^- complex [94] have been spectroscopically detected as short-lived species. Hexazine N_6 **18** isoelectronic to benzene was suggested to be a product of photochemical reductive elimination of *cis*-diazidobis(triphenylphosphine) platinum(II) in solution at 77 K [95].

The chemistry of hydronitrogens [96] and polynitrogens [90, 91] is still less advanced than the chemistry of hydrocarbons. Unknown hydronitrogens may also be of potential utility as the known hydronitrogens suggest. There are many questions to be answered about the chemical and physical properties of hydronitrogens and polynitrogens. In this section, we briefly review the chemistry of some hydronitrogens and polynitrogens, including the fundamental nature of chemical bonding between the nitrogen atoms and recent advances.

4.1 Triazene $HN=NNH_2$ and 2-Tetrazene $H_2NN=NNH_2$

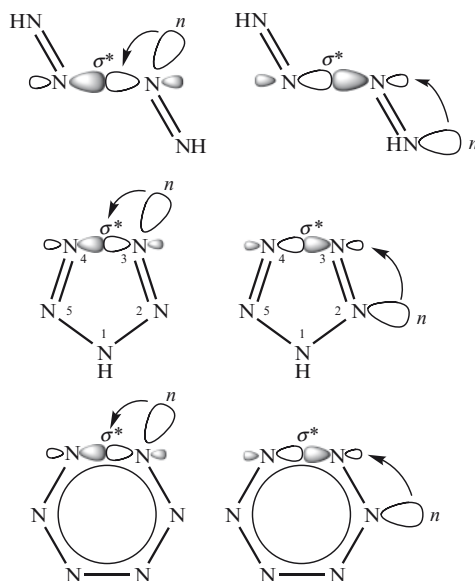
The delocalization of lone pair electrons on NH_2 group to an adjacent $N=N$ bond was suggested by some calculations [97] to be appreciable in triazene **12** and 2-tetrazene **13**. The N–N single bond is shorter than the isolated N–N single bond in NH_2NH_2 . The $N=N$ bond is longer than in $NH=NH$. The $n-\pi$ conjugation stabilizes hydronitrogens.

There are six π electrons in **13**. The delocalization of six π electrons in the four *p*-orbitals of the linear conjugation is disfavored by the orbital phase discontinuity

(Sects. 2.1 and 3.1 in Chapter “A Orbital Phase Theory” by Inagaki in this volume) [98, 99]. The $n-\pi$ conjugation is weaker relative to that in **12** where a similar phase restriction is absent. In fact, the rotational barriers about the single RNH-NH=bond have been observed to be lower for derivatives of **13** than for those of **12** [100].

4.2 Tetraazabutadiene (Tetrazadiene) $\text{HN}=\text{NN}=\text{NH}$

The geometry optimization and the analysis of electronic structure [97] suggested that the single N–N bond could be unusually weak in tetraazabutadiene (tetrazadiene) **14**.



Scheme 9 Electron donation from lone pairs weakening the single bond

The $\sigma_{\text{N-N}}$ -bond is weakened by the acceptance of electrons in the antibonding orbital $\sigma_{\text{N-N}}^*$ from geminal lone pairs on the inner nitrogen atoms as well as vicinal lone pairs on the terminal nitrogen atoms (Scheme 9). The electron donation from the geminal lone pairs occurs more readily in unsaturated hydronitrogens than in saturated ones. The interaction between sp^2 orbitals on the same atom is stronger than that between sp^3 orbitals since sp^2 has a high s-character [97] (For the importance of the interaction between the geminal σ -bonds, see Chapter “Relaxation of Ring Strain” by Naruse and Inagaki in this volume).

Hexaaza-1,5-dienes $\text{RN}=\text{NNRN}=\text{NR}$, derivatives of **15** [96], are unusual high-energy molecules. Very recently, Cowley, Holland, and co-workers [101] fairly well stabilized the dianion RN_6R^{2-} **16** as a ligand in a transition metal complex. These species are stabilized by such conjugations as those in allyl anions, which are special conjugations of the $n-\pi$ conjugations.

4.3 Pentazole RN_5 and Hexazine N_6

The effects of cyclic 6π electron conjugation have been found in the optimized geometries of pentazole **17** [102] and hexazine **18** [97]. The N=N bond is longer than the isolated double bond in NH=NH. The N–N single bond in the tetrazadiene moiety is shorter than the single bond in NH_2NH_2 . The bond lengths in **18** are nearly intermediate between those in NH_2NH_2 and NH=NH. The aromatic character of pentazoles was supported by the effect of electron donating substituents on the thermodynamic and kinetic stabilization [103].

Analysis suggested that cyclic delocalization could, however, occur in **17** and **18** to a lesser extent than in pyrrole and benzene, respectively [97]. This suggests low aromaticity of **17** and **18**. Donation from sp^2 lone pairs (Scheme 9) weakens the N–N (sp^2 – sp^2) single bonds in the cyclic conjugated hydronitrogens and polynitrogens.

A recent theory of pentagon stability [68, 77] suggests thermodynamic stability of **17** and **18** relative to hexazine. Lone pair electrons in the molecular plane are promoted by the orbital phase continuity to delocalize in a cyclic manner through σ bonds of five-membered rings (Scheme 6). The n - π conjugations also contribute to the relative stability of **17**.

The kinetic stability of **17** increases on deprotonation. The half-life times of **17** and its anion N^{5-} **19** have been estimated [104] from the observed [105, 106] and computed free energy to be only 10 min and 2.2 days, respectively. The high kinetic stability of the anion **19** can be understood in terms of enhanced pentagon stability and aromaticity. The deprotonation raises the energy of lone pair orbitals and promotes cyclic delocalization of σ - and π -electrons.

The kinetic stability of pentazole has been estimated by the activation energy of decomposition or retro-[3 + 2]-cycloaddition reaction of 19.8 kcal mol⁻¹ [107] and 19.5 kcal mol⁻¹ [108] with a half-life of only 14 s at 298 K [108].

The anion **19** has been generated by high-energy collision of the *p*-pentazolylphenolate anion with an inert gas [109] and by laser desorption ionization time-of-flight mass spectroscopy of solid *p*-dimethylaminophenylpentazole [110]. N_5AsF_6 , N_5SbF_6 , and $[N_5]_2SnF_6$ have been used by Gordon, Christie et al. [111] in their attempt to observe N_5F .

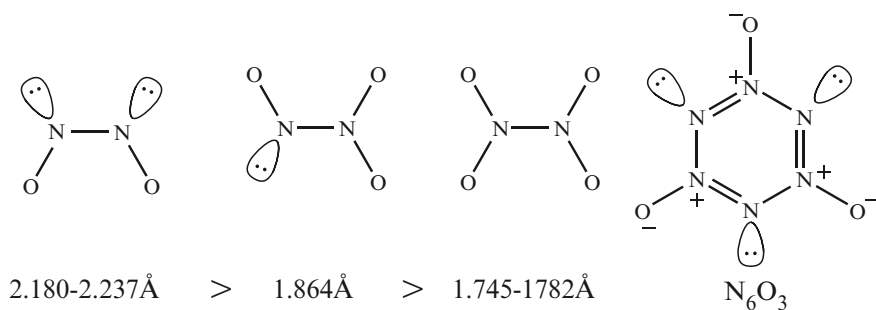
Notable in the series of homoleptic polynitrogen systems is the absence of the N_6 ring. The structure of hexaazabenzene strongly depends on the choice of theoretical model and basis set: D_{6h} , [97] D_2 [112], van der Waals type structure of two N_3 units [113]. There is a common recognition that open chain hexaazadiazide lies on the global minima of the potential energy surface.

The planar hexagons of P_6 [114] and As_6 [115] have the highest energies of the five valence isomers.

The chemistry of binary nitrogen compounds is currently a topic of intensive investigations. Polynitrogen ion N_5^+ was synthesized 10 years ago [116] as the second homonuclear polynitrogen species after N_3^- [117]. The first structural characterization of hexaazidoarsenate anion $As(N_3)_6^-$ [118] was another highlight of the synthetic efforts. Frenking et al. [119] proposed that iron bispentazole could be a promising target for synthesis.

4.4 Nitrogen Oxides

Dinitrogen dioxide ONNO is an isoelectronic molecule of **14**. If the similar effects of lone pairs are predominant, the N–N bond is weak and long. In fact, the observed bond length is 2.180 Å in the solid phase [120] and 2.237 Å in the gas phase [121]. The dissociation energy is very low (1.6 kcal mol⁻¹) [122]. The N–N atomic distances of nitrogen oxides support the importance of the geminal lone pairs relative to the vicinal lone pairs (Scheme 10). Dinitrogen trioxide ONNO₂ and dinitrogen tetroxide O₂NNO₂ have one and two less geminal lone pairs and two and four more vicinal lone pairs than ONNO. The N–N distance decreases in the order of ONNO > ONNO₂ [123] > O₂NNO₂ [124]. The still remaining long N–N bond in O₂NNO₂ without any geminal lone pairs on the nitrogen atoms supports the effect of vicinal lone pairs predicted for **14** [97] and proposed for O₂NNO₂ [125].

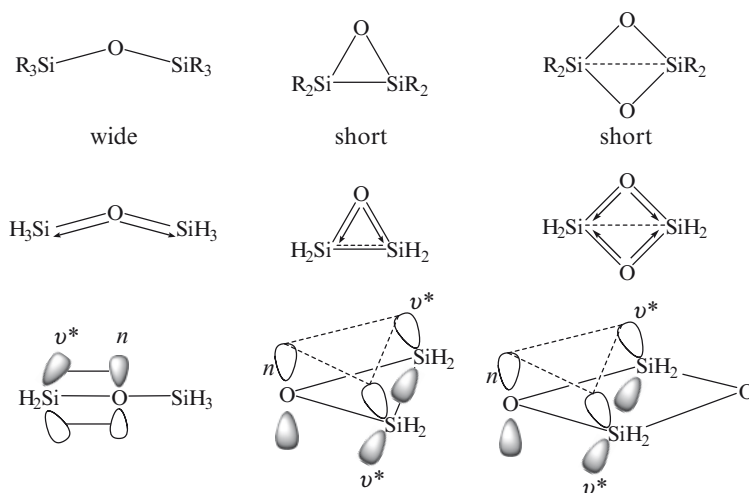


Scheme 10 Nitrogen oxides and N₆O₃

The results of calculations of N₆O₃ (Scheme 10) by Bartlett et al. [126] are in agreement with the prediction [97] that donation from nitrogen lone pairs weakens the geminal N–N single bonds in the hydronitrogens and polynitrogens. Half numbers of the nitrogen lone pairs in **18** are used for the bonding with oxygen atoms in N₆O₃. The stabilization is expected. The optimized structure is planar with equal N–N bond lengths between those of single and double bonds. The computed heat of formation (154.7 kcal mol⁻¹) and the barrier to unimolecular dissociation (62.4 kcal mol⁻¹) suggested thermodynamic and kinetic stabilities. The long-sought N₆ ring can be formed by adding coordinate-covalent bonds from oxygen.

5 Short Atomic Distances in Metallacycles

Some inorganic molecules containing metal–oxygen bonds have unusual properties (Scheme 11). In disiloxane, Si–O–Si angles between the single bonds are wider than those of ethers. The bond angle is 144.1° for $\text{H}_3\text{Si–O–SiH}_3$ [127] and 111.5° for $\text{H}_3\text{C–O–CH}_3$ [128]. The Si–Si bond distance in the three-membered

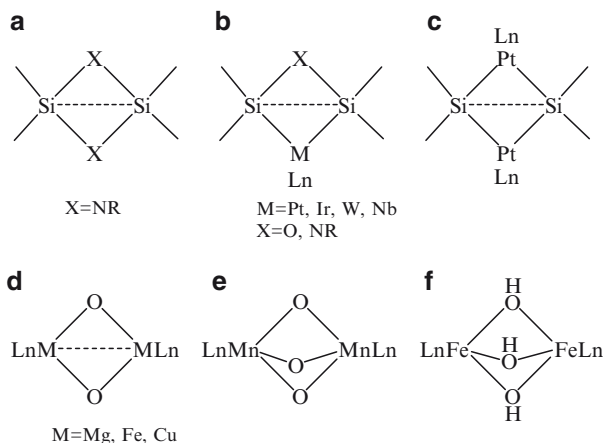


Scheme 11 Orbital interactions for unusual geometries of inorganic molecules

ring molecule, disilaoxirane, is unusually short. The Si–Si bond length (2.227 Å) in 1,1,2,2-tetramesityldisilaoxirane is closer to a typical Si=Si bond length (ca. 2.16 Å) than to a normal Si–Si bond (ca. 2.38 Å) [129]. The nonbonded Si–Si distance in the four-membered ring molecules, 1,3-cyclodisiloxane, is also short. The distance (2.31 Å) [130] in the tetramesityl derivative is shorter than the normal Si–Si single bond (2.34 Å) and, surprisingly, also shorter than the nonbonded O---O distance (2.47 Å). Our chemical orbital theory gives us insight into the unusual properties of molecules containing the Si–O bonds [131] and related metallacycles.

5.1 Small Ring Molecules Containing Si–O Bonds

The lone pairs on the oxygen atom in disiloxane, disilaoxirane, and 1,3-cyclodisiloxane have been shown [131] by the bond model analysis [132–134] to delocalize significantly to the silicon atoms through the interaction of the *n*-orbital



Scheme 12 Short nonbonded distances between metal atoms

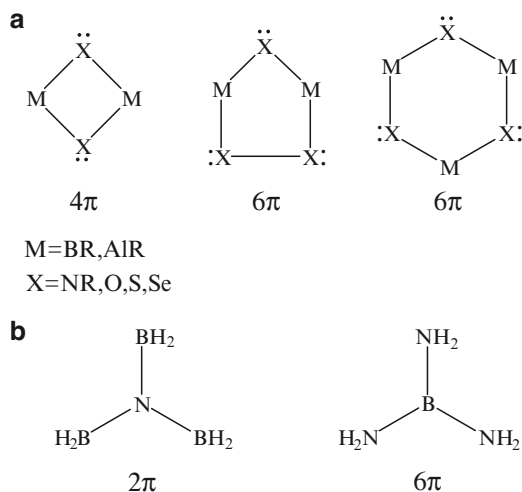
on the oxygen atom with a vacant orbital (denoted by v^* in Scheme 11) on the silicon atoms. The v^* orbital is a vacant $3d$ orbital in the well known but disputed oldest ($d-p$) π bonding model [135]. The oxygen atoms form dative π bonds with the Si atoms. In the ring systems the oxygen lone pairs delocalize in a cyclic manner through the cyclic interactions of the n -orbital with the v^* orbitals favored by the continuity of the orbital phase (Chapter “An Orbital Phase Theory” by Inagaki in this volume). The v^*-v^* interactions as well as the dative π bonding contribute to the shortening of the Si–Si distances in disiloxirane [131]. The transannular delocalization of the oxygen lone pairs through the Si atoms can account for the short Si–Si distance relative to the O–O separation in 1,3-cyclodisiloxane, but the shortening of Si–O single bond by the dative π bonds alone cannot.

5.2 Related Metallacycles

There are many four-membered metallacycles containing short metal---metal nonbonded distances. Cyclodisilazanes (Scheme 12a) isoelectronic to 1,3-cyclodisiloxanes also have short Si---Si distances [136, 137].

Short nonbonded Si---Si distances have been observed in four membered metallacycles (Scheme 12b) with a Pt, Ir, W, or Nb atom [138–142] in place of one of the oxygen (nitrogen) atoms of 1,3-cyclodisilazanes (1,3-cyclodisilazanes) and in μ -silylene-bridged dinuclear platinum complexes (Scheme 12c) [143, 144]. Electron donating occupied orbitals are expected to be on the platinum atoms like lone pair orbitals on the oxygen atoms in cyclodisiloxanes.

The bis(μ -oxo)dimetal $[M_2(\mu-O)_2]^{n+}$ core (Scheme 12d) has been proposed as a common motif for oxidation chemistry mediated by manganese, iron, and copper



Scheme 13 π conjugations and number of π electrons in inorganic molecules

metalloenzymes [145, 146]. Short metal-metal distances have been reported for Mn---Mn [147–152], for Fe---Fe [153–155], and for Cu---Cu [156–160]. Three μ -oxo bridges (Scheme 12e) shorten the Mn---Mn distance [161]. Three hydroxyl bridges (Scheme 12f) also result in a short Fe---Fe distance [162, 163]. Low-lying vacant orbitals are available on metal atoms bonded to highly electronegative oxygen atoms. Delocalization of oxygen lone pairs (Scheme 11) contributes to the short M---M distances in the bis(μ -oxo)dimetal $[M_2(\mu-O)_2]^{n+}$ core.

6 π -Conjugation in B–N and Related Systems

π -Type interaction occurs between the nonbonding orbitals on the nitrogen atom and the vacant orbital on the boron atom in single B–N bonds. The π -electron system in a B–N bond is isoelectronic to that of a C=C bond in alkenes. However, the Hückel rule cannot be applied (Chapter “An Orbital Phase Theory” by Inagaki in this volume) [164] to inorganic heterocycles (Scheme 13a) containing B or Al atoms as acceptors with a vacant orbital and N, O, S, Se atoms as donors with one or two lone pairs. Donors and acceptors are alternately disposed along the cyclic chains. In such molecules π electrons cannot effectively delocalize in a cyclic manner: cyclic conjugation is discontinuous [165] (Chapter “An Orbital Phase Theory” by Inagaki in this volume). The number of π electrons is not a predominant factor of stability for such discontinuous conjugations. Interaction between neighboring pairs of donors and acceptors is more important.

π -Conjugation between B and N makes a difference from that between C atoms in noncyclic conjugations. Cross conjugate systems (trimethylenemethane dication and anion) with two and six π electrons in four p -orbitals are more stable than their linear isomers (1,3-butene-2-yl dication and dianion) in organic chemistry [166] due to cyclic orbital interaction in a noncyclic conjugation [167] (Chapter “An Orbital Phase Theory” by Inagaki in this volume). This is not the case with the B–N systems, $\text{N}(\text{BH}_2)_3$ and $\text{B}(\text{NH}_2)_2$ [168]. These inorganic molecules have two or six π electrons. However, appreciable stabilization of the cross conjugate B–N systems has not been found [168], in line with the rationale for cyclic B–N systems that neighboring donor–acceptor interaction is more dominant than the number of electrons.

Acknowledgements The author thanks Prof. Hisashi Yamamoto of Chicago University for his reading of the manuscript and his encouragement, Messrs. Hiroki Murai and Hiroki Shimakawa for their assistance in preparing the manuscript, and Ms. Jane Clarkin for her English suggestions.

Note added in proof Trinuclear arsenic compounds, $\text{L}_2\text{As}=\text{As}=\text{AsL}$, related to the triazene derivatives in Sect. 4.1 were reported very recently (Hitchcock PB, Lappert MF, Li G, Protchenko AV (2009) Chem Commun 428).

References

1. Lewis GN (1916) J Am Chem Soc 38:762
2. Sidgwick NV (1923) Trans Faraday Soc 19:469
3. Wade K (1971) J Chem Soc Chem Commun 792
4. Wade K (1976) Adv Inorg Chem Radiochem 18:1
5. Hückel E (1931) Z Phys 70:204
6. Woodward RB, Hoffman R (1965) J Am Chem Soc 87:395
7. Ding YH, Takeuchi K, Inagaki S (2004) Chem Lett 33:934
8. Takeuchi K, Shirahama Y, Inagaki S (2008) Inorg Chim Acta 361:355
9. Zimmerman HE (1966) J Am Chem Soc 88:1564; 1566
10. Zimmerman HE (1966) Science 153:837
11. Hamilton TP, Schaefer HF III (1990) Chem Phys Lett 166:303
12. Honea EC, Ogura A, Murray CA, Raghavachari K, Sprenger WO, Jarrold MF, Brown WL (1993) Nature 366:42
13. Kuznetsov AE, Birch KA, Boldyrev AI, Li X, Zhai HJ, Wang LS (2003) Science 300:622
14. Billmers RI, Smith AL (1991) J Phys Chem 95:4242
15. Kuznetsov A, Boldyrev A (2002) Struct Chem 13:141
16. Balasubramanian K, Sumathi K, Dai D (1991) J Chem Phys 95:3494–505
17. Martinez A, Vela A (1994) Phys Rev B 49:17464
18. Cuthbertson AF, Glidewell C (1981) Inorg Chim Acta 49:91
19. Li X, Kuznetsov AE, Zhang HF, Boldyrev AI, Wang LS (2001) Science 291:859
20. Kuznetsov AE, Boldyrev AI, Li X, Wang LS (2001) J Am Chem Soc 123:8825
21. Li X, Zhang HF, Wang LS, Kuznetsov AE, Cannon NA, Boldyrev AI (2001) Angew Chem Int Ed 40:1867
22. Juselius J, Straka M, Sundholm D (2001) J Phys Chem A 105:9939
23. Fowler PW, Havenith RWA, Steiner E (2001) Chem Phys Lett 342:85
24. Zhan CG, Zheng F, Dixon DA (2002) J Am Chem Soc 124:14795

25. Zhai HJ, Kuznetsov AE, Boldyrev AI, Wang LS (2004) *Chem Phys Chem* 5:1885
26. Kuznetsov AE, Zhai HJ, Wang LS, Boldyrev AI (2002) *Inorg Chem* 41:6062
27. Kraus F, Aschenbrenner JC, Korber N (2003) *Angew Chem Int Ed* 42:4030
28. Roziere F, Seigneurin A, Belin C, Michalowicz A (1985) *Inorg Chem* 24:3710
29. Jin Q, Jin B, Xu WG (2004) *Chem Phys Lett* 396:398
30. Kraus F, Korber N (2005) *Chem Eur J* 11:5945
31. Critchlow SC, Corbett JD (1984) *Inorg Chem* 23:770
32. Cisar A, Corbett JD (1977) *Inorg Chem* 16:2482
33. Janssen RAJ (1993) *J Phys Chem* 97:6384
34. Murchie MP, Johnson JP, Passmore J, Sutherland GW, Tajik M, Whidden TK, White PS, Grein F (1992) *Inorg Chem* 31:273
35. Clark RJH, Dines TJ, Ferris LTH (1982) *J Chem Soc Dalton Trans* 11:223
36. Lin YC, Juselius J, Sundholm D, Gauss J (2005) *J Chem Phys* 122:214308
37. Havenith RWA, van Lenthe JH (2004) *Chem Phys Lett* 385:198
38. Havenith RWA, Fowler PW, Steiner E, Shetty S, Kanhere D, Pal S (2004) *Phys Chem Chem Phys* 6:285
39. Santos JC, Tiznado W, Contreras R, Fuentealba P (2004) *J Chem Phys* 120:1670
40. Bishop DM, Chailler M, Larrieu K, Pouchan C (1984) 51:179
41. Lee TJ, Rendel AP, Taylor PR (1990) *J Chem Phys* 92:489
42. Alexandrova AN, Boldyrev A (2003) *J Phys Chem A* 107:554
43. Beckman HO, Koutecky J, Bonacic-Koutecky V (1980) *J Chem Phys* 73:6182
44. Kornath A, Kaufmann A, Zoerner A, Ludwig R (2003) *J Chem Phys* 118:6957
45. Kornath A, Ludwig R, Zoerner A (1998) *Angew Chem Int Ed* 37:1575
46. Kornath A, Zoerner A, Ludwig R (2002) *Inorg Chem* 41:6206
47. Jones RO (1993) *J Chem Phys* 99:1194
48. Jug K, Schluff HP, Kupka H, Iffert R (1988) *J Comput Chem* 9:803
49. Baulder M, Duester D, Ouzounis D (1987) *Z Anorg Allg Chem* 544:87
50. Glukhovtsev MN, Schleyer PVR, Maerker C (1993) *J Phys Chem* 97:8200
51. Chen MD, Huang RB, Zheng LS, Zhang QE, Au CT (2000) *Chem Phys Lett* 325:22
52. Gausa M, Kaschner R, Lutz HO, Seifert G, Meiwes-Broer KH (1994) *Chem Phys Lett* 230:99
53. Gausa M, Kaschner R, Seifert G, Faehrmann JH, Lutz HO, Meiwes-Broer KH (1996) *J Chem Phys* 104:9719
54. Teo BK (1984) *Inorg Chem* 23:1251
55. Teo BK, Longoni G, Chung FRK (1984) *Inorg Chem* 23:1257
56. Mingos DMP (1985) *Inorg Chem* 24:114
57. Slee T, Lin Z, Mingos DMP (1989) *Inorg Chem* 28:2256
58. Balakrishnarajan MM, Jemmis ED (2000) *J Am Chem Soc* 122:4516
59. Balakrishnarajan MM, Hoffmann R, Pancharatna PD, Jemmis ED (2003) *Inorg Chem* 42:4650
60. Kuznetsov AE, Boldyrev AI, Zhai HJ, Wang LS (2002) *J Am Chem Soc* 124:11791
61. Upton TH (1987) *J Chem Phys* 86:7054
62. Petterson LGM, Bauschlicher CW Jr, Halicioglu T (1987) *J Chem Phys* 87:2205
63. Zhao C, Balasubramanian K (2002) *J Chem Phys* 116:3690
64. Zhao C, Balasubramanian K (2001) *J Chem Phys* 115:3121
65. Fuke K, Tsukamoto K, Misaizu F, Sanekata M (1993) *J Chem Phys* 99:7807
66. Yoshida S, Fuke K (1999) *J Chem Phys* 111:3880
67. Kircher P, Huttner G, Heinze K, Renner G (1998) *Angew Chem Int Ed* 37:1664
68. Ma J, Hozaki A, Inagaki S (2002) *Inorg Chem* 41:1876
69. Schiffer H, Ahlrichs R, Häser M (1989) *Theor Chim Acta* 75:1
70. Gimarc BM, Zhao M (1994) Phosphorus, sulfur, and silicon 93–94:231
71. Yoshifuji M, Inamoto N, Ito K, Nagase S (1985) *Chem Lett* 14:437
72. Baudler M (1982) *Angew Chem Int Ed Engl* 21:492
73. Baudler M (1987) *Angew Chem Int Ed Engl* 26:419

74. Baudler M, Glinka K (1993) *Chem Rev* 93:1623
75. Häser M (1994) *J Am Chem Soc* 116:6925
76. Böcker S, Häser M (1995) *Z Anorg Allg Chem* 621:258
77. Ma J, Hozaki A, Inagaki S (2002) Phosphorus, sulfur and silicon 177:1705
78. Levinson AS (1977) *J Chem Educ* 54:98
79. Lloyd NC, Morgan HW, Nicholson BK, Ronumus RS (2005) *Angew Chem Int Ed* 44:941
80. Breslow R (1957) *J Am Chem Soc* 79:1762 (C & EN, March 22, 1999, 33)
81. House HO (1972) *Modern synthetic reactions*. Benjamin, CA, Chap 4
82. Feher F, Linke KH (1966) *Z Anorg Allg Chem* 344:18
83. Clarke DA, Barclay RK, Stock CC, Rondestvedt CS (1955) *Proc Soc Exp Biol Med* 90:484
84. Rice FO, Luckenbach TA (1960) *J Am Chem Soc* 82:2681
85. Wiberg N, Bayer H, Bachhuber H (1975) *Angew Chem Int Ed* 14:177
86. Hayon E, Simic M (1972) *J Am Chem Soc* 94:42
87. Milligan DE, Jacox ME (1964) *J Chem Phys* 41:2838
88. Clusius K, Huerzeler H (1954) *Helv Chim Acta* 37:798
89. Butler RN, Hanniffy JM, Stephens JC, Burke LA (2008) *J Org Chem* 73:1354
90. Kwon O, McKee ML (2003) *Theor Compt Chem* 12:405
91. Nguyen MT (2003) *Coord Chem Rev* 244:93
92. Friedmann A, Soliva AM, Nizkorodov SA, Bieske EJ, Maier JP (1994) *J Phys Chem* 98:8896
93. Hiraoka K, Nakajima G (1988) *J Chem Phys* 88:7709
94. Workentin MS, Wagner BD, Luszytk J, Wayner DDM (1995) *J Am Chem Soc* 117:119
95. Vogler A, Wright RE, Kunkey H (1980) *Angew Chem* 92:745
96. Benson FR (1984) *The high nitrogen compounds*. Wiley, New York
97. Inagaki S, Goto N (1987) *J Am Chem Soc* 109:3234
98. Inagaki S, Kawata H, Hirabayashi Y (1982) *Bull Chem Soc Jpn* 55:3724
99. Inagaki S, Iwase K, Goto N (1986) *J Org Chem* 51:362
100. Wiberg N (1984) *Adv Organomet Chem* 24:179
101. Cowley RE, Elhaik J, Eckert NA, Brennessel WW, Bill E, Holland PL (2008) *J Am Chem Soc* 130:6074
102. Sana M, Leroy G, Nguyen MT, Elguero J (1979) *Nouv J Chim* 3:607
103. Hammerl A, Klapoetke TM, Schwerdtfeger P (2003) *Chem Eur J* 9:5511
104. Benin V, Kaszynski P, Radziszewski JG (2002) *J Org Chem* 67:1354
105. Ugi I, Huisgen R (1958) *Chem Ber* 91:531
106. Butler RN, Collier S, Fleming AFM (1996) *J Chem Soc Perkin Trans 2* 801
107. Ferris KF, Bartlett RJ (1992) *J Am Chem Soc* 114:8302
108. da Silva G, Bozzelli JW (2008) *J Org Chem* 73:1343
109. Vij A, Pavlovich JG, Wilson WW, Vij V, Christe KO (2002) *Angew Chem Int Ed* 41:3051
110. Oestmark H, Wallin S, Brinck T, Carlqvist P, Claridge R, Hedlund E, Yudina L (2003) *Chem Phys Lett* 379:539
111. Netzloff HM, Gordon MS, Christe K, Wilson WW, Vij A, Vij V, Boatz JA (2003) *J Phys Chem A* 107:6638
112. Glukhovtsev MN, Schleyer PVR (1992) *Chem Phys Lett* 198:547
113. Wilson KJ, Perera SA, Bartlett RJ (2001) *J Phys Chem A* 105:4107
114. Warren DS, Gimarc BM (1992) *J Am Chem S* 114:5378
115. Warren DS, Gimarc BM, Zhao M (1994) *Inorg Chem* 33:710
116. Christe KO, Wilson WW, Sheehy JA, Boatz J (1999) *Angew Chem Int Ed* 38:2004
117. Curtius T (1890) *Ber Dtsch Chem Ges* 23:3023
118. Klapoetke TM, Noeth H, Schuett T, Warchhold M (2000) *Angew Chem Int Ed* 39:2108
119. Lein M, Frunzke J, Timoshkin A, Frenking G (2001) *Chem Eur J* 7:4155
120. Dulmage WJ, Meyers EA, Lipscomb WN (1953) *Acta Crystallogr* 6:760
121. Kukolich SG (1982) *J Am Chem Soc* 104:4715

122. Billingsley J, Callear AB (1971) *Trans Faraday Soc* 67:589
123. Brittain AH, Cox AP, Kuczkowski RL (1969) *Trans Faraday Soc* 1963
124. Smith DW, Hedberg K (1956) *J Chem Phys* 25:1282
125. Brown RD, Harcourt RD (1961) *Proc Chem Soc* 216
126. Wilson KJ, Perera SA, Bartlett RJ (2001) *J Phys Chem A* 105:7693
127. Almenningen A, Bastiansen O, Ewing V, Hedberg K, Traetteberg M (1963) *Acta Chem Scand* 17:2455
128. Kimura K, Kubo M (1959) *J Chem Phys* 30:151
129. Yokelson HB, Millevolte AJ, Gillette GR, West R (1987) *J Am Chem Soc* 109:6865
130. Fink MJ, Haller KJ, West R, Michl J (1984) *J Am Chem Soc* 106:822
131. Ma J, Inagaki S (2000) *J Phys Chem A* 104:8989
132. Iwase K, Inagaki S (1996) *Bull Chem Soc Jpn* 69:2781
133. Inagaki S, Yamamoto T, Ohashi S (1997) *Chem Lett* 26:977
134. Ikeda H, Inagaki S (2001) *J Phys Chem A* 47:10711
135. Cotton FA, Wilkinson G, Gaus PL (1995) *Basic inorganic chemistry*. Wiley, New York, p 383
136. Wheatley PJ (1962) *J Chem Soc* 1721
137. Jaschke B, Herbst-Irmer R, Klingebiel U, Pape T (2000) *J Chem Soc Dalton Trans* 1827
138. Greene J, Curtis MD (1977) *J Am Chem Soc* 99:5176
139. Pham EK, West R (1990) *Organometallics* 9:1517
140. Hong P, Damrauer NH, Carroll PJ, Berry DH (1993) *Organometallics* 12:3698
141. Tanabe M, Osakada K (2001) *Organometallics* 20:2118
142. Nikonov GI, Vyboishchikov SF, Kuzmina LG, Howard JAK (2002) *Chem Commun* 568
143. Shimada S, Rao MLN, Li YH, Tanaka M (2005) *Organometallics* 24:6029
144. Shimada S, Tanaka M (2006) *Coord Chem Rev* 250:991
145. Que L Jr, Dong Y (1996) *Acc Chem Res* 29:190
146. Tolman WB (1997) *Acc Chem Res* 30:227
147. Plaskin PM, Stoufer RC, Mathew M, Palemik GJ (1972) *J Am Chem Soc* 94:2121
148. DeRose VJ, Mukerji I, Latimer MJ, Yachandra VK, Sauer K, Klein MP (1994) *J Am Chem Soc* 116:5239
149. Larson EJ, Pecoraro VL (1991) *J Am Chem Soc* 113:3810
150. Gohdes JW, Armstrong WH (1992) *Inorg Chem* 31:368
151. Waldo GS, Yu S, Penner HJE (1992) *J Am Chem Soc* 114:5869
152. Yachandra VK, Sauer K, Klein MP (1996) *Chem Rev* 96:2927
153. Teo BK, Shulman RG (1982) In: Spiro T (ed) *Iron-sulfur proteins*. Wiley, New York
154. Zang Y, Dong Y, Que L Jr, Kauffman K, Muenck E (1995) *J Am Chem Soc* 117:1169
155. Dong Y, Fujii H, Hendrich MP, Leising RA, Pan G, Randal CR, Wilkinson EC, Zang Y, Que L Jr, Fox B, Kauffmann K, Muenck E (1995) *J Am Chem Soc* 117:2778
156. Blackburn NJ, Barr ME, Woodruff WH, van der Oost J, de Vries S (1994) *Biochemistry* 33:10401
157. Iwata S, Ostermeier C, Ludwig B, Michel H (1995) *Nature* 376:660
158. Mahapatra S, Halfen JA, Wilkinson EC, Pan G, Wang X, Young VG Jr, Cramer CJ, Que L Jr, Tolman WB (1996) 118:11555
159. Mahapatra S, Young VG Jr, Kaderli S, Zuberbuehler AD, Tolman WB (1997) *Angew Chem Int Ed* 36:130
160. Mahadevan V, Hou Z, Cole AP, Root DE, Lal TK, Solomon EI, Stack TDP (1997) *J Am Chem Soc* 119:11996
161. Wieghardt K, Bossek U, Nuber B, Weiss J, Bonvoisin J, Corbella M, Vitols SE, Girerd JJ (1988) *J Am Chem Soc* 110:7398
162. Drueeke S, Chaudhuri P, Pohl K, Wieghardt K, Ding XQ, Bill E, Sawaryn A, Trautwein AX, Winkler H, Gurman SJ (1989) *J Chem Soc Chem Commun* 59
163. Gamelin DR, Bominaar EL, Kirk ML, Wieghardt K, Solomon EI (1996) *J Am Chem Soc* 118:8085
164. Inagaki S, Hirabayashi Y (1982) *Inorg Chem* 21:1798

Index

A

Acetylene, 7
Acetylene dicarboxylate, 105
Acetylenes, conformers, 104
1,8-Acridinedione dyes, 50
Acrylonitrile, 50
Adamantan-2-one, 134
Alkali metals, $4N+2$ valence electron rule, 299
Alkaline earth metals, $4N+2$ valence electron rule, 299
Alkanes, preferential branching, 105
Alkenes, [2+2] cycloadditions, 26
HOMO energy, 15
Alkyl species, isomeric, relative stabilities, 108
7-Alkylidenenorbornenes, 77
Allenecarboxylates, 29
Allylsilanes, *Z*-selectivity, 120
Aluminum clusters, 110
Amine nitrogen atom, 129
Amine non-bonding orbital, facial selectivity, 174

B

β -Arylenamines, [2+2] cycloaddition, 40
 β -Arylenol ethers, [2+2+2] cycloaddition, 40
B–N systems, π -conjugation, 310
Bent unsaturated bonds, [2+2] cycloadditions, 43
Benzene, cyclic orbital interaction, 94
Benzo[*b*]fluorene, 167
Benzobicyclo[2.2.2]octadienes, 79
Benzobicyclo[2.2.2]octan-2-ones, 139
Benzonorbornadienes, 163
Benzonorbornene, 163
1,4-Benzoquinone, 98
1,4-Benzoquinone 4-oximes, 113
Benzzyne, 43

Bicyclic systems, 171
Bicyclo[2.2.1]hepta-2,5-diene-2,3-dicarboxylic anhydride, 162
Bicyclo[2.2.1]heptane, unsaturated, 148
Bicyclo[2.2.1]heptanones, 135
Bicyclo[2.2.1]hept-2-ene-2,3-dicarboxylic anhydride, 162
Bicyclo[2.2.2]octene, 149, 153
Bis(trifluoromethyl)ketene, 46, 47
Bond orbitals, 2, 11
Bond orbitals, interactions, 11
Borazine, 115
Butadiene, bond orbitals, 11, 12
2-Buten-1,4-diyl (BD), 90
Butenes, 26, 107
n-Butyllithium, 108

C

Carbonyl compounds, [2+2] cycloadditions, 29
LUMO, 16
Carbonyl π^* orbitals, orbital phase environment unsymmetrization
CH/ π interactions, 211
Chemical orbital theory, 1, 23, 73, 83
Chemical reactions, interactions of frontier orbitals, 13
Ciplak effect, 183
Composite molecules, arrangements, 153
Conformational stability, 104
Cyclic conjugations, 83, 94, 97, 111
Cycloadditions, 23
[2+2]Cycloadditions, 26, 43, 44, 48
[4+2]Cycloadditions, 30, 35
Cycloalkanes, 132, 284
Cycloalkynes, [2+2] cycloaddition, 44
Cyclobutadiene, antiaromatic, 112

Cyclobutanones, 44, 45
 1,3-Cyclodisiloxane, 293
 Cyclohexadiene, 169
 Cyclohexanones, 79, 132, 133
 Cyclopentane, 166
 Cyclopentanone, 134
 Cyclopentaphosphane, 293
 Cyclopentene, 147
 Cyclopentyne, 44
 Cyclopolysilenes, 284

D

Delocalization band, 26, 34
 5,5-Diarylcyclopentadienes, 166
 2,2-Diarylcyclopentanone, 134
 Diazadiborane, 116
 Dibenzobicyclo[2.2.2]octadienone, 144
 Dibenzobicyclo[2.2.2]octatrienes, 158
 1,2-Dicyano-1,2-bis(trifluoromethyl) ethylene, 27
 Diels–Alder dienes, 129
 Diels–Alder dienes, stereoselection, 166
 Diels–Alder dienophiles, 129
 Diels–Alder reactions, 65, 183
 exo-addition, 35
 stereoselection, 161
 Dienophiles, 161
 dibenzobicyclo[2.2.2]octatriene structure, 164
 norbornane structure, 162
 1,2-Dihydro-1,2-azaborane, 115
 1,4-Dihydropyridines, 50
 2,5-Dimethyl-2,4-hexadiene, 28
 Dimethylenecyclobutene, 113
 2,5-Dimethylpyrazolone-*N,N*-dioxide, 123
 1,1-Diphenylbutadiene, 28
 Diphenylmethylenecyclobutane, 41
 Diradicals, 83, 109, 219, 222
 acyclic, 244
 bicyclic, σ -type, 252
 cyclic orbital interactions, 227
 cyclic π -conjugated, 238
 Kekulé vs. non-Kekulé, 235
 localized, 243
 monocyclic, ring strain, 249
 π -conjugated, 233, 235
 substituent effects on S-T gaps, 245
 substituent effects on stability, 248
 Disilaoxirane, 293
 Disiloxane, 293
 Disposition isomers, 83
 Donor–acceptor disposition isomers, 113
 Donor–acceptor interaction, 23, 83

E

Electron delocalization band, 23
 Electron density, frontier orbital amplitude, 14
 Electron donors/acceptors, chemical reactions, 24
 Electron transfer band, 23
 Electron-accepting group (EAG), 99
 Electron-donating group (EDG), 99
 Electronic spectra, 13
 Electrons, delocalization, 1, 8, 25, 83
 number of, 9
 Electrophilic additions, 64
 regioselectivities, 99
 Electrophilic aromatic substitutions, 33, 72, 100
 Electrostatic interaction, 183, 207
 Electrostatic mixing, 62
 Ethylene, 7, 11, 16
 Exchange repulsion, 9

F

Facial selection, 129
 π -Facial selectivity, 57, 183
 origin, 185
 Fluorene derivatives, nitration, 172
 5-Fluoro-2-methyleneadamantane, 147
 2-Fluorodibenzobicyclo[2.2.2]octatriene, 158
 Frontier orbitals, 1, 13, 14, 23
 Furazano[3,4-*d*]pyridazine 5,6-dioxide, 124

G

Geminal bond participation, 116
 Geminal interaction, 265, 269

H

Heterocycles, inorganic, 83, 293
 Hexazine N_6 , 293, 306
 HOMO/LUMO, 11, 12
 Hydrazine NH_2-NH_2 , 4
 Hydride equivalent transfers, 52
 Hydrogen molecule, bond orbitals, 3
 Hydronitrogens, 293, 304

I

Indoles, unsaturated acceptors, 34
 Inverted bonds, 265, 272
 Ionization energies, 13
 Isobutane, 107
cis-Isomers, relative stabilities, 122
 7-Isopropylidenebenzonorbomadiene, 163

11-Isopropylidenedibenzonorbornadienes, 153
7-Isopropylidenenorbornadiene, 163
7-Isopropylidenenorbornanes, 2-*exo*-
monosubstituted, 148

K

Kekulé vs. non-Kekulé diradicals, 235
Ketenes, [2+2] cycloadditions, 44
[4+2] cycloadditions, 35
Ketones, 129
stereoselection, 132
Kinetic stability, 219

L

Lone pair effect, 265

M

Maleic anhydride (MA), 18, 168
norbornadiene derivative, 162
Mechanistic spectrum, 23
Metal clusters, 293
Metal complexes, acute coordination angle, 110
Metal rings, 26, 27, 29, 31–34, 293
Metallacycles, 293, 310
short atomic distances, 308
Methyl benzenes, TCNQ, 52
N-Methyl-1,3,5-triazoline-2,4-dione (MTD), 168
Methylenecyclohexane, 145
Methylenemalononitriles, 28
7-Methylenenorbornanes, 149
2,3-*exo,exo*-disubstituted, 148
Methylketene, dimerization, 47
2-Methylpropene, 107
Michael acceptor, 129
Molecular orbitals, 11

N

N_3H , cyclic unsaturated, 284
NAD(P)H reactions, 23, 49
Naphthalene, 15, 16
Nicotinamide–adenine dinucleotide (NADH), 49
3-Nitrodibenzobicyclo[2.2.2]octadienones, 144
2-Nitrodibenzobicyclo[2.2.2]octatriene, 158
Nitrogen oxides, 293, 307
N-Nitrosamines, N–NO bond cleavage, 175
N-Nitroso bond, bond strength, 174
Non-cyclic conjugation, 85, 98
2-Norbornanone, 140
7-Norbornanone, 135
Norbornenes, 77, 152

Norbornyne, 44
Nucleophilic conjugate addition,
stereoselection, 171

O

Octahedrons, M_6 clusters, 300
Olefin π orbitals, π orbitals, β positions, 157
 σ orbitals, β -position, 147
Olefins, 129
stereoselection, 145
Oligosilenes, polycyclic, 286
Orbital amplitude, 1, 15, 23, 57
Orbital deformation, 57
Orbital energy 1
Orbital interactions, 1, 2, 23, 185
chemical bonds, 2
secondary, 129, 131, 183
strength, 6
Orbital mixing, 57
rules, 1, 21, 58, 183
Orbital phase, 1, 3, 23, 57, 83, 129, 222
continuity, 1, 83, 88, 227, 265
environment, 1, 17, 18, 130, 131, 183
theory, 21, 83, 219, 221
Orbital polarization, 57
Orbital symmetry, 1, 16
Orbital unsymmetrization, 129
overlapping, 130
Orbitals, amplitude, 1, 4, 6, 12
energy, 1, 3, 12
Overlap mixing, 59
3-Oxacyclobutene ring, 120
Oxetanes, 19
2-Oxopropane-1,3-diyl, 93

P

P_3H molecules, cyclic unsaturated, 284
Pseudoexcitation band, 26, 36
Pentagon stability, 293, 302
Pentazole RN_3 , 293, 306
N-Phenyl-1,3,5-triazoline-2,4-dione
(PTD), 168
N-Phenylmaleimide (PMI), 168
N-Phenyltriazolinedione, 169
Photochemical reactions, 19
Polarization, 83
Polycyclic molecules, 274
Polyenes, conjugate, cycloisomerization, 32
Polynitrogens, 293, 304
Preferential branching, 83
Propellanes, heterocyclic, 169
Propyl propenyl ether, 27

- Pseudoexcitation, 25
band, 23, 36
Pyrazolone *N,N*- dioxide ring, 123
- Q**
Quasi-intermediate, 23
- R**
Radical reactions, copolymerizations, 18
Reactivity, 1, 15, 23, 83
Regioselectivities, 57, 64
 π -Relaxation, 265, 268
applications, 276
 σ -Relaxation, 265, 268
Ring strain, 83, 265
relaxation, 266
- S**
Secondary orbital interaction (SOI), 170
Selectivity, 1, 16, 23, 83
2-Siloxybutadienes, 29
Singlet molecular oxygen O₂, 23, 36
Si–O bonds, small ring molecules, 309
Spin preference, 219
Spiro[cyclopentane-1,9'-fluorene], 153
Spiro-1,3-cyclopentadienes, 167
Spirocyclopentanone, 142
Spirofluorene–diene system, 168
Stability, 83, 108, 122, 219, 248
Stereoselectivity, 57
Steric repulsion, 9, 183, 205
Strain relaxation, small ring molecules, 121
Styrene, 18
- Surface reactions, 23
Surfaces, [2+2] cycloadditions, 47
[4+2] cycloadditions, 36
- T**
Tautomerism, 83
TCNE, 29
TCNQ, methyl benzenes, 52
Tetraazabutadiene (tetrazadiene)
HN=NN=NH, 293, 305
Tetrakis (dimethylamino)ethylene, 29
2-Tetrazene H₂NN=NNH₂, 293, 305
Thiophene 1-oxides, Diels-Alder
reaction, 213
Torquoselectivities, 120
Torsional control, 183, 207
Transfer band, 26, 29, 49
Triazene HN=NNH₂, 293, 305
Tricyclo[3.2.1.0]octan-8-one, 135
Trimethylenemethane (TMM), 90
- V**
Valence electron rules, 293, 294
2-Vinylideneadamantanes, 147
Vinylidenenorbornanes, 150
- X**
Xylylenes, orbital phase properties, 103
- Z**
Z-selectivity, 83, 119, 120
Zeolites, photooxygenation, 43